Bayesian Framework for Multi-Stage Transmission Expansion Planning Under Uncertainty via Emulation

Antony Lawson

A Thesis presented for the degree of
Doctor of Philosophy

Statistics and Probability
Department of Mathematical Sciences
Durham University
United Kingdom

February 2018

Dedicated to

Pauline Turnbull

and

John “Jack” Lawson

Bayesian Framework for Multi-Stage Transmission Expansion Planning Under Uncertainty via Emulation

Antony Lawson

Submitted for the degree of Doctor of Philosophy

February 2018

Abstract:

Effective transmission expansion planning is necessary to ensure a power system can satisfy all demand both reliably and economically. However, at the time reinforcement decisions are made many elements of the future power system background are uncertain, such as demand level, type and location of installed generators, and plant availability statistics. In the current power system planning literature, making decisions which account for such uncertainties is usually done by considering a small set of plausible scenarios, and the resulting limited coverage of parameter space limits confidence that the resulting decision will be a good one with respect to the real world.

This thesis will consider a Bayesian approach to transmission expansion planning under uncertainty, which uses statistical emulators to approximate how input affects output of expensive simulators using a small number of training runs (evaluations from the simulator), as well as quantifying uncertainty in the simulator output for all points at which it has not been evaluated. In addition, expert judgement is used to formulate probability density functions to describe the uncertainties which exist in the power system, which can then be used alongside the emulator to estimate expected costs under uncertainty whilst also giving credible intervals for the resulting estimate.

Further, the methodology will be expanded to consider multi-stage transmission expan-

sion problems under uncertainty, where uncertainty can be reduced in various aspects of the power system between decisions. In the existing power system planning literature, multi-stage decisions under uncertainty are handled by considering a small number of possible projections of the future power system, which gives a very limited coverage of the space of all possible projections of the future power system. This thesis will consider how emulation can be used alongside backwards induction to calculate costs across all stages as a function of the first stage decision only, whilst also accounting for the uncertainties which exists in the future power system. As part of this, the future state of the power system is modelled using continuous variables which effectively allows for an infinite number of possible projections to be considered.

Throughout this thesis, the methodology used is detailed in quite general terms, which should allow for the methodology to be applied to problems of interest other than the transmission expansion planning problem considered in this thesis with relative ease.

Declaration

The work in this thesis is based on research carried out in the Statistics and Probability, Department of Mathematical Sciences, Durham University, United Kingdom. No part of this thesis has been submitted elsewhere for any other degree or qualification and it is all my own work unless referenced to the contrary in the text.

Acknowledgements

First, a big thank you to my supervisors, Michael Goldstein and Chris Dent, for their time, patience and expertise throughout my studies and for giving me the opportunity to study towards a PhD, and further thanks to Chris for continuing to travel to Durham for meetings after his move to Edinburgh. In addition, I would like to thank Paul Plumptre for his help and expertise with regards to the particular transmission expansion problem considered, in particular for helping to formulate prior information about uncertainties and appropriate assumptions to make, as well as travelling to Durham for several meetings throughout my studies.

I am also very grateful to Jochen Einbeck for working with me on both a project in the summer of 2011 as well as my undergraduate fourth year project, which prepared me for my postgraduate studies, as well as setting up the initial meeting with Michael Goldstein which led to me studying this project.

I would like to thank everyone in the maths department for all the help they have offered me, both as an undergraduate and a postgraduate, which has helped me get to where I am today.

Thank you to the Durham CDT in Energy for allowing me to participate in many interesting activities throughout my studies, such as field trips to various power stations, as well as organising many very interesting lectures and discussions, which allowed me to acquire a much broader view of energy, climate and technology issues than would otherwise have been possible, as well as funding an additional 6 months of my studies.

Finally, many thanks to The Autonomic Power System Project and EPSRC for funding this project and making my studies possible. This work was funded by EPSRC grant EP/I031650/1.

Contents

List of Figures

List of Tables

Chapter 1

Introduction

1.1 Introduction

In life we are often confronted with a need to make decisions. Statistics can provide us with a methodological framework for making good decisions in the face of uncertainty, such as to maximise expected utility or minimise expected losses.

In the simplest examples, this amounts to taking an appropriately weighted average using known probabilities of all outcomes that can occur. For example, suppose there is a biased die with n faces indexed by $i = 1, ..., n$, with the probability of observing face i known to be p_i. If we are offered a gamble to pay a price, C, to roll the die and receive reward r_i if the die lands on face i, the expected reward of such a gamble could be calculated as

$$R = \sum_{i=1}^{n} r_i p_i \tag{1.1.1}$$

The decision of whether or not to take the gamble can be made to maximise expected profits, by taking the gamble if $R > C$, not taking the gamble if $R < C$ and being indifferent to taking the gamble if $R = C$. This could be extended by considering the attitude to risk of the decision maker (the person offered the gamble) and making a decision to maximise expected utility.

Unfortunately, real world examples are rarely this simple. The most obvious difference is that we rarely know exactly how likely each particular outcome is. Further, the outcome itself may contain a random element, going back to the die example it could

be that if a 6 is rolled, instead of receiving a set prize we instead receive a random prize from some distribution. The primary factor of interest in this thesis, however, is when it takes vast statistical calculation to calculate the profit/loss of a particular outcome.

As a general problem, consider making decisions, $\mathbf{d}$, with variables, $\mathbf{v}$, that can affect the outcome of a situation, and a function $f(\mathbf{v}, \mathbf{d})$ which estimates the costs/profits for particular values of $\mathbf{v}$ and $\mathbf{d}$. If $f(\mathbf{v}, \mathbf{d})$ is very expensive (i.e. it takes a long time to evaluate the function) we will not be able to evaluate it for every set of values of $\mathbf{v}$ and $\mathbf{d}$ that we would like. The primary focus of this thesis is to develop a method of making good decisions which adequately account for the uncertainty which exists when working with expensive simulators, $f(\mathbf{v}, \mathbf{d})$.

In this thesis the particular application of making transmission expansion decisions applied to Britain's power system is considered. As a very simple overview of what will be detailed in the coming chapters, the objective is to identify reinforcement decisions, $\mathbf{d}$, (which equate to building new power lines) which minimise the expected mean constraint costs of a power system (detailed in Chapter 2, for now it suffices to think of these as the additional costs of generating electricity due to bottlenecks in the transmission network) plus the reinforcement costs of the decision, when uncertainty exists in the variables which define Britain's power system, $\mathbf{v}$. In this example, $f(\mathbf{v}, \mathbf{d})$ would be the expensive simulator which calculates total costs (mean constraint costs plus reinforcement costs) for given values of the variables containing uncertainty, $\mathbf{v}$, and decision variables, $\mathbf{d}$. The objective of the problem is to identify the values of $\mathbf{d}$ which minimise the expected value of $f(\mathbf{v}, \mathbf{d})$ when accounting for the uncertainty which exists in $\mathbf{v}$.

The transmission expansion planning problem is one which is considered extensively in the engineering literature. A full literature review will be given in Section 2.3, but an overview is that many applications ignore the uncertainty which exists in the variables which describe the power system background and decisions are identified based on the best projections of the power system available, i.e. the values of variables $\mathbf{v}$ are treated as if their values are known precisely. Further, the articles which do consider uncertainty do so by considering considering a finite (and usually small) set of possible scenarios, i.e. consider a small set of values which $\mathbf{v}$ could possibly take. Such a finite

set of scenarios may give sparse coverage of the space of model inputs, and hence an optimal decision within the model which is strongly dependent on the particular choice of scenarios rather than the underlying uncertainty in model inputs.

Our primary goal is to overcome this limited scope of uncertainty, and present a methodology which can be used to make decisions which account for any possible scenario that could occur (not just a single scenario or limited finite set). In this thesis we will present how emulation can be used as an approximation to simulation. This is achieved by taking a small number of training runs of the simulator, $f(\mathbf{v}, \mathbf{d})$, which vary the model input (values of $\mathbf{v}$ and $\mathbf{d}$) to construct an alternative function, the emulator $\tilde{f}(\mathbf{v}, \mathbf{d})$, which approximates how input affects output of the simulator whilst being much faster to evaluate. Further, an estimate of the uncertainty in the approximation for values not simulated is also given by the emulator.

In addition, expert judgement can be used to specify a probability density function (PDF) to describe a distribution for the possible values the variables containing uncertainty, $\mathbf{v}$, take. This allows for a Bayesian expectation of total costs under uncertainty to be calculated.

This methodology will then be extended further to consider making decisions over multiple stages in time, with the uncertainty in the values of $\mathbf{v}$ reduced between each decision stage based on observations made between each stage. Further, consideration will also be given to how costs estimated and the resulting estimates of optimal decision are sensitive to many underlying assumptions made about the power system not considered in $\mathbf{v}$ (such as National Grid's assumed seasonal model for wind generation or the assumed discount rate of future costs).

1.2 Chapter Summary

The remainder of this thesis is arranged as follows: Chapter 2 defines the constraint cost problem (the main problem of interest in this thesis) in Section 2.1 and demonstrates in Section 2.2 how the constraint costs calculated can be sensitive to many assumptions made about the power system. Section 2.3 then gives an overview of the available literature on transmission expansion planning under uncertainty.

Chapter 3 defines the simulator used to calculate mean annual constraint costs for Britain's power system using the freely available data of National Grid's online reference [69] and shows how the mean annual constraint costs calculated for Britain's power system are also sensitive to many of the assumptions made by National Grid. As the simulator used to calculate constraint costs can be expensive to evaluate for a single set of input data, Chapter 4 shows how importance sampling can be used to acquire an estimate of mean annual constraint costs to a given level of precision whilst expecting to do less work in comparison to using full simulator evaluations.

Chapter 5 details how emulation can be used as part of a methodology for decision making under uncertainty, where a set of training runs from the full simulator are used to approximate how input affects output for values not simulated. Section 5.3 applies this methodology to a simple example, where a single reinforcement decision is to be made whilst considering the uncertainty which exists in a single variable, and Section 5.4 goes on to show how the decision made is sensitive to other assumptions about the power system (such as the cost of reinforcement and the attitude to risk of the decision maker).

Chapter 6 expands on the example of Chapter 5, illustrating how the same methodology can be used to make 2 simultaneous reinforcement decisions whilst considering the uncertainty which exists in three variables. Further, Section 6.2 shows how a consideration of the credible intervals for the estimates of expected total costs can be used to eliminate decisions from consideration which have evidence against them being optimal, which allows for a more accurate emulator model to be fitted over a smaller range of values of the decision variables which were not eliminated. The sensitivity of the estimated optimal decisions to various assumptions made about the power system is again considered in Section 6.4.

An article based on the work of Chapter 6 titled "Bayesian Framework for Power Network Planning Under Uncertainty" has been published in the Elsevier journal "Sustainable Energy, Grids and Networks (SEGAN)" [52].

A consideration to how sensitive cost estimates and the resulting estimated optimal reinforcement decisions are to various underlying assumptions made about the power system is given in Chapter 7. These assumptions include the underlying seasonal

model (which affects the output of wind generation) assumed by National Grid and the assumed future projections for installed generating capacity given by [69].

Chapter 8 gives consideration to how the emulation methodology can be used alongside backwards induction to make multiple stage decisions, which allows for the system to be observed between each decision and make later decisions more suited to the observed state of the future power systems. Section 8.1 gives an overview of the existing literature for multi-stage transmission expansion planning. A methodology for a two stage problem is proposed in Section 8.2, which improves on the existing literature by using continuous variables to model the future scenario observed, effectively allowing for an infinite number of possible future scenarios. The methodology of Section 8.2 is then applied to an example two stage decision problem in Sections 8.3 to 8.5.

This is extended further to a general M stage problem in Chapter 9. An application of this methodology to a three stage problem is considered in Sections 9.2 to 9.5. Section 9.6 then goes on to show how the estimated optimal multi-stage decisions are sensitive to many modelling assumptions made (such as the assumed discount rate of future costs and the assumed planning horizon considered).

It is noted that the methodology presented in Section 9.1.2 of Chapter 9 makes use of quite a useful simplification, where the costs in stage m onwards are dependent on the total reinforcement decisions in the previous $m-1$ stages, $\mathbf{d}_{T_{m-1}}$, and not the individual reinforcement decisions in stages 1 to $m-1$, i.e. $\mathbf{d}_1, ..., \mathbf{d}_{m-1}$. This makes the M stage problem more tractable, as the number of variables the emulator model is fitted over in each stage does not need to grow with the number of decision stages considered. However, Section 9.1.3 notes how the methodology of Section 9.1.2 can be adapted to consider problems where the costs in stage m onwards are dependent on the individual decisions in the previous $m-1$ stages (i.e. $\mathbf{d}_1, ..., \mathbf{d}_{m-1}$) and not just the total reinforcement in the previous $m-1$ stages, $\mathbf{d}_{T_{m-1}}$.

Finally, a discussion of the work presented throughout this thesis is given in Chapter 10.

Throughout the thesis a large amount of notation is used, so a notation appendix is given in Appendix E to assist the reader.

Chapter 2

Decision Making and The Constraint Cost Problem

2.1 The Constraint Cost Problem

This thesis is concerned with decision making under uncertainty. Our primary concern is with the constraint cost problem applied to Britain's power system. This section will introduce the constraint cost problem, and illustrate how constraint costs can be calculated on a simple power system. Further, it will be shown how even in the simple example presented the estimated mean constraint costs are highly sensitive to many assumptions made about the power system.

2.1.1 Power Systems

This subsection gives details of how power systems are modelled for the purpose of the examples presented in this thesis. A power system represents an interconnected geographical region with demand for electricity that must be satisfied. This thesis considers the power system to be made up of several zones which are interconnected via a transmission system (power lines). Not every zone is necessarily directly connected to every other zone.

Each zone is supposed to contain some installed generating capacity (electricity generation) and demand for generating capacity (demand for electricity). Often, installed

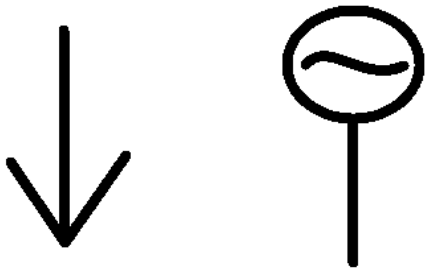

(a) Demand symbol. (b) Generation symbol.

Figure 2.1: Illustrations of symbols used in engineering diagrams.

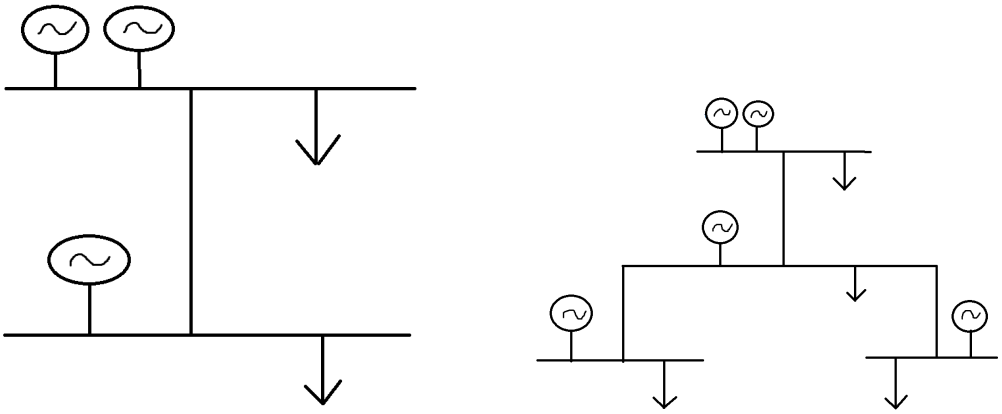

(a) A simple 2 zone power system. (b) A 4 zone power system.

Figure 2.2: Illustrations of power systems as engineering diagrams.

generating capacity in a zone will not be equal to demand in a zone. For this reason, available generating capacity can be traded between any two connected zones. However, the amount of capacity that can be traded between two zones is limited by how much transmission capacity (transmission lines) exist between the zones.

Figure 2.1 illustrates symbols used within diagrams which illustrate power systems. In addition to these, horizontal lines are used to illustrate zones and vertical lines are used to illustrate connections between these zones.

Figure 2.2 gives illustrations of two power systems. Figure 2.2 (a) is a simple 2 zone model, where the two zones are connected to one another and each have a demand to be satisfied. The zone at the top has 2 types of installed generators, the bottom contains just 1 type of installed generating capacity.

Figure 2.2 (b) has 4 zones, where each zone has a demand to be satisfied. The top zone is modelled as having 2 types of generation with the other three zones modelled as having a single generation type. In this example not every zone is directly connected to every other zone. The central zone is connected to each zone, but the other three zones are only connected to this central zone. Of course, the other zones are connected indirectly. The bottom left zone would still be able to import capacity from the bottom right zone, but it would have to be transmitted via the central zone.

2.1.2 Constraint Costs

Constraint costs are calculated on a snapshot by snapshot basis. For the rest of this section it will be assumed that constraint costs are being calculated for a single snapshot in time. A power system has demand spread across its zones, all of which must be satisfied. However, the generating capacity is not free, and not all generating capacities are equally priced. The desire is to satisfy all demand as cheaply as possible. The ideal situation would be to use all of the cheapest generating capacity available across the whole power system to satisfy this demand. However, due to the installed transmission capacity being limited we will not necessarily always be able to use all of the cheapest capacity available to satisfy demand.

In simple terms, constraint costs are the costs that arise due to there being insufficient installed transmission capacity to utilise all of the cheapest generation capacity available. Calculating these costs is actually quite complicated. Generating capacity is associated with two costs: an offer price, $\mathfrak{c}^+$, and a bid price, $\mathfrak{c}^-$. The offer price is the amount which a generator demands to produce an additional MW of capacity, whereas the bid price is the amount which a generator will pay to produce 1 less MW of capacity. The bid and offer prices are dependent on the type of generating technology (e.g. wind, coal, gas etc), such that $\mathfrak{c}_\mathfrak{t}^+$ is the offer price of generating technology type $\mathfrak{t}$ and $\mathfrak{c}_\mathfrak{t}^-$ is the bid price of generating technology type $\mathfrak{t}$.

Initially, the system operator will seek to satisfy demand with generating capacity with the lowest offer price. This results in an unconstrained schedule which satisfies all demand whilst assuming there is infinite transmission capacity (i.e. as if as much as is desired can be traded between zones). This unconstrained schedule first schedules all

available generating capacity with the lowest offer price, then schedules the capacity with the next lowest offer price and so on until all demand is satisfied.

Of course, when actually satisfying demand, the system operator cannot simply trade as much as they would like between zones, as they are restricted by the installed transmission capacity between zones. Therefore, it may be necessary to constrain off (not use) some generating capacity from the unconstrained schedule and constrain on (use instead) some alternative capacity so that demand is met without transmitting more between zones than is physically allowed. In order to do this, the bid price is received of the capacity constrained off, but the offer price must be paid of the capacity constrained on to replace it.

Let $\mathfrak{g}_t^+$ represent the amount (in MW) of generating technology $\mathfrak{t}$ constrained on and $\mathfrak{g}_t^-$ represent the amount (in MW) of generating technology $\mathfrak{t}$ constrained off across the whole system in order to satisfy demand whilst obeying transmission constraints. The constraint costs are then calculated as

$$\sum_{\mathfrak{t}} (\mathfrak{c}_t^+ \mathfrak{g}_t^+ - \mathfrak{c}_t^- \mathfrak{g}_t^-) \tag{2.1.1}$$

In words, this is the sum of the offer prices of generating technology constrained on minus the sum of the bid prices of generating technology constrained off across the whole system. The constraint costs we work with are those that arise from minimising Equation 2.1.1, whilst satisfying all demand.

The importance to consider constraint costs was highlighted in [102]. It was noted how a local generator monopoly may be able to manipulate its bid strategy if insufficient transmission exists in order to sell its generating capacity at a very high price. Further, it was noted that an increase in renewable sources (which have a volatile availability) could result in a large increase in costs occurring due to an insufficient transmission system. Planning a transmission system to minimise Equation 2.1.1 plus the cost of expanding the transmission system would protect against price manipulation as far as is economically justifiable, and will give protection against the constraint costs that occur due to increased renewable generation capacity being built.

One thing that has been overlooked is it will not always be possible to satisfy all demand in the system. In this thesis we concentrate on the economics of the system (minimising

costs) whilst neglecting the security of the system (the reliability to satisfy all demand). The way this thesis handles the fact that it may not always be possible to satisfy all demand is to add an additional generating capacity of curtailment, which would equate to simply not satisfying the demand. However, this capacity will generally come with a huge offer price, making this option very unattractive.

In the next subsection it is illustrated how constraint costs are calculated on a simple power system. Details of the linear program used to solve the constraint cost problem for a general power system will be given later in Chapter 3.

2.2 A Simple Example to Illustrate Constraint Cost Calculations

2.2.1 Simple Example

To illustrate how to calculate constraint costs, a very simple example will be presented in this section. Figure 2.3 illustrates a very simple representation of Britain's power system, which roughly divides Britain into one region of Scotland and one region of England and Wales. In this example values for the available generating capacity and the demand for it are simply assumed. Demand is separated into a one to nine ratio, which is quite accurate in peak demand. The numbers for demand and generation given are supposed to represent a peak snapshot in winter.

Generation Type	Offer Price	Bid Price
Wind	£0 per MW	£-50 per MW
Coal	£50 per MW	£25 per MW
Gas	£120 per MW	£80 per MW
Curtailment	£120 per MW	£120 per MW

Table 2.1: Table detailing bid and offer prices of generating capacity.

In addition to the power system illustrated in Figure 2.3, values are required for the bid and offer prices of each generating capacity, which are detailed in Table 2.1. One interesting thing to note is that under this model if wind capacity is constrained off we would actually pay wind £50 per MW for doing nothing, highlighting the importance

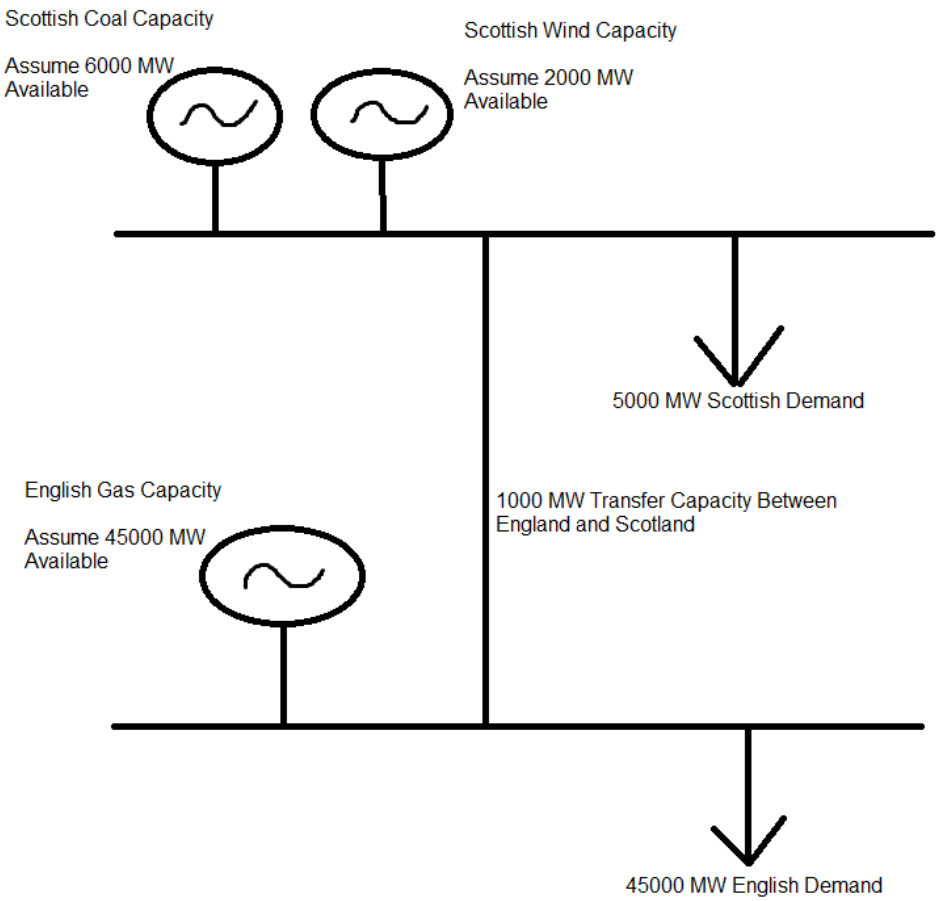

Figure 2.3: Plot to illustrate a simplified representation of Britain's power system.

to have sufficient transmission capacity to make use of all the cheapest generating capacity available. This also addresses the point made by [102] of needing to have a transmission system suitable for renewable generation, by incurring a large economic punishment for failing to utilise available renewable (wind in this case) capacity.

As wind and coal have the lowest and second lowest offer price respectively, the unconstrained schedule will use all wind and coal capacity available, with the rest of demand being met with gas generation capacity. Constraint costs will thus arise due to the fact only 1 GW of coal capacity can be traded between Scotland and England.

In this example, 2 GW of wind capacity, 6 GW of coal capacity and 45 GW of gas capacity is available. As wind has the lowest offer price and coal has the next lowest offer price, the unconstrained schedule would use all 2 GW of wind capacity, all 6 GW of coal capacity and 42 GW of gas capacity. Then, when it came to actually satisfying demand, 2 GW of wind capacity and 3 GW of coal capacity would be used to satisfy Scottish demand. 1 GW of coal capacity would be transferred to England and the remainder of English demand is made up of 44 GW of gas capacity.

In this example, 2 GW of coal was constrained off (receiving $£(2000 \times 25) = £50,000$ from its bid price) and 2 GW of gas constrained on (costing $£(2000 \times 120) = £240,000$ from its offer price). This gives constraint costs for this example as $£240,000 - £50,000 = £190,000$.

The real problem is not as simple as assuming what capacity will be available. Figure 2.4 illustrates a power system where the availability of all generators are random. In practice, a binomial distribution based on these figures would be used to randomly simulate the available generating capacities. For example, with coal generation there are 12 units each with a 0.85 chance of being available. Therefore, a random draw from a binomial distribution with n=12 and p=0.85 would be taken to randomly simulate the number of units available. The available capacity can then be calculated as the number of units available multiplied by the unit size. For example, suppose 8 available units is randomly drawn from the binomial distribution with n=12 and p=0.85. The available coal capacity is then calculated as 8×500MW=4000MW. After the availabilities have been randomly drawn for all 3 generators, constraint costs will be calculated based on these availabilities.

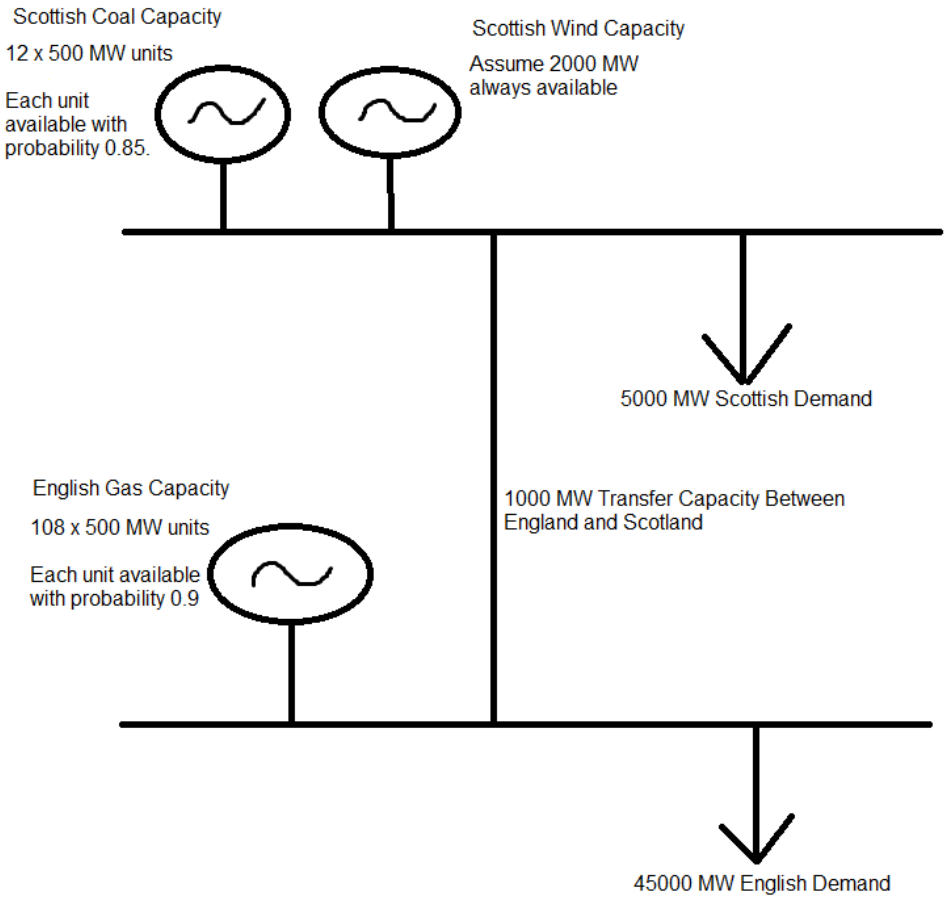

Figure 2.4: Plot to illustrate Britain's power system with random generator availabilities.

Note that these figures are a decent representation for coal and gas generation, but the model for wind generation has been extremely simplified for the purpose of this example.

Table 2.1 also gives pricing details for curtailment, which is the price that must be paid when we are unable to satisfy all demand. Note that by design curtailment can actually be included in the unconstrained schedule. This would mean that if there was no further curtailment included in the constrained schedule there would not be any constraint costs incurred for this. Whilst this may seem like a poor design, it is actually useful for the problems considered in this thesis. This is because this thesis considers the transmission expansion planning problem, not the generation expansion planning problem. If curtailment is in the unconstrained schedule that means that there is not enough generating capacity available to satisfy demand and an infinite transmission system would not solve this problem.

As available capacity is random, this means that the realisation of constraint costs each time the simulator is run will also be random, thus an average of many simulator evaluations must be taken. In this simple example, an extremely accurate estimate of the mean constraint costs of the power system can be acquired very quickly by taking the average of millions of simulator evaluations. For the full simulator this is not possible, and Chapter 4 considers how to get an accurate measure of mean simulator output (mean constraint costs) using importance sampling.

It is noted that what is referred to in this thesis as the mean constraint costs of a power system (the long run average of constraint costs of a given power system) would be more commonly referred to as the expected constraint costs of a power system. However, we avoid the term expected constraint costs when referring to the long run average of a given power system to avoid any confusion when we later considering estimating an expected response whilst considering uncertainty in the variables which define the power system background (as will be detailed in Section 5.2 of Chapter 5). For example, if uncertainty is considered in the peak demand level of a power system, an expectation of mean constraint costs under uncertainty is calculated (rather than the expected constraint costs under uncertainty which would be more accurately referred to as the expectation of the expected constraint costs under uncertainty).

The mean constraint costs of the power system illustrated in Figure 2.4 are £106,000 to 3 significant figures. The examples considered throughout this thesis are only concerned with the mean constraint costs of power systems, which is the standard practice of National Grid (and broadly the case elsewhere). Further, the full simulator, which will be detailed in Chapter 3, does not take into account the temporal correlation between half hour snapshots (such as if a generator is available in one snapshot that will have an effect on its availability in the next snapshot) as is also standard practice of National Grid. By not doing this the PDF of the annual constraint costs that arise from the simulator would not be a good approximation to the PDF of annual constraint costs in reality (and is not of interest in this thesis). However, the mean of the annual constraint costs (which is of interest) is preserved.

For interest, the probability of the system being unable to satisfy all demand is 0.23%.

2.2.2 Uncertainty Analysis of the Simple Example

Even ignoring how simple the structure of the model is, values have been assumed for all the variables of the model. Many of these variables cannot be known exactly in reality, such as what the demand will be in any given snapshot or the availability probability of the generators. If the assumed values are varied, it would be natural to expect the estimate of mean constraint costs to also vary.

Model Variable	Mean Constraint Costs at -10%	Mean Constraint Costs at +10%
Boundary Transfer Capacity	£115,000	£97,300
Unit Size	£106,000	£107,000
Coal Availability Probability	£64,700	£153,000
Gas Availability Probability	£106,000	£106,000
Installed Coal Generating Capacity	£61,700	£153,000
Installed Gas Generating Capacity	£106,000	£106,000
Scottish Demand level	£152,000	£63,800
English Demand level	£106,000	£106,000

Table 2.2: Table detailing how mean constraint costs vary as model variables' values are varied.

Table 2.2 considers how estimates of mean constraint costs vary when any of the model inputs are varied by +/-10%. As can be seen, English demand has no effect on the costs

estimated. This is because (on the +/-10% range) England will always want to import as much cheap coal capacity as possible. The same is true as to why gas availability probability and installed gas generating capacity have no effect on the estimate of mean constraint costs.

Variables relating to Scottish demand or coal generation can be seen to have a large effect on estimated mean constraint costs. The largest of these is installed coal generating capacity, with costs rising to £153,000 when installed coal generating capacity is 10% higher and falling to £61,700 when installed coal generating capacity is 10% lower. These are changes of 44.3% and -41.8% respectively.

The reason that these variables have a large impact is as follows. If Scottish demand was lower or more coal generation was installed, there would be a greater surplus of coal capacity in Scotland which would be utilised in the unconstrained schedule. However, there remains a 1 GW transmission capacity between England and Scotland, meaning that, despite this surplus, this additional capacity cannot be utilised in practice and thus mean constraint costs rise.

This indicates that, even on this relatively simple example, certain factors can have a huge impact on the resulting cost estimates. Therefore, any uncertainty in input data should be accurately accounted for in order to make a good decision. Conversely, it has also been shown that not every variable has a relevant effect on costs, so we do not need to account for every single variable (of which there are hundreds in the full model) when modelling how input affects output when making decisions.

Figure 2.5 illustrates how installed coal generating capacity, coal availability probability and Scottish demand affect estimates of mean constraint costs over the +/- 10% range. As can be seen, varying any of these factors affects mean constraint cost estimates in a linear way of almost the exact same magnitude. This linear pattern is not surprising, because in this simple example the three factors illustrated all directly affect the expected surplus of coal generating capacity in Scotland in a linear manner. England would demand as much coal generating capacity as is available, and under most circumstances gas is brought on in a one to one ratio to replace any coal capacity that can't be used due to transmission constraints.

It could also be interesting to compare how constraint costs vary as multiple factors are

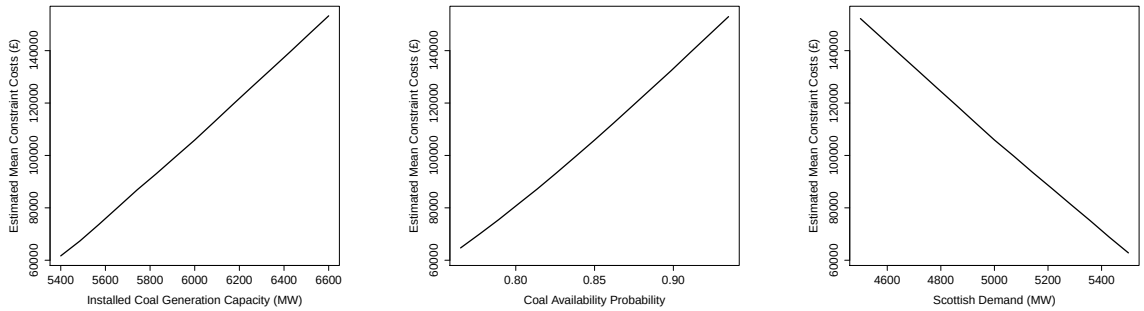

(a) Varying installed coal generating capacity.

(b) Varying coal availability probability.

(c) Varying Scottish demand level.

Figure 2.5: Graphs to demonstrate how mean constraint costs vary as simulator inputs are varied.

varied simultaneously. Illustrations of this are given in Figure 2.6, where installed coal capacity and coal availability probability are varied simultaneously for three different demand levels. Again, it can be seen that mean constraint costs increase as Scottish demand decreases, due to the increased probability that there will be a surplus of coal generating capacity to export. However, all 3 plots approximately form 2 dimensional planes, with minimal interaction between installed coal capacity and coal availability probability.

2.2.3 Uncertainty Analysis of the Simple Example When Assuming a Larger Cost of Curtailment

In the previous subsection there was relatively little punishment for failing to satisfy demand, with gas and curtailment having the same offer price and thus being just as cheap to constrain on. In reality, it is much more reasonable to assume that the cost of failing to satisfy demand would be much greater than the cost of bringing on the most expensive generating capacity. This is reflected in Table 2.3, where larger bid and offer prices of £1000 per MW are assumed for curtailment.

With these new assumed bid and offer prices for curtailment, the mean constraint costs of the power system illustrated in Figure 2.4 are £107,000, which is very slightly greater than the £106,000 of the model which assumes a lower cost of curtailment. This is a small rise, but what would reasonably be expected considering the probability of

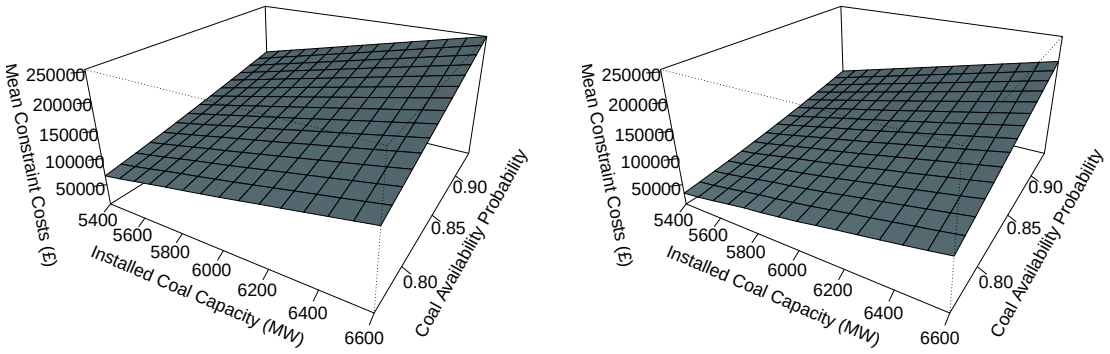

(a) 90% Scottish demand assumed.

(b) 100% Scottish demand assumed.

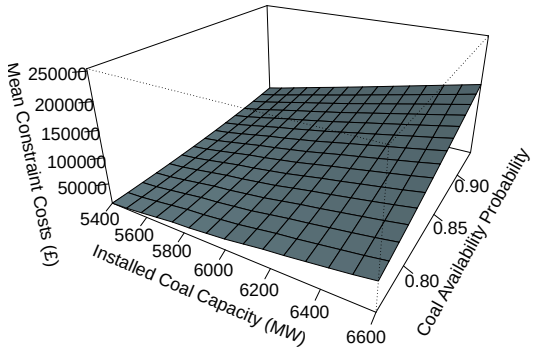

(c) 110% Scottish demand assumed.

Figure 2.6: Graphs to demonstrate how mean constraint costs vary as installed coal capacity and coal availability probability are varied for three demand levels.

Generation Type	Offer Price	Bid Price
Wind	£0 per MW	£-50 per MW
Coal	£50 per MW	£25 per MW
Gas	£120 per MW	£80 per MW
Curtailment	£1000 per MW	£1000 per MW

Table 2.3: Table detailing an alternative set of bid and offer prices of generating capacity.

curtailing any demand is low (0.23%) and some of this curtailment will be due to insufficient generation not transmission. However, this increased cost of curtailment does have an interesting effect on results as assumed model inputs are varied.

Model Variable	Mean Constraint Costs at -10%	Mean Constraint Costs at +10%
Boundary Transfer Capacity	£117,000	£98,400
Unit Size	£107,000	£109,000
Coal Availability Probability	£65,700	£155,000
Gas Availability Probability	£505,000	£106,000
Installed Coal Generating Capacity	£62,600	£155,000
Installed Gas Generating Capacity	£473,000	£106,000
Scottish Demand level	£154,000	£63,800
English Demand level	£107,000	£399,000

Table 2.4: Table detailing how mean constraint costs vary as model variables' values are varied when there is a larger cost of curtailment.

Table 2.4 shows how mean constraint costs vary as any of the assumed values of model inputs are varied by 10%, when assuming the bid and offer prices of detailed in Table 2.3. All estimates are at least as large as the corresponding estimates in Table 2.2, which is to be expected as the only model difference is the increased curtailment cost for failing to satisfy demand.

It can be seen that Scottish demand, installed coal generating capacity and coal availability probability behave very similarly to how they behaved at a low cost of curtailment. This is because these three factors affect the availability of the relatively cheap coal resource. If all other factors of the system are unchanged, unused surplus coal capacity is usually constrained off for gas capacity.

English demand, installed gas generating capacity and gas availability probability on

the other hand now show a huge variation as their assumed value is varied, whereas at the lower curtailment cost they showed no variation at all. This is because gas capacity is constrained on when there is a surplus of coal capacity in Scotland but insufficient transmission capacity to utilise it. If all other simulator inputs take their assumed values, there is usually enough gas capacity available to satisfy the additional capacity demand. However, if English demand rises, or there is less gas capacity available (through less total capacity being built or that capacity having a lower probability of being available) then that increases the likelihood of replacing the coal capacity constrained off with curtailment instead of gas, thus raising mean constraint costs.

It is worth noting that the largest costs in this table (from decreasing gas availability probability by 10%) are over £500,000. This is more than triple the largest cost noted in Table 2.2.

Figure 2.7 shows how costs vary with installed gas generating capacity, gas availability probability and English demand when assuming the larger cost of curtailment. Whilst Figure 2.5 of the previous subsection showed that the effect of installed coal generating capacity, coal availability probability and Scottish demand to be linear at the lower cost of curtailment, the effects of varying gas generating capacity, gas availability probability and English demand level here are clearly non-linear

When the difference is favourable to the power system (i.e. less English demand or gas available more often), there appears to be next to no effect on the system (as this reduces the probability of curtailment). When the difference is unfavourable to the power system, the rise in costs actually appears to be quite small for all factors with a variation of 5% or less. However, beyond this we see a very sharp rise in mean constraint costs, eventually leading to the extreme values noted in Table 2.4.

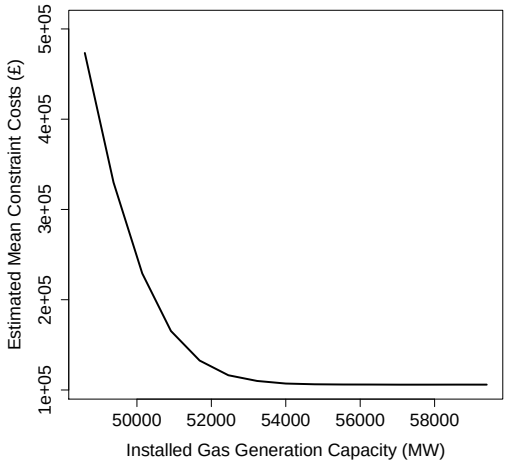

(a) Varying installed gas generating capacity.

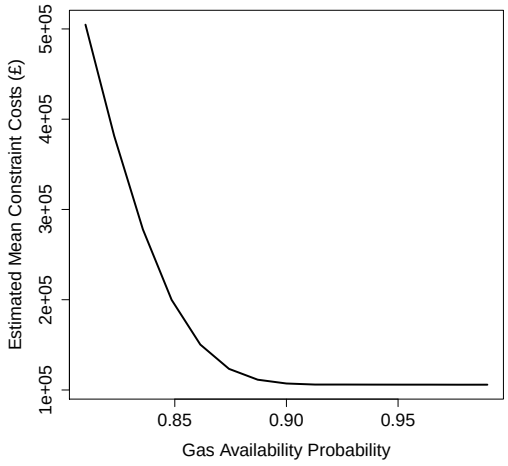

(b) Varying gas availability probability.

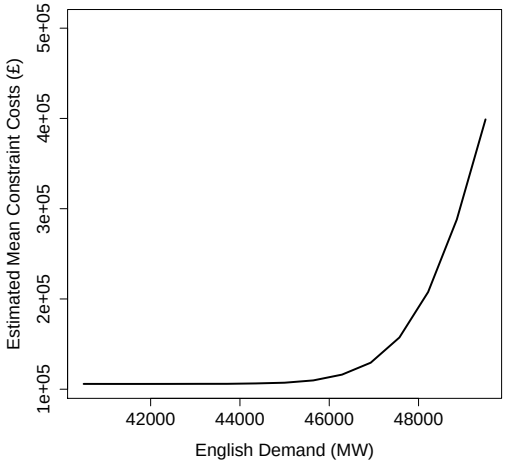

(c) Varying English demand level.

Figure 2.7: Graphs to demonstrate how mean constraint costs vary as simulator inputs are varied for a larger curtailment cost.

2.3 Literature Review for Decision Making Under Uncertainty for Power Systems

2.3.1 Decision Making Under Uncertainty

In the previous section it was illustrated how to calculate the mean constraint costs of a power system. These costs exist because there is insufficient transmission capacity to utilise all of the cheapest generation capacity available. In reality the situation can be improved by expanding the transmission system (building new transmission lines), however, there are considerable reinforcement costs involved in expanding the transmission system. Therefore, the aim is not to eliminate constraint costs, but rather to find an economic balance which minimises the sum of the mean constraint costs plus the costs of reinforcement over a given period of time.

The previous section also illustrated how the assumed input can have a large effect on the mean constraint costs of a power system. When making decisions we must accurately account for these uncertainties and their effect on cost estimates in order to make good decisions. This thesis is concerned with decision making under uncertainty, particularly the transmission expansion problem. Our objective is to minimise the sum of reinforcement costs plus the expected mean constraint costs whilst accounting for the uncertainty that exists in many variables of the power system. Further, we aim to improve on the pre-existing methodology from decision making under uncertainty in the engineering literature in order to give a more complete consideration to the uncertainty that exists within a power system.

2.3.2 Transmission Expansion Planning Overview

Transmission expansion planning (the particular application we are considering) has been covered quite extensively in engineering literature. Historically, systems were planned to maintain continuity of supply with any α components on outage, α commonly being 1; this is known as an N-α planning criterion [12, 91, 61, 55]. More recently, a number of authors (e.g. [12, 57, 58]) have suggested that the likelihood of

events occurring must also be considered, because it would typically be deemed undesirable to make a large investment to protect against a very unlikely event, or one whose consequences are very small. Further, in an economic setting, as will be presented in this thesis, it would be similarly undesirable to make a decision that alleviates costs in a handful of negligible scenarios, whilst resulting in a substantial over-investment in any scenario that could plausibly occur. Therefore, it would be more relevant to consider problems which not only satisfy the N-α criterion, but also make decisions to optimise some secondary economic/welfare function.

[39] is a good introductory article which gives a brief history of transmission expansion planning before giving a comprehensive review of a wide range (33 in total) different potential criteria to be considered when making transmission expansion decisions. [39] also state key market characteristics to be efficiency, competitiveness and customer choice; and classifies each of the 33 criteria depending on their effect on these three characteristics. Finally, an example is given which briefly considers how a subset of these characteristics vary with various transmission expansion decisions applied to the Pennsylvania, New Jersey and Maryland electricity market.

2.3.3 Transmission Expansion Planning to Meet Specific Criteria

The majority of literature gives examples with an in depth investigation of decisions dependant upon a single criterion. For example, [94] consider a criterion which minimises the present worth of investment costs and expected outage and production costs. These costs were calculated using a generalized Benders decomposition to solve a stochastic non-linear mixed integer programming problem. An application was presented on a 24 bus system, which made certain projections of how the system might change over a 20 year period. For an unfamiliar reader, it is sufficient to think of buses as the zones of Section 2.1 in order to understand the literature of this section. The projections include the rate at which gas prices grow and oil generating units come off-line. However, no results were presented to illustrate how these decisions may be sensitive to the particular projections made, although, it was demonstrated that the decisions made were somewhat sensitive if a linearisation was used within the model (by linearising

power flow over lines in the stochastic non-linear mixed integer programming problem) to improve computation time.

A novel approach using co-operative game theory is given in [19]. This approach allows (but does not necessitate) coalitions to be formed between multiple agents (autonomous decision makers) of the power system which gives the potential for each agent to benefit from the decisions of others in the coalition. This in turn could reduce the number of lines needed to expand the network. This methodology was applied to several 6 bus systems and a 24 bus system, though the paper did not consider how uncertainties in any of aspects of any of these systems might affect the coalitions formed or decisions made.

A very holistic view is presented by [40], which consider making an expansion decision when there are transmission expansion cost limits, as well as reliability criteria (system value of loss of load) and congestion criteria (system congestion revenue which is the difference between what customers pay and what generators take from the market) that must be satisfied. Several expansion options are available, and performance indices are calculated for each. However, all market stakeholders are given the ability to express preference for each expansion option on a 5 point scale, and regulatory authorities in turn give weights to the preferences of each stakeholder. This allows for a weighted performance index to be calculated, which is used to identify the optimal decision to make. Whilst the resulting plan gives a very thorough consideration to all market participants, no uncertainties in any elements of the power system are considered.

[91] considers using investment sensitivities, defined as the ratio at which an objective function is improved to the capital cost of investment, to make decisions. Many such sensitivities are considered, such as the satisfying of the supply-demand curves or power exchange deviations. To calculate the investment sensitivities, first a linear program is used to determine the behaviour of the system operator (which seeks to minimise power exchange deviations, non-fulfilment of network $n-1$ criterion and system unserved demand). Then, investment sensitivities are calculated using the linear program post optimal information, dual variables and reduced costs of the system operator model. Decisions which result from accounting for multiple investment sensitivities are then presented for a 6 bus system and the Spanish power system.

A cost-benefit analysis (CBA) approach can also be taken [49, 56, 50]. [50] consider transmission expansion on a pan-European grid, with particular attention placed on expanding the transmission system between countries. An overview is given to the main criteria for transmission expansion planning for several European countries. The paper then lists several benefits to consider for decision making, such as value of lost load, social welfare (sum of generator and consumer surplus) and reduction of conventional generation external costs (a measure of benefit to environmental sustainability). A weighted average of these is taken for any decision considered with the investment costs of such a decision subtracted, which is then used to identify optimal decisions.

[42] provides an example which was inspired by how transmission systems across Europe are set to change greatly in the next 20 years, due to targets relating to increased renewable generation and reduction of fossil fuel emissions. They highlight how intermittent generation such as wind will greatly increase in this period, which will also increase the importance of hydro generation. An expansion decision is made to account for the marginal profits of reinforcements made against the marginal cost to reinforce. These costs are calculated as a stochastic dynamic problem using the EFIs Multi-Area Power-market simulator. Then, investment decisions are iteratively considered with the capacity increases added or rejected based on the marginal profits of the reinforcement in comparison to the system without the investment. The costs calculated do acknowledge the variation in estimates due to the intermittent (uncertain) generation of wind and solar. However, despite the acknowledgement that the system is set for great changes, they do not consider the uncertainty in any aspects of the projected 2030 system. Due to the importance placed on wind in their paper it would have been interesting to see how decisions vary if the assumed amount or location of future installed wind capacity was varied.

2.3.4 Articles Which Consider the Sensitivity of the Decision to Various Assumptions

The previous subsection considers a range of articles which make transmission expansion decisions for power systems when considering a wide range of different criteria that it may be desirable to optimise. However, all of these examples require a model

of a power system, which makes many assumptions about the power system in reality. It is therefore of interest to consider resources which demonstrate how assumptions in the input can affect the costs estimated and decisions made as a result.

[4] is one such article, which considers minimising the sum of investment costs and operation costs, whilst also acknowledging this sum could be weighted to the preference of the system planner. This linear sum of costs is subject to linear constraints in expansion and operation. A Benders decomposition is used to find an optimal solution using costs and constraints associated with the expansion as a master problem and the costs and constraints associated with operation as a sub-problem. The problem was applied to a reduced version of the Spanish power system based on a 2005 horizon from 1996. Uncertainty in demand was considered for 2 different scenarios, though it was stated that the methodology could handle up to 10. Further, as assumptions had to be made about installed generating capacities, results were also presented for two different sets of installed generation possibilities. This article is an improvement on those of the previous subsection, as it acknowledge uncertainties in the projections of the future system, and also mentions how the farther into the future we attempt to predict, the larger the uncertainties will be.

[49] present an example which considers increasing the capacity of one particular component of Manitoba hydro system, with the goal of minimising the sum of the costs of increasing the capacity of this component plus energy replacement costs (akin to our constraint costs) related to that component. Many assumptions about the system are made, though a small amount of the sensitivity of the decision is illustrated by considering how the optimal decision varies for two different costs of energy and 4 periods of time considered. Expected costs were calculated probabilistically based on historic data (such as capacity outage probabilities) and the optimum was identified simply by calculating these expected costs for a number of expansion options and picking the expansion which gives the smallest expectation.

[15] consider minimising the sum of construction costs, operation costs and stand-by costs of transmission expansion decisions. Decisions resulting from applications to two systems, a 5 bus system and a 21 bus system based on south-eastern South Korea's system, were presented. Further, it was demonstrated how the decisions were

sensitive to the security level required (i.e. value of α in N-α) as well as considering the separation of α to specify a number of generator and a number of transmission components. Solutions were acquired through an integer programming problem which uses a branch and bound method to identify which additional transmission lines it would be optimal to build.

An example applied to the Western Interconnection system is considered by [65], with decisions based on the adjusted delivered cost. The adjusted delivered cost is the delivered cost of a resource to a load zone which considers bus-bar and transmission (investment, operation and line losses) costs and also adjusts for key market value factors (such as integration costs, avoided resource adequacy costs and avoided time-of-delivery costs). These costs were calculated using the Western Renewable Energy Zone (WREZ) generation and transmission model (GTM) which was developed by many organizations (including Black & Veatch Corp and the Lawrence Berkeley National Laboratory) which is a user friendly excel based tool which can be used to show how input affects the economic attractiveness (i.e. the adjusted delivered cost) of resources and transmission capacities. Transmission expansion decisions are presented based on a case where 33% of future demand must be met with renewable resources. However, transmission expansion results are also given to compare how the resulting decisions would vary if this figure was a lower 12% or 25%, and the resulting decisions showed huge variation. Questions are also raised about how other factors (for example: what if the integration cost of wind was doubled) would affect cost estimates and decisions.

2.3.5 Articles Which Consider Decision Making Which Accounts for Uncertainty in Input Data

The previous two subsections have considered a wide variety of existing literature which considers a wide variety of different criteria and methods for expanding transmission systems. However, not all consider how sensitive the decisions identified could be to assumptions made about the power system. Even the resources which do encompass some aspects of uncertainty have merely shown how decisions differ as certain aspects of the system are altered. Whilst it is interesting to investigate such sensitivities, this

is insufficient when it comes to making decisions in reality as we must settle on a single set of decisions to be implemented in the face of uncertainty.

Few resources exist which attempt to tackle the issue of decision making under uncertainty. [87] is one such resource which does, and plans to maximise generation company and transmission company expected profits, subject to a reliability check from the independent system operator. The problem is solved using a Benders decomposition with maximising generator and transmission company profits as the master problem and the system operator reliability check as the sub-problem. This example accounts for the uncertainty that exists in future load growth and outages by taking an expectation over multiple scenarios. A scenario is defined as a possible future state of the power system, which in the example provided relates to characteristics (generator and transmission availabilities) of the system and load growth.

An example is then presented where decisions are made on a 6 bus system when 10 scenarios are considered. These 10 scenarios are given different weights, with the particular weights (and scenarios themselves) acquired through scenario reduction applied to Monte Carlo simulation from 1000 possible scenarios. Additional sensitivity of the decisions is also considered to various factors, such as the cost of imaginary units (akin to our curtailment costs). The scenario reduction technique means that the 10 scenarios give a much more dense coverage of the sample space in comparison to a random sample of size 10, and the weights given to the scenarios also improve the estimate of expectation. However, 10 scenarios is still a small number considering multiple factors are varied in each scenario, suggesting the overall coverage is still quite poor.

[75] considers a transmission expansion problem which accounts for the uncertainty that exists due to the varying availability of hydro power. The objective is to identify the decision which minimises the cost of investment, plus a weighted average of expected costs due to load shedding across multiple scenarios. The problem is initially formulated as a mixed integer non-linear programming problem with a disjunctive formulation then used to transform the problem into a mixed integer linear programming problem (MILP) which can be solved more easily. Constraints are repeated in the MILP problem for each scenario considered, though it is stated the problem remains feasible to solve through MILP techniques as the same investment decision variables

apply to all scenarios. Two examples were presented, one of the Bolivian system which considered 15 dispatch scenarios for hydro power; and one of the south-eastern Brazilian power system, which considered only a single hydro inflow scenario. Further, both examples broke each scenario down further into single contingency scenarios (i.e. scenarios with single circuit outages). This meant that a large number of total scenarios were considered in the Bolivian power system (52 for each of the 15 dispatch scenarios).

[105] seeks to minimise expansion investment whilst maximising system reliability and security for each of several scenarios which vary system load and additional capacity installations. Initially, each scenario is considered separately as multi-objective optimization problems. These problems are then reformulated as mixed integer linear programming problems using goal programming, which can then be solved to identify optimal transmission reinforcements for each scenario. Then, the expansion with the lowest adaptation cost (i.e. the cost for additional reinforcement to meet system objectives if the initial scenario is incorrect) is selected. Two examples applied to a 14 bus system are presented. The first considers 3 different scenarios of system load, whilst the second considers six scenarios which vary system load and installed generating capacity. The load levels considered are three evenly spaced increases in load (10%, 20% or 30%), and the second example considers a 200 MW increase in generation in one of two buses for each of these load levels. This is equivalent to considering a three dimensional space with 6 points (with the points forming a 3 by 2 grid within that space), which is an extremely sparse coverage.

[97] presents an example which considers 6 different scenarios occurring on the British power system between 2010 and 2030; and considers the decisions of generation operation as well as transmission expansion. Initially, the problem is formulated stochastically as a mixed integer linear programming problem, with the objective of minimising the total expected costs of generation operation and investment, and transmission investment across all 6 scenarios. These 6 scenarios greatly vary the values of 6 aspects of the future system, such as renewable targets, demand change and cost of conventional generation. Whilst these 6 scenarios do represent very different states that the future system could be in, just 6 scenarios which have a large variation in the values of 6 factors (which have many sub-factors e.g. cost of conventional generation could

be broken down further into cost of CCGT generation and cost of OCGT generation, which are two forms of gas generation) gives a very sparse coverage and may be of limited use if the scenario which occurs in reality has some aspects of one scenario and some aspects of another.

Thought is also given to the expected value of perfect information, which is the expected reduction in costs if the future scenario could be known exactly and serves as an upper bound of how much should be spent to acquire better information, as well as presenting an interesting example of how transmission decisions would vary if any particular scenario was assumed to occur. The expected cost of ignoring uncertainty and regret analysis are also performed, as well as considering how accounting for an attitude to risk might affect the decisions made.

This example is particularly interesting as it considers making decisions over multiple stages. Making decisions over multiple stages allows the decision maker to learn about uncertainties as time progresses, and make amendments to the transmission system accordingly. This could potentially allow for a smaller investment to be made in the present, knowing that if an unfavourable set of circumstances occur in the future we can expand the transmission system as appropriate, instead of having to make an overly large investment now in case an unfavourable future scenario occurs. In this thesis we will eventually consider multiple stage decisions in Chapters 8 and 9 and will give a full literature review on multi-stage transmission expansion planning in Section 8.1.

However, a common feature to all of these methodologies is that uncertainty is handled by considering a finite (and usually small) set of possible scenarios. [87] does attempt to account for this via scenario reduction, but nevertheless the end example still used only 10 scenarios (albeit with weights attached). Particularly where the uncertainty in planning is high dimensional, such a finite set of scenarios may give sparse coverage of the space of model inputs, and hence an optimal decision within the model which is strongly dependent on the particular choice of scenarios rather than the underlying uncertainty in model inputs. Further, almost all the examples detailed (those that do and do not consider uncertainty) consider selecting the best from a finite set of decisions. In the remainder of this thesis a methodology will be developed to give a more complete model for how input affects output of cost estimates, which in turn can

be used to make better decisions under uncertainty.

Chapter 3

Simulating Power System Constraint Costs

This chapter gives a complete description of the simulation model used throughout the rest of this thesis. This simulator is used as a method for estimating mean annual constraint costs for a given power system background, which in turn will be used to make transmission reinforcement decisions. However, we must additionally account for how various factors of the system background affect the output of the simulator when making decisions. Therefore, a brief investigation of the sensitivity of the simulator output to various input factors is also given, with particular problems of interest outlined to be considered in the remainder of this thesis.

Sections 3.1 to 3.6 of this chapter will specify the simulator used in this thesis to estimate constraint costs for a given power system. This is broken down as follows. Section 3.1 gives some preliminary information to help an unfamiliar reader understand some of the standard practices used when estimating constraint costs, such as breaking a year down into snapshots and National Grid's model of snapshot demand. Section 3.2 then gives an overview of the notation that will be used to specify the simulator. Section 3.3 defines the linear program that can be used to calculate constraint costs for a given system background and generator availabilities. Section 3.4 specifies the simulator used to estimate mean annual constraint costs for a given power system background. Section 3.5 then defines the random model of generator availabilities used in the simulator. Section 3.6 then gives some information about the data used

to estimate constraint costs in this thesis, with further details on this data given in Appendix F.

3.1 Preliminary Information

3.1.1 Snapshots

In Section 2.2 it was stated the simple example represented a snapshot in peak demand in winter. In this thesis, when estimating constraint costs for a given period of time, that period of time is first broken down into half hour snapshots (giving 17520 snapshots per year). Data which describes the power system background for a particular half hour (such as demand level in that snapshot, installed generating capacity in that snapshot, model for wind availability in that snapshot, etc.) can then be used to estimate constraint costs for that particular snapshot (as will be explained in the remainder of this chapter).

When estimating constraint costs, snapshots are treated independently of one another (i.e. there is no stochastic element in generator availabilities or demand level), as is standard practice of National Grid. This means that the distribution of total constraint costs for a given year is not a perfect representation of reality (and is not of interest in this thesis), though the mean of the total constraint costs for the year is preserved. As mentioned in Section 2.2.1, it is standard practice of National Grid to work with mean annual constraint costs (and broadly the case elsewhere), rather than the distribution of annual constraint costs.

3.1.2 Zones

The example of Section 2.2 was a simple example which used just 2 zones. The methodology presented will be suitable to solve a general system of $\mathfrak{R}$ Zones, indexed by $\mathfrak{r}$. Further, the methodology will allow for constraint costs to be calculated for any potential arrangement of the zones (i.e. the methodology generalises to any amount of zones and any set of connections between the zones).

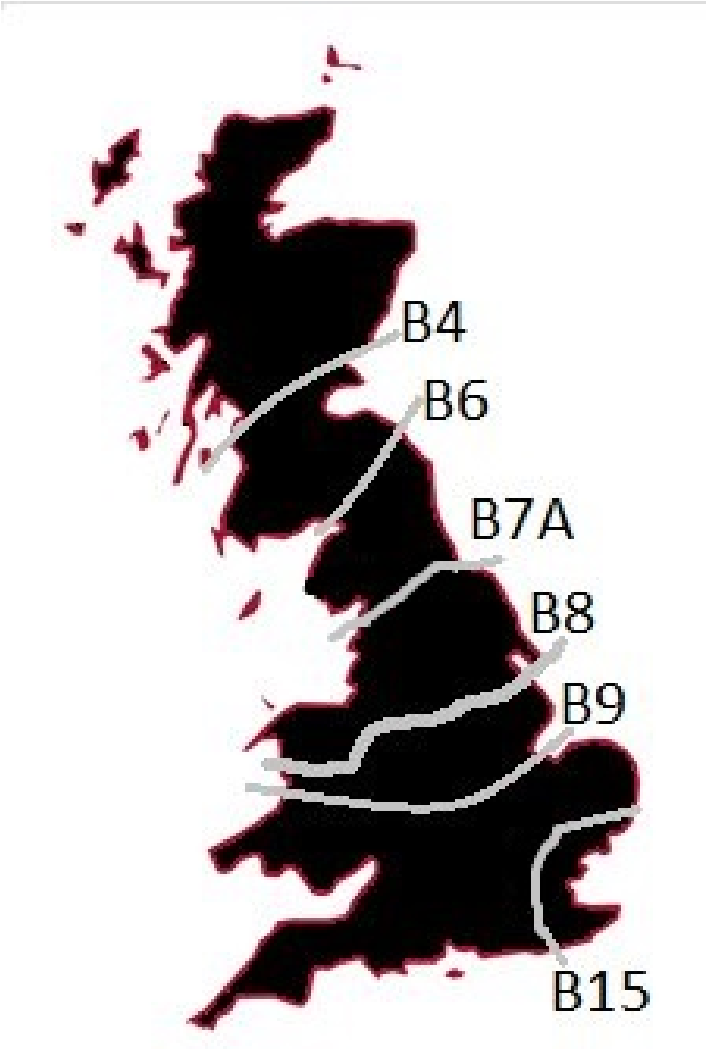

Figure 3.1: Graph displaying the structure of zones and boundaries of the power system used in this thesis.

Figure 3.1 illustrates the particular zone structure used in this thesis, which has 7 zones with a linear pattern of connections between the zones, i.e. each zone is only connected to the zone(s) directly north and/or south of itself.

3.1.3 Demand

Demand is not explicitly specified by stating the demand in MW in each zone in each snapshot. Instead, a peak demand for the year is specified as $\mathfrak{d}^y$, the proportion of peak demand in snapshot τ is specified as $\mathfrak{d}^\tau$, and the proportion of demand in zone $\mathfrak{r}$ is specified as $\mathfrak{d}^\mathfrak{r}$. The demand in a particular zone in a particular snapshot for a particular year can then be calculated as

$$\mathfrak{d}_{y,\tau,\mathfrak{r}} = \mathfrak{d}^y \times \mathfrak{d}^\mathfrak{r} \times \mathfrak{d}^\tau \tag{3.1.1}$$

No interaction term is included between zone or snapshot, which means the ratio of demand between snapshots is treated as if it were consistent throughout the year (relating this back to the simple example of Section 2.2, this would mean that a ratio of 9 to 1 for English to Scottish demand would be used in each snapshot of the year). This calculation of demand is closely based on the modelling of demand used by National Grid.

A vector detailing the peak demand for each snapshot in a year (i.e. a vector of length 17520 which details each value of $\mathfrak{d}^\tau$) is referred to in the engineering literature as a load duration curve (LDC). Examples and more details about LDCs will be given in Section 4.1.2.

In reality, what the demand will be in a particular snapshot could be considered a random variable. Using an LDC to specify the demand for each snapshot would seemingly treat demand of a particular snapshot as a deterministic variable. However, it is more practical to treat the LDC as a specification of the distribution for demand at a random point in time. This in turn means that the mean of the constraint costs over a year is preserved when using of Equation 3.1.1 to calculate snapshot demand.

There could potentially be a problem if other factors in the power system vary with snapshot. However, other than a seasonal effect (which will be detailed in Section 7.2

which differentiates wind generation between winter and not-winter) for a given year demand is the only factor of the power system considered to vary in each snapshot. This means that if the LDC accurately describes the distribution of demand for each season the effect of this is minimised.

3.2 Notation Definitions

In order to give a specification of the model, the following notation is first required.

Sets

- $\mathfrak{T}$ Generating technologies, indexed by $\mathfrak{t}$ (such as wind, coal and gas from Section 2.2)
- $\mathfrak{R}$ Zones, indexed by $\mathfrak{r}$ (or $\mathfrak{s}$ when describing an interaction such as transferring capacity from zone $\mathfrak{r}$ to a general, alternative zone)
- $\mathscr{T}$ Time intervals (half hour snapshots) indexed by τ
- n_Z Number of elements in set Z

Parameters

It is assumed that bid and offer prices depend only on technology type, not zone. As such our bid/offer prices have only a single subscript.

- $\mathfrak{c}_{\mathfrak{t}}^{+}$ Offer price of technology $\mathfrak{t}$
- $\mathfrak{c}_{\mathfrak{t}}^{-}$ Bid price of technology $\mathfrak{t}$
- $\mathfrak{g}_{\mathfrak{r}\mathfrak{t}}^{\mathfrak{M}}$ Installed capacity of generating technology $\mathfrak{t}$ in zone $\mathfrak{r}$
- $\mathfrak{d}^{\tau}$ Proportion of peak demand in time interval (snapshot) τ
- $\mathfrak{d}^{\mathfrak{r}}$ Proportion of time interval demand in zone $\mathfrak{r}$
- $\mathfrak{d}^{y}$ Peak demand level in year y

- $\mathfrak{f}^{\mathfrak{M}}_{\mathfrak{r},\mathfrak{s}}$ Boundary transmission capacity between zones $\mathfrak{r}$ and $\mathfrak{s}$ (i.e. maximum power flow between zones $\mathfrak{r}$ and $\mathfrak{s}$)

Variables

- $x_{\mathfrak{r}\mathfrak{t}}$ Available capacity from technology $\mathfrak{t}$ in zone $\mathfrak{r}$
- $\mathfrak{g}^0_{\mathfrak{r}\mathfrak{t}}$ Generation level (MW) of technology $\mathfrak{t}$ in zone $\mathfrak{r}$ in the unconstrained schedule (recall, from Section 2.1.2 the unconstrained schedule is the schedule which uses all the cheapest technology available to satisfy demand, assuming as much as necessary can be traded between zones)
- $\mathfrak{f}_{\mathfrak{r},\mathfrak{s}}$ Power flow from zone $\mathfrak{r}$ to $\mathfrak{s}$. Note, $\mathfrak{f}_{\mathfrak{r},\mathfrak{s}}$ can be negative, which would represent a positive flow from zone $\mathfrak{s}$ to $\mathfrak{r}$
- $\mathfrak{g}^+_{\mathfrak{r}\mathfrak{t}}$ Volume of accepted offers from technology $\mathfrak{t}$ in zone $\mathfrak{r}$ in the constrained schedule
- $\mathfrak{g}^-_{\mathfrak{r}\mathfrak{t}}$ Volume of accepted bids from technology $\mathfrak{t}$ in zone $\mathfrak{r}$ in the constrained schedule

Recall from Section 2.1.2 that the bid price is the amount which a generator will pay to produce 1 less MW of capacity. The offer price is the amount which a generator demands to produce an additional MW of capacity. More information about the particular values of these variables is given in Appendix F.3.2.

3.3 Snapshot Constraint Cost Estimation

The objective of the simulator is to estimate mean constraint costs of a given power system over a given period of time. As mentioned in Section 3.1, this is done by breaking the year down into a series of snapshots and estimating the constraint costs in each. This section will detail how costs are calculated for a single snapshot when the available capacities of all generators across all zones, $x_{\mathfrak{r}\mathfrak{t}}$, and the demands in each zone for that snapshot, $\mathfrak{d}_{y,\tau,\mathfrak{r}}$, are given as an input.

3.3.1 The Unconstrained Schedule

To calculate constraint costs, first an unconstrained schedule must be created. The unconstrained schedule is an initial schedule which seeks to satisfy all demand with the cheapest available capacity whilst acting as if an unlimited amount of generating capacity can be traded between zones, just as in Section 2.1.2.

The cheapest way to satisfy all demand is to schedule generating capacity in order of offer price (lowest first) until the magnitude of scheduled capacity is equal to the sum of demand across all zones. In Section 2.2 this was easy to calculate, as it would consist of all wind and coal capacity available with the remainder of the unconstrained schedule being made up of enough gas to satisfy the remainder of demand.

The unconstrained schedule is still simple to calculate for a general power system. The unconstrained schedule for technology $\mathfrak{t}$ in zone $\mathfrak{r}$ is denoted by $\mathfrak{g}^0_{\mathfrak{r},\mathfrak{t}}$. For a fixed snapshot, τ, generating capacity is scheduled, starting from the lowest offer price, until all demand across all zones would be satisfied, i.e.

$$\sum_{\mathfrak{r}} \mathfrak{d}_{y,\mathfrak{r},\tau} = \sum_{\mathfrak{r},\mathfrak{t}} \mathfrak{g}^0_{\mathfrak{r},\mathfrak{t}} \tag{3.3.1}$$

The generation scheduled must not be more than the available capacity, i.e.

$$0 \leq \mathfrak{g}^0_{\mathfrak{r},\mathfrak{t}} \leq x_{\mathfrak{r},\mathfrak{t}} \tag{3.3.2}$$

There is one marginal technology, $\mathfrak{t}_M$, whose scheduled generation is between 0 and its availability. The scheduled output for this technology is allocated between all zones in proportion to the available capacity $x_{\mathfrak{r},\mathfrak{t}_M}$.

Just as in Section 2.2, there will be a curtailment technology with very high bid and offer prices, which means the unconstrained schedule can always be calculated (though part of this schedule may involve curtailing demand).

3.3.2 The Constrained Schedule

The system is split into $n_{\mathfrak{R}}$ zones, indexed by $\mathfrak{r}$. Generating capacity can be transferred between zones, but only up to the transfer capacity between the two zones, $\mathfrak{f}^{\mathfrak{M}}_{\mathfrak{s},\mathfrak{r}}$. A

transfer capacity of zero would mean two zones aren't connected (i.e. cannot directly transfer capacity) but may transfer capacity indirectly (through intermediate zones).

As mentioned in Section 2.1.2, it will not always be possible to satisfy all demand in the cheapest way possible (i.e. to follow the unconstrained schedule) whilst obeying the limits of transfer capacity between zones. In this case, it is necessary to constrain off (not use) some generating capacity and constrain on (use instead) some alternative capacity so that demand is met without transmitting more between zones than is physically allowed.

The constrained schedule is the cheapest way to satisfy all demand when taking into account the transfer capacities that exist between zones. In Section 2.2 it was feasible to give a blueprint of how to calculate the constrained schedule, and resulting constraint costs, for any possible state of the system. If there was a power flow from Scotland to England resulting from the unconstrained schedule and this flow exceeded the transfer capacity, then gas capacity (or curtailment if no gas was available) would be constrained on and coal capacity would be constrained off. If there was a power flow from England to Scotland resulting from the unconstrained schedule and the power flow exceeded the transfer capacity, then gas capacity would be constrained off and curtailment would be constrained on in its place.

For a more general system (with more than two zones and tens of generating technologies in each zone) it is not feasible to manually calculate the constrained schedule for any possible state of the system. This subsection will give details of the linear program that can be used to calculate the constraint costs of a general system.

Objective Function

The objective of the constrained schedule is to minimise the constraint costs that arise. This is calculated by minimising the sum of the offer prices of generating technology constrained on, $\mathfrak{c}_t^+ \mathfrak{g}_{rt}^+$, minus the sum of the bid prices for generating technology constrained off, $\mathfrak{c}_t^- \mathfrak{g}_{rt}^-$, i.e.

$$\min \sum_{rt} (\mathfrak{c}_t^+ \mathfrak{g}_{rt}^+ - \mathfrak{c}_t^- \mathfrak{g}_{rt}^-) \tag{3.3.3}$$

Variable Bounds

There are several constraints that must be satisfied when minimising Equation 3.3.3. The first are the bounds of the values the variables describing the power system can take:

$$0 \leq \mathfrak{g}^{+}_{\mathfrak{r}\mathfrak{t}} \leq x_{\mathfrak{r}\mathfrak{t}} - \mathfrak{g}^{0}_{\mathfrak{r}\mathfrak{t}} \tag{3.3.4}$$

$$0 \leq \mathfrak{g}^{-}_{\mathfrak{r}\mathfrak{t}} \leq \mathfrak{g}^{0}_{\mathfrak{r}\mathfrak{t}} \tag{3.3.5}$$

$$-\mathfrak{f}^{\mathfrak{M}}_{\mathfrak{s},\mathfrak{r}} \leq \mathfrak{f}_{\mathfrak{s},\mathfrak{r}} \leq \mathfrak{f}^{\mathfrak{M}}_{\mathfrak{s},\mathfrak{r}} \tag{3.3.6}$$

$$0 = \sum_{\mathfrak{r},\mathfrak{t}} (\mathfrak{g}^{+}_{\mathfrak{r},\mathfrak{t}} - \mathfrak{g}^{-}_{\mathfrak{r},\mathfrak{t}}) \tag{3.3.7}$$

Equation 3.3.4 describes the bounds for the volume of offers constrained on, $\mathfrak{g}^{+}_{\mathfrak{r}\mathfrak{t}}$. We cannot constrain on negative amounts, nor can we constrain on more than the available capacity, $x_{\mathfrak{r}\mathfrak{t}}$, minus what is already scheduled, $\mathfrak{g}^{0}_{\mathfrak{r}\mathfrak{t}}$.

Equation 3.3.5 describes the bounds for the volume of bids constrained off, $\mathfrak{g}^{-}_{\mathfrak{r}\mathfrak{t}}$. We cannot constrain off negative amounts, nor can we constrain off more than we have scheduled, $\mathfrak{g}^{0}_{\mathfrak{r}\mathfrak{t}}$.

Equation 3.3.6 describes the bounds of transfer of generating capacity (flow), $\mathfrak{f}_{\mathfrak{s},\mathfrak{r}}$, from zone $\mathfrak{s}$ to $\mathfrak{r}$. A positive value indicates a flow from zone $\mathfrak{s}$ to $\mathfrak{r}$, whereas a negative value indicates a flow from zone $\mathfrak{r}$ to $\mathfrak{s}$. The flow cannot exceed the boundary capacity, $\mathfrak{f}^{\mathfrak{M}}_{\mathfrak{s},\mathfrak{r}}$.

Equation 3.3.7 is the demand balance constraint. This equation ensures that the sum of the volume of offers constrained on is equal to the sum of the volume of bids constrained off. As we initially schedule enough energy to satisfy demand, this equation ensures our final solution satisfies all demand. Again, in each snapshot there will be the very expensive curtailment technology available, meaning this equation can always be satisfied.

Boundary Flow and Satisfying Demand

In addition to the variable bounds of the previous sub-subsection, $n_{\mathfrak{R}}$ further constraints are required to ensure demand in each zone of the power system is satisfied. In words, these $n_{\mathfrak{R}}$ equations are:

Flow into zone - Flow out of zone + Generation constrained on in zone - Generation constrained off in zone = Demand in zone - Generation scheduled in zone

These $n_{\mathfrak{R}}$ equations can be written as:

$$\sum_{\mathfrak{s}\neq\mathfrak{r}} \mathfrak{f}_{\mathfrak{s},\mathfrak{r}} + \sum_{\mathfrak{t}} (\mathfrak{g}^{+}_{\mathfrak{r}\mathfrak{t}} - \mathfrak{g}^{-}_{\mathfrak{r}\mathfrak{t}}) = \mathfrak{d}_{y,\tau,\mathfrak{r}} - \sum_{\mathfrak{t}} \mathfrak{g}^{0}_{\mathfrak{r}\mathfrak{t}} \tag{3.3.8}$$

Linear Program and the Calculation of Constraint Costs

Constraint costs (and the constrained schedule) can then be calculated by using a linear program. The linear program first assumes the unconstrained schedule has been formed as in Section 3.3.2.

A linear program is then formulated, which has the objective function defined in Equation 3.3.3. The linear program also has constraints defined in Equations 3.3.4 to 3.3.8. Once this linear program has been solved Equation 3.3.3 defines the constraint costs for the snapshot. The R code of the implementation of the linear program used in this thesis is given in Appendix G.2.

Again, in each snapshot there will be the very expensive curtailment technology available, meaning the linear program can always be solved. In reality using this curtailment would signify not satisfying the demand for a very high penalty cost.

3.4 Simulator Specification

The aim is to estimate the mean costs arising due to constraints over a given period of time. This section will define how this is achieved, by first breaking the time down into a series of snapshots. For each snapshot, available generating capacity is randomly simulated and these availabilities are then used to estimate constraint costs via the linear program defined in Section 3.3. As the available generating capacity is random, the constraint costs are themselves random and therefore an average of the process is required.

3.4.1 Estimation of Snapshot Constraint Costs

First, consider estimating constraint costs for a fixed snapshot in time, τ. Let $\underline{\mathbf{X}}_\tau$ denote a vector containing information of all available capacity (across all zones) for the snapshot τ. Let $\mathfrak{B}_\tau$ denote a vector containing all information of the system background for snapshot τ . This is a vector of fixed numbers of boundary transmission capacities and demand.

$\underline{\mathbf{X}}_\tau$ and $\mathfrak{B}_\tau$ are then used to create the unconstrained schedule detailed in Section 3.3.1. This is in turn used to calculate constraint costs using the linear programming problem described in Section 3.3.2.

$\mathfrak{c}^{\text{con}}(\underline{\mathbf{X}}_\tau, \mathfrak{B}_\tau)$ is defined to be a function which calculates constraint costs resulting from the solution to this linear programming problem for the given information about the power system.

This calculation required the available generating capacities for the snapshot, $\underline{\mathbf{X}}_\tau$. This is a random vector to be realised in each individual snapshot. Define $h(\mathfrak{G}_\tau) = \underline{\mathbf{X}}_\tau$ to be a function which simulates the random availabilities of generating capacity for given information about installed generating technology in the snapshot, $\mathfrak{G}_\tau$. The model of this function will be detailed in Section 3.5. $\mathfrak{C}^{\text{con}}(\mathfrak{G}_\tau, \mathfrak{B}_\tau)$ is then defined as a function which randomly simulates the available capacity using $h(\mathfrak{G}_\tau) = \underline{\mathbf{X}}_\tau$, and then calculates the corresponding constraint costs for a particular snapshot.

3.4.2 Estimation of Yearly Constraint Costs

The estimation of constraint costs for an entire year requires a vector containing all information required to estimate constraint costs across all snapshots, defined as $\mathfrak{X} = (\mathfrak{G}, \mathfrak{B})$ where $\mathfrak{G} = (\mathfrak{G}_1, \mathfrak{G}_2, ..., \mathfrak{G}_{\mathscr{T}})$ and $\mathfrak{B} = (\mathfrak{B}_1, \mathfrak{B}_2, ..., \mathfrak{B}_{\mathscr{T}})$. Constraint costs will be calculated for each snapshot in sequence, then summed to give constraint costs over the entire year:

$$g(\mathfrak{X}) = \sum_{\tau=1}^{\mathscr{T}} \mathfrak{C}^{\text{con}}(\mathfrak{G}_\tau, \mathfrak{B}_\tau) \tag{3.4.1}$$

This easily extends to estimating costs for a number of years as

$$g(\mathfrak{X}) = \sum_{y=1}^{Y} \sum_{\tau=1}^{\mathscr{T}} \mathfrak{C}^{\text{con}}(\mathfrak{G}_{y,\tau}, \mathfrak{B}_{y,\tau}) \tag{3.4.2}$$

where the subscript y, τ denotes snapshot τ of year y.

3.4.3 Estimation of Mean Constraint Costs

Finally, it is important to consider that the output from $g(\mathfrak{X})$ (the estimate of constraint costs for a given period of time) is random, as the availability of generators across that time is random. As mentioned in Section 2.2.1, this thesis is concerned with the mean constraint costs, as is standard practice of National Grid and broadly the case elsewhere.

This can be handled by using a function $f_c(\mathfrak{X})$ which takes an expectation of $g(\mathfrak{X})$, i.e.

$$f_c(\mathfrak{X}) = E(g(\mathfrak{X})) \tag{3.4.3}$$

The simplest way to take this expectation would be to take an average of many repetitions of $g(\mathfrak{X})$. As noted in Section 2.2.1, such an expectation is referred to as the mean constraint costs in this thesis. However, $g(\mathfrak{X})$ takes approximately 3 minutes to give one estimate for a single year, which can potentially make this an expensive procedure if the output of $g(\mathfrak{X})$ has a high level of variability (the level of variability in the estimate is highly dependent on the power system background and will be detailed in Section 4.1.1). Section 4.3 will demonstrate how importance sampling can be used to greatly improve this.

Again, the use of mean constraint costs (and not working with the distribution of constraint costs) is standard practice by National Grid which is used to account for the fact that the simulator lacks a stochastic element (i.e. snapshots are simulated independently of one another, so correlation of the available capacities or demand between snapshots is ignored).

3.5 Random Simulation of Available Generating Capacity

Section 3.4.1 indicated that the available generating capacity, $\underline{\mathbf{X}}_\tau$, in a snapshot must be randomly simulated. The available capacity is randomly simulated using either

a binomial distribution, a normal distribution or a wind distribution depending on technology type, $\mathfrak{t}$. Appendix F.3.1 gives a summary of how the random availability model varies with technology type.

If the availability of technology $\mathfrak{t}$ in a zone $\mathfrak{r}$ is assumed to follow a binomial distribution with availability probability $a_{\mathfrak{t}}$, installed capacity $\mathfrak{g}^{\mathfrak{M}}_{\mathfrak{r}\mathfrak{t}}$ and unit size $u_{\mathfrak{t}}$ (both in MW), the following simulation technique is used, which is the same approach used by National Grid. The number of installed units are calculated as $n_{\mathfrak{r},\mathfrak{t}} = \frac{\mathfrak{g}^{\mathfrak{M}}_{\mathfrak{r}\mathfrak{t}}}{u_{\mathfrak{t}}}$, which is rounded to an integer if necessary. A random drawing from the binomial distribution with $n_{\mathfrak{r},\mathfrak{t}}$ trials and probability of success $a_{\mathfrak{t}}$ is simulated, with $s_{\mathfrak{r},\mathfrak{t}}$ denoting the randomly drawn number of successes. Then, the available capacity of technology $\mathfrak{t}$ in zone $\mathfrak{r}$ is calculated as $\frac{s_{\mathfrak{r},\mathfrak{t}}}{n_{\mathfrak{r},\mathfrak{t}}} \times \mathfrak{g}^{\mathfrak{M}}_{\mathfrak{r}\mathfrak{t}}$.

If the availability of technology $\mathfrak{t}$ in a zone $\mathfrak{r}$ is assumed to follow a Gaussian distribution with mean availability $\mu_{\mathfrak{t}}$, standard deviation $\sigma_{\mathfrak{t}}$ and installed capacity $\mathfrak{g}^{\mathfrak{M}}_{\mathfrak{r}\mathfrak{t}}$, the following simulation technique is used. One result, $q_{\mathfrak{r},\mathfrak{t}}$, is randomly drawn from a normal distribution with mean $\mu_{\mathfrak{t}}$ and standard deviation σ_t, with $q_{\mathfrak{r},\mathfrak{t}}$ being constrained to be no greater than 1 and no less than 0 to ensure the available capacity simulated is non-negative and the available capacity does not exceed the installed capacity. The available capacity of technology $\mathfrak{t}$ in zone $\mathfrak{r}$ is then calculated as $\mathfrak{g}^{\mathfrak{M}}_{\mathfrak{r}\mathfrak{t}} \times q_{\mathfrak{r},\mathfrak{t}}$.

Wind availability follows a more complicated model, which we have been given permission to use by National Gird. This is used to reflect the fact that whilst it is reasonable to assume generator availabilities in different zones may be independent for conventional generators (such as coal or gas), Britain's weather and thus wind generation is highly correlated. In addition, a binomial or normal distribution are poor approximations for the availability of wind generation, so an entirely separate availability model is used.

To simulate wind availability, first a correlation matrix is specified for wind availability between different zones as well as the correlation between onshore and offshore wind availability within each zone, $\kappa_{\mathfrak{R}}$. A random drawing is then taken from a multivariate normal distribution with mean 0 and covariance matrix determined by $\kappa_{\mathfrak{R}}$. This random drawing, $\mathbf{w}_1$, has $2\mathfrak{R}$ elements, such that the $(2(\mathfrak{r}-1)+1)$th element can be used to calculate onshore wind availability in zone $\mathfrak{r}$ and the $2\mathfrak{r}$th element can be used

to calculate offshore wind availability in zone $\mathfrak{r}$. The CDF of the standard normal distribution is then used to transform each element of $\mathbf{w}_1$ to a value in the range [0,1], with $\mathbf{w}_2$ denoting the resulting transformation. National Grid then have functions $\mathfrak{w}_\mathfrak{r}$ which can transform a given input to an availability proportion of onshore or offshore wind generation in zone $\mathfrak{r}$. Let $\mathbf{w}_{3,\mathfrak{r},1}$ and $\mathbf{w}_{3,\mathfrak{r},2}$ be the resulting transformations of $\mathbf{w}_2$ to give estimates of the availability proportion of onshore and offshore wind respectively in zone $\mathfrak{r}$.

The available capacity of onshore and offshore wind respectively is then calculated as $\mathfrak{g}^{\mathfrak{M}}_{\mathfrak{r}\mathfrak{t}_{won}} \times \mathbf{w}_{3,\mathfrak{r},1}$ and $\mathfrak{g}^{\mathfrak{M}}_{\mathfrak{r}\mathfrak{t}_{woff}} \times \mathbf{w}_{3,\mathfrak{r},2}$ where $\mathfrak{t}_{won}$ represents onshore wind generation and $\mathfrak{t}_{woff}$ represents offshore wind generation.

There is also a seasonal effect in the availability of wind generating capacity, and the output of $\mathfrak{w}_\mathfrak{r}$ is dependent on whether the snapshot considered is classified as summer or winter. National Grid classify snapshots in December, January and February as winter snapshots and all other snapshots as summer snapshots. The effects of this seasonal assumption will be considered in Section 7.2.

The available capacity of technology $\mathfrak{t}$ in zone $\mathfrak{r}$ is denoted $x_{\mathfrak{r},\mathfrak{t}}$.

3.6 Particular Input Data

The previous sections of this chapter detail how to calculate constraint costs for given information about a power system. This section will give information about the power system that will be used as the basis for investigation in the remainder of this thesis.

The zone structure used in this thesis was detailed in Section 3.1.2, where Figure 3.1 illustrated the linear structure of the zones, with the north-most zone connected only to the 2nd north-most zone and the south-most zone connected only to the 2nd south-most, with all other zones connected to the zone immediately north and immediately south of them. This is an accurate representation of the zone structure used by National Grid in calculations for Britain's power system.

As well as the zone structure of the power system, information about the system background is required to estimate constraint costs. This includes the installed transmission

capacity between each zone, factors relating to demand (peak demand level, LDC, regional breakdown of demand), the installed generating capacities and factors relating to these generators to simulate available capacity as in Section 3.5.

For everything that follows in this thesis, data will be taken from the Electricity Scenarios Illustrator (ELSI) published by National Grid on their consultation and engagement website [69]. This resource gives full details about the system background for 20 consecutive years. We will refer to these as year 1 to year 20 in this thesis. These years are based on actual projections for Britain's power system for the 20 years between 2011 and 2030. A summary of this information is given in Appendix F. Section 3.7 will calculate mean constraint costs using this information, as well as illustrate how the mean constraint costs vary as the values given by [69] are varied.

Throughout this thesis, variables which detail the system background (such as installed generating capacities, generator availability probabilities, peak demand levels, etc.) will generally be referred to as input variables of the simulator.

3.7 Variation of Mean Constraint Cost Estimates and Uncertainties of Input Data

As mentioned in Section 2.3, this thesis investigates how to make transmission expansion decisions under uncertainty. For the examples presented in this thesis, this means making decisions to minimise the sum of the expected mean constraint costs plus the costs of any reinforcement made when there is uncertainty in the assumed background of the power system.

This section will give an overview to how assumptions about the power system background affect the resulting estimates of mean constraint costs. This includes investigating how mean constraint costs vary with each system background year detailed in [69] and also how mean constraint costs vary if one particular aspect of an assumed power system background (such as peak demand level) is varied.

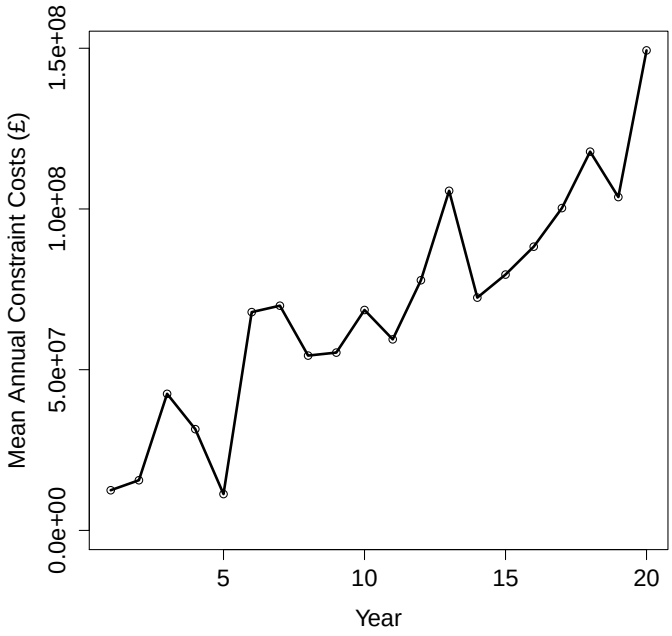

Figure 3.2: Plot to show how mean annual constraint costs vary with power system background year.

3.7.1 Power System Background Year

Assumed Power System Backgrounds

Section 3.6 stated that [69] details power system background data for 20 consecutive years. The estimate of peak demand level and installed generating capacities are the main differences between each of these years. This can have a large impact on the costs estimated. [69] also gives values for the installed transmission capacities for each boundary for each year, which includes scheduled reinforcements (increases to the installed capacity) for years 2 to 20.

Figure 3.2 illustrates how mean annual constraint costs vary with the projections made for each year of the dataset. As can be seen, the cost estimates vary greatly with year, with the lowest estimate coming in year 5 and their magnitude being just one fourteenth of those in year 20. This is the simplest way to illustrate how input can have a large impact on the output of the simulator.

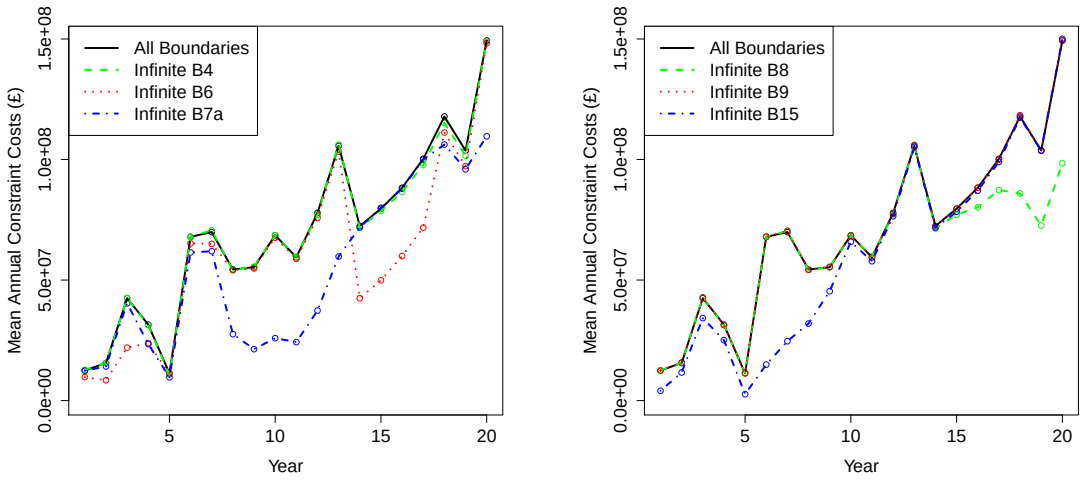

Figure 3.3: Plots to show how mean annual constraint costs vary with power system background year as the transmission capacity of particular boundaries is raised to infinity.

Increasing Transmission Capacity Between Zones

In the power system there are 6 connections (boundaries) between zones and the transmission capacity across each of these boundaries could be increased to decrease constraint costs. Making 6 simultaneous decisions to optimise constraint costs is a large task, especially when considering additional uncertainty in the power system background (as is the case for the examples that will be presented). However, just because a boundary can be reinforced (the transmission capacity can be increased) does not necessarily mean doing so will reduce constraint costs (as if the power flow across a boundary never exceeds the transfer capacity, increasing the capacity across that boundary will not affect constraint costs). Further, there are considerable costs associated with increasing the transmission capacity of a boundary, so if the reduction in constraint costs is small, the reinforcement would not be justified economically.

In order to get some initial information on which boundaries are most relevant to consider for reinforcement, it is first considered how mean annual constraint costs differ from Figure 3.2 if each boundary is treated in turn as if it had infinite transmission capacity (as much capacity as desired could be traded across that boundary). This will give some initial insight into which boundaries will give the greatest reduction in constraint costs if reinforced.

Figure 3.3 displays how mean annual constraint costs vary as the transmission capacity of each boundary is taken to be infinity. A plot which does not take any boundary to infinity is given as reference. As can be seen, not all boundaries have a relevant effect on costs at all times. B4 and B9 seem to have next to no effect at all times, meaning we are quite unconcerned with them as reinforcing them does not appear to reduce mean annual constraint costs.

In years 5 to 9 it can be seen that B15 has the largest reduction on costs, with increasing B15 also notably reducing costs in years 1 to 4. B8 on the other hand appears to have little to no effect in early years, but has the largest effect on estimated cost for years 15 onwards, with a particularly large effect in years 19 and 20.

The boundaries B6 and B7a are of particular interest. This is because whilst B15 is very relevant early and has no effect late on, and B8 has no effect in early years but is quite relevant for late years, B6 and B7a together have non negligible effects across all years. B6 is particularly interesting in year 5 and earlier and between years 14 and 17, with B7a having a particularly large reduction in costs between years 6 and 13.

These boundaries make for an especially interesting example, as they are adjacent boundaries. This means it would be reasonable to expect an interaction to exist, i.e. to expect reinforcing both of these boundaries to result in a greater reduction in mean constraint costs than simply the sum of their individual reductions. Figure 3.4 displays how mean annual constraint costs vary when both the B6 and B7a boundaries are taken to infinite capacity.

This is interesting, as there is far more interaction than might have been expected. Between the years 8 and 17, it appears that only either B6 or B7a give a substantial reduction of mean annual constraint costs with the other having next to no effect on costs. However, the combined effect of increasing both boundaries gives a much greater reduction in mean annual constraint costs in comparison to just reinforcing the one boundary that gave a cost reduction.

Overall, in this subsection it has been shown how mean constraint costs vary greatly with the system background year used. Further, which boundaries would give the most benefit when reinforced also changes year on year. In early years, B15 alone appears to have the largest effect, with B8 alone having the largest effect in later years. However,

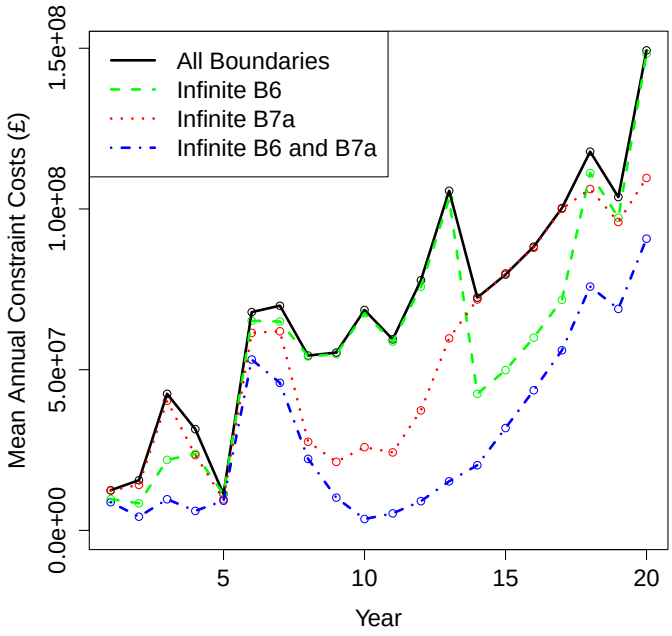

Figure 3.4: Plot to show how mean annual constraint costs vary with power system background year when considering taking the transmission capacity of the B6 and B7a boundaries to infinity.

the interaction between boundaries B6 and B7a seems to provide an interesting example across all years.

Explanations for These Observations

From the data, some explanation can be offered for these results. South of the B15 boundary lies the zone which is modelled as having a small proportion of snapshot demand (3.5%) whereas north of the B15 boundary lies a zone which has a large proportion of snapshot demand (41%). The zone south of the B15 boundary also has a quite a lot of high merit order generating capacity installed, such as wind and CCGT (i.e. gas), whereas the zone North of the B15 boundary has relatively little generating capacity installed. This means that there will often be a power flow from south to north across the B15 boundary, and reinforcing this boundary allows for more of the cheap capacity installed south of the B15 boundary to be used more often in the constrained schedule.

Between the years 8 and 11, a lot of high merit order capacity, such as off-shore wind and CCGT, are scheduled to be built in the zone immediately north of the B15 boundary.

This means that there will be a power flow across the B15 boundary less often, leading to the observed lack of benefit from reinforcing the B15 boundary in later years.

The reasons for the B8 boundary being more relevant in later years is less easy to tell directly from the data, as the boundaries north and south of it have reasonably high proportions of demand (21.1% and 18.5% of total system demand respectively) and have quite a large amount of generating capacity installed in all years. However, several GW of CCS (carbon capture and storage) CCGT and coal are scheduled to be built in the zone immediately north of the B8 boundary in years 14 and 15 which would coincide with the increased benefit from reinforcing the B8 boundary.

The reason the B6 and B7a boundaries are relevant for all 20 years is there is a lot of high merit order capacity (especially on and off-shore wind) in the three zones north of the B7a boundary (especially the zone directly north of the B7a boundary and the zone north directly of the B6 boundary) across all years. Further, the sum of the demand across all three zones is just 15.9% of the total system demand, meaning there will often be a power flow south across these boundaries. However, power can only flow south of the B7a boundary from north of the B6 boundary if both the B6 and B7a boundaries are sufficiently reinforced, which explains the interaction between the two.

3.7.2 Uncertainty in The Power System Background

The Sum of Constraint Costs Across All 20 Years

In the previous subsection it was shown how mean annual constraint costs vary for particular power system backgrounds. However, it is unreasonable to think an entire power system background can be known precisely; there will be uncertainty in some (or all) variables. Not every variable has a large effect on costs, and which variables have the most relevant effect on costs may change year on year. In addition, the relative magnitude of uncertainty in a variable will also vary with which variable is considered. For example, it is reasonable to assume the current installed amounts of generating capacity can be known very accurately (though there will be at least some uncertainty in later years) though their availability probabilities will be known much less accurately.

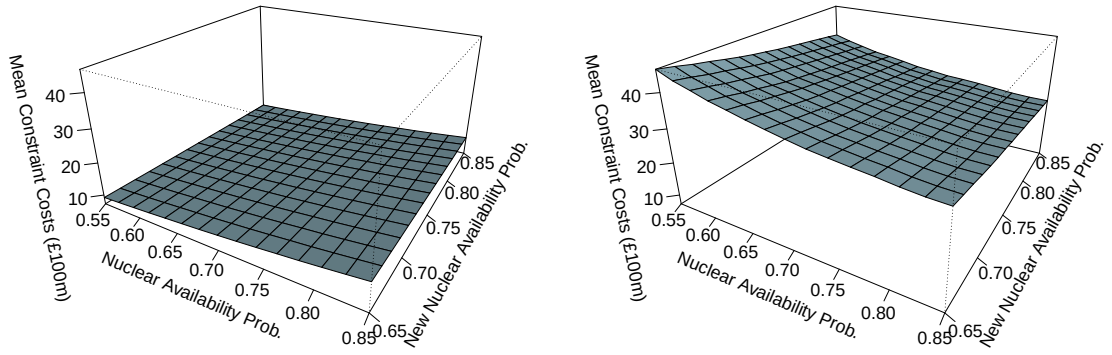

(a) Peak demand level magnified by a factor of 0.85.

(b) Peak demand level magnified by a factor of 1.15.

Figure 3.5: Graphs of how the sum of mean constraint costs across all 20 years varies as nuclear and new nuclear availability probabilities are varied for two different levels of peak demand.

When considering the sum of constraint costs across all 20 years, 3 variables of particular interest are peak demand level, nuclear availability probability and new nuclear availability probability. Figure 3.5 displays how mean constraint costs vary as these factors are varied. The variation of peak demand is specified as a factor of magnification. For example, if the peak demand of a year was 10000 MW a peak demand magnification of 1.15 would mean increasing the peak demand to 10000 MW $\times 1.15 = 11500$ MW.

The availability probabilities of different generators are the variables used when randomly simulating the available generating capacity, i.e. values of a_t in Section 3.5. In simple terms, the larger the availability probability the more likely a particular generating unit will be available. This in turn means that larger availability probabilities increase the expected available capacity of a particular generating technology. If sufficient transmission capacity exists to utilise this generating capacity, the larger availability probabilities will generally decrease mean constraint costs. However, if a high merit order technology (i.e. a technology with a low offer price that would likely be included in the unconstrained schedule such as wind or nuclear) has more capacity available more often and the transmission is insufficient to utilise this capacity, then

the increased availability would increase mean constraint costs. Section 2.1.2 indicated that this is because the constraint costs are a measure of a power system's ability to utilise the cheapest generating capacity available and are not a measure of the total amount spent on generating capacity.

Figure 3.5 illustrates how the peak demand level assumed has a large effect on the mean constraint costs (up to a factor of 4). There is also an interaction between the peak demand level and the availability probabilities. At low peak demand levels it can be seen that the mean constrain costs generally increase as nuclear and new nuclear availability probabilities are increased. However, at high peak demand levels it is seen that mean constraint costs generally decrease as nuclear and new nuclear availability probabilities are increased. The effect of nuclear and new nuclear availability on the mean constraint costs also appears to be greater at the higher peak demand level.

The Use of Only 1 Future Year When Estimating Constraint Costs

It can be quite expensive to acquire an accurate estimate of mean constraint costs, even when making use of the importance sampling technique which will be outlined in Section 4.4.2. As a result, when estimating mean constraint costs for a period of time, it is common practice to simply evaluate one future year and use it to extrapolate an estimate of mean constraint costs across a longer period of time [78, 97, 66, 81]. This thesis will initially consider transmission expansion problems where constraint costs are extrapolated from a single future year to remain consistent with this and to make results comparable to the existing literature.

However, the variables which the estimate of mean constraint costs is most sensitive to vary depending on which power system background year is considered. For example, the graphs in Figure 3.5 consider varying nuclear and new nuclear availability probabilities. However, no generating technology classified "new nuclear" is included in the projections of [69] until year 9. Therefore, if any extrapolation is made from years 1 to 8 this variable would not be of interest.

Initial examples in this thesis will consider transmission expansion decisions based on the power system backgrounds of year 1 and year 6 (presented in Chapters 5 and 6 re-

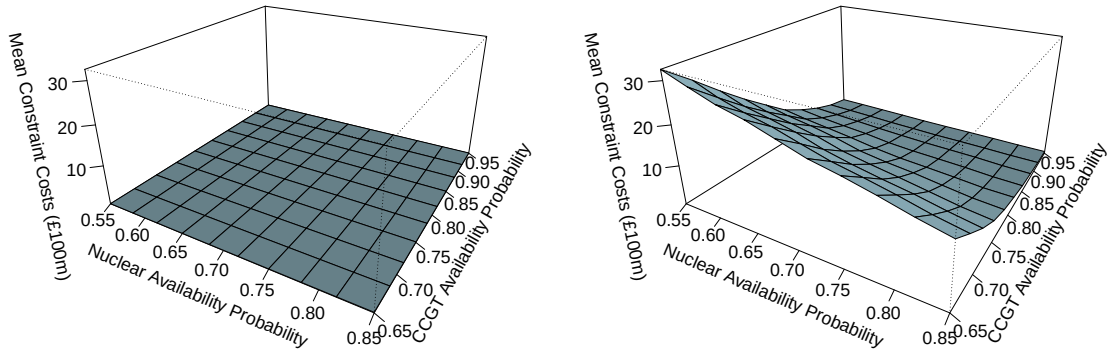

(a) Peak demand level magnified by a factor of 0.85.

(b) Peak demand level magnified by a factor of 1.15.

Figure 3.6: Graphs of how mean constraint costs vary in year 1 as nuclear and CCGT availability probabilities are varied for 2 different peak demand levels.

spectively). Therefore, the following two sub-subsections consider how mean constraint costs are sensitive to input variables in these years.

However, Figure 3.2 of Section 3.7.1 would suggest that basing estimates of future constraint costs on a single future year may not a particularly accurate method of estimating costs over a given period of time. Therefore, Section 7.6 will consider using multiple future years to estimate mean constraint and present how this affects costs estimated and the resulting decisions made. Chapter 8 will then go on to consider decision making over multiple stages, which requires mean constraint costs to be estimated separately for each stage which requires the evaluation of multiple future years.

Constraint Costs for a Year 1 Power System Background

Figure 3.6 displays how mean constraint costs vary with peak demand level, nuclear availability probability and CCGT (gas) availability probability when using a year 1 power system background. As can be seen, the costs are dominated by the particularly high mean constraint costs that can occur when peak demand is magnified by a factor of 1.15 and CCGT availability probability is low. Mean constraint costs for all conditions when peak demand is magnified by a factor of 0.85 seem flat and negligible in comparison.

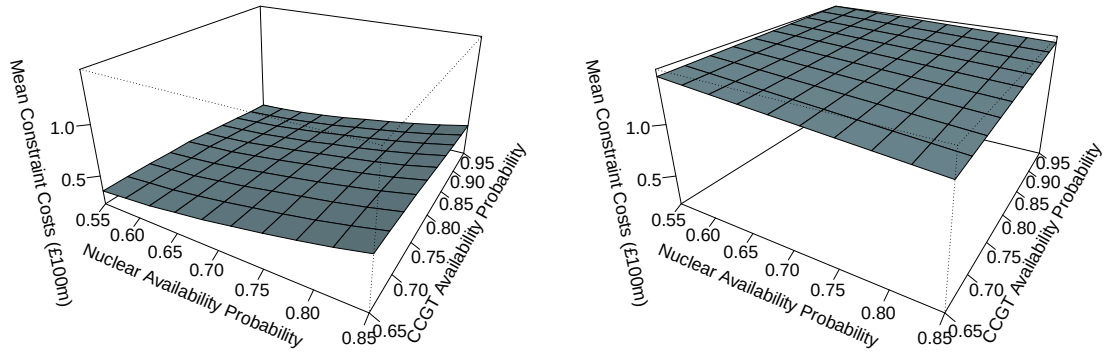

(a) Peak demand level magnified by a factor of 0.85.

(b) Peak demand level magnified by a factor of 1.15.

Figure 3.7: Graphs of how mean constraint costs vary in year 6 as nuclear and CCGT availability probabilities are varied for 2 different peak demand levels.

This means that when it comes to decision making under uncertainty, if sufficient weight is given to cases where peak demand is magnified by a factor of 1.15, reinforcement decisions made could be very different to decisions which assume the projections of [69] to be 100% accurate. A transmission expansion planning problem based off a year 1 system background will be considered in Chapter 5. This will be a simple initial example to illustrate how emulators can be used to approximate simulators and make decisions under uncertainty.

Constraint Costs for a Year 6 Power System Background

Figure 3.7 considers how mean constraint costs vary with peak demand level, nuclear availability probability and CCGT availability probability if a year 6 power system background was assumed. Again, we see a difference in behaviour as peak demand magnification is varied, though high peak demand assumptions do not dominate costs in the way they do when assuming a year 1 power system background.

Further, mean constraint costs actually seem less sensitive to the values for CCGT and nuclear availability probabilities at the higher peak demand level in comparison to the lower peak demand level. This would mean that if a higher level of peak demand was assumed we may expect the resulting decision to be less sensitive to the

decision maker's attitude to risk than if a lower peak demand level was assumed. A transmission expansion planning problem based off a year 6 power system background will be considered in Chapter 6. This example will be more complicated than the example presented in Chapter 5, as it will consider making multiple simultaneous decisions with uncertainty being considered in multiple variables.

Again, making a reinforcement decision based off a constraint cost estimate for a single future year is quite poor, so the example will be extended in Section 7.6 to estimate constraint costs and make decisions using multiple future years. Further, Chapters 8 and 9 will consider decision making over multiple stages, with costs for each stage simulated separately using different power system backgrounds.

Chapter 4

The Use of Importance Sampling to Estimate Mean Constraint Costs

Chapter 3 defined the simulator used to estimate mean constraint costs in this thesis. Due to the random availabilities of generating technology, the output of the simulator each time it is run (evaluation of annual constraint costs) is itself a random variable, and it was noted in Section 3.4.3 that an average of many annual evaluations must therefore be calculated. Recall, this thesis is only concerned with the calculation of mean constraint costs for a given power system background which is the standard practice of National Grid, and broadly the case elsewhere.

However, a single estimate of constraint costs from the simulator for a given power system background can be quite expensive to evaluate. Further, the value of constraint costs calculated in each simulator evaluation can vary greatly, as will be illustrated in Section 4.1.1. This means that calculating an accurate estimate of mean constraint costs for a fixed power system background by taking an average of many evaluations of constraint costs for that power system can be a very expensive procedure.

Part of the methodology of Chapter 3 was to break the year down into 17520 half hour snapshots. Some of these snapshots contain more relevant information to the estimate of mean annual constraint costs than others (as will also be demonstrated in this chapter). This chapter proposes a method of importance sampling which can be used to estimate mean constraint costs for a given power system background, which evaluates certain snapshots with a greater frequency than others. This importance

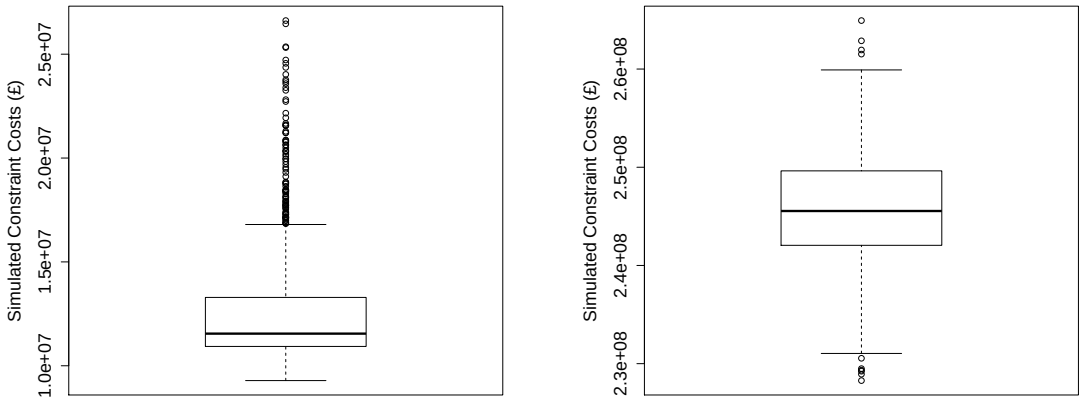

(a) Year 1 power system background. (b) Year 6 power system background.

Figure 4.1: Boxplots to show how evaluations of constraint costs from the simulator vary each time the simulator is run for a fixed power system background.

sample will have the same expectation as using the full simulator, but will require fewer snapshots to be evaluated to reach a given level of accuracy in the estimate.

4.1 Variation in Constraint Costs Estimates

4.1.1 Variation in Annual Constraint Cost Estimates

Section 3.1 detailed how constraint costs for a year are calculated by first breaking the year down into 17520 snapshots, with Section 3.5 going on to give details about how the available generating capacity is randomly simulated in each snapshot. This means that the constraint costs calculated for these randomly drawn availabilities of generating capacities are themselves random, which in turn means the evaluation of annual constraint costs (which is simply the sum of constraint costs from all 17520 snapshots) each time the simulator is evaluated is itself random. As mentioned, this thesis is concerned with mean constraint costs (as is standard practice of National Grid) and as such an average of many annual evaluations must be taken. This section gives details of how the evaluation of annual constraint cost varies each time the simulator is run.

Power System Background	Year 1	Year 6
Mean of Constraint Cost Evaluations	£12,600,000	£246,000,000
Standard Deviation of Constraint Cost Evaluations	£2,780,000	£5,740,000
Standard Deviation as a Percentage of Mean	22.1%	2.34%
Range of Constraint Cost Evaluations	£17,300,000	£36,700,000

Table 4.1: Table giving details of simulated annual constraint costs for two power system backgrounds.

Figure 4.1 displays boxplots of how 1000 evaluations of annual constraint costs from the full simulator vary for two fixed power system backgrounds, whilst Table 4.1 details some statistics about these simulator evaluations. Results are presented for a year 1 and year 6 power system background, with data for these power system backgrounds being taken from National Grid's freely available online reference [69]. As mentioned in Section 3.7.2, these power system backgrounds are of interest for the examples presented in Chapters 5 and 6. As can be seen, there is the potential for costs to vary greatly with each evaluation of the simulator.

For both power system backgrounds, there is considerable variation in the evaluation of annual constraint costs each time the simulator run. For a year 6 power system background, it is observed that costs can vary by tens of millions of pounds each time the simulator is run. However, it should be noted that the mean of these evaluations was £246,000,000, so the standard deviation of the simulations is quite small in comparison (2.34% of the mean). The boxplot also shows that there are long tails to both the right and left.

For a year 1 power system background, the mean constraint costs are 20 times smaller than the mean for a year 6 power system background, yet the standard deviation is just half the size. This results in the standard deviation of the simulator evaluations being large in comparison to the mean of the simulator evaluations (22.1%) for a year 1 power system background. This implies that if an estimate of mean annual constraint costs is required such that the standard error of the estimate is small relative to the mean, a lot more work is necessary to acquire such an estimate of constraint costs for a year 1 power system background in comparison to a year 6 power system background, and this will be demonstrated in Section 4.3.3. However, if it is required that the value of the standard error of the estimate itself be below a given value, more work

will be required to acquire such an estimate for a year 6 power system background, as will be demonstrated in Section 4.3.5. The boxplot for annual constraint costs for a year 1 system background also shows a very long tail to the right, implying it is not uncommon for an evaluation of annual constraint costs from the simulator to be far greater than the mean.

4.1.2 The Load Duration Curve

Section 3.1 stated that annual constraint costs are calculated by breaking the year down into half hour snapshots, simulating each snapshot separately and taking a sum of the constraint costs which arise in each to acquire an estimate of constraint costs for the entire year. It was also stated that the main differences between these snapshots are a seasonal effect (which affects the distribution for wind generating capacity and will be explored in greater detail in Section 7.2) and the proportion of peak demand used in that snapshot (which is of interest in this subsection).

A load duration curve (LDC) is used to specify the distribution of demand for generating capacity throughout a year. This is achieved by specifying demand in each snapshot as a proportion of the peak demand level, which can then be used to calculate the demand for the snapshot via Equation 3.1.1. These demands can then in turn be used to simulate constraint costs as outlined in Chapter 3.

Figure 4.2 (a) displays the LDC used in this thesis. In this plot, it is shown how many snapshots exceed a particular proportion of peak demand. The plot shows how a small proportion (1906 of 17520, or 10.8%) of snapshots use a demand level which exceeds 80% of peak demand, and an even smaller amount (328 of 17520, or 1.8%) exceed 90% of peak demand. The majority of snapshots have a demand level which is between 40% and 80% of peak demand.

The LDC used in this thesis is also taken from [69] and is based on the observed load duration curve from the years 2009 and 2010. This LDC will be used in the examples presented in Chapters 5, 6, 8 and 9 on the advice of Paul Plumptre (formerly of National Grid) [78]. However, Section 3.7.2 illustrated how peak demand level has a large effect on estimated mean constraint costs, which would imply the LDC would also have a

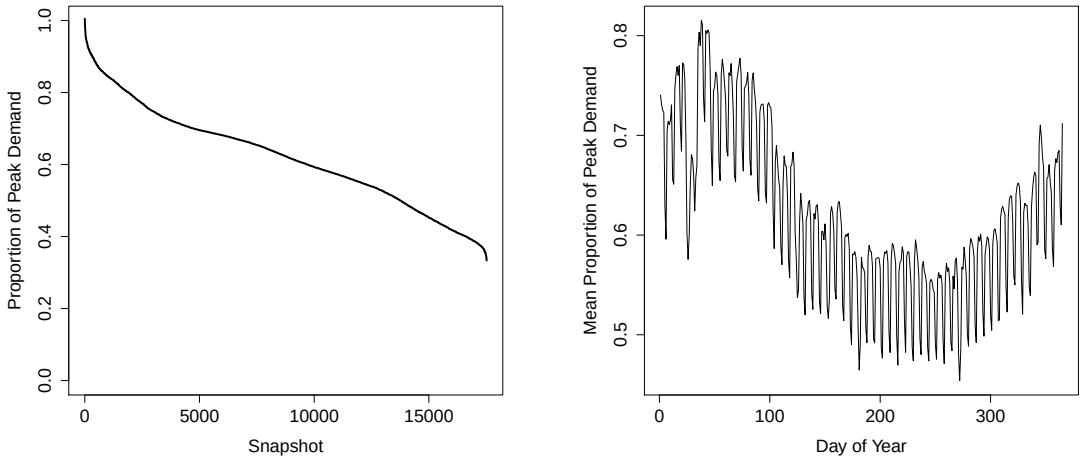

(a) Load duration curve.

(b) Illustration of how mean daily snapshot demand varies chronologically.

Figure 4.2: Graphs to illustrate a load duration curve.

large effect. The effect of the assumed LDC on cost estimates, and resulting decisions, will be investigated in Section 7.3.

Figure 4.2 (b) is an alternative way to display the yearly demand data. This plot shows how the mean snapshot demand for each day varies chronologically, beginning on the 1st of December and ending on the 30th of November. Whilst the graph is not particularly clear, there are some important patterns to be observed. First, it is illustrated how daily snapshot demand can fluctuate quite a lot over a short period of time. This is due to a weekly pattern in demand, where demand is greater throughout the week in comparison to weekends.

Secondly, there is a seasonal pattern in the demand data, where demand is generally greater in December, January, February and November in comparison to other months. This is what may be expected for British demand, where there is a greater demand for electricity in these colder months (for example, due to a greater need for electrical heating). Further, even within this seasonal pattern there is an interesting relative lack of demand over the Christmas period.

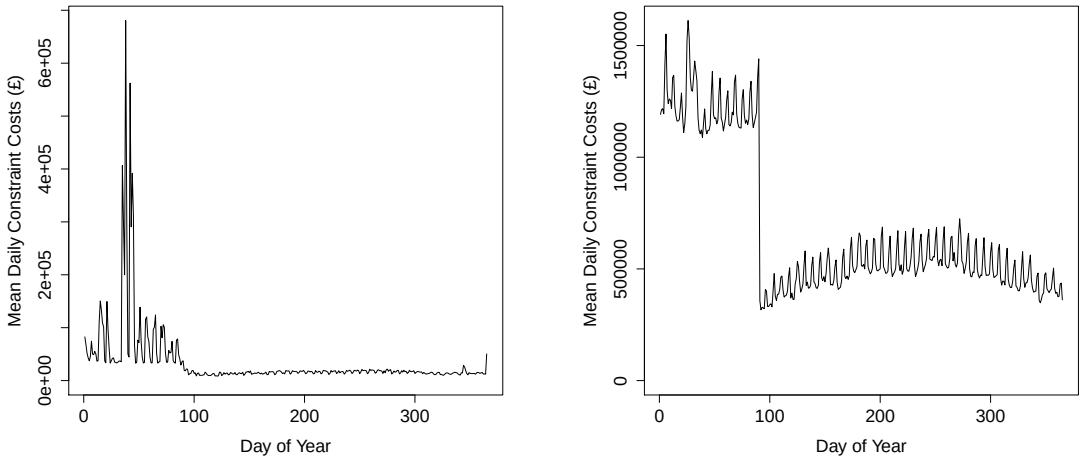

(a) Mean constraint costs by day, for a year 1 power system background.

(b) Mean constraint costs by day, for a year 6 power system background.

Figure 4.3: Graphs to show how mean constraint costs vary by day for two power system backgrounds.

4.1.3 Constraint Cost Estimation By Day

Figure 4.2 (a) shows that snapshot demand level varies greatly throughout the year, with Figure 4.2 (b) going on to show this variation on a day to day basis. However, it is important to consider what effect this variation has on mean constraint costs for a given power system.

Figure 4.3 displays how mean constraint costs vary with day for both a year 1 and year 6 power system background from [69]. These daily means are plotted chronologically, beginning on the 1st of December and ending on the 30th of November. Again, as generator availabilities are random there can be a great deal of variation in the constraint costs calculated in each simulator evaluation, even for a fixed snapshot. Therefore, the estimates given in Figure 4.3 are averages of 1000 repetitions.

For a year 1 power system background it can be seen that the mean constraint costs of a small number of days greatly exceed the mean constraint costs of the vast majority of days. In particular, just 9 of the days (2.47% of the year) have mean constraint costs greater than £200,000, and these 9 days account for 27.3% of the mean constraint costs of the year. By comparison to Figure 4.2 (b), it is clear that these constraint costs correlate with demand, but in a very non-linear manner.

Further, between March and November the daily mean constraint costs appear negligible in comparison to those of December, January of February. This is partially due to the decrease in demand over this period, which can be observed in Figure 4.2 (b). The decrease in mean constraint costs over this period is also due to the seasonal effect mentioned in Chapter 3, where a different model is used for the availability of wind generating capacity for winter months (December, January and February) in comparison to the model used for summer months (all other months). This will be considered in greater detail in Section 7.2.

Mean constraint costs estimates by day for a year 6 power system background, displayed in Figure 4.3 (b), indicate that all snapshots have a somewhat similar contribution to the estimate of mean annual costs, especially in comparison to Figure 4.3 (a). This could contribute to explaining what was noted in Table 4.1, where the year 6 estimate of mean annual constraint costs was relatively much more consistent than the estimate of mean annual constraint costs in year 1. This is because when all snapshots behave similarly with a similar contribution to the yearly estimate (as in year 6), the variations in each snapshot can somewhat be averaged out across all 17520 snapshots. However, in year 1, where there are less snapshots with a large contribution to the yearly estimate, the random variation within snapshots is effectively averaged across fewer snapshots.

Figure 4.3 (b) also illustrates a steep drop in mean constraint costs at the beginning of March. Again, this is due to the seasonal model for wind generating capacity, which uses a different model for winter months (January, February and December) in comparison to summer months (March to November). However, unlike the year 1 power system background where mean constraint costs were negligible between March and November, the costs between March and November for a year 6 power system background are far from negligible, with all daily estimates of constraint costs being greater than £316,000.

4.2 Importance Sampling

4.2.1 Brief Overview of Applications of Importance Sampling in the Existing Literature

The previous section demonstrated how there is a great deal of variation of constraint costs in each simulator evaluation for a given power system background, both on an annual and snapshot basis. Section 3.4.3 stated that an average of many annual simulator evaluations is used to acquire an estimate of mean annual constraint costs. This is to remain consistent with National Grid methodology of working with mean constraint costs. However, acquiring an estimate of annual constraint costs which evaluates all 17520 snapshots of the year is quite expensive. In turn, this means taking an average of many such annual evaluations is very expensive.

Figure 4.3 shows how the mean constraint costs of a snapshot can vary greatly with snapshot, and suggests that when estimating mean constraint costs for a year, certain snapshots contain more relevant information to the estimate of mean annual constraint costs than others. Therefore, when aiming to acquire an accurate estimate of mean annual constraint costs it may be more important to have accurate estimates of costs in certain snapshots more than others. This is the fundamental principle behind importance sampling, where a careful selection of sampling density can reduce the work necessary to achieve a given level of accuracy in an estimate [29, 6, 31, 77].

In order to detail how importance sampling is commonly applied in the existing literature, consider a problem where the expected value of a function, $f(\mathbf{x})$, of a set of discrete random variables, $\mathbf{x}$, is of interest. The expectation can be calculated as

$$\mu = \sum_{\mathbf{x}} f(\mathbf{x})p(\mathbf{x}) \tag{4.2.1}$$

where $p(\mathbf{x})$ is the probability density function of $\mathbf{x}$.

However, if the function $f(\mathbf{x})$ is expensive to evaluate it will not be feasible to calculate μ exactly via Equation 4.2.1. Therefore, Monte Carlo simulation is commonly used to approximate Equation 4.2.1 by randomly drawing values of $\mathbf{x}$ from the distribution of $p(\mathbf{x})$ to estimate μ [104, 28, 86, 6]. If n random drawings of $\mathbf{x}$ are sampled from the

distribution $p(\mathbf{x})$ such that $\mathbf{x}_i$ is the ith value sampled, an estimate of μ via Monte Carlo simulation can be acquired as

$$\hat{\mu}_p = \frac{1}{n}\sum_{i=1}^{n} f(\mathbf{x}_i) \tag{4.2.2}$$

However, certain values of $\mathbf{x}$ may be more relevant to the estimate of μ than others. This is particularly true when estimating the probability of a rare event occurring (i.e. μ is the probability of a rare event occurring with $f(\mathbf{x})$ acting as an indicator function, taking the value 1 if the rare event occurs for a particular value of $\mathbf{x}$ and 0 otherwise) as is considered in the examples of [9, 36, 104, 96]. In such examples, sampling values of $\mathbf{x}$ from the distribution $p(\mathbf{x})$ will be very inefficient, as the rare event will not be observed for the majority of values of $\mathbf{x}$. In particular, [96] notes that if μ corresponds to a rare event with a probability of 10^{-6} of occurring it would require a Monte Carlo sample size of the order of hundreds of millions to acquire an estimate of μ with an error of 10%.

Therefore, importance sampling can be applied by instead sampling values of $\mathbf{x}_i$ from some alternative distribution $q(\mathbf{x})$, where $q(\mathbf{x})$ gives more weight to values of $\mathbf{x}$ more relevant to the estimate of μ. If n random drawings of $\mathbf{x}$ are sampled from the distribution $q(\mathbf{x})$ such that $\mathbf{x}_i$ is the ith value sampled, an estimate of μ using importance sampling can be calculated as [77, 36, 16, 96]

$$\hat{\mu}_q = \frac{1}{n}\sum_{i=1}^{n} f(\mathbf{x}_i)\frac{p(\mathbf{x}_i)}{q(\mathbf{x}_i)} \tag{4.2.3}$$

It can be shown that such a method has the same expectation as the estimate from Monte Carlo simulation as

$$E(\hat{\mu}_q) = E_{q(\mathbf{x})}\left(\frac{f(\mathbf{x})p(\mathbf{x})}{q(\mathbf{x})}\right) = \sum_{\mathbf{x}} \frac{f(\mathbf{x})p(\mathbf{x})}{q(\mathbf{x})}q(\mathbf{x}) = \sum_{\mathbf{x}} f(\mathbf{x})p(\mathbf{x}) = E_{p(\mathbf{x})}(f(\mathbf{x})) = E(\hat{\mu}_p) \tag{4.2.4}$$

When applying importance sampling to estimate the probability of a rare event it is desirable that the alternative density, $q(\mathbf{x})$, results in an increased probability of the rare event occurring [104, 16, 82], with there being several potential methods of achieving this such as exponential twisting [9, 36] or iterative schemes such as the cross-entropy method [104, 96] or adaptive importance sampling [47]. An iterative scheme suitable for estimating mean annual constraint costs (as considered in this thesis) via

importance sampling will be proposed in Section 4.4.2.

There are a wide variety of applications of importance sampling to various examples in the existing literature. For example, [47] consider an application to fishery stock assessment, where importance sampling is used to estimate the biomass stock of the orange roughy (a type of fish), as well as to estimate the probability that the stock exceeds a particular value. Further, these estimates are then used to make policy decisions for the fisheries, with consideration also given to how the policy maker's attitude to risk affects the decision made.

The safety of lane change events of automated vehicles is considered in [104], where importance sampling is used to estimate the probabilities of conflict, crashes and injuries during the lane change events. A comparison is also given to show the benefit of using importance sampling over Monte Carlo sampling without importance sampling. An application related to power systems is presented in [96], where importance sampling is used to estimate the loss of load probability (the probability that a power system will not be able to satisfy all demand) and expected power not served (the expected demand, in MW, that will not be satisfied) for a variety of power system backgrounds.

Many other applications of importance sampling to a wide variety of topics exist, including estimating the probability of failure of the Data Communication System (DCS) of large scale passenger rail systems [82]; predicting the yield of an integration circuit (i.e. the probability of failure of a complex circuit) under variability due to the manufacturing process [16]; biological/medical applications (such as testing for distinctive charge clusters in proteins or identifying cancer indicators in mammograms) [68] and path tracing using the photon map [43].

As importance sampling is not the main focus of this thesis, but rather a tool used within the simulation process to estimate mean annual constraint costs, this section is not intended to be taken as a full literature review, but rather a brief overview of applications of importance sampling in the existing literature.

4.2.2 Using Importance Sampling to Estimate Mean Annual Constraint Costs

As noted at the beginning of Section 4.2.1, the application of importance sampling in this thesis will consider reducing the number of snapshots which must be evaluated to acquire an estimate of mean annual constraint costs.

In order to consider applying importance sampling to estimate mean annual constraint costs for a given power system background, define $f_{c,\tau}(\tau)$ as the function which randomly simulates constraint costs for snapshot τ for a given power system background. As the simulator defined in Chapter 3 calculates an evaluation of annual constraint costs by randomly simulating constraint costs in each snapshot, then taking a sum of the simulated constraint costs across all snapshots, importance sampling is not applied as described in Section 4.2.1.

Instead, an alternative method is used where a smaller number of snapshots are evaluated when acquiring an evaluation of annual constraint costs. This requires a vector of snapshot weights, $\boldsymbol{\omega}$, which is a vector of length $\mathscr{T}$ (i.e. of length 17520 as there are 17520 half hour snapshots in a year) where ω_τ (the τth element of $\boldsymbol{\omega}$) is the probability that snapshot τ is actually simulated, with $0 < \omega_\tau \leq 1$. By randomly simulating whether or not to simulate each snapshot based on $\boldsymbol{\omega}$, an evaluation of annual constraint costs using importance sampling can be acquired as

$$\sum_{\tau=1}^{17520} \frac{f_{c,\tau}(\tau)}{\omega_\tau} X(\tau) \tag{4.2.5}$$

where $X(\tau)$ is an indicator function which takes the value 1 if snapshot τ was actually simulated and 0 otherwise. The R-code for the simulator which uses such an importance sampling method is given in Appendix G.2. It is trivial to show this gives the same expectation as simulating every snapshot, as

$$\begin{aligned} E\left(\sum_{\tau=1}^{17520} \frac{f_{c,\tau}(\tau)}{\omega_\tau} X(\tau)\right) &= \sum_{\tau=1}^{17520} \frac{E(f_{c,\tau}(\tau)X(\tau))}{\omega_\tau} \\ &= \sum_{\tau=1}^{17520} \left(\frac{E(f_{c,\tau}(\tau) \times 1)\omega_\tau}{\omega_\tau} + \frac{E(f_{c,\tau}(\tau) \times 0)(1-\omega_\tau)}{\omega_\tau}\right) \\ &= \sum_{\tau=1}^{17520} \frac{E(f_{c,\tau}(\tau))\omega_\tau}{\omega_\tau} = \sum_{\tau=1}^{17520} E(f_{c,\tau}(\tau)) \end{aligned} \tag{4.2.6}$$

However, it would be possible to consider applying importance sampling as described in Section 4.2.1 by using an equivalent alternative method to randomly simulate annual constraint costs where the snapshot to be simulated, τ, is modelled as a discrete random variable with probability mass function, $p(\tau)$, which describes the probability of τ taking a particular value as

$$p(\tau) = \begin{cases} \frac{1}{17520} & \text{for } \tau \text{ in 1,2,...,17520} \\ 0 & \text{Otherwise} \end{cases}$$

i.e. a discrete uniform distribution over the integers 1 to 17520.

Under this model, constraint costs for a year are simulated by first randomly drawing a snapshot, τ, to be simulated from the distribution $p(\tau)$, then using the function $f_{c,\tau}(\tau)$ to randomly simulate constraint costs for that snapshot. As there are 17520 half hour snapshots in a year, an estimate of annual constraint costs based on such a simulation is

$$f_{c,\mathscr{T}}(\tau) = 17520 \times f_{c,\tau}(\tau) \tag{4.2.7}$$

By defining the simulator in this way, the importance sampling methodology described in Section 4.2.1 can then be applied, where the density $p(\tau)$ is replaced by some alternative density $q(\tau)$. Importance sampling can then be applied by sampling values of τ according to the distribution of $q(\tau)$. If n values of τ are sampled according to the distribution of $q(\tau)$, such that τ_i is the ith value of τ in the sample, an estimate of mean annual constraint costs, $\hat{\mu}_q$, can be calculated as

$$\hat{\mu}_q = \frac{1}{n} \sum_{i=1}^{n} \frac{f_{c,\mathscr{T}}(\tau_i) p(\tau_i)}{q(\tau_i)} \tag{4.2.8}$$

For given weights, ω_τ, to apply importance sampling using Equation 4.2.5, an equivalent alternative density, $q(\tau)$, to apply importance sampling using Equation 4.2.8 is

$$q(\tau) = \frac{\omega_\tau}{\sum_\tau \omega_\tau} \tag{4.2.9}$$

Similarly, for a given specification of $q(\tau)$, an equivalent set of weights, ω_τ, to apply importance sampling using Equation 4.2.5 could be calculated as

$$\omega_\tau = \frac{q(\tau)}{q^*} \tag{4.2.10}$$

where q^* is the maximum value of $q(\tau)$ across all snapshots. This is given some further thought in Appendix A.1.

It is also important to consider how the selection of the weights, ω_τ, affects the variance of the estimate arising when using Equation 4.2.5 to acquire an evaluation of annual constraint costs. This is detailed in Appendix A.1.

As an overview, if y is used to represent a single evaluation of annual constraint costs using the full simulator (i.e. evaluating each snapshot in each yearly evaluation) and $y_{\boldsymbol{\omega}}$ is a single evaluation of annual constraint costs from Equation 4.2.5 using importance sampling weights $\boldsymbol{\omega}$, the variance of these evaluations can be calculated as

$$\text{var}(y) = \sum_{\tau=1}^{17520} \text{var}(f_{c,\tau}(\tau)) \tag{4.2.11}$$

and

$$\begin{aligned}\text{var}(y_{\boldsymbol{\omega}}) &= \sum_{\tau=1}^{17520} \left(\frac{\text{var}(f_{c,\tau}(\tau))\text{var}(X(\tau))}{\omega_\tau^2} + \text{var}(f_{c,\tau}(\tau)) + \frac{(E(f_{c,\tau}(\tau)))^2\text{var}(X(\tau))}{\omega_\tau^2} \right) \\ &\geq \sum_{\tau=1}^{17520} \text{var}(f_{c,\tau}(\tau))\end{aligned} \tag{4.2.12}$$

with equality if and only if $\omega_\tau = 1$ for all τ (or more precisely, with equality if and only if $\omega_\tau = 1$ for all τ except for snapshots where $E(f_{c,\tau}(\tau)) = 0$ with zero variance). Naively, this would suggest that any choice of importance sampling weights other than $\omega_\tau = 1$ for all τ increases the variance of the estimate. However, this is because Equation 4.2.12 simply calculates the variance of the output of the simulator, and does not consider the amount of work required (number of snapshots evaluated) to acquire the estimate of constraint costs.

Therefore, when considering the optimal choice of importance sampling weights it is more useful to consider the importance sampling methodology detailed in Section 4.2.1. As detailed above, an application of this to the constraint cost problem considered in this thesis would model the snapshot to be simulated, τ, as a random variable, which can subsequently be used to evaluate annual constraint costs via Equation 4.2.7, thus each evaluation of annual constraint costs would simulate only a single random snapshot. Consideration to this is given in Appendix A.1, where it is shown that an

optimal choice of $q(\tau)$ to minimise the variance of $\hat{\mu}_q$ from Equation 4.2.8 is

$$q(\tau) = \frac{f_{c,\mathscr{T}}(\tau)p(\tau)}{\mu} \tag{4.2.13}$$

where μ is the mean of the full simulator (mean annual constraint costs). As μ is an unknown constant (it is the what is being estimated) and $p(\tau)$ has a constant value of $\frac{1}{17520}$ for all τ, Equation 4.2.13 implies that an optimal alternative density, $q(\tau)$, to minimise the variance of the estimate of mean constraint costs is to select values of $q(\tau)$ in proportion to the mean constraint costs in each snapshot. This in turn implies an optimal choice of weights, ω_τ, (which can be calculated via Equation 4.2.10 for given $q(\tau)$) when applying importance sampling using Equation 4.2.5, is to select the weights in proportion to the mean constraint costs of the snapshot.

4.3 Initial Application of Importance Sampling to Estimate Mean Constraint Costs

4.3.1 Selection of Weights for Importance Sampling

The previous section detailed how importance sampling can be used to reduce the expected amount of work required to acquire an evaluation of annual constraint costs, whilst giving the same mean as when using the full simulator (i.e. evaluating each snapshot). This section will consider the application of importance sampling to estimate mean constraint costs for a year 1 and year 6 power system background. As stated in Section 3.7, these are the two power system backgrounds that will be used for the decision problems considered in Chapters 5 and 6 respectively.

Equation 4.2.5 defines how to acquire an estimate of constraint costs for a power system, which has the same expectation as evaluating all 17520 snapshots whilst only evaluating a smaller subset of the snapshots. However, this equation relies on weights, $\boldsymbol{\omega}$, to be given to acquire this estimate. Whilst all selections of weights give the same mean of costs (as was verified in Equation 4.2.6) certain selections of weights will give a more consistent estimate of constraint costs than others. This was considered in Section 4.2.2 and Appendix A.1 where it is shown that the variance of the estimate of mean constraint

costs is minimised (when evaluating an equivalent number of snapshots) when the importance sampling weights are proportional to the mean constraint costs in each snapshot.

This implies that the optimal choice of weights, $\boldsymbol{\omega}$, to be used for importance sampling are proportional to the mean constraint costs of each snapshot. By defining ϕ_τ as the mean constraint costs in snapshot τ, with the largest value of mean constraint costs across all snapshots defined as Φ, such a selection of weights based on the mean constraint costs in each snapshot can be calculated as

$$\omega_\tau = \frac{\phi_\tau}{\Phi} \tag{4.3.1}$$

These weights could then be used in Equation 4.2.5 to estimate mean annual constraint costs.

However, basing the weights on the mean constraint costs of each snapshot is problematic, as this requires prior estimates of these quantities in order to calculate the resulting importance sampling weights, ω_τ. Further, if the mean constraint costs for each snapshot were known accurately in advance, then mean annual constraint costs (the value we are trying to estimate) would also be known accurately (as it is simply the sum of the mean constraint costs in each snapshot).

Therefore, it may be worthwhile considering other criteria for importance sampling weights, $\boldsymbol{\omega}$, which do not depend on the mean constraint costs in each snapshot. Section 3.1 stated that other than a seasonal effect, the only variable which is varied between snapshots for a given power system background was the proportion of peak demand used in that snapshot. An alternative solution could therefore be to base the importance sampling weights on snapshot demand level by defining ϕ_τ as the demand level of snapshot τ and Φ as the peak demand level (i.e. largest demand level of all snapshots). Weights to be used for importance sampling based on the demand level of each snapshot could then be calculated by using these values of ϕ_τ and Φ in Equation 4.3.1.

However, Figure 4.3 indicated that the estimate of constraint costs in a snapshot may have a greater level of variation than the peak demand alone may have suggested. This means that basing importance sampling weights on snapshot demand may not

result in a great improvement in the efficiency of estimating mean annual constraint costs for a given power system background in comparison to using the full simulator. The remainder of this section will consider how the choice of weights for importance sampling, $\boldsymbol{\omega}$, affects the work required to acquire an estimate of mean annual constraint costs to a given level of precision, and also compare the resulting estimates to the actual mean of the full simulator.

4.3.2 Initial Application of Importance Sampling

Initial Application of Importance Sampling

Sections 4.3.3 to 4.3.5 will consider how much work (i.e. how many snapshot evaluations) are required to estimate mean annual constraint costs to a given level of precision for a year 1 and year 6 power system background. Results are given when basing the weights for importance sampling on snapshot demand level and the mean of constraint costs in each snapshot. For comparison, results are also given when basing the importance sampling weights on the standard deviation of constraint costs in each snapshot or when evaluating each snapshot (i.e. not using importance sampling).

However, in Section 4.3.1 it was noted that importance sampling methods based on snapshot mean or snapshot standard error require prior estimates of these quantities before importance sampling can be applied. Therefore, the results of these sections can be considered to be a pilot study, where it is assumed these quantities can be known accurately in advance in order to show the potential benefit of importance sampling if appropriate weights, $\boldsymbol{\omega}$, were already known accurately. For this pilot study, weights are calculated using 1000 initial evaluations of each snapshot. In practice, it would be very expensive and inefficient to first estimate importance sample weights using 1000 full simulator evaluations, so Sections 4.4.1 and 4.4.2 will go on to consider applications of importance sampling which use a small number of initial full simulations to estimate weights.

It is possible that no constraint costs are expected to occur in a given snapshot (i.e. the mean constraint costs of a snapshot are zero), which would result in ω_τ for the snapshot being calculated as 0 via Equation 4.3.1. However, Equation 4.2.5 requires

ω_τ to be greater than zero to apply importance sampling. Therefore, a minimum value of ω_τ was set to 0.001.

Metric for Work Done

Naively, to compare the different importance sampling methods, it may be considered how many evaluations of Equation 4.2.5 are necessary to acquire an estimate of mean annual constraint costs to a given level of precision. However, Section 4.2.2 and Appendix A.1 indicate that this is a misleading metric as it does not account for the amount of snapshots actually evaluated (actual work done) to acquire the estimate. For example, 20 evaluations from importance sampling which evaluate on average 2000 snapshots actually expects to evaluate fewer snapshots than 3 simulations which evaluate each snapshot.

Therefore, λ, a metric which accounts for the amount of snapshots actually simulated, will be considered instead. λ is a measure of how many snapshots were actually evaluated in terms of the 17520 half hour snapshots in a single year. For example, suppose 3 yearly simulator runs using importance sampling are performed which evaluate 11000, 9950 and 11572 snapshots respectively. Then for these three evaluations the total work done is

$$\lambda = \frac{11000 + 9950 + 11572}{17520} = \frac{32522}{17520} = 1.856279 \text{ EFSE}$$

The unit used for λ in this thesis is equivalent full simulator evaluations (EFSE).

Precision of Estimates

Results of this section will consider how much work must be done to acquire an estimate of mean annual constraint costs with an accuracy of at least 1%. Suppose $\mathbf{c} = (c_1, ..., c_n)$ represents a vector of n estimates of annual constraint costs utilising importance sampling via Equation 4.2.5. An accuracy of one percent will be defined as when the ratio of the standard error of the estimate of annual constraint costs to the mean of the estimate of annual constraint costs is 0.01 or less. That is, if $\mu_{\mathbf{c}} = \frac{1}{n}\sum_{i=1}^{n} c_i$ and $s_{\mathbf{c}} = \frac{\sqrt{\frac{1}{n-1}\sum_{i=1}^{n}(c_i - \mu_{\mathbf{c}})^2}}{\sqrt{n}}$ an accuracy of 1% requires $\frac{s_{\mathbf{c}}}{\mu_{\mathbf{c}}}$ to be 0.01 or less.

However, for a year 6 power system background it was noted that mean annual constraint costs are £246,000,000. Therefore, an estimate where the standard error of the estimate is less than 1% of the mean of the estimate will expect to have a standard error of £2,460,000, which is very large in real terms. Therefore, an alternative criterion will also be considered where the standard error of the estimate, $s_{\mathbf{c}}$, must be less than £100,000. Whilst this may still seem quite high, £100,000 will later be defined in Section 5.1 as the equivalent cost of making a very small increase of 1 MW to transmission capacity [5, 78].

It is also important to recall that simulations of annual constraint costs acquired from importance sampling (and the average of many simulations) is still a random variable. Therefore, the amount of work required to reach a given level of accuracy will not be perfectly consistent if one were to repeat the process. For example, it could be that one estimate of mean annual constraint costs with an accuracy of 1% is acquired after the equivalent work of 53.24 full simulator evaluations. However, if the process was repeated for the same power system background, an estimate with an accuracy of 1% may take more or less work than the equivalent of 53.24 full simulator evaluations to acquire.

Therefore, this section will perform 200 separate repetitions of how much work is required for an accuracy of 1%. The mean amount of work required for an accuracy of 1% across these repetitions will be calculated to give an estimate of the expected work required to reach an estimate of mean annual constraint costs with an accuracy of 1%. Boxplots of the work required for all 200 repetitions will also be given to illustrate how even for a fixed importance sampling technique there will be variation in the amount of work required to acquire an estimate of given precision.

Accuracy of Estimates

As well as considering the work required to acquire an estimate of mean annual constraint costs, it is also important to give consideration to how the resulting estimates of mean annual constraint costs compare to the actual mean of the full simulator. This is considered in Section 4.3.6 with further details being given in Appendix A.2, which

compare the estimates that will be acquired in Sections 4.3.3 to 4.3.5 to highly accurate estimates of the simulator mean.

This is because whilst all estimates of mean annual constraint costs are unbiased (as Equation 4.2.6 verifies), it is possible that if too few simulator evaluations are used to acquire an estimate of constraint costs then the resulting estimate will typically differ quite substantially from the actual mean of the simulator. Therefore, the goal is not necessarily to minimise the expected work required to acquire an estimate of mean constraint costs, but to find a feasible balance between the work required to acquire an estimate of mean constraint costs and the accuracy one could expect in the resulting estimate.

4.3.3 Initial Application of Importance Sampling Results

Importance Sample Basis	Year 6 Results	Year 1 Results
All Snapshots	4.595 EFSE	442.1 EFSE
Snapshot Demand	4.356 EFSE	283.3 EFSE
Snapshot Standard Error	4.197 EFSE	30.88 EFSE
Snapshot Mean	4.119 EFSE	28.29 EFSE

Table 4.2: Table showing how the amount of work done (λ, in terms of equivalent full simulator evaluations) to estimate mean annual constraint costs to an accuracy of 1% varies with the basis used for importance sampling weights.

Table 4.2 gives details of the expected value of λ (i.e. expected work done expressed as an equivalent number of full simulator evaluations) to acquire an estimate of mean annual constraint costs with an accuracy of 1%. It can be seen that when not using importance sampling (i.e. evaluating each snapshot) around 100 times more snapshot evaluations are required for a year 1 power system background in comparison to a year 6 power system background. For both power system backgrounds, using importance sampling with weights, $\boldsymbol{\omega}$, based on the mean snapshot constraint costs yields the best results.

For a year 6 system background this improvement is small, as all methods (including evaluating all snapshots) require less than the work of 5 equivalent full simulator evaluations on average. For a year 1 system background, however, importance sampling

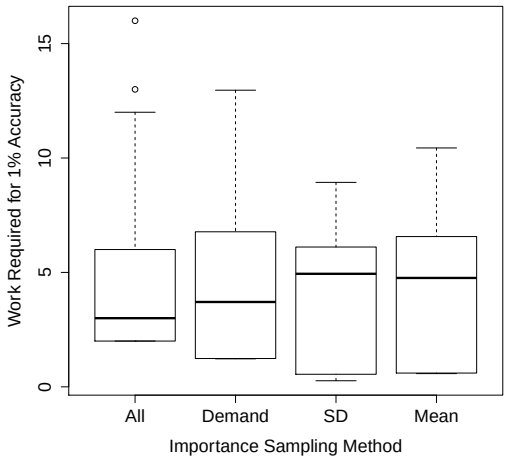

(a) Year 6 power system background.

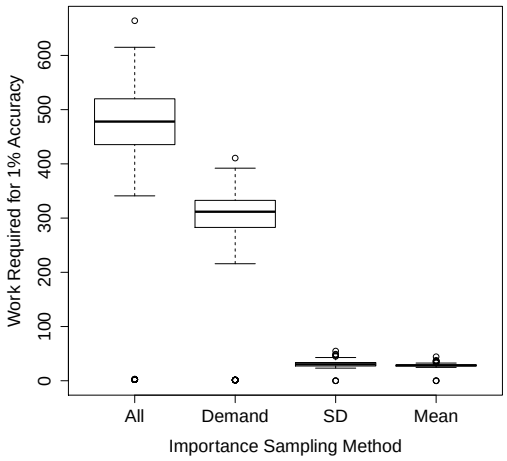

(b) Year 1 power system background.

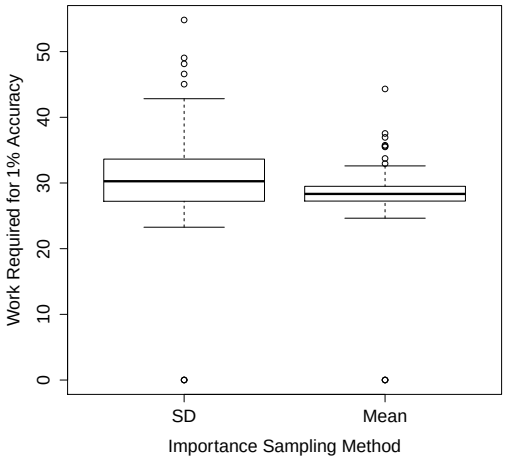

(c) Year 1 power system background.

Figure 4.4: Boxplots to illustrate the variation of work done (λ, in terms of equivalent full simulator evaluations) to reach an estimate of mean annual constraint costs to an accuracy of 1% for a variety of choices of importance sampling weights.

has great benefits. Using importance sampling with weights based on the demand of the snapshot decreases the expected work done to acquire an estimate of mean annual constraint costs by 36%. An even greater reduction in the expected work done is achieved by basing the importance sample weights on the standard deviation or mean of constraint costs of the snapshots, with both methods giving reductions of over 93%, with the weights based on snapshot mean resulting in marginally better results.

Figure 4.4 helps illustrate these results, by providing boxplots of the amount work done to reach an error of less than 1% for each of the 200 repetitions of each condition. For a year 6 power system background, displayed in Figure 4.4 (a), it is again illustrated that the use of importance sampling has little effect, with all boxplots being quite similar. However, it is worth noting that the boxplots display shorter tails for importance sampling methods with weights based on snapshot standard deviation or mean of constraint costs, indicating these methods reduce the frequency of which it takes substantially longer than average to acquire an accuracy of 1% in the estimate.

Figure 4.4 (b) displays results for a year 1 power system background, which illustrates the great benefits from using importance sampling with weights based on snapshot standard deviation or mean. Due to the great improvement in the results, the boxplots using these two importance sampling methods are difficult to visualise in Figure 4.4 (b), so Figure 4.4 (c) was constructed to give a clear illustration of the boxplots for these two conditions.

The boxplots of Figure 4.4 also raise a point of concern. It can be seen (much more clearly for a year 1 power system background) that there are several occurrences of estimates with an error of less than 1% being acquired for very small values of λ (i.e. evaluating very few snapshots in total), whilst the vast majority of estimates of mean annual constraint costs are acquired for much greater values of λ (i.e. evaluating a much greater number of snapshots in total).

To show where this problem arises, Figure 4.5 illustrates how the error of the estimate varies with work done for one repetition for an estimate of mean annual constraint costs for a year 6 power system background which uses the mean constraint costs of each snapshot as the basis for importance sampling weights. It can be seen that after a small amount of work has been done, the standard error of the estimate is less than

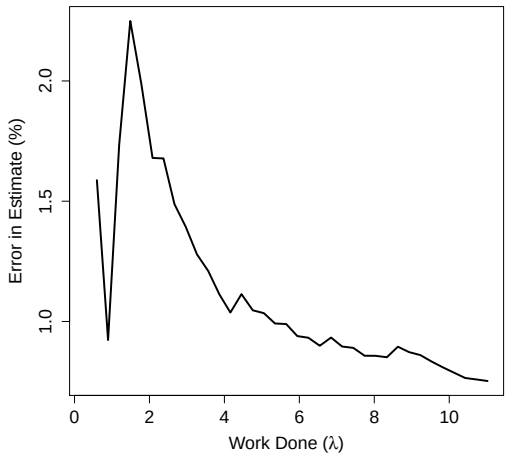

Figure 4.5: Plot to illustrate how error in the estimated response varies with work done for one particular repetition of a year 6 power system background, using mean snapshot constraint costs as the basis of importance sampling weights.

1% of the mean of the estimate. However, the error soon rises above 2%, and further work is required before the error in the estimate drops below 1% again.

This shows how when a small amount of work has been done, if the simulations happen to give similar estimates of annual constraint costs (even if they differ greatly from a very accurate estimate of the simulator mean) the standard error of the sample will be small in comparison to the mean of the sample. This could potentially give misleading results, and further evaluations would give a more accurate estimate of mean annual constraint costs. This implies it may be wise to impose some minimum amount of work to be done before an estimate is accepted, to avoid misleading results from a small sample. Further consideration to the accuracy of the estimates of mean constraint costs is given in Section 4.3.6 and Appendix A.2.

Importance Sample Basis	Year 6 Results	Year 1 Results
All Snapshots	10.16 EFSE	479.9 EFSE
Snapshot Demand	10.59 EFSE	317.2 EFSE
Snapshot Standard Error	10.09 EFSE	31.12 EFSE
Snapshot Mean	10.14 EFSE	28.82 EFSE

Table 4.3: Table showing how the amount of work done (λ, in terms of equivalent full simulator evaluations) to estimate mean annual constraint costs to an accuracy of 1% varies with the basis used for importance sampling weights, when setting a minimum work of 10 EFSE to be done.

Table 4.3 gives details of the expected work done to reach an accuracy of 1%, when a minimum work of 10 EFSE is set. It can be seen that all methods for estimating constraint costs for a year 6 power system background give estimates just above 10 EFSE. This is to be expected, as Figure 4.4 shows the work required is usually below the minimum bound of 10 EFSE.

For a year 1 power system background, there is actually very little increase in expected work done for an importance sampling method based on snapshot mean or standard deviation, indicating that these methods are less susceptible to giving false estimates of accuracy. However, when performing full yearly evaluations or using an importance sampling method based on snapshot demand level, an increase in expected work of 37 and 34 equivalent full simulator evaluations respectively is noted. This indicates that previously a lot of estimates of constraint costs may have been falsely accepted, and when it is imposed that estimates must also have performed a certain amount of work, as well as the standard error of the estimate being less than 1% of the mean of the estimate, more work is required on average to acquire an estimate of mean annual constraint costs.

4.3.4 Using a Poor Estimate of Importance Sampling Weights

Section 4.3.2 noted that for this pilot study, it was assumed that importance sampling weights based on the mean constraint costs or standard deviation of constraint costs in a snapshot could be known accurately in advance, with 1000 full simulator evaluations used to calculate such weights. However, for a general problem it may be inefficient to take such a large number of full simulator evaluations before applying importance sampling.

One possible solution could be to use a small number of full simulations to estimate importance sample weights for use in subsequent simulator evaluations, as will be considered in Section 4.4. Alternatively, importance sampling weights could be calculated based off one particular power system background, then used in all future power system problems. For good results, this would require the weights to be somewhat similar for all power system backgrounds.

What has already been presented in this chapter would suggest this is not the case. For example, Figure 4.3 of Section 4.1.3 shows how the distribution of mean constraint costs by day differs greatly between a year 1 and year 6 power system background. Further, when the weights for the importance sample are based on the mean snapshot constraint costs for a year 1 power system background, it is expected that 74.68 (0.427% of the total 17520) snapshots will be used in each yearly evaluation. However, when the weights for the importance sample are based on the mean snapshot constraint costs for a year 6 power system background, it is expected that 5220 (29.8% of the total 17520) snapshots will be evaluated. This difference implies that the two different sets of weights will give very different levels of consistencies in the resulting estimates.

Importance Sample Basis	Year 6 Results	Year 1 Results
All Snapshots	4.595 EFSE	442.1 EFSE
Snapshot Demand	4.356 EFSE	283.3 EFSE
Snapshot Standard Error of Alternative Power System Background	9.499 EFSE	275.6 EFSE
Snapshot Mean of Alternative Power System Background	11.93 EFSE	288.0 EFSE

Table 4.4: Table showing how the amount of work done (λ, in terms of equivalent full simulator evaluations) to estimate mean annual constraint costs to an accuracy of 1% varies with the basis used for importance sampling weights.

Table 4.4 gives results of the expected work required to acquire an estimate of mean annual constraint costs with less than 1% error when using weights calculated for a year 6 power system background in year 1 and using weights calculated for a year 1 power system background in year 6. As the same LDC is assumed for both power system backgrounds, results using snapshot demand as the basis of the weights are the same as in Table 4.2.

For both power system backgrounds, it is seen that using a poor selection for the weights yields poor results. For the year 6 power system background, the expected work required to acquire an estimate of mean annual constraint costs with an error of less than 1% more than doubles (though still less than 12 equivalent full simulator evaluations is expected to acquire an estimate of mean annual constraint costs). For a year 1 power system background, when using weights calculated from a year 6 power system background it can be seen that the expected work required increases by a factor

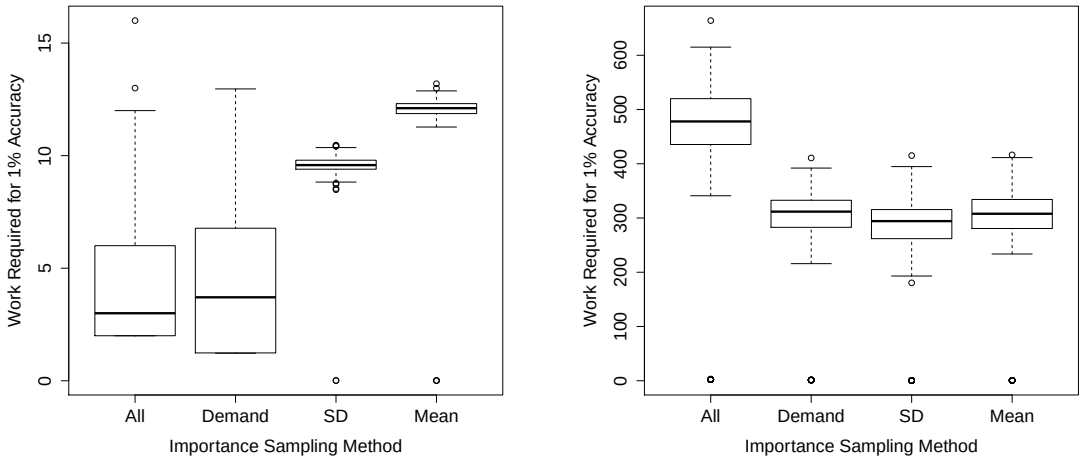

(a) Year 6 power system background.

(b) Year 1 power system background.

Figure 4.6: Boxplots to illustrate the variation of work done (λ, in terms of equivalent full simulator evaluations) to reach an estimate of mean annual constraint costs to an accuracy of 1% for a variety of choices of importance sampling weights.

of 8.9 and 10.2 when using importance sampling weights based on snapshot mean and snapshot standard error respectively.

This is evidence that it is insufficient to simply estimate weights for importance sampling based off a single power system background and expect good results when applying them to any problem to be considered. However, it is also noted that for a year 1 system background, even using weights calculated for a year 6 power system background gave an improvement in the expected amount of work required for an estimate of mean annual constraint costs with an error of less than 1% in comparison to evaluating every snapshot, though using these weights would still expect for 8.9 times as many snapshots to be evaluated in comparison to using importance sampling weights calculated using a year 1 system background.

Again, there is the potential that estimates could be misleading if a small number of initial samples give similar estimates. Table 4.5 gives results when a minimum amount of work of 10 EFSE is imposed before an estimate of mean annual constraint costs can be accepted.

Importance Sample Basis	Year 6 Results	Year 1 Results
All Snapshots	10.16 EFSE	479.9 EFSE
Snapshot Demand	10.59 EFSE	317.2 EFSE
Snapshot Standard Error of Alternative Power System Background	10.13 EFSE	293.8 EFSE
Snapshot Mean of Alternative Power System Background	12.11 EFSE	311.8 EFSE

Table 4.5: Table showing how the amount of work done (λ, in terms of equivalent full simulator evaluations) to estimate mean annual constraint costs to an accuracy of 1% varies with the basis used for importance sampling weights, when setting a minimum of work of 10 EFSE to be done.

4.3.5 Estimating Mean Annual Constraint Costs with a Standard Error Less than £100,000

The previous 2 subsections considered how much work, λ, was expected to acquire an estimate of mean annual constraint costs such that the standard error of the estimate was less than 1% of the mean of the estimate. This results in estimates of mean annual constraint costs with a standard error which is small relative to the estimate itself. However, Table 4.1 of Section 4.1.1 shows that the mean annual constraint costs for a year 6 power system background are £246,000,000, which in turn means that an estimate with an error of 1% will still have a standard error of around £2,460,000, which is far from a negligible cost in real terms.

Importance Sample Basis	Year 6 Results	Year 1 Results
All Snapshots	3534 EFSE	778.0 EFSE
Snapshot Demand	3846 EFSE	508.1 EFSE
Snapshot Standard Error	3462 EFSE	51.25 EFSE
Snapshot Mean	3363 EFSE	45.93 EFSE

Table 4.6: Table showing how the amount of work (λ, in terms of equivalent full simulator evaluations) required to estimate mean annual constraint costs with a standard error less than £100,000 varies with the basis used for importance sampling weights.

Therefore, it may be desirable to acquire an estimate with a standard error smaller than some specified value. Table 4.6 displays the expected amount of work, λ, required to estimate mean annual constraint costs such that the standard error of the estimate is less than £100,000 and that the work of at least 10 equivalent full simulator evaluations

has been done. As was noted, this value is selected as this is the equivalent cost of making a very small (1 MW) increase to transmission capacity [5, 78]. Again, each of the values in the table is the average value of λ from 200 repetitions, as each yearly simulator evaluation of constraint costs is random and therefore the amount of work required to acquire an estimate to a given level of precision is also random.

For a year 1 power system background, results are similar to what was observed in Section 4.3.3, where a large amount of work is expected (the work of 778 equivalent full simulator evaluations) when evaluating each snapshot. This is reduced slightly to the equivalent work of over 508 full simulator evaluations when using an importance sample with weights based on snapshot demand. The expected work required is reduced by over 93% when using importance sampling methods based on snapshot mean or standard error. For a year 1 system background, the values in Table 4.6 are approximately 60% larger than those in Table 4.3 for all importance sampling methods.

The similarities of results in comparison to those of Section 4.3.3 are what may have been expected based on Table 4.1, which states that the mean annual constraint costs for a year 1 power system background are £12,600,000. This means that in Section 4.3.3, which considered estimating mean annual constraint costs such that that the standard error of the estimate is less than 1% of the mean of the estimate, it is expected that the standard error will be around £126,000. This is only 26% greater in comparison to acquiring an estimate such that the standard error is less than £100,000, as is considered in this subsection.

For a year 6 power system background, however, mean annual constraint costs are much greater, at £246,000,000 as detailed in Table 4.1. This means that the standard error of an estimate with an accuracy of 1% will be around £2,460,000. Therefore, to acquire an estimate of mean annual constraint costs such that the standard error of the estimate is less than £100,000 requires a much greater amount of work in comparison. This can be seen in Table 4.6, where the expected amount of work, λ, required is now greater than 3360 equivalent full simulator evaluations for any choice of importance sample weights. This is over 750 times greater in comparison to the values of Table 4.2 which consider how much work is expected to acquire an estimate of mean constraint costs such that the standard error of the estimate is less than 1% of the estimate mean.

When requiring the standard error of the estimate to be less than 1% of the mean of the estimate, Table 4.2 showed that the choice of weights for importance sampling made very little difference to the expected work required to acquire an estimate of mean annual constraint costs for a year 6 power system background. Table 4.6 shows that this is also the case when estimating such that the standard error of the estimate is less than £100,000, with importance sampling using weights based on the standard deviation or mean of snapshot constraint costs resulting in quite small decreases of 2.0% and 4.8% of the expected value of λ (work done) respectively in comparison to not using importance sampling (evaluating all snapshots).

However, using importance sampling with snapshot weights based on the demand level of each snapshot actually increases the expected work done by 8.8%. This can be explained by comparing Figure 4.2 (b), which displays how mean daily demand varies throughout the year, to Figure 4.3 (b), which displays how the mean constraint costs of each day vary throughout the year for a year 6 power system background. As can be seen, it appears that the seasonal effect has a much greater effect than that of demand on mean constraint costs. Further, throughout summer months it does not appear as if mean daily demand and mean daily constraint costs positively correlate. This indicates that for a year 6 power system background, using snapshot weights, $\boldsymbol{\omega}$, for importance sampling which are proportional to the demand level of each snapshot will yield poor results.

It is noted that whilst requiring standard error of the estimate to be less than £100,000 does result in a substantial increase in the expected work required to acquire the estimate, it would be possible to consider alternative criteria which are more strict than requiring the standard error of the estimate to be less than 1% of the mean of the estimate, in order to find a feasible balance between the accuracy of the estimate and the amount of work required to acquire the estimate. For example, estimates which require the error of the estimate to be less than 0.5%, 0.25% or 0.1% of the mean of the estimate can be acquired with the equivalent of approximately 21, 90 or 577 full simulator evaluations respectively, which represent more feasible balances between the accuracy of the estimate and the work required to acquire the estimate.

Figure 4.7 displays boxplots for how much work, λ, was required to acquire an estimate

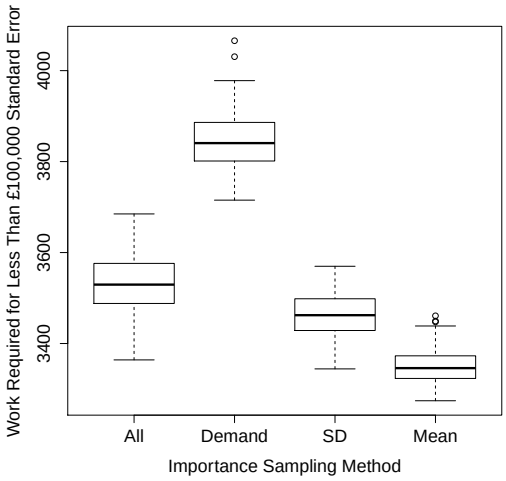

(a) Year 6 power system background.

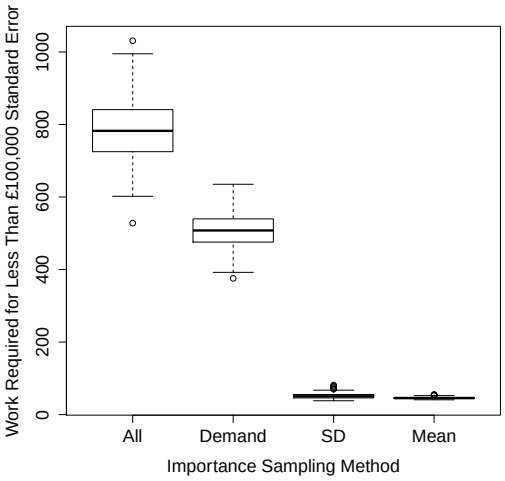

(b) Year 1 power system background.

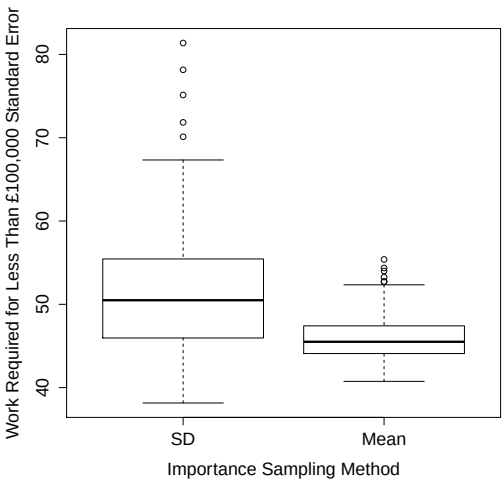

(c) Year 1 power system background.

Figure 4.7: Boxplots to illustrate the variation of work done (λ, in terms of equivalent full simulator evaluations) to reach an estimate of mean annual constraint costs with an error less than £100,000 for a variety of choices of importance sampling weights.

of mean constraint annual costs with a standard error of less than £100,000 for each of the repetitions. For a year 1 power system background, things are very similar to what was illustrated in Figure 4.4, where all repetitions using an importance sampling method based on the standard deviation or mean of snapshot constraint costs required substantially less work to acquire an estimate of mean constraint costs in comparison to when basing the importance sample weights on demand or evaluating each snapshot. Therefore, Figure 4.7 (c) allows for a more accurate comparison of boxplots for when importance sampling weights were based on the standard deviation of snapshot or mean constraint costs of snapshot. As can be seen, not only is the median value of λ lower when basing the importance sample weights on the mean of each snapshot, but the range of values of λ is also smaller, indicating that the number of equivalent full simulator evaluations required to acquire an estimate of mean annual constraint costs with an error of less than £100,000 is also more consistent.

Figure 4.7 (a), which considers boxplots for a year 6 power system background, illustrates how all estimates which use importance sample weights based on snapshot demand level resulted in a greater value of λ than the highest value of λ for any other choice of weights considered, giving further evidence to how poor a choice of weights this is for a year 6 power system background.

4.3.6 Accuracy of Estimates From Importance Sampling

In addition to considering how much work, λ, is required to acquire an estimate of mean annual constraint costs to a given level of precision, it is also important to consider how accurate these estimates are in comparison to the "true" mean of the full simulator. Equation 4.2.6 of Section 4.2.2 shows that estimates of mean constraint costs when applying importance sampling are unbiased, i.e. they have the same expectation as using the full simulator. Further, as many evaluations of Equation 4.2.5 are being averaged for each repetition, and each yearly simulator evaluation is conditionally independent and identically distributed, this means that the estimates of mean constraint costs should form a normal distribution around the mean of the full simulator by the central limit theorem.

However, as the output of the simulator each time the simulator is run is random,

each estimate of mean annual constraint costs will differ from the "true" mean of the simulator. Whilst a Bayesian approach to modelling may reject the concept of a "true" mean of annual constraint costs of a power system in reality, the simulator itself does have a true mean, in the sense that for each snapshot a probabilistic expectation of constraint costs which arise from all possible permutations of generator availabilities could theoretically be calculated, with the process repeated and a sum taken across all snapshots. However, this calculation would be extremely expensive, and infeasible for the resources available to us in this thesis.

An estimate of mean annual constraint costs for a given power system background can be calculated to a high degree of accuracy by taking a very large number of full simulations and calculating the average value of all the simulator evaluations. Table 4.7 details such estimates of mean annual constraint costs for year 1 and year 6 power system backgrounds by calculating the average of 100,000 such full yearly evaluations of the simulator (i.e. 1,752,000,000 snapshots evaluated in total). Error in the estimate of mean annual constraint costs for a year 1 power system background has been reduced to just £8,862 (0.0699% of the estimated mean) whereas error in the estimate of mean annual constraint costs for a year 6 power system background has been reduced to just £18,806 (0.00765% of the estimated mean).

Power System Background	Year 1	Year 6
Estimate of Mean Annual Constraint Costs	£12,673,885	£245,706,816
Standard Error of Estimate	£8,862	£18,806
Standard Error as a Percentage of Mean	0.0699%	0.00765%

Table 4.7: Table detailing accurate estimates of mean annual constraint costs for a year 1 and year 6 power system background.

Consideration will be given to how the estimates of mean annual constraint costs when using importance sampling compare to $\hat{\mu}_1$ and $\hat{\mu}_6$, the highly accurate estimate of mean annual constraint costs for a year 1 and year 6 power system background respectively from Table 4.7. In this section results will be presented for a year 6 power system background when importance sampling weights are based on the mean constraint costs of each snapshot. Further details on the accuracy of estimated constraint costs for other choices of importance sampling weights for both a year 1 and year 6 power

system background are given in Appendix A.2.

Accuracy of Estimates with a Standard Error Less Than 1% of the Mean of the Estimate

Figure 4.8 displays graphs to show how 200 estimates of mean annual constraint costs vary for a year 6 power system background. These are the costs estimated in Section 4.3.3, where it was required that the standard error of the estimate was less than 1% of the mean of the estimate, and that a minimum of 175200 snapshots (the equivalent of 10 full simulator evaluations) had been evaluated. As noted in the previous sub-subsection, the importance sampling weights used when acquiring these estimates were based on the mean constraint costs of each snapshot.

Figure 4.8 (a) shows a scatter plot for the final estimate of mean annual constraint costs for each of the 200 repetitions, with a horizontal line also shown to represent $\hat{\mu}_6$. As can be seen, estimates are fairly evenly scattered around $\hat{\mu}_6$ with costs being over-estimated as often as they are under-estimated.

The normal quantile plot of Figure 4.8 (d) shows that the estimates approximately follow a normal distribution. As mentioned, this is what should be expected by the central limit theorem, as simulations of annual constraint costs using importance sampling via Equation 4.2.5 are conditionally independent and identically distributed, with an expectation equal to the expected annual constraint costs from the full simulator. Therefore, when using multiple simulations to estimate mean annual constraint costs, the estimates of mean annual constraint costs form a normal distribution centred around the mean of the simulator.

Figure 4.8 (b) shows the difference between the estimates of mean annual constraint costs and $\hat{\mu}_6$ ($\hat{\mu}_6$ minus the estimate of mean annual constraint costs acquired from importance sampling), with Figure 4.8 (c) showing this difference as a percentage of $\hat{\mu}_6$. As can be seen, all estimates lie within +/-2.21% of $\hat{\mu}_6$, with 99% of estimates lying within 2% of $\hat{\mu}_6$ and 78% lying within 1% of $\hat{\mu}_6$. These differences are smaller than what may have been expected for a normal distribution with an error of 1% of $\hat{\mu}_6$. The reason for this is the estimates displayed in Figure 4.8 required that a minimum level of work of the equivalent of 10 full simulator evaluations had been performed.

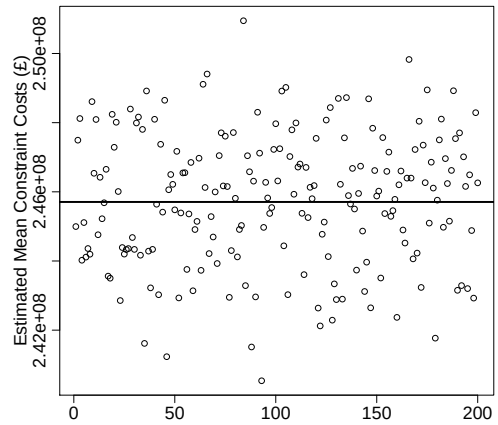

(a) Scatter plot of cost estimates.

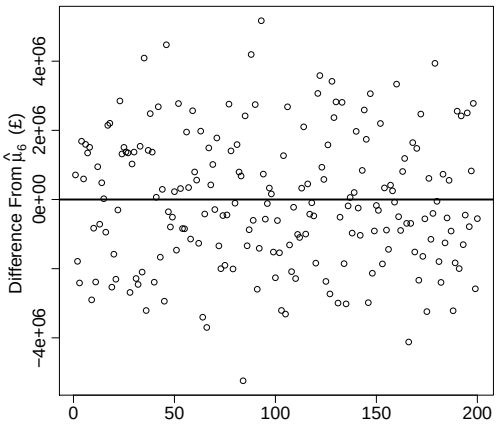

(b) Scatter plot of differences from $\hat{\mu}_6$.

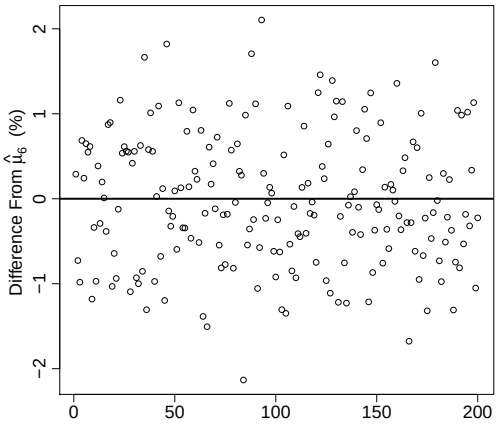

(c) Scatter plot of relative differences from $\hat{\mu}_6$.

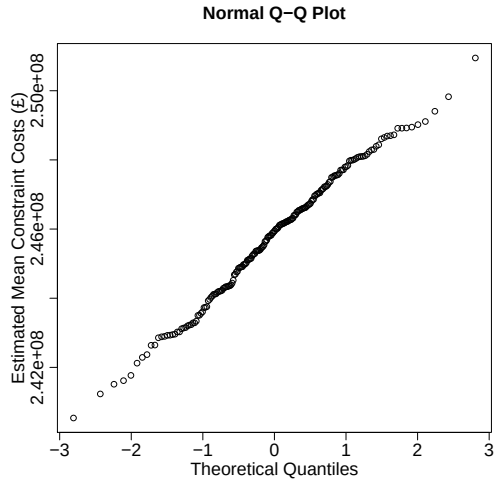

(d) Normal QQ plot.

Figure 4.8: Plots to compare estimates of mean annual constraint costs from importance sampling to $\hat{\mu}_6$ for a year 6 power system background, when it is required that the standard error of the estimate is less than 1% of the mean of the estimate.

However, in Section 4.3.3 it is shown how for a year 6 power system background an estimate with an error less than 1% typically requires fewer than 10 EFSE, meaning additional information is acquired which improves the accuracy of the estimate even further.

Importance Sample Basis	Mean Difference	Mean Absolute Difference	Mean Percentage Difference	Mean Absolute Percentage difference
All Snapshots	£122,000	£1,540,000	0.0496 %	0.626%
Demand	£133,000	£1,620,000	0.0540%	0.659%
Snapshot Mean	£58,400	£1,570,000	0.0238%	0.639%
Snapshot Standard Deviation	- £39,300	£1,370,000	-0.0160%	0.564%

Table 4.8: Table comparing estimated mean annual constraint costs from importance sampling to $\hat{\mu}_6$ for a year 6 power system background, when it is required that the standard error of the estimate is less than 1% of the mean of the estimate.

Table 4.8 gives a comparison of the estimates of mean annual constraint costs from importance sampling to $\hat{\mu}_6$, with consideration given to all choices of importance sampling weights. As can be seen, the largest difference between $\hat{\mu}_6$ and the average of all 200 estimates from an importance sampling condition is £133,000 (which is a difference of just 0.054% of $\hat{\mu}_6$) when basing the importance sampling weights on the demand of each snapshot. It is to be expected that the relative difference (i.e. difference as a percentage of $\hat{\mu}_6$) is small as Equation 4.2.6 shows each estimate is unbiased so the expectation of all estimates of mean annual constraint costs is the same as the mean of the full simulator, which $\hat{\mu}_6$ is a very accurate estimate of.

It is also useful to consider the mean absolute difference of the estimates from $\hat{\mu}_6$, to consider how much an estimate of mean constraint costs will typically differ from the true mean of the simulator by. Table 4.8 shows how the mean absolute difference of an estimate from $\hat{\mu}_6$ is between £1,370,000 and £1,620,000. As $\hat{\mu}_6$ is over £245,000,000 such differences are still less than 0.66% of $\hat{\mu}_6$. However, a difference of £1,620,000 is a large amount of money, which is why Section 4.3.5 considered the stricter criterion of estimating mean annual constraint costs such that the standard error of the estimate is less than £100,000, and the resulting cost estimates from such a method are considered

in the next sub-subsection.

Accuracy of Estimates With a Standard Error Less Than £100,000

Graphs to illustrate how 200 estimates of mean annual constraint costs vary for a year 6 power system background (when basing importance sampling weights on the mean constraint costs of each snapshot) are displayed in Figure 4.9. These are the 200 estimates acquired in Section 4.3.5, where it was required that the standard error of the estimate is less than £100,000, and that a minimum level of work of at least 10 equivalent full simulator evaluations had been performed.

A scatter plot of the 200 estimates of mean constraint costs is illustrated in Figure 4.9 (a), with a horizontal line also shown to represent $\hat{\mu}_6$. Figure 4.9 (b) shows the difference between these estimates and $\hat{\mu}_6$, with Figure 4.9 (c) showing this difference as a percentage of $\hat{\mu}_6$. As can be seen, the vast majority of estimates vary from $\hat{\mu}_6$ by less than £200,000, which is less than 0.1% of $\hat{\mu}_6$ (and all estimates vary from $\hat{\mu}_6$ by less than £300,000). Estimates appear to over-estimate costs as often as they are under-estimated, with a fairly even scatter around $\hat{\mu}_6$.

These results can be contrasted with the corresponding plot of Figure 4.8 of the previous sub-subsection, where estimates were acquired such that the standard error of the estimate was less than 1% of the mean of the estimate, where estimates typically differed from $\hat{\mu}_6$ by up to 2% (an increase by a factor of 20). This is due to the mean annual constraint costs being greater than £245,000,000 for a year 6 power system background. Therefore, an estimate with a standard error of 1% of the mean will expect to have a standard error of around £2,450,000, which is 24.5 times greater than the £100,000 used for the estimates displayed in Figure 4.9. This shows how the accuracy of estimates of mean annual constraint costs has been greatly improved by the stricter convergence required for the estimate.

The normal quantile plot illustrated in Figure 4.9 (d) shows that the estimates of mean annual constraint costs approximately follow a normal distribution, which again is what would be expected by the central limit theorem.

Table 4.9 gives further evidence that the resulting estimates of mean annual constraint costs are very accurate when it is required that the standard error of the estimate is

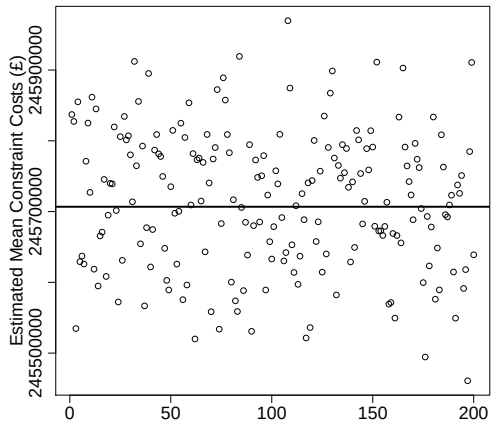

(a) Scatter plot of cost estimates.

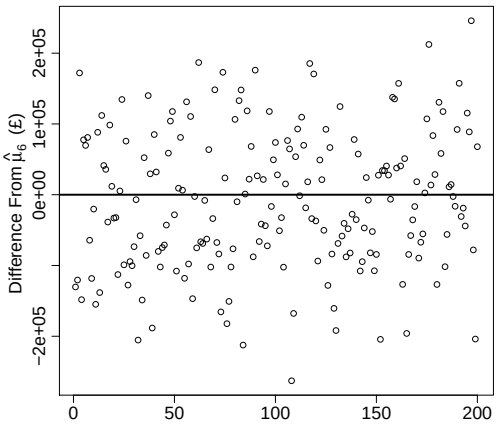

(b) Scatter plot of differences from $\hat{\mu}_6$.

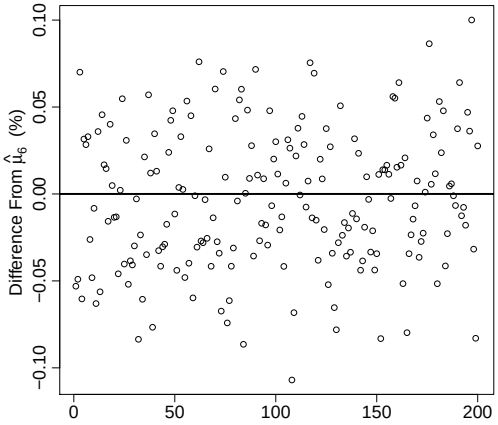

(c) Scatter plot of relative differences from $\hat{\mu}_6$.

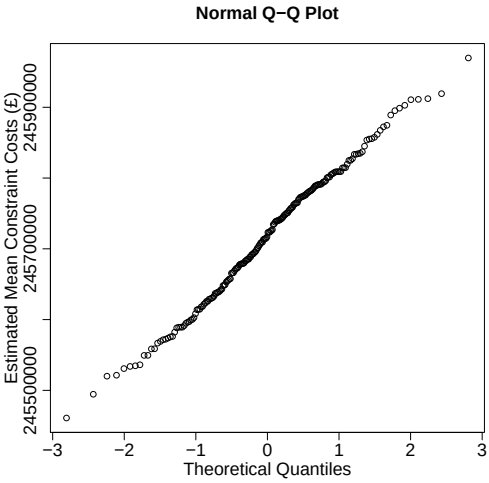

(d) Normal QQ plot.

Figure 4.9: Plots to compare estimates of mean annual constraint costs from importance sampling to $\hat{\mu}_6$ for a year 6 power system background, when it is required that the standard error of the estimate is less than £100,000.

Importance Sample Basis	Mean Difference	Mean Absolute Difference	Mean Percentage Difference	Mean Absolute Percentage difference
All Snapshots	-£6,900	£77,700	-0.00281 %	0.0316%
Demand	£2,500	£83,200	0.00104%	0.0339%
Snapshot Mean	-£17,300	£81,700	-0.00702%	0.0332%
Snapshot Standard Deviation	-£14,700	£72,800	-0.00598%	0.0296%

Table 4.9: Table comparing estimated mean annual constraint costs from importance sampling to $\hat{\mu}_6$ for a year 6 power system background, when it is required that the standard error of the estimate is less than £100,000.

less than £100,000, with the mean difference between the estimates of mean annual constraint costs and $\hat{\mu}_6$ being less than 0.008% for all importance sampling methods, and the mean absolute difference being less than 0.034%.

This table contrasts greatly with Table 4.8, the equivalent table when estimating mean annual constraint costs such that the standard error of the estimate is less than 1% of the mean of the estimate, where the mean absolute differences are more than 18 times larger for all importance sampling methods. Again, this is due to the estimates considered in Table 4.8 having an expected error of around £2,450,000 in comparison to the error of £100,000 of the estimates considered in Table 4.9.

However, it should also be considered that in Section 4.3.5 it was shown that estimates with a standard error less than £100,000 require over 330 times more simulator evaluations in comparison to estimates where it is required the standard error of the estimate is less than 1% of the estimate. This means that despite the improvement in the accuracy of the estimates of mean annual constraint costs demonstrated in this subsection, it is infeasible to take many such evaluations in practice for the resources available to us in this thesis. However, for an organisation such as National Grid it may be plausible and of benefit to perform such calculations.

For the resources available to us it would, however, still be possible to reduce the error in the estimate for a year 6 power system background below the 1% of the mean of the estimate considered in Section 4.3.3. For example, an estimate can be acquired where

the standard error of the estimate is less than 0.5%, 0.25% or 0.1% of the mean of the estimate when expecting to do the work of just 21, 90 or 577 EFSE respectively.

Further Results

This section has given some consideration to how the estimates of mean annual constraint costs for a year 6 power system background from Sections 4.3.3 and 4.3.5 compare to the "true" mean of the full simulator when using importance sampling with weights, $\boldsymbol{\omega}$, based on the mean constraint costs of each snapshot. Further thought to the accuracy of estimates for both a year 1 and year 6 power system background for all choices of importance sampling weights is given in Appendix A.2.

As a brief overview, for a year 6 power system background, results are very similar to what has been presented in this section regardless of the choice of importance sample weights, in that although estimates are quite accurate (almost always within 2% of the very accurate estimate, $\hat{\mu}_6$) when estimating such that the standard error of the estimate is less than 1% of the mean of the estimate, the accuracy is greatly improved (by around a factor of 20) when using the stricter convergence criteria of requiring the standard error of the estimate to be less than £100,000.

For a year 1 power system, however, less improvement is observed when estimating mean constraint costs such that the standard error of the estimate is less than £100,000 in comparison to 1% of the mean. The reason for this is 1% of the mean annual constraint costs for a year 1 power system is £126,000, so there is relatively little benefit in reducing the standard error of the estimate to less than £100,000 in comparison to a year 6 power system background, where the stricter convergence criteria would reduce the standard error of the estimate by more than a factor of 20.

4.3.7 Why Importance Sampling Has Relatively Little Benefit for a Year 6 Power System Background

In Sections 4.3.3 and 4.3.5 it was shown that when estimating mean annual constraint costs for a year 1 power system background to a given level of precision, basing the

importance sampling weights on the mean constraint costs in each snapshots can substantially reduce the amount of work required to reach a given level of precision in the estimate. However, it was also shown that for a year 6 power system background there was relatively little benefit from an application of importance sampling in comparison to using full simulator evaluations, with the best results being a 4.8% reduction in EFSE when basing importance sampling weights on the mean constraint costs of each snapshot.

As Section 4.2.2 and Appendix A.1 showed that basing importance sampling weights on the mean constraint costs of each snapshot minimises the variance of the resulting estimate (when evaluating an equivalent number of snapshots) it may have been expected that a greater reduction in the expected work required would have been observed for a year 6 power system background.

However, it is important to consider that just because a certain selection of weights minimises the variance of an estimate, it does not necessarily mean that the variance of the estimate is substantially reduced in comparison to simply evaluating every snapshot. To illustrate this, 1000 further full simulator evaluations (i.e. evaluating each snapshot) were taken. Then, these simulations were used to acquire an estimate of how the variance varies depending on whether or not importance sampling was used. In Section 4.2.2 it was noted that applying importance sampling using Equation 4.2.5 results in an increase in the variance of evaluations of annual constraint costs for all choices of importance sampling weights, $\boldsymbol{\omega}$, as the work required to acquire an estimate of annual constraint costs is not accounted for and instead the alternative importance sampling methodology detailed in Section 4.2.1 must be used to compare variance estimates when an equivalent amount of work (number of snapshots) have been evaluated.

Using the alternative importance sampling method outlined in Section 4.2.1, Appendix A.1 states that the variance of a particular choice of importance sampling weights can be calculated as

$$\sigma^2_{q(\tau)} = E_{q(\tau)}\left[\left(\frac{f_{c,\mathscr{T}}(\tau)p(\tau)}{q(\tau)} - \mu\right)^2\right] \tag{4.3.2}$$

where $f_{c,\mathscr{T}}(\tau)$ was defined in Equation 4.2.7 as an estimate of annual constraint costs based on a single simulation of snapshot τ; $p(\tau)$ is the probability mass function used

when treating the snapshot, τ, as if it were a random variable (defined in Section 4.2.2 as $\frac{1}{17520}$ for all snapshots) and $q(\tau)$ is the alternative density used to sample values of τ to simulate, with Equation 4.2.9 defining an equivalent $q(\tau)$ for given values of ω_τ as

$$q(\tau) = \frac{\omega_\tau}{\sum_\tau \omega_\tau}$$

The variance detailed in Equation 4.3.2 can be estimated using the additional 1000 full simulations as

$$\hat{s}^2_{q(\tau)} = \frac{1}{1000} \sum_{i=1}^{1000} \sum_{\tau=1}^{17520} q(\tau) \left(\frac{f_{c,\mathscr{T},i}(\tau) p(\tau)}{q(\tau)} - \hat{\mu} \right)^2 \tag{4.3.3}$$

where $f_{c,\mathscr{T},i}(\tau)$ is the ith simulated value of $f_{c,\mathscr{T}}(\tau)$ for snapshot τ and $\hat{\mu}$ is the mean value of $f_{c,\mathscr{T},i}(\tau)$ across all 17520 snapshots and 1000 repetitions.

	Year 6 Results	Year 1 Results
Estimate of variance when evaluating each snapshot (call this $\hat{s}^2_{p(\tau)}$)	6.37×10^{17}	1.31×10^{17}
Estimate of variance when using importance sampling with weights based on snapshot mean (call this $\hat{s}^2_{q(\tau)}$)	6.02×10^{17}	8.27×10^{15}
$\frac{\hat{s}^2_{q(\tau)}}{\hat{s}^2_{p(\tau)}}$	0.945	0.063

Table 4.10: Table detailing how variance estimates vary depending whether or not importance sampling is used.

Table 4.10 details how the estimate of the variance from Equation 4.3.3 varies depending on whether or not importance sampling is used (with importance sample weights based on snapshot mean constraint costs). As can be seen, for a year 1 power system background the variance of the estimate is reduced by 93.7% when using importance sampling with weights based on the mean constraint costs of each snapshot in comparison to not using importance sampling, which is in line with the reductions of over 93% in the amount of work required to estimate to a given level of precision in Tables 4.3 and 4.6. However, for a year 6 power system background, the variance estimate is only reduced by around 5.5% when using importance sampling, which is also in line with the reductions in expected work required to acquire an estimate to a given level of precision previously observed.

Further evidence of this can be seen by considering Figure 4.10 (a), which illustrates

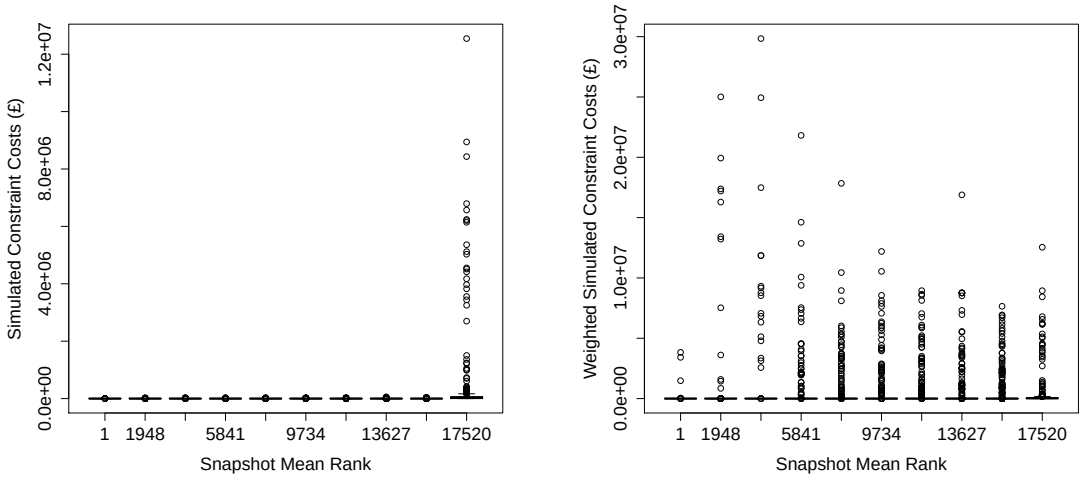

(a) Simulated constraint costs.

(b) Weighted simulated constraint costs.

Figure 4.10: Boxplots to illustrate the variation in simulated constraint costs for 1000 simulations for 10 snapshots for a year 1 power system background.

boxplots for 1000 simulator evaluations of constraint costs for 10 snapshots for a year 1 power system background. The snapshots chosen for illustration in Figure 4.10 (a) are 10 equally spaced snapshots when snapshots are ranked from the lowest mean of constraint costs to the greatest mean of constraint costs.

As can be seen, the snapshot with the greatest mean of constraint costs dominates the graph, with the costs in the other 9 snapshots being negligible in comparison. Intuitively, it would therefore be expected that this snapshot is most important to the estimate of mean annual constraint costs, and when using importance sampling this snapshot should be sampled much more frequently than others. This is reflected in Figure 4.11, which illustrates how importance sampling weights, $\boldsymbol{\omega}$, vary from smallest weight to largest for a year 1 power system background when basing importance sampling weights on the mean constraint costs of each snapshot. As can be seen, the vast majority of snapshots have very little weight due to the mean of constraint costs in these snapshots being very low, with only 520 (3.02%) of the snapshots having a weight greater than 0.01.

Figure 4.10 (b) illustrates boxplots for the 1000 simulations of each of the snapshots of Figure 4.10 (a) when each of the simulations of constraint costs has been weighted using Equation 4.2.5 (i.e. the value that would be used when estimating constraint costs if

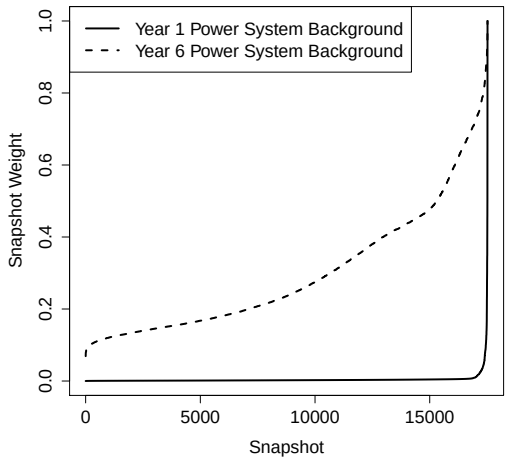

Figure 4.11: Plot to compare importance sampling weights for a year 1 and year 6 power system background, when basing the weights on the mean constraint costs of each snapshot.

that particular snapshot was simulated when using importance sampling). As can be seen, the plots for each snapshot are now much more similar to one another, with no particular snapshot dominating. This illustrates the benefit of importance sampling for a year 1 power system background, as snapshots less relevant to the estimate of annual constraint costs are sampled much less frequently, with the weighted estimates of constraint costs from Equation 4.2.5 accounting for this when the snapshot is actually simulated.

Figure 4.12 displays the equivalent graphs to Figure 4.10 for a year 6 power system background (i.e. boxplots for 1000 simulator evaluations of constraint costs for 10 equally spaced snapshots when snapshots are ranked from the snapshot with the lowest mean of constraint costs to the snapshot with the greatest mean of constraint costs). As can be seen in Figure 4.12 (a), even without an application of importance sampling the distribution of constraint costs across all snapshots is somewhat similar, with the constraint costs from the snapshot with the greatest mean not dominating simulated costs from the other snapshots, unlike what was seen for a year 1 power system background. Further, the weighted estimates of constraint costs from these simulations displayed in Figure 4.12 (b) do not appear to be a great improvement on Figure 4.12 (a). In particular, it can be seen that for the snapshot with the lowest mean of constraint costs, due to the small weight of this snapshot (0.069) several simulator evaluations

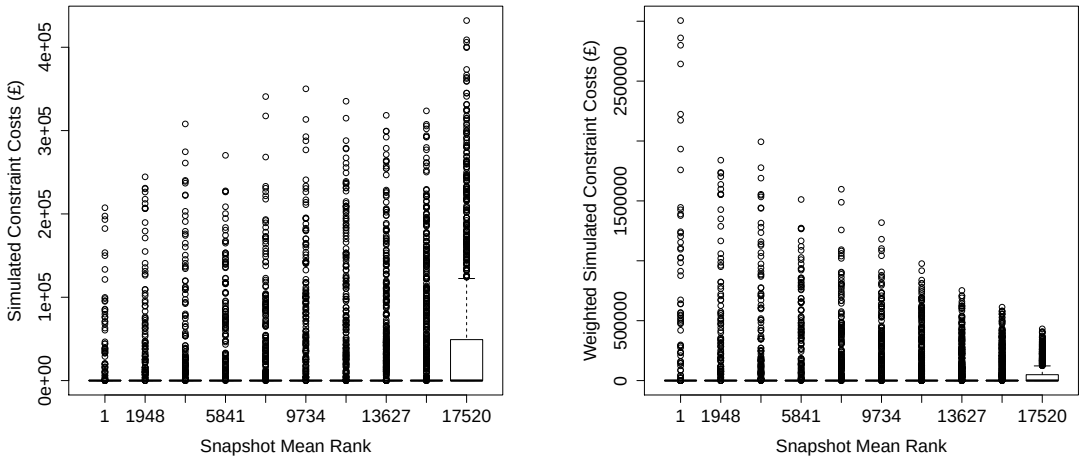

(a) Simulated constraint costs.

(b) Weighted simulated constraint costs.

Figure 4.12: Boxplots to illustrate the variation in simulated constraint costs for 1000 simulations for 10 snapshots for a year 6 power system background.

which gave a larger than average evaluation of constraint costs for this snapshot result in very large weighted estimates of constraint costs.

Further evidence to this can be seen in Figure 4.11, which also displays how importance sampling weights, $\boldsymbol{\omega}$, vary from smallest weight to largest for a year 6 power system background when basing importance sampling weights on the mean constraint costs of each snapshot. For a year 6 power system background it can be seen that whilst only a small amount of snapshots are given weight greater than 0.8 or 0.7 (1.0% and 3.9% of snapshots respectively) the weights are much more evenly distributed amongst snapshots in comparison to a year 1 power system background. In particular, a yearly simulation of constraint costs which uses importance sampling would expect to evaluate just 74.68 snapshots for a year 1 power system background (0.43% of the year) in comparison to the 5220 that would be expected to be evaluated for a year 6 power system background (29.80% of the year).

4.3.8 Conclusions of Pilot Investigation

This section has considered how the expected value of λ (the amount of work expressed as equivalent full simulator evaluations) required to acquire an estimate of mean annual constraint costs to a given level of precision varies with weights, $\boldsymbol{\omega}$, used when using

importance sampling to estimate annual constraint costs. For both the year 1 and year 6 power system backgrounds, the two power system backgrounds which are of interest for the examples which will be presented in Chapters 5 and 6, the best results were acquired when basing the weights to be used on the mean constraint costs for each snapshot, which is consistent with the results of Section 4.2.2 and Appendix A.1. For a year 1 power system background, Table 4.3 shows how using an importance sample with weights based on the mean constraint costs of each snapshot expected to evaluate 16.6 times less snapshots in comparison to not using importance sampling (i.e. evaluating each snapshot in each yearly simulation).

However, for this pilot investigation 1000 full evaluations of the simulator were used to estimate the weights used for the applications of importance sampling in this section, and this initial work outweighs the benefits of importance sampling. Further, it was shown in Section 4.3.4 that it was insufficient to calculate weights for one particular power system background, then use those weights when estimating mean annual constraint costs for other power system backgrounds. Therefore, from this initial experiment it can be concluded that if the mean snapshot constraint costs could be known accurately, applying importance sampling based on these means gives the best results. The next section will consider how to efficiently estimate mean annual constraint costs when the importance sampling weights are not known accurately in advance.

4.4 A General Importance Sampling Methodology

The previous section presented a pilot study to demonstrate how importance sampling can be used to estimate mean annual constraint costs, whilst expecting to evaluate fewer snapshots in comparison to evaluating each snapshot in each simulator evaluation. Basing importance sample weights on the mean constraint costs of each snapshot gave the best results, expecting to evaluate 16.6 times fewer snapshots on average to acquire an estimate of mean annual constraint costs to a given level of precision, in comparison to using the full simulator for a year 1 power system background.

However, for the pilot study it was assumed that the weights used for importance sampling were known accurately in advance, with mean snapshot constraint costs estimated

from 1000 full simulator evaluations. This section will consider if it is possible to use a small number of full simulator evaluations to estimate the weights used for importance sampling to reduce the total number of snapshots evaluated when estimating mean annual constraint costs for a given power system background. All results in this section will use the mean constraint costs of each snapshot as the basis for the weights used in importance sampling. As the importance sampling methodology of Section 4.2.2 requires each snapshot to have strictly positive weight, a minimum weight of 0.01 will be given to each snapshot (i.e. each snapshot will expect to be evaluated at least once in every 100 yearly simulations).

Further, Section 4.2.1 noted that several references use iterative schemes within applications of importance sampling to improve results [104, 96, 47]. Therefore, Section 4.4.2 will detail an iterative scheme suitable for the application of importance sampling when estimating mean annual constraint costs, where a small number of initial simulations are taken to estimate initial importance sampling weights, with these weights then continuously updated after each subsequent simulator evaluation.

As the results of the previous section showed that there is relatively little benefit in using importance sampling for a year 6 power system background, this section will only present results when estimating mean annual constraint costs for a year 1 power system background, though in omitted work the applications proposed in this section were also applied to a year 6 power system background.

4.4.1 Using a Small Number of Initial Simulations

Table 4.11 displays how the expected work, λ, required to acquire an estimate of mean annual constraint costs such that the standard error of the estimate is less than 1% of the mean of the estimate (accuracy of 1%) varies with the initial number of snapshots used to estimate the weights used for importance sampling. The results displayed do not include the work done to acquire the initial simulator evaluations used to estimate importance sample weights. As was the case throughout Section 4.3, the work required to acquire an estimate of mean constraint costs to a given level of precision varies each time an estimate is acquired, so the results of Table 4.11 are based on the average work required to acquire an estimate for 200 repetitions.

Number of Initial Simulations	Expected work, λ, for a Year 1 Power System Background
Full Simulation	484.1 EFSE
10	152.7 EFSE
25	88.31 EFSE
50	67.06 EFSE
100	55.01 EFSE

Table 4.11: Table showing how the amount of work done (λ, in terms of equivalent full simulator evaluations) to estimate mean annual constraint costs to an accuracy of 1% varies with the initial number of simulations used to estimate importance sample weights.

There appears to be great benefit in using importance sampling in comparison to using full simulation. Using just 10 initial full simulations to estimate the importance sampling weights requires just one third of the work in comparison to using the full simulator on average to acquire an estimate of mean annual constraint costs with an accuracy of 1%. Table 4.11 shows further improvement when the number of initial full simulations used to estimate importance sample weights is increased, with the use of 25 initial full simulations decreasing the expected value of λ from 153 EFSE to 88 EFSE.

However, it is also observed that the benefit of using additional initial simulations to estimate importance sample weights decreases as the number of initial simulations increases. For example, increasing the number of initial simulations used to estimate weights from 50 to 100 decreases the expected work required to achieve an estimate of mean annual constraint costs with an error less than 1% from 67 EFSE to 55 EFSE (i.e. a decrease of 12 equivalent full simulator evaluations). However, an additional 50 initial full simulation evaluations were required to estimate the initial weights, indicating that the total work done (i.e. the work done to calculating the weights plus the work to estimate mean constraint costs such that the standard error of the estimate is less than 1% of the mean of the estimate) would have been less if just 50 initial simulations were used to estimate the importance sample weights.

Figure 4.13 displays boxplots to show how much variation there was in the estimate of the work required for 1% accuracy across all 200 repetitions of each condition. This shows clearly how the work required to achieve a 1% error in the estimate decreases with the number of initial simulations used to estimate importance sampling weights.

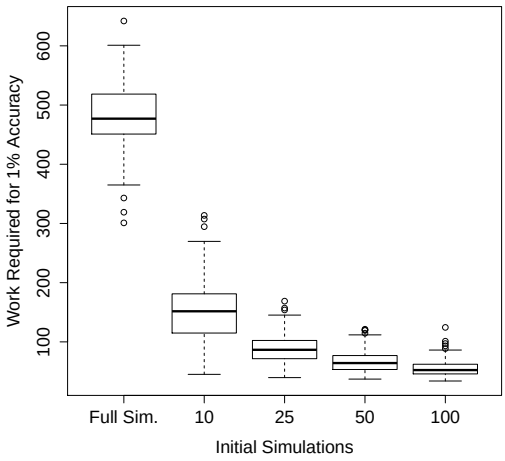

Figure 4.13: Boxplots to illustrate the variation of work done (λ, in terms of equivalent full simulator evaluations) to reach an estimate of mean annual constraint costs to an accuracy of 1% for varying numbers of initial simulations to estimate weights.

Further, with the exception of a few outliers when using 10 initial simulations to estimate weights, all estimates when using importance sampling were acquired by evaluating fewer total snapshots in comparison to all estimates when not using importance sampling. This illustrates that even when importance sampling weights are estimated from a small number of initial full simulator evaluations, there is great benefit to using importance sampling when estimating mean annual constraint costs for a year 1 power system background.

4.4.2 Updating Importance Sampling Weights

The previous subsection considered the possibility of using a small number of initial full simulator evaluations to estimate weights, $\boldsymbol{\omega}$, to be used for importance sampling. For a year 1 power system background, even using just 10 initial simulations to estimate the weights reduced the expected number of snapshot evaluations required to estimate mean annual constraint costs by 68.46% in comparison to not using importance sampling, with further improvement noted as the number of initial simulations to estimate weights was increased.

However, in the examples of the previous subsection the importance sampling weights were calculated based on an initial set of full simulations, and no information from

subsequent simulations was taken into account. The importance sampling methodology could be greatly improved if information from each sample was taken into account when taking the next sample, as described in the following algorithm:

1. Set a minimum value of λ (i.e. work done in terms of equivalent full simulator evaluations) before an estimate of mean annual constraint costs can be accepted (10 EFSE for the results of this section) and set a level of error in the estimate to be achieved (such that the standard error of the estimate is less than 1% of the mean of the estimate for the results of this section).

2. Take an initial set of simulations from the full simulator (an appropriate size for this initial sample will be explored in this section).

3. Note the number of times snapshot τ was evaluated in the initial set of simulations as N_τ and the mean of the evaluations in snapshot τ as $\hat{\phi}_\tau$

4. Estimate an initial set of weights, $\boldsymbol{\omega}$, to use in importance sampling via Equation 4.3.1 based on the values of $\hat{\phi}_\tau$ from these initial simulations.

5. Use the weights, $\boldsymbol{\omega}$, to take N_{y_ω} additional simulations of annual constraint costs, y_ω, via importance sampling as outlined in Section 4.2.2. Denote the number of times snapshot τ was simulated in this additional sample as $N_{\tau,+}$ and the mean of these additional $N_{\tau,+}$ evaluations as $\hat{\phi}_{\tau,+}$.

6. Calculate an estimate of mean annual constraint costs as an average of the simulated annual constraint costs from importance sampling (mean of all the y_ω), and also calculate the standard error of the estimate (standard error of all the y_ω).

7. Check, have the convergence criteria of step 1 been met? If so, stop; else go to step 8.

8. Update the mean of each snapshot such that

$$\hat{\phi}_\tau \leftarrow \frac{\hat{\phi}_\tau N_\tau + \hat{\phi}_{\tau,+} N_{\tau,+}}{N_\tau + N_{\tau,+}}$$

and the total number of times each snapshot has been evaluated as

$$N_\tau \leftarrow (N_\tau + N_{\tau,+})$$

9. Recalculate the importance sampling weights to be used, $\boldsymbol{\omega}$, using the updated snapshot means, $\hat{\phi}_\tau$, via Equation 4.3.1.

10. Go back to Step 5.

The above algorithm means that the weights used for importance sampling, $\boldsymbol{\omega}$, always take into account the maximum amount of information available. In this thesis, estimating annual constraint costs using importance sampling via Equation 4.2.5 is much more expensive than updating the weights via step 8 of the above algorithm so it is sufficient to set N_{y_ω} to 1, i.e. update the important sampling weights after each yearly estimate of constraint costs. This means that if the initial sample over or under-estimated the importance of a particular snapshot, subsequent information from subsequent samples could be taken into account in order to improve future sampling. Appendix G.3 gives the R code used to implement this algorithm.

It is noted that in the above algorithm the evaluations of annual constraint costs from the initial simulations used to estimate initial importance sampling weights are not subsequently used in the estimate of mean annual constraint costs. This is given further thought at the end of this subsection.

Number of Initial Simulations	Expected work, λ, for a Year 1 Power System Background
Full Simulation	484.1 EFSE
10	48.21 EFSE
25	45.38 EFSE
50	45.82 EFSE
100	44.06 EFSE

Table 4.12: Table showing how the amount of work done (λ, in terms of equivalent full simulator evaluations) to estimate mean annual constraint costs to an accuracy of 1% varies with the initial number of simulations used to estimate importance sample weights when the weights are updated after each subsequent simulation.

Table 4.12 shows how the expected work required to estimate mean annual constraint costs, λ, varies when using an importance sampling method which updates the weights

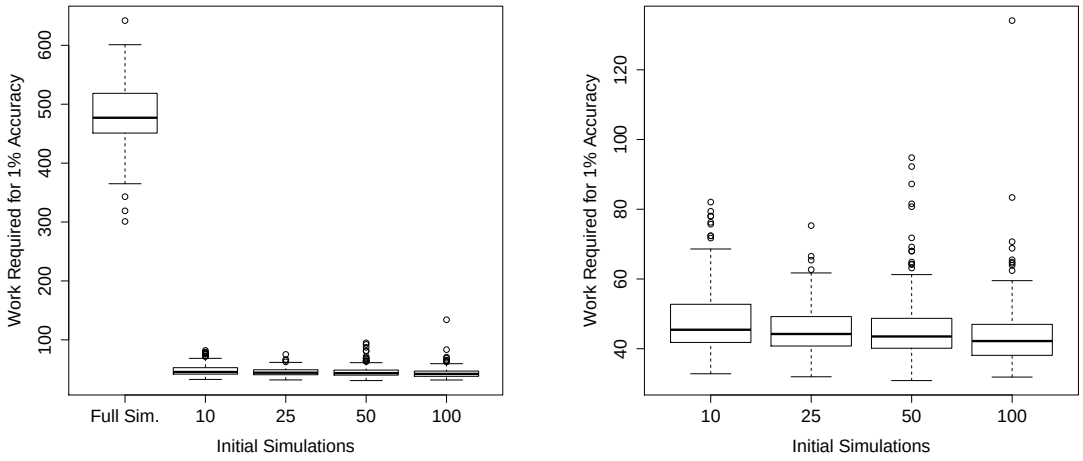

(a) All Methods.

(b) Only Applications of Importance Sampling.

Figure 4.14: Boxplots to illustrate the variation of work done (λ, in terms of equivalent full simulator evaluations) to reach an estimate of mean annual constraint costs to an accuracy of 1% for varying amounts of initial simulations to estimate weights.

used for importance sampling after every yearly simulation (not including the work done to acquire the initial simulator evaluations used to estimate the initial importance sampling weights). By comparison to Table 4.11 it can be seen it can be seen that these results are great improvement in comparison to when the importance sampling weights were not continually updated. For example, using 10 initial full simulator evaluations to estimate the initial weights would require over 152 EFSE to estimate mean annual constraint costs when the importance sample weights are not continually updated, which can be reduced to just over 48 EFSE (a reduction of over 68%) when the importance sampling weights are updated after each yearly evaluation.

The expected equivalent number of full simulator evaluations appears to decrease as the number of initial simulations used to estimate importance sampling weights increases, but at a very slow rate. As mentioned, using 10 initial full simulator evaluations to estimate the initial weights expects to give an estimate of mean annual constraint costs after the equivalent of just 48 further full simulator evaluations. However, increasing the number of initial full simulator evaluations used to estimate initial weights to 100 expects to give an estimate of mean annual constraint costs after the equivalent of 44 further full simulator evaluations, a reduction of just 4 EFSE despite using an

additional 90 initial full simulations. Therefore, it appears as if it is sufficient to use a small number of initial simulations to estimate initial importance sampling weights when allowing the weights to be updated after each subsequent yearly simulation.

The reason a small number of initial full simulator evaluations is sufficient is partially explained by Figure 4.3 (a) of Section 4.1.3. In this plot it is seen how a small number of days give a much greater contribution to the estimate of annual constraint costs than the rest of the year (in particular in Section 4.1.3 it was noted that 2.47% of days account for 27.3% of annual costs). Further, Figure 4.11 of Section 4.3.7 shows that the accurate estimates of importance sampling weights based on 1000 full simulator evaluations would expect to evaluate 0.42% of the 17520 snapshots in a full year. This explains what is observed in Table 4.12, as a small number of initial simulations can be used to identify the snapshots with the largest means of constraint costs, and once identified these snapshots will actually be simulated more often than others when evaluating annual constraint costs using importance sampling. Then, when applying importance sampling these snapshots will be continually sampled, meaning very accurate weights can be estimated for them very quickly. When doing extra initial work, however, all 17520 snapshots are repeatedly sampled, meaning a substantial amount of work is performed to accurately estimate weights for snapshots of negligible importance.

It is noted that the algorithm proposed in this subsection takes an initial set of full simulator evaluations to estimate initial importance sampling weights, but the corresponding evaluations of annual constraint costs of these initial simulations are not used when estimating mean annual constraint costs. This is part of a (perhaps overly) cautious approach, to account for the fact that although evaluations of annual constraint costs obtained via importance sampling have the same mean as evaluations of the full simulator (as is verified in Equation 4.2.6 of Section 4.2.2), the variance of the evaluations of annual constraint costs when using importance sampling may be very different to the variance of the full simulator (especially if very few snapshots are evaluated when using importance sampling). However, it would be possible to use the initial simulations as part of the estimation process, and Appendix G.3.2 notes how to achieve this through a minor adjustment to the R code.

4.5 Importance Sampling Conclusions

This chapter has considered how importance sampling can be used as a method of estimating mean annual constraint costs for a given power system, whilst evaluating fewer snapshots in comparison to using the full simulator. Section 4.3.3 showed that using importance sampling weights, $\boldsymbol{\omega}$, based on the mean constraint costs of each snapshot can reduce the expected number of snapshots to be evaluated to acquire an estimate of mean annual constraint costs to a given level of precision. However, this requires initial evaluations of the full simulator to estimate these weights. Further, Section 4.3.4 showed that weights estimated for one particular power system background do not generalise well to a different power system background. Section 4.4.2 showed how this problem can be overcome by using a small number of initial full simulator evaluations to estimate some initial weights to be used, with the weights subsequently updated after each yearly evaluation from importance sampling to account for subsequent estimations of mean constraint costs in each snapshot. For the remainder of this thesis the algorithm proposed in Section 4.4.2 will be used when estimating mean constraint costs for a given power system background, using 10 initial simulations to estimate initial importance sampling weights.

It was stated that throughout Section 4.4 that a minimum weight for each snapshot was set to 0.01. This is because Equation 4.2.5 requires each snapshot to have a non-zero weight in order to apply importance sampling. Further, as a small number of initial snapshots are used to estimate initial weights it was important not to set this value too low to avoid under-estimating the importance of a snapshot due to a poor initial sample. A weight of 0.01 means the particular snapshot will expect to be sampled every 1 in 100 times. Setting the value higher than this would mean a lot of work would be spent evaluating constraint costs for snapshots where the best evidence available suggested they were of less importance. An investigation omitted from this thesis was carried out to verify this was an appropriate lower bound for importance sample weight.

Chapter 5

The Use of Emulation as Part of Decision Making Under Uncertainty

Chapter 3 defined the simulator used to estimate constraint costs in this thesis. Further, Section 3.7 showed how details about the power system background (input variables of the simulator) have an effect on the mean constraint costs estimated.

As discussed in Section 2.3, this thesis will provide a methodology to make transmission expansion decisions when uncertainty exists in the values of the variables which are used to describe the power system. Further, this thesis gives a more complete consideration to uncertainty of the simulator input variables, which improves on the existing transmission expansion planning literature, which only handles uncertainty by considering a small number of possible values for the input variables.

This chapter will introduce the concept of emulators, which can be used to approximate simulators whilst being much less expensive to evaluate. Further, details will be given of how the emulators can then be used alongside prior beliefs about uncertainties (which quantify expert judgement about the possible values which variables containing uncertainty may take) to make decisions which give a careful consideration to the uncertainty which exists in the power system background. This chapter will end with an application of the emulation methodology presented to a simple example of transmission expansion planning under uncertainty.

5.1 Structure of the Uncertainty Problem

Section 3.4 gave the specification of the simulator, $f_c(\mathfrak{X})$, which is used to estimate the mean constraint costs of power systems in this thesis (recall $\mathfrak{X}$ contains all relevant information about the power system background such as installed generating capacities, peak demand levels, etc). Recall, constraint costs are the additional operational costs, conditional on the level of transmission network investment, which arise due to finite network capacity restricting the ability to use the cheapest generating capacity available.

In reality, it is possible to increase the transmission capacity between zones (build more transmission lines) which would allow more generating capacity to be traded between zones. This would in turn decrease the constraint costs expected to arise. The magnitude and location of transmission reinforcements (i.e. the magnitude of increase of transmission capacity between two specific zones) are decisions to be made. Therefore, such decisions could be quantified as decision variables and included in $\mathfrak{X}$. Increasing the transmission capacity of certain boundaries was also given consideration in Section 3.7.

It is also important to note that there are considerable costs associated with expanding the transmission system. Therefore, decisions to expand the transmission network must also account for the construction costs of such a reinforcement, $f_\rho(\mathfrak{X})$. This means that the goal of transmission expansion planners is not to eliminate constraint costs from the system, but rather to find an economic balance between the mean constraint costs expected to arise and the reinforcement costs of expanding the transmission system. Therefore, the quantity of interest in this thesis is the total costs of the power system, defined as the sum of the mean constraint costs plus the cost of any reinforcement made, i.e.

$$f_T(\mathfrak{X}) = f_c(\mathfrak{X}) + f_\rho(\mathfrak{X}) \tag{5.1.1}$$

In this thesis it will initially be assumed that it costs £100,000 to increase the transmission capacity between two zones by 1 MW [5, 78]. This calculation is based on the assumption that it would cost £1000 per MW per km to reinforce, and assuming that each boundary between zones is 100 km. Further thought is given to this figure in

Sections 5.4.1 and 6.4.2, which additionally consider how sensitive particular decisions about the power system are to this figure.

This thesis will present a methodology for decision making whilst accounting for the uncertainty that exists in the input data of the simulator (i.e. decision making whilst accounting for the uncertainty in values contained in $\mathfrak{X}$). Section 3.7 showed how the estimates of constraint costs from the simulator, f_c, are dependent on the system background assumed for the power system, which is defined by the data contained in $\mathfrak{X}$.

In total, $\mathfrak{X}$ contains hundreds of variables which define the power system background. As was noted, there are varying amounts of uncertainty in the true values of these variables (for example, currently installed generating capacities can be known very accurately whereas future peak demand levels can be known much less accurately). Further, the effect on the estimate of mean constraint costs as the assumed value of a variable is varied also varies with the variable considered (for example, in Section 3.7.2 it was shown that the assumed level of peak demand had a large effect on the mean constraint costs estimated, but the transfer capacity of the B9 boundary had very little effect on the estimate of mean constraint costs). This means it is neither feasible nor necessary to consider uncertainty in every single variable when estimating optimal reinforcement decisions to be made for the transmission system.

It is therefore useful to think of $\mathfrak{X}$ as $(\mathbf{v}, \mathbf{a}, \mathbf{d})$, where $\mathbf{v}$ represents the inputs in which uncertainty is modelled explicitly; $\mathbf{a}$ represents the inputs which are either known with certainty or in which uncertainties are not of interest, so their values are treated as fixed as if they are known precisely (the effect of assuming fixed values for these variables is investigated in Chapter 7); and $\mathbf{d}$ represents the decision variables. To link this back to the examples presented in Section 3.7, $\mathbf{v}$ would represent variables which have a large impact on the mean constraint costs estimated, such as the peak demand level and certain generator availability probabilities. $\mathbf{a}$ would represent variables shown to have little impact on the estimate of mean constraint costs, such as the B9 transmission capacity or variables which it is reasonable to think could be known very precisely, such as current levels of installed generating technology. $\mathbf{d}$ quantifies the transmission expansions decisions which are of interest. In this thesis $\mathbf{d}$ will represent the amount

(in MW) of additional transmission capacity built between two zones, which in turn represents the amount (in MW) of additional generating capacity that can be traded between two zones.

With this formulation, if $\mathbf{d} = (d_1, ..., d_{N_d})$, the cost of reinforcement for a particular power system background from Equation 5.1.1 can then be redefined as

$$f_\rho(\mathfrak{X}) = f_\rho(\mathbf{d}) = f_\rho(d_1, ..., d_{N_d}) = £100,000 \times \sum_{i=1}^{N_d} d_i \tag{5.1.2}$$

5.2 Emulation

5.2.1 Fitting an Emulator

Section 2.3 gave an overview for the existing literature on transmission expansion planning. It was noted that a large amount of the literature gave little thought to uncertainty in the power system background when identifying optimal expansion decisions of the power system's transmission system. Further, the literature which did consider uncertainty did so by considering a small number of possible states of the power system. This thesis will overcome this by treating the variables which define the power system as continuous variables, which would allow the variables to take any potential value over a given range (e.g. we could model the peak demand level to be anywhere between 62100 MW and 63600 MW) instead of a small number of possible values.

As mentioned, in the problem presented there is uncertainty in the values of the input variables, $\mathfrak{X}$. However, the function $f_T(\mathfrak{X})$ (the simulator of total costs), is far too expensive to evaluate at every set of input parameters desired. Therefore, it is necessary to evaluate f_T a small number of times for particular values of $\mathfrak{X}$, and approximate f_T everywhere else as carefully as possible by some alternative function, $\tilde{f}_T$. $\tilde{f}_T$ should be much less computationally demanding to evaluate in order to allow for efficient estimation for input values not simulated. An estimate of the uncertainty that exists in the response when approximating f_T by $\tilde{f}_T$ is also required. The process of approximating f_T by $\tilde{f}_T$ is known as emulation [74, 45, 89].

Suppose there are N_v variables with uncertainty of interest, labelled $v_1, ..., v_{N_v}$ and N_d decision variables, $d_1, ..., d_{N_d}$. The goal is to fit a model to the output of f_T (the sum

of mean constraint costs plus reinforcement costs) based on these $N_v + N_d$ variables. As this process assumes all other variables are considered fixed as if known, $\tilde{f}_T$ can be treated as if it is a function of $v_1, ..., v_{N_v}$ and $d_1, ..., d_{N_d}$ only.

A small set of training runs of the simulator are used to construct the function $\tilde{f}_T$ which approximates f_T. These training runs vary the values of $v_1, ..., v_{N_v}$, and $d_1, ..., d_{N_d}$ over a given range. Details on how training runs are selected to give a dense coverage of the space defined by $v_1, ..., v_{N_v}$ and $d_1, ..., d_{N_d}$ are given in Section 5.2.4.

Suppose y_T represents the response of the simulator (f_T) for the training data. For simplicity in the following notation, also suppose $\mathbf{x} = (\mathbf{v}, \mathbf{d}) = (v_1, ..., v_{N_v}, d_1, ..., d_{N_d})$. The emulator, $\tilde{f}_T$, is usually constructed such that $\tilde{f}_T$ is the sum of a parametric model plus a non-parametric smoother applied to the residuals of the parametric model [45, 89, 84, 92], i.e.

$$\tilde{f}_T(\mathbf{x}) = g(\mathbf{x})^{\mathrm{T}}\boldsymbol{\beta} + e(\mathbf{x}) \tag{5.2.1}$$

where $g(\mathbf{x})^{\mathrm{T}}\boldsymbol{\beta}$ is the parametric portion of the emulator and $e(\mathbf{x})$ is the non-parametric smoother applied to the residuals of $g(\mathbf{x})^{\mathrm{T}}\boldsymbol{\beta}$. The emulator used in this thesis will use a polynomial regression model as the parametric portion (i.e. $g(\mathbf{x})^{\mathrm{T}}\boldsymbol{\beta}$ from Equation 5.2.1) of the emulator model. This can be thought of as

$$y_T(v_1, ...v_{N_v}, d_1, ..., d_{N_d}) = y_T(\mathbf{x}) = \beta_0 + \sum_{t=1}^{p}\sum_{i=1}^{N_v+N_d}\beta_{t,i}x_i^t + \sum_{t=1}^{p}\sum_{i=1}^{N_v+N_d}\sum_{j\neq i}\beta_{t,i,j}x_i^t x_j^t + ... + \varepsilon(\mathbf{x}) \tag{5.2.2}$$

i.e. the dot product of a coefficient vector with the polynomial form of the predictor variables with error term $\varepsilon(v_1, ..., v_{N_v}, d_1, ..., d_{N_d})$. This thesis only considers interactions between equal powers of variables (e.g. the polynomial may include an interaction between v_1 and d_2 but not between v_1 and d_2^2). Values of $\boldsymbol{\beta}$ are estimated via least squares regression, as will be detailed in Section 5.2.2.

Whilst this methodology applies very generally, the terms included in the polynomial regression model should be carefully selected based on the specifics of the example considered. This is considered in Sections 5.3.3 and 6.1.3, where both the R^2 value of the polynomial regression model and a measure of the resulting emulator's predictive power for a second set of training data which was not used to fit the model are used

to identify terms to be included in the model.

If the residual of the polynomial regression model, $\varepsilon(\mathbf{x}^*)$, is positive for a given set of input values, $\mathbf{x}^*$, this indicates that the polynomial regression model under-estimates the response of the simulator, $y_T(\mathbf{x})$, at $\mathbf{x}^*$. As $y_T(\mathbf{x})$ is modelled as a continuous variable, $\varepsilon(\mathbf{x})$ is also modelled as a continuous variable. By the continuity of $y_T(\mathbf{x})$, the polynomial model will also under-estimate the response for values of $\mathbf{x}$ close to $\mathbf{x}^*$, i.e. values of $\varepsilon(\mathbf{x})$ are not independent but rather contain information about the response of the simulator near $\mathbf{x}$.

This means that the fit of the model can be improved further by using a Gaussian process model to smooth the residuals, $\varepsilon(v_1, ..., v_{N_v}, d_1, ..., d_{N_d})$. This is important as the polynomial model will aim to give a good fit over the entire range of the variables considered, whereas the Gaussian process model can model local behaviour much more accurately. The idea of a Gaussian process is to smooth the residuals in order for the model to agree with the training data and provide an accurate estimate of response (and variance of the estimated response) for values where training data is unavailable. In this sense, the Gaussian process model can be thought of as a smooth interpolator of the residuals [74]. In simple terms, the idea of the Gaussian process is if a response is to be estimated at point $\mathbf{x}_p$, training data closer to $\mathbf{x}_p$ carries more relevant information and should be given more weight when making an estimation. Further details on Gaussian process models are given in Section 5.2.3.

In this thesis, the polynomial portion of the emulator model will be denoted by $\tilde{f}_{T_1}$ and the Gaussian process model fitted to the resulting residuals of the polynomial model will be denoted by $\tilde{f}_{T_2}$. Thus, the emulator model for given inputs is the sum of these two, denoted $\tilde{f}_T$, such that

$$\tilde{f}_T(v_1, ..., v_{N_v}, d_1, ..., d_{N_d}) = \tilde{f}_{T_1}(v_1, ..., v_{N_v}, d_1, ..., d_{N_d}) + \tilde{f}_{T_2}(v_1, ..., v_{N_v}, d_1, ..., d_{N_d}) \tag{5.2.3}$$

That is to say $\tilde{f}_T$ is our emulator which approximates the simulator, and the estimated response of the emulator is acquired by evaluating the sum of the estimated responses of the fitted polynomial regression model and the corresponding Gaussian process model for given input values.

After the emulator has been fitted to a set of training data, a second set of training

data will then be simulated. The emulator model fitted to the first set of training data, $\tilde{f}_T$, will then be used to estimate a response for the output of the simulator at the second set of training data. By comparing the estimated response of the emulator to the value simulated the predictive power of the emulator can be assessed, as will be demonstrated in Section 5.3.3.

5.2.2 Polynomial Regression Modelling

Section 5.2.1 mentioned that polynomial regression models are used as part of the emulation process. Equation 5.2.2 detailed the form of the polynomial regression model. However, in practice it is more useful to use a design matrix, X_{dp}, and a vector of parameters, $\boldsymbol{\beta}$, to represent this polynomial regression model. The ith row of the design matrix details the polynomial form of the ith training run, with n training runs acquired in total (i.e. X_{dp} has n rows). For example, suppose a polynomial regression model is to be fitted to two variables which contain uncertainties of interest and one decision variable, and the form of the polynomial regression model is

$$\beta_0 + \beta_1 v_1 + \beta_2 v_2 + \beta_3 d_1 + \beta_4 d_1^2 + \beta_5 v_2 d_1$$

The design matrix of such a polynomial regression model would be

$$X_{dp} = \begin{pmatrix} 1 & v_{1,1} & v_{1,2} & d_{1,1} & d_{1,1}^2 & v_{1,2}d_{1,1} \\ 1 & v_{2,1} & v_{2,2} & d_{2,1} & d_{2,1}^2 & v_{2,2}d_{2,1} \\ \vdots & \vdots & \vdots & \vdots & \vdots & \vdots \\ 1 & v_{i,1} & v_{i,2} & d_{i,1} & d_{i,1}^2 & v_{i,2}d_{i,1} \\ \vdots & \vdots & \vdots & \vdots & \vdots & \vdots \\ 1 & v_{n,1} & v_{n,2} & d_{n,1} & d_{n,1}^2 & v_{n,2}d_{n,1} \end{pmatrix}$$

where $v_{i,1}$, $v_{i,2}$ and $d_{i,1}$ are the values of the two uncertain variables and decision variable respectively for the ith training run.

Equation 5.2.2 could then be rewritten as

$$\mathbf{y}_T = X_{dp}\boldsymbol{\beta} + \boldsymbol{\varepsilon} \tag{5.2.4}$$

where $\mathbf{y}_T = (y_{1,T}, y_{2,T}, ..., y_{n,T})^{\mathrm{T}}$ such that the ith entry of $\mathbf{y}_T$ is the simulated response

of the ith training run, $\boldsymbol{\varepsilon} = (\varepsilon_1, \varepsilon_2, ..., \varepsilon_n)^{\mathrm{T}}$ such that the ith entry of $\boldsymbol{\varepsilon}$ is the residual of the ith training run when fitting the polynomial regression model and $\boldsymbol{\beta}$ is the vector of parameters of the polynomial regression model, i.e. $\boldsymbol{\beta} = (\beta_0, \beta_1, ..., \beta_5)^{\mathrm{T}}$.

The values of the parameters of the polynomial regression model in this thesis are estimated using least squares regression. That is, values of $\boldsymbol{\beta}$ are estimated to minimise the sum of squares of the model residuals:

$$\hat{\boldsymbol{\beta}} = \arg\min_{\boldsymbol{\beta}} \sum_{i=1}^{n} \varepsilon_i^2 \tag{5.2.5}$$

$\hat{\boldsymbol{\beta}}$ can be calculated as

$$\hat{\boldsymbol{\beta}} = (X_{dp}^{\mathrm{T}} X_{dp})^{-1} X_{dp}^{\mathrm{T}} \mathbf{y}_T \tag{5.2.6}$$

For a polynomial regression model, the covariance matrix of these estimated parameters is

$$cov(\hat{\boldsymbol{\beta}}) = \sigma^2 (X_{dp}^{\mathrm{T}} X_{dp})^{-1} \tag{5.2.7}$$

where σ^2 is the variance of the residuals in the regression model which can be estimated as

$$\sigma^2 \approx s^2 = \frac{\sum_i^n \varepsilon_i^2}{n - q} \tag{5.2.8}$$

where q is the number of parameters in the polynomial regression model (i.e. the length of $\boldsymbol{\beta}$). For a standard polynomial regression model, it is then assumed that the estimated model parameters are multivariate normally distributed with some unknown true mean $\boldsymbol{\beta}$ and covariance matrix $cov(\hat{\boldsymbol{\beta}})$.

These results are used to inform our beliefs about the values of $\boldsymbol{\beta}$ used in the polynomial portion of the emulator model, which for a given set of training data form a multivariate normal distribution with mean $\hat{\boldsymbol{\beta}}$, as defined by Equation 5.2.5, and variance matrix $cov(\hat{\boldsymbol{\beta}})$, as defined by Equation 5.2.7.

If an estimated response is required at some new set of values $\mathbf{x}_o = (v_{o,1}, ..., v_{o,N_v}, d_{o,1}, ..., d_{o,N_d})^{\mathrm{T}}$, first a vector describing the polynomial terms of $\mathbf{x}_o$ is formed as $\mathbf{x}_{op}$. $\mathbf{x}_{op}^{\mathrm{T}}$ is written as if it were a row in the design matrix of the polynomial X_{dp}, so for the example given at the beginning of this section $\mathbf{x}_{op}^{\mathrm{T}}$ would have the form

$$\mathbf{x}_{op}^{\mathrm{T}} = (1, v_{o,1}, v_{o,2}, d_{o,1}, d_{o,1}^2, v_{o,2} d_{o,1})$$

An estimated response for values for these input values can then be calculated as

$$\mathbf{x}_{op}^{\mathrm{T}}\hat{\boldsymbol{\beta}} \tag{5.2.9}$$

The model parameters, $\hat{\boldsymbol{\beta}}$, and covariance matrix of these parameters will be calculated in this thesis using the lm function in R.

5.2.3 Gaussian Process Modelling

As mentioned in Section 5.2.1, Gaussian process models are used when fitting an emulator model, specifically to smooth the residuals of the fitted polynomial regression model. Technically, a Gaussian process is a collection of random variables, of which any finite subset have a joint Gaussian distribution [84, 10, 60]. For the example presented, this means that the Gaussian process fitted will model $\boldsymbol{\varepsilon}$ as a multivariate Gaussian distribution dependent on $\mathbf{x}$, as will be described in the remainder of this subsection.

[74] gives an accessible introduction to Gaussian processes models. The exemplar model is a simple function of a single variable (specifically $x + 3\sin(\frac{x}{2})$), acting in place of a complicated simulator for demonstration purposes. The function is evaluated exactly a small number of times (training runs) and it is demonstrated how a smooth interpolation (the Gaussian process) of these training runs acts as a good approximation to the true function, as well as illustrating the approximation error at inputs where the model has not been evaluated. This tutorial reference also demonstrates how the Gaussian process model can be improved by using additional training runs, and how the parameters of the Gaussian process itself affect the quality of the resulting approximation.

In this thesis, Gaussian process models are used to smooth the residuals of the polynomial regression model fitted in Section 5.2.2. As was noted in Section 5.2.1, this is to account for the fact that the simulated total cost, $y_T(\mathbf{x})$, is a continuous variable, and therefore $\varepsilon(\mathbf{x})$ (the difference between the simulated costs and the polynomial regression model fitted in Section 5.2.2, $\tilde{f}_{T_1}(\mathbf{x})$) is also modelled as a continuous variable dependent on $\mathbf{x}$.

A Gaussian process model fitted to model a response, ε, dependent on a set of variables, $\mathbf{x}$, uses a mean function, $m(\mathbf{x})$, and a covariance function, $\kappa(\mathbf{x}, \mathbf{x})$, to specify a mean-variance relationship (i.e. expected value of response and uncertainty in that expectation) for ε based on $\mathbf{x}$, as will be detailed in the remainder of this subsection. The Gaussian process model is completely defined by its mean and covariance function, and is denoted $\varepsilon \sim GP(m(\mathbf{x}), \kappa(\mathbf{x}, \mathbf{x}))$.

This thesis will use the mean function

$$m(\mathbf{x}) = \mu_{GP} \tag{5.2.10}$$

and covariance function

$$\kappa(\mathbf{x}_1, \mathbf{x}_2) = \sigma^2_{GP}\text{cor}(\mathbf{x}_1, \mathbf{x}_2) \tag{5.2.11}$$

where $\mathbf{x}_1^{\text{T}} = (x_{1,v_1}, ..., x_{1,v_{N_v}}, x_{1,d_1}, ..., x_{1,d_{N_d}})$ and $\mathbf{x}_2^{\text{T}} = (x_{2,v_1}, ..., x_{2,v_{N_v}}, x_{2,d_1}, ..., x_{2,d_{N_d}})$ are two sets of predictor variables; σ^2_{GP} is a variance parameter of the Gaussian process and $\text{cor}(\mathbf{x}_1, \mathbf{x}_2)$ is the value of a correlation function between $\mathbf{x}_1$ and $\mathbf{x}_2$. The correlation function used in this thesis is defined as:

$$\text{cor}(\mathbf{x}_1, \mathbf{x}_2) = e^{-\sum_{i=1}^{N_v+N_d} \gamma_i (x_{1,i} - x_{2,i})^2} \tag{5.2.12}$$

where $\gamma_1, ..., \gamma_{N_v+N_d}$ are the hyper-parameters of the correlation function to be estimated.

In practice the correlation between 2 matrices is required. Suppose X_1 and X_2 are two matrices where each row of each matrix is a set of predictor variables. Further, suppose that X_1 has I rows where $\mathbf{x}_{1,i}$ is the ith row of X_1, and that X_2 has J rows where $\mathbf{x}_{2,j}$ is the jth row of X_2. The correlation matrix between these two matrices would be a matrix K_{X_1,X_2} with I rows and J columns, where the jth entry of the ith row of K_{X_1,X_2} is $\text{cor}(\mathbf{x}_{1,i}, \mathbf{x}_{2,j})$.

Defining $m(\mathbf{x})$ as in Equation 5.2.10 (i.e. a constant mean function) is a common choice of mean function, which is a simple extension to a zero mean function, $m(\mathbf{x}) = 0$, which greatly simplifies calculations involved without the loss of generality [84, 93, 103]. Defining the correlation function as in Equation 5.2.12 means that the fitted correlation function is infinitely differentiable, which in turn means that the resulting Gaussian process model will be very smooth. This is also a very common choice of

correlation function [84, 17, 83].

For given values of the hyper-parameters of the correlation function, $\gamma_1, ..., \gamma_{N_v+N_d}$, a Gaussian process model can then be used to estimate the mean and variance of the response, ε. To do so, the design matrix, X_{dg}, of the training runs is required, as well as a vector of calculated responses, $\boldsymbol{\varepsilon}$. The ith row of X_{dg} describes the input values used for the ith training run, and the ith entry of $\boldsymbol{\varepsilon}$ is the corresponding residual of the polynomial regression model for that training run. Note, X_{dg} differs from X_{dp} as it simply gives the values of the training data of the $N_v + N_d$ input variables of interest, not the polynomial form of the polynomial regression model, i.e.

$$X_{dg} = \begin{pmatrix} v_{1,1} & v_{1,2} & \dots & v_{1,N_v} & d_{1,1} & d_{1,2} & \dots & d_{1,N_d} \\ v_{2,1} & v_{2,2} & \dots & v_{2,N_v} & d_{2,1} & d_{2,2} & \dots & d_{2,N_d} \\ \vdots & \vdots & \vdots & \vdots & \vdots & \vdots & \vdots & \vdots \\ v_{i,1} & v_{i,2} & \dots & v_{i,N_v} & d_{i,1} & d_{i,2} & \dots & d_{i,N_d} \\ \vdots & \vdots & \vdots & \vdots & \vdots & \vdots & \vdots & \vdots \\ v_{n,1} & v_{n,2} & \dots & v_{n,N_v} & d_{n,1} & d_{n,2} & \dots & d_{n,N_d} \end{pmatrix}$$

Suppose an estimated response is desired at a new set of n_2 data-points. A matrix X_* is created, where each row details the input values for which an estimated response is required. Note, X_* can be a single set of input values and will be treated as if it were a matrix with a single row. The vector for estimated responses of the Gaussian process for the input values of X_* is then modelled as a normal distribution with expectation [84, 41]

$$\boldsymbol{\varepsilon}_* = \boldsymbol{\mu}^*_{GP} + K_{X_*,X_{dg}}(K_{X_{dg},X_{dg}})^{-1}(\boldsymbol{\varepsilon} - \boldsymbol{\mu}_{GP}) \tag{5.2.13}$$

with the covariance matrix of these estimates

$$var(\boldsymbol{\varepsilon}_*) = \sigma^2_{GP}(K_{X_*,X_*} - K_{X_*,X_{dg}}(K_{X_{dg},X_{dg}})^{-1}K_{X_{dg},X_*}) \tag{5.2.14}$$

where $\boldsymbol{\mu}_{GP}$ is a vector of length n (the number of observations used to fit the Gaussian process) where each entry is μ_{GP}, i.e.

$$\boldsymbol{\mu}_{GP} = (\mu_{GP}, ..., \mu_{GP}) \tag{5.2.15}$$

and similarly $\boldsymbol{\mu}^*_{GP}$ is a vector of length n_2 (the number of points where a new estimated response is required) where each entry is μ_{GP}.

The parameters $\gamma_1, ..., \gamma_{N_v+N_d}$ in Equation 5.2.12 control how much weight is given to each training run when estimating a response using the Gaussian process model. The larger the values of these parameters, the faster the relative weight given to a training runs decreases with distance from the point where an estimate is required. In simple terms, larger values of these parameters will result in a function which is more sensitive to the local behaviour of training runs than smaller values.

In this thesis, the Gaussian process model is fitted using the function mlegp in R. This function identifies maximum likelihood estimates for the values of μ_{GP} and the correlation function hyper-parameters, $\gamma_1, ..., \gamma_{N_v+N_d}$, using numerical methods (specifically the Nelder-Mead Simplex and the L-BFGS method).

Sections 5.2.1 to 5.2.3 have presented the methodology for fitting an emulator model considered in this thesis. However, it is noted that other approaches to emulation can be taken, such as a fully Bayesian approach (as is considered in [45, 72, 10]) or a Bayes linear approach (as is considered in [37, 23, 98]).

5.2.4 Latin Hypercube Sampling

Section 5.2.1 stated that a set of training runs is used to create the emulator model which approximates the simulator. These training runs are acquired using Latin hypercube (LHC) sampling [76].

A hyper-rectangle (also called an n-orthotope) is the generalisation of a rectangle to a general number of dimensions. Just as the 2 dimensional rectangle could be extended to a cuboid by specifying a range for a third variable over a third axis, this cuboid could be extended into even higher dimensions, for example, by specifying n_d ranges for n_d variables over n_d axes.

Latin hypercube sampling is a method of taking a sample of n points from a specified hyper-rectangle. When taking the sample, each axis of the hyper-rectangle formed by the variables of interest (i.e. $v_1, ..., v_{N_v}, d_1, ..., d_{N_d}$) is divided into n intervals. A sample of size n is then taken which varies the values of the $N_v + N_d$ variables such that for

each variable exactly one of the samples has a corresponding value in each of the n intervals of that variable's axis.

Figure 5.1 illustrates this process when taking an LHC sample of size 6 from 2 variables of interest. The first variable is supposed to take a value in the range 0.95 to 1.05 and the second in the range 0 to 1500. An LHC sample can be acquired for any given ranges of two (or more) variables, but these particular choices mean this illustration is an application for the example that will be detailed in Section 5.3.1.

As the desired sample size is 6, Figure 5.1 (a) shows how first each axis is divided into 6 intervals. Figure 5.1 (b) then illustrates how the sample is taken such that exactly one value in the sample lies in each row and column of the axes. Using the centre point of each of these intervals is known as Lattice sampling [101].

It is not necessary for each point to lie in the centre of the grid. For example, the LHC sample of Figure 5.1 (b) could be used to identify which interval each point of the sample lies in. Then, a uniform sample within that interval could be taken to determine the actual values of the sample. Such a sample is illustrated in Figure 5.1 (c), where the points lie in the same row and column as Figure 5.1 (b), but the points have been randomly sampled (from a uniform distribution) within those intervals.

The Latin hypercube sample gives the input values to be used when simulating training runs, which in turn are used to fit the emulator model. An appropriate number of training runs must be selected and is considered in Sections 5.3.3 and 6.1.3 by considering how the predictive power of a fitted model varies with the size of the LHC sample used.

A potential flaw of LHC sampling is that it is possible for the values of the variables to be highly correlated, which would give a sparse coverage of the sample space. This is illustrated in Figure 5.2, which shows a 6 point sample. This is still technically an LHC sample as each row and column contains exactly one point, but the coverage of the space is very poor in comparison to that of Figure 5.1 (c).

As a result, there are many methods available which can reduce the pairwise correlation between variables in an LHC sample, to give a better coverage of the sample space. For example, [76] consider using a Cholesky decomposition to transform the sample to reduce correlation between the variables, [11] propose two genetic algorithms to

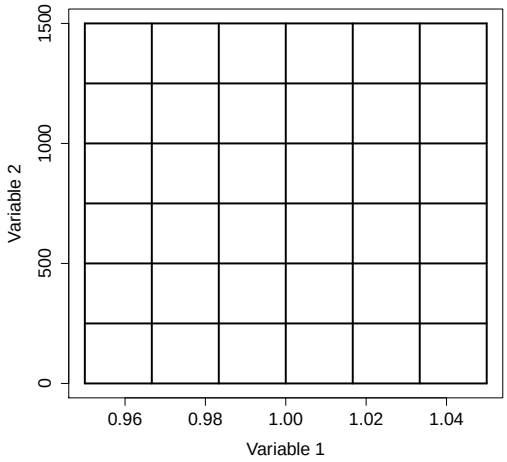

(a) Plot to illustrate how the Latin hypercube sample first breaks the hyper-rectangle into n intervals.

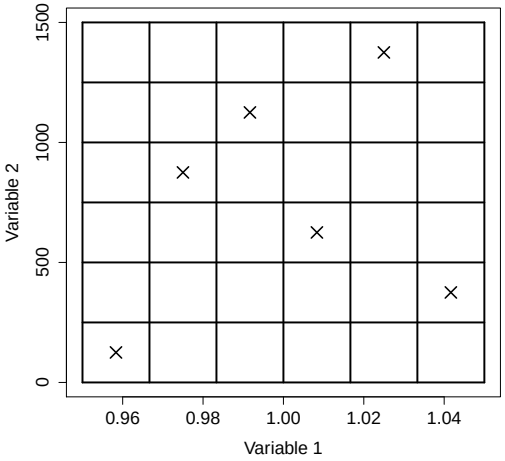

(b) Plot to illustrate a possible Latin hypercube sample of size 6.

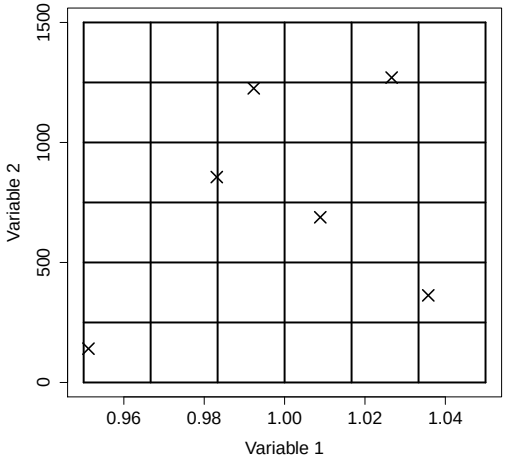

(c) Plot to illustrate an alternative possible Latin hypercube sample of size 6.

Figure 5.1: Plots to illustrate how to take Latin hypercube samples.

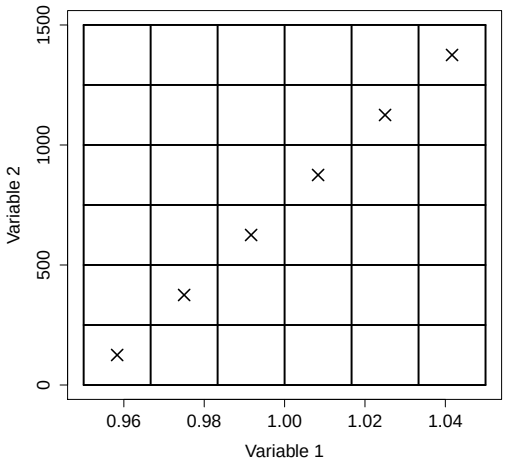

Figure 5.2: Plot to illustrate a poor Latin hypercube sample.

improve the Latin hypercube sample and [99] detail how orthogonal sampling could be used, which would divide the sample space into several subspaces, and take separate LHC samples in each subspace. A very simple alternative would be to simply take many LHC samples, calculate pair-wise correlation values between the values of the sample and then actually simulate training runs with the LHC sample which gives the smallest pair-wise correlation. Another common, simple alternative is to take many LHC samples and select the sample with the maximum minimum distance between points [74, 98, 23].

Latin hypercubes are very advantageous in comparison to grids (i.e. evenly distributed points over a given range). First, a more dense coverage of the region sampled is given, in the sense that a wider range of values of the variables is taken. For example, Figure 5.3 (a) illustrates a sample of size 16 when using a 4 by 4 grid to determine the input values of training runs, whilst Figure 5.3 (b) illustrates a 16 point LHC sample. For the grid, only 4 unique values are used of each variable (repeated 4 times), whereas for the 16 point Latin hypercube sample 16 unique values are sampled for each variable. The problem is even worse in higher dimensions. For example, in 3 dimensions a 4 by 4 by 4 grid would would use 64 points, though each variable would consider only 4 unique values (which would have each value repeated 16 times for other points in the sample). However, in Latin hypercube sampling a sample of size 64 would use 64 unique values for each variable, which should allow models to give a better fit.

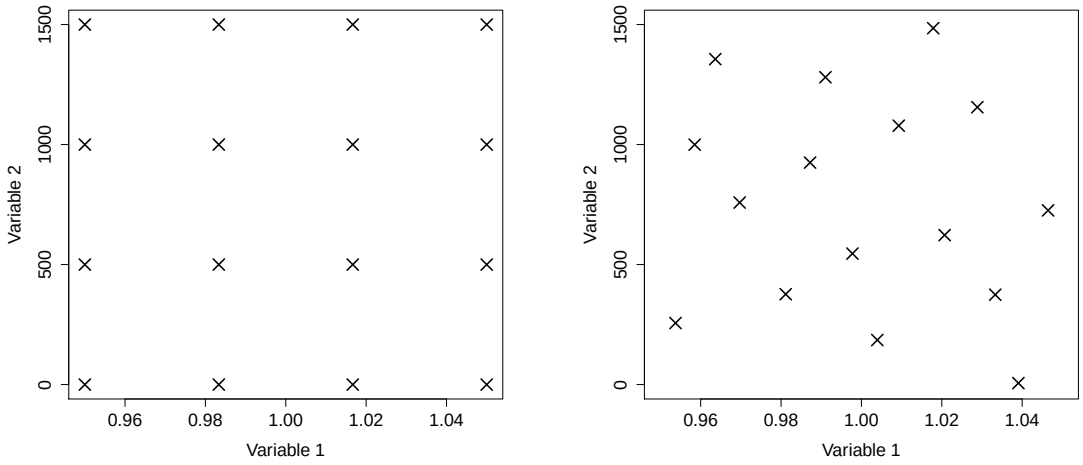

(a) Plot to illustrate points which form a 4 by 4 grid.

(b) Plot to illustrate a 16 point LHC sample.

Figure 5.3: Plots to compare a Latin hypercube sample to a grid of points.

In addition, the structure of a grid can be very limiting to the sample sizes that can be considered. For example, in 3 dimensions a 4 by 4 by 4 grid would use 64 points, whereas a 5 by 5 by 5 grid would use 225 points. However, an LHC sample can be of any size we desire. Further, grid sizes increase exponentially with dimension, whereas this is not necessarily the case for LHC samples.

5.2.5 Estimation of Expected Costs Under Uncertainty

The expectation of a function of a continuous random variable is calculated as the integral of the product of the function and the probability density function (PDF) of the random variable. Applying this to emulation, if the PDF of the distribution of the uncertain variables (i.e. $v_1, ..., v_{N_v}$) was known to be $p(v_1, ..., v_{N_v})$, the estimate of expected total costs under uncertainty for a given decision, $\mathbf{d}^* = d_1^*, ..., d_{N_d}^*$, is

$$\tilde{F}_T(d_1^*, ..., d_{N_d}^*) = \int_{v_1,...,v_{N_v}} \tilde{f}_T(v_1, ..., v_{N_v}, d_1^*, ..., d_{N_d}^*) \times p(v_1, ..., v_{N_v}) \mathrm{d}v_1 ... \mathrm{d}v_{N_v} \quad (5.2.16)$$

where $\tilde{f}_T(v_1, ..., v_{N_v}, d_1^*, ..., d_{N_d}^*)$ is the estimated response of the fitted emulator model (i.e. the estimate of total costs from the fitted emulator model for the examples considered in this thesis) for given values of variables containing uncertainty, $v_1, ..., v_{N_v}$, and decision variables, $d_1^*, ..., d_{N_d}^*$.

In real world problems, such as the constraint cost problem presented, the PDF of the uncertain variables is often not assessed exactly. In particular, in cases such as this, assessment of uncertainty in the planning background relies to a large extent on expert judgment [25, 34], and in a Bayesian formulation the prior judgment of uncertainty should be expressed as a PDF of the variables $v_1, ..., v_{N_v}$. The expected total costs under uncertainty can then be estimated as in Equation 5.2.16, where $p(v_1, ..., v_{N_v})$ would represent the prior judgement of the expert expressed as a PDF. Examples of prior beliefs for the constraint cost problem are given in Sections 5.3.1 and 6.1.3.

When making a decision it is often desirable to identify the value of the decision variable which minimises/maximises (as appropriate) Equation 5.2.16, as an estimate of the optimal decision to be made.

5.2.6 Credible Intervals for Cost Estimates from Emulators

As mentioned in Section 5.2.1, uncertainty exists in the fitted emulation model itself. Recall, the polynomial portion of the model, $\tilde{f}_{T_1}$, has model parameters $\boldsymbol{\beta}$. Our beliefs about the values of these parameters are modelled as a multivariate normal distribution with mean $\hat{\boldsymbol{\beta}}$, estimated via Equation 5.2.5, and covariance matrix $cov(\hat{\boldsymbol{\beta}})$, estimated via Equation 5.2.7.

To model the variation in the fitted emulator model, a new set of parameters, $\hat{\boldsymbol{\beta}}_r$, could be randomly drawn from the multivariate normal distribution with mean $\hat{\boldsymbol{\beta}}$ and covariance matrix $cov(\hat{\boldsymbol{\beta}})$. The estimated response of $\tilde{f}_{T_1,r}(\mathbf{x})$ (the resulting polynomial model using parameters $\hat{\boldsymbol{\beta}}_r$ instead of $\hat{\boldsymbol{\beta}}$) for given input can be calculated by replacing $\hat{\boldsymbol{\beta}}$ with $\hat{\boldsymbol{\beta}}_r$ in Equation 5.2.9, such that the estimated response of $\tilde{f}_{T_1,r}(\mathbf{x})$ at $\mathbf{x}_o$ (where $\mathbf{x}_{op}^{\mathrm{T}}$ details the form of the polynomial at $\mathbf{x}_o$ as outlined in Section 5.2.2) is

$$\tilde{f}_{T_1,r}(\mathbf{x}_o) = \mathbf{x}_{op}^{\mathrm{T}} \hat{\boldsymbol{\beta}}_{\boldsymbol{r}} \tag{5.2.17}$$

Corresponding residuals of this randomly drawn polynomial model can then be calculated as

$$\varepsilon_r(\mathbf{x}) = y_T(\mathbf{x}) - \tilde{f}_{T_1,r}(\mathbf{x})$$

The methodology of Section 5.2.3 could then be used to fit a Gaussian process model

to model ε_r based on $\mathbf{x}$, with $\tilde{f}_{T_2,r}(\mathbf{x})$ denoting this Gaussian process model.

A random variation of the emulator model could thus be the sum of the polynomial model with a random draw of parameters and the corresponding Gaussian process fitted to the resulting residuals such that:

$$\tilde{f}_{T,r}(v_1, ...v_{N_v}, d_1, ..., d_{N_d}) = \tilde{f}_{T_1,r}(v_1, ...v_{N_v}, d_1, ..., d_{N_d}) + \tilde{f}_{T_2,r}(u_1, ...u_{N_v}, d_1, ..., d_{N_d}) \tag{5.2.18}$$

However, such variations in the model parameters can have a large effect on the fitted model. Further, using $\tilde{f}_{T,r}$ instead of $\tilde{f}_T$ in Equation 5.2.16 could also have a large effect on the estimated expected total costs under uncertainty. By carefully considering how the cost estimates vary as the model parameters are varied, credible bounds can be formed which give a range in which we would expect the expected total costs to lie for a given level of confidence.

To do this, consider creating a randomly drawn model, $\tilde{f}_{T,r}$, as described above. For a given decision, $d_1^*, ..., d_{N_d}^*$, an estimate of expected response using the randomly drawn model can be calculated by integrating over uncertainties, as in Equation 5.2.16, as:

$$\tilde{F}_{T,r}(d_1^*, ..., d_{N_d}^*) = \int_{v_1,...,v_{N_v}} \tilde{f}_{T,r}(v_1, ..., v_{N_v}, d_1^*, ..., d_{N_d}^*) \times p(v_1, ..., v_{N_v}) \mathrm{d}v_1 ... \mathrm{d}v_{N_v} \tag{5.2.19}$$

By considering how $\tilde{F}_{T,r}(d_1^*, ..., d_{N_d}^*)$ varies with the randomly drawn models, credible intervals can be formed for $\tilde{F}_T(d_1^*, ..., d_{N_d}^*)$. To do this, suppose a large number of models, N_r, have been randomly drawn and an $\alpha\%$ credible interval is desired. Such an interval could be formed by taking the lower bound as the value which $\frac{100-\alpha}{2}\%$ of the $\tilde{F}_{T,r}(d_1^*, ..., d_{N_d}^*)$ are less than, and the upper bound as the value which $\frac{100-\alpha}{2}\%$ of the $\tilde{F}_{T,r}(d_1^*, ..., d_{N_d}^*)$ are greater than. It is convenient to label the lower and upper bounds as $\tilde{F}_{T,L}(d_1^*, ..., d_{N_d}^*)$ and $\tilde{F}_{T,U}(d_1^*, ..., d_{N_d}^*)$ respectively.

Section 6.2 will later detail how the credible bounds of the estimates from emulation can be used to reduce the range of values considered for the decision variables. This in turn allows for a second, more accurate emulator model to be fitted over a smaller range of values of the decision variables, which increases confidence in the estimates and allows for a better decision to be made.

5.3 Application of Emulation to a Simple Example

5.3.1 Details of the Example

This section will give an initial, simple example to illustrate how emulators can be used to approximate how input affects output of simulators. Further, it will illustrate how the resulting emulators can be used to make decisions which account for the uncertainty which exists in the input to the simulator.

Section 3.7.2 stated that it is common practice to estimate constraint costs for a given period of time using a power system background of a single future year. This example will therefore use a single future year to estimate constraint costs, with that year being year 1 from [69] (recall this is National Grid's freely available online reference which gives projections for all aspects of Britain's power system over a 20 year period). Section 7.6 will consider how cost estimates and the resulting estimates of optimal decisions are affected by using multiple future years to estimate constraint costs.

The initial example will consider treating just one variable of the simulator as containing uncertainty (i.e. $v_1, ..., v_{N_v}$ is just a single variable, v) and making just one decision (i.e. $d_1, ..., d_{N_d}$ is just a single variable, d). The variable containing uncertainty, v, is the peak demand level of the power system. The decision variable is the reinforcement magnitude of the B15 boundary. Section 3.7.1 indicated that reinforcing the B15 boundary can greatly reduce costs in year 1, and Section 3.7.2 showed how peak demand level has a large effect on the estimated constraint costs in year 1. This makes these particular variables suitable for this initial investigation.

Recall from Section 3.7.2, v will not explicitly specify the peak demand level of the power system. Instead, v will specify a magnification of the peak demand level projected by [69] (which gives equivalent results to working directly with peak demand level). For example, if the peak demand level of a year was 10000 MW, a peak demand magnification of 1.15 would mean increasing the peak demand level to
10000 MW $\times 1.15 = 11500$ MW. Under this model, a value of $v = 1$ would represent the peak demand level projected by [69].

The objective is therefore to form an emulator model, $\tilde{f}_T(v, d)$, which accurately approximates how the input values of v and d affect the output of $f_T(v, d)$ (i.e. the

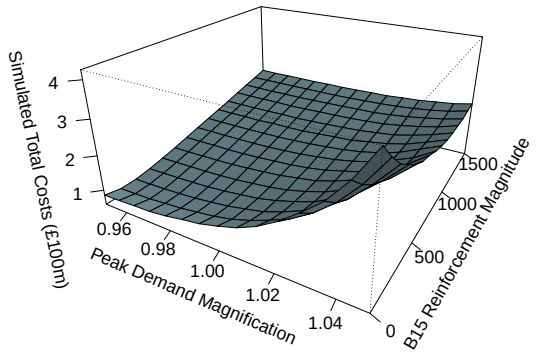

Figure 5.4: Plot to show how total costs calculated using the simulator vary with peak demand magnification and B15 reinforcement magnitude.

simulator of total costs of the power system).

It will be assumed that the peak demand level realised can differ from the projected peak demand level from [69] by 5% (i.e. the peak demand could be between 95% and 105% of the projection given in [69], meaning v takes a value between 0.95 and 1.05) and that the B15 boundary reinforcement can be between 0 and 1500 MW (i.e. d can take a value between 0 and 1500).

5.3.2 Sensitivity of the Simulator

Figure 5.4 illustrates how the simulated total costs (mean constraint costs plus reinforcement costs) varies with peak demand magnification and B15 reinforcement magnitude. It can be seen that if B15 reinforcement magnitude is low, total costs steeply rise as peak demand magnification rises. However, as B15 reinforcement magnitude rises, there is much less variation in total costs as peak demand magnification is varied. The total costs simulated for high peak demand magnifications initially begin to fall as B15 reinforcement magnitude is increased (indicating that the decrease in mean constraint costs outweighs the cost of the reinforcement), though as B15 reinforcement magnitude is increased even further, total costs level out and even begin to rise again. This would indicate that, for high levels of B15 reinforcement magnitude, the benefits from the reduction in constraint costs is outweighed by the expenditure of the reinforcement.

5.3.3 Constructing an Emulator

Selection of an Appropriate Emulator Model

Once an appropriate problem to consider has been identified (i.e. decision variables and variables containing uncertainty of interest) an emulator must be constructed to accurately approximate how the input values of the variables of interest affect the output of the simulator. There are two aspects to consider: the number of training runs used to construct the emulator model and the emulator model fitted to those training runs.

Section 5.2.1 indicated this thesis will use an emulator model which uses a polynomial regression model with a Gaussian process model applied to smooth the residuals of the resulting polynomial model.

For the problem outlined in Section 5.3.1, Table 5.1 shows how the R^2 value of the polynomial portion of the emulator model varies with the polynomial model fitted and number of training runs used to fit the emulator model. Table 5.2 gives details of the terms included in the polynomial regression portion of the emulator models considered.

For every polynomial degree it can be seen that the R^2 value is much greater when including interaction terms in comparison to when not. This indicates that it is important to include these terms in order to accurately model the output of the simulator. This is supported by Figure 5.4 which clearly shows an interaction between peak demand magnification and B15 reinforcement magnitude. It also appears that a polynomial with second degree terms of v and d and interactions between terms of equal degree (polynomial 4) is sufficient, with little improvement in R^2 when including 3rd degree terms of v and d (polynomials 5 and 6).

It also appears as if sample size (the number of training runs used) has little effect on the value of R^2. This is to be expected, as R^2 is a measure of how well a given model fits a set of data, and not necessarily a measure of how well it predicts a response outside of the training data.

This indicates a limitation of using R^2 alone as a measure of goodness of fit of the emulator. A further limitation is the R^2 value gives no indication of the predictive power of the full emulator model, $\tilde{f}_T$, which also includes the Gaussian process model

Training Run Sample Size	25	50	100	200	300
Polynomial 1	0.7547	0.6908	0.6499	0.6557	0.6380
Polynomial 2	0.8819	0.8267	0.7931	0.7865	0.7807
Polynomial 3	0.8616	0.8044	0.7558	0.7462	0.7511
Polynomial 4	0.9840	0.9671	0.9504	0.9508	0.9438
Polynomial 5	0.8715	0.8203	0.7657	0.7560	0.7606
Polynomial 6	0.9884	0.9745	0.9622	0.9631	0.9579

Table 5.1: Table detailing how the R^2 value of the polynomial portion of the fitted emulator model varies with polynomial model fitted and sample size of training runs.

Polynomial Model	Model Description
Polynomial 1	$\beta_0 + \beta_1 v + \beta_2 d$
Polynomial 2	$\beta_0 + \beta_1 v + \beta_2 d + \beta_3 vd$
Polynomial 3	$\beta_0 + \beta_1 v + \beta_2 d + \beta_3 v^2 + \beta_4 d^2$
Polynomial 4	$\beta_0 + \beta_1 v + \beta_2 d + \beta_3 v^2 + \beta_4 d^2 + \beta_5 vd + \beta_6 v^2 d^2$
Polynomial 5	$\beta_0 + \beta_1 v + \beta_2 d + \beta_3 v^2 + \beta_4 d^2 + \beta_5 v^3 + \beta_6 d^3$
Polynomial 6	$\beta_0 + \beta_1 v + \beta_2 d + \beta_3 v^2 + \beta_4 d^2 + \beta_5 v^3 + \beta_6 d^3 + \beta_7 vd + \beta_8 v^2 d^2 + \beta_9 v^3 d^3$

Table 5.2: Table which describes the terms included in the polynomial portion of the emulator model.

applied to smooth the residuals of the polynomial regression model. Therefore, a secondary criteria must be used in order to assess the predictive power of a fitted model for values where training data was unavailable.

As mentioned in Section 5.2.1, for this thesis this involves simulating a second set of training data. Suppose n_2 is the sample size of this second set of training data, such that $y_{2,i}$ is the response of the ith simulation in this second set of training data and $\mathbf{x}_{2,i}$ are the values of the input variables for this second set of training data. A measure of the predictive power of the full emulator model (both the polynomial regression model and the Gaussian process model applied to its residuals) fitted to the first set of training data, $\tilde{f}_T$, can then be acquired as

$$P = \frac{1}{n_2} \sum_{i=1}^{n_2} (y_{2,i} - \tilde{f}_T(\mathbf{x}_{2,i}))^2 \tag{5.3.1}$$

This would represent the mean squared error of estimating the response of the second dataset from the emulator model fitted to the first dataset, and a smaller value of P

would indicate a greater level of predictive power.

It may also be useful to normalise this value by the variance in the response of the second sample, i.e.

$$\tilde{P} = \frac{P}{var(\mathbf{y}_2)} \tag{5.3.2}$$

This would represent a measure of the predictive power of the fitted emulator normalised by the predictive power of the sample mean of the response of the second set of training data. Again, smaller values of $\tilde{P}$ indicate a greater level of predictive power of $\tilde{f}_T$.

Training Run Sample Size	25	50	100	200	300
Polynomial 1	3.862×10^{14}	2.827×10^{14}	2.095×10^{14}	3.958×10^{13}	2.522×10^{13}
Polynomial 2	2.469×10^{14}	1.823×10^{14}	1.218×10^{14}	1.235×10^{13}	1.280×10^{13}
Polynomial 3	3.515×10^{14}	2.453×10^{14}	1.856×10^{14}	3.401×10^{13}	2.448×10^{13}
Polynomial 4	2.050×10^{14}	8.546×10^{13}	4.844×10^{13}	6.252×10^{12}	5.457×10^{12}
Polynomial 5	3.417×10^{14}	2.435×10^{14}	1.753×10^{14}	3.729×10^{13}	2.215×10^{13}
Polynomial 6	2.094×10^{14}	9.284×10^{13}	5.161×10^{13}	7.680×10^{12}	6.506×10^{12}

Table 5.3: Table detailing how the value of P of the fitted model varies with model fitted and sample size.

Training Run Sample Size	25	50	100	200	300
Polynomial 1	0.1547	0.1133	0.08391	0.01586	0.01011
Polynomial 2	0.09895	0.07307	0.04882	0.004950	0.005128
Polynomial 3	0.1409	0.09831	0.07437	0.01363	0.009809
Polynomial 4	0.08216	0.03425	0.01941	0.002505	0.002187
Polynomial 5	0.1369	0.09719	0.07026	0.01494	0.008880
Polynomial 6	0.08393	0.03720	0.02068	0.003072	0.002607

Table 5.4: Table detailing how the value of $\tilde{P}$ of the fitted model varies with model fitted and sample size.

Table 5.3 displays how the value of P varies with the form of the polynomial portion of the emulator model (with a Gaussian process then applied to the residuals of that polynomial) and number of training runs used to fit the model, with Table 5.4 displaying the same information when the value of P has been normalised by the variance in the response in the second set of training data. All results in this table were acquired by comparing how well the fitted models estimated the response of a second sample

of training data of size 50. First, it is noted that the information in this table also supports the previous observation that it is important to include the interaction terms in the polynomial model.

For this example, it is also noted that the predictive power of the model does increase when using 200 training runs over 25, 50 or 100 training runs, though there appears to be little benefit in using additional training runs beyond this. Also, there does not appear to be a benefit from using a polynomial model which includes third degree terms of v and d over one which only includes second degree terms of v and d, with the table even suggesting that for larger sample sizes (200 or greater) the models give a slightly poorer fit when including these additional terms.

For this initial example, the fitted emulator model will use a polynomial which includes second order terms of v and d and interactions between equal powers of v and d (i.e. polynomial 4 from Table 5.2) as the polynomial regression portion of the emulator, with a Gaussian process applied to the residuals of this model as outlined in Section 5.2.1. This emulator will be fitted using 200 training runs.

However, it is noted that it cannot therefore be assumed that 200 training runs and a polynomial of the form of polynomial 4 from Table 5.2 is appropriate to use for any example of using an emulator to approximate a simulator to be considered. Each time a new problem is considered (which may vary the simulator used, the variables which are assumed to contain uncertainty and/or the decision variables considered) it is required that an appropriate number of training runs and an appropriate polynomial portion of the emulator model be identified. This will be demonstrated in Section 6.1.3 and Appendices B.1, C.3 and D.1, which consider fitting emulator models for the examples of Chapters 6, 8 and 9, where the number of training runs identified to be used to fit the emulator models varies between 50 and 300, and the optimal form of the polynomial model (i.e. how high a degree and which interactions, if any, to include) is also shown to vary with the example considered.

Comparing the Fitted Emulator Model to the Simulator

Figure 5.5 illustrates fitted emulator models (i.e. the sum of fitted polynomial regression model and a Gaussian process model applied to its residuals) when using 50, 200

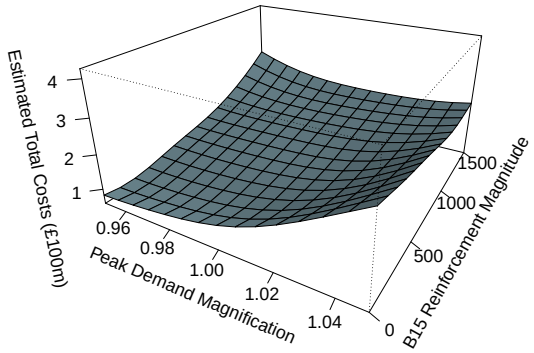

(a) 50 training runs

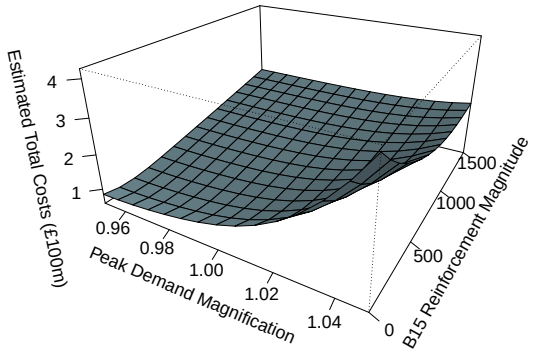

(b) 200 training runs

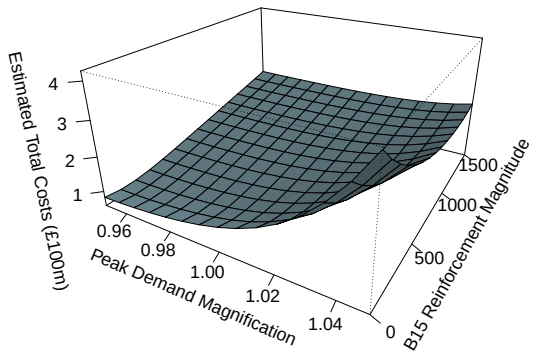

(c) 300 training runs

Figure 5.5: Plots to show how estimates of total costs from the fitted emulator models vary with peak demand magnification and B15 reinforcement magnitude.

or 300 initial training runs and using a polynomial of the form Polynomial 4 from Table 5.2 for the polynomial portion of the emulator model. By comparison to Figure 5.4 (the equivalent plot using the simulator), it is seen that all of these models are reasonably good approximations to the simulator.

However, it can be seen that fitting a model using just 50 training runs tends to under-estimate costs when peak demand magnification is high and B15 reinforcement magnitude is low, whilst over-estimating costs when peak demand magnification is low and B15 reinforcement magnitude is high. The model which uses 200 training runs shows a noticeable improvement over the model using 50 training runs in these two areas, being a very good approximation to the simulator. Comparing the use of 300 to 200 initial training runs shows little difference between these two models, though the model using 300 training runs is slightly better than the model using 200 training runs when peak demand magnification is very high and little to no B15 reinforcement has been made.

These results are what one would expect from Table 5.3, which show the predictive power of an emulator model increases with number of training runs used to fit the model up to 200 training runs, with little improvement beyond this.

Figure 5.6 illustrates how cost estimates from the emulators differ from the estimates from simulation when using 50, 200 or 300 simulations to fit the emulator model, to support the conclusions reached about Figure 5.5. As can be seen, when using only 50 training runs the total costs are considerably under-estimated when B15 reinforcement is low and peak demand magnification is high, and considerably over-estimated when B15 reinforcement magnitude is high and peak demand magnification is low.

Using 200 training runs to fit the emulator model also appears to under-estimate costs when B15 reinforcement magnitude is low and peak demand magnification is very high, though the difference between the emulator is 10 times less in comparison to when using only 50 training runs to fit the emulator. Using 300 training runs to fit the emulator model decreases the difference between the emulator and simulator even further.

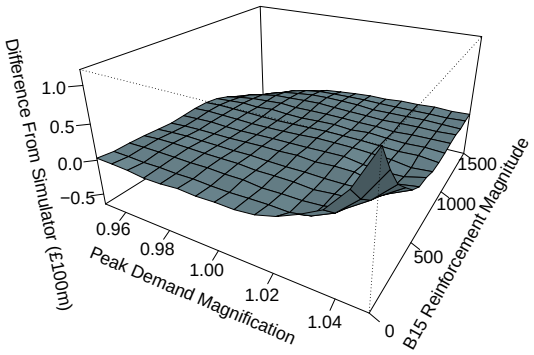

(a) 50 training runs

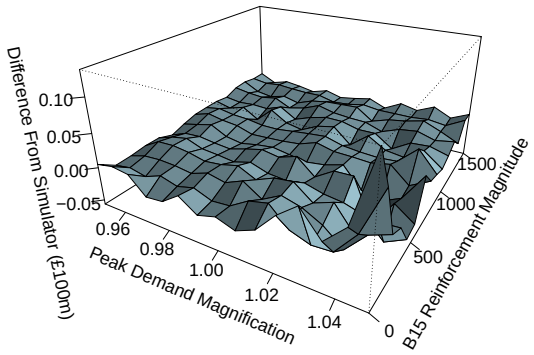

(b) 200 training runs

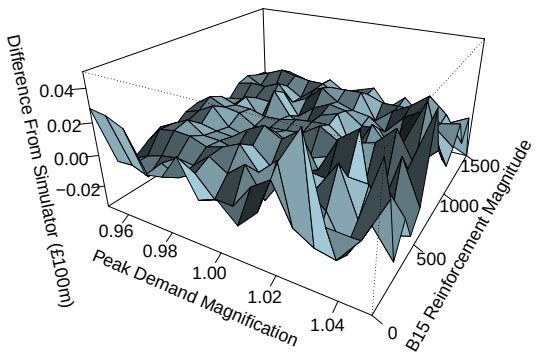

(c) 300 training runs

Figure 5.6: Plots to show how differences between calculations from simulation and estimates from the fitted emulator models vary with peak demand magnification and B15 reinforcement magnitude.

5.3.4 Expected Total Cost Estimation Under Uncertainty

Section 5.2.5 detailed how to estimate expected total costs under uncertainty using an emulator. This requires an emulator model and a set of prior beliefs which describe a probability density function for the variables containing uncertainty.

For this initial example, there is one variable containing uncertainty, the peak demand magnification. Section 5.3.1 stated the peak demand level would be modelled as having a value between 95% and 105% of the value projected by [69] (i.e. peak demand magnification between 0.95 and 1.05). However, no distribution for the value taken was specified.

For this initial example, a uniform distribution between 0.95 and 1.05 will be used to represent prior beliefs about peak demand magnification, $p(v)$. That is to say, for the initial example, any value of peak demand level between 95% and 105% of the projection given by [69] will be deemed equally likely to be observed, but any value outside of that range will be deemed impossible to occur. This uniform distribution is simple, but it is also consistent with the interpretation of expert judgement that will be used when a more complicated example is presented in Section 6.1.

Figure 5.7 displays how the estimate of expected total costs under uncertainty varies with reinforcement magnitude when these prior beliefs are used in combination with the emulator fitted using 200 training runs (the sum of the polynomial regression model plus the Gaussian process model applied to its residuals) from Section 5.3.3 in Equation 5.2.16 of Section 5.2.5. Figure 5.7 (a) shows how the estimate of expected total costs from the fitted emulator model varies with B15 reinforcement magnitude, whereas Figure 5.7 (b) illustrates 95% credible intervals for the estimates of expected total costs as B15 reinforcement magnitude is varied. In Figure 5.7 (b), each grey curve represents the expected total costs estimated when using a random variation of the fitted emulator model using the methodology outlined in Section 5.2.6.

Initially, estimates of expected total costs decrease with reinforcement magnitude as the increased transmission capacity greatly reduces expected mean constraint costs. However, estimates of expected total costs eventually begin to rise again. This is due to the rate of decrease of expected mean constraint costs decreasing with each additional MW of transmission capacity, and eventually the increase in reinforcement costs

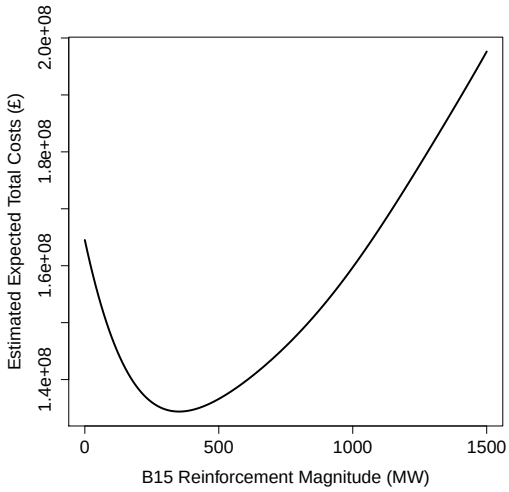

(a) Plot of how estimated expected total costs vary with B15 reinforcement magnitude.

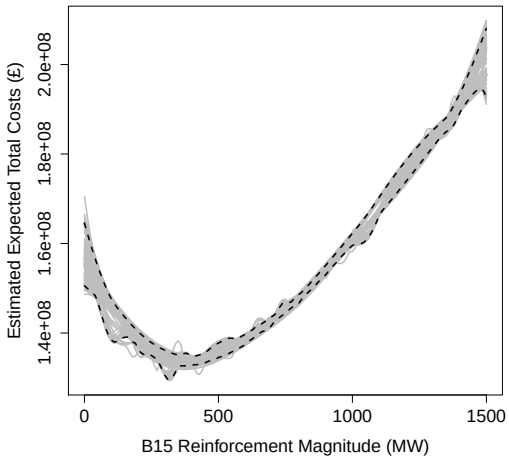

(b) Plot to illustrate how estimates of expected total costs vary with B15 reinforcement magnitude when using random variations of the fitted emulator model, with the resulting 95% credible bounds also illustrated.

Figure 5.7: Plot to show how estimated expected total costs vary with B15 reinforcement magnitude.

is greater than the decrease in expected mean constraint costs. For high reinforcement magnitudes the curve appears quite linear as the reduction in constraint costs from further reinforcement is very small, but reinforcement costs continue to increase linearly.

For this initial example the estimate of the optimal decision (i.e. the reinforcement magnitude which minimises the estimate of expected total costs) would be to increase the transfer capacity of the B15 boundary by 350 MW.

5.3.5 Diagnostic Test For Credible Bounds

Figure 5.7 (b) illustrates credible bounds for the estimates of expected total costs when integrating over uncertainty. However, it is possible that the credible intervals illustrated are too narrow or too wide (meaning error in the estimate may have been under or over estimated). Therefore, it is necessary to test how well credible intervals from randomly drawing the emulator model parameters act as intervals for the value acquired under simulation.

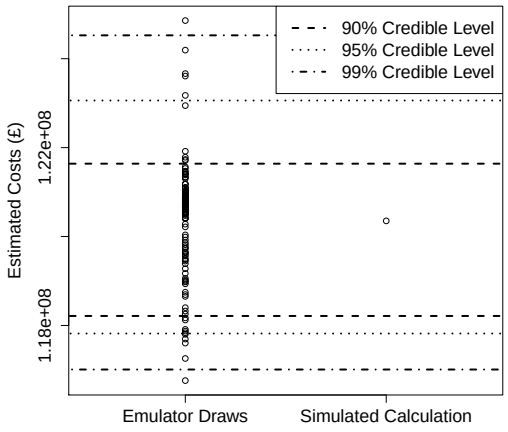

(a) Comparison of credible intervals to the calculation from simulation when assuming peak demand magnification of 0.9676 and B15 reinforcement of 739.5 MW.

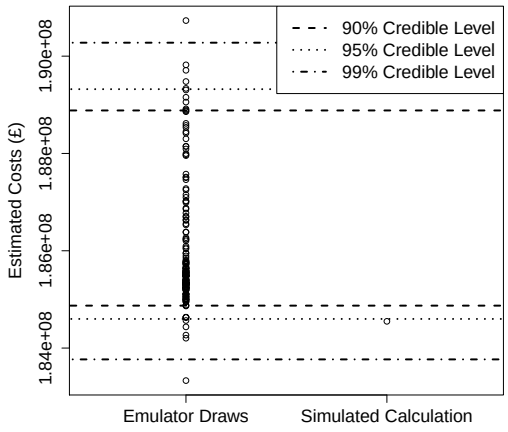

(b) Comparison of credible intervals to the calculation from simulation when assuming peak demand magnification of 1.0364 and B15 reinforcement of 862.7 MW.

Figure 5.8: Plots to compare credible intervals for estimates of total costs from the fitted emulator to the calculation of total costs from the simulator.

Figure 5.8 (a) displays how 200 randomly drawn emulator evaluations vary when assuming peak demand magnification of 0.9676 and B15 reinforcement of 739.5 MW, as well as the evaluation of total costs from the simulator. Credible intervals at the 90%, 95% and 99% level are shown for comparison, where 10%, 5% and 1% of the estimates from randomly drawn emulator models lie outside the respective credible intervals. As can be seen, the evaluation from the simulator lies between the credible bounds at all 3 credibility levels shown.

An equivalent plot is shown in Figure 5.8 (b), which compares estimates from randomly drawn emulator models and the calculation from the simulator for a peak demand magnification of 1.0364 and a B15 reinforcement magnitude of 862.7 MW. For these inputs, the simulated value is smaller than all but 4 of the 200 random draws from the emulator, and therefore lies between lower bounds of the 95% and 99% credibility intervals. This means that the value calculated from simulation would be contained in the credible interval for the estimated response at the 99% level, but not the 95% and 90% level.

In order to test how well the credible intervals model the error in the estimated response, full simulator evaluations were performed at 500 new sets of inputs, and credible bounds

were formed for each set of inputs based on the fitted emulator model. If these credible bounds are a good model for error in the estimation from emulation, it is expected that 495 of the simulated values (99%) will lie between the credible bounds at the 99% credibility level, 475 of the simulated values (95%) will lie between the credible bounds at the 95% credibility level and 450 of the simulated values (90%) of the simulated values will lie between the credible bounds and the 90% credibility level.

Credible Level	Expected Simulations Falling Into Credible Intervals	Observed Simulations Falling Into Credible Intervals
99%	495	491
95%	475	470
90%	450	438

Table 5.5: Table detailing how many of the simulated values lie in the credibility intervals of the estimate.

Table 5.5 details how many evaluations of the simulator lie in the credibility intervals for the estimates from the emulator in comparison to how many would be expected if the credibility bounds accurately model uncertainty in the estimated response from the emulator. As can be seen, the credibility bounds appear to be slightly too narrow, as fewer evaluations from simulation lie within them than would be expected. For example, at the 99% credibility level it would be expected that all but 5 simulated values are contained within the credible intervals, but in practice 9 of the simulated values did not lie within the credible intervals of the emulator.

The credibility intervals at the 95% and 90% levels also contain fewer simulator evaluations than would be expected, with the credibility bounds at the 95% level containing 470 in comparison to the expected 475, and the the credibility bounds at the 90% level containing 438 in comparison to the expected 450. This would suggest being slightly cautious when using the credibility bounds of Figure 5.7 (b), and acknowledging that the variation in the estimate is slightly under-estimated.

5.4 Sensitivity of the Estimate of Optimal Decisions From Emulation

The simple example of Section 5.3.3 has illustrated how emulation can be used to make decisions under uncertainty when working with expensive simulators. This simple example could be expanded by fitting the emulator over additional variables (such an example will be presented in Chapter 6). However, even without emulating over additional variables, there are other factors/assumptions which affect the estimates of expected total costs and the resulting decisions made. This section will illustrate how the estimated optimal decisions from the emulator are sensitive to three factors: the cost to reinforce, the attitude to risk of the decision maker and the prior beliefs used to quantify uncertainty.

5.4.1 Cost to Reinforce

As noted in Section 5.1, the initial assumption is that it costs £100,000 per MW to increase the transfer capacity between two zones (i.e. to reinforce the B15 boundary in the example presented), which is based on the assumption that it costs £1000 per MW per km to reinforce each boundary and assuming that each boundary between zones is 100 km thick. Based on our interpretation of discussions with Paul Plumptre (formerly of National Grid) [78], this was an appropriate cost of reinforcement to assume which is consistent with [5]. However, estimates of this cost vary, even within the same organisation, with [70] stating an appropriate value to be £750 per MW per km, whilst [95] state an appropriate value to be £1500 per MW per km. Such differences can have an obvious effect on cost estimates, which may in turn have an effect on the decision made.

Figure 5.9 displays how estimated expected total costs vary with B15 reinforcement magnitude for a variety of assumed costs to reinforce. As to be expected, the curves are very similar for low reinforcement magnitudes (where there are less reinforcement costs) but estimates vary greatly at higher levels of reinforcement. The reinforcement magnitude which gives the lowest estimate of expected total costs also appears to

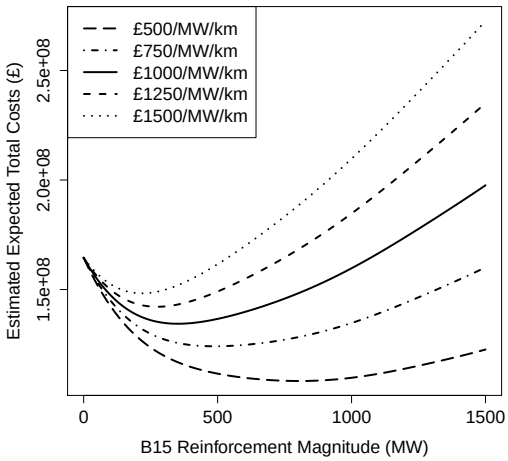

Figure 5.9: Plot to show how estimated expected total costs vary with B15 reinforcement magnitude and the assumed cost to reinforce.

Cost to Reinforce	Estimated Optimal B15 Reinforcement Magnitude
£500/MW/km	800 MW
£750/MW/km	490 MW
£1000/MW/km	350 MW
£1250/MW/km	270 MW
£1500/MW/km	220 MW

Table 5.6: Table detailing how the estimated optimal reinforcement magnitude of the B15 boundary varies with the assumed cost to reinforce.

change with cost to reinforce assumed, indicating the decision made is sensitive to the cost to reinforce assumed.

Table 5.6 details how the estimated optimal reinforcement magnitude (i.e. the reinforcement magnitude which minimises estimated expected total costs under uncertainty via Equation 5.2.16) varies with the assumed cost to reinforce. As can be seen, the estimated optimal decision is very sensitive to the assumed cost to reinforce, with a decrease of 130 MW (over 37.1%) when assuming a cost of £1500 per MW per km to reinforce (in comparison to when assuming a cost of £1000 per MW per km to reinforce), and more than doubling to 800 MW when assuming a cost of £500 per MW per km to reinforce.

Although it is reasonable to think that the cost of reinforcement can be known quite accurately at the time a decision is made, if poor information is available this could have

quite substantial consequences. For example, if the cost of reinforcement is assumed to be £500/MW/km then the expected total costs of the optimal reinforcement decision of 800 MW are estimated to be £108,000,000. However, if a reinforcement of 220 MW was built (from assuming the cost of reinforcement to be £1500/MW/km) when the actual cost of reinforcement is £500/MW/km, then the expected total costs of the decision are estimated to be £126,000,000, a 17% increase.

Conversely, if the cost of reinforcement is assumed to be £1500/MW/km then the expected total costs of the optimal reinforcement decision of 220 MW are estimated to be £148,000,000. However, if an 800 MW reinforcement was built due to the cost of reinforcement incorrectly being assumed to be £500/MW/km when the actual cost of reinforcement is £1500/MW/km, then the expected total costs of the decision would increase by an estimated 27% to £188,000,000.

5.4.2 Prior Beliefs

Initially, a uniform distribution between 0.95 and 1.05 was used to represent prior beliefs about the value of peak demand magnification. Figure 3.6 of Section 3.7.2 and Figure 5.4 of Section 5.3.2 illustrate how high levels of peak demand can greatly increase the costs estimated by the simulator.

The prior beliefs describe how plausible particular values of input variables (in this case peak demand magnification) are. If these prior beliefs were changed to give more or less weight to extreme values of these variables, this in turn could have a large impact on the decision made.

This section will consider how estimated expected total costs and the resulting estimates of optimal decision to be made would be affected if a uniform distribution to represent beliefs about the values peak demand magnification was fitted over a smaller or larger range. Two alternative sets of prior beliefs are considered: a narrow prior which fits a uniform distribution over the range 0.975 to 1.025 and a wide prior which fits a uniform distribution over the range 0.925 to 1.075 for peak demand magnification.

Figure 5.10 displays how estimated expected total costs vary with reinforcement magnitude and prior beliefs when assuming a cost of £1000 per MW per km to reinforce,

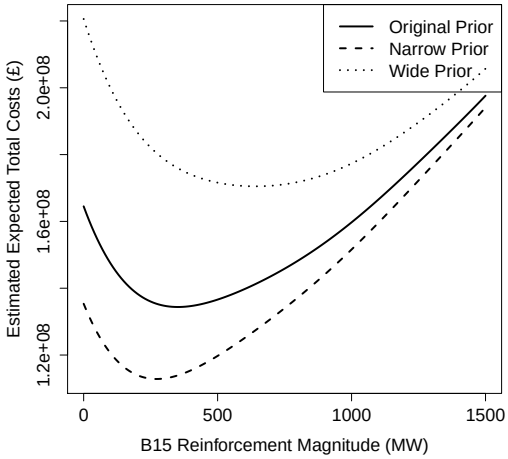

Figure 5.10: Plot to show how estimated expected total costs vary with B15 reinforcement magnitude and prior beliefs.

Prior Beliefs	£500/MW/km	£1000/MW/km	£1500/MW/km
Narrow Prior	510 MW	270 MW	170 MW
Original Prior	800 MW	350 MW	220 MW
Wide Prior	1130 MW	640 MW	330 MW

Table 5.7: Table detailing how the estimated optimal reinforcement magnitude of the B15 boundary varies with prior beliefs and the assumed cost of reinforcement.

and Table 5.7 shows how the estimated optimal decision varies with both prior beliefs and the assumed cost to reinforce. From Figure 5.10 it can be seen that the prior beliefs about the uncertain variable do have a noticeable effect on the costs estimated. Further, Table 5.7 shows how the prior beliefs assumed also have a quite large effect on the resulting estimates of optimal reinforcement decision, with an increase of 290 MW (82.9%) when assuming a wider set of prior beliefs (in comparison to when assuming the original prior) and a decrease of 80 MW (22.9%) when assuming a narrow set of prior beliefs and a cost of £1000 per MW per km to reinforce.

If the cost to reinforce was assumed to be the larger £1500 per MW per km, the decision made is less sensitive to the prior beliefs, with an increase of 110 MW (50%) when assuming the wide set of prior beliefs and a decrease of 50 MW (22.7%) when assuming the narrow set of prior beliefs. When a smaller cost to reinforce is assumed, reinforcement decreases by 290 MW (36.3%) if the narrow prior is assumed over the original and increases by 330 MW (41.3%) if the wide prior is assumed over the original.

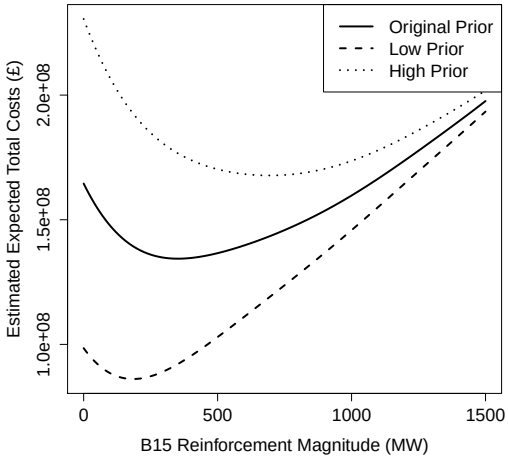

Figure 5.11: Plot to show how estimated expected total costs vary with B15 reinforcement magnitude and prior beliefs.

However, the prior beliefs of both of these alternatives have the same distribution centre (at 100% of the projected peak demand level). An alternative would be to use a set of prior beliefs which are not centred around the projected peak demand level. Therefore, two further alternative sets of prior beliefs are considered: a low prior which fits a uniform distribution over the range 0.95 to 1 and a high prior which fits a uniform distribution over the range 1 to 1.05 for peak demand magnification.

Prior Beliefs	£500/MW/km	£1000/MW/km	£1500/MW/km
Low Prior	300 MW	180 MW	110 MW
Original Prior	800 MW	350 MW	220 MW
High Prior	1130 MW	690 MW	390 MW

Table 5.8: Table detailing how the estimated optimal reinforcement magnitude of the B15 boundary varies with prior beliefs and the assumed cost of reinforcement.

Figure 5.11 displays how estimated expected total costs vary with reinforcement magnitude and prior beliefs when assuming a cost of £1000 per MW per km to reinforce, and Table 5.8 shows how the estimated optimal B15 reinforcement decision varies with both prior beliefs and assumed cost to reinforce. From Figure 5.11 it can be seen that these two alternative prior beliefs about the uncertain variable also have a noticeable effect on the costs estimated. Further, Table 5.8 indicates that these prior beliefs have a greater effect on decision made in comparison to those considered in Table 5.7.

The largest increase in reinforcement (in comparison to when assuming the original

prior) comes from assuming the high prior and a cost of £1000 per MW per km to reinforce, which increases B15 reinforcement by 340 MW (97.1%). The largest decrease in reinforcement (again, in comparison to when assuming the original prior) is 500 MW (62.5%) which is observed when assuming the low prior and a cost of £500 per MW per km to reinforce.

5.4.3 Attitude to Risk

Attitude to Risk: Methodology

So far, the methodology of Section 5.2.5 has been used to estimate optimal reinforcement decisions to be made by minimising Equation 5.2.16 (the estimate of expected total costs under uncertainty) for a given emulator model, $\tilde{f}_T(\mathbf{v}, \mathbf{d})$, and given prior beliefs about uncertainties, $p(v_1, ..., v_{N_v})$.

However, it is often desirable to take an attitude to risk into account when making planning decisions, as investors commonly place more weight on avoiding extreme negative outcomes (e.g. very large total costs) than positive benefits (e.g. lower expected total costs). An attitude to risk can be taken into account by applying a loss function, l, which represents the decision maker's attitude to risk to the total cost estimates from $\tilde{f}_T(v_1, ..., v_{N_v}, d_1, ..., d_{N_d})$ to give an estimate of the expected loss under uncertainty as

$$\tilde{F}_{T,l}(d_1, ..., d_{N_d}) = \int_{v_1,...,v_{N_v}} l(\tilde{f}_T(v_1, ..., v_{N_v}, d_1, ..., d_{N_d})) \times p(v_1, ..., v_{N_v}) \mathrm{d}v_1 ... \mathrm{d}v_{N_v} \quad (5.4.1)$$

Optimal decisions under an attitude to risk can then be identified as those which minimise the resulting estimate of expected loss (i.e. the values of decision variables $d_1, ..., d_{N_d}$ which minimise the value of $\tilde{F}_{T,l}(d_1, ..., d_{N_d})$).

The examples presented in this section will consider the loss function, l, to apply a power to the total costs such that

$$l(\tilde{f}_T(v_1, ..., v_{N_v}, d_1, ..., d_{N_d}), p) = \left(\tilde{f}_T(v_1, ..., v_{N_v}, d_1, ..., d_{N_d})\right)^p \quad (5.4.2)$$

where $\tilde{f}_T(v_1, ..., v_{N_v}, d_1, ..., d_{N_d})$ is the total cost estimate from the emulator and p is the power of the loss function. p=1 represents a risk neutral attitude, $0 < p < 1$ represents a risk prone attitude and $1 < p$ represents a risk averse attitude. In reality,

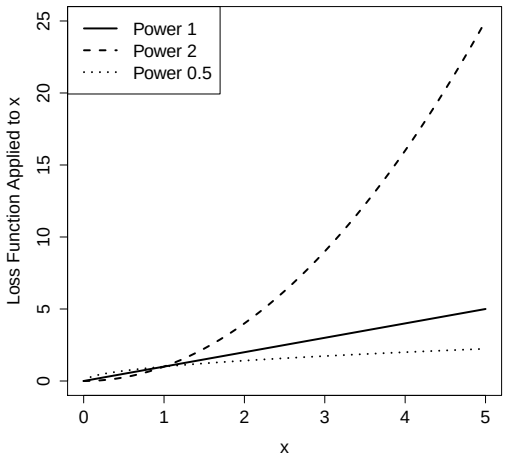

Figure 5.12: Plot to illustrate how the loss function varies with power, p, and the value it is applied to.

transmission expansion planners should never be risk prone due to the importance of maintaining a reliable electricity supply in society, though this section will provide an illustration of how a risk prone attitude affects decisions made.

The purpose of a loss function is to represent the decision maker's preference for potential outcomes. In the example presented, this means representing the decision maker's preference for different values of total costs.

For example, if p is set to 2 in Equation 5.4.2 (i.e. using a square loss function) this would penalise larger costs more than smaller ones (when the costs are greater than 1, which all costs considered are). This is illustrated in Figure 5.12, where the value of the loss function applied to costs increases much faster than the costs (costs are equivalent to the loss function of Equation 5.4.2 with $p = 1$) when using a square loss function. This would encourage the decision maker to make a decision which avoids large costs to minimise the expected square loss (even if this means increasing the expected costs).

Referring back to Figure 5.4, it can be seen that large total costs occur when peak demand magnification is high and B15 reinforcement magnification is low. This would mean that these large costs are penalised more severely than the low costs which arise when peak demand magnification is low. This would encourage the decision maker to make a larger B15 reinforcement under this attitude to risk as this avoids the large total costs which occur when peak demand magnification is high, even though this slightly

increases the total costs that occur when peak demand magnification is low (and in turn increases the resulting estimate of expected total costs under uncertainty).

Alternatively, if $p = 0.5$, larger costs would not be punished as severely in comparison to working directly with costs, which is again illustrated in Figure 5.12, where costs rise much more quickly than the loss function applied to the costs. As the large costs which occur when peak demand magnification is high are less severely penalised, this encourages the decision maker to make a smaller B15 reinforcement.

Attitude to Risk: Decisions

It would be interesting to provide a graphical comparison of how loss varies with reinforcement decision for different attitudes to risk. However, the losses which arise from applying a power to total costs, as is the case in Equation 5.4.2, would mean that these attitudes operate on very different scales (for example, under a risk neutral attitude, i.e. $p = 1$, costs operate on the order of 10^8 whilst a squared loss function, i.e. $p = 2$, results in losses which operate on the magnitude of 10^{16}). In order to provide a graphical comparison we could apply the inverse of the loss function to the resulting estimate of expected losses as:

$$l^{-1}(\tilde{F}_{T,l}(d_1^*, ..., d_{N_d}^*)) = \\ l^{-1}\left(\int_{v_1,...,v_{N_v}} l(\tilde{f}_T(v_1, ..., v_{N_v}, d_1^*, ..., d_{N_d}^*)) \times p(v_1, ..., v_{N_v}) \mathrm{d}v_1 ... \mathrm{d}v_{N_v}\right) \quad (5.4.3)$$

As the inverse of the loss function is applied after the integration, the shape (and resulting minimum) of how expected losses vary with reinforcement decision is preserved.

Figure 5.13 shows how the inverted expected loss varies with reinforcement magnitude for a variety of attitudes to risk. It is seen that the more risk averse the attitude, the higher the curve lies and the greater the magnitude of reinforcement of the minimum point. This indicates the more risk averse the position, the greater the estimated optimal magnitude of reinforcement.

Table 5.9 also compares how the estimated optimal decision to be made varies with both attitude to risk and the assumed cost to reinforce. As one would expect, the more risk averse the decision maker becomes the greater the reinforcement magnitude of the

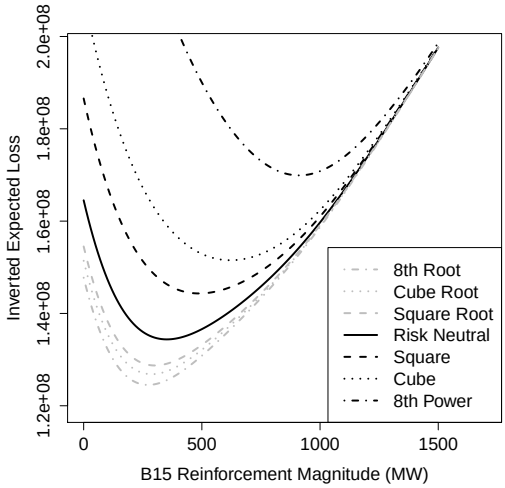

Figure 5.13: Plot to show how inverted expected losses vary with B15 reinforcement magnitude and attitude to risk.

Loss Function Power	£500/MW/km	£1000/MW/km	£1500/MW/km
$\frac{1}{8}$	590 MW	270 MW	170 MW
$\frac{1}{3}$	660 MW	290 MW	180 MW
$\frac{1}{2}$	710 MW	300 MW	190 MW
1	800 MW	350 MW	220 MW
2	920 MW	490 MW	300 MW
3	1000 MW	620 MW	390 MW
8	1240 MW	910 MW	690 MW

Table 5.9: Table detailing how the estimated optimal reinforcement magnitude of the B15 boundary varies with attitude to risk and assumed cost of reinforcement.

estimated optimal decision. For example, when assuming a cost of £1000 per MW per km to reinforce and taking the most risk averse attitude increases B15 reinforcement magnitude by 560 MW (over 160%) whereas the most risk prone position resulted in an 80 MW decrease in B15 reinforcement magnitude (over 22.8%) in comparison to the estimated risk neutral optimal.

Attitude to risk is observed to be a relevant factor to decision made as the assumed cost to reinforce is varied, with estimated optimal B15 reinforcement ranging from 170 MW when assuming the most risk prone position to 690 MW when assuming the most risk averse position when assuming a greater cost of £1500 per MW per km to reinforce, whereas estimated optimal B15 reinforcement ranges from 590 MW with the most risk prone position to 1240 MW with the most risk averse position when assuming the lower

cost of £500 per MW per km to reinforce.

Note, in the real life applications under-reinforcing the transmission system could have serious consequences, as this could lead to a significant chance of blackouts across the system (or very high constraint costs, which are the more direct concern in this thesis). As such, risk prone attitudes are extremely unrealistic for system planners. Therefore, for all risk prone attitudes give interesting results, they will not be considered in the further examples presented in this thesis.

Chapter 6

Emulating Over Multiple Waves as a Method to Solve a Typical Real World Transmission Expansion Planning Problem

Chapter 5 gave details on statistical emulation, the method in which an expensive function such as a simulator can be accurately approximated by a function which is computationally much less expensive to evaluate. A simple example was then presented in Section 5.3 to illustrate an application of this methodology. In this simple example, it was assumed that there was uncertainty in only a single variable and only a single decision was to be made.

Section 5.3.3 illustrated how the constructed emulator model was a very good approximation to the simulator with Sections 5.3.4 and 5.4 then showing how decisions can be made under uncertainty using the fitted emulator as an approximation to the simulator.

However, the problem considered was very simple, considering uncertainty in only a single variable whilst making only a single decision. This chapter will consider a more complicated transmission expansion planning problem, where multiple simultaneous reinforcement decisions are to be made whilst considering uncertainty in multiple simulator input variables. Further, an expert was consulted when formulating the problem

in an attempt to make the problem considered be somewhat representative of a typical problem a transmission expansion planner would consider.

For the example presented in Chapter 5, the full simulator could be approximated very accurately by an emulator over the variations considered in the variables of interest. However, as the problem that will be presented in this chapter fits an emulator to approximate the simulator over a larger number of variables, the approximation is less accurate. Therefore, additional methodology is required where the decision space can be reduced and a second emulator fitted over this reduced decision space. As the second emulator is fitted over a smaller range of values of the decision variables, this allows for the emulator to more accurately approximate the simulator over that range, which in turn allows for a better decision to be made. Sensitivities of the estimated optimal decision to various assumptions will also be presented.

6.1 Second Emulation Example: An Application to a Typical Real World Transmission Expansion Planning Problem

6.1.1 Details of the Transmission Expansion Planning Problem Considered

The example of decision making under uncertainty in this chapter will consider making two simultaneous decisions, i.e. $\mathbf{d} = (d_1, d_2)$, whilst considering uncertainty in three of the input variables of the simulator, i.e. $\mathbf{v} = (v_1, v_2, v_3)$. Data for all other input to the power system, $\mathbf{a}$, will be taken from year 6 of [69] (recall, this is National Grid's freely available online reference), which will initially be treated as fixed, as if known precisely. However, Chapter 7 will give consideration to how variations in $\mathbf{a}$ affect costs estimated and the resulting decisions made.

The two decisions to be made are the reinforcement magnitudes (increase in transmission capacity) of the B6 and B7a boundaries. Further, Figure 3.1 of Section 3.6 showed that the two boundaries considered are adjacent boundaries, and Figure 3.4

of Section 3.7 showed that there is an interaction between the two when simulating mean constraint costs. As in Chapter 5, it will initially be assumed that it costs £1000 per MW per km to reinforce each boundary [5, 78]. However, the sensitivity of costs estimated (and the resulting decisions made) to this assumed cost of reinforcement will be considered in Section 6.4. Initially, it will be assumed that the magnitude of reinforcement of both boundaries (i.e. values of d_1 and d_2) can be between 0 MW (do nothing) and 4000 MW.

The three variables which are modelled as containing uncertainty of interest are nuclear availability probability, CCGT availability probability and peak demand level, which can be considered as v_1, v_2 and v_3 respectively. Section 3.7.2 showed that the values assumed for these three variables can have a large impact on the resulting mean constraint costs simulated.

When developing this example, Paul Plumptre, formerly of National Grid, was consulted to help inform the prior beliefs about uncertainty and other assumptions that will be applied to this example. The prior beliefs and assumptions used for this example are our interpretation of what was discussed in these meetings and are not intended in any way to directly reflect the views of Paul Plumptre or National Grid.

Our interpretation of the information discussed is that a suitable range to consider for Nuclear availability probability is 0.55 to 0.85 and a suitable range to consider for CCGT availability probability is 0.8 to 0.95. Further, our interpretation is that an appropriate level of uncertainty in peak demand level is 1% for each future year used. Therefore, we interpret this by modelling the peak demand level to be between 95% and 105% of the peak demand level given by [69] for year 6 (which is five years ahead of year 1). Further, our interpretation of the information discussed suggests that an appropriate set of prior beliefs about uncertainties would be to use a uniform distribution across each range.

One further model assumption made is that boundaries which are not of interest (i.e. B4, B8, B9 and B15) are treated as if they have infinite transmission capacity (i.e. they will be treated as if as much generating capacity as desired can be traded across them). This assumption is consistent with National Grid and transmission expansion planners elsewhere.

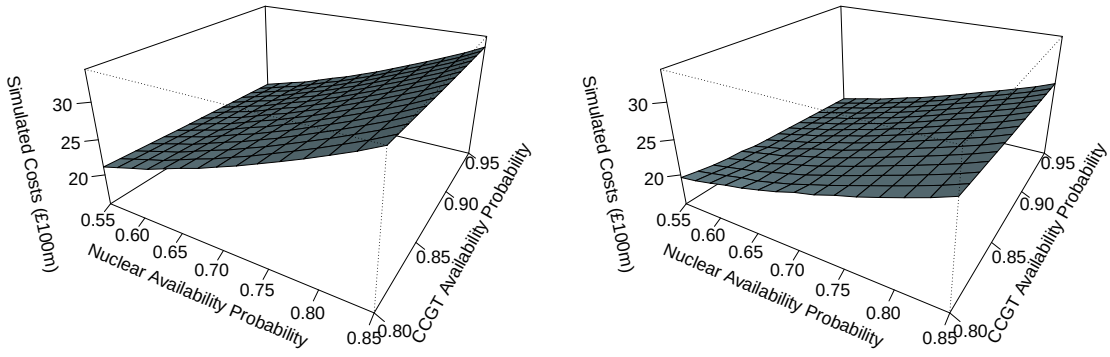

(a) 0.95 peak demand magnification assumed. (b) 1.05 peak demand magnification assumed.

Figure 6.1: Plots to show how calculations of mean constraint costs from the simulator vary with nuclear and CCGT availability probabilities.

A further note with respect to the boundaries is that the initial transmission capacity for the B6 and B7a boundaries will be treated as if it is the transmission capacity given by [69] for year 1, not year 6. This assumption, in combination with the prior beliefs outlined above, means that the problem being considered represents making a reinforcement decision for a year 6 transmission system based on the best information that is available in year 1.

6.1.2 Variations of Cost Estimates from Simulation

This subsection will consider how calculations of total costs from the simulator vary with assumed values for the variables of interest (variables containing uncertainty and decision variables).

Figure 6.1 illustrates how calculations of mean constraint costs from the simulator vary with nuclear availability probability and CCGT availability probability. Plots are shown for two peak demand levels and assume no B6 or B7a reinforcement was made. Both plots appear quite linear in shape, with constraint costs being greater for the lower peak demand level.

Figure 6.2 illustrates how calculations of total costs (mean constraint costs plus reinforcement costs) from the simulator vary with the reinforcement magnitude of the

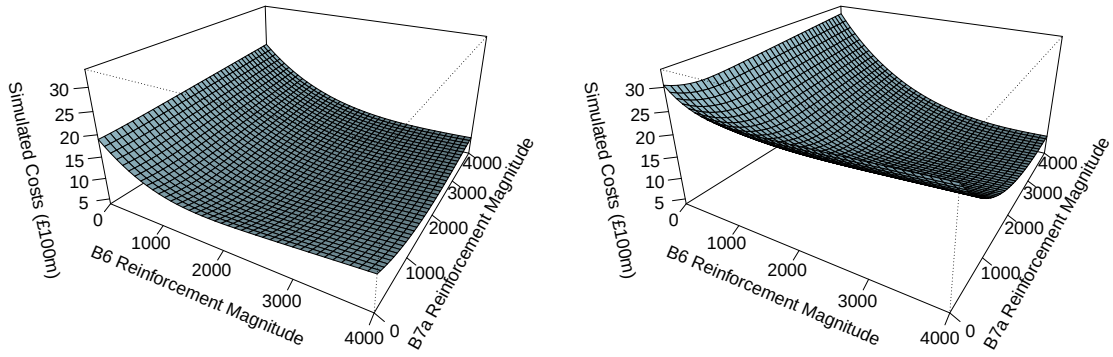

(a) Nuclear availability probability of 0.55 assumed.

(b) Nuclear availability probability of 0.85 assumed.

Figure 6.2: Plots to show how calculations of total costs from the simulator vary with reinforcement magnitude of the B6 and B7a boundaries. These plots assume a CCGT availability probability of 0.875 and the year 6 peak demand level projected by [69].

B6 and B7a boundaries. It can be seen that estimates of total costs are very high when both reinforcement magnitudes are low, with total costs sharply declining as reinforcement magnitude increases. Further, costs appear to be greater when nuclear availability probability is greater, indicating that there may exist an interaction between the decision variables and the nuclear availability probability.

Figure 6.3 considers how calculations of mean constraint costs (not total costs) vary with reinforcement magnitude of the B6 and B7a boundaries. In this plot it is clear that expanding only the B7a boundary has very little impact on reducing the constraint costs, whereas reinforcing only the B6 boundary does result in a large reduction in constraint costs. However, when both boundaries are reinforced, the reduction in mean constraint costs is greater in comparison to when only the B6 boundary is reinforced, illustrating the interaction between the B6 and B7a transfer capacities that was first noted in Section 3.7.

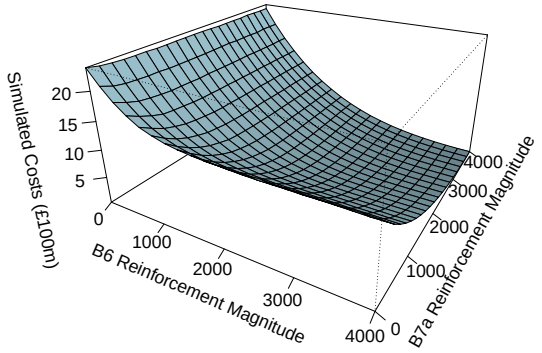

Figure 6.3: Plot to show how calculations of mean constraint costs from the simulator vary with reinforcement magnitude of the B6 and B7a boundaries. Nuclear and CCGT availability probabilities were assumed to be 0.7 and 0.875 respectively, whilst peak demand level was fixed at the year 6 projection from [69].

6.1.3 Constructing an Emulator Model for This Example

Fitting the Emulator Model

An emulator model must be fitted to accurately approximate how input affects output of the simulator of total costs. Just as in Section 5.3.3, this requires an appropriate number of training runs and an appropriate model to be fitted to these training runs to be identified. Recall from Section 5.2.1, this thesis considers fitting emulator models which consist of a polynomial regression model with a Gaussian process model applied to smooth the resulting residuals from this polynomial regression model.

The form of the polynomial regression portion of the emulator model in this chapter is

$$\beta_0 + \beta_1 v_1 + \beta_2 v_2 + \beta_3 v_3 + \beta_4 d_1 + \beta_5 d_2 + \beta_6 v_1^2 + \beta_7 v_2^2 + \beta_8 v_3^2 + \beta_9 d_1^2 + \beta_{10} d_2^2 + \beta_{11} v_1 d_1 + \beta_{12} v_1 d_2 + \beta_{13} d_1 d_2 + \beta_{14} v_1^2 d_1^2 + \beta_{15} v_1^2 d_2^2 + \beta_{16} d_1^2 d_2^2 + \beta_{17} v_1 d_1 d_2 + \beta_{18} v_1^2 d_1^2 d_2^2$$

Details about the selection of an appropriate polynomial regression portion of the emulator model are given in Appendix B.1.

This polynomial regression model is consistent with what was illustrated in Figures 6.1 and 6.2 of Section 6.1.2, where there was a clear interaction between the two decision variables, a possible interaction between the decision variables and nuclear

availability probability and no interaction between the three variables which contain uncertainty.

Training Run Sample Size	Value of R^2	Value of P	Value of $\tilde{P}$
50	0.9870	1.257×10^{16}	0.04418
100	0.9787	7.378×10^{15}	0.02594
200	0.9768	4.314×10^{15}	0.01517
300	0.9714	2.177×10^{15}	0.007652
400	0.9712	1.561×10^{15}	0.005488
500	0.9737	1.632×10^{15}	0.005736

Table 6.1: Table of how the model selection criteria vary with the number of training runs used to fit the emulator.

Table 6.1 considers how the value of R^2 varies with the number of training runs used to fit the polynomial regression portion of the emulator model. Values of P and $\tilde{P}$ (defined in Equations 5.3.1 and 5.3.2 of Section 5.3.3 respectively) are also given for when the fitted emulator model (polynomial model plus Gaussian process applied to its residuals) is used to estimate a response for a second set of 50 training runs which were not used to fit the model.

For all sample sizes, the value of R^2 is greater than 0.97, which indicates that an excellent fit is given, even without the inclusion of a Gaussian process model. The value of P gradually decreases as sample size increases, though there is little improvement in predictive power when using more than 300 training runs to construct the emulator model, implying it would be sufficient to use 300 training runs. Further details on the selection of the emulator model are given in Appendix B.1 and B.2.

Comparison to the Simulator

Figure 6.4 compares how calculations of total costs from simulation (in Figure 6.4 (a)) and estimates from the fitted emulator model using 300 training runs (in Figure 6.4 (b)) vary as B6 and B7a reinforcement magnitudes are varied. As can be seen, the emulator model is quite a good approximation to the simulator, though far from perfect.

The differences between the calculations from the simulator and the estimates from the emulator (i.e. the difference between Figure 6.4 (a) and Figure 6.4 (b)) are shown

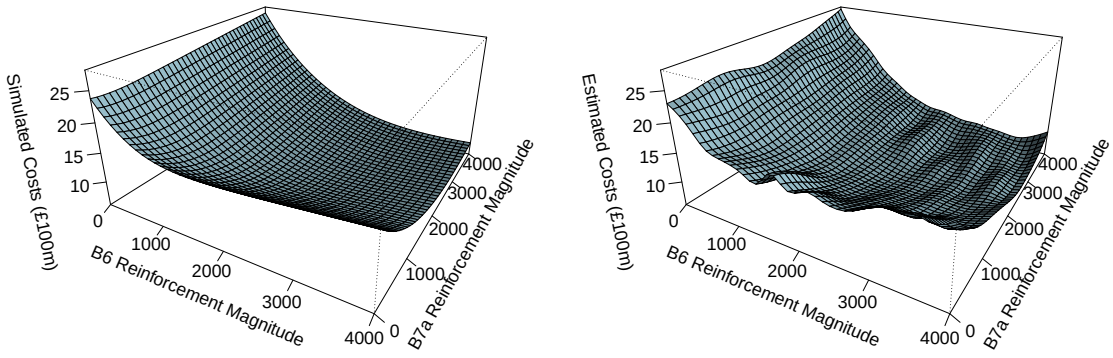

(a) Calculations from the simulator.

(b) Estimates from the emulator.

Figure 6.4: Plots to show how total costs vary with B6 and B7a reinforcement magnitude. Nuclear and CCGT availability probabilities were assumed to be 0.7 and 0.875 respectively, whilst peak demand level was fixed at the year 6 projection from [69] (i.e. the central values for the variables containing uncertainty).

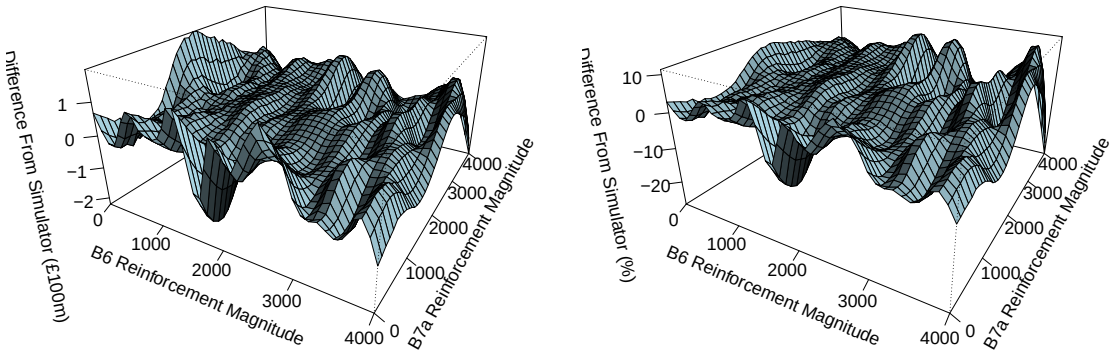

(a) Difference.

(b) Relative difference.

Figure 6.5: Plots to show how the difference between total cost calculations from the simulator and estimates from the emulator vary with B6 and B7a reinforcement magnitude. Nuclear and CCGT availability probabilities were assumed to be 0.7 and 0.875 respectively, whilst peak demand level was fixed at the year 6 projection from [69].

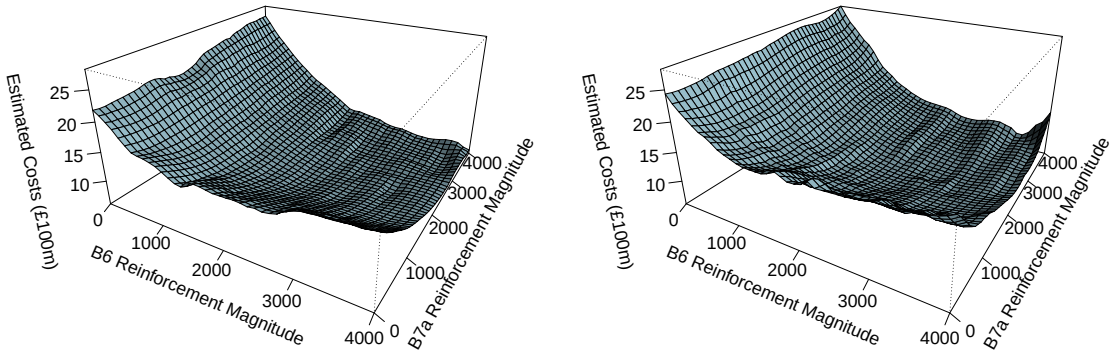

(a) Lower bound.

(b) Upper bound.

Figure 6.6: Plots to show how credible bounds of the estimates of total costs from the emulator vary with B6 and B7a reinforcement magnitude, when assuming central values for the variables containing uncertainty.

in Figure 6.5. As can be seen, the difference between the two is generally relatively small (with the vast majority of differences being less than 7% of total costs), though a particularly large over-estimation of total costs from the emulator is noted when the reinforcement magnitude of both the B6 and B7a boundaries is assumed to be 4000 MW (the largest reinforcement considered).

Figure 6.6 displays 95% credible intervals for the estimates of total costs from the emulator (i.e. 95% credible intervals for Figure 6.4 (b)). There is a notable spike in the upper bound and dip in the lower bound when both the B6 and B7a reinforcement magnitudes are close to 4000 MW, with the calculations from the simulator lying somewhere in between. This shows that although the emulator considerably over-estimates total costs in this range, when accounting for uncertainty due to the emulation approximation, the credible bounds of the estimate contain the value acquired via simulation.

Of the simulated values used to construct construct Figure 6.4 (a), all but 0.3% lay within the credible bounds of Figure 6.6. This means that fewer evaluations from simulation than the 5% that would be expected for a 95% credible interval lie outside the credible intervals, which suggests that the credible intervals considered may over-estimate error in the emulation approximation and be too wide.

Further thought is given to the credible intervals in Appendix B.2 and B.3. An

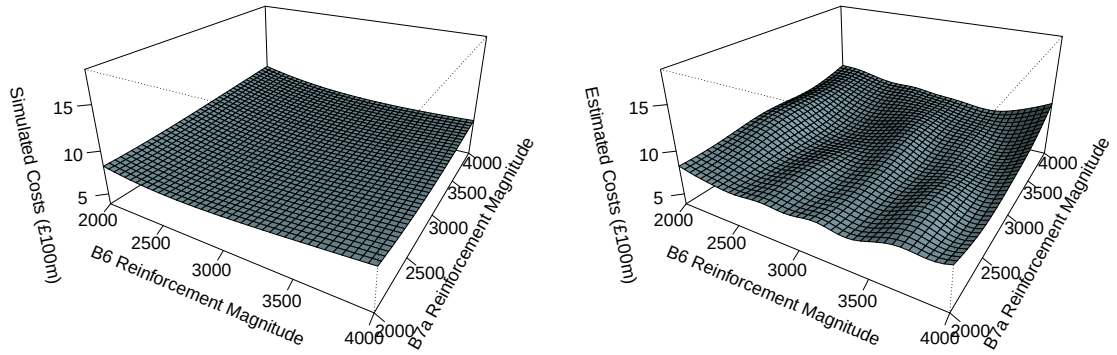

(a) Calculations from the simulator.

(b) Estimates from the emulator.

Figure 6.7: Plots to show how total costs vary with B6 and B7a reinforcement magnitude, for reinforcement magnitudes greater than 2000 MW on both boundaries. Nuclear and CCGT availability probabilities were assumed to be 0.7 and 0.875 respectively, whilst peak demand level was fixed at the year 6 projection from [69].

overview is that in general the credible intervals over-estimate uncertainty in the emulator, though too a much lesser extent than for the values used to construct Figure 6.4 (a). This is partly due to the central values of nuclear availability probability, CCGT availability probability and peak demand magnification being used to construct Figure 6.4 (a), where the emulation approximation is most accurate. When extreme values for multiple variables are taken simultaneously the credible intervals contain a value closer to the 95% of the simulated values that would be expected.

Figure 6.7 compares calculations of total costs from simulation to estimates from the fitted emulator model when only reinforcement magnitudes greater than 2000 MW were considered, with Figure 6.8 illustrating the differences between the two. These plots allow for a closer comparison of the emulator to the simulator where total costs are lowest (i.e. close to where the optimal reinforcement decision lies).

Over this range the emulator is still a good approximation to the simulator, though with noticeable differences between the emulator and simulator, in particular the over-estimation of costs from the emulator when both boundaries are reinforced by 4000 MW (which is also present in Figure 6.4).

Figure 6.9 displays how estimates of mean constraint costs from the emulator vary

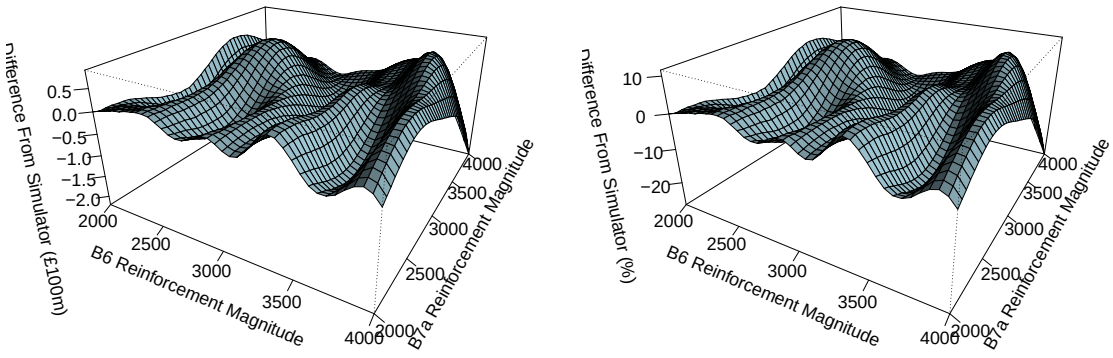

(a) Difference. (b) Relative difference.

Figure 6.8: Plots to show how the difference between total cost calculations from the simulator and estimates from the emulator vary with B6 and B7a reinforcement magnitude, for reinforcement magnitudes greater than 2000 MW on both boundaries. Nuclear and CCGT availability probabilities were assumed to be 0.7 and 0.875 respectively, whilst peak demand level was fixed at the year 6 projection from [69].

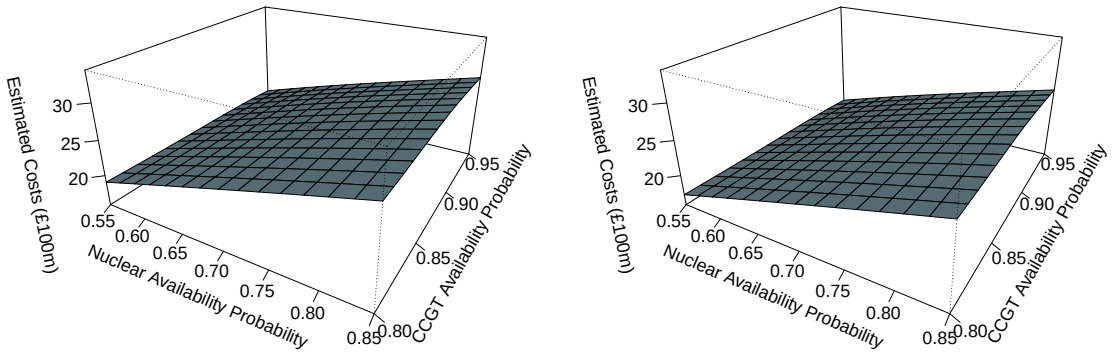

(a) 0.95 peak demand magnification assumed. (b) 1.05 peak demand magnification assumed.

Figure 6.9: Plots to show how estimates of mean constraint costs from the emulator vary with nuclear and CCGT availability probabilities, assuming no B6 or B7a reinforcement has been made.

with nuclear availability probability and CCGT availability probability. These are the emulation approximations to the graphs of Figure 6.1.

By comparing the two sets of plots it can be seen that the effect of varying nuclear availability probability and CCGT availability probability is modelled quite well. However, costs do tend to be underestimated by the emulator, especially when peak demand level is low and nuclear availability probability is high.

This limitation arises due to the fact that the emulator approximates the simulator over a large range of reinforcement magnitudes, and not just when no reinforcement was made (as was assumed for both sets of graphs). However, Figure 6.2 shows how costs everywhere are much lower when there has been even a small amount of B6 reinforcement made. Further, the approximation is weakest where 4 of the 5 variables considered take extreme values. Therefore, even though the Gaussian process model is used to improve the local fit of the data, most training runs will consider less extreme values of at least one of the input variables (which will give a lower corresponding calculation of total costs), causing costs to be under-estimated by the emulator when all variables simultaneously take extreme values. This could be partially overcome by extending the ranges of the variables used for training runs beyond the ranges required for estimation (for example, the range for nuclear availability probability could be extended from 0.55 to 0.85, to 0.5 to 0.9). However, this would result in the emulator giving a less good approximation to the simulator in general in order to improve the fit at the extremes.

Further thought is given to this in Appendix B.3, where credible bounds for the estimates illustrated in Figure 6.9 are considered, with Appendix B.3 going on to illustrate how the emulation approximation to the simulator as nuclear and CCGT availability probabilities are varied is greatly improved when even a small amount of B6 and B7a reinforcement is considered.

Figure 6.10 illustrates how estimates of total costs from the emulator vary with B6 and B7a reinforcement magnitude. It is the emulation approximation to Figure 6.2 and further illustrates that the emulator is actually quite a good approximation to the simulator, though far from perfect. Figures 6.11 and 6.12 give a further comparison when only considering reinforcement magnitudes greater than 2000 MW. Over this

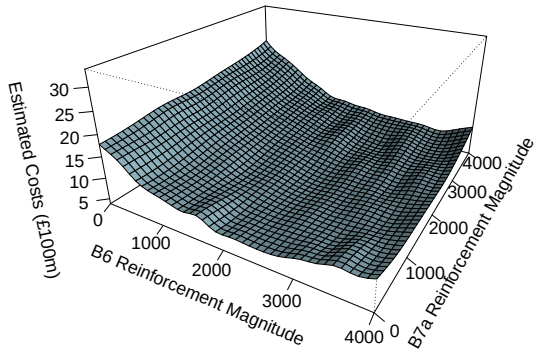

(a) Nuclear availability probability of 0.55 assumed.

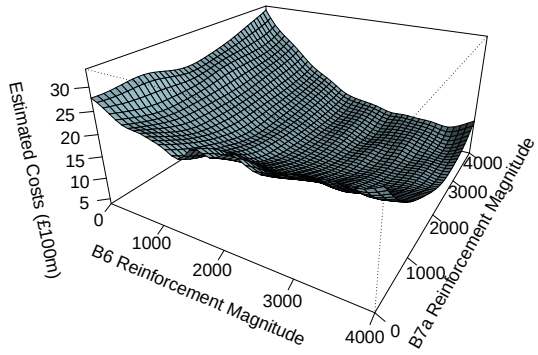

(b) Nuclear availability probability of 0.85 assumed.

Figure 6.10: Plots to show how estimates of total costs from the emulator vary with the reinforcement magnitudes of the B6 and B7a boundaries. These plots assume a CCGT availability probability of 0.875 and the year 6 peak demand level projected by [69].

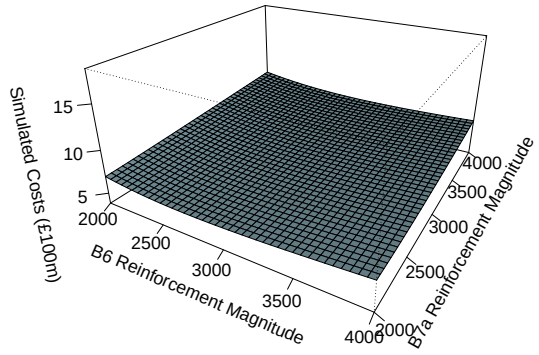

(a) Nuclear availability probability of 0.55 assumed.

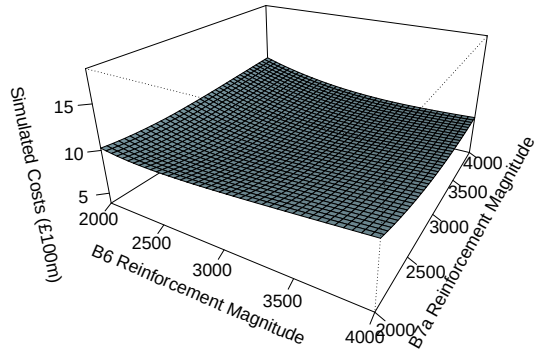

(b) Nuclear availability probability of 0.85 assumed.

Figure 6.11: Plots to show how calculations of total costs from the simulator vary with the reinforcement magnitudes of the B6 and B7a boundaries, for reinforcement magnitudes greater than 2000 MW on both boundaries. These plots assume a CCGT availability probability of 0.875 and the year 6 peak demand level projected by [69].

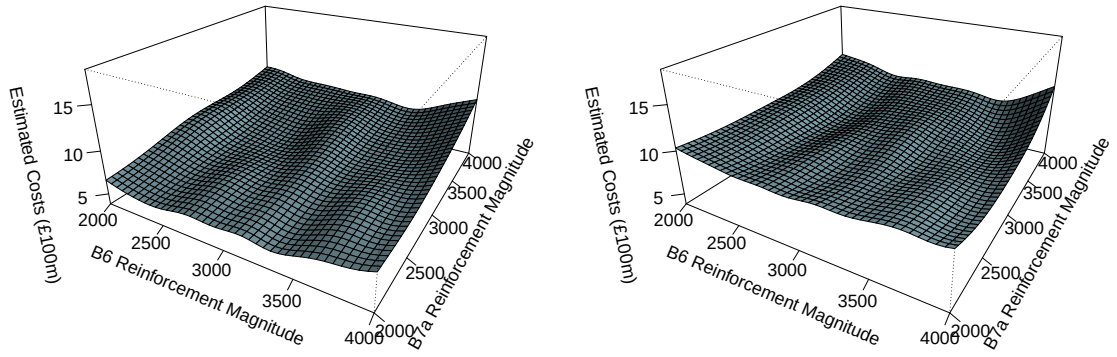

(a) Nuclear availability probability of 0.55 assumed.

(b) Nuclear availability probability of 0.85 assumed.

Figure 6.12: Plots to show how estimated total costs from the emulator vary with the reinforcement magnitudes of the B6 and B7a boundaries, for reinforcement magnitudes greater than 2000 MW on both boundaries. These plots assume a CCGT availability probability of 0.875 and the year 6 peak demand level projected by [69].

range the emulator is still quite a good approximation to the simulator. However, there are some noticeable differences between the calculations from simulation and the estimates from emulation, such as total costs being considerably over-estimated when both B6 and B7a reinforcement magnitude are very large (close to 4000 MW).

Further, the ranges of the reinforcement considered in Figures 6.11 and 6.12 are where the lowest values of total costs occur (i.e. where the optimal reinforcement decision would lie). This means that it would be desirable for the emulator to be as accurate as possible over this range, in order to make the best decision possible. Therefore, an improvement in this current emulator model would be required before a reliable decision can be made, and this will be considered further in Section 6.2.

A further comparison of Figure 6.2 to Figure 6.10 is given in Appendix B.3.2. In particular, it is noted that when the reinforcement magnitude of both boundaries exceeds 2000 MW all calculations of total costs from the simulator are contained within the credible bounds of the estimates from the emulator. This indicates that although the emulator model is not give a perfect approximation to the simulator over this range, the error in the estimate is adequately accounted for.

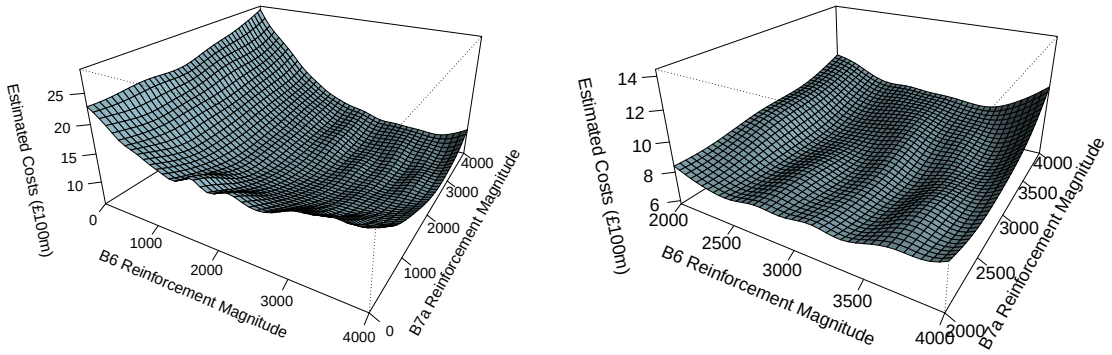

(a) Plot of how estimated expected total costs from the emulator vary with reinforcement of the B6 and B7a boundaries, considering reinforcement decisions between 0 MW and 4000 MW on each boundary.

(b) Plot of how estimated expected total costs from the emulator vary with reinforcement of the B6 and B7a boundaries, considering reinforcement decisions between 2000 MW and 4000 MW on each boundary.

Figure 6.13: Plots to show how estimated expected total costs from the emulator vary with reinforcement magnitudes of the B6 and B7a boundaries.

Estimating Expected Total Costs Under Uncertainty Using the Fitted Emulator Model

Figure 6.13 (a) displays how estimates of expected total costs under uncertainty (calculated via Equation 5.2.16 from Section 5.2.5 using the PDF of beliefs about the 3 uncertainties detailed in Section 6.1.1) vary with B6 and B7a reinforcement magnitude. The shape of the plot (i.e. very high costs when little reinforcement is made with an interaction between the two decisions) is what would be expected based on the results of this section (such as from Figures 6.4 and 6.10).

In particular, it can be seen that all decisions of 2000 MW reinforcement or more of both boundaries result in similar, relatively low estimates of expected total costs, indicating that the optimal decision lies somewhere in this range. Figure 6.13 (b) displays the estimates of expected total costs under uncertainty when only considering decisions of at least 2000 MW reinforcement for both boundaries, with Figure 6.14 illustrating the 95% credible bounds for the estimate of expected total costs in that region.

Over this range it can be seen that the variation in the estimate of expected total costs as the reinforcement magnitudes are varied is not particularly smooth. Further, over

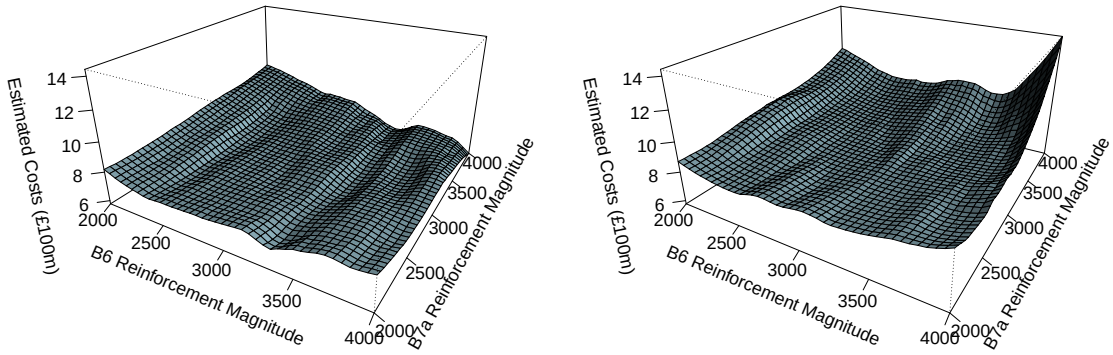

(a) Lower bound.

(b) Upper bound.

Figure 6.14: Plots to illustrate how credible bounds for the estimated expected total costs vary with reinforcement magnitudes of the B6 and B7a boundaries.

this range it can be seen that the variation in the estimates of expected total costs as the reinforcement magnitudes are varied is relatively small in comparison to the width of the credible intervals (as will be demonstrated further in Figure 6.18 of Section 6.3). This means it would be unwise to identify any one decision as optimal.

The quality of the emulator could be improved if the emulator was fitted to model simulator behaviour over a smaller range of values of the input variables, which in turn would result in narrower credible intervals for the estimated response.

6.2 Improving the Emulator Model

6.2.1 Wave Process for Decision Making

The objective is to make a reinforcement decision which minimises the expected total costs in the system (the sum of expected mean constraint costs plus the expected costs of reinforcement) under uncertainty. So far, this thesis has demonstrated how emulators can be used to approximate simulators. Estimates can then be acquired for expected total costs under uncertainty by integrating the product of the fitted emulator model and prior beliefs about uncertainties using Equation 5.2.16. Decisions could then be

identified to minimise Equation 5.2.16 (i.e. to minimise the estimate of expected total costs under uncertainty).

However, Section 6.1.3 showed that whilst the emulator fitted in this chapter is a decent approximation to the simulator it is far from perfect. Therefore, there will be error in the estimates that arise from evaluating Equation 5.2.16. If the emulator model was fitted over a smaller range of values for the decision variables, it would be able to fit a more accurate model over that range.

This motivates a wave process for making decisions, where in each wave decisions which are unlikely to be optimal (i.e. unlikely to minimise expected total costs under uncertainty) are eliminated and a new, smaller range for the decision variables is identified where the optimal decision could potentially lie. This is summarised in the following algorithm:

1. Set an initial range of values to be considered for the decision variables.

2. Simulate training runs based on a Latin hypercube (LHC) sample using the current limits on the decision variables.

3. Fit an emulator model to the latest simulated sample and use it to eliminate decisions from consideration (details below).

4. Repeat until uncertainty about the optimal decision reaches an acceptable level (such as when the range of values considered for the decision variables can be reduced no further or when the error in the estimate of expected total costs reaches a given level of precision). The estimated optimal decision is the decision which minimises Equation 5.2.16 (i.e. minimises the estimate of expected total costs under uncertainty).

To do this, an LHC sample will be taken over a specified initial range of reinforcements to consider. This LHC sample gives the values of input variables to be used for the training data. Simulations are then taken using these input values to give the training data. Then, the emulation process of Section 5.2 uses this training data to create an emulator model of how input affects output of the simulator.

The methodology of Section 5.2.6 is then used to estimate expected total costs and corresponding credible intervals as the values of the decision variables are varied, such that if $\tilde{F}_T(d_1, ..., d_{N_d})$ is the value of the estimate of expected total costs when integrating over uncertainty using Equation 5.2.16, $\tilde{F}_{T,L}(d_1, ..., d_{N_d})$ would represent a lower bound of that estimate and $\tilde{F}_{T,U}(d_1, ..., d_{N_d})$ would represent an upper bound for that estimate. The values of the decision variables which give the minimum value of $\tilde{F}_{T,U}(d_1, ..., d_{N_d})$ are then identified as $d_1^o, ..., d_{N_d}^o$, with the corresponding upper bound for the estimate of expected total cost under uncertainty when making this decision being $F_{T,U}(d_1^o, ..., d_{N_d}^o)$. For any alternative set of decisions, $d_1^a, ..., d_{N_d}^a$, such that $F_{T,L}(d_1^a, ..., d_{N_d}^a) > F_{T,U}(d_1^o, ..., d_{N_d}^o)$ it can be said that there is evidence against that decision being optimal, as the lower bound of the estimate is not better than the minimum point of the upper bounds. That decision can thus be eliminated from the decision space.

A new set of training runs is taken where the values of the decision variables are only those not eliminated. This space will not necessarily form a hypercube, so Section 6.2.2 will detail a method of how to take a second sample of input values for decision variables to be used for training runs. A new emulator model is fitted to this new set of training runs, and credible intervals are estimated for decisions which were not previously ruled out. This allows for further poor decisions to be identified and eliminated. The process continues iteratively until the uncertainty about the optimal decision reaches an acceptable level (such as when the range of values considered for the decision variables can be reduced no further or when the error in the estimate of expected total costs reaches a given level of precision).

The use of a wave process is usually very efficient. Initially, global behaviour is modelled, so an area where the optimal decision is likely to lie can be identified. Subsequent waves can then model local behaviour much more accurately, meaning a more accurate decision can be made. Further, a much better model (and therefore better decision) can be obtained from several waves of a relatively small numbers of observations than a single wave of a relatively large number of observations.

The iterative scheme proposed in this section is used to iteratively eliminate decisions from consideration which are unlikely to be optimal. It is noted that similar iterative

schemes are considered elsewhere in the existing literature as part of a preliminary or alternative to model calibration, to iteratively rule out values of uncertain input parameters (which are said to give implausible matches to observations about a system in reality) via a technique known as history matching [7, 21, 22, 98].

6.2.2 Sampling Training Runs Beyond the First Wave

It is noted that when eliminating decisions from consideration as outlined in Section 6.2.1 the remaining decision space will not necessarily form a hypercube (as will be illustrated in Section 6.3.1). A poor solution to overcome this would be to extend the region of decisions not eliminated to a hypercube when sampling input values for training runs in the next wave. However, this would mean that the next wave would considers a larger range of values for the decision variables than necessary, and therefore result in a less accurate emulator model.

A more appropriate method would be one which preserves the shape of the decision space. To achieve this, values for $d_1, ..., d_{N_d}$ are sampled from a uniform distribution, with $d_1^r, ..., d_{N_d}^r$ denoting the values randomly sampled. A lower bound for the estimated expected total costs of decisions $d_1^r, ..., d_{N_d}^r$ are calculated using the methodology of Section 5.2.6, and with $F_{T,L}(d_1^r, ..., d_{N_d}^r)$ representing this lower bound. If $F_{T,L}(d_1^r, ..., d_{N_d}^r) \leq F_{T,U}(d_1^o, ..., d_{N_d}^o)$ then the decision set $d_1^r, ..., d_{N_d}^r$ would not have been eliminated from consideration, so $d_1^r, ..., d_{N_d}^r$ can be used as a set of values for decision variables for training data. If $F_{T,L}(d_1^r, ..., d_{N_d}^r) > F_{T,U}(d_1^o, ..., d_{N_d}^o)$, then $d_1^r, ..., d_{N_d}^r$ is rejected as a set of values for training data. A new sample for the values of $d_1, ..., d_{N_d}$ is then drawn from a uniform distribution. This is repeated iteratively until a sample of desired size is acquired.

This method of uniformly sampling points is adequate for the examples considered in this thesis. For the emulator model fitted in Section 6.1.3, Figure 6.15 (a) illustrates decisions which would not be eliminated from consideration in a second wave using the method of Section 6.2.1. Decisions can then be uniformly sampled from the space enclosing this region illustrated in Figure 6.15 (b).

Figure 6.16 (a) illustrates 200 decisions uniformly sampled from the space illustrated in Figure 6.15 (b). As described in the methodology of this subsection, for each of these

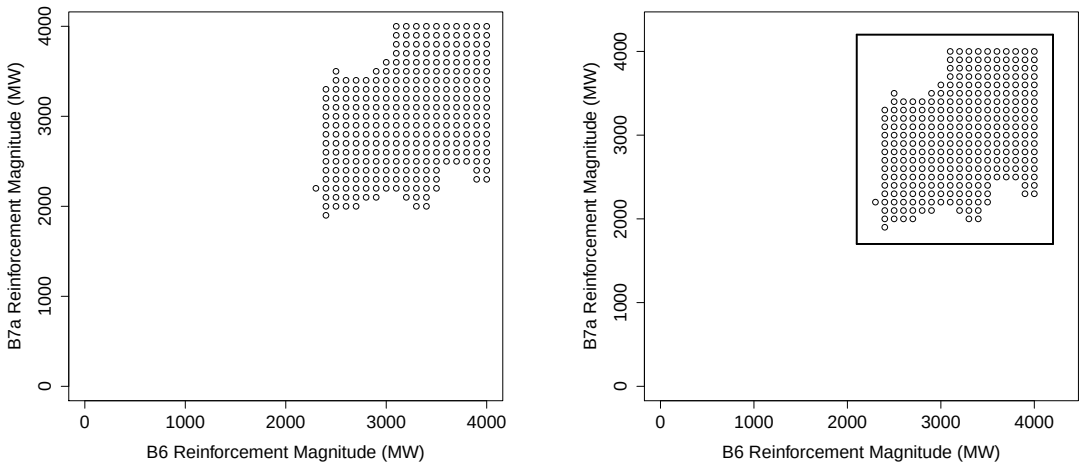

(a) Illustration of decisions not eliminated from consideration in the second wave.

(b) Region to be uniformly sampled for input values of decision variables in the second wave.

Figure 6.15: Plots to illustrate decisions considered in the second wave, and the region uniformly sampled when acquiring input values for the decision variables for training runs for the second wave.

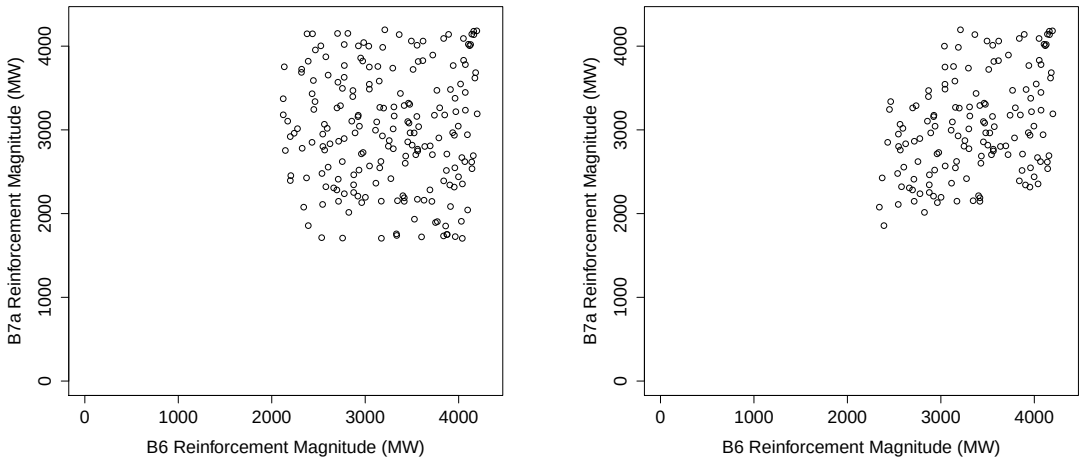

(a) 200 decisions uniformly sampled.

(b) Decisions from the sample of 200 which were not rejected.

Figure 6.16: Plots to illustrate decisions sampled as potential input decisions for the second wave, and which decisions of the sample were not rejected.

200 decisions a lower bound for the estimate of expected total costs under uncertainty is calculated as $F_{T,L}(d_1^r, ..., d_{N_d}^r)$. If $F_{T,L}(d_1^r, ..., d_{N_d}^r)$ is greater than $F_{T,U}(d_1^o, ..., d_{N_d}^o)$ the decision is rejected for use in the second wave, otherwise the decision can be used as input for training data in the second wave. Figure 6.16 (b) illustrates which of the 200 decisions of Figure 6.16 (a) were not eliminated (i.e. suitable for use as input data in the second wave), which shows how the shape of the region illustrated in Figure 6.15 (a) is preserved.

However, if the shape of decisions considered in the second wave took the shape illustrated in Figure 6.17 (a), sampling from a uniform distribution of the space illustrated in Figure 6.17 (b) would be very inefficient, as the majority of decisions sampled would lie away from the region of decisions which merit further consideration illustrated in Figure 6.17 (a), and $F_{T,L}(d_1^r, ..., d_{N_d}^r)$ can be quite expensive to evaluate. Therefore, it would be more appropriate to sample from the region illustrated in Figure 6.17 (c). Principle component analysis could be used to identify such regions.

Alternative, less accurate methods could also be considered to greatly increase the speed at which decisions are sampled. For example, the regions illustrated in Figure 6.16 (a) or Figure 6.17 (a) could be parametrised in some way, which would make it much faster to check if a randomly sampled set of decisions, $(d_1^r, ..., d_{N_d}^r)$, lie in that region.

Note, as values of variables containing uncertainty (i.e. $v_1, ..., v_{N_v}$) are not being eliminated, values for these variables in training data can still be acquired via Latin hypercube sampling.

6.3 Wave Process Application and Estimate of Optimal Decision for the Example Presented

6.3.1 Wave Process Applied to the Example

Figure 6.18 shows how credible bounds for the estimated expected total costs under uncertainty vary with B6 reinforcement magnitude for the emulator model fitted in Section 6.1.3. For this plot, B7a reinforcement was fixed at 2890 MW (which is what

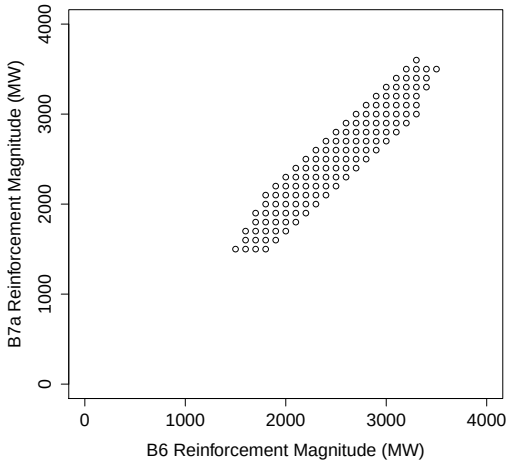

(a) Plot to illustrate a potential decision space for second wave decisions.

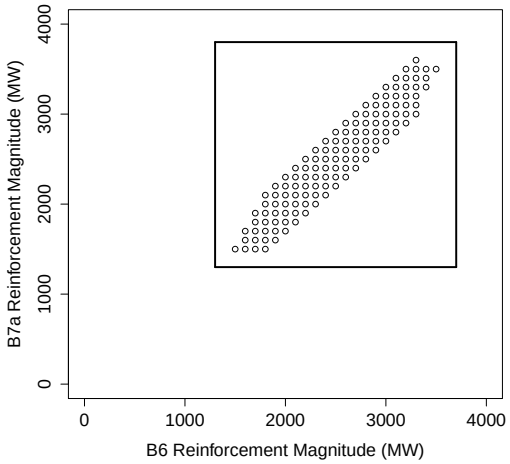

(b) Plot to show a region which it would be inefficient to uniformly sample decisions from.

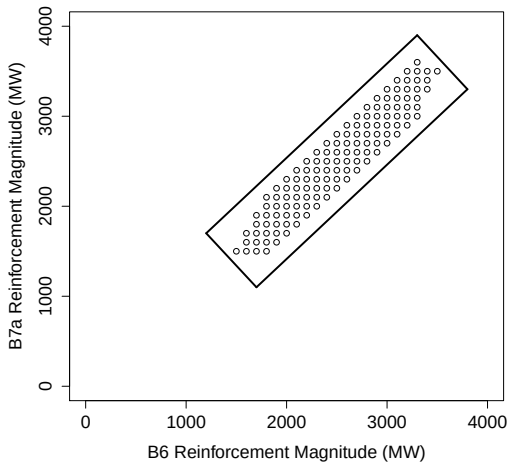

(c) Plot to illustrate a space which would be much more efficient to sample from.

Figure 6.17: Plots to illustrate a decision space which it would be inefficient to uniformly sample second wave decisions from.

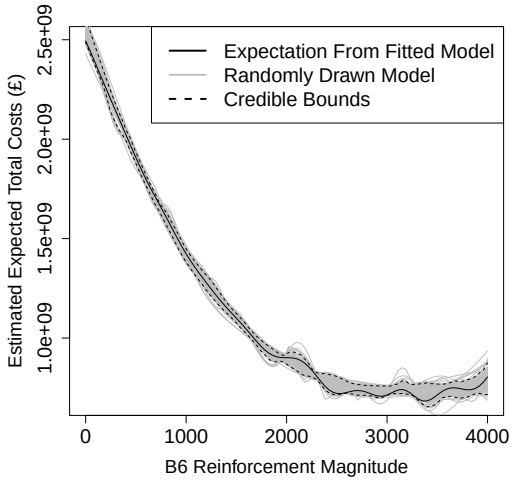

Figure 6.18: Plot of credible bounds for estimates of expected total costs from the emulator model fitted in the first wave.

will later be identified as the estimated optimal reinforcement). It can be seen that these estimated credible bounds capture the majority of the variation of the estimates.

Figure 6.19 (a) shows which decisions seemed to merit further consideration in the second wave (i.e. based on the methodology of Section 6.2.1 there was no significant evidence against them being optimal). This is still a quite large region, though it has eliminated 82.7% of the decisions considered in the first wave.

A new emulator model is then fitted to a new set of training runs sampled from the region illustrated in Figure 6.19 (a). This allows for further decisions to be eliminated by considering the credible bounds of the resulting estimates of expected total costs from this second emulator model, as outlined in Section 6.2.1. Figure 6.19 (b) displays the reinforcement combinations that would merit further consideration in a third wave of emulation. If sufficient resources are available, the wave process can be continued, eliminating even more decisions.

Alternatively, after sufficient decisions have been eliminated a final decision could be taken to minimise the estimate of expected total costs for the current wave. The reason to make such a decision is the uncertainty in the estimate of expected total costs when integrating over uncertainties, $\tilde{F}_T(\mathbf{d})$, will not always allow for all but a single decision to be eliminated, but in practice it will often be necessary to identify a decision to actually be implemented (e.g. for the transmission expansion problem considered it

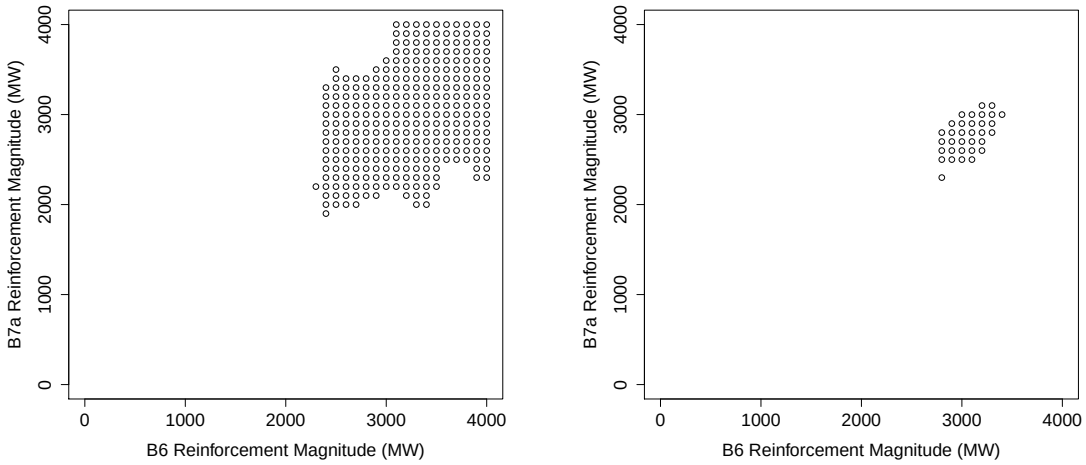

(a) After wave 1.

(b) After wave 2.

Figure 6.19: Plots to illustrate decisions not eliminated as the wave process progresses.

is necessary in practice to identify a reinforcement to actually be built). Note, this would not be a definitive optimum, as uncertainty is always present in the model and consequently any decision not eliminated in this wave could also potentially be optimal.

For this example, applying another wave of elimination did not result in any significant reduction in the decision space, so an optimal decision was estimated after this third wave. This is due to cost estimates being very flat over the range of decisions considered in the third wave, in the sense that there is little variation in the estimates of expected total costs as the reinforcement decision is varied, as will be demonstrated in the following subsection. It could be noted that the 95% credible bounds were used when performing the wave process, so using a lower credibility level (e.g. 90%) would result in narrower bounds which would allow further decisions to be eliminated, though this would come with an increased risk of incorrectly eliminating an optimal decision.

6.3.2 Graphical Comparison of Cost Estimates from Emulation by Wave and Estimate of Optimal Reinforcement Decision

Figure 6.20 compares how estimates of expected total costs from the emulator model vary with reinforcement decision when taking an expectation over the variables which

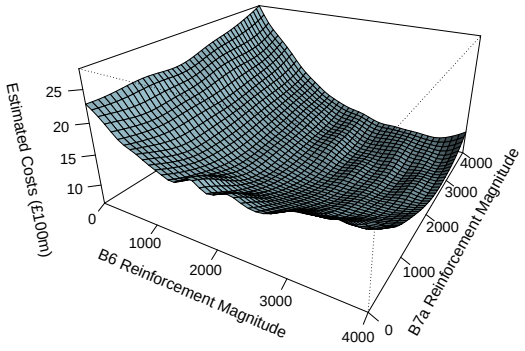

(a) Wave 1.

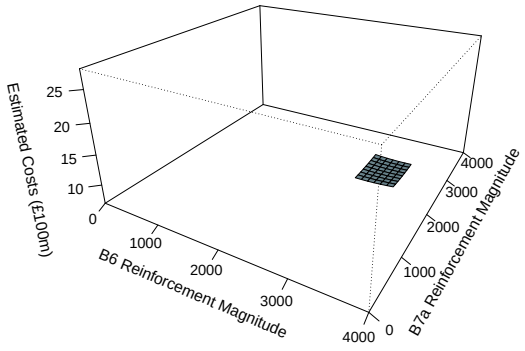

(b) Wave 3.

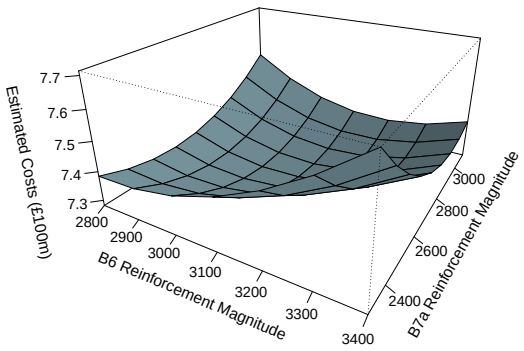

(c) Wave 3.

Figure 6.20: Plots to show how estimated expected total costs vary with reinforcement decisions and fitted emulator model.

contain uncertainty using Equation 5.2.16 for the first and third wave models. Making a decision to minimise the estimate of expected total costs under uncertainty from the emulator fitted in the third wave would result in a decision of 3060 MW B6 reinforcement and a 2890 MW B7a reinforcement. As Figure 6.20 (b) and (c) show that all decisions considered in the third wave result in similar, relatively low estimates of expected total costs, there is little risk of making a poor decision by making such a decision. If the decision was made based on the emulator from the first wave the resulting decision would have been 3370 MW B6 reinforcement and 2830 MW B7a reinforcement, which is somewhat different and would cost an additional £25,000,000 to build.

Figure 6.21 (a) and (b) compare estimates of expected total cost from the wave 1 and 3 emulator models over the range of decisions considered in the third wave, with cost estimates from the third wave model varying much more smoothly. This is an improvement due to the fact that the third wave model is fitted over a much smaller range of decisions, allowing it to be much more accurate over that range. This is demonstrated further in Figure 6.21 (c), which also illustrates how the credible intervals are much narrower for the third wave model than the first. This indicates the increased level of confidence within the estimate as a result of fitting the emulator model over a smaller range of values of the decision variables. This increased confidence then allows for more decisions to be eliminated, or if a decision is to be taken it allows for a narrower range to be given that could possibly contain the optimal.

The power of the presented methodology of emulation through several waves is demonstrated by the fact that a much better model is achieved by taking 3 separate waves of 300 observations, with the final one being over a much narrower range, than attempting to fit one model to a single set of 900 training runs. In this final wave, the fitted emulator model is a very accurate approximation of the simulator, whilst being much less expensive to evaluate.

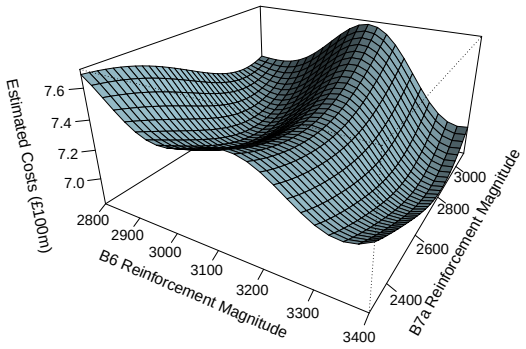

(a) Plot of how estimated expected total costs vary with reinforcement decisions for the emulator model fitted in the first wave, over the range of decisions considered in the third wave.

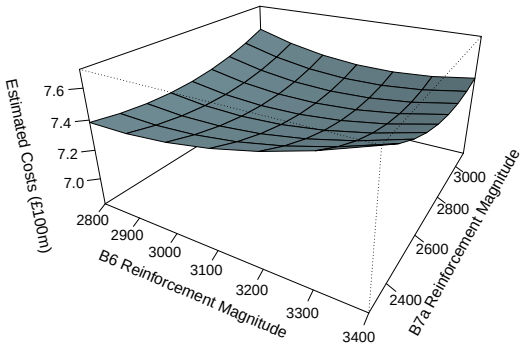

(b) Plot of how estimated expected total costs vary with reinforcement decisions for the emulator model fitted in the third wave, over the range of decisions considered in the third wave.

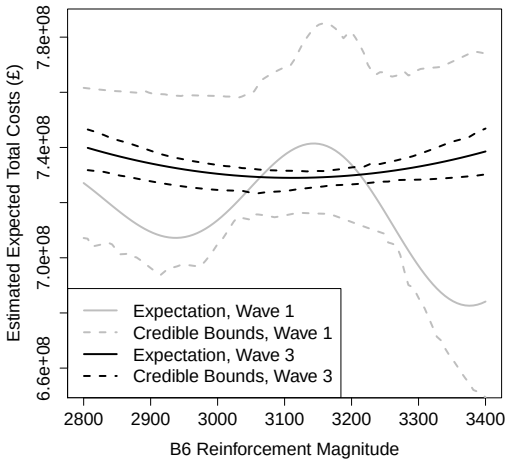

(c) Plot to compare credible intervals for the estimated expected total costs from the fitted emulator models for waves 1 and 3.

Figure 6.21: Plots to compare the fitted emulator models in wave 1 and wave 3.

6.3.3 Offering Decision Support to Real Life Transmission Expansion Planners

It is noted that reinforcement decisions in practice are often discrete and "lumpy" [44, 67, 78], such as building a discrete number of transmission lines of a specified capacity, meaning that reinforcement magnitudes could be modelled as discrete variables of a specified precision (e.g. building a discrete number of 250 MW transmission lines) rather than as (quasi) continuous variables. This means that in practice, such a precise reinforcement decision of 3060 MW and 2890 MW (i.e. the estimated optimal reinforcement decision in the third wave as identified in the previous subsection) may not be a decision the transmission system planner would consider making.

However, the results presented in this chapter can still be of use to offer decision support in such cases. This is because an application of the wave process detailed in Section 6.2 to the example detailed in Section 6.1.1 was used to identify a quite small region of reinforcement decisions where the optimal reinforcement could potentially lie, illustrated in Figure 6.19 (b). Further, a comparison of Figure 6.20 (b) to Figure 6.20 (a) shows how estimates of expected total costs are relatively flat over the range of decisions considered in the final third wave, in the sense that there is little variation in the estimate of expected total costs as the reinforcement decision is varied over this range, especially in comparison to estimates of expected total costs over the range of decisions initially considered in the first wave, where estimates of expected total costs exceed £2 billion when little to no reinforcement is made.

This means that decision support can be offered by showing these results to the transmission system planner and explaining how the small region illustrated in Figure 6.19 (b) represents a region of near-optimal decisions which all result in similar, relatively low estimates of expected total costs under uncertainty. The transmission system planner can then make an appropriate decision based on these results. For example, if the transmission system planner considers making a reinforcement decision in terms of making a number of discrete 250 MW additions to the power system, an appropriate decision could therefore be to reinforce both the B6 and B7a boundaries by 3000 MW (which would be 12×250 MW additions on both boundaries), which was considered in third wave (i.e. was not eliminated from consideration using the

methodology of Section 6.2).

A further consideration could be that the transmission system planner could have a preference for reinforcing one boundary more than the other, for example, it may be easier to reinforce the B6 boundary in comparison to the B7a boundary for various reasons (such as tighter building regulations over the B7a boundary). In such cases decision support could be offered by estimating optimal B6 reinforcement magnitudes for a variety of B7a reinforcement magnitudes (e.g. estimating optimal B6 reinforcement magnitudes for 250 MW increments of B7a reinforcement), as well as noting the estimate of expected total costs of each decision. The transmission system planner could then use these estimates to balance their preferences of minimising expected total costs and making a smaller reinforcement of the B7a boundary.

6.4 Sensitivity of the Estimate of Optimal Decision

6.4.1 The Necessity for a New Wave Process for Each Sensitivity Considered

When considering the sensitivity of the optimal decision to a factor such as the assumed cost of reinforcement or the attitude to risk of the decision maker, it is necessary to carry out a separate wave process for each assumption to avoid incorrectly eliminating the optimal decision. This is illustrated in Figure 6.22, which shows how the decisions considered in the third wave vary with the assumed cost to reinforce. As can be seen, there is very little overlap between the three regions, implying the optimal decision varies greatly with the assumed cost of reinforcement. Further, Figure 6.23 displays how the corresponding estimates of expected total costs in wave 3 vary as the assumed cost to reinforce is varied. This gives further evidence to how the fitted model varies greatly with the assumptions made and why it is necessary to carry out a separate wave process for each scenario.

In all further results presented in this section, when varying particular assumptions an optimal decision will be identified by performing 2 waves of elimination, then identifying decisions to minimise the estimate of expected total costs in the third wave, just as

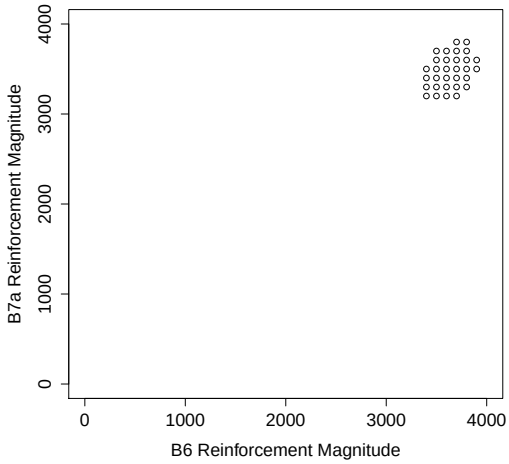

(a) £500 per MW per km.

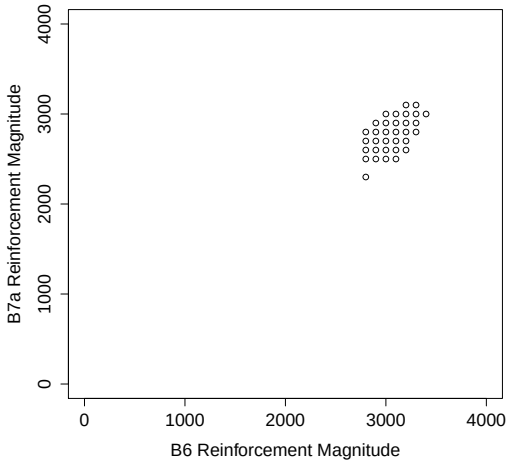

(b) £1000 per MW per km.

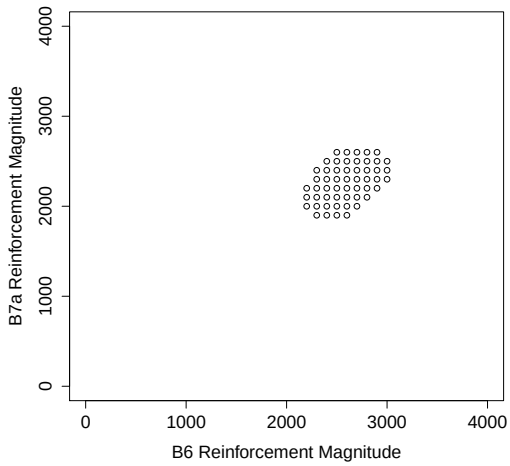

(c) £1500 per MW per km.

Figure 6.22: Plots to show how decisions considered in the third wave vary with the assumed cost to reinforce.

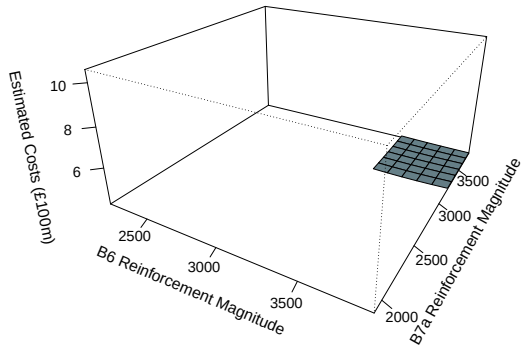

(a) £500 per MW per km.

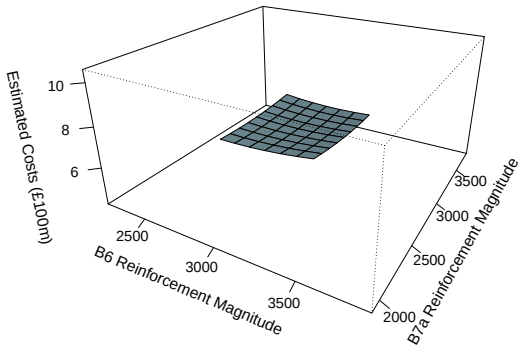

(b) £1000 per MW per km.

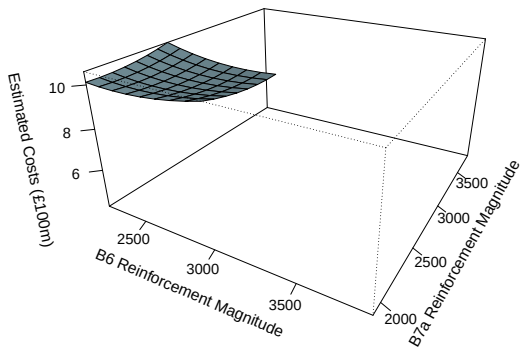

(c) £1500 per MW per km.

Figure 6.23: Plots to show how estimated expected total costs vary with B6 and B7a reinforcement magnitude for the emulator models fitted in the third wave for three different values of the assumed cost to reinforce.

in Section 6.3. For all variations on assumptions, this was appropriate as the decision space had been substantially reduced by this third wave and the reduction in the decision space from any further waves was negligible, with all decisions considered in the final wave resulting in similar, relatively low estimates of expected total costs.

6.4.2 Assumed Cost of Reinforcement

Assumed Cost of Reinforcement	Optimal B6 Reinforcement	Optimal B7a Reinforcement	Total Cost of Reinforcement
£500/MW/km	3690 MW	3420 MW	£355,500,000
£750/MW/km	3300 MW	3110 MW	£480,750,000
£1000/MW/km	3060 MW	2890 MW	£595,000,000
£1250/MW/km	2850 MW	2420 MW	£658,750,000
£1500/MW/km	2580 MW	2240 MW	£723,000,000

Table 6.2: Table of how estimated optimal reinforcement strategy varies with assumed cost of reinforcement.

Table 6.2 displays how the optimal decision estimated in wave 3 varies as the cost of reinforcement is varied from the assumed £1000 per MW per km. There appears to be a quite smooth general trend of around 100 MW reinforcement less being made on each boundary for each additional £100 per MW per km it costs to reinforce, with total reinforcement across both boundaries increasing by 1130 MW MW when the cost to reinforcement is decreased to £500 per MW per km and decreasing by 1160 MW when the cost to reinforcement is increased to £1500 per MW per km.

6.4.3 Prior Beliefs About Uncertainties

Results of this chapter have so far assumed the set of prior beliefs about uncertainties detailed in Section 6.1.1. However, Figures 6.1 and 6.2 illustrated how total costs are dependent on the uncertain variables, which in turn means the estimate of expected total costs under uncertainty is dependent on the assumed prior beliefs about these variables. Therefore, four alternative sets of prior beliefs about uncertainties, detailed in Table 6.3, will be considered in this section.

Prior Beliefs	Range Considered for Nuclear Availability Probability	Range Considered for CCGT Availability Probability	Range Considered for Peak Demand Magnification
Original Prior	0.55 to 0.85	0.8 to 0.95	0.95 to 1.05
Narrow Prior	0.625 to 0.775	0.8375 to 0.9125	0.975 to 1.025
Wide Prior	0.475 to 0.925	0.7625 to 0.9875	0.925 to 1.075
Low Prior	0.55 to 0.7	0.8 to 0.875	0.95 to 1
High Prior	0.7 to 0.85	0.875 to 0.95	1 to 1.05

Table 6.3: Table detailing the ranges considered for variables containing uncertainty for five potential sets of prior beliefs about uncertainty. A uniform distribution is fitted across each range to represent prior beliefs, $p(\mathbf{v})$.

Prior Beliefs	B6 Reinforcement Magnitude	B7a Reinforcement Magnitude
Original Prior	3060 MW	2890 MW
Narrow Prior	3050 MW	2700 MW
Wide Prior	3180 MW	2990 MW
Low Prior	3030 MW	2380 MW
High Prior	3130 MW	3020 MW

Table 6.4: Table of how the estimated optimal decision varies with prior beliefs about uncertainties, assuming it costs £1000 per MW per km to reinforce.

Table 6.4 shows how the estimated optimal decision varies with the assumed set of prior beliefs about uncertainties. Varying the width of the uncertainty window considered appears to have a quite small effect on the estimate of optimal decision, with total reinforcement decreasing by 200 MW for the narrow prior and increasing by 220 MW for the wide prior. However, varying the centre of the uncertainty distribution appears to have a greater effect, with total reinforcement decreasing by 540 MW when assuming the low prior in comparison to when assuming the original prior.

6.5 Attitude to Risk

6.5.1 Applying a Loss Function

Results for this chapter have so far assumed a risk neutral attitude. A loss function can be used to account for an attitude risk when making decisions. However, using

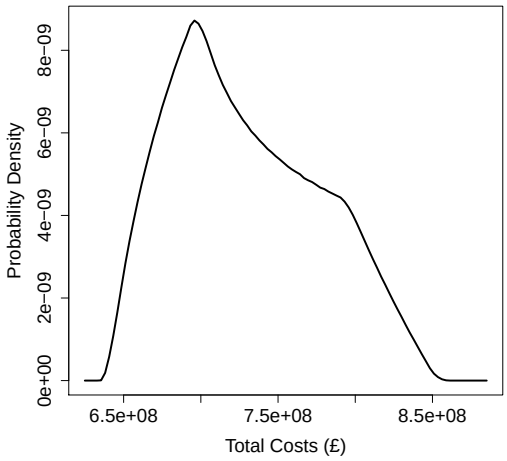

(a) Risk profile when making the estimated optimal risk neutral decision.

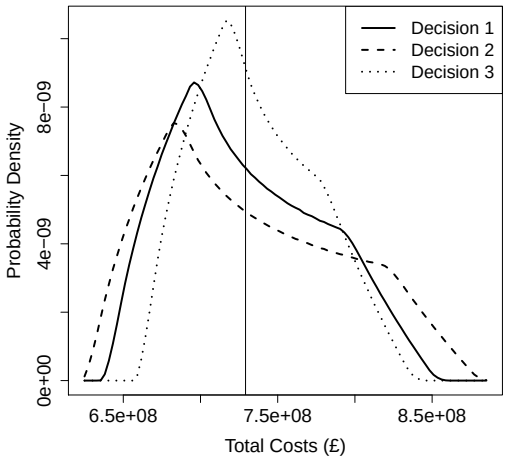

(b) Comparison of risk profiles when varying decisions from the estimated optimal risk neutral decision. The vertical line represents the estimate of expected total costs when making the risk neutral optimal decision.

Figure 6.24: Plots to illustrate risk profiles for various decisions.

a power loss function, as was considered in Equation 5.4.2 of Section 5.4.3, does not give interesting results for the example of Section 6.1.1, even when large powers are considered. For example, using a loss function which uses an 8th power loss would result in a decision of 3090 MW B6 reinforcement and 2950 MW B7a reinforcement, an increase of just 90 MW in comparison to a risk neutral attitude.

Reinforcement Decision	B6 Reinforcement Magnitude	B7a Reinforcement Magnitude
Decision 1	3060 MW	2890 MW
Decision 2	2860 MW	2690 MW
Decision 3	3260 MW	3090 MW

Table 6.5: Summary of decisions used in Figure 6.24 (b).

The reasons for this can be explained by considering Figure 6.24, which compares risk profiles for three reinforcement decisions. The decisions, detailed in Table 6.5, are the risk neutral optimal decision of 3060 MW B6 and 2890 MW B7a, as well as two alternative decisions which consider either increasing or decreasing the reinforcement of both boundaries by 200 MW in comparison to the risk neutral optimal. These plots illustrate that when the risk neutral optimal decision is made, a loss of at least

£636,000,000 will occur no matter what values the variables containing uncertainty take (the reinforcement costs alone, which are modelled deterministically, amount to £595,000,000), with the largest costs that can occur being just 35% larger.

Further, when increasing the reinforcement magnitude beyond the risk neutral optimal, the probability of the most extreme costs occurring (beyond £800,000,000) are not greatly reduced (losses of up to £800,000,000 are in fact more common when making the larger reinforcement). This shows how a large cost will occur no matter what, and (within the model) the decision maker is quite indifferent to the relatively small benefits of reinforcing beyond the risk neutral optimal decision.

In a real application this would mean that this particular example is insensitive to the decision maker's attitude to when working directly with total costs (unless a very large power of the loss function is used), whereas the example of Section 5.4.3 was sensitive to the decision maker's attitude to risk. The following subsection will illustrate how an atypical loss function can be used to assess the relative losses in comparison to the risk neutral expectation, resulting in the estimate of the optimal decision being more sensitive to the decision maker's attitude to risk.

6.5.2 Attitude to Risk: Methodology

For the methodology of accounting for an attitude to risk that will be used in this section, first the optimal values of the decision variables under a risk neutral attitude, $\mathbf{d}^o = d_1^o, ..., d_{N_d}^o$, are estimated, along with the resulting estimate of expected total costs, $\tilde{F}_T(\mathbf{d}^o)$. A model, $\tilde{f}_b$, is then fitted such that:

$$\tilde{f}_b(\mathbf{v}, \mathbf{d}) = \tilde{f}_T(\mathbf{v}, \mathbf{d}) - \tilde{F}_T(\mathbf{d}^o) \tag{6.5.1}$$

$\tilde{f}_b(\mathbf{v}, \mathbf{d})$ is the relative loss when uncertain variables take values $\mathbf{v} = v_1, ..., v_{N_v}$ and decision $\mathbf{d} = d_1, ..., d_{N_d}$ is made in comparison to the estimated expected total costs of the risk neutral estimated optimal decision.

Section 6.5.1 noted that because extremely large costs (hundreds of millions) occur regardless of the decision made, the use of a power loss function will not result in a substantial change to the optimal decision unless a very large power is considered,

despite the variations in costs as the uncertain variables are varied being quite large in real terms. Working with $\tilde{f}_b$ allows for the relative losses as the uncertain variables are varied when making a particular decision to be adequately assessed. A negative value of $\tilde{f}_b$ indicates a smaller loss in comparison to the expected loss when a reinforcement equal to the risk neutral optimal has been made.

For a loss function, l, which describes an attitude to risk, the expected loss of a decision can then be calculated as:

$$\tilde{F}_{b,l}(\mathbf{d}) = \int_{\mathbf{v}} l\left(\tilde{f}_b(\mathbf{v},\mathbf{d})\right) \times p(\mathbf{v})\mathrm{d}\mathbf{v} \tag{6.5.2}$$

The objective is to minimise Equation 6.5.2 (i.e. minimise the estimate of expected loss). It is necessary to carry out a separate wave process for each attitude to risk. This is because risk averse attitudes would consider decisions of larger magnitude than a risk neutral attitude, so it is better to work with several models fitted more accurately over a smaller range of values of decision variables than one model fitted less accurately over a larger range.

The loss function applied in Equation 6.5.2 is, for relative loss $\tilde{f}_b(\mathbf{v},\mathbf{d})$ and risk attitude parameter p:

$$l(\tilde{f}_b(\mathbf{v},\mathbf{d}),p) = \begin{cases} -|\tilde{f}_b(\mathbf{v},\mathbf{d})|^{\frac{1}{p}} & \text{if } \tilde{f}_b(\mathbf{v},\mathbf{d}) < 0 \\ \left(\tilde{f}_b(\mathbf{v},\mathbf{d})\right)^p & \text{if } \tilde{f}_b(\mathbf{v},\mathbf{d}) \geq 0 \end{cases}$$

This loss function is illustrated in Figure 6.25. $p > 1$ represents a risk averse attitude, $0 < p < 1$ represents a risk prone attitude and $p = 1$ represents a risk neutral attitude. In practice, real world decision makers are rarely risk prone.

Under risk averse conditions, this loss function will harshly penalise a scenario for doing worse than the expectation of the risk neutral optimal, thus placing in the decision process great emphasis on avoiding scenarios where extremely large losses occur. The loss function also rewards improvement on the risk neutral optimal, however this reward is relatively smaller than the penalty for doing worse than the risk-neutral optimum.

6.5.3 Decisions Under an Attitude to Risk

Tables 6.6 and 6.7 show how the estimated optimal decision to be made varies as the assumed attitude to risk of the decision maker is varied, when assuming a cost

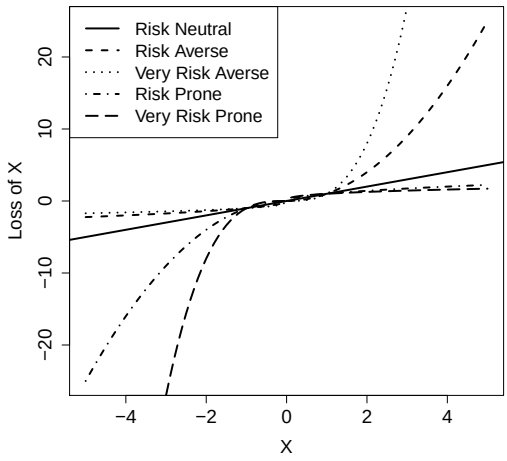

Figure 6.25: Plot to illustrate the loss function as attitude to risk is varied.

of £1000 and £1500 per MW per km to reinforce respectively. Results are generally much more sensitive to attitude to risk when assuming a cost of £1500 per MW per km to reinforce, particularly when assuming a less severe risk averse position or only considering the B6 boundary.

For example, taking the least risk averse position ($p = 1.5$) results in a total of 200 MW additional reinforcement (in comparison to the risk neutral optimal decisions) when assuming a cost of £1000 per MW per km to reinforce, but a total additional reinforcement of 410 MW when assuming a cost of £1500 per MW per km to reinforce. Under the most severe risk averse position considered ($p = 3$) the increases to total reinforcement were 630 MW and 850 MW in comparison to the estimated risk neutral optimal decision when assuming a cost to reinforce of £1000 per MW per km or £1500 per MW per km respectively.

Loss Function Power	B6 Reinforcement Magnitude	B7a Reinforcement Magnitude
1	3060 MW	2890 MW
1.5	3120 MW	3030 MW
2	3140 MW	3190 MW
2.5	3220 MW	3230 MW
3	3160 MW	3420 MW

Table 6.6: Table of how the estimated optimal decision varies with the assumed attitude to risk of the decision maker, assuming it costs £1000 per MW per km to reinforce.

Loss Function Power	B6 Reinforcement Magnitude	B7a Reinforcement Magnitude
1	2580 MW	2240 MW
1.5	2660 MW	2570 MW
2	2740 MW	2660 MW
2.5	2770 MW	2730 MW
3	2840 MW	2830 MW

Table 6.7: Table of how the estimated optimal decision varies with the assumed attitude to risk of the decision maker, assuming it costs £1500 per MW per km to reinforce.

6.6 Using a Smaller Number of Training Runs

Based on the results of Section 6.1.3 and Appendix B.1, this chapter has so far used 300 training runs to fit the emulation model in each wave. However, it would be possible to use a smaller number of training runs to approximate the simulator (albeit less accurately), which would still allow for decisions to be identified which have evidence against them being optimal using the methodology of Section 6.2. This section will consider whether it is plausible to reduce the number of training runs used in each wave to 50 in order to reduce the computation requirements to identify a small region where the optimal decision lies. It was verified that when using 50 training runs the optimal form of the polynomial portion of the emulator model remains as

$$\beta_0 + \beta_1 v_1 + \beta_2 v_2 + \beta_3 v_3 + \beta_4 d_1 + \beta_5 d_2 + \beta_6 v_1^2 + \beta_7 v_2^2 + \beta_8 v_3^2 + \beta_9 d_1^2 + \beta_{10} d_2^2 + \beta_{11} v_1 d_1 + \beta_{12} v_1 d_2 + \beta_{13} d_1 d_2 + \beta_{14} v_1^2 d_1^2 + \beta_{15} v_1^2 d_2^2 + \beta_{16} d_1^2 d_2^2 + \beta_{17} v_1 d_1 d_2 + \beta_{18} v_1^2 d_1^2 d_2^2$$

6.6.1 The Wave Process Using 50 Training Runs Per Wave

Figure 6.26 illustrates the decisions considered in each wave when using 50 training runs per wave to fit the emulator model. Of the decisions initially considered in each wave; 65.7%, 64.9% and 55.0% were eliminated in waves 1, 2 and 3 respectively. Reduction in the decision space was negligible from further waves. As in Section 6.3, this is due to the cost estimates being relatively flat in the final wave, with all decisions considered resulting in similar, relatively low estimates of expected total costs.

Figures 6.27 and 6.28 illustrate how estimates of expected total costs from the emulator model vary with reinforcement decision in the first and fourth wave, when using 50

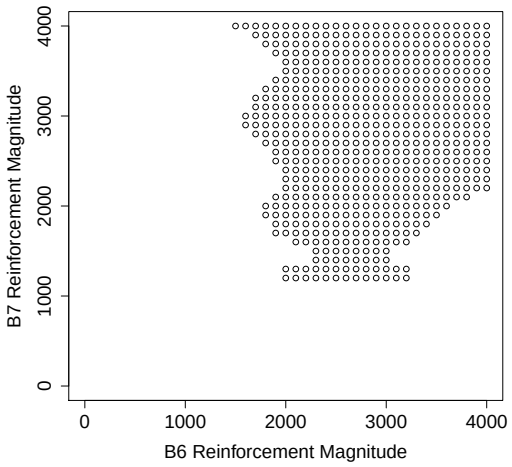

(a) Wave 2.

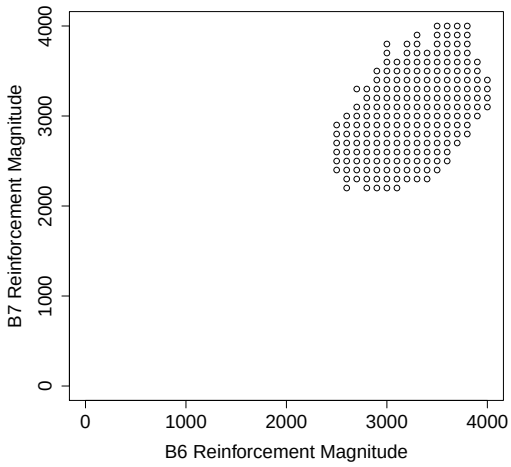

(b) Wave 3.

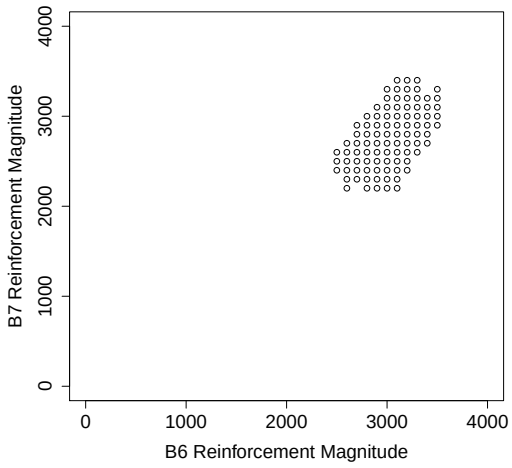

(c) Wave 4.

Figure 6.26: Plots to illustrate the ranges of decisions considered in each wave when using 50 training runs in each wave to construct the emulator model.

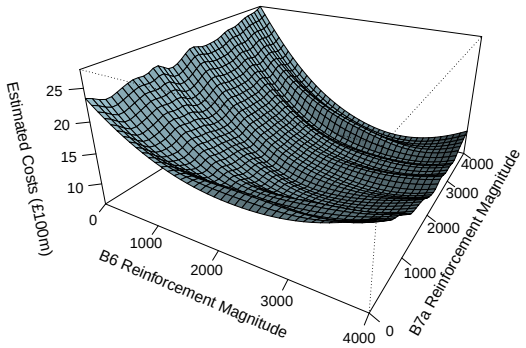

(a) Wave 1.

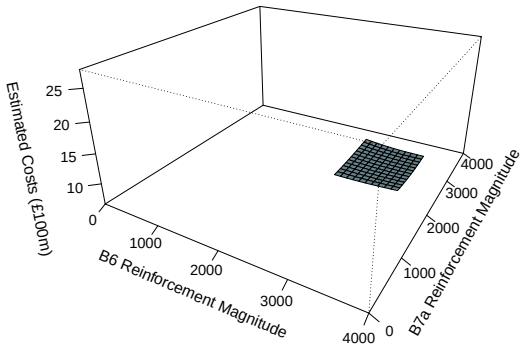

(b) Wave 4.

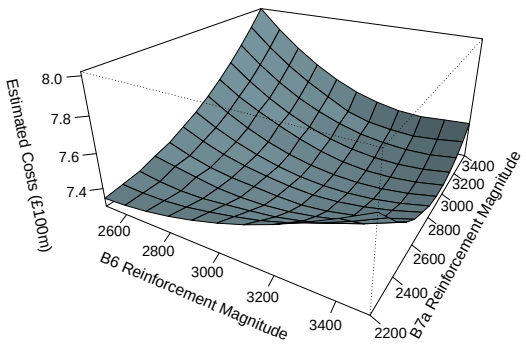

(c) Wave 4.

Figure 6.27: Plots to show how estimates of expected total costs vary with reinforcement decisions and fitted emulator model, when using 50 training runs per wave to construct the emulator.

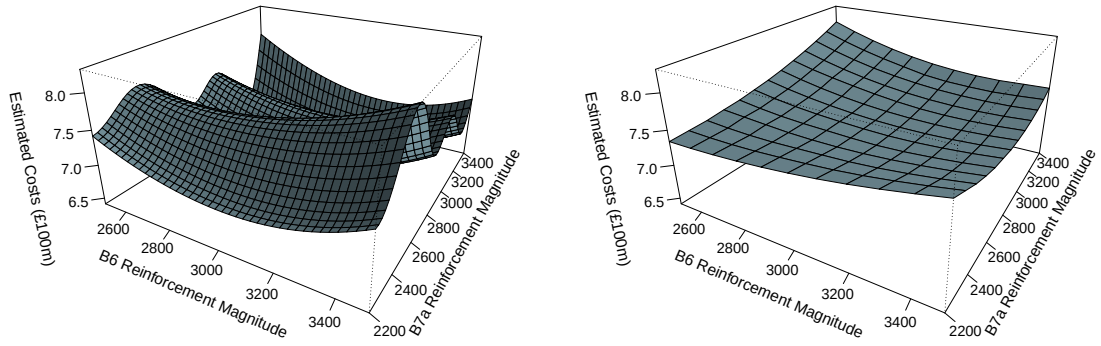

(a) Wave 1. (b) Wave 4.

Figure 6.28: Plots to show how estimates of expected total costs vary with reinforcement decisions and fitted emulator model over the range of decisions considered in wave 4, when using 50 training runs per wave to construct the emulator.

training runs to construct the emulator model in each wave. Figure 6.27 (b) shows how all decisions considered in the fourth wave result in similar, relatively low estimates of expected total costs. In Figure 6.28 it is shown how the fourth wave emulator model varies much more smoothly in comparison to the emulator model fitted in the first wave, indicating how eliminating decisions from consideration has allowed for a more accurate model to be fitted over a smaller range of values of the decision variables.

In the fourth wave, the estimate of the optimal decision (i.e. the decision which minimises the estimate of expected total costs under uncertainty using Equation 5.2.16) is 3170 MW B6 and 2830 MW B7a reinforcement, which is somewhat different to the 3060 MW B6 and 2890 MW B7a which would be made when using the third wave emulator model when using 300 training runs per wave (though only a 50 MW total difference across both boundaries).

6.6.2 Comparison to Using 300 Training Runs Per Wave

In the previous subsection it was shown how 50 training runs per wave instead of 300 could be used in the emulation process. By comparing Figure 6.26 to Figure 6.19 it can be seen that decisions are eliminated at a faster rate when using 300 training runs per

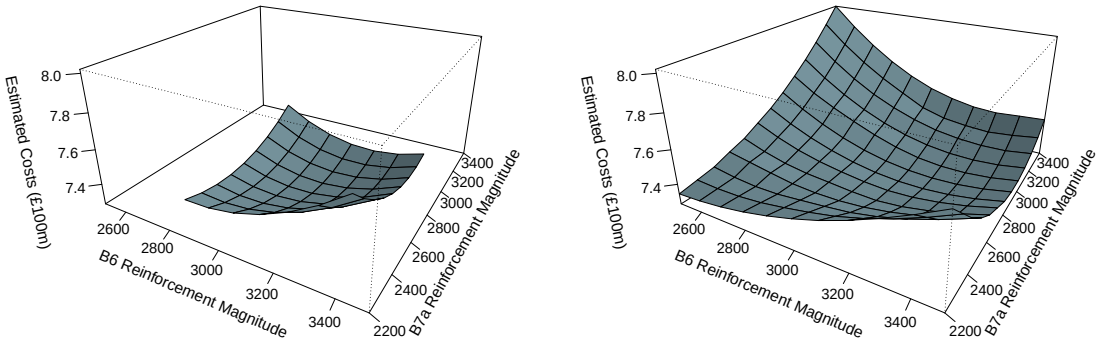

(a) 300 training runs, wave 3.

(b) 50 training runs, wave 4.

Figure 6.29: Plots to compare the estimated expected total costs from the final wave emulator models when using 50 or 300 training runs to fit the emulator model.

wave to fit the emulator model. This is to be expected, as a greater number of training runs means a more accurate emulator model can be fitted in each wave with a greater level of confidence in the estimates from the emulator. 2.75 times more decisions are considered in the final wave when using 50 training runs per wave in comparison to using 300 training runs per wave. However, 4 waves of 50 training runs requires 77.8% fewer total training runs to be acquired across all waves in comparison to using 3 waves of 300 training runs, indicating there is a trade-off between the amount of work done and the amount of decisions eliminated.

This is considered further in Figure 6.29 compares the estimates of expected total costs under uncertainty for the final wave models when using 50 or 300 training runs per wave to fit the emulator models. It is shown that the models appear to be very similar over the range of decisions considered by both models. This is clearer in Figure 6.30, which plots the differences in the estimates of expected total costs between the two models. These plots show how fitting an emulator model using 50 training runs generally underestimates total costs in comparison to the model fitted using 300 training runs, though this difference is generally quite small (less than 1.5% of the total costs).

A further comparison between the two models and their respective credible bounds is given in Figure 6.31. It is again shown that estimates of expected total costs are

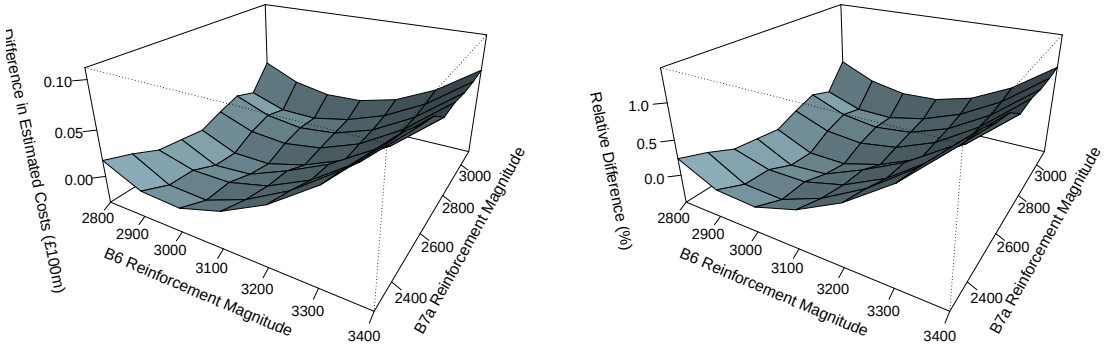

(a) Difference between estimates from emulator models fitted using 300 and 50 training runs in the final wave.

(b) Relative difference between estimates from emulator models fitted using 300 and 50 training runs in the final wave.

Figure 6.30: Plots of the differences in estimated expected total costs as decision is varied when using 50 or 300 training runs per wave to fit the emulator model.

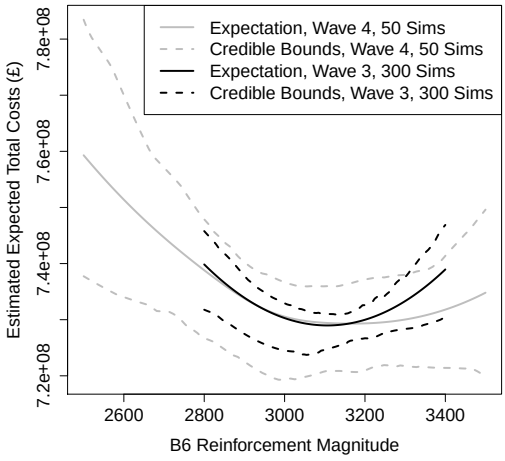

Figure 6.31: Plot to compare estimates of expected total costs and corresponding credible intervals for the final wave emulator models fitted using 50 and 300 training runs. B7a reinforcement magnitude fixed at 2890 MW (the estimated optimal when using 300 training runs).

generally quite similar, though a greater difference is noted towards the higher and lower limits of B6 reinforcement magnitude. Also, the credible intervals are much narrower for the model fitted using 300 training runs. This is to be expected, as the model was fitted over a smaller range of decisions when using a greater number of training runs to fit the model. This indicates there is a greater level of confidence in the estimates of expected total costs when using 300 training runs to fit the model in comparison to 50.

However, the estimates of expected total costs from the model fitted using 50 training runs do lie within the credible intervals for the model fitted using 300 training runs. This would imply that the estimated expected total cost under uncertainty when using the model fitted from 50 training runs are not significantly different to those from the model fitted using 300 training runs.

By comparing these results to Figure 6.21 (c) it can be seen that the emulator model of the fourth wave when using 50 training runs per wave gives a much better comparison to the emulator model of the third wave when using 300 training runs per wave, than the emulator model of the first wave when using 300 training runs per wave. This is despite the fact that 100 fewer training runs are required in total to fit the fourth wave model when using 50 training runs per wave in comparison to the first wave when using 300 training runs per wave.

6.6.3 Conclusions on Number of Training Runs Used to Fit the Emulator Model

This section has demonstrated that when just 50 training runs are used to fit an emulator in each wave, the decision space can still be greatly reduced over a number of waves. However, using 300 training runs does allow for a greater reduction of the decision space and the resulting credible bounds of the estimate are narrower in comparison to when using 50 training runs to fit the model. This would imply that there are benefits to using a larger number of training runs to fit the emulator model, though if it is not feasible to fit a model using 300 training runs, then progress can still be made using only 50 training runs to fit the emulator model.

Chapter 7

Investigating the Effects of Model/Data Assumptions for the Example of Chapter 6

7.1 Model and Data Assumptions

Chapters 5 and 6 gave examples of how emulators can be used to approximate simulators to make decisions under uncertainty. The particular examples presented were transmission expansion planning problems (building more power lines) to optimise constraint costs (costs which arise when there is insufficient installed transmission capacity to utilise all the cheapest available generating technology) for given power systems. These examples depended on the simulator defined in Chapter 3, which estimates the mean constraint costs that arise for given input information about the power system.

Whilst the examples of Chapters 5 and 6 do consider decision making whilst accounting for uncertainty in certain aspects of the power system, there were many other assumptions that were made when defining the simulator in Chapter 3. These assumptions include data assumed for many aspects of the power system (such as installed generators, bid/offer prices, generator availabilities, etc), with several modelling assumptions also made (such as the use of estimation via half hour snapshots, the seasonal model used to simulate available wind generating capacity, etc). These assumptions could

have an effect on the costs estimated from the simulator, and the resulting decisions made. This chapter will investigate how four assumptions (the seasonal model, the assumed load duration curve, the installed wind generating capacity and yearly constraint cost model) affect costs estimated and the resulting decisions made.

7.2 Assumption One - Seasonal Model

7.2.1 The Simulator Seasonal Model

Section 3.1 indicated that constraint costs for a year are simulated by breaking the year down into half hour snapshots, simulating each snapshot independently and calculating the sum of the constraint costs across all snapshots. There are two factors which vary between snapshots: a seasonal effect and the demand level of the snapshot. The demand level assumed for each snapshot was first considered in Section 4.1.2 when considering an application of importance sampling to improve the efficiency of estimating mean annual constraint costs. Further consideration to the effects of the assumed demand of each snapshot will be considered later in Section 7.3, where the effects of the assumed load duration curve on mean constraint cost estimates and the resulting estimates of optimal decisions is considered.

This section will consider the seasonal effect on estimates of mean constraint costs. The seasonal effect was detailed in Section 3.5, where it is stated that a different distribution is assumed for available wind generating capacity in summer and winter. Aside from this, all other factors (other than the aforementioned snapshot demand level) are consistent in each snapshot.

Section 3.5 also noted that any snapshot in December, January or February was classified as a winter snapshot, and all other snapshots were classified as summer snapshots. However, this is quite a rigid assumption, with the distribution of wind capacity changing very abruptly between 23:30 on the 28th of February and 00:00 on the 1st of March. This effect was very clear in Figure 4.3 (b) of Section 4.1.3.

In reality, the weather (and thus wind generation) will not change so abruptly and there would not be such a clear divide between winter and summer. Sections 7.2.2 and 7.2.3

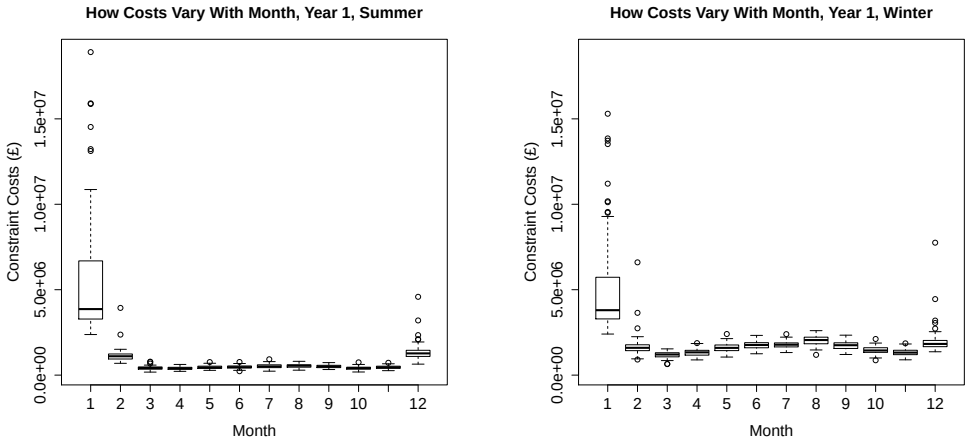

(a) Summer model assumed for available wind generating capacity.

(b) Winter model assumed for available wind generating capacity.

Figure 7.1: Boxplots to show how simulations of constraint costs vary with month and assumed seasonal model for a year 1 power system background.

will consider how the classification of months as summer or winter affects the estimates of mean constraint costs. Section 7.2.4 will then consider how the estimate of optimal reinforcement decision is affected by assuming a particular seasonal model, with Section 7.2.5 going on to consider how mean constraint costs can be estimated when accounting for the uncertainty which exists in the seasonal model, and how accounting for such uncertainty affects the resulting estimates of optimal reinforcement decisions.

7.2.2 Graphical Illustration of the Effect of Assumed Seasonal Model on Cost Estimates

To investigate how the assumed seasonal model affects estimates of mean constraint costs, 100 full simulations of constraint costs for each combination of month and seasonal model were evaluated for a year 1 and year 6 power system background (to consider how constraint costs would vary for the examples presented in Chapters 5 and Chapter 6 respectively). Comparisons between the mean and variation of these simulations as seasonal model is varied can then be used to consider the effect of seasonal model on constraint cost estimation.

Figure 7.1 displays boxplots of how simulated constraint costs vary with month when assuming a year 1 system background from [69], with Figure 7.1 (a) showing how

simulated constraint costs vary if each month uses the summer model for available wind generating capacity and Figure 7.1 (b) shows how simulated constraint costs vary if each month uses the winter model for available wind generating capacity. The graphs are numbered in order of calendar month, such that 1 refers to January, 2 refers to February,...,12 refers to December.

The first thing to note is that the extremely large costs in January dominate this graph, meaning it would be most important to model January as accurately as possible as it is the most important month to the estimate of mean annual constraint costs. As few would argue against classifying January as a winter month, the risk of error from misclassifying January is minimal.

Figure 7.1 also shows that constraint costs are generally greater when the winter model is used in comparison to the summer model. This implies that if a month is incorrectly classified as a summer month then mean constraint costs for the year will be underestimated, which may affect the resulting decision.

The relative importance of the months also changes depending on which seasonal model was used. For example, when a summer model is used for all months, the largest constraint costs by some margin occur in January, but February and December also contribute a lot more to the annual constraint costs than the other nine months. However, when a winter model is used for all months, January still gives the greatest contribution to annual constraint cost estimates, but all other months now have a comparable contribution to one another (with the 9 months classified as summer months having a much greater contribution to annual constraint costs when using a winter model for available wind generating capacity in comparison to when using a summer model). August appears to have the largest contribution to costs (after January) when using the winter model, despite being a month which few would argue against classifying as a summer month.

Figure 7.2 shows boxplots of how simulated constraint costs vary with month for a year 6 power system background, with Figure 7.2 (a) showing how constraint costs vary if each month uses the summer model for available wind generating capacity and Figure 7.2 (b) shows how constraint costs vary if each month uses the winter model for available wind generating capacity. There is clearly a large increase in costs for every

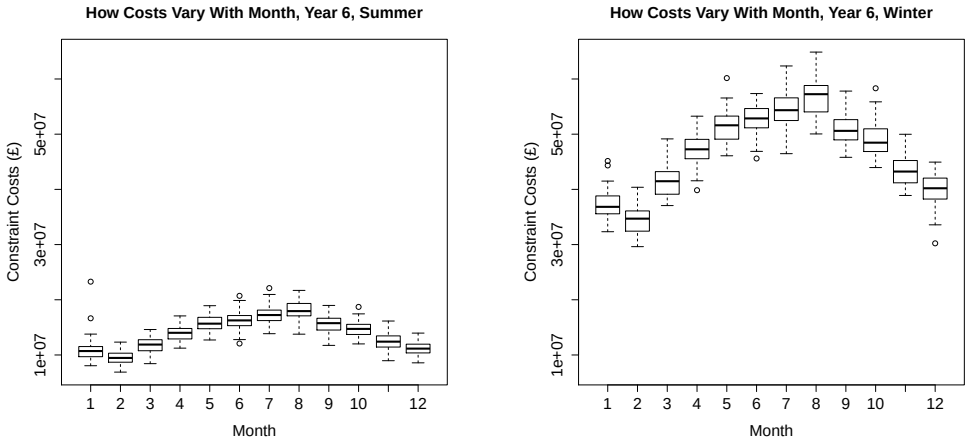

(a) Summer model assumed for available wind generating capacity.

(b) Winter model assumed for available wind generating capacity.

Figure 7.2: Boxplots to show how simulations of constraint costs vary with month and assumed seasonal model for a year 6 power system background.

month when a winter model for available wind generating capacity is assumed for that month over assuming a summer model. This not only applies to the mean of constraint costs, but it can also be clearly seen that there is no overlap between the spread of the 100 summer simulations and the 100 winter simulations.

One thing that is interesting to note is that the simulator as described in Chapter 3 classified December, January and February as winter months, and all others as summer months. Handling snapshots in this manner results in the majority of annual constraint costs occurring in the winter. However, Figure 7.2 shows that when the same seasonal model is applied to all months, the nine months originally classified as summer months all have higher estimates of constraint costs than the three months classified as winter months. As a winter model results in greater mean constraint cost estimates for each month, if additional months were included in the winter model this would increase the estimate of mean annual constraint costs. As the transmission system is expanded (B6 and B7a boundaries reinforced) to reduce constraint costs this would suggest that including additional months as winter months would increase the optimal reinforcement magnitude of the transmission system expansion, and this will be investigated in Section 7.2.4.

7.2.3 Figures on the Effect of Assumed Seasonal Model on Cost Estimates

Month	Estimated Mean Constraint Costs Under Assumed Seasonal Model	Change in Mean Constraint Costs When Using Alternative Season	Percentage Change in Monthly Mean Constraint Costs	Change in Mean as a Percentage of Mean Annual Constraint Costs
January	£4,992,000	£290,000	5.82%	2.27%
February	£1,667,000	-£534,000	-32.0%	-4.17%
March	£420,000	£767,000	183%	5.99%
April	£403,000	£916,000	227%	7.15%
May	£460,000	£1,139,000	248%	8.89%
June	£478,000	£1,269,000	265%	9.90%
July	£521,000	£1,258,000	241%	9.82%
August	£541,000	£1,501,000	278%	11.7%
September	£512,000	£1,230,000	240%	9.60%
October	£407,000	£1,049,000	258%	8.19%
November	£458,000	£872,000	190%	6.81%
December	£1,953,000	-£617,000	-31.6%	-4.81%

Table 7.1: Table detailing how mean constraint cost estimates vary with assumed seasonal model for a year 1 power system background.

Tables 7.1 and 7.2 detail how mean constraint cost estimates for each month vary with the assumed seasonal model for a year 1 and year 6 power system background respectively. Original estimate refers to the estimate using the seasonal model assigned by National Grid (i.e. modelling January, February and December as winter months and all other months as summer months) with the change in the estimate indicating how much the estimate of mean constraint costs would change if the alternative seasonal model was used instead. Each of these cost estimates were acquired using the 100 evaluations of the full simulator used to construct the boxplots in Section 7.2.2.

With the exception of January for a year 1 power system background, it is seen that using a summer model instead of a winter model results in a large reduction in mean constraint costs and using a winter model instead of a summer model results in a large increase in mean constraint costs for all months for both power system backgrounds. This is consistent with what was observed in Section 7.2.2.

Month	Estimated Mean Constraint Costs Under Assumed Seasonal Model	Change in Mean Constraint Costs When Using Alternative Season	Percentage Change in Monthly Mean Constraint Costs	Change in Mean as a Percentage of Mean Annual Constraint Costs
January	£37,210,000	-£26,370,000	-70.9%	-10.7%
February	£34,550,000	-£24,990,000	-72.3%	-10.1%
March	£11,890,000	£29,630,000	249%	12.0%
April	£13,910,000	£33,240,000	239%	13.4%
May	£15,760,000	£35,730,000	227%	14.4%
June	£16,200,000	£36,400,000	225%	14.7%
July	£17,230,000	£37,260,000	216%	15.1%
August	£18,070,000	£38,770,000	215%	15.7%
September	£15,520,000	£35,280,000	227%	14.3%
October	£14,670,000	£34,250,000	233%	13.8%
November	£12,430,000	£30,880,000	249%	12.5%
December	£39,940,000	-£28,730,000	-71.9%	-11.6%

Table 7.2: Table detailing how mean constraint cost estimates vary with assumed seasonal model for a year 6 power system background.

It also appears that winter months are more robust to cost estimates with change in season, with changes in constraint cost estimates being 32% or less for winter months for a year 1 power system background and 73% or less for a year 6 power system background. The changes in mean constraint cost estimates for months classified by National Grid as summer are much greater, with all changes being greater than 183%, the largest of which was a 278% increase in August for a year 1 power system background.

Whilst the change in mean constraint costs is quite large for each individual month, it is important to consider that there are 12 months in a year and therefore if the seasonal model of a single month is changed it may not necessarily have a great effect on the estimate of mean annual constraint costs. Therefore, Tables 7.1 and 7.2 also detail the percentage change in the estimate of mean annual constraint costs if the seasonal model for a single month is changed.

For a year 6 power system background, changing the seasonal model assumed for any individual month has quite a large effect on the estimate of mean annual constraint costs, with each month changing the annual estimate by at least 10%, with August having the largest effect of a 15.7% increase.

Things are less extreme for a year 1 power system background with the use of a summer model for months National Grid classify as winter months having an effect on mean annual constraint costs of less than 5%. The effect of using a winter model for months National Grid assume to follow a summer model is greater, with all changes in the estimate of mean annual constraint costs being greater than 5%, and August giving the largest change at an 11.7% increase.

7.2.4 The Effect of Assumed Seasonal Model on the Estimated Optimal Reinforcement Decisions

Alternative Seasonal Models

This section has shown how the seasonal model assumed can have a large effect on the estimated mean constraint costs for a particular month. Further, it was shown that if the seasonal model was changed for just a single month, the effect on the mean annual constraint costs was not negligible. This subsection will consider how changing the assumed seasonal model of particular months affects the estimated optimal reinforcement decisions for a year 6 power system background.

However, it must also be considered how realistic certain changes to the seasonal model are. For example, the modelling of January as a winter month and July as a summer month seem to be very reasonable classifications that few would argue against. However, there would be much less consensus on the classification of November or March as summer months.

Therefore, instead of presenting results for every possible seasonal breakdown, results will be presented for four potential seasonal models:

1. December, January and February classified as winter months, all other months classified as summer months (National Grid's assumption).

2. November, December, January and February classified as winter months, all other months classified as summer months.

3. December, January, February and March classified as winter months, all other months classified as summer months.

4. November, December, January, February and March classified as winter months, all other months classified as summer months.

These assumptions consider whether or not to additionally include the months November, March or both in the seasonal model for winter. As these two months are the closest months to those classified as winter months, they are the two most logical choices for additional inclusion for winter month classification.

In order to investigate how such assumptions of seasonal model affect the estimate of optimal decisions to be made, the example of Chapter 6 detailed in Section 6.1.1 was repeated when assuming each of the four seasonal models detailed above, instead of just assuming the National Grid seasonal model. Recall, the example of Section 6.1.1 considers reinforcing the B6 and B7a boundaries whilst considering uncertainty in the nuclear availability probability, CCGT availability probability and peak demand level of the power system.

Estimates of Expected Total Costs for Each Seasonal Model

Figure 7.3 illustrates how estimates of expected total costs vary with B6 and B7a reinforcement magnitude when repeating the example of Section 6.1.1 for each of the four seasonal models considered and assuming a cost of £1000 per MW per km to reinforce. For each of the four seasonal models assumed, the estimate of expected total costs were acquired, as detailed in Section 5.2, by integrating the product of a fitted emulator model and prior beliefs about uncertainties via Equation 5.2.16. As these graphs intend to represent how results vary for the example detailed in Section 6.1.1 when varying the seasonal model assumed, the prior beliefs used are those outlined in Section 6.1.3 based on our interpretation on the expert judgement of Paul Plumptre [78], where a uniform distribution was fitted over a specified plausible range for each variable containing uncertainty (nuclear availability probability, CCGT availability probability and peak demand level).

For all four seasonal models, the variation in the estimates of expected total costs as reinforcement decision is varied is similar to what was noted in Section 6.1.3 when National Grid's seasonal model was assumed. That is, estimates of expected total costs

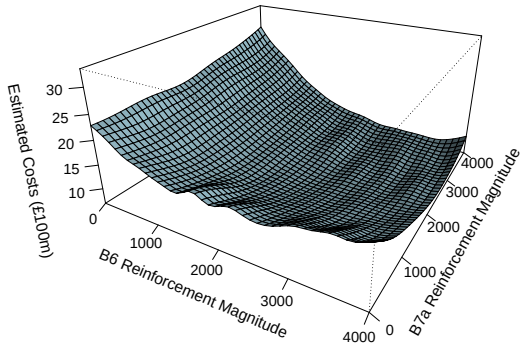

(a) Seasonal model 1 assumed.

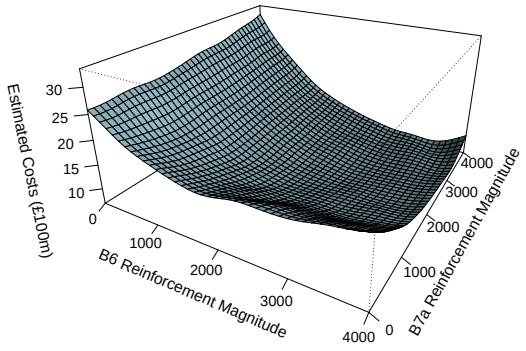

(b) Seasonal model 2 assumed.

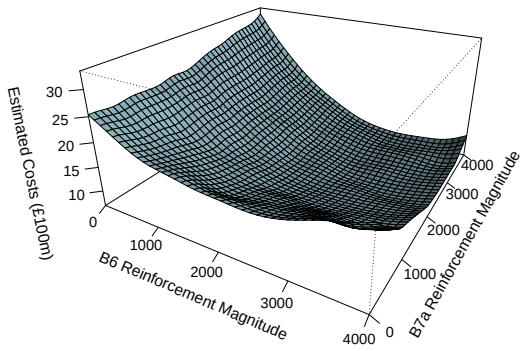

(c) Seasonal model 3 assumed.

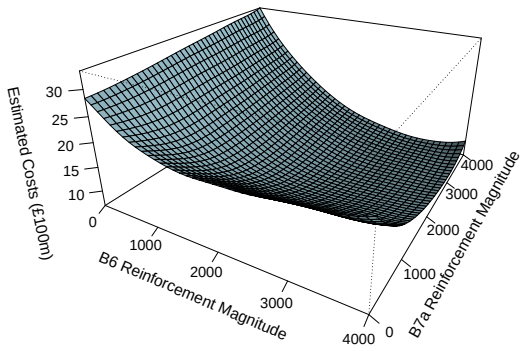

(d) Seasonal model 4 assumed.

Figure 7.3: Plots to show how estimates of expected total costs vary with B6 and B7a reinforcement magnitude and assumed seasonal model.

are very high when B6 reinforcement magnitude is low, with costs greatly decreasing as the B6 boundary is reinforced. Further, as was also noted in Section 6.1.3, expected total costs begin to rise when the B7a boundary alone is reinforced, though reinforcing both the B6 and B7a boundaries results in a greater decrease in estimated expected total costs in comparison to reinforcing the B6 boundary alone, indicating that an interaction exists between the two boundaries.

It can also be seen that estimates of expected total costs appear to rise as more seasons are included in the winter model. This is consistent with results from Section 7.2.2 and Section 7.2.3, which showed how estimated mean constraint costs increase when using a winter model instead of a summer model for all months.

For all seasonal models, it is also seen that all decisions which make at least 2000 MW B6 and 2000 MW B7a reinforcement result in similar, relatively low estimates of expected total costs, which indicates that the optimal reinforcement decision lies somewhere in this range for all seasonal models. Just as in the example presented in Chapter 6, a wave process must be carried out for each assumed seasonal model, in order to fit a more accurate emulation approximation to the simulator over a smaller range of decisions using the methodology of Section 6.2. In doing so, after several waves of elimination, it is likely that both the estimates of expected total costs and the ranges of decisions considered will vary with the assumed seasonal model. This is illustrated in Figure 7.4, which shows how estimated expected total costs when integrating over uncertainty using Equation 5.2.16 vary with the assumed seasonal model for decisions considered in the third wave (i.e. after 2 waves of elimination) when assuming a cost of £1000 per MW per km to reinforce.

It is seen that as more months are included in the winter model, the estimate of expected total costs rises (which again is consistent with results from Section 7.2.2 and Section 7.2.3). Further, it is seen that as more months are included in the winter model, the reinforcement magnitudes of decisions considered in the third wave generally increase slightly. This is what one would likely expect, as greater mean constraint costs indicate there is a greater potential benefit from reinforcement, which may justify a larger reinforcement being built.

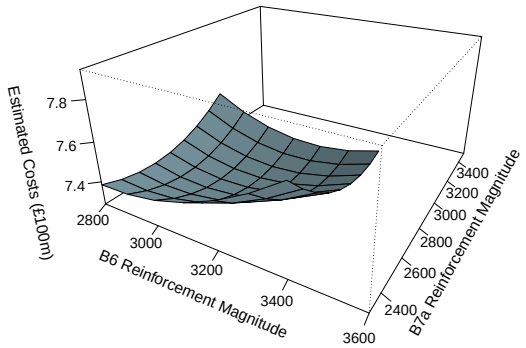

(a) Seasonal model 1 assumed.

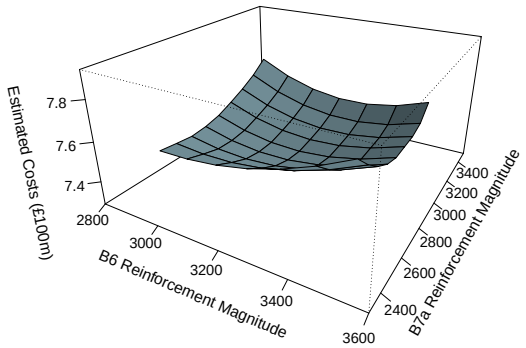

(b) Seasonal model 2 assumed.

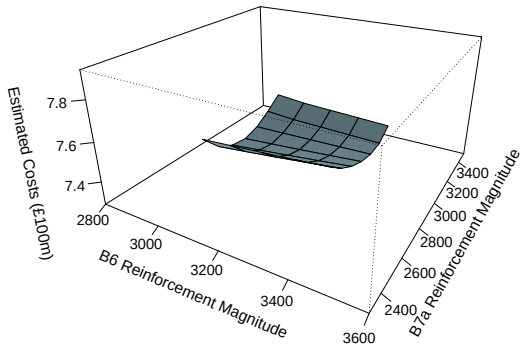

(c) Seasonal model 3 assumed.

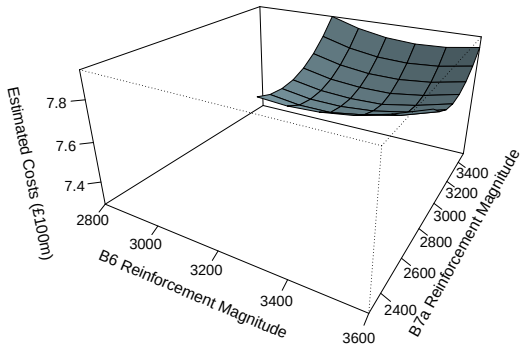

(d) Seasonal model 4 assumed.

Figure 7.4: Plots to show how estimates of expected total costs vary with B6 and B7a reinforcement magnitude and assumed seasonal model, after two waves of eliminating decisions which have evidence against them being optimal.

Estimated Optimal Decisions for Each Seasonal Model

Seasonal Model Assumed	B6 Reinforcement Magnitude	B7a Reinforcement Magnitude	Increase in Total Reinforcement
Seasonal Model 1	3060 MW	2890 MW	N/A
Seasonal Model 2	3060 MW	2980 MW	90 MW
Seasonal Model 3	3170 MW	2870 MW	90 MW
Seasonal Model 4	3230 MW	3030 MW	310 MW

Table 7.3: Table of how the estimated optimal reinforcement decision varies with the assumed seasonal model, when assuming it costs £1000 per MW per km to reinforce.

Table 7.3 displays how the estimated optimal decision to be made varies with assumed seasonal model, with decisions being made to minimise the estimated expected total costs from the emulator model fitted in the third wave, just as in Sections 6.3.2 and 6.4. As can be seen, including any additional months as winter months in the model increases the total amount of reinforcement built. Including only March or November results in quite a small change of 90 MW (in comparison to the estimate of optimal decision when assuming National Grid's seasonal model), with the inclusion of November only increasing the B7a boundary reinforcement magnitude, and the inclusion of March only increasing the B6 boundary reinforcement magnitude. However, modelling both March and November as winter months results in a total increase in reinforcement of 310 MW across both boundaries.

It is noted that whilst Figure 7.4 indicates that expected total costs rise as additional months are included in the winter model, there are several decisions which are considered (not eliminated) in the final wave of all four seasonal models. In particular, seasonal models 2 and 3 consider very similar ranges of decisions in the final wave. This means that although the estimated optimal reinforcement magnitudes appear to rise as additional months are included in the seasonal model, it has not been definitively proven that including these additional months in the winter model necessarily increases the optimal reinforcement magnitude.

Table 7.4 displays how the estimated optimal reinforcement decision to be made varies with assumed seasonal model, when assuming a larger cost of £1500 per MW per km to reinforce. As can be seen, at this higher cost to reinforce the decision made is more

Seasonal Model Assumed	B6 Reinforcement Magnitude	B7a Reinforcement Magnitude	Increase in Total Reinforcement
Seasonal Model 1	2580 MW	2240 MW	N/A
Seasonal Model 2	2710 MW	2470 MW	360 MW
Seasonal Model 3	2730 MW	2390 MW	300 MW
Seasonal Model 4	2850 MW	2570 MW	600 MW

Table 7.4: Table of how the estimated optimal reinforcement decision varies with the assumed seasonal model, when assuming it costs £1500 per MW per km to reinforce.

sensitive to the seasonal model assumed, with all changes being at least a total of 300 MW across both boundaries in comparison to the estimate of optimal decision when assuming National Grid's seasonal model. Including both March and November as winter months increases the estimated optimal reinforcement magnitude by a total of 600 MW, which would cost an additional £90,000,000 to build.

7.2.5 A Better Decision When Considering Uncertainty in Assumed Seasonal Model

Methodology

The decisions of Chapter 6 assumed the seasonal model of National Grid when estimating optimal reinforcement decisions to be made. However, it has been shown in this section that modelling additional months (March, November or both) as winter months can have quite a large effect on costs estimated and the resulting decisions made. Therefore, it would be desirable to acquire an estimate of expected costs which accounts for uncertainties that might exist in the seasonal model, as well as the resulting estimates of optimal reinforcement decisions.

The simplest way to acquire this would to repeat the problem of Section 6.1.1 when including the seasonal model as a fourth variable containing uncertainty of interest, v_4, such that $\mathbf{v}$ is now modelled as $\mathbf{v} = (v_1, v_2, v_3, v_4)$. v_4 would be modelled as a discrete random variable taking a value 1, 2, 3 or 4 to indicate observing seasonal model 1, 2, 3, or 4 from Section 7.2.4. The methodology of Section 5.2 could then be used to create an emulator to approximate how input affects output when considering uncertainty

in four variables (nuclear availability probability, CCGT availability probability, peak demand level and seasonal model) and making two decisions (B6 and B7a reinforcement magnitudes), which could in turn be used to estimate expected total costs under uncertainty via Equation 5.2.16 of Section 5.2.5.

However, the more variables an emulator is fitted over, the less accurate an approximation it will be to the simulator (as was noted in Section 6.1.3). Recall, Equation 3.4.1 of Section 3.4.2 details how constraint costs are calculated for an entire year. This is achieved by performing a separate simulation for each snapshot (a discrete variable) and taking a sum of constraint costs across all snapshots to get an estimate of constraint costs across the entire year. The same principle can be applied here, where instead of taking a sum across a discrete variable, an expectation is taken across the discrete variable which contains uncertainty (the seasonal model).

When considering variation in a discrete variable with a small number of variations (such as the four variations on seasonal model considered in Section 7.2.4) it is easier and more accurate to take such an expectation (or weighted expectation if all variations are not deemed to have equal probability of occurring) over the discrete possibilities as part of the simulation process.

For example, suppose $f_{c,Q}(\mathfrak{X}, q)$ represents a simulator of constraint costs when some discrete variable which affects the estimate constraint costs takes value q, with the simulator otherwise being equivalent to the simulator $f_c(\mathfrak{X})$ defined in Chapter 3. For the example of this section, q would describe the seasonal model used, with a value of 1, 2, 3 or 4 used to indicate the seasonal model as in Section 7.2.4.

A simulator which takes an expectation of constraint costs over the discrete variable can then be defined as:

$$f_c(\mathfrak{X}) = \sum_q f_{c,Q}(\mathfrak{X}, q) p_Q(q) \tag{7.2.1}$$

where $p_Q(q)$ is the probability the discrete variable takes value q. The emulation methodology of Section 5.2 can then be applied to model how input affects output of this simulator, f_c, for the remaining continuous variables which contain uncertainty, $\mathbf{v}$, and decision variables, $\mathbf{d}$.

Estimates of Expected Total Costs

This sub-subsection will compare the estimated expected total costs under uncertainty for the example detailed in Section 6.1.1 of Chapter 6 when using the assumed National Grid seasonal model, or using a simulator which takes an expectation over the four seasonal models of Section 7.2.4 using Equation 7.2.1 of the previous sub-subsection (with both approaches additionally considering uncertainty in nuclear availability probability, CCGT availability probability and peak demand level as detailed in Section 6.1.1). Taking an expectation over the four seasonal models will assume each seasonal model is equally likely to be observed, i.e. $p_Q(q) = \frac{1}{4}$ for $q = 1, 2, 3$ or 4 where observing a particular value of q indicates observing seasonal model 1 to 4 of Section 7.2.4.

Figure 7.5 (a) and (b) display how estimated expected total costs vary with reinforcement decision (when assuming a cost of £1000 per MW per km to reinforce) when using National Grid's seasonal model or the model taking an expectation over the four proposed seasonal models of Section 7.2.4 respectively (with both estimates also calculating an expectation over uncertainties in nuclear availability probability, CCGT availability probability and peak demand level as outlined in Section 5.2.5). Again, the methodology of Section 6.2 is used to eliminate decisions from consideration which have evidence against them being optimal in order to fit a more accurate emulator model over a smaller range of decisions, and therefore Figure 7.5 (c) and (d) are included to compare estimates of expected total costs from the emulator models fitted in the third wave (i.e. after 2 waves of eliminating decisions which have evidence against them being optimal).

It is seen that in the first wave, both models are quite similar with costs being a little higher when using the model which additionally takes an expectation across all seasonal models. However, in the third wave (near the optimal decision), it is seen that estimates of expected total costs are noticeably larger when additionally taking an expectation across the 4 seasonal models, with the magnitudes of reinforcement considered in this final wave being quite similar though generally a little larger when taking an expectation across the 4 seasonal models.

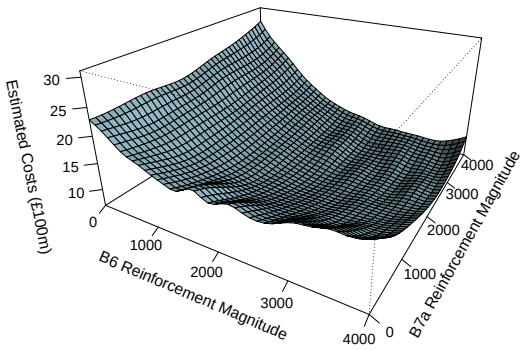

(a) National Grid's seasonal model, wave 1.

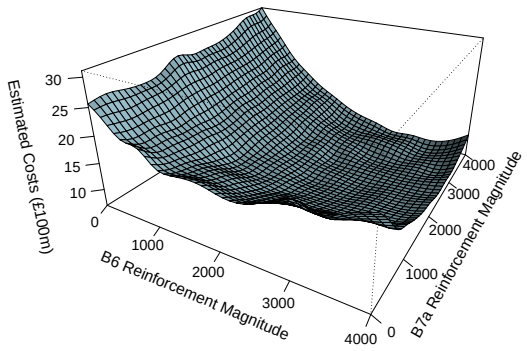

(b) Taking an expectation over the 4 seasonal models of Section 7.2.4, wave 1.

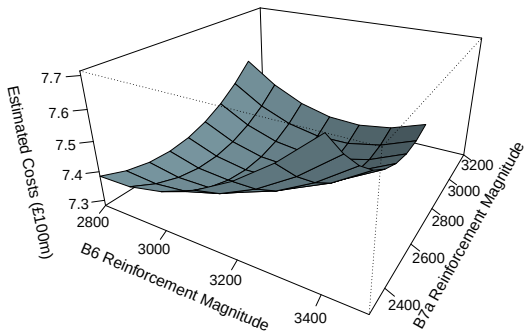

(c) National Grid's seasonal model, wave 3.

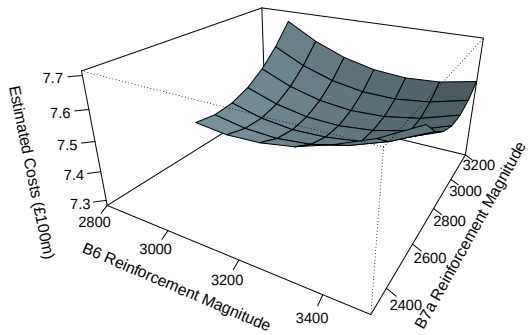

(d) Taking an expectation over the 4 seasonal models of Section 7.2.4, wave 3.

Figure 7.5: Plots to show how estimated expected total costs vary with reinforcement decisions and fitted emulator model.

Seasonal Model	B6 Reinforcement Magnitude	B7a Reinforcement Magnitude
Original Seasonal Model Assumed	3060 MW	2890 MW
Expectation Calculated Over All 4 Seasonal Models	3160 MW	2880 MW

Table 7.5: Table of how the estimated optimal decision varies depending on whether or not uncertainty is considered in the seasonal model, when assuming it costs £1000 per MW per km to reinforce.

Seasonal Model	B6 Reinforcement Magnitude	B7a Reinforcement Magnitude
Original Seasonal Model Assumed	2580 MW	2240 MW
Expectation Calculated Over All 4 Seasonal Models	2790 MW	2500 MW

Table 7.6: Table of how the estimated optimal decision varies depending on whether or not uncertainty is considered in the seasonal model, when assuming it costs £1500 per MW per km to reinforce.

Estimates of Optimal Decisions

Table 7.5 displays how the estimate of optimal decision varies depending on whether National Grid's seasonal model is assumed, or whether an expectation over the four seasonal models of Section 7.2.4 is used when estimating expected total costs. This table assumes a cost of £1000 per MW per km to reinforce, with Table 7.6 showing the corresponding information when assuming a cost of £1500 per MW per km to reinforce.

When assuming a cost of £1000 per MW per km to reinforce, taking an expectation over the four seasonal models has little effect in comparison to using National Grid's seasonal assumed model, with estimated optimal B6 reinforcement increasing by 100 MW, but estimated optimal B7a reinforcement decreasing by 10 MW. The estimated optimal decision is more sensitive to whether National Grid's seasonal model is assumed or an expectation across the four seasonal models is taken when assuming a cost of £1500 per MW per km to reinforce, with B6 reinforcement magnitude increasing by 210 MW and B7a reinforcement magnitude increasing by 260 MW when taking an expectation

over the four seasonal models. This is consistent with the results of Section 7.2.4, where the estimated optimal reinforcement decision was more sensitive to the assumed seasonal model when a larger cost to reinforce was assumed, so there is more incentive to increase reinforcement when taking an expectation over the four possible season models considered.

7.3 Assumption Two - Load Duration Curve

Section 3.1 states that constraint costs are calculated by first breaking the year down into half hour snapshots. Constraint costs are then simulated for each snapshot independently and a sum is taken to give an estimate of constraint costs for the entire year. There are two factors which vary between snapshots: a seasonal effect (discussed in Section 7.2) and the demand level of the snapshot.

As outlined in Section 4.1.2, the variation in demand between snapshots is handled via a load duration curve (LDC). Recall, the LDC specifies the proportion of peak demand used in each snapshot, which can then be used to calculate snapshot demand via Equation 3.1.1. Peak demand level was noted to have a large effect on mean constraint costs in Section 3.7.2, and was considered as a variable containing uncertainty of interest in Chapters 5 and 6. Therefore, it is reasonable to expect variations to the assumed LDC to also have an effect of interest on mean constraint costs.

The examples of Chapters 5 and 6 used the LDC which is included in the primary data reference for this thesis, [69], and this LDC was illustrated in Figure 4.2 (a) of Section 4.1.2. This load duration curve is based on demand data from September 2009 to August 2010. Based on our interpretation of the expert judgement of Paul Plumptre [78], formerly of National Grid, the use of this LDC alone was deemed to be sufficient for calculations for the examples of Chapters 5 and 6.

However, National Grid also have historical records for load duration curves dating back to 2002 [71]. No two yearly demand patterns are exactly the same, and basing data on a particularly yearly pattern may have an effect on the mean constraint costs estimated and the resulting estimates of optimal decisions. This effect will be investigated in this section.

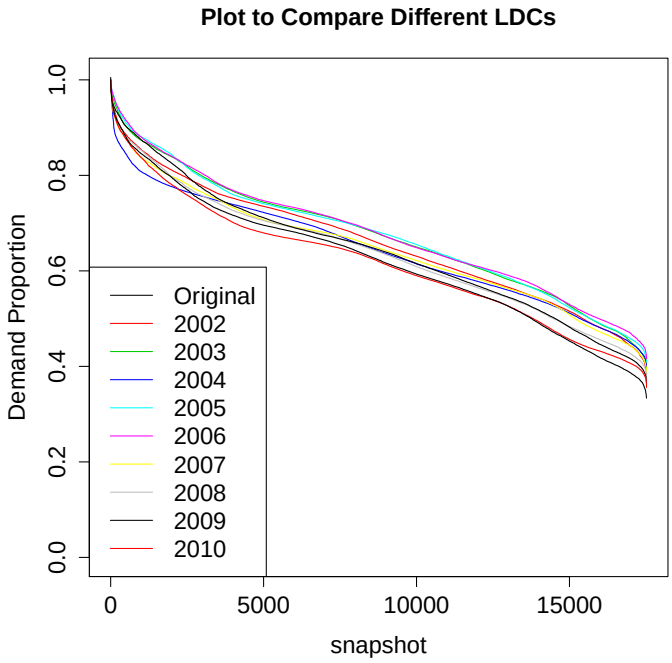

Figure 7.6: Plot to compare observed LDCs from different years.

7.3.1 Comparison of LDCs

Figure 7.6 displays the LDC which has been assumed so far in this thesis, as well as the nine alternative LDCs based on demand data from the years 2002 to 2010. It can be seen that all curves have a similar general shape with a small proportion of snapshots having extremely high demand. Then, the proportion of snapshots exceeding a particular demand level declines steadily in an almost linear fashion before a fairly steep decline which indicates a small proportion of snapshots experience a relatively low demand level.

Despite the similar general shapes, however, the curves are far from identical. Differences in the curves indicate a different distribution in demand throughout the year, which will likely affect the estimate of mean constraint costs and may affect the resulting estimate of optimal reinforcement decision.

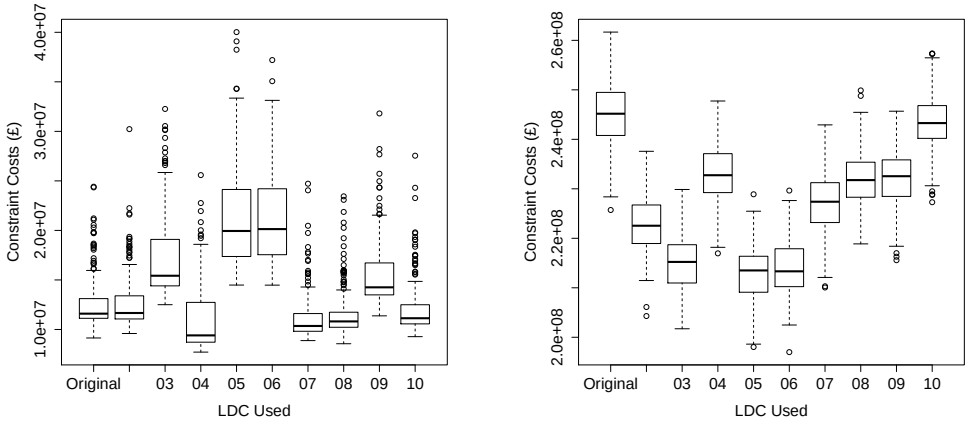

(a) Year 1 power system background. (b) Year 6 power system background.

Figure 7.7: Boxplots to show how simulations of constraint costs vary with assumed LDC.

7.3.2 Graphical Illustration of the Effect of Assumed LDC on Mean Constraint Cost Estimates

To compare how estimates of mean constraint costs vary with assumed LDC, 200 evaluations of the full simulator were acquired for our "original" LDC (the LDC from [69] used in the examples of Chapters 5 and 6) and for the LDC of the years 2002 to 2010 detailed in [71]. Figures 7.7 (a) and (b) show boxplots for the 200 evaluations of the full simulator for each assumed LDC, with Figure 7.7 (a) showing results for a year 1 power system background and Figure 7.7 (b) showing results for a year 6 power system background.

The first thing to note is that there are a lot of outliers with large annual constraint cost evaluations for all LDCs when assuming a year 1 power system background, and all boxplots show positive skew (a long tail to the right). However, when assuming a year 6 power system background the boxplots are much more symmetrical and the outliers are much less extreme. This is consistent with what was observed in Section 4.1.1, where it was shown that the variation in constraint costs with each simulation is greater (relative to the mean constraint costs) for a year 1 power system background in comparison to a year 6 power system background. As it is standard practice of National Grid (and broadly the case elsewhere) to work with mean constraint costs only, these outliers are not of great interest in this thesis.

The boxplots also indicate that the LDC assumed has an effect on the mean annual constraint costs. For a year 6 power system background it appears that the originally assumed LDC (which is based on 2009 and 2010 demand data) results in the simulations with the greatest magnitude of constraint costs. The next highest simulated constraint costs come from assuming the 2010 LDC (which is not too surprising as the original LDC is partially based on this data) with the simulations from assuming the 2004 LDC also being quite high. However, the simulations using most other LDCs result in considerably lower evaluations of constraint costs, with LDCs based on demand data from 2003, 2005 and 2006 appearing to be particularly low.

For a year 1 power system background, it can be seen that varying the assumed LDC can both raise and lower the median of constraint costs evaluations in comparison to the originally assumed LDC, whereas for a year 6 power system background the original LDC gave the greatest median of constraint cost simulations. This indicates that there is an interaction between power system background and LDC. Further, for a year 1 power system background the LDCs which resulted in the greatest median simulation of constraint costs were the LDCs based on years 2005 and 2006, whereas these LDCs resulted in the lowest median simulation of constraint costs for a year 6 power system background. These figures are explored further in the next subsection.

7.3.3 Figures on the Effect of Assumed LDC on Cost Estimates

Table 7.7 details how estimates of mean annual constraint costs vary with the assumed LDC for a year 1 power system background. As can be seen, the LDC assumed appears to have quite a large impact on the estimate of mean annual constraint costs, with the 2005 and 2006 LDCs increasing expected costs by over £8 million in comparison to the originally assumed LDC from [69].

The relative changes of the estimate of mean annual constraint costs in comparison to the estimate when using the LDC originally assumed are also given. The largest changes in comparison to the estimate from the original LDC were noted in 2005 and 2006 which were equivalent to increases of 69.5% and 66.3% respectively.

LDC Used	Estimated Mean Annual Constraint Costs	Difference in Comparison to Using Original LDC	Percentage Difference in Comparison to Using Original LDC
Original LDC	£12,650,000	N/A	N/A
2002 LDC	£12,720,000	£72,620	0.574%
2003 LDC	£17,270,000	£4,620,000	36.5%
2004 LDC	£10,980,000	- £1,674,000	-13.2%
2005 LDC	£21,440,000	£8,787,000	69.5%
2006 LDC	£21,040,000	£8,390,000	66.3%
2007 LDC	£11,230,000	- £1,422,000	-11.2%
2008 LDC	£11,640,000	- £1,010,000	-7.99%
2009 LDC	£15,420,000	£2,770,000	21.9%
2010 LDC	£12,110,000	- £536,000	-4.24%

Table 7.7: Table of how estimates of mean annual constraint cost vary with assumed LDC for a year 1 power system background.

LDC Used	Estimated Mean Annual Constraint Costs	Difference in Comparison to Using Original LDC	Percentage Difference in Comparison to Using Original LDC
Original LDC	£245,400,000	N/A	N/A
2002 LDC	£222,500,000	- £22,920,000	-9.33%
2003 LDC	£215,000,000	- £30,440,000	-12.4%
2004 LDC	£233,000,000	- £12,450,000	-5.07%
2005 LDC	£213,000,000	- £32,400,000	-13.2%
2006 LDC	£213,800,000	- £31,670,000	-12.9%
2007 LDC	£226,800,000	- £18,600,000	-7.58%
2008 LDC	£231,800,000	- £13,620,000	-5.54%
2009 LDC	£232,100,000	- £13,310,000	-5.42%
2010 LDC	£243,400,000	- £1,996,000	-0.813%

Table 7.8: Table of how estimates of mean annual constraint costs vary with assumed LDC for a year 6 power system background.

Table 7.8 shows how estimates of mean annual constraint costs vary with assumed LDC for a year 6 power system background. The absolute differences in estimated costs are much greater in comparison to those observed for a year 1 power system background, with all LDCs other than the 2010 LDC decreasing constraint costs by at least £12 million and up to £32 million.

However, for a year 6 power system background all LDCs result in estimates of mean annual constraint costs of at least £213 million, so the relative difference of the estimates must also be considered. Table 7.8 shows that the relative differences in mean annual constraint costs in comparison to the mean annual constraint costs when assuming the original LDC vary between a 5.07% decrease and a 13.2% decrease (except for the 2010 LDC which resulted in a decrease of just 0.81%), with 3 of the LDCs giving changes of more than 12% in comparison to the estimate when assuming the original LDC from [69]. This indicates that for our example it could have been very worthwhile to consider using multiple LDCs to estimate expected mean annual constraint costs under uncertainty. Again, it is noted that the largest changes come from using the LDCs of 2005 and 2006, though for the year 6 power system background assuming these LDCs results in a decrease in the estimate of mean annual constraint costs, whereas for the year 1 power system background an increase in the estimate of mean annual constraint costs was observed. How these changes affect the estimate of optimal decision to be made will be explored in the next subsection.

7.3.4 The Effect of Assumed LDC on the Estimated Optimal Reinforcement Decision

Assuming a Particular LDC

Just as when the seasonal model was considered in the Section 7.2, it is important to consider how assuming a particular LDC affects the decision made of a reinforcement problem. As in Section 7.2.4, this subsection will consider how the estimated optimal reinforcement decision would vary if the example detailed in Section 6.1.1 of Chapter 6 (considering uncertainty in nuclear availability probability, CCGT availability probability and peak demand level whilst reinforcing the B6 and B7a boundaries) was repeated whilst assuming a different LDC.

Figure 7.8 illustrates how estimated expected total costs under uncertainty vary with reinforcement decision and assumed LDC. Graphs are shown for three different assumed LDCs: the 2006 LDC (which Sections 7.3.2 and 7.3.3 showed gave the lowest estimates of mean constraint costs), the 2010 LDC (which Sections 7.3.2 and 7.3.3

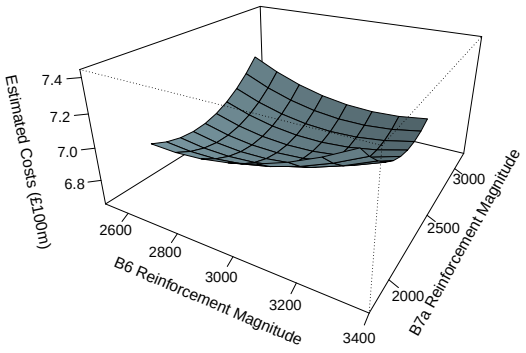

(a) 2002 LDC assumed.

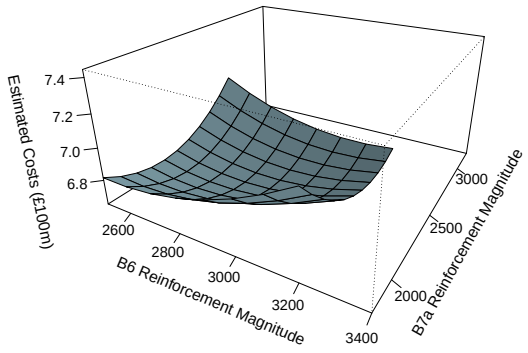

(b) 2006 LDC assumed.

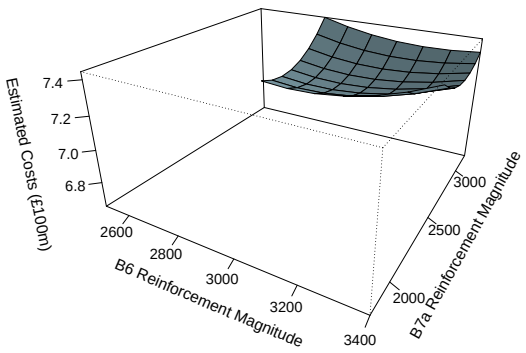

(c) 2010 LDC assumed.

Figure 7.8: Plots to show how estimates of expected total costs vary with B6 and B7a reinforcement magnitude and assumed LDC, when assuming it costs £1000 per MW per km to reinforce.

showed gave the greatest estimates of mean constraint costs) and the 2002 LDC (which Sections 7.3.2 and 7.3.3 showed gave estimates between the two extremes). As was the case for the example presented in Chapter 6, it is necessary to carry out a wave process using the methodology of Section 6.2 to fit a more accurate emulation approximation to the simulator over a smaller range of decisions for each assumed LDC. As such, the cost estimates displayed from Figure 7.8 are those acquired after two waves of elimination have been performed to fit a more accurate emulator model over a smaller range of decisions.

It can be seen that in this final wave the estimates of expected total costs are lowest when the 2006 LDC is assumed and greatest when the 2010 LDC is assumed (again, as may have been expected based on the Table 7.8 of Section 7.3.3) with estimates when assuming the 2002 LDC lying somewhere in between. Further, it can be seen that in the final wave larger magnitudes of reinforcements are considered when assuming the 2010 LDC in comparison to the 2006 LDC, indicating the increase in constraint costs appears to justify a larger reinforcement, as may be expected.

Assumed LDC	B6 Reinforcement Magnitude	B7a Reinforcement Magnitude
Original LDC	3060 MW	2890 MW
2002 LDC	2900 MW	2430 MW
2003 LDC	2850 MW	2360 MW
2004 LDC	2820 MW	2530 MW
2005 LDC	2760 MW	2380 MW
2006 LDC	2800 MW	2350 MW
2007 LDC	2840 MW	2410 MW
2008 LDC	2910 MW	2550 MW
2009 LDC	2930 MW	2530 MW
2010 LDC	2950 MW	2730 MW

Table 7.9: Table of how the estimated optimal decision varies with the assumed LDC, when assuming it costs £1000 per MW per km to reinforce.

Table 7.9 displays how the estimated optimal reinforcement decision varies with the assumed LDC when assuming a cost of £1000 per MW per km to reinforce, with results displayed for all 10 LDCs considered, including the LDC from [69] originally assumed for the example of Chapter 6. The original LDC gives the largest estimate of optimal reinforcement magnitudes, which may have been expected as it gave the

largest estimates of mean constraint costs. However, this would not necessarily have to be the case, as it could be that an LDC which gave a lower estimate of constraint costs when no reinforcement is made would experience a greater decrease in constraint costs as the boundaries were reinforced, which would result in a greater reinforcement being justified.

Using a 2005 LDC gives the largest decrease in estimated optimal B6 reinforcement in comparison to the estimated optimal decision when assuming the original LDC from [69] (300 MW less), though the other 8 alternative LDCs show quite little variation in estimated optimal B6 reinforcement, with decisions varying between 2800 MW and 2950 MW. The B7a boundary appears more sensitive to the assumed LDC, with the smallest decrease in B7a reinforcement occurring when using a 2010 LDC, building 160 MW less reinforcement in comparison to when assuming the original LDC. All other decreases in estimated optimal B7a reinforcement are at least 340 MW in comparison to when assuming the original LDC, with the largest decrease being 540 MW when assuming a 2006 LDC.

Modelling Uncertainty in the Assumed LDC

As in Section 7.2.5, a decision can be made for the example detailed in Section 6.1.1 of Chapter 6 which minimises the estimate of expected total costs when additionally taking an expectation of mean constraint costs over all possible LDCs as part of the simulation process via Equation 7.2.1 (as well as considering uncertainty in peak demand level, nuclear availability probability and CCGT availability probability as outlined in Section 6.1.1). For the application of this section, an expectation will be taken over the 2002 to 2010 LDCs, with each LDC given equal weight (i.e. $p_Q(q) = \frac{1}{9}$ for all LDCs) when calculating an expectation of costs as the LDC is varied as part of the simulation process via Equation 7.2.1. The original LDC was not included in this expectation, as it is formed from 2009 and 2010 data, which would bias results by including both the original LDC and the LDCs from the years 2009 and 2010.

Figure 7.9 illustrates graphs to compare how estimates of expected total costs under uncertainty vary with reinforcement decision for the example detailed in Section 6.1.1 of Chapter 6, depending whether the LDC from [69] was assumed (as was the case in

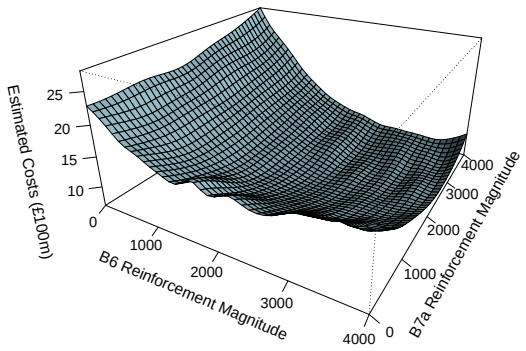

(a) Assuming the LDC from [69], wave 1.

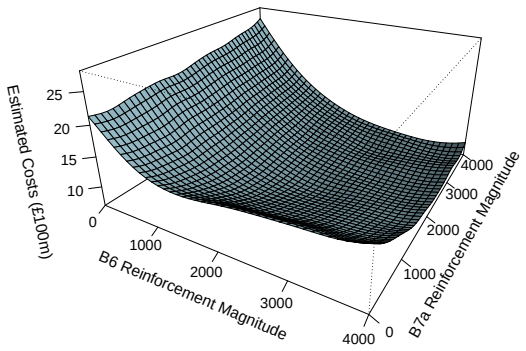

(b) Taking an expectation over the 2002 to 2010 LDCs, wave 1.

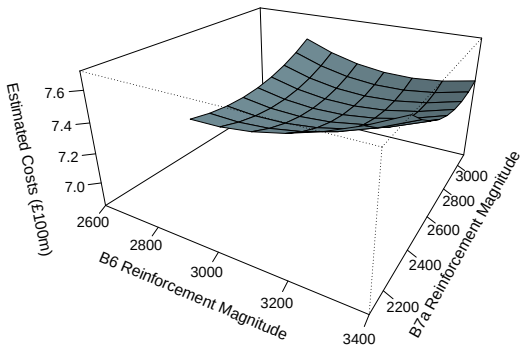

(c) Assuming the LDC from [69], final wave.

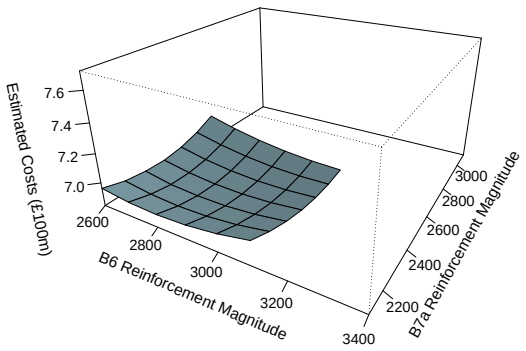

(d) Taking an expectation over the 2002 to 2010 LDCs, final wave.

Figure 7.9: Plots to show how estimated expected total costs vary with reinforcement decisions and fitted emulator model.

Chapter 6) or an expectation is taken over the estimates from the 2002 to 2010 LDCs. Again, a wave process must be performed using the methodology of Section 6.2 to eliminate decisions from consideration which have evidence against them being optimal, in order to fit a more accurate emulator model over a smaller range of decisions. Figure 7.9 (a) and (b) compare estimates from the emulator models fitted in the first wave, whereas Figure 7.9 (c) and (d) compare estimates from the emulator models fitted in the final wave.

As can be seen, estimates of expected total costs are greater when the LDC from [69] is assumed, which again is consistent with Table 7.8 of Section 7.3.3 which showed this LDC to result in greater estimates of mean constraint costs for a year 6 power system background in comparison to estimates from any of the 9 alternative LDCs considered. Further, it can be seen that in the final wave larger magnitudes of reinforcement are considered when assuming the LDC from [69] in comparison to taking an expectation of costs from the 2002 to 2010 LDCs, indicating that this increase in total costs justifies a larger reinforcement being built.

LDC Model	B6 Reinforcement Magnitude	B7a Reinforcement Magnitude
Original LDC Assumed	3060 MW	2890 MW
Expectation Calculated Over 2002 to 2010 LDCs	2910 MW	2420 MW

Table 7.10: Table of how the estimated optimal reinforcement decision varies with the assumed LDC, when assuming it costs £1000 per MW per km to reinforce.

Table 7.10 compares the estimates of optimal reinforcement decisions to minimise the estimate of expected total costs depending on whether or not the LDC from [69] was assumed, as was the case in Chapter 6, or whether an expectation of costs across the 2002 to 2010 LDCs is taken. A decision which takes an expectation of costs across the 9 LDCs results in an estimated optimal decision with lower reinforcement magnitudes of both boundaries in comparison to when simply using the original LDC. This is quite predictable from Table 7.9, where all LDCs result in a decision less than the original LDC. Further, the decrease in estimated optimal B6 reinforcement is quite small (150 MW) whereas the decrease in estimated optimal B7a is somewhat larger (470 MW) which is also consistent with what was observed in Table 7.9.

7.4 Assumption Three - Installed Wind Generating Capacity

In Section 5.1 it was stated that the input variables to the simulator, $\mathfrak{X}$, could better be thought of as $(\mathbf{v}, \mathbf{a}, \mathbf{d})$, where $\mathbf{v}$ represents the inputs in which uncertainty is modelled explicitly; $\mathbf{a}$ represents the inputs which are either known with certainty or in which uncertainties are not of interest, so their values are treated as fixed as if they are known precisely; and $\mathbf{d}$ represents the decision variables.

Amongst the variables included in $\mathbf{a}$ were the installed generating capacities. It is reasonable to think that the installed generating capacities in a power system at the present moment can be known very accurately, with projections in the near future still being accurate. However, the further into the future projections are made, the less accurate these projections will be. This section will consider how error in these projections affects the mean constraint costs estimated.

As it is reasonable to think currently installed levels of generating capacities can be known very accurately, results for a year 1 power system background will not be presented. Further, only the change in installed capacity between year 1 and year 6 will be assumed to contain error, again due to the fact that it is reasonable to think the installed capacity in year 1 can be known very accurately.

This section will consider how projections of installed wind generating capacities affect the costs estimated. Installed wind generating capacity is of particular interest as it is a high merit order capacity (it is cheap so is desirable to use). Further, a large amount of wind generating capacity is scheduled to be installed between year 1 and year 6 which makes these variables of particular interest.

7.4.1 Graphical Illustration of the Effect of Installed Wind Generating Capacity on Cost Estimates

Figure 7.10 (a) illustrates how boxplots of annual constraint costs for a year 6 power system background vary with the projected increase in installed wind generating capacity between year 1 and year 6, with 200 evaluations of the full simulator used for each

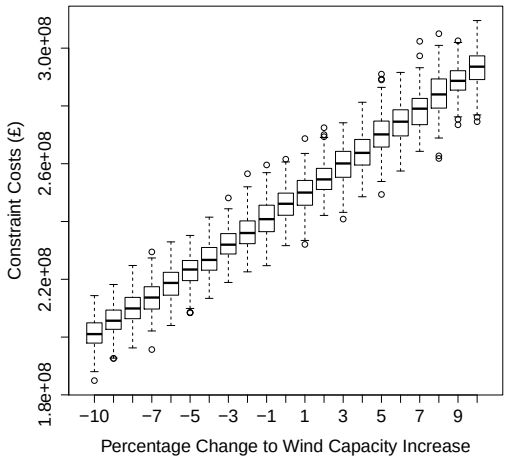

(a) Boxplots to show how simulations of constraint costs vary with assumed installed wind generating capacity, for a year 6 power system background.

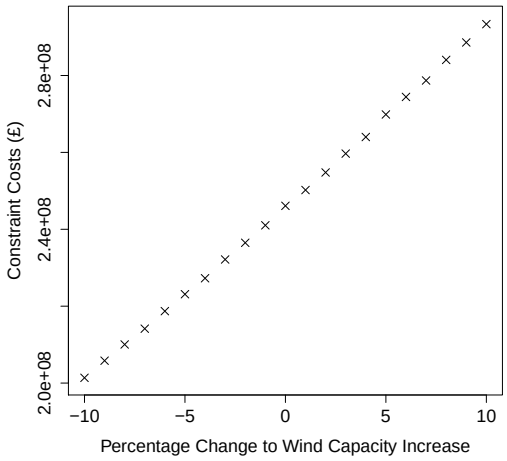

(b) Plot to show how mean constraint costs vary with assumed installed wind generating capacity, for a year 6 power system background.

Figure 7.10: Graphs to compare how estimates of mean annual constraint costs vary with the change in the projected increase in installed wind generating capacity.

variation of installed wind generating capacity considered. The resulting estimates of mean annual constraint costs are displayed in Figure 7.10 (b).

The first thing to note is that the relationship between the increase in installed wind generating capacity and the estimated mean annual constraint costs appears to be very linear, with constraint costs increasing as installed wind generating capacity increases. Whilst this increase may seem counter intuitive, as wind is a high merit order (cheap) capacity, this is explained by the fact that constraint costs are a measure of a power system's ability to use the cheapest generating capacity available and not the total amount spent on generating capacity as was noted in Section 3.7.2. Therefore, increasing the total installed wind generating capacity will increase mean annual constraint costs if there is insufficient installed transmission technology to use this available capacity.

In particular, to help understand this, recall the simple example of Section 2.2.1 of Chapter 2, where it was noted that if there was insufficient transmission capacity installed to make use of all available wind generating capacity, wind would be paid £50 for every MW which was produced but could not be used to satisfy demand due to the limitations of the installed transmission capacity. This would mean that if, for example, an extra 2000 MW of wind generating capacity was installed but could

not be used due to a small amount of installed transmission capacity, then potentially $2,000 \times £50 = £100,000$ of additional constraint costs could occur in each snapshot.

7.4.2 Figures on the Effect of Installed Wind Generating Capacity on Cost Estimates

Change in Projected Increase of Installed Wind Capacity	Estimated Mean Annual Constraint Costs	Difference in Comparison to Using Projected Wind Generating Capacity	Percentage Difference in Comparison to Using Projected Wind Generating Capacity
-10%	£201,400,000	- £44,530,000	-18.2%
-5%	£223,100,000	- £22,790,000	-9.35%
0%	£245,900,000	N/A	N/A
+5%	£270,100,000	£24,220,000	9.77%
+10%	£293,400,000	£47,460,000	19.2%

Table 7.11: Table of how estimates of mean annual constraint costs vary with the change in the projected increase in installed wind generating capacity for a year 6 power system background.

Table 7.11 details how estimates of mean annual constraint costs for a year 6 power system background vary with the change in the projected increase in installed wind generating capacity between year 1 and year 6. This table indicates that there is a general linear trend of around £4,500,000 increase in mean annual constraint costs for every 1% increase in installed wind generating capacity increase. However, it can also be seen that the decrease in mean annual constraint costs when wind generating capacity is increased by 10% less than the projection (£44.5 million) is slightly smaller than the increase in mean annual constraint costs when wind generating capacity is increased by 10% more than the projection (£47.5 million) indicating that this relationship is not perfectly linear.

All changes in the table are non-negligible, with the smallest changes in estimates of mean annual constraint costs being a decrease of 9.35% when the increase in installed wind generating capacity is 5% lower than projected, whilst increasing the projected increase in installed wind generating capacity by 10% gives the largest change, with

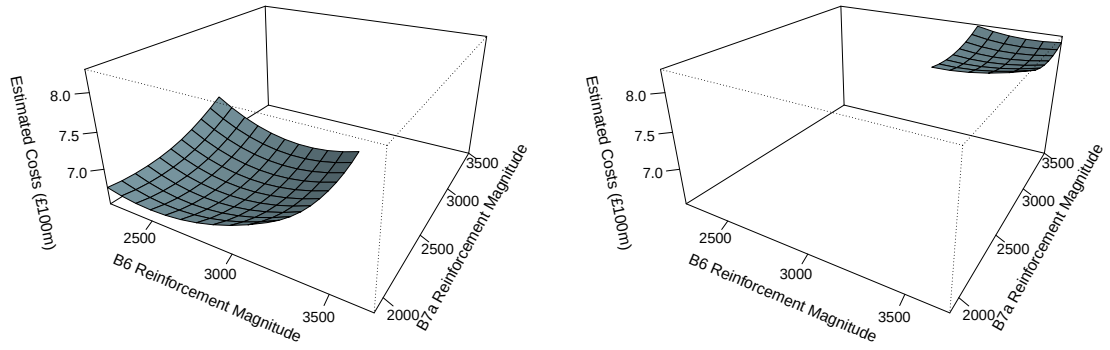

(a) 10% decrease in projected wind generating capacity increase.

(b) 10% increase in projected wind generating capacity increase.

Figure 7.11: Plots to show how estimates of expected total costs vary with B6 and B7a reinforcement magnitude and assumed wind generating capacity projection.

an increase of mean annual constraint costs of 19.2%. Further, such changes are not entirely implausible, especially as these are changes in the projected increases in wind generating capacity not total installed wind generating capacity.

7.4.3 Effect of Installed Wind Generating Capacity on the Estimates of Optimal Reinforcement Decisions

Assuming a Different Projection of Installed Wind Generating Capacity

It is also important to also consider how assuming a particular projection of installed wind generating capacity affects the resulting estimate of optimal reinforcement decision. As was the case when considering the assumed seasonal model or assumed LDC in Sections 7.2.4 and 7.3.4 respectively, this section will consider how the estimated optimal reinforcement decision varies if the example of Section 6.1.1 of Chapter 6 is repeated with various assumed projections of increase in installed wind generating capacity.

Figure 7.11 illustrates how estimates of expected total costs under uncertainty vary with reinforcement decision if the assumed increase in installed wind generating capacity

between years 1 and 6 was 10% lower or higher than the projected increase from [69], after the methodology of Section 6.2 was applied to fit a more accurate emulator model over a smaller range of decisions. As can be seen, estimates of expected total costs are greater when the assumed increase in installed wind generating capacity between years 1 and 6 is greater, which is consistent with Table 7.11 of Section 7.4.2. Further, it can be seen that the reinforcement magnitudes considered in the final wave are greater when the increase to installed capacity is 10% greater than the projections of [69] in comparison to when the increase to installed capacity is 10% lower than the projections of [69], indicating that the increase in constraint costs justifies a greater reinforcement.

Change in Projected Increase of Installed Wind Generating Capacity	B6 Reinforcement Magnitude	B7a Reinforcement Magnitude	Increase in Total Reinforcement
-10%	2710 MW	2390 MW	-850 MW
-5%	2950 MW	2620 MW	-380 MW
0%	3060 MW	2890 MW	N/A
+5%	3180 MW	2920 MW	150 MW
+10%	3560 MW	3070 MW	680 MW

Table 7.12: Table of how the estimated optimal decision varies with the assumed installed wind generating capacity, when assuming it costs £1000 per MW per km to reinforce.

Table 7.12 displays how estimated optimal reinforcement decisions vary with the assumed increase in installed wind generating capacity between year 1 and year 6. It is seen that the assumed change in installed wind generating capacity can have quite a large effect on the estimated optimal reinforcement decision made, with the change in total reinforcement ranging from a decrease of 850 MW total reinforcement when assuming 10% less wind generating capacity is installed than projected between year 1 and year 6 (in comparison to the estimate of optimal decision when assuming the projected levels of installed wind generating capacity), with an increase of 680 MW total reinforcement when assuming 10% more wind generating capacity is installed than projected between year 1 and year 6.

Modelling Uncertainty in The Projected Wind Generating Capacity

As was the case when considering the assumed seasonal model and LDC, the example detailed in Section 6.1.1 of Chapter 6 could be repeated whilst additionally considering uncertainty in the projected increase in wind generating capacity between year 1 and year 6. In Sections 7.2.5 and 7.3.4 such decisions when considering uncertainty in the seasonal model or LDC were handled by taking an expectation over all seasonal models or LDCs considered as part of the simulation process via Equation 7.2.1, which was appropriate as a small discrete set of alternative seasonal models or LDCs were considered.

However, it would be more appropriate to treat the increase in installed wind generating capacity as a (quasi) continuous variable, v_4, which takes a value in the range 90 to 110, such that observing $v_4 = v_4^*$ would indicate observing an increase of installed wind generating capacity of $v_4^*\%$ of the amount projected by [69]. The example detailed in Section 6.1.1 would then be extended to model uncertainty in four variables: nuclear availability probability, CCGT availability probability, peak demand level and increase in installed wind generating capacity, which make up $\mathbf{v} = (v_1, v_2, v_3, v_4)$.

To give a comparison to estimates of expected total costs under uncertainty when considering this additional variable, prior beliefs about the observed increase in installed wind generating capacity, $p(v_4)$, are required. $p(v_4)$ will be modelled as a uniform distribution between 90 and 110, i.e. assuming any increase in installed wind generating capacity between 90% and 110% of the amount projected by [69] to be equally likely to occur. This is partially to remain consistent with our interpretation of information discussed with Paul Plumptre [78] in Section 6.1.1 when modelling uncertainty in other variables (i.e nuclear availability probability, CCGT availability probability and peak demand level) and also to reflect our lack of knowledge of an appropriate distribution for future projections of installed wind generating capacity.

Figure 7.12 illustrates how estimates of expected total costs under uncertainty vary with reinforcement decision, with Figure 7.12 (a) illustrating estimates when the projected increase in installed wind generating capacity from [69] is assumed and Figure 7.12 (b) illustrating estimates when uncertainty is considered in the projected increase in installed wind generating capacity. As can be seen both plots are very similar. This is

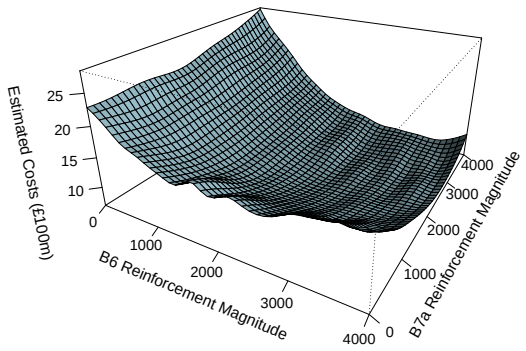

(a) Assuming projected wind generating capacity, first wave.

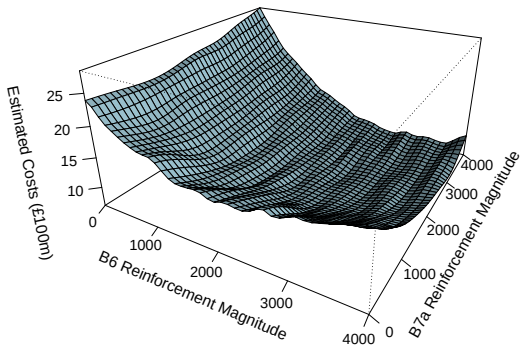

(b) Considering uncertainty in projected wind generating capacity, first wave.

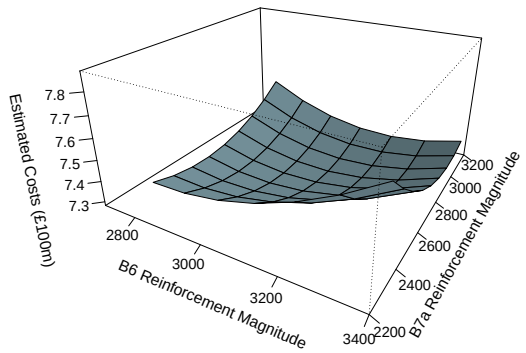

(c) Assuming projected wind generating capacity, final wave.

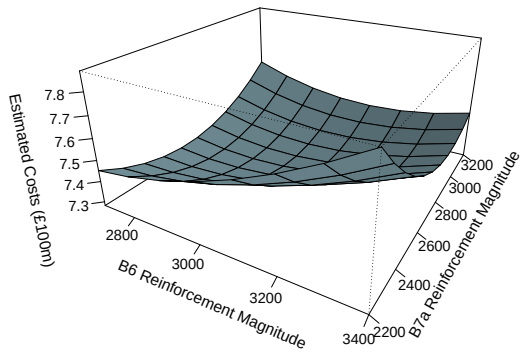

(d) Considering uncertainty in projected wind generating capacity, final wave.

Figure 7.12: Plots to show how estimated expected total costs vary with reinforcement decisions and fitted emulator model.

what may have been expected based on Sections 7.4.1 and 7.4.2, which showed that variation in mean constraint costs as the installed wind generating capacity is varied is symmetrical and linear around the projected capacity, which suggests taking an expectation over this projection will have little effect on the expectation of total costs.

Again, a wave process must be performed using the methodology of Section 6.2 in order to fit more accurate emulator models over a smaller range of decisions, with Figure 7.12 (c) and (d) displaying the resulting estimates of expected total costs in the final wave (after two waves of elimination when assuming the projected installed wind generating capacity and three waves of elimination when considering uncertainty in projections of installed wind generating capacity). In the final wave it can be seen that the model which additionally considers uncertainty in the projected increase in wind generating capacity is fitted over a slightly larger range of decisions, due to the additional uncertainty being modelled. However, the estimates of expected total costs for both models are quite similar over the range of decisions considered by both, which again is consistent Sections 7.4.1 and 7.4.2.

Wind Generating Capacity Considered	B6 Reinforcement Magnitude	B7a Reinforcement Magnitude
Assuming Projected Wind Generating Capacity	3060 MW	2890 MW
Considering Uncertainty in Projected Wind Generating Capacity	3090 MW	2730 MW

Table 7.13: Table of how the estimated optimal decision varies with depending on whether or not uncertainty is considered in projections of installed wind generating capacity, when assuming it costs £1000 per MW per km to reinforce.

Table 7.13 displays the estimated optimal reinforcement decisions when also emulating over the projected increase in installed wind generating capacity. As can be seen, the overall estimate of optimal reinforcement decision is not greatly impacted by emulating over this additional variable, with a quite small increase of 30 MW B6 reinforcement and decrease of 160 MW B7a reinforcement noted. Again, this is what may have been expected due to the estimates of expected total costs being very similar regardless of whether or not uncertainty is modelled in future projections of installed wind generating capacity, as the increase in constraint costs when the projections of installed wind

generating capacity is greater than expected is of similar magnitude to the decrease in constraint costs when the projections of installed wind generating capacity is lower than expected.

7.5 Further Discussion Regarding These Three Assumptions

7.5.1 The Additive Effect of These Three Assumptions

Sections 7.2, 7.3 and 7.4 considered how the assumed seasonal model, LDC or projection of installed wind generating capacity can affect estimates of mean constraint costs and the resulting decisions made. This could be taken a step further by considering the additive effect of all three assumptions. This subsection will give a brief consideration to such effects by considering the best and worst case scenarios across all three conditions.

The best case scenario will assume National Grid's seasonal model (i.e. December, January and February modelled as winter months, all other months modelled as summer months), the 2006 LDC and an increase of installed wind generating capacity between years 1 and 6 which is 10% lower than the amount projected by [69], which were the conditions which gave the lowest estimates of mean constraint costs for their respective assumptions. The worst case scenario will assume seasonal model 4 from Section 7.2.4 (i.e. December, January, February, March and November modelled as winter months, all other months modelled as summer months), the originally assumed LDC from [69] and an increase of installed wind generating capacity between years 1 and 6 which is 10% greater than the amount projected by [69], which were the conditions which gave the greatest estimates of mean constraint costs for their respective assumptions.

The Additive Effect on Mean Constraint Costs

Figure 7.13 illustrates boxplots of 200 simulator evaluations of constraint costs for a year 6 power system background for the best and worst case scenarios, as well as a comparison to simulations using the assumptions made throughout Chapter 6 (i.e.

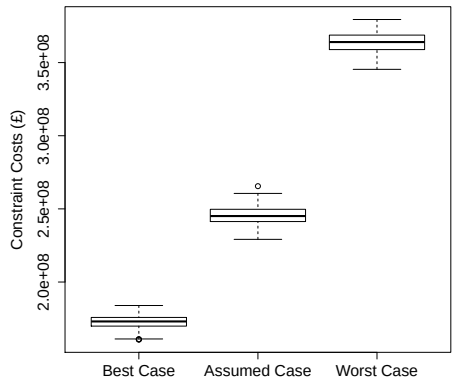

Figure 7.13: Boxplots to show how simulations of constraint costs vary with assumptions made.

Assumptions Made	Estimated Mean Annual Constraint Costs	Difference in Comparison to Using Original Assumptions	Percentage Difference in Comparison to Using Original Assumptions
Best Case	£172,800,000	-£72,700,000	-29.6%
Assumed Case	£245,500,000	N/A	N/A
Worst Case	£363,700,000	£118,200,000	48.2%

Table 7.14: Table of how estimates of mean annual constraint cost vary with assumptions made about the power system for a year 6 power system background.

National Grid's assumed seasonal model, the LDC originally assumed from [69] and the assumed increase in projected wind generating capacity from [69]). Further details about these simulator evaluations are given in Table 7.14.

As can be seen, varying multiple factors at once can have a very large effect on the resulting estimate of mean annual constraint costs, with mean annual constraint costs decreasing by over £72 million (29.6%) in the best case scenario and increasing by over £118 million (48.2%) in the worst case scenario.

When only varying a single assumption, the most extreme results were acquired when varying the assumed projected increase in installed wind generating capacity, which was detailed in Table 7.11 of Section 7.4.2, with the largest increase observed being £47.5 million (when increasing projected wind generating capacity increase by 10%) and the largest decrease being £44.5 million (when decreasing projected wind generating

capacity increase by 10%). This shows how the additive effect of varying multiple factors at once is much greater than varying any single factor alone.

The Additive Effect on Estimated Optimal Reinforcement Decisions

Assumptions Made	B6 Reinforcement Magnitude	B7a Reinforcement Magnitude
Best Case	2370 MW	1830 MW
Assumed Case	3060 MW	2890 MW
Worst Case	3660 MW	3380 MW

Table 7.15: Table of how the estimated optimal decision varies with the assumptions made about the power system, when assuming it costs £1000 per MW per km to reinforce.

As was the case when varying any single factor, the example detailed in Section 6.1.1 of Chapter 6 could be repeated when using a combination of the best and worst assumptions about seasonal model, LDC and increase in projected wind generating capacity. Table 7.15 details how the resulting estimate of optimal reinforcement decision would be affected when making such assumptions. As would be expected, assuming the best case scenario (i.e. the scenario which minimises the mean constraint costs) results in a large decrease in reinforcement of 690 MW B6 and 1060 MW B7a in comparison to the decision identified using the assumptions made in Chapter 6, a total decrease of 1750 MW. Conversely, assuming the worst case scenario results in an increase of 600 MW B6 and 490 MW B7a reinforcement, a total increase of 1090 MW.

It is noted that the total increase in reinforcement in the worst case scenario (1090 MW) in comparison to the assumed case is 660 MW less than the total decrease in reinforcement in the best case (1750 MW) in comparison to the assumed case. This indicates that if the seasonal model, LDC and increase in future wind generating capacity could be known precisely there is a larger potential decrease in reinforcement made if a favourable set of circumstances are known in comparison to the potential increase in reinforcement if an undesirable set of circumstance are known.

These reinforcement decisions can also be compared to the reinforcement decisions when the assumed increase in installed wind generating capacity alone was varied,

detailed in Table 7.12 of Section 7.4.3, which resulted in the most extreme decisions when only a single factor was varied. It can be seen that the lowest reinforcement of 2710 MW B6 and 2390 MW B7a (when the assumed increase in installed wind generating capacity is 10% lower than the projected increase of [69]) is a total 900 MW greater than the lowest reinforcement of Table 7.15 (i.e. the reinforcement under the best case scenario). Conversely, it can be seen that the greatest reinforcement of 3560 MW B6 and 3070 MW B7a (when the assumed increase in installed wind generating capacity is 10% greater than the projected increase of [69]) is 410 MW smaller than the greatest reinforcement of Table 7.15 (i.e. the reinforcement under the worst case scenario). This shows that the additive effect of varying three factors at once is greater than the effect of varying just a single factor (as would be expected). Further, it also shows how this effect is greater when multiple variables take favourable values (i.e. lower constraint costs simultaneously) as opposed to unfavourable values (i.e. increase constraint costs simultaneously).

7.5.2 Possible Further Consideration Regarding These and Other Assumptions

Alternative Methods of Decision Making to Account for These Uncertainties

For all the examples of Sections 7.2 to 7.4, as well as showing how the estimated costs and resulting estimated optimal decisions varied as the assumptions made were varied, consideration was also given to how the estimated optimal decision would vary if an expectation was taken across all possible assumptions. Alternative methods of decision making could also have been considered. For example, instead of making a decision to minimise the estimate of expected total costs across the four seasonal models considered in Section 7.2.4, the minimax decision across the four proposed seasonal models could have been made. However, this is not the most useful method of decision making to consider for the problems considered in Sections 7.2 to 7.4. This is because, for the examples considered, one condition (such as the condition which models November, December, January, February and March as winter months for Section 7.2) tends to dominate cost estimates, and a minimax problem simply

amounts to minimising expected total costs for that particular condition.

Further Consideration to the Seasonal Model and Correlation Within the Simulator

Section 7.2 considered how National Grid have a summer and winter model for available wind generating capacity, with December, January and February following the winter model and all other months following the summer model. It was shown how including additional months in the winter model increased estimates of expected total costs and increased the magnitudes of the estimated optimal reinforcement decisions. However, it could be argued that such a rigid classification is poor, regardless of the months included, as in reality the weather would not undergo such an abrupt change. An improved model could be one where the available wind generating capacity is modelled stochastically from one snapshot to the next, which may incorporate underlying seasonal effects into the stochastic model. However, constructing such a model in itself would be a large task beyond the scope of this thesis. Whilst the construction of such a model is beyond the scope of this thesis it is noted that if such a model was available, the emulation methodology presented in this thesis could still be used to approximate how input affects output of the resulting simulator, which can in turn be used to estimate optimal reinforcement decisions, meaning such a problem is not beyond the scope of the method.

This is part of a larger problem where National Gird (and broadly the case elsewhere) are only concerned with mean constraint costs, and not the distribution of constraint cost simulations. As such, correlation between snapshots for all factors is for the most part ignored (though the load duration curve (LDC) is based on chronological historical demand data so does account for this to an extent). Therefore, this could be extended even further by building a model which accounts for correlation between snapshots for all generation types.

Further Consideration to the Assumed LDC

Section 7.3 considered how estimates of mean constraint costs and the resulting estimates of optimal reinforcement decision vary depending on the assumed LDC. However,

one thing to note is that while all LDCs assume that the peak snapshot has 100% of peak demand, the lowest proportion of peak demand used in a snapshot actually varies with assumed LDC (as in reality the lowest demand level observed also varies year on year). It is possible to also set a lower limit for snapshot demand for a year and scale each LDC accordingly to consider the same range of snapshot demand for each LDC. An omitted experiment did consider this and it was noted that the LDCs are much more similar in shape when doing so (as may be expected) which resulted in the estimates of mean constraint costs and the resulting estimates of optimal reinforcement decisions being much more similar.

Further Assumptions to Consider

In addition to the assumptions considered in Sections 7.2 to 7.4, there are many additional model and data assumptions that could have been considered. For example, the same bid and offer prices were assumed for every problem considered throughout this thesis. Whilst such an assumption is reasonable for renewable and nuclear generation, the assumption is less reasonable for conventional generation such as coal, gas and oil, where prices may fluctuate on a short term (daily/weekly) basis as well as a longer yearly basis.

Fairly small changes in the bid/offer prices may have a fairly uninteresting, linear effect on mean constraint costs, but there is the potential that larger changes may effect the merit order (i.e. the order which generating capacity is scheduled in the unconstrained schedule from Section 3.3.1) which may have a much larger effect on mean constraint costs (especially if a capacity which was previously constrained off quite regularly would no longer included in the unconstrained schedule as a result in increased offer price, which could actually reduce constraint costs).

However, accounting for this would require a separate model to be incorporated into our simulator to model short term price fluctuations and long term trends. Such a model was unavailable to us and the construction of one was beyond the scope of this thesis. As noted earlier, if such a model was available, the emulation methodology presented could still be used to approximate how input affects output of the resulting simulator

and in turn estimate optimal reinforcement decisions for the resulting model, again indicating that such a problem is not beyond the scope of the methodology considered.

7.6 Assumption Four - Yearly Constraint Cost Estimation

7.6.1 Using Multiple Future Years to Estimate Constraint Costs Over a Period of Time

In Section 3.7.2 it was noted that it was common practice in the existing literature to estimate costs over a given period of time using only data for a single year (i.e. simulating based on a single power system background). Therefore, Chapters 5 and 6 presented examples which estimated mean constraint costs using a single future year to remain consistent with this practice.

However, Figure 3.2 of Section 3.7.1 would suggest that it is necessary to use multiple future years in order to estimate costs over a given period of time, and simply using a single future year will give an inaccurate cost estimate which in turn could result in poor decisions being made.

The example of Chapter 6 considered estimating constraint costs over a 10 year period using an estimate of mean constraint costs based on a year 6 power system background (by assuming a year 6 power system background for each of the 10 years). A more accurate estimate of the mean constraint costs in the 10 year period between years 6 and 15 could be acquired if estimates of mean constraint costs were acquired for each of the 10 years between years 6 and 15. However, simulating constraint costs for just one future year can be an expensive procedure, as was outlined in Chapter 4, which is why the quite poor practice of using just a single year is common in the engineering literature. Therefore, this section will illustrate how an improved estimate can be acquired without requiring each year to be evaluated, by evaluating a subset of the future years, and using a piece-wise linear interpolation to estimate costs for years not simulated.

This section will consider estimating costs for the 10 year period between years 6 and 15 of the dataset used throughout this thesis [69], based on a piece-wise linear interpolation from estimates of years 6, 9, 12 and 15 (4 evenly spaced years over the 10 year period). If $f_{c,i}$ represents an estimate of mean constraint costs in year i for given information about the power system background, then an estimate of mean constraint costs across the 10 year period using the piecewise linear interpolation would be acquired as

$$f_c = \sum_{i=6}^{9}\left(f_{c,6} + \frac{(i-6)(f_{c,9}-f_{c,6})}{3}\right) + \sum_{i=10}^{12}\left(f_{c,9} + \frac{(i-9)(f_{c,12}-f_{c,9})}{3}\right) + \sum_{i=13}^{15}\left(f_{c,12} + \frac{(i-12)(f_{c,15}-f_{c,12})}{3}\right) \quad (7.6.1)$$

This will give a more accurate estimate than simply simulating mean constraint costs for a year 6 power system background, but will do 60% less work in comparison to simulating each year.

Other than using multiple future years to estimate constraint costs, the problem will remain the same as the one outlined in Section 6.1.1. One exception to this is the initial ranges considered for the decision variables (values of B6 and B7a reinforcement magnitude). As reinforcing the B6 and B7a boundaries seems to reduce constraint costs by a greater amount in future years, this would suggest that a greater amount of reinforcement may be justified (and preliminary investigations confirmed this). Therefore, this example will initially consider B6 reinforcement magnitudes between 0 and 7000 MW and B7a reinforcement magnitudes between 0 and 6000 MW.

7.6.2 The Wave Process Applied to This Example

Figure 7.14 (a) shows how estimates of expected total costs vary with B6 and B7a reinforcement magnitude when integrating over uncertainty using Equation 5.2.16 from Section 5.2.5.

This plot is visually similar in shape to Figure 6.13 (a) from Section 6.1.3 (the equivalent plot when estimating costs using a year 6 power system background only). Both show how costs decrease greatly when B6 reinforcement magnitude is increased, though total costs actually rise when B7a alone is reinforced (owing to the large reinforcement costs

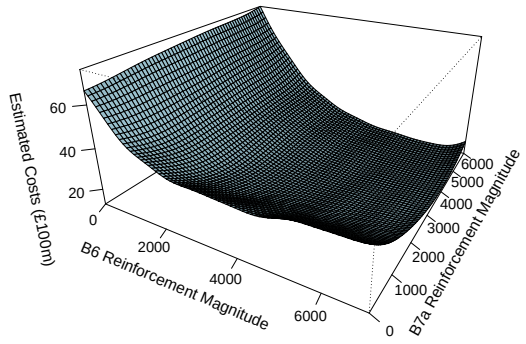

(a) Wave 1.

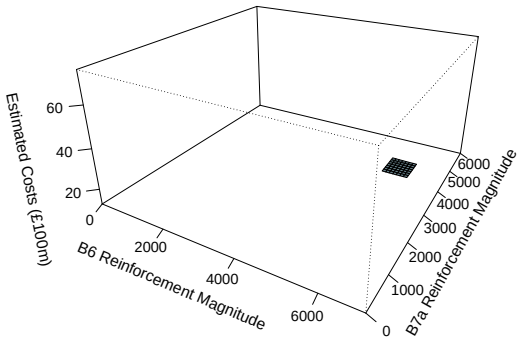

(b) Wave 3.

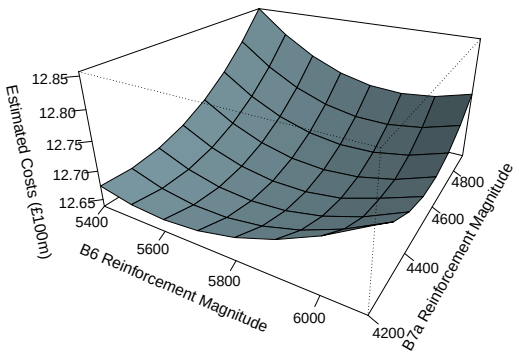

(c) Wave 3.

Figure 7.14: Plots to show how estimated expected total costs vary with reinforcement decisions and fitted emulator model, when assuming a cost of £1000 per MW per km to reinforce.

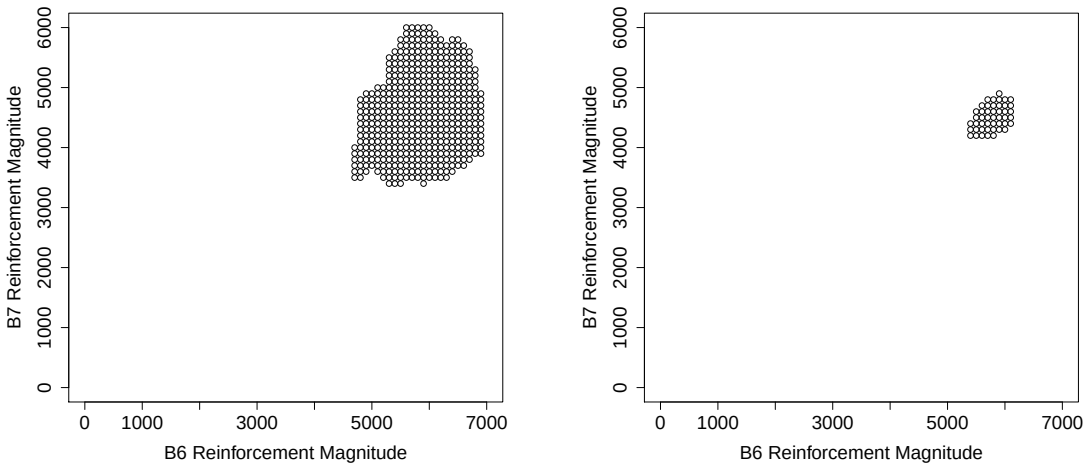

(a) Wave 2.

(b) Wave 3.

Figure 7.15: Plots to illustrate decisions not eliminated as the wave process progresses, when assuming a cost of £1000 per MW per km to reinforce.

and relatively low reduction in constraint costs). However, reinforcing both boundaries gives a much greater reduction in total costs in comparison to reinforcing only the B6 boundary, indicating that an interaction exists between the two decisions. However, the estimates of expected total costs are greater when using the piecewise linear interpolation between years in comparison to using an extrapolation from year 6 alone.

Just as for the example of Chapter 6, the fitted emulator model can be improved by fitting it over a smaller range of decisions, with the methodology of Section 6.2.1 used to eliminate decisions from consideration which have evidence against them being optimal. Figure 7.15 illustrates the decisions considered when the wave process is applied to this example. Despite the initial decision space being around 2.64 times greater than the example considered in Chapter 6, the initial decision space has been reduced to a very small region after just two waves of elimination.

Figure 7.14 (b) displays how the estimates of expected total costs vary with reinforcement decision in the third wave. This indicates that over the ranges of decisions considered in the third wave, all decisions result in similar, relatively low estimates of expected total costs indicating there is little risk of making a poor decision by minimising costs over this range. In particular, the very large estimates of expected total costs which occur when little to no reinforcement has been made have been eliminated from

consideration. Just as in the example of Chapter 6, the third wave fits a model over a much smaller range, with cost estimates being much smaller than the greatest cost estimate of the first wave, so Figure 7.14 (c) gives a more detailed display of behaviour over this range.

7.6.3 Estimated Optimal Decisions for This Example

Constraint Costs Considered	B6 Reinforcement Magnitude	B7a Reinforcement Magnitude
Extrapolation from year 6	3060 MW	2890 MW
Piecewise linear interpolation	5710 MW	4380 MW

Table 7.16: Table to compare the estimated optimal reinforcement decisions from a year 6 extrapolation or a piecewise linear interpolation between years 6 and 15, when assuming a cost of £1000 per MW per km to reinforce.

Constraint Costs Considered	B6 Reinforcement Magnitude	B7a Reinforcement Magnitude
Extrapolation from year 6	2580 MW	2240 MW
Piecewise linear interpolation	5140 MW	3870 MW

Table 7.17: Table to compare the estimated optimal reinforcement decisions from a year 6 extrapolation or a piecewise linear interpolation between years 6 and 15, when assuming a cost of £1500 per MW per km to reinforce.

Table 7.16 details the estimates of optimal reinforcement decisions when using or not using the piecewise linear interpolation of Equation 7.6.1 to estimate mean constraint costs between years 6 and 15 and assuming a cost of £1000 per MW per km to reinforce. The estimated optimal reinforcement decision is much greater when using the piecewise interpolation to estimate expected total costs in comparison to when an extrapolation from year 6 is used, with B6 reinforcement increasing by 2650 MW and B7a reinforcement increasing by 1490 MW. Table 7.17 details these results when assuming a cost of £1500 per MW per km to reinforce, with B6 reinforcement increasing by 2560 MW and B7a reinforcement increasing by 1630 MW when using the piecewise interpolation to estimate expected total costs in comparison to when an extrapolation from year 6 is used.

These results show how the reinforcement magnitudes are greatly increased when using the piece-wise interpolation to estimate costs, which is what may have been expected due to the increase in the estimate of expected total costs noted in Figure 7.14 (a). In reality, if the extrapolation from year 6 only was used to estimate constraint costs, the resulting reinforcement decisions would leave the power system with an inadequate transmission system, which aside from the huge economic costs could possibly leave the power system vulnerable to severe consequences such as blackouts.

The increased reinforcement observed in Tables 7.16 and 7.17 is because there is a greater benefit from reinforcing the B6 and B7a boundaries for years later than year 6. In reality, it is not necessary to make all transmission reinforcements at once. One reinforcement decision could be made now and another at a later date (or dates). Making decisions in multiple stages has two main benefits. First, future costs are discounted (something neglected in the model so far) which means it can be economically beneficial to postpone part (or all) of a reinforcement until it is needed instead of making an overly large outlay now. Secondly, things can be learnt about the uncertainties (i.e. uncertainty reduced) between making decisions, which should allow for a decision made in 5 years time to be better suited for the power system in 10 years time, in comparison to a decision made now for the power system in 10 years time. This motivates the next chapter, which considers making reinforcement decisions over multiple stages.

Chapter 8

Two Stage Modelling and Decision Making, Using Emulation and Backwards Induction

Up until this point, this thesis has considered making transmission expansion decisions at a single point in time, based on a single quantification of beliefs about uncertainties in the future power system at the time the decision is made. Under this model, once a decision has been made the power system must be operated with the particular reinforcement made, regardless of what is learnt about the uncertainties in the power system in the future. However, in real life applications, information will be learnt about the power system which reduces uncertainty as time progresses. Further, as well as making an initial decision, there will often be an opportunity for an amendment to the decision (further reinforcement) at a later date (or the ability to delay some/all of the initial reinforcement) which can make the transmission system more suited to to the observed state of the future power system background (i.e. the ability to make further decisions which account for what has been learnt about uncertainties since the first decision).

Backwards induction is a commonly used method to handle multi-stage decision making. However, applications are only feasible when there is a finite number of decisions that can be made in each stage and a finite number of possible scenarios (states of the future power system) at each stage. This chapter will consider the use of emulators

to improve the backwards induction methodology and allow for the variables which describe decisions made and scenarios to be treated as continuous variables, effectively allowing for an infinite number of potential future scenarios and decisions, rather than a small finite set as backwards induction alone allows.

8.1 Multi-Stage Power System Planning Literature Review

Section 2.3 described results from a wide variety of literature on transmission expansion planning. These papers presented different methodologies for how to make transmission expansion decisions, which considered uncertainty in the input data to varying degrees. Amongst this literature was [97] which gave thought to making decisions over multiple stages.

There are two main advantages to decision making over multiple stages. Firstly, it could be that, with the projected changes in generation and demand, certain reinforcements of the transmission system which are of little value in the near future (e.g. 5 years) are of much greater benefit in the more distant future (e.g. 15 years). Therefore, it would be worth delaying this expansion instead of making an overly large outlay of costs now.

Secondly, uncertainties exist in projections of the future power system. Waiting to make a decision allows the decision maker to observe the power system in the intermediate time, learn about certain values (thus reducing uncertainty) and make a better decision which is more suited to the improved projections of the power system.

This section will give an overview to the existing literature which considers transmission expansion planning over multiple stages.

8.1.1 Multiple Stage Decision Making Without Considering Uncertainty

[54] is one example of multi-stage transmission expansion planning from the existing literature which seeks to identify optimal decisions to minimise the net present value

of the investment costs, operational costs of the system and load shedding costs of the system over a given period of time. For any given expansion strategy (i.e. a plan of what to build and when to build it) total costs are calculated via a linear programming problem. Several algorithms are proposed to find the optimal reinforcement strategy, based on evolutionary algorithms (such as one based on artificial immune systems), swarm intelligence (such as an algorithm based on ant colony optimisation) and the tabu search metaheuristic. Two applications of the proposed algorithms are considered, the first of which considers a multi-stage transmission expansion problem of a 6 bus power system where reinforcement decisions can be made at any point over an 8 year horizon, whilst the second considers an application to the Minas Gerais power system of south-east Brazil where reinforcements can be made at any point over a 10 year horizon. For both of these applications a single projection is used to model how the system is expected to change over the given horizon.

[8] details a methodology which utilises a branch and bound algorithm to make reinforcement decisions over multiple stages for given projections of a power system. The objective considered is to minimise the net present value of the cost of expanding the transmission system whilst satisfying network constraints. The optimal reinforcement strategy is solved via a branch and bound algorithm which is formulated as a mixed-integer linear programming problem. An example is presented of the methodology applied to the Columbian power system with three sequential decisions to be made in 2002, 2005 and 2009, with these decisions being based on the projected power system for the years 2005, 2009 and 2012 respectively.

[81] consider multi-stage transmission expansion planning whilst also allowing for the system planner to make use of fixed series compensation (FSC). FSC is where the topology of the transmission network is altered to reduce bottlenecks in the network (such as if one power line is often overloaded but other parallel transmission lines are not) to get more benefit from the existing transmission system without the need for expansion. The problem is formulated as a linear mixed binary programming problem with an optimal solution identified by using a branch and cut solver. The objective of the problem is to minimise the total cost of network expansion and FSC subject to network constraints. Two examples to illustrate an application are given of a 24 bus

power system and the Columbian power system, where three sequential decisions are to be made. A comparison is also given between expansion decisions depending on whether or not FSC was utilised.

Multi-stage transmission planning which seeks to minimise the net present value of expansion and operational costs is considered by [30]. The problem is formulated as a mixed integer non-linear programming problem, and a genetic algorithm is used to identify the optimal reinforcement strategy. Applications of the methodology to the Brazilian and Columbian power systems are given. The application to the Columbian power system considers making reinforcement decisions in three stages (with decisions in 2002 for the 2005 system, in 2005 for the 2009 system and in 2009 for the 2012 system) whilst the application to the Brazilian power system considers making decisions in two stages (in 1998 for the 2002 system and in 2002 for the 2008 system).

However, all of the examples from papers considered in this subsection provide a methodology which considers making sequential transmission expansion decisions based on a single set of projections about the future power system. This ignores the fact that there will be uncertainties in many aspects of the future power system, and does not not consider the fact that updated information will be available when making second stage decisions, which allows for future decisions to be better suited to the state of the power system that is observed.

8.1.2 Multiple Stage Decision Making With Some Consideration of Uncertainty

Within the existing literature there are examples which do consider uncertainty in the assumed projections of future power system when making multi-stage transmission expansion decisions. This is often handled by a somewhat limited approach of making several plausible projections about the future power system, then either comparing how decisions vary when any particular scenario is assumed to be true or outlining a single multi-stage expansion plan which takes an expectation of costs across all scenarios.

One such example is considered in [62], which presents a multi-objective transmission expansion problem, which seeks to identify optimal transmission expansion decisions

across multiple stages when there are multiple scenarios (possible states of the future power system) that could occur as time progresses. A non-dominated genetic algorithm (NDGA) is used to solve the multi-objective problem which minimizes the sum of investment plus congestion costs across all stages as the primary problem, whilst also accounting for risk metrics such as minimising maximum adjustment cost and minimizing maximum regret.

An application is presented which considers making three sequential decision over a 15 year period. For this example, the power system is initially modelled based on the 2007 Iranian power system. Two scenarios are considered for how the power system might develop over the 15 year period, with an optimal reinforcement strategy for the 15 year period identified to optimize the multi-objective criteria by taking a weighted average across both scenarios. However, a limitation of this methodology is that it does not consider learning about which scenario is actually observed when it comes to actually making the second and third decisions, it simply makes a decision which minimises the expected costs across all possible scenarios. If information could be learnt about which scenario has occurred between making the first and second decision, this would allow for the second decision to be much better suited to the state the power system is actually in, which in turn would reduce the expected costs in the second stage and beyond.

[26] consider a multi-stage transmission expansion problem to minimise the sum of investment plus congestion costs. The problem is formulated as a mixed integer linear programming problem which is solved via a Benders decomposition which minimizes the total cost of investment and network congestion as the master problem, whilst giving consideration to the security of the system and market competitiveness of the system as two sub-problems. An application of the method to the Iranian power system is presented, where the initial state of the power system is based on the 2008 Iranian power system. 12 possible projections of the future power system are considered which vary the discount rate of costs and the projections of future installed generating capacity. Half the scenarios consider a 5 year horizon and half a 10 year horizon, with the ability to expand the transmission system in any year. Results are presented which give the optimal transmission system expansion strategy when assuming any

one scenario to be true, which show how the optimal transmission expansion plan is sensitive to assumptions made about the future power system. However, the paper does not consider making a decision when there is uncertainty into which particular scenario is true.

[80] present a co-planning problem, which allows for both the transmission system and the energy storage system to be expanded. The objective is to minimise the net present value of the sum of investment in the transmission and storage system plus the expected costs of operation over a given period of time subject to network, generator and storage constraints. An example is presented which considers a 24 bus system and three projections of how installed wind capacity and demand will grow over a 25 year period. The system is formulated stochastically, taking an expectation over all three projections, but the example does not consider learning about which of the three projections is more likely to be true as time progresses. Result are also given to show the benefit of co-planning transmission and storage in comparison to only planning storage expansion and also how the decisions would vary if one of the scenarios (referred to as the base scenario) was assumed to occur with certainty in comparison to taking a stochastic optimisation across the three scenarios.

The articles considered in this subsection are an improvement on the previous subsection as they consider uncertainty in the projections of the future power system and how they affect the decisions made. However, none of the examples presented in either subsection are ideal, as none of the examples consider making a decision at one point in time then reducing the uncertainty in any aspects of the future power system before the next decision in order to make a decision best suited to the observed state of the power system.

8.1.3 Multiple Stage Decision Making Which Accounts for Uncertainty

There are some articles in the existing power system literature which consider multi-stage transmission expansion planning under uncertainty where uncertainties are reduced between each decision, such as [66] which presents an example which considers

a multi-stage problem with the objective of minimising the sum of investment and expected operational costs across all scenarios that could occur. The problem is formulated stochastically as a mixed integer linear programming problem. An example is then applied to the 240 bus West Electricity Coordinating Council (WECC) power system of western USA, with costs being considered between the years 2023 and 2063. The first decision is to be made in 2013 (when there is uncertainty about the state of the future system) and a second decision can be made in 2023 (when information about the state of the future system has been learned), with the resulting reinforcements from these decisions becoming available in years 2023 and 2033 respectively. Three scenarios which describe the state of the 2023 power system are considered, with emission limits, generating costs and installed renewable generators varying between the three scenarios. Results are compared to deterministic planning, where a single future scenario would be assumed to occur with certainty, to illustrate the necessity to account for uncertainty in the future scenario.

[79] consider a co-planning problem, which allows for both the transmission system and gas generation system (both gas generating units and necessary expansions to gas pipelines required for those generating units) to be expanded over multiple stages. Initially, an expansion decision is to be made with the lowest adaptation cost, which is defined as the the additional costs required to adapt the system if an unexpected scenario occurs (quantified as the maximum cost across all possible future scenarios). When the future state of the power system is realised, further network expansion is available to maximise the net present value of social welfare of the system. This is formulated stochastically as a mixed integer non-linear programming problem, which is solved using a modified differential evolution algorithm. An example is presented which considers an application to a 14 bus system, which gives projections for the power system over a 12 year period. There is considered to be uncertainty in the projections of the installed generating capacities and 6 different potential future scenarios are considered which vary the projections of installed generating capacities.

[48] consider a multi-stage planning problem which allows for the use of energy storage (to store generation capacity during periods of low demand to be used during periods of high demand) and demand-side management (DSM, such as rescheduling flexible load).

The use of energy storage and DSM can allow for investments in the transmission system to be delayed, and a later investment can be made when more information has been learnt about uncertainties in the transmission system. The problem is formulated stochastically as a mixed integer linear programming problem, which is solved using a Benders decomposition with the master problem to minimise the probabilistic expectation of discounted investment and operating costs subject to network constraints and the sub-problem of minimising the sum of generating costs and penalized demand curtailment costs subject to operational constraints.

An example is applied to a 24 bus system with a 15 year planning horizon in which 3 sequential decisions are to be made (an initial decision with two further decisions spaced 5 years apart). Uncertainty is considered in the amount of installed wind generating capacity over the 15 year period, with 4 potential scenarios for future installed wind generating capacity considered. These four scenarios form a probability tree, with the initial installed wind generating capacity assumed to be known with certainty. When the second decision is to be made it is assumed that one of two scenarios for installed wind generating capacity will have been observed, with these two scenarios each branching into a further two scenarios when the final third decision is to be made. Results are presented which compare how the multi-stage decisions vary depending on whether or not energy storage and DSM are used, as well as a comparison to multi-stage decisions in a deterministic setting, where the future scenario is known with certainty.

From the wider power system planning literature, [64] is an example which considers distribution network (the connection between the transmission system and consumers) planning over multiple years under uncertainty. The problem is formulated as a stochastic mixed integer linear programming problem with the objective of minimising the total expected investment and operation costs over a given time horizon subject to constraints. An optimal solution is identified using real options methods from mathematical finance which assess the flexibility of decisions in each stage by calculating expected costs in future stages assuming the current decision will limit which future decisions can be made. An application to a neighbourhood of the UK power system with 1000 consumers is presented, which considers a 3 stage decision problem over a 15 year horizon, where an immediate decision is to be made with 2 further opportunities

for investment available in 5 years time and 10 years time respectively. Uncertainty is considered in 4 variables over the planning horizon, with future electricity consumption and gas consumption assumed to stay the same or rise by 5% after each decision and electricity and gas prices assumed to rise by 50% or fall by 50% after each decision. This is quite a limiting model, as electricity and gas prices, for example, are assumed to rise by 50% with probability 0.6 or decrease by 50% with probability 0.4 at each stage, with the probability of observing any price between these two extremes being 0.

Decisions are compared to decisions under the "best view philosophy" where a single future scenario is considered, where variables containing uncertainty are assumed to take their mean value across all future time periods. This best view scenario actually differs from any of the original 12 scenarios considered. For example, in the second stage it is assumed electricity and gas consumption will either stay the same, with a 30% chance, or increase by 5%, with a 70% chance. This means that the best view scenario would consider an increase of 3.5% with certainty, which is considered in neither of the potential changes in the stochastic problem. A comparison is also given to a case where decisions are made as a series of three single stage investments, with each decision made to minimise the expected costs across the remainder of the horizon whilst assuming there will be no further decisions.

An example which considers generation expansion planning (building new generators) over multiple decisions stages is [38], which aims to devise a strategy which minimises the sum of investment and operational costs that are expected to arise after each decision is made. The problem is formulated stochastically as a mixed integer linear programming problem which is solved via a Benders decomposition. The Benders decomposition uses the investment problem as the master problem and the operational problem as a sub-problem. An example is presented which decides where, when and how many new hydro power plants should be built on the South-South Eastern Brazilian power system between 1995 and 2000, with expansion decisions to be made in each year. A total of 16 scenarios are considered each of which vary load (demand) level slightly over the five year period. These scenarios form a probability tree, with one scenario known in the first year and each scenario branching into two different scenarios in each subsequent year, leading to 16 scenarios being considered by the fifth year.

Deterministic results are also presented for comparison, when power system expansion decisions are made when assuming a particular scenario will occur with certainty.

However, all of these examples consider a small number of possible future scenarios, which can differ greatly from one another. Further, the examples assume that once a particular scenario has been realised that there is no uncertainty in any aspect of the power system, which is also overly simplistic, as many variables which define a power system can never be known absolutely, so there will always remain uncertainty in some aspects of the power system.

8.1.4 Summary of Available Multi-Stage Power System Planning Literature

This section has given an overview of the existing literature for transmission expansion planning across multiple stages, with consideration as to how the uncertainty that exists in projections of future power systems is handled to varying degrees in the literature. The simplest examples simply make a single set of projections about the future power system which are assumed to be correct, and make multi-stage decisions based on this single set of projections, whilst the more complicated examples consider multiple scenarios (possible states of the future power system) and making an initial decision to minimise the expectation across all future scenarios whilst allowing for a second decision to be made when more has been learnt about the future powers system.

However, the articles which do consider uncertainty in the projections of the future power system do so by considering a small number of possible future scenarios whilst varying the projections of multiple variables. This is very limiting as this gives a very poor coverage of the space of the potential scenarios for the future power system that could occur. Further, as more stages for reinforcement are considered, or uncertainty is considered in more variables, the number of scenarios considered would either have to grow exponentially or give an increasingly sparse coverage of the sample space of all possibilities of the future power system.

This problem is often compounded by the fact that the probabilistic aspect of generating future scenarios is often neglected or not given deep enough thought. It is often the

case that the scenarios will assume an uncertainty takes one of two extreme values and all intermediate values are modelled as impossible (as was highlighted when considering [64] where electricity and gas prices were assumed to rise by 50% with probability 0.6 or decrease by 50% with probability 0.4, with the probability of observing any price between these two extremes being 0).

This exposes the need for a more Bayesian approach to scenario modelling, where instead of considering a small number of possible projections for the power system, probability density functions (PDFs) are used to specify continuous distributions which quantify prior beliefs about the uncertainties that exists in the projections of the future power system. Further, conditional PDFs of the uncertainties for given observations (which can also be quantified continuously) as time progresses can also be specified (for example, specifying a PDF for peak demand 16 years into the future conditional on the observed peak demand 11 years into the future). This modelling of uncertainties and observations as continuous variables essentially models an infinite number of possible states for the future power system, probabilistically modelling any state of the future power system deemed possible by the expert judgement.

This thesis will demonstrate how backwards induction [88, 33, 100, 1] can be combined with such a Bayesian approach to give a multi-stage decision methodology which gives a more complete consideration to the uncertainties of the projected future power system each time a decision is made. Further, future decisions can account for what has been observed about the power system since the first decision and as a result make decisions which are better suited to the observed state of the power system. This chapter will present the solution for a 2-stage decision problem, which will be generalised to an M-stage problem in Chapter 9.

8.2 Formulation of the M-Stage Decision Problem and a Solution for 2 Stages

8.2.1 Preliminary Modelling Information for the M-Stage Problem

Before giving details about the methodology used to solve the M-stage decision problem, this subsection will give some preliminary information and justifications for modelling choices used in this thesis.

Simulator Models For Mean Constraint Costs in Each Stage

Chapter 3 defined the simulator, $f_c(\mathfrak{X}) = f_c(\mathbf{v}, \mathbf{a}, \mathbf{d})$, which is used to simulate mean constraint costs for given information about a power system, where $\mathbf{v}$ represents variables containing uncertainties of interest (i.e. variables which have a large effect on the estimate of constraint costs), $\mathbf{a}$ represents variables which it is either reasonable to think can be known very accurately or variables which have little effect on the estimate of constraint costs and $\mathbf{d}$ represents decision variables. As the values of $\mathbf{a}$ are kept fixed, as if known precisely, $f_c(\mathbf{v}, \mathbf{a}, \mathbf{d})$ can be treated as if it is a function of $\mathbf{v}$ and $\mathbf{d}$ only, i.e. $f_c(\mathbf{v}, \mathbf{a}, \mathbf{d})$ can be treated as $f_c(\mathbf{v}, \mathbf{d})$.

This notation must be extended when making decisions over M stages, indexed by m. $f_{c,m}(\mathbf{v}_m, \mathbf{d}_m | \mathbf{d}_1, ..., \mathbf{d}_{m-1})$ is used to represent the simulator which simulates mean constraint costs for given information about the power system background in stage m, where $\mathbf{v}_m$ represents variables which contain uncertainty in stage m, $\mathbf{d}_m$ represents decision variables in stage m and $\mathbf{d}_1, ..., \mathbf{d}_{m-1}$ represent the decisions that were previously made in stages 1 to $m-1$.

Estimating Expected Mean Constraint Costs Under Uncertainty in Each Stage and Reducing Uncertainty Between Decisions

For the single stage decision problems considered in Chapters 5 and 6, Equation 5.2.16 of Section 5.2.5 detailed how an estimate of expected total costs under uncertainty

can be calculated by integrating the product of the fitted emulator and a set of prior beliefs which describe the probabilities of the uncertain variables taking particular values, $p(\mathbf{v})$. For the M-stage methodology that will be presented it is assumed that information will be learnt about the variables which contain uncertainty between each stage. This will allow future decisions to take into account information that has been observed, in order to make a decision which is more suited to the observed state of the power system. This means that the beliefs about the variables which contain uncertainty in the mth stage, $\mathbf{v}_m$, will be dependent upon what was observed up until the point the mth decision is made.

Therefore, $\boldsymbol{\psi}_m$ is used to quantify what was observed about the variables which contain uncertainty by the time mth decision is to be made. $\boldsymbol{\psi}_m$ is cumulative and in some way quantifies what was observed in the previous $m-1$ stages. $\boldsymbol{\psi}_m$ is in turn used to specify $p(\mathbf{v}_m|\boldsymbol{\psi}_m)$ as the beliefs about the values of the variables which contain uncertainty in stage m, given that the information quantified in $\boldsymbol{\psi}_m$ has been observed up until the time the mth decision is to be made. An estimate of expected mean constraint costs under uncertainty in stage m can then be calculated as

$$F_{c,m}(\mathbf{d}_m|\mathbf{d}_1,...,\mathbf{d}_{m-1},\boldsymbol{\psi}_m) = \int_{\mathbf{v}_m} f_{c,m}(\mathbf{v}_m,\mathbf{d}_m|\mathbf{d}_1,...,\mathbf{d}_{m-1}) \times p(\mathbf{v}_m|\boldsymbol{\psi}_m)\mathrm{d}\mathbf{v}_m \quad (8.2.1)$$

How $\boldsymbol{\psi}_m$ and in turn $p(\mathbf{v}_m|\boldsymbol{\psi}_m)$ are specified will depend on the particular variables of interest. For example, if uncertainty is considered in stage m peak demand level, $\boldsymbol{\psi}_m$ could represent the estimate of expected peak demand level in stage m based on the observed peak demand in the previous $m-1$ stages. Such an expectation could be that if the observed peak demand level in the previous stage was δ% larger than initially projected at the beginning of stage 1 (or alternatively, if peak demand level in the previous m stages was on average δ% larger than initially projected), $\boldsymbol{\psi}_m$ could be specified as $(100+\delta)$% of the stage m peak demand level which was projected at the beginning of year 1. This could then be used to specify a distribution for the beliefs about the stage m peak demand level, for example, $p(\mathbf{v}_m|\boldsymbol{\psi}_m)$ could represent a uniform distribution between $0.95\boldsymbol{\psi}_m$ and $1.05\boldsymbol{\psi}_m$ (i.e. a uniform distribution over a +/-5% range, which is consistent with what was earlier considered in Section 6.1.1).

If uncertainty is considered in the availability probability of nuclear generation, $\boldsymbol{\psi}_m$

could be defined as $\boldsymbol{\psi}_m = (\psi_{m,1}, \psi_{m,2})$, where $\psi_{m,1}$ denotes the average observed nuclear availability probability in stages 1 to $m-1$ and $\psi_{m,2}$ denotes how much weight is given to these observations. These values can then be used to specify $p(\mathbf{v}_m|\boldsymbol{\psi}_m)$ as a (scaled) beta distribution for nuclear availability probability in stage m, as described in Appendix C.1.

When considering uncertainty in the bid (or offer) price of a particular type of generating technology, it is possible that a model for the bid price in stage m considers longer term trends from the previous stages which requires the most recent N_{M_2} observations to be specified. Therefore, $\boldsymbol{\psi}_m$ could be defined as $\boldsymbol{\psi}_m = (\psi_{m,1}, ..., \psi_{m,N_{M_2}})$, where $\psi_{m,1}$ to $\psi_{m,N_{M_2}}$ represent the latest N_{M_2} observations, which are then used to specify $p(\mathbf{v}_m|\boldsymbol{\psi}_m)$ via an appropriate time series model.

For an example which considers uncertainty in the reinforcement costs of transmission expansion, $\boldsymbol{\psi}_m$ could be the observed cost of reinforcement at the time the mth decision is made. Beliefs about the cost to reinforce at the time the mth decision is made could then be defined such that $p(\mathbf{v}_m|\boldsymbol{\psi}_m) = 1$ when $\mathbf{v}_m = \boldsymbol{\psi}_m$, and 0 otherwise, as it is reasonable to assume that the cost of reinforcement can be known accurately at the time the decision is made.

Uncertainty can be reduced in more aspect of the future power system between decisions. This would model $\boldsymbol{\psi}_m$ as $\boldsymbol{\psi}_m = (\boldsymbol{\psi}_{m,1}, ..., \boldsymbol{\psi}_{m,N_\psi})$, where uncertainty is reduced in N_ψ variables between decisions and $\boldsymbol{\psi}_{m,i}$ quantifies what was learnt about the ith uncertainty in an appropriate way.

Although the specification of $\boldsymbol{\psi}_m$ and in turn $p(\mathbf{v}_m|\boldsymbol{\psi}_m)$ depends on the particular variables considered, the methodology that will be presented is otherwise written in general terms, meaning it can be applied for any given specification of $\boldsymbol{\psi}_m$ and $p(\mathbf{v}_m|\boldsymbol{\psi}_m)$. Specifications for $\boldsymbol{\psi}_m$ and $p(\mathbf{v}_m|\boldsymbol{\psi}_m)$ for the multi-stage problems considered in this thesis will later be given in Sections 8.3.3 and 9.2.3.

Quantifying Beliefs About $\boldsymbol{\psi}_m$

As $\boldsymbol{\psi}_m$ describes the observed state of the power system (i.e. quantifies what was learnt about uncertainties) by the time the mth decision is to be made, it is itself unknown at

the times when the previous $m-1$ decisions were made. Therefore, it is necessary to specify prior beliefs for the value of $\boldsymbol{\psi}_m$ that will be observed. In the methodology that will be presented, it is sufficient to specify $p_{\boldsymbol{\psi}_{m|m-1}}(\boldsymbol{\psi}_m|\boldsymbol{\psi}_{m-1})$, i.e. to specify beliefs about the observed state of the power system at the time mth decision is made, $\boldsymbol{\psi}_m$, given the observed state of the power system at the time the $m-1$th decision is made, $\boldsymbol{\psi}_{m-1}$, only.

In particular, it is noted that beliefs about $\boldsymbol{\psi}_m$ do not depend on the decisions made in the previous $m-1$ stages (i.e. $\mathbf{d}_1, ..., \mathbf{d}_{m-1}$). For the multi-stage decision examples considered in this thesis (which will be detailed in Sections 8.3 and 9.2) this is sufficient as the decisions made in each stage are reinforcement decisions of the transmission system (i.e. building new transmission lines) whilst the future scenario, $\boldsymbol{\psi}_m$, describes the expected peak demand level and the availability probabilities of generating technologies in stage m, and it is reasonable to think of these variables as being independent from one another.

However, in a more general example it is possible that the decision made in stage $m-1$ affects the scenario observed in stage m. For example, if uncertainty is considered in the total installed renewable generating capacity in each stage and the stage $m-1$ decision was the total value of government incentives that would be made available in order to encourage investment in renewable generation, it is reasonable to think that the stage $m-1$ decision may have an effect on the observed scenario (total installed renewable generating capacity) in stage m. This would lead to the prior beliefs about the stage m scenario at stage $m-1$ being dependent on the scenario observed in stage $m-1$, $\boldsymbol{\psi}_{m-1}$, and the previous decisions made, $\mathbf{d}_1, ..., \mathbf{d}_{m-1}$. This would result in $p_{\boldsymbol{\psi}_{m|m-1}}(\boldsymbol{\psi}_m|\mathbf{d}_1, ..., \mathbf{d}_{m-1}, \boldsymbol{\psi}_{m-1})$ being used to express beliefs in stage $m-1$ about the scenario that will be observed in stage m in place of $p_{\boldsymbol{\psi}_{m|m-1}}(\boldsymbol{\psi}_m|\boldsymbol{\psi}_{m-1})$, with the methodology that will be presented being otherwise unchanged.

8.2.2 Our Intractable M-Stage Problem

Our Intractable M-Stage Problem

The methodology for multi-stage decision making used in this thesis will adapt the methodology of backwards induction. Backwards induction is a methodology for identifying an optimal decision strategy for a multi-stage decision problem with M sequential decisions to be made, where optimal decisions are first identified for the final Mth stage which maximise expected profits (or alternatively minimise expected losses) conditional on the observed state when the Mth decision is to be made and the decisions made in the previous $M-1$ stages. Then, optimal decisions are identified for the previous stage (stage $M-1$) to maximise expected profits for stages $M-1$ plus M (conditional on the observed state when the $M-1$th decision is to be made and the decisions made in previous $M-2$ stages), assuming the decision maker acts optimally in stage M. This is done for each stage iteratively, until eventually the optimal stage 1 decision is identified to maximise expected profits across all M stages, assuming the decision maker will act in an optimal manner in stages 2 to M.

For an unfamiliar reader, further details on backwards induction can be found in [88, 33, 100]. Further, formulation for a general backwards induction problem and an example to illustrate an application of the backwards induction methodology are given in Appendix C.2.

For the transmission expansion problem considered in this thesis, the objective is to present a methodology for making M sequential decisions, where each decision is made to minimise the expected value of all future costs. The methodology for making such decisions will seek to use backwards induction as the basis for achieving this. This means first identifying the optimal reinforcement decisions to be made in the final stage. Then, at each previous stage, optimal reinforcement decisions are identified to minimise the expected total costs of the current stage plus the expected total costs of all future stages, whilst assuming that the decision maker behaves optimally in all future stages.

Estimating Expected Total Costs and Optimal Decisions in Stage M

The previous subsection detailed how $f_{c,m}(\mathbf{v}_m, \mathbf{d}_m|\mathbf{d}_1, ..., \mathbf{d}_{m-1})$ represents the simulator which calculates mean constraint costs in stage m for given information about the power system background, which could subsequently be used to estimate expected mean constraint costs under uncertainty in stage m, $F_{c,m}(\mathbf{d}_m|\mathbf{d}_1, ..., \mathbf{d}_{m-1}, \boldsymbol{\psi}_m)$, via Equation 8.2.1.

The reinforcement costs of decisions in each stage must also be accounted for, with $f_{\rho,m}(\mathbf{d}_m|\mathbf{d}_1, ..., \mathbf{d}_{m-1}, \boldsymbol{\psi}_m)$ representing the costs of making decision $\mathbf{d}_m$ in stage m when decisions $\mathbf{d}_1, ..., \mathbf{d}_{m-1}$ were previously made in stages 1 to $m-1$ and $\boldsymbol{\psi}_m$ describes what has been observed up until the time when the mth decision is to be made.

At each stage the aim is to make the decision that will minimise the sum of expected total costs in the current stage and across all future stages. We seek to make these decisions via backwards induction, which requires starting at the final (Mth) stage, identifying optimal decisions and iteratively working backwards. In the Mth stage the expected total costs of a decision across the Mth stage and all future stages (i.e. just stage M as it is the final stage) are

$$F_{T,M}(\mathbf{d}_M|\mathbf{d}_1, ..., \mathbf{d}_{M-1}, \boldsymbol{\psi}_M) = F_{c,M}(\mathbf{d}_M|\mathbf{d}_1, ..., \mathbf{d}_{M-1}, \boldsymbol{\psi}_M) + f_{\rho,M}(\mathbf{d}_M|\mathbf{d}_1, ..., \mathbf{d}_{M-1}, \boldsymbol{\psi}_M) \tag{8.2.2}$$

i.e. the sum of expected mean constraint costs, $F_{c,M}(\mathbf{d}_M|\mathbf{d}_1, ..., \mathbf{d}_{M-1}, \boldsymbol{\psi}_M)$, plus reinforcement costs, $f_{\rho,M}(\mathbf{d}_M|\mathbf{d}_1, ..., \mathbf{d}_{M-1}, \boldsymbol{\psi}_M)$, in stage M. If information was given about the current state of the power system in the Mth stage (i.e. values of $\mathbf{d}_1, ..., \mathbf{d}_{M-1}, \boldsymbol{\psi}_M$), then the value of the decision, $\mathbf{d}_M$, which minimised Equation 8.2.2 would be the estimate of the optimal stage M decision.

Estimating Expected Total Costs in Stage $M-1$ Onwards

Suppose a function can be created, $d^o_M(\mathbf{d}_1, ..., \mathbf{d}_{M-1}, \boldsymbol{\psi}_M)$, which returns the optimal decision to be made in the Mth stage for given information about the current state of the power system. The backwards induction methodology would then seek to identify optimal decisions to be made which minimise the estimate of expected total costs in stage $M-1$ onwards (i.e. stages $M-1$ and M).

For a given observed stage $M-1$ scenario (value of $\boldsymbol{\psi}_{M-1}$) and reinforcement decisions in the previous $M-2$ stages (values of $\mathbf{d}_1, ..., \mathbf{d}_{M-2}$) the expected total costs in stage $M-1$ can be calculated as the sum of the expected constraint costs in stage $M-1$, $F_{c,M-1}(\mathbf{d}_{M-1}|\mathbf{d}_1, ..., \mathbf{d}_{M-2}, \boldsymbol{\psi}_{M-1})$ calculated via Equation 8.2.1, and the reinforcement costs in stage $M-1$, $f_{\rho,M-1}(\mathbf{d}_{M-1}|\mathbf{d}_1, ..., \mathbf{d}_{M-2}, \boldsymbol{\psi}_{M-1})$.

For a given stage M scenario, $\boldsymbol{\psi}_M$, the expected total costs in stage M can be calculated as $F_{T,M}(\mathbf{d}^o_M(\mathbf{d}_1, ..., \mathbf{d}_{M-2}, \mathbf{d}_{M-1}, \boldsymbol{\psi}_M)|\mathbf{d}_1, ..., \mathbf{d}_{M-2}, \mathbf{d}_{M-1}, \boldsymbol{\psi}_M)$ via Equation 8.2.2, by assuming the decision maker acts optimally in stage M. However, at the time the $M-1$th decision is made, the stage M scenario is unknown. Therefore, expected total costs in stage M at the time the $M-1$th decision is made are calculated by taking a probabilistic expectation of costs over all possible stage M scenarios that could be observed, whilst assuming the decision maker in stage M would make the optimal decision, $d^o_M(\mathbf{d}_1, ..., \mathbf{d}_{M-2}, \mathbf{d}_{M-1}, \boldsymbol{\psi}_M)$, in each scenario. An estimate of expected total costs in stage M at the time the $M-1$th decision is made can thus be calculated as

$$\int_{\psi_M} F_{T,M}(\mathbf{d}^o_M(\mathbf{d}_1, ..., \mathbf{d}_{M-2}, \mathbf{d}_{M-1}, \boldsymbol{\psi}_M)|\mathbf{d}_1, ..., \mathbf{d}_{M-1}, \boldsymbol{\psi}_M) \times p_{M|M-1}(\boldsymbol{\psi}_M|\boldsymbol{\psi}_{M-1}) \mathrm{d}\boldsymbol{\psi}_M \tag{8.2.3}$$

where $p_{M|M-1}(\boldsymbol{\psi}_M|\boldsymbol{\psi}_{M-1})$ is the probability of observing the scenario described by $\boldsymbol{\psi}_M$ in stage M if the scenario described by $\boldsymbol{\psi}_{M-1}$ is observed in stage $M-1$.

An estimate of expected total costs in stage $M-1$ onwards which depends only on the stage $M-1$ decision and state of the power system in stage $M-1$ (i.e. value of $\boldsymbol{\psi}_{M-1}$) can then be acquired as

$$\begin{aligned} F_{T,M-1}(\mathbf{d}_{M-1}|\mathbf{d}_1, ..., \mathbf{d}_{M-2}, \boldsymbol{\psi}_{M-1}) &= F_{c,M-1}(\mathbf{d}_{M-1}|\mathbf{d}_1, ..., \mathbf{d}_{M-2}, \boldsymbol{\psi}_{M-1}) \\ &\quad + f_{\rho,M-1}(\mathbf{d}_{M-1}|\mathbf{d}_1, ..., \mathbf{d}_{M-2}, \boldsymbol{\psi}_{M-1}) \\ + \int_{\psi_M} F_{T,M}(\mathbf{d}^o_M(\mathbf{d}_1, ..., \mathbf{d}_{M-2}, \mathbf{d}_{M-1}, \boldsymbol{\psi}_M)|\mathbf{d}_1, ..., \mathbf{d}_{M-1}, \boldsymbol{\psi}_M) &\times p_{M|M-1}(\boldsymbol{\psi}_M|\boldsymbol{\psi}_{M-1}) \mathrm{d}\boldsymbol{\psi}_M \end{aligned} \tag{8.2.4}$$

Optimal decisions to be made in stage $M-1$ for given information about the power system can then be estimated as the stage $M-1$ decisions which minimise Equation 8.2.4. This allows for a function, $d^o_{M-1}(\mathbf{d}_1, ..., \mathbf{d}_{M-2}, \boldsymbol{\psi}_{M-1})$, to be created which identifies the optimal decision to be made in the $M-1$th stage for given information

about the current state of the system (i.e. for given decisions in the previous $M-2$ stages, $\mathbf{d}_1, ..., \mathbf{d}_{M-2}$, and stage $M-1$ scenario, $\boldsymbol{\psi}_{M-1}$).

Estimating Expected Total Costs in a General Stage m Onwards

The methodology of the previous sub-subsections leads to the recursion

$$F_{T,m}(\mathbf{d}_m|\mathbf{d}_1, ..., \mathbf{d}_{m-1}, \boldsymbol{\psi}_m) = F_{c,m}(\mathbf{d}_m|\mathbf{d}_1, ..., \mathbf{d}_{m-1}, \boldsymbol{\psi}_m) + f_{\rho,m}(\mathbf{d}_m|\mathbf{d}_1, ..., \mathbf{d}_{m-1}, \boldsymbol{\psi}_m)$$
$$+ \int_{\psi_{m+1}} F_{T,m+1}(\mathbf{d}^o_{m+1}(\mathbf{d}_1, ..., \mathbf{d}_m, \boldsymbol{\psi}_{m+1})|\mathbf{d}_1, ..., \mathbf{d}_m, \boldsymbol{\psi}_{m+1}) \times p_{m+1|m}(\boldsymbol{\psi}_{m+1}|\boldsymbol{\psi}_m)\mathrm{d}\boldsymbol{\psi}_{m+1} \tag{8.2.5}$$

where expected total costs are estimated for stages m to M depending only on the decision at stage m (for given information about the system at stage m), as the sum of the expected mean constraint costs in stage m, $F_{c,m}(\mathbf{d}_m|\mathbf{d}_1, ..., \mathbf{d}_{m-1}, \boldsymbol{\psi}_m)$ calculated via Equation 8.2.1; reinforcement costs in stage m, $f_{\rho,m}(\mathbf{d}_m|\mathbf{d}_1, ..., \mathbf{d}_{m-1}, \boldsymbol{\psi}_m)$; plus the estimate of expected total costs in stage $m+1$ onwards,

$$\int_{\psi_{m+1}} F_{T,m+1}(\mathbf{d}^o_{m+1}(\mathbf{d}_1, ..., \mathbf{d}_m, \boldsymbol{\psi}_{m+1})|\mathbf{d}_1, ..., \mathbf{d}_m, \boldsymbol{\psi}_{m+1}) \times p_{m+1|m}(\boldsymbol{\psi}_{m+1}|\boldsymbol{\psi}_m)\mathrm{d}\boldsymbol{\psi}_{m+1}$$

where $p_{m+1|m}(\boldsymbol{\psi}_{m+1}|\boldsymbol{\psi}_m)$ is the probability of observing the scenario described by $\boldsymbol{\psi}_{m+1}$ in stage $m+1$ if the scenario described by $\boldsymbol{\psi}_m$ is observed in stage m.

Solving each stage in reverse would eventually identify the optimal decisions to be made in stages 1 to M for all possible states across all stages.

8.2.3 Computational Challenge of Solving the Problem Outlined in Section 8.2.2

This thesis uses backwards induction as the basis for solving the multi-stage planning problem. If there were a small set of decisions and scenarios it would actually be possible to solve the problem as outlined in the previous subsection, where at each stage the function $\mathbf{d}^o_m(\mathbf{d}_1, ..., \mathbf{d}_{m-1}, \boldsymbol{\psi}_m)$ is formed which returns the optimal decisions to be made in stage m for given information about the current state of the power system (with the use of emulation to approximate the simulator $f_{c,m}(\mathbf{v}_m, \mathbf{d}_m|\mathbf{d}_1, ..., \mathbf{d}_{m-1})$ by

an emulator $\tilde{f}_{c,m}(\mathbf{v}_m, \mathbf{d}_m|\mathbf{d}_1, ..., \mathbf{d}_{m-1})$ in each stage to allow for an efficient evaluation of Equation 8.2.1).

However, the decision variables, $\mathbf{d}_m$, and variables which describe the state of the power system in stage m, $\boldsymbol{\psi}_m$, are modelled as continuous variables (i.e. effectively allowing for an infinite number of scenarios and decisions in each stage). This means that whilst decisions to minimise Equation 8.2.2 can be identified for any given values of $\boldsymbol{\psi}_M$ and $\mathbf{d}_1, ..., \mathbf{d}_{M-1}$, solving it accurately for general inputs is not possible.

Consequently, it is not possible to construct the function $d^o_M(\mathbf{d}_1, ..., \mathbf{d}_{M-1}, \boldsymbol{\psi}_M)$ which precisely identifies the optimal decision to be made in Stage M for any possible stage 1 to $M-1$ decisions $(\mathbf{d}_1, ..., \mathbf{d}_{M-1})$ and stage $M-1$ scenario $(\boldsymbol{\psi}_M)$. This in turn means we are unable to evaluate

$$\int_{\psi_M} F_{T,M}(\mathbf{d}^o_M(\mathbf{d}_1, ..., \mathbf{d}_{M-1}, \boldsymbol{\psi}_M)|\mathbf{d}_1, ..., \mathbf{d}_{M-1}, \boldsymbol{\psi}_M) \times p_{M|M-1}(\boldsymbol{\psi}_M|\boldsymbol{\psi}_{M-1})\mathrm{d}\boldsymbol{\psi}_M$$

which is required in order to estimate expected total costs in Stage $M-1$ onwards as a function of stage $M-1$ decision and scenario only via Equation 8.2.4. As a result, optimal decisions to be made in stage $M-1$ cannot be identified, which in turn means optimal decisions to be made in all previous stages cannot be identified.

In order to solve this problem, emulation will be used to approximate how costs vary in stage m onwards as a function of the decisions made in the previous $m-1$ stages (assuming the decision maker acts optimally in each future stage for whatever scenario arises). This means that as well as fitting emulator models, $\tilde{f}_{c,m}(\mathbf{v}_m, \mathbf{d}_m|\mathbf{d}_1, ..., \mathbf{d}_{m-1})$, to approximate the simulator, $f_{c,m}(\mathbf{v}_m, \mathbf{d}_m|\mathbf{d}_1, ..., \mathbf{d}_{m-1})$, in each stage, these emulator models will subsequently be used to fit another emulator model, $\tilde{G}_{T,m,\boldsymbol{\psi}_m}(\mathbf{d}_1, ..., \mathbf{d}_{m-1}, \boldsymbol{\psi}_m)$, to approximate how expected total costs in stage m onwards vary as a function of the previous $m-1$ decisions and observed scenario in stage m only, when assuming the decision maker acts optimally in stages $m+1$ to M. The methodology for achieving this for the two stage problem will be presented in the next subsection, which will be generalised to a general M stage problem in Section 9.1.2.

8.2.4 A Solution for Two Stages

Overview of the Methodology

This section will present a solution for decision making over two stages when there exists uncertainty in the future system. Section 9.1.2 will expand this methodology to account for a general number of M decision stages.

In the two stage problem there exists the simulator $f_{c,1}(\mathbf{v}_1, \mathbf{d}_1)$, which calculates mean constraint costs in the first stage for given values of variables which contain uncertainty in stage 1, $\mathbf{v}_1$, and stage 1 decision variables, $\mathbf{d}_1$; and the simulator $f_{c,2}(\mathbf{v}_2, \mathbf{d}_2|\mathbf{d}_1)$, which calculates mean constraint costs in the second stage for given values of variables which contain uncertainty in stage 2, $\mathbf{v}_2$, and stage 2 decision variables, $\mathbf{d}_2$, given that the decision $\mathbf{d}_1$ was previously made in the first stage. Emulator models are then fitted to approximate the simulator in each stage, such that $\tilde{f}_{c,1}(\mathbf{v}_1, \mathbf{d}_1)$ approximates $f_{c,1}(\mathbf{v}_1, \mathbf{d}_1)$ and $\tilde{f}_{c,2}(\mathbf{v}_2, \mathbf{d}_2|\mathbf{d}_1)$ approximates $f_{c,2}(\mathbf{v}_2, \mathbf{d}_2|\mathbf{d}_1)$, as described in Section 5.2.

As an outline of the methodology that will be presented, backwards induction will be used as the basis of the method, by first considering the expected total costs in the final (second) stage. Although Section 8.2.3 noted that a full backwards induction application is not possible, it will be shown how estimated optimal stage 2 decisions, and the resulting estimates of expected total costs, can be acquired for a small number of given stage 1 decisions, $\mathbf{d}_1$, and stage 2 scenarios, $\boldsymbol{\psi}_2$. The resulting estimates of expected total stage 2 costs can subsequently be used as a set of training runs to fit an emulator model, $\tilde{G}_{T,2,\boldsymbol{\psi}_2}(\mathbf{d}_1, \boldsymbol{\psi}_2)$, to approximate how expected total costs vary in stage 2 as a function of stage 1 decision, $\mathbf{d}_1$, and stage 2 scenario, $\boldsymbol{\psi}_2$, only. This model can subsequently be used along with prior beliefs about the stage 2 scenario that will be observed, $p_{\boldsymbol{\psi}_{2|1}}(\boldsymbol{\psi}_2)$, to estimated expected total costs in stage 2 as a function of the first stage decision only. After considering expected total costs in the first stage, an estimate of expected total costs across both stages can then be acquired as a function of the first stage decision only.

Estimating Expected Total Costs in Stage 2

When the time comes to make the second decision, there are a number of possible states the power system could be in. As noted in Section 8.2.1, $\boldsymbol{\psi}_2$ is a vector of variables which describe the observed state of the power system at the time the second decision is to be made. An estimate of expected mean constraint costs under uncertainty in stage 2 for a given state of the power system, $\boldsymbol{\psi}_2$, and a given first stage decision, $\mathbf{d}_1$, can then be acquired as

$$\tilde{F}_{c,2}(\mathbf{d}_2|\mathbf{d}_1, \boldsymbol{\psi}_2) = \int_{\mathbf{v}_2} \tilde{f}_{c,2}(\mathbf{v}_2, \mathbf{d}_2|\mathbf{d}_1) \times p(\mathbf{v}_2|\boldsymbol{\psi}_2) \mathrm{d}\mathbf{v}_2 \tag{8.2.6}$$

where $\tilde{f}_{c,2}(\mathbf{v}_2, \mathbf{d}_2|\mathbf{d}_1)$ is the emulator model which approximates the simulator of stage 2 constraint costs and $p(\mathbf{v}_2|\boldsymbol{\psi}_2)$ represents beliefs about the values the variables which contain uncertainty will take in stage 2 for a given value of $\boldsymbol{\psi}_2$. An estimate of the expected total costs (expected mean constraint costs plus reinforcement costs) in stage 2 can then be calculated as

$$\tilde{F}_{T,2}(\mathbf{d}_2|\mathbf{d}_1, \boldsymbol{\psi}_2) = \tilde{F}_{c,2}(\mathbf{d}_2|\mathbf{d}_1, \boldsymbol{\psi}_2) + f_{\rho,2}(\mathbf{d}_2|\mathbf{d}_1, \boldsymbol{\psi}_2) \tag{8.2.7}$$

where $f_{\rho,2}(\mathbf{d}_2|\mathbf{d}_1, \boldsymbol{\psi}_2)$ (which may be simplified to $f_{\rho,2}(\mathbf{d}_2|\mathbf{d}_1)$ if the cost to reinforce in the second stage does not depend on the scenario observed) is the calculation of reinforcement costs in the second stage for decision $\mathbf{d}_2$ in the second stage when $\boldsymbol{\psi}_2$ describes the observed state of the power system when the second decision is made, given that reinforcement decision $\mathbf{d}_1$ was previously made in the first stage.

Estimating Expected Total Costs in Stage 2 as a Function of Stage 1 Decision Only

To estimate how expected total costs across stage 1 and stage 2 vary as a function of the decision made in the first stage only, a model is required of how expected total costs in the second stage vary as a function of the decision made in the first stage only. This model is fitted by taking a sample of N_θ stage 1 decisions (values of $\mathbf{d}_1$) and stage two scenarios (values of $\boldsymbol{\psi}_2$) from all possible decisions being considered in stage 1 and all possible stage 2 scenarios that can occur. This gives a random sample of stage 1 decisions as $\mathbf{d}_{1,\theta}$ and stage 2 scenarios as $\boldsymbol{\psi}_{2,\theta}$ for $\theta = 1, ..., N_\theta$.

For each stage 1 decision and stage 2 scenario in the sample, an estimate for the optimal decision that would be made in stage 2 is calculated by minimising Equation 8.2.7 (i.e. minimising the estimate of expected total costs in stage 2 for the given stage 1 decision and stage 2 scenario), such that $\mathbf{d}_{2|\theta}$ is the estimate for the optimal decision to be made in stage 2, when decision $\mathbf{d}_{1,\theta}$ was previously made in stage 1 and $\boldsymbol{\psi}_{2,\theta}$ is observed in stage 2. The estimate of expected total stage 2 costs of such a decision can be calculated as the resulting evaluation of Equation 8.2.7, such that

$$\tilde{F}_{T,2,\theta} = \tilde{F}_{T,2}(\mathbf{d}_{2|\theta}|\mathbf{d}_{1,\theta}, \boldsymbol{\psi}_{2,\theta}) \tag{8.2.8}$$

is the estimate of expected total costs that arise in stage 2 based on decision $\mathbf{d}_{1,\theta}$ being made in stage 1, $\boldsymbol{\psi}_{2,\theta}$ being observed in stage 2 and the estimated optimal decision $\mathbf{d}_{2|\theta}$ being made in stage 2.

The estimates of expected total stage 2 costs, $\tilde{F}_{T,2,\theta}$, for the N_θ sampled values of stage 1 decision, $\mathbf{d}_{1,\theta}$, and stage 2 scenario, $\boldsymbol{\psi}_{2,\theta}$, can then be used as a set of N_θ training runs used to fit an emulator model, $\tilde{G}_{T,2,\boldsymbol{\psi}_2}(\mathbf{d}_1, \boldsymbol{\psi}_2)$, which models how expected total costs in stage 2 vary as a function of stage 1 decision, $\mathbf{d}_1$, and stage 2 scenario, $\boldsymbol{\psi}_2$, only.

If $p_{\boldsymbol{\psi}_{2|1}}(\boldsymbol{\psi}_2)$ represents the prior beliefs in stage 1 about the value of $\boldsymbol{\psi}_2$ being observed at the time the second decision is to be made, the expected total costs in stage 2 as a function of the stage 1 decision only can be calculated as

$$\tilde{G}_{T,2}(\mathbf{d}_1) = \int_{\boldsymbol{\psi}_2} \tilde{G}_{T,2,\boldsymbol{\psi}_2}(\mathbf{d}_1, \boldsymbol{\psi}_2) \times p_{\boldsymbol{\psi}_{2|1}}(\boldsymbol{\psi}_2) \mathrm{d}\boldsymbol{\psi}_2 \tag{8.2.9}$$

Estimating Expected Total Costs Across Both Stages as a Function of Stage 1 Decision Only

An estimate of expected mean constraint costs in the first stage when reinforcement decision $\mathbf{d}_1$ is made in the first stage can be calculated as

$$\tilde{F}_{c,1}(\mathbf{d}_1) = \int_{\mathbf{v}_1} \tilde{f}_{c,1}(\mathbf{v}_1, \mathbf{d}_1) \times p(\mathbf{v}_1) \mathrm{d}\mathbf{v}_1 \tag{8.2.10}$$

where $\tilde{f}_{c,1}(\mathbf{v}_1, \mathbf{d}_1)$ is the emulator model which approximates the simulator of stage 1 constraint costs and $p(\mathbf{v}_1)$ represents prior beliefs about the variables which contain

uncertainty in stage 1.

An estimate of expected total costs across both stages when decision $\mathbf{d}_1$ is made in stage 1 (i.e. expected mean constraint costs plus reinforcement costs in stage 1 plus expected total costs in stage 2) can then be acquired as

$$\tilde{G}_T(\mathbf{d}_1) = \tilde{F}_{c,1}(\mathbf{d}_1) + f_{\rho,1}(\mathbf{d}_1) + \tilde{G}_{T,2}(\mathbf{d}_1) \tag{8.2.11}$$

where $f_{\rho,1}(\mathbf{d}_1)$ are the reinforcement costs of making decision $\mathbf{d}_1$ in stage 1.

The decision which minimises Equation 8.2.11 is thus the estimate for the optimal decision to be made in stage 1.

In a real application, after making the first decision, $\mathbf{d}_1$, a given number of years will pass and the second decision, $\mathbf{d}_2$, must be made. At this time $\mathbf{d}_1$ will be known and it is assumed $\boldsymbol{\psi}_2$ will have been observed. This problem can then be treated as a single stage decision problem and an estimate for the optimal decision to be made in the second stage can be acquired using the methodology of Sections 5.2 and 6.2.

8.2.5 Uncertainty in The Estimates of Expected Total Costs and a Wave Process for Eliminating Decisions from Consideration

Just as in the case of decision making in a single stage, the fitted emulator models are not perfect approximations to the simulators. Section 5.2.6 detailed how variation in the parameters of the fitted emulator model can be used to form credible intervals for estimated costs, which could then be used to fit a more accurate emulator model over a smaller range of decisions using the methodology of Section 6.2.1.

In the multi-stage setting, the estimate of expected total costs depending on the first decision only is dependent on three models: the calculation of reinforcement costs for a given stage 1 decision, $f_{\rho,1}(\mathbf{d}_1)$; the estimate of expected mean constraint costs under uncertainty in stage 1 for a given stage 1 decision, $\tilde{F}_{c,1}(\mathbf{d}_1)$, and the estimate of expected total costs beyond the first stage for a given stage 1 decision, $\tilde{G}_{T,2}(\mathbf{d}_1)$. $f_{\rho,1}(\mathbf{d}_1)$ is modelled deterministically and consequently it is assumed to have no error. An estimate

for the error in $\tilde{F}_{c,1}(\mathbf{d}_1)$ can be acquired using the methodology of Section 5.2.6 (as will be detailed later in this section).

However, $\tilde{G}_{T,2,\boldsymbol{\psi}_2}(\mathbf{d}_1, \boldsymbol{\psi}_2)$ (which is used to evaluate $\tilde{G}_{T,2}(\mathbf{d}_1)$ via Equation 8.2.9) was fitted by identifying the optimal decision to be made in stage 2 for a sample of N_θ stage 2 scenarios and stage 1 decisions. This means that the fitted model is dependent on both the estimates for optimal stage 2 decisions for each scenario, $\mathbf{d}_{2|\theta}$, and the resulting estimates of expected total costs in stage 2 when making such decisions, $\tilde{F}_{T,2,\theta}$, both of which contain error.

It would be an extremely expensive procedure to reduce the error in $\mathbf{d}_{2|\theta}$, as this would require N_θ separate wave processes to be performed within each stage 1 wave to fit the emulator model for stage 2 constraint costs over a smaller range of decisions, and performing the process just once is an expensive procedure. Further, this would be even worse for a general M stage problem, which would require a total of $\sum_{m=2}^{M} N_{\theta_m}$ separate wave processes to be performed within each stage 1 wave. For the resources we have available to us for this thesis this is not feasible, though in practice for a company such as National Grid it may be necessary if $\mathbf{d}_{2|\theta}$ contains great error. The accuracy of the estimated optimal stage 2 decisions, $\mathbf{d}_{2|\theta}$, and corresponding estimates of expected costs will be considered later in Section 8.7.

However, the error in the resulting estimates' expected total costs for such decisions, $\tilde{F}_{T,2,\theta}$, can be accounted for by considering how the value of $\tilde{F}_{T,2,\theta}$ varies as the fitted emulator model of stage 2 constraint costs, $\tilde{f}_{c,2}(\mathbf{v}_2, \mathbf{d}_2|\mathbf{d}_1)$, is varied. This can then be used to model the error in $\tilde{G}_{T,2}(\mathbf{d}_1)$.

8.2.6 Forming Credible Intervals for Expected Total Costs Across Both Stages

Estimating Credible Bounds for the Expected Total Costs in Stage 2

To estimate the uncertainty in $\tilde{G}_T(\mathbf{d}_1)$, first, the methodology of Section 5.2.6 is adapted to model the variation in $\tilde{G}_{T,2}(\mathbf{d}_1)$. As is outlined in Section 5.2.6, this is achieved by considering how the estimated response of the emulator varies as the

model parameters of the emulator are varied. As a very brief recap, model parameters for the polynomial portion of the emulator are modelled as following a normal distribution with mean $\hat{\boldsymbol{\beta}}$ and covariance matrix $cov(\hat{\boldsymbol{\beta}})$. Random variations of these model parameters, $\hat{\boldsymbol{\beta}}_r$, can be drawn from this normal distribution and a new Gaussian process model fitted to smooth the resulting residuals of the polynomial portion of the emulator when using $\hat{\boldsymbol{\beta}}_r$ instead of $\hat{\boldsymbol{\beta}}$. $\tilde{f}_{c,2,r}(\mathbf{v}_2, \mathbf{d}_2|\mathbf{d}_1)$ can then be used as a randomly drawn variation of $\tilde{f}_{c,2}(\mathbf{v}_2, \mathbf{d}_2|\mathbf{d}_1)$ when using $\hat{\boldsymbol{\beta}}_r$ as the parameters of the polynomial portion of the emulator and the resulting Gaussian process model.

These randomly drawn models can then be used in Equation 8.2.7 to randomly draw estimates for $\tilde{F}_{T,2,\theta}$ (the estimated expected total costs in stage 2 when making the estimated optimal stage 2 decision, $\mathbf{d}_{2|\theta}$, in stage 2 given that reinforcement decision $\mathbf{d}_{1,\theta}$ was previously made in stage 1 and that scenario $\boldsymbol{\psi}_{2,\theta}$ is observed when the second decision is made) as

$$\tilde{F}_{T,2,\theta,r} = \tilde{F}_{c,2,r}(\mathbf{d}_{2|\theta}|\mathbf{d}_{1,\theta}, \boldsymbol{\psi}_{2,\theta}) + f_{\rho,2}(\mathbf{d}_{2|\theta}|\mathbf{d}_{1,\theta}, \boldsymbol{\psi}_{2,\theta}) \tag{8.2.12}$$

where

$$\tilde{F}_{c,2,r}(\mathbf{d}_{2|\theta}|\mathbf{d}_{1,\theta}, \boldsymbol{\psi}_{2,\theta}) = \int_{\mathbf{v}_2} \tilde{f}_{c,2,r}(\mathbf{v}_2, \mathbf{d}_{2|\theta}|\mathbf{d}_{1,\theta}) \times p(\mathbf{v}_2|\boldsymbol{\psi}_{2,\theta}) \mathrm{d}\mathbf{v}_2 \tag{8.2.13}$$

Credible intervals for $\tilde{F}_{T,2,\theta}$ can then be estimated using the methodology of Section 5.2.6, such that if an $\alpha\%$ credible interval is desired a lower bound is formed as the value which $\frac{100-\alpha}{2}\%$ of the $\tilde{F}_{T,2,\theta,r}$ are smaller than, and the upper bound as the value which $\frac{100-\alpha}{2}\%$ of the $\tilde{F}_{T,2,\theta,r}$ are greater than. $\tilde{F}_{T,2,\theta,L}$ and $\tilde{F}_{T,2,\theta,U}$ are used to denote the lower and upper bounds respectively.

In Section 8.2.4 the values of $\tilde{F}_{T,2,\theta}$ were used as a set of N_θ training runs to fit an emulator model, $\tilde{G}_{T,2,\boldsymbol{\psi}_2}(\mathbf{d}_1, \boldsymbol{\psi}_2)$, of how expected total costs in stage 2 vary as a function of the first stage decision, $\mathbf{d}_1$, and stage 2 scenario, $\boldsymbol{\psi}_2$, only. Similarly, the values of $\tilde{F}_{T,2,\theta,L}$ and $\tilde{F}_{T,2,\theta,U}$ can be used as two sets of N_θ training runs which can be used to fit respective emulator models of how lower and upper bounds of the expected total costs in stage 2 vary as a function of $\mathbf{d}_1$ and $\boldsymbol{\psi}_2$ only, such that $\tilde{G}_{T,2,\boldsymbol{\psi}_2,L}(\mathbf{d}_1, \boldsymbol{\psi}_2)$ and $\tilde{G}_{T,2,\boldsymbol{\psi}_2,U}(\mathbf{d}_1, \boldsymbol{\psi}_2)$ represent the fitted emulator models which act as lower and upper bounds respectively for $\tilde{G}_{T,2,\boldsymbol{\psi}_2}(\mathbf{d}_1, \boldsymbol{\psi}_2)$.

Estimating Credible Bounds for the Expected Total Costs in Both Stages as a Function of Stage 1 Decision

Estimates of lower and upper bounds for the expected total costs in stage 2 as a function of stage 1 decision only can then be calculated as

$$\tilde{G}_{T,2,L}(\mathbf{d}_1) = \int_{\boldsymbol{\psi}_2} \tilde{G}_{T,2,\boldsymbol{\psi}_2,L}(\mathbf{d}_1, \boldsymbol{\psi}_2) \times p_{\boldsymbol{\psi}_{2|1}}(\boldsymbol{\psi}_2) \mathrm{d}\boldsymbol{\psi}_2 \tag{8.2.14}$$

and

$$\tilde{G}_{T,2,U}(\mathbf{d}_1) = \int_{\boldsymbol{\psi}_2} \tilde{G}_{T,2,\boldsymbol{\psi}_2,U}(\mathbf{d}_1, \boldsymbol{\psi}_2) \times p_{\boldsymbol{\psi}_{2|1}}(\boldsymbol{\psi}_2) \mathrm{d}\boldsymbol{\psi}_2 \tag{8.2.15}$$

Further, the emulator used to approximate the simulator in stage 1, $\tilde{f}_{c,1}(\mathbf{v}_1, \mathbf{d}_1)$, contains error. This can be handled in the same manner as in Section 5.2.6, where the model parameters of $\tilde{f}_{c,1}(\mathbf{v}_1, \mathbf{d}_1)$ are randomly varied such that $\tilde{f}_{c,1,r}(\mathbf{v}_1, \mathbf{d}_1)$ represents a random drawing of $\tilde{f}_{c,1}(\mathbf{v}_1, \mathbf{d}_1)$. $\tilde{f}_{c,1,r}(\mathbf{v}_1, \mathbf{d}_1)$ can then be used to estimate expected mean constraint costs under uncertainty in stage 1 as

$$\tilde{F}_{c,1,r}(\mathbf{d}_1) = \int_{\mathbf{v}_1} \tilde{f}_{c,1,r}(\mathbf{v}_1, \mathbf{d}_1) \times p(\mathbf{v}_1) \mathrm{d}\mathbf{v}_1 \tag{8.2.16}$$

Random variations for the costs that occur across stage 1 and stage 2, when fitting a lower bound for the estimated stage 2 total costs, can be estimated as

$$\tilde{G}_{T,L,r}(\mathbf{d}_1) = \tilde{F}_{c,1,r}(\mathbf{d}_1) + f_{\rho,1}(\mathbf{d}_1) + \tilde{G}_{T,2,L}(\mathbf{d}_1) \tag{8.2.17}$$

whilst random variations for the costs that occur across stage 1 and stage 2, when fitting an upper bound for the estimated stage 2 total costs, can be estimated as

$$\tilde{G}_{T,U,r}(\mathbf{d}_1) = \tilde{F}_{c,1,r}(\mathbf{d}_1) + f_{\rho,1}(\mathbf{d}_1) + \tilde{G}_{T,2,U}(\mathbf{d}_1) \tag{8.2.18}$$

Credible intervals can then be estimated for $\tilde{G}_T(\mathbf{d}_1)$ such that if an $\alpha\%$ credible interval is desired for $\tilde{G}_T(\mathbf{d}_1)$, a lower bound is formed as the value which $\frac{100-\alpha}{2}\%$ of the $\tilde{G}_{T,L,r}(\mathbf{d}_1)$ are smaller than, and the upper bound as the value which $\frac{100-\alpha}{2}\%$ of the $\tilde{G}_{T,U,r}(\mathbf{d}_1)$ are greater than. These lower and upper bounds are represented as $\tilde{G}_{T,L,L}(\mathbf{d}_1)$ and $\tilde{G}_{T,U,U}(\mathbf{d}_1)$ respectively.

This methodology for estimating credible bounds will be generalised to a general M stage problem in Section 9.1.4, with a further discussion of the methodology given in

Section 9.1.5.

8.2.7 Wave Process for Decision Making

Section 6.2.1 outlined a wave process to iteratively eliminate decisions from consideration for the single stage problem. This allows for a more accurate emulator model to be fitted over a smaller range of values for the decision variables. This can be adapted to the multi-stage problem, where first stage decisions, $\mathbf{d}_1$, are iteratively eliminated from consideration in order to fit more accurate emulator models over a smaller range of decisions. This is summarised in the following algorithm:

1. Set an initial range of values to be considered for the decision variables in each stage (i.e. values of $\mathbf{d}_1$ and $\mathbf{d}_2$ in the 2 stage problem).

2. Simulate training runs based on a Latin hypercube (LHC) sample using the current limits on the decision variables.

3. Fit emulator models to the latest simulated samples and use them to eliminate decisions from consideration (details below).

4. Repeat until uncertainty about the optimal first stage decision (i.e. optimal choice of values for $\mathbf{d}_1$) reaches an acceptable level (such as when the range of values considered for the decision variables can be reduced no further or when the error in the estimate of expected total costs reaches a given level of precision). The estimate of the optimal decision is the decision which minimises Equation 8.2.11 (i.e. the stage 1 decision which minimises the estimate of expected total costs).

To do this, an LHC sample will be taken over a specified initial range of reinforcements to consider. This LHC sample gives the values of input variables to be used for the training data. Simulations are then taken using these input values to give the training data. Then, the emulation process of Section 5.2 is used to fit emulator models $\tilde{f}_{c,1}(\mathbf{v}_1, \mathbf{d}_1)$ and $\tilde{f}_{c,2}(\mathbf{v}_2, \mathbf{d}_2|\mathbf{d}_1)$ to model how simulator input affects output for the mean constraint costs in stage 1 and 2 respectively. These can in turn be used to form $\tilde{G}_T(\mathbf{d}_1)$ using the methodology of Section 8.2.4 to estimate expected total costs across both stages as a function of the first stage decision, $\mathbf{d}_1$, only.

The methodology of Section 8.2.6 can then be used to estimate corresponding credible intervals as the values of the decision variables are varied, such that if $\tilde{G}_T(\mathbf{d}_1)$ is the value of estimated expected total costs across both stages from Equation 8.2.11, $\tilde{G}_{T,L,L}(\mathbf{d}_1)$ would represent a lower bound of that estimate and $\tilde{G}_{T,U,U}(\mathbf{d}_1)$ would represent an upper bound for that estimate. The values of the decision variables which give the minimum value of $\tilde{G}_{T,U,U}(\mathbf{d}_1)$ are then identified as $\mathbf{d}_1^o = d_{1,1}^o, ..., d_{1,N_d}^o$, with the corresponding upper bound for expected total costs across both stages under uncertainty when making this decision being $\tilde{G}_{T,U,U}(\mathbf{d}_1^o)$. For any alternative set of decisions, $\mathbf{d}_1^a = d_{1,1}^a, ..., d_{1,N_d}^a$, such that $\tilde{G}_{T,L,L}(\mathbf{d}_1^a) > \tilde{G}_{T,U,U}(\mathbf{d}_1^o)$ it can be said that there is evidence against that decision being optimal, as the lower bound of the estimate is greater than the minimum upper bound. That decision can thus be eliminated from the decision space considered.

A new set of training runs is taken where the values of the decision variables are only those not eliminated. As was the case in Section 6.2.1, this space will not necessarily form a hypercube, so the methodology of Section 6.2.2 is used to sample values of first stage decision variables, $\mathbf{d}_1$, to be used for training runs beyond the first wave. A new emulator model is then fitted to this new set of training runs, and credible intervals are estimated for decisions which were not previously ruled out. This allows for further poor decisions to be identified and eliminated. The process continues iteratively until the uncertainty about the optimal decision reaches an acceptable level (such as when the range of values considered for the decision variables can be reduced no further or when the error in the estimate of expected total costs reaches a given level of precision).

Note, as part of this methodology the range of values considered for the second stage decision, $\mathbf{d}_2$, is not directly reduced. However, values of $\mathbf{d}_2$ considered are indirectly reduced, as the emulator model for mean constraint costs in the second wave, $\tilde{f}_{c,2}(\mathbf{v}_2, \mathbf{d}_2|\mathbf{d}_1)$, only needs to consider decisions, $\mathbf{d}_2$, which are possible for any stage 1 decision, $\mathbf{d}_1$, still considered in the current wave.

For the examples presented in this thesis it is noted that the simulator of mean constraint costs in stage 2, $f_{c,2}(\mathbf{v}_2, \mathbf{d}_2|\mathbf{d}_1)$, is dependent on the total reinforcement after the second decision, i.e. $\mathbf{d}_{T_2} = \mathbf{d}_1 + \mathbf{d}_2$, and not the individual reinforcements in stages 1 and 2. For example, if 4000 MW of total B6 reinforcement is built after the second

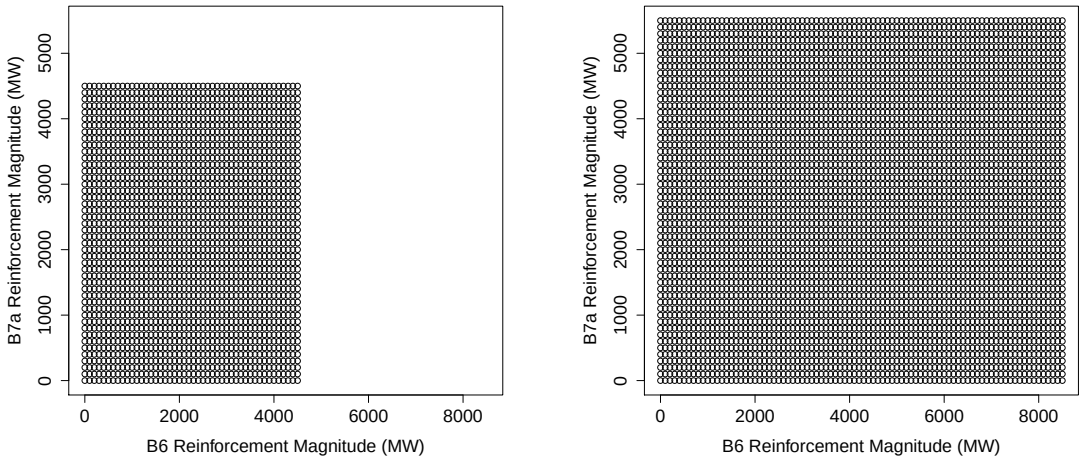

(a) Values of $\mathbf{d}_1$ considered in wave 1.

(b) Values of $\mathbf{d}_{T_2}$ considered in wave 1.

Figure 8.1: Plots to illustrate values of $\mathbf{d}_1$ and $\mathbf{d}_{T_2}$ considered in the first wave.

decision, the simulator would not distinguish between 1000 MW being built in stage 1 and 3000 MW in stage 2 or 3000 MW in stage 1 and 1000 MW in stage 2 (or any other combination of reinforcements which result in a total of 4000 MW after the second decision). Therefore, the range of decisions considered in the second stage are considered in terms of $\mathbf{d}_{T_2}$.

All values of $\mathbf{d}_{T_2}$ considered should be at least as large as the values considered for $\mathbf{d}_1$ (as the total reinforcement in stage 2 will be at least as large as the smallest possible reinforcement in stage 1), which indirectly reduces the range of values the emulator to estimate mean constraint costs in the second stage, $\tilde{f}_{c,2}$, is fitted over. For example, if all values of $\mathbf{d}_1$ in the second wave consider making at least 1000 MW B6 reinforcement, all values of $\mathbf{d}_{T_2}$ should consider a total of at least 1000 MW B6 reinforcement after the second decision.

This is illustrated in Figures 8.1 and 8.2. Figure 8.1 shows the values of $\mathbf{d}_1$ and $\mathbf{d}_{T_2}$ initially considered in the first wave, which are 0 to 4500 MW B6 and 0 to 4500 MW B7a reinforcement in stage 1 and 0 to 8500 MW B6 and 0 to 5500 MW B7a total reinforcement after stage 2. These are the values that will actually be considered for the example which will be detailed in Section 8.3.

Figure 8.2 (a) illustrates the values of $\mathbf{d}_1$ considered in the second wave using the methodology of this section. These decisions consider a minimum of 2000 MW B6

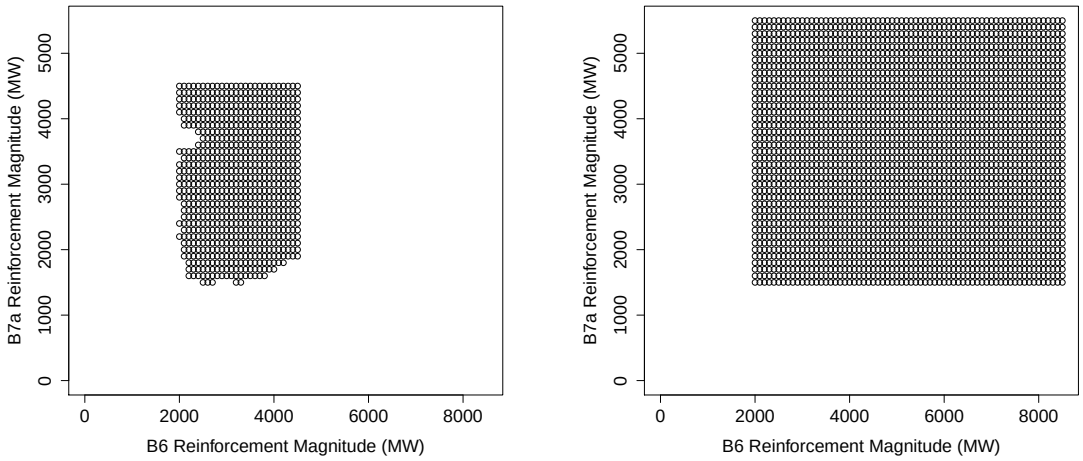

(a) Values of $\mathbf{d}_1$ considered in wave 2.

(b) Values of $\mathbf{d}_{T_2}$ considered in wave 2.

Figure 8.2: Plots to illustrate values of $\mathbf{d}_1$ and $\mathbf{d}_{T_2}$ considered in the second wave.

and a minimum of 1500 MW B7a reinforcement. Therefore, in the second wave, only values of total reinforcements of at least 2000 MW B6 and 1500 MW B7a in the second stage (values of $\mathbf{d}_{T_2}$) need to be considered, as at least that much reinforcement will be made in the first stage. An appropriate set of values of $\mathbf{d}_{T_2}$ to therefore consider in the second wave is illustrated in Figure 8.2 (b). This has eliminated 44% of the values of $\mathbf{d}_{T_2}$ initially considered in the first wave.

8.3 Details of a Two Stage Transmission Expansion Planning Problem

An initial application will present the methodology of Sections 8.2.4 and 8.2.6 applied to an example which considers making 2 sequential decisions over a 25 year period. This example will be an extension of the example detailed in Section 6.1.1 to a multi-stage setting. As in Section 6.1.1, uncertainty will be considered in three variables (nuclear availability probability, CCGT availability probability and peak demand level) and two decision variables will be considered at each stage (increasing the transfer capacity of the B6 and B7a boundaries). A comparison to the corresponding problem that only allows for a single investment opportunity is given in Section 8.6.

8.3.1 Time Frame of Problem

For the problem considered, the first decision will be made at the beginning of year 1 and the reinforcement made will be available at the beginning of year 6. The second decision will be made at the beginning of year 11 and the reinforcement made will be available at the beginning of year 16. This is summarised in Table 8.1.

Decision	Time Decision is Made	Time Reinforcement is Available
First Decision	Beginning of Year 1	Beginning of Year 6
Second Decision	Beginning of Year 11	Beginning of Year 16

Table 8.1: Table of when decisions are made and when the resulting reinforcement becomes available.

The cost of the first reinforcement and the cost of the second reinforcement represent the reinforcement costs of the first and second stage respectively. Constraint costs for the first stage are the constraint costs of the power system between years 6 and 15 and constraint costs for the second stage are the constraint costs of the power system between the years 16 and 25 (as these are the years which are directly affected by the first and second decisions respectively). For the example presented, constraint costs do not need to be calculated for years 1 to 5 as they will be the same regardless of what decision was made in year 1 (as the reinforcement is not available until year 6). However, in a real-world application the system would still be observed during this period in order to learn about the variables which contain uncertainty over this period, and reduce uncertainty as much as possible by the time the second decision is to be made.

At each decision stage, it is assumed that two decisions are to be made, namely the reinforcement magnitude (increase in transfer capacity) of the B6 and B7a boundaries. Therefore, $\mathbf{d}_1 = (d_{1,1}, d_{1,2})$ and $\mathbf{d}_2 = (d_{2,1}, d_{2,2})$ where $d_{m,1}$ represents B6 reinforcement magnitude in stage m and $d_{m,2}$ represents B7a reinforcement magnitude in stage m.

Initially this thesis will follow the methodology of [97, 66, 81] where the power system of year 6 (i.e. peak demand level, installed generators, availability probability of generators etc.) is assumed to be representative of the power system for the entirety of the first stage (i.e. the period between year 6 and year 15) and the power system of year

16 is assumed to be representative of the power system for the entirety of the second stage (i.e. the period between year 16 and year 25).

8.3.2 Assumed Cost of Reinforcement

As was the case in Chapters 5 and 6, it will initially be assumed that it costs £1000 per MW per km to reinforce each boundary [78, 5]. For the 2 stage problem detailed in this section it is assumed that all reinforcement costs are incurred at the time each decision is made. That is, it is assumed that the reinforcement costs of the first decision are incurred at the beginning of year 1 and the reinforcement costs of the second decision are incurred at the beginning of year 11.

This is consistent with how costs are modelled when assuming a fixed capital cost, such as £1000 per MW per km, to reinforce [78, 5, 70, 95], though reinforcement costs could alternatively be modelled as annualised costs, with an annual payment to be made at the beginning of each year over a given period of time.

8.3.3 Uncertainties

Stage 1 Uncertainties

In both stages, uncertainty will be considered in three variables: peak demand level, nuclear availability probability and CCGT availability probability. These three variables make up $\mathbf{v}_1$ and $\mathbf{v}_2$, i.e. $\mathbf{v}_1 = (v_{1,1}, v_{1,2}, v_{1,3})$ and $\mathbf{v}_2 = (v_{2,1}, v_{2,2}, v_{2,3})$, where $v_{m,1}$ represents nuclear availability probability in stage m, $v_{m,2}$ represents CCGT availability probability in stage m and $v_{m,3}$ represents peak demand level in stage m.

At year 1 there will be prior beliefs about the values these variables take. Nuclear availability probability is supposed to have a value between 0.55 and 0.85 and CCGT availability probability is supposed to have a value between 0.8 and 0.95. [69] has been used throughout this thesis to give projections of values for many aspects of the future power system, one of which is peak demand level over a 20 year period. Peak demand in stage 1 is supposed to have a value between 95% and 105% of the projected year 6 peak demand level from [69] and peak demand in stage 2 is supposed to have

a value between 85% and 115% of the projected year 16 peak demand level from [69]. This is summarised in Table 8.2. The range of 85% to 115% is an extrapolation from our interpretation of the expert judgement as outlined in Section 6.1.1, where an appropriate level of uncertainty in future peak demand was modelled as +/-1% uncertainty for each future year of projection in peak demand level. As the problem considers starting in year 1, and stage 2 constraint costs are modelled based on a year 16 power system background (15 years in the future) a range of +/- 15% is appropriate.

Variable	Lower Limit of Beliefs	Upper Limit of Beliefs
Stage 1 Nuclear Availability Probability	0.55	0.85
Stage 1 CCGT Availability Probability	0.8	0.95
Stage 1 Peak Demand Level	95%	105%
Stage 2 Nuclear Availability Probability	0.55	0.85
Stage 2 CCGT Availability Probability	0.8	0.95
Stage 2 Peak Demand Level	85%	115%

Table 8.2: Table summarising the beliefs about the uncertain variables in year 1.

It is also necessary to specify a distribution to describe prior beliefs about the values the variables take across these ranges. In stage 1 a uniform distribution is fitted between the lower and upper limits for the values of nuclear availability probability, CCGT availability probability and year 6 peak demand level detailed in Table 8.2. That is $p(\mathbf{v}_1)$ forms a uniform distribution, such that prior beliefs about nuclear availability probability in stage 1 form a uniform distribution between 0.55 and 0.85, prior beliefs about CCGT availability probability in stage 1 form a uniform distribution between 0.8 and 0.95 and prior beliefs for peak demand level in stage 1 form a uniform distribution between 95% and 105% of the projected year 6 peak demand level in [69]. These are equivalent to the prior beliefs about these uncertainties for the example detailed in Section 6.1.1, which also considered making a decision to minimise the expected total costs between years 6 and 15.

From the methodology of Section 8.2.4, an explicit specification for the beliefs about the values the uncertain variables take in stage 2 at the time the first decision is made is not required. Only prior beliefs about $\boldsymbol{\psi}_2$ (which describes the observed state of the power system at the time the second decision is made) is required, which can be used

to estimate total costs in stage 2 via Equation 8.2.9. $p_{\boldsymbol{\psi}_{2|1}}(\boldsymbol{\psi}_2)$, which will be specified in the next sub-subsection, could be used to calculate an explicit formula for the beliefs about the values of $\mathbf{v}_2$ at year 1 as

$$p(\mathbf{v}_2) = \int_{\boldsymbol{\psi}_2} p(\mathbf{v}_2|\boldsymbol{\psi}_2) p_{\boldsymbol{\psi}_{2|1}}(\boldsymbol{\psi}_2) \mathrm{d}\boldsymbol{\psi}_2 \tag{8.3.1}$$

but the explicit evaluation of Equation 8.3.1 is never required for the two stage problem.

It is further noted that the methodology of Section 8.2.4 does not even require ranges to be explicitly specified for $\mathbf{v}_2$ at the time the first decision is made, though these were earlier specified in Table 8.2 to illustrate the level of uncertainty considered in the future power system. However, $p(\mathbf{v}_2)$ will later be explicitly evaluated in Section 8.6.1, which will verify that the ranges for $\mathbf{v}_2$ detailed in Table 8.2 are consistent with the ranges that arise when explicitly evaluating $p(\mathbf{v}_2)$ via Equation 8.3.1.

Stage 2 Uncertainties

It is assumed that the state of the power system has been observed between year 1 and year 11 (between making the first and second decisions), and that information has been learnt about the variables which contain uncertainty. This information is quantified in $\boldsymbol{\psi}_2$.

For the introductory example, it will be assumed that nothing is learnt about the availability probabilities of nuclear and CCGT between years 1 and 11. This means that $p(v_{2,1}|\boldsymbol{\psi}_2)$ is a uniform distribution between 0.55 and 0.85 for all values of $\boldsymbol{\psi}_2$ and $p(v_{2,2}|\boldsymbol{\psi}_2)$ is a uniform distribution between 0.8 and 0.95 for all values of $\boldsymbol{\psi}_2$.

However, it will be assumed that information will be learnt about the peak demand level in year 16 between year 1 and year 11. To remain consistent with our interpretation of the expert judgement of Paul Plumptre [78], $\boldsymbol{\psi}_2$ will be used to represent the estimated expected level of peak demand in year 16, as a proportion of the year 16 peak demand level projected by [69], based on what has been observed about the power system when the second decision is to be made in year 11. For example, $\boldsymbol{\psi}_2 = 0.97$ would mean that the estimate of expected year 16 peak demand level at year 11 is 97% of the year 16 peak demand projected by [69].

This is then used to define a probability distribution to describe the prior beliefs about the possible values year 16 peak demand could take based on what has been observed by year 11 (i.e. to describe $p(v_{2,3}|\boldsymbol{\psi}_2)$) which is modelled as uniform distribution fitted between $(100\boldsymbol{\psi}_2 - 5)\%$ and $(100\boldsymbol{\psi}_2 + 5)\%$ of the year 16 peak demand level projected by [69]. This is consistent with our earlier interpretation of the expert judgement of Paul Plumptre [78] used in Section 6.1.1, as the second decision is made at the beginning of year 11 for the year 16 power system (5 years ahead) and the prior beliefs represent a uniform distribution across a +/-5% range. Again, it is stressed that this is our interpretation of what was discussed in meetings with Paul Plumptre and in no way directly reflects the views of Paul Plumptre.

For example, if at year 11 it is believed that the expected value for peak demand level in year 16 is now 8% greater than the value projected by [69], $\boldsymbol{\psi}_2$ would take a value of 1.08, which would result in the beliefs about peak demand level in year 16 forming a uniform distribution across the range of 103% to 113% of the projection given by [69].

Prior beliefs about the value of $\boldsymbol{\psi}_2$ that will be observed in year 11 are required to estimate expected total costs in stage 2 at the time the first decision is to be made via Equation 8.2.9. For this example, $p_{\boldsymbol{\psi}_{2|1}}(\boldsymbol{\psi}_2)$ (the prior beliefs at the beginning of year 1 about the value of $\boldsymbol{\psi}_2$ that will be observed in year 11) is taken to be a uniform distribution between 0.9 and 1.1.

8.3.4 Assumed Discount Rate of Future Costs

For the examples of Chapters 5 and 6, the effect of discounting future costs was ignored when decision making (i.e. results were equivalent to using a discount rate of 0%). Even for these single stage examples, the simplification of ignoring the discounting of future costs would have an effect on decision made, as the present value of future constraint costs would be reduced. This in turn would reduce the benefit from building reinforcements and result in an estimated optimal reinforcement decision of lower magnitude.

The effect is potentially even greater for a multi-stage example, where a greater discount rate may give more incentive to postpone part (or all) of a reinforcement to nearer the

time the system will benefit from such a reinforcement, whereas a lower discount rate may encourage the majority of a reinforcement to be built earlier.

Within the multi-stage transmission expansion planning literature a discount rate of 5% is common [2, 26, 3, 80]. However, a discount rate of 10% (which increases the discounting effect) is also common [30, 85, 62]. Initially, a discount rate of 5% will be assumed. However, the effect of the assumed discount rate will later be considered in Chapter 9, where results will be presented for how cost estimates and the resulting estimates of optimal decisions vary if the higher discount rate of 10% is assumed instead, as well as comparing results to an example which assumes a low discount rate of 1%.

8.4 Stage 1 Decision

8.4.1 Fitted Emulator Models

In order to present results for the example of Section 8.3, emulator models must be fitted to approximate the simulator to estimate stage 1 mean constraint costs, stage 2 mean constraint costs and total stage 2 costs as a function of the stage 1 decision only. As is detailed in Section 5.2, the emulators used in this thesis take a small number of training run evaluations from the simulator, then use a polynomial regression model with a Gaussian process smoother applied to the residuals of the polynomial regression model to approximate how input affects output of the simulator.

As was demonstrated in Sections 5.3.3 and 6.1.3, the number of training runs to use and the terms to include in the polynomial regression portion of the emulator model must be carefully considered for each example, and are selected based on the values of R^2 (a measure of how well the model fits the training data) and P (a measure of how well the model predicts a response for simulator evaluations not used to fit the emulator) of the resulting emulator model. Further, Sections 5.3.3 and 5.3.5 of Chapter 5 and Section 6.1.3 of Chapter 6 also gave graphical comparisons of estimates of costs from the fitted emulator models, and the corresponding credible intervals, to calculations of costs from the simulator.

As the fitting of emulator models was covered in quite a bit of detail in

Sections 5.3.3 and 5.3.5 of Chapter 5 and Section 6.1.3 of Chapter 6, this section gives a brief overview of the details of the emulator models fitted to avoid substantial repetition and to concentrate on presenting the application of the methodology of Section 8.2.4 to the two stage planning problem detailed in Section 8.3. However, further details of how appropriate terms to include in the polynomial portion of the model and number of training runs used to fit the emulator are given in Appendix C.3. As a brief overview, the results of this model selection were that the emulator model which approximates the simulator calculation of mean constraint costs in the first stage, $\tilde{f}_{c,1}(\mathbf{v}_1, \mathbf{d}_1)$, is fitted using 300 training runs, and the polynomial portion of the emulator model takes the form

$$\beta_0 + \beta_1 v_{1,1} + \beta_2 v_{1,2} + \beta_3 v_{1,3} + \beta_4 d_{1,1} + \beta_5 d_{1,2} + \beta_6 v_{1,1}^2 + \beta_7 v_{1,2}^2 + \beta_8 v_{1,3}^2 + \beta_9 d_{1,1}^2 + \beta_{10} d_{1,2}^2 + \beta_{11} v_{1,1} d_{1,1} + \beta_{12} v_{1,1} d_{1,2} + \beta_{13} d_{1,1} d_{1,2} + \beta_{14} v_{1,1}^2 d_{1,1}^2 + \beta_{15} v_{1,1}^2 d_{1,2}^2 + \beta_{16} d_{1,1}^2 d_{1,2}^2 + \beta_{17} v_{1,1} d_{1,1} d_{1,2} + \beta_{18} v_{1,1}^2 d_{1,1}^2 d_{1,2}^2$$

The R^2 of the polynomial portion of the emulator model is 0.972. A Gaussian process model is then used to smooth the residuals of this polynomial regression model. The emulator model which approximates the simulator calculation of mean constraint costs in the second stage, $\tilde{f}_{c,2}(\mathbf{v}_2, \mathbf{d}_2|\mathbf{d}_1)$, is fitted using 300 training runs, and the polynomial potion of the emulator model takes the form

$$\beta_0 + \beta_1 v_{2,1} + \beta_2 v_{2,2} + \beta_3 v_{2,3} + \beta_4 d_{T_2,1} + \beta_5 d_{T_2,2} + \beta_6 v_{2,1}^2 + \beta_7 v_{2,2}^2 + \beta_8 v_{2,3}^2 + \beta_9 d_{T_2,1}^2 + \beta_{10} d_{T_2,2}^2$$

The R^2 of the polynomial portion of the emulator model is 0.968. A Gaussian process model is then used to smooth the residuals of this polynomial regression model. The emulator model for expected total stage 2 costs as a function of stage 1 decision and stage 2 scenario only, $\tilde{G}_{T,2,\boldsymbol{\psi}_2}(\mathbf{d}_1, \boldsymbol{\psi}_2)$, is fitted using 50 training runs and the polynomial portion of the emulator model takes the form

$$\beta_0 + \beta_1 \boldsymbol{\psi}_2 + \beta_2 d_{1,1} + \beta_3 d_{1,2} + \beta_4 \boldsymbol{\psi}_2^2 + \beta_5 d_{1,1}^2 + \beta_6 d_{1,2}^2$$

The R^2 of the polynomial portion of the emulator model is 0.995. A Gaussian process model is then used to smooth the residuals of this polynomial regression model. Again, further details on how each of these emulator models were fitted are given in Appendix C.3.

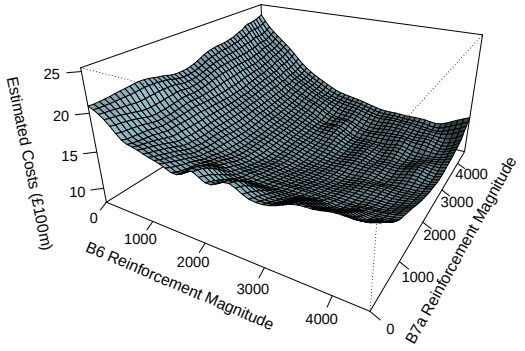

Figure 8.3: Plot to illustrate how estimates of expected total costs across both stages vary with B6 reinforcement magnitude and B7a reinforcement magnitude in the first wave of stage 1.

8.4.2 Estimates of Expected Total Costs Across Both Stages as a Function of Stage 1 Decision

Figure 8.3 shows how estimates of expected total costs vary with stage 1 B6 and B7a reinforcement magnitude for the example outlined in Section 8.3.3, using the methodology of Section 8.2.4 to estimate expected total costs across both stages. However, just as for the single stage example of Chapter 6, the emulators used to estimate total costs are not perfect approximations to the simulators, and therefore the estimates of expected total costs displayed in Figure 8.3 contain error. Credible bounds for the estimates of expected total costs of Figure 8.3 were therefore calculated using the methodology of Section 8.2.6 and are illustrated in Figure 8.4. These credible bounds are in turn used to apply the wave process of Section 8.2.7 to eliminate decisions from consideration which have evidence against them being optimal in order to fit a more accurate emulator model over a smaller range of decisions.

Figure 8.5 illustrates the decisions considered in the second, third and fourth waves and shows how after 3 waves of elimination quite a small region where the optimal stage 1 decision could potentially lie has been identified. The first wave of elimination eliminated 64.9% of the decisions initially considered, with the second wave of elimination eliminating 58.9% of what remained after the first wave and a third wave of

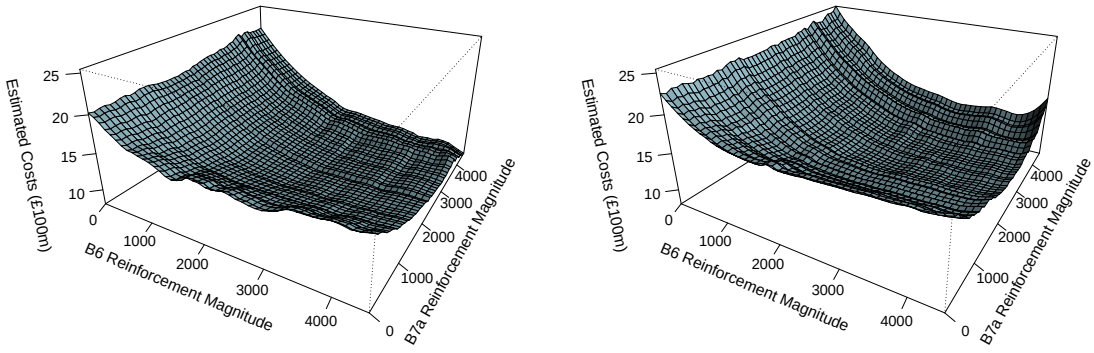

(a) Lower Bound. (b) Upper Bound.

Figure 8.4: Plots to show credible bounds for the estimates of expected total costs from the emulator models fitted in the first wave.

elimination eliminating 44.2% of what remained remained after the second wave.

However, there was negligible elimination of the decisions considered beyond this. The reason a negligible number of values for the decision variables were eliminated beyond the fourth wave is the estimates of expected total costs from the emulators fitted in the fourth wave are relatively flat over the region illustrated in Figure 8.5 (c) in the sense that the variation in the estimates of expected total costs as the values of the stage 1 decision variables are varied is relatively small. Therefore, even though the credible bounds of the estimate from the emulator model fitted in the fourth wave are also narrow over this region, there is insufficient evidence to eliminate any further decisions as potentially optimal stage 1 decisions, as will be demonstrated in the remainder of this section.

Figure 8.6 displays how estimated expected total costs across both stages vary with stage 1 B6 and B7a reinforcement magnitude in each wave. However, as in the example of Chapter 6, the total costs estimated are much greater when little to no reinforcement has been made in comparison to when substantial reinforcement has been made, making the wave 4 plot appear very flat in comparison.

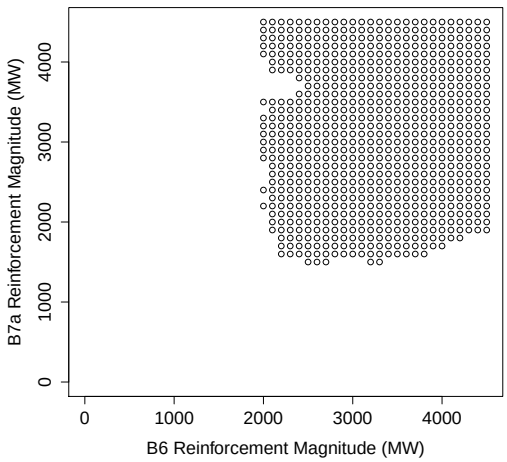

(a) Wave 2.

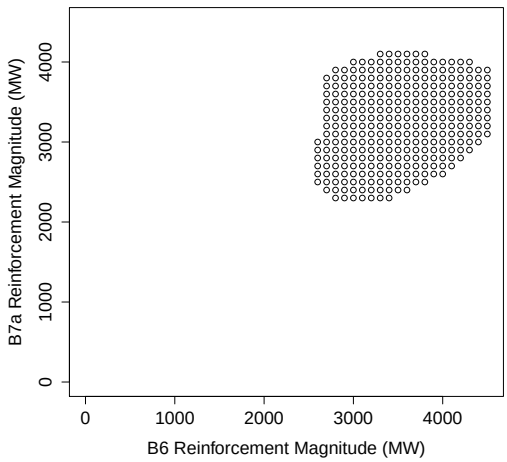

(b) Wave 3.

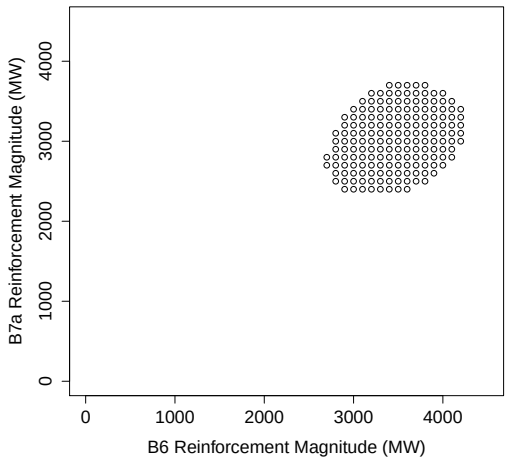

(c) Wave 4.

Figure 8.5: Plots to show decisions not eliminated from consideration in the second, third and fourth waves.

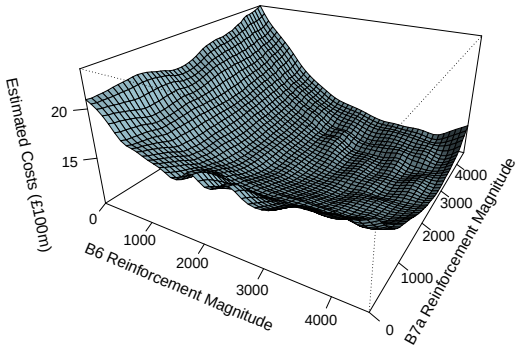

(a) Wave 1.

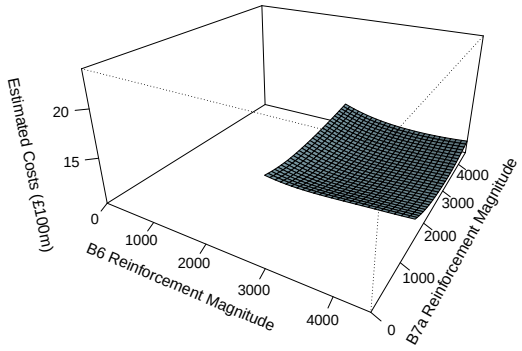

(b) Wave 2.

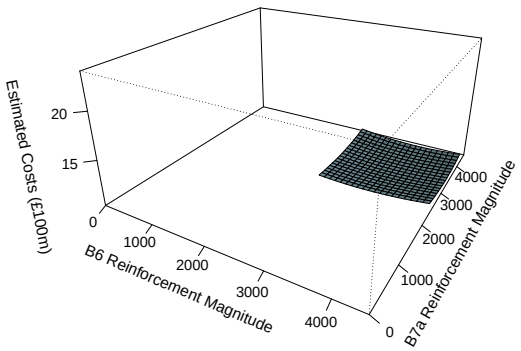

(c) Wave 3.

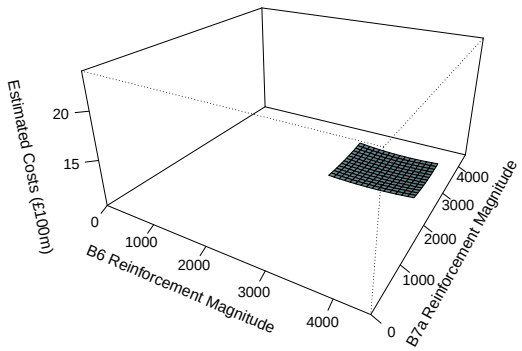

(d) Wave 4.

Figure 8.6: Plots to show how estimates of expected total costs across both stages vary with stage 1 reinforcement decisions and fitted emulator model.

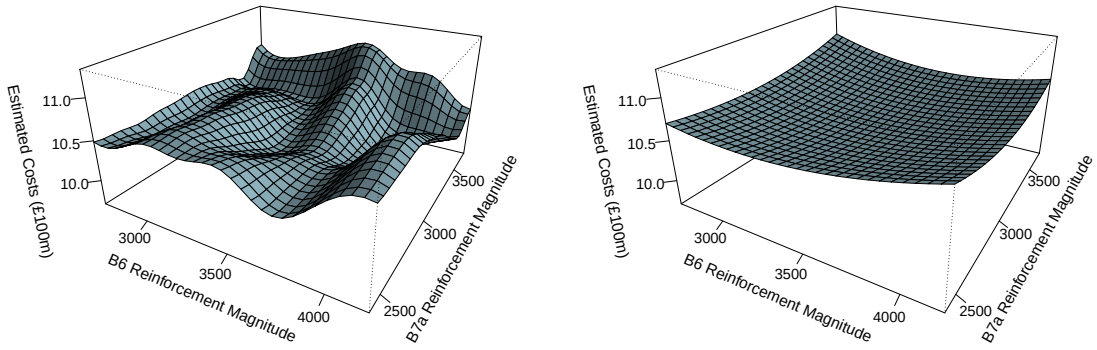

(a) Wave 1.

(b) Wave 4.

Figure 8.7: Plots to show how estimates of expected total costs across both stages vary with stage 1 reinforcement decisions and fitted emulator model.

8.4.3 Comparison of Cost Estimates in the First and Final Wave

As Figure 8.6 shows that cost estimates are much flatter in the fourth wave in comparison to the first, Figure 8.7 was therefore created, which compares the estimates of expected total costs from the wave 1 and wave 4 emulator models over the range of decisions considered in the fourth wave. As was the case in Section 6.3, the models fitted in wave 4 result in a smoother variation in estimates of expected total costs as the B6 and B7a reinforcement magnitudes are varied in comparison to estimates of expected costs from the first wave models. This is an indication of the improvement that arises from fitting the final wave model over a smaller range of values of the decision variables. The estimate for the optimal reinforcement decision to be made in first stage (i.e. the values of the decision variables which minimise the estimate of expected total costs across both stages from Equation 8.2.11) based on the emulator models fitted in the fourth wave is to increase the transfer capacity of the B6 boundary by 3360 MW and the B7a boundary by 3130 MW.

Further evidence of the improvement in the emulator model fitted in the fourth wave can be seen by comparing Figure 8.8 to Figure 8.9, which compare credible intervals for the estimated expected total costs for the first and fourth wave emulator models

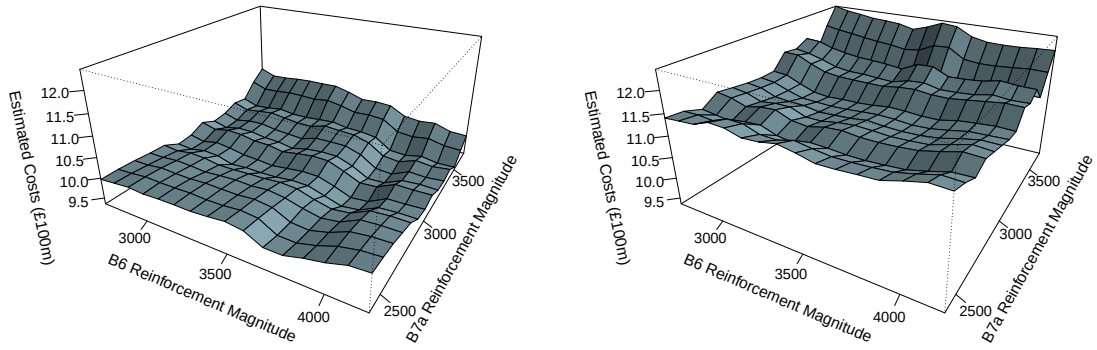

(a) Lower Bound. (b) Upper Bound.

Figure 8.8: Plots to show credible bounds for the estimates of expected total costs from the emulator models fitted in the first wave over the range of decisions considered in the fourth wave.

respectively (over the range of decisions considered in the fourth wave). As can be seen, the credible intervals are much narrower for the emulator model fitted in the fourth wave in comparison to the first, indicating the increased level of confidence in the estimate that arises from fitting the emulator model over a smaller range of decisions. Despite the credible intervals of these estimates in the fourth wave, illustrated in Figure 8.9, being very narrow, the lower bound of the estimate is lower than the smallest estimate of the upper bound for all decisions, indicating that there is insufficient evidence to further reduce the decision space using the methodology of Section 8.2.7.

This is illustrated further in Figure 8.10. Figure 8.10 (a) illustrates how estimated expected total costs vary with B6 reinforcement magnitude, along with credible intervals for these estimates, for the emulator models fitted in the first wave. For this plot B7a reinforcement magnitude was fixed at 3130 MW (the value which minimises the estimate of expected total costs in the fourth wave). Over this range it can be seen that when no B6 reinforcement is made, estimates of expected total costs are around £2.2 billion, with estimates of expected total costs decreasing as B6 reinforcement magnitude increases until over 2000 MW B6 reinforcement has been made. However, when the B6 reinforcement magnitude exceeds 2000 MW, the credible intervals are wide in comparison to the variation in the estimate of expected total costs, meaning

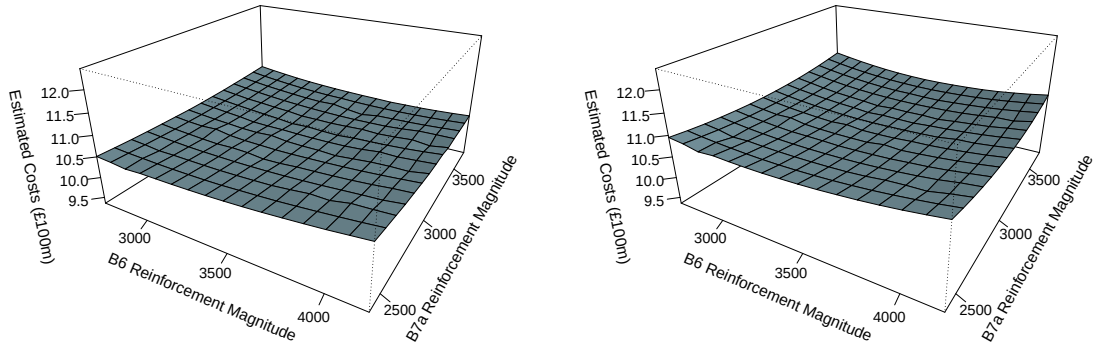

(a) Lower Bound.

(b) Upper Bound.

Figure 8.9: Plots to show credible bounds for the estimates of expected total costs from the emulator models fitted in the fourth wave.

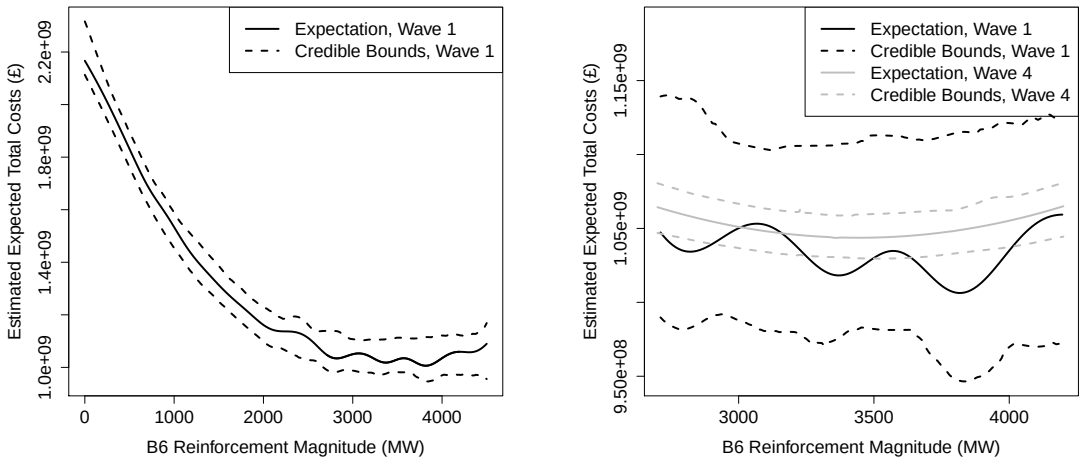

(a) Credible Intervals for the emulator fitted in wave 1.

(b) Comparison of credible intervals for the emulator models fitted in waves 1 and 4.

Figure 8.10: Plot to illustrate how credible intervals for the estimated expected total costs vary as B6 reinforcement magnitude is varied.

no single decision can be identified as optimal. Using the methodology of Section 8.2.7 this means that reinforcement decisions with less than 2000 MW B6 reinforcement can be eliminated from consideration and a more accurate emulator model fitted over a smaller range of decisions.

Figure 8.10 (b) compares how estimates of expected total and the corresponding credible intervals vary with B6 reinforcement magnitude for the emulator models fitted in the first and fourth waves over the range of decisions considered in the fourth wave. Again, for this plot B7a reinforcement magnitude was fixed at 3130 MW (the value which minimises the estimate of expected total costs in the fourth wave). It can be seen that the credible interval for the fourth wave model is much narrower than that of the first wave, indicating the increased level of confidence in the estimate from fitting the emulator model over a smaller range of values of the decision variables. However, it is also clear that over this range there is little variation in the estimate of expected total costs as B6 reinforcement magnitude is varied. Therefore, even though the credible interval is quite narrow for the emulator model fitted in the fourth wave, there is insufficient evidence to eliminate any further decisions from consideration.

8.4.4 Estimate of Optimal Stage 1 Decision

As mentioned earlier, an estimate of optimal first stage decision which minimises the estimate of expected total costs across both stages based on the emulator models fitted in the fourth wave is to increase the transfer capacity of the B6 boundary by 3360 MW and the B7a boundary by 3130 MW. The fact that there is little variation in the estimate of expected total costs as reinforcement decision is varied indicates there is little risk of making a poor reinforcement decision by minimising the expectation arising from the fourth wave emulator models, as all decisions give similar, relatively low estimates of expected total costs with similarly narrow credible intervals. In particular, the large estimates of expected total costs which arise when little to no B6 reinforcement is made (which give twice the estimate of expected total costs at £2.2 billion as can be seen in Figure 8.10 (a)) have been avoided (i.e. eliminated from consideration).

This section has demonstrated how an estimate for the optimal reinforcement decision to be made in year 1 can be acquired using the methodology of Section 8.2.4. As

part of this methodology it is assumed that there exists an opportunity for further reinforcement of the transmission system in year 11. Section 8.6 will provide an example to illustrate how the estimate of optimal reinforcement decision to be made in year 1 varies if it is assumed that no further opportunity for reinforcement is available and the problem of Section 8.3.3 is solved as a single stage decision problem, with the decision to be made at the beginning of year 1.

8.5 Stage 2 Decisions

8.5.1 Stage 2 Decision Based on a Particular Observation

Observing A Particular Scenario

The stage 2 scenario is defined by the continuous variables contained in $\boldsymbol{\psi}_2$. This allows for an infinite number of potential stage 2 scenarios. When making the stage 1 decision using the methodology of Section 8.2.4, this is accounted for via Equation 8.2.9, which estimates an expectation of total stage 2 costs across all possible stage 2 scenarios by integrating over $\boldsymbol{\psi}_2$.

In a real life application, after the first decision is made a number of years will pass and the second decision must be made based on the observed state of the power system. For the example outlined in Section 8.3, 10 years pass between when the first decision is made at the beginning of year 1 and when the second decision is to be made at the beginning of year 11 based on the observed value of $\boldsymbol{\psi}_2$.

In a real application, an optimal stage 2 decision only needs to be identified for the value of $\boldsymbol{\psi}_2$ actually observed. For example, suppose it is observed that $\boldsymbol{\psi}_2 = 0.987$ (i.e. in year 11 the best estimate for peak demand level in year 16 is 98.7% of that projected by [69]). The prior beliefs for peak demand level in stage 2, $v_{2,3}$, would then be a uniform distribution between 93.7% and 103.7% of the projected year 16 peak demand level given by [69]. Optimal stage 2 decisions can then be identified to minimise Equation 8.2.7, given that $\boldsymbol{\psi}_2 = 0.987$, $d_{1,1} = 3360$ and $d_{2,2} = 3130$ (the estimated optimal stage 1 reinforcement magnitudes).

This subsection will demonstrate how an estimate of optimal second stage decision can be acquired once a particular stage 2 scenario has been observed, though later Sections 8.5.2 and 8.5.3 will present results to illustrate how the estimated optimal stage 2 decision varies with the observed stage 2 scenario.

Note, this thesis gives results for the second stage (and later stages when considering the examples of Chapter 9) as the total reinforcement made across both stages. This allows for an easier comparison of the state of the transmission system after the second reinforcement between decisions arrived at through different assumptions (such as comparing the total reinforcement made after 2 stages when varying the assumed discount rate or cost to reinforce).

Initially, this second decision is assumed to be made such that the total reinforcement magnitude after the second decision will be between the reinforcement after the first decision (i.e. do nothing in stage 2) and 8500 MW B6 and 5500 MW B7a reinforcement. However, this means that the initial stage 2 emulator model is fitted over a large range of reinforcement decisions, so the methodology of Section 6.2.1 is used to fit a more accurate model over a smaller range of decisions.

Wave Process For a Particular Scenario

Figure 8.11 (a) illustrates the decisions initially considered for the second stage reinforcement, assuming decisions of 3360 MW B6 and 3130 B7a reinforcement were made in stage 1 and that $\boldsymbol{\psi}_2 = 0.987$ was observed when the second decision was made. This region considers all decisions between the stage 1 estimated optimals (i.e. 3360 MW B6 and 3130 MW B7a) and 8500 MW B6 and 5500 MW B7a reinforcement.

Figure 8.11 (b) and (c) show the reinforcement decisions considered in waves 2 and 3 respectively for the stage 2 decision. As can be seen, the decision space is reduced at a very fast rate. The decisions that remain in the third wave all consider at most a 270 MW increase in B7a reinforcement in comparison to the first stage decision, though all decisions considered in the third wave would increase B6 reinforcement by at least 2340 MW in comparison to the first stage decision. This implies that in stage 2 the reinforcement of the B6 boundary is more important than the reinforcement of the B7a boundary.

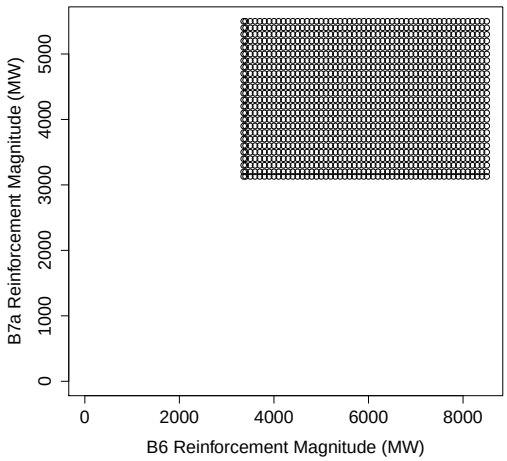

(a) Wave 1.

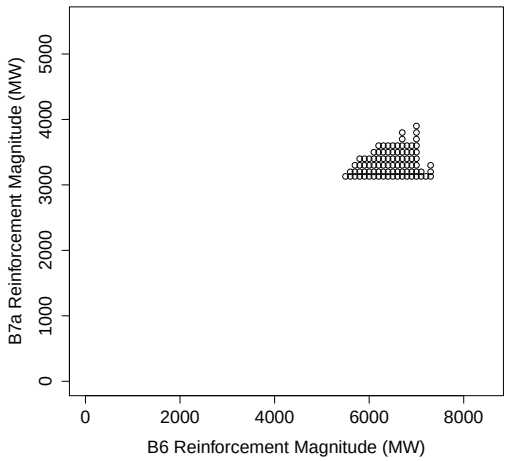

(b) Wave 2.

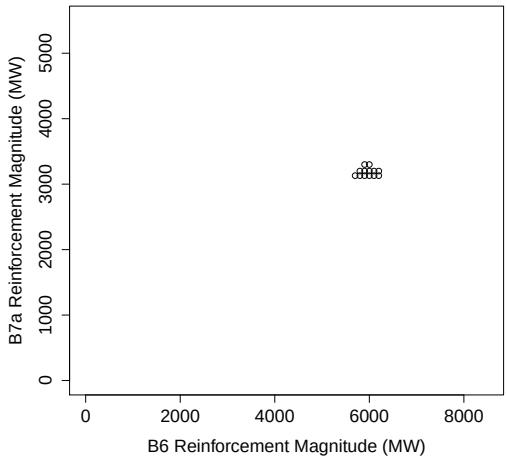

(c) Wave 3.

Figure 8.11: Plots to show decisions considered in each wave for the second stage.

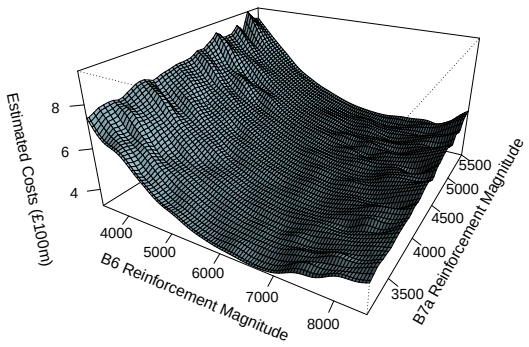

Figure 8.12: Graph to show how estimated expected total costs in stage 2 vary with total B6 and B7a reinforcement for the emulator model fitted in the first wave of the second stage.

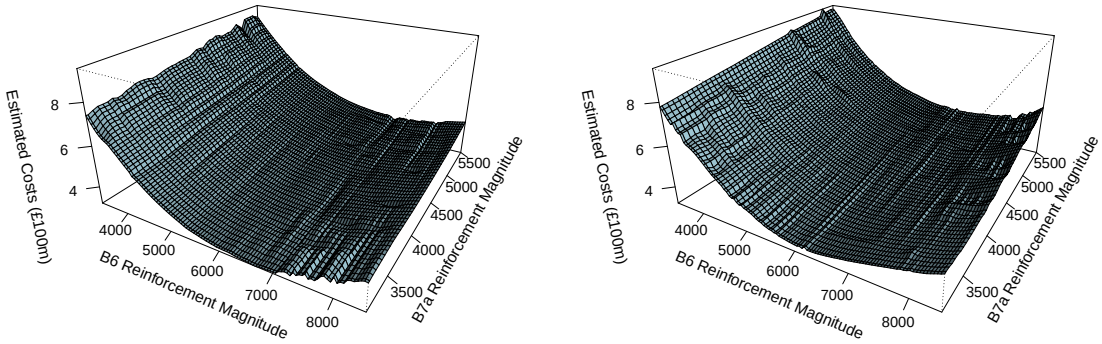

(a) Lower Bound.

(b) Upper Bound.

Figure 8.13: Plots to show how credible bounds for the estimated expected total costs in stage 2 vary with total reinforcement decisions for the emulator model fitted in the first wave of the second stage.

Figure 8.12 displays how estimated expected total costs in stage 2 (from evaluating Equation 8.2.7 assuming $\boldsymbol{\psi}_2 = 0.987$, and that 3360 MW B6 and 3130 B7a reinforcement were made in stage 1) vary with total B6 and B7a reinforcement magnitude after the second decision. Credible bounds for these estimates of expected total costs are illustrated in Figure 8.13. In Figure 8.12, it appears that costs rise fairly linearly as B7a reinforcement magnitude increases, which supports what was seen in Figure 8.11, where it was noted that later waves only consider decisions which make little to no further B7a reinforcement.

Figure 8.14 displays how estimates of expected total costs vary with total B6 and B7a reinforcement magnitude for each wave. As was the case when considering the decision to make in the first stage, costs are much lower over the range of values of the decision variables considered in the third wave, with the variation in costs with decision appearing relatively flat over this range in comparison to the estimates of expected total costs considered in the first wave. Therefore, Figure 8.15 was created to compare the estimates of expected total costs over only the range of decisions considered in the third wave.

As can be seen, there is quite of bit of difference in the estimates of expected total costs over this range when comparing estimates from the emulator model fitted in the first wave, displayed in Figure 8.15 (a), to the estimates from the emulator model fitted in the third wave, displayed in Figure 8.15 (b), as a result of the improvement in the third wave model from being fitted over a smaller range of decisions. Further evidence of this improvement in the fitted emulator model can be seen by comparing the credible intervals of the estimates of expected total costs from the first wave, displayed in Figure 8.16, to the credible intervals of the estimates of expected costs from the third wave, displayed in Figure 8.17. As can be seen, the credible intervals are much narrower in the third wave in comparison to the first indicating the improved level of confidence in the estimate that arises from fitting the emulator model over a smaller range of decisions.

An estimate of optimal stage 2 decision (minimising Equation 8.2.7 based on the emulator model fitted in the third wave) for the observed scenario (observing $\boldsymbol{\psi}_2 = 0.987$ and assuming that 3360 MW B6 and 3130 MW B7a reinforcement was previously made)

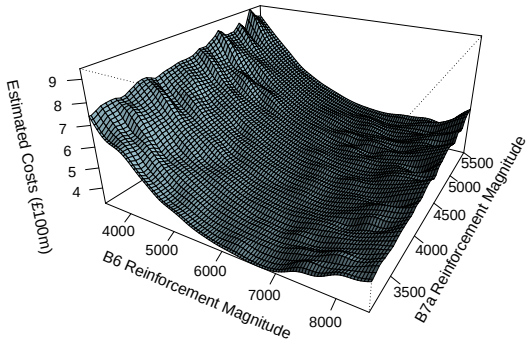

(a) Wave 1.

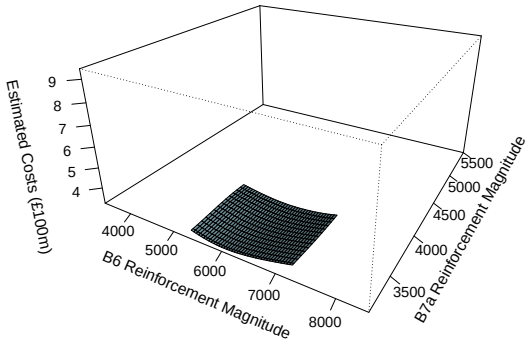

(b) Wave 2.

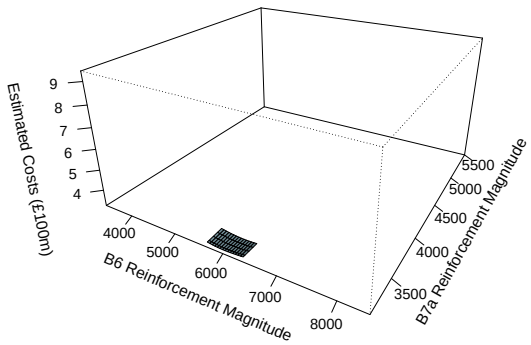

(c) Wave 3.

Figure 8.14: Plots to show how estimated expected total costs in stage 2 vary with total B6 and B7a reinforcement decisions and fitted emulator model in the second stage.

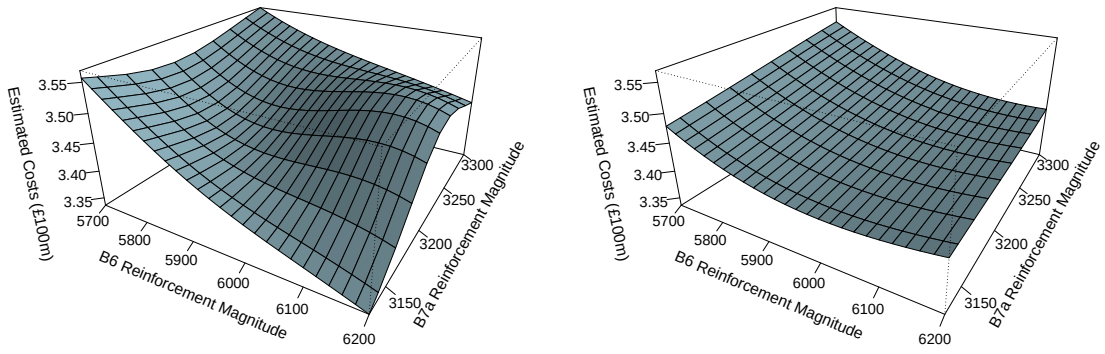

(a) Wave 1.

(b) Wave 3.

Figure 8.15: Plots to show how estimated expected total costs vary with total B6 and B7a reinforcement magnitudes and fitted emulator model in the second stage, over the range of values for the decision variables considered in the third wave.

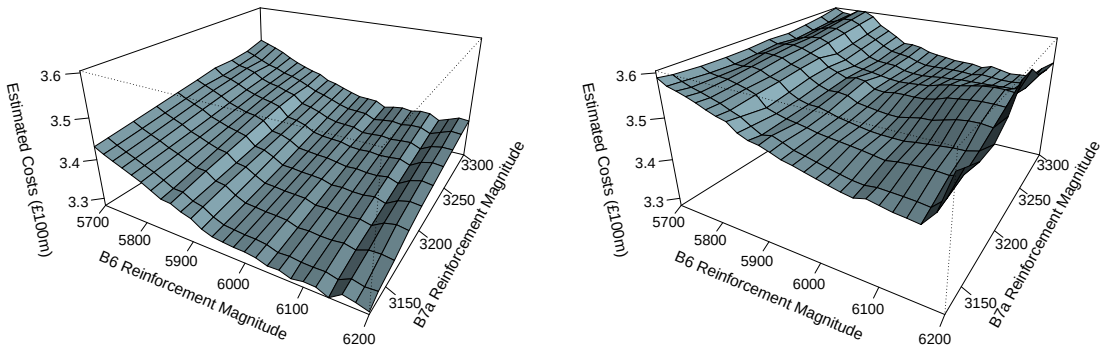

(a) Lower Bound.

(b) Upper Bound.

Figure 8.16: Plots to show how credible bounds for the estimated expected total costs vary with total B6 and B7a reinforcement decisions for the emulator model fitted in the first wave of the second stage, over the range of values for the decision variables considered in the third wave.

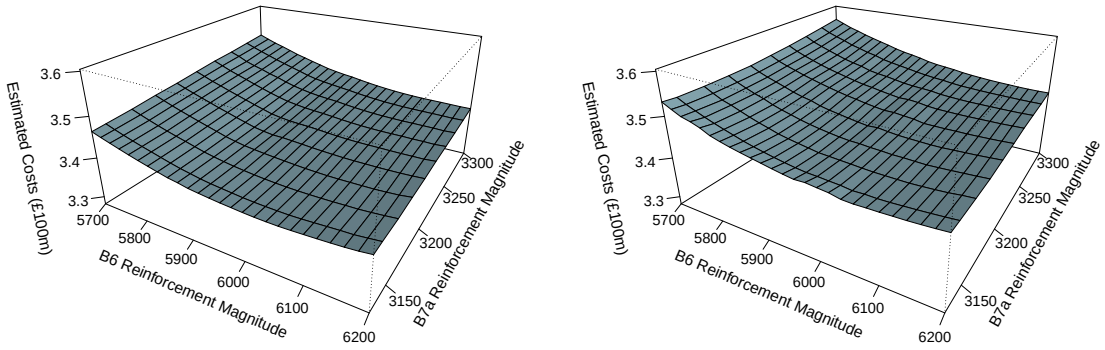

(a) Lower Bound. (b) Upper Bound.

Figure 8.17: Plots to show how credible bounds for the estimated expected total costs vary with total B6 and B7a reinforcement decisions for the emulator model fitted in the third wave of the second stage.

is to increase total B6 reinforcement to 6030 MW (an increase of 2670 MW from stage 1) and make no further B7a reinforcement.

8.5.2 Illustration of Continuous Stage 2 Scenario

The previous subsection noted how the optimal stage 1 decision is estimated by taking an expectation across all potential stage 2 scenarios via Equation 8.2.9, and went on to show how an optimal stage 2 decision can be estimated for the stage 2 scenario (value of $\boldsymbol{\psi}_2$) actually observed when the time comes to make the second decision.

$\boldsymbol{\psi}_2$ is modelled as a continuous variable, with a value between 0.9 and 1.1 that will be learnt when it is time to make the second decision. This continuous model essentially allows for an infinite number of stage 2 scenarios that could be observed (and when the stage 1 decision is made an expectation of the total costs in stage 2 across all of the scenarios that could potentially arise is estimated using the methodology of Section 8.2.4). Any value of $\boldsymbol{\psi}_2$ in the range 0.9 to 1.1 could be observed, though a real life application only needs to make a decision for the value of $\boldsymbol{\psi}_2$ actually observed.

However, it is interesting to compare how the stage 2 decision varies depending on the observed value of $\boldsymbol{\psi}_2$. This would ideally involve creating some function $d_2^o(\boldsymbol{\psi}_2|\mathbf{d}_1)$

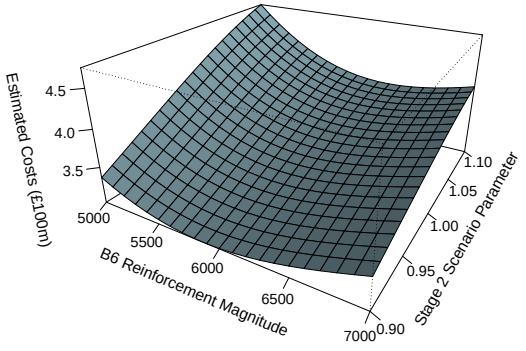

Figure 8.18: Plot to illustrate how expected total cost estimates vary with total B6 reinforcement magnitude and $\boldsymbol{\psi}_2$ (stage 2 scenario).

which would return the optimal stage 2 decision to be made for any stage 2 scenario, for a given stage 1 decision. However, the previous subsection showed how a wave process is required to identify an accurate estimate of optimal stage 2 decision, which is an expensive procedure. This means it is not feasible to acquire an accurate estimate of stage 2 decision for any stage 2 scenario that could possibly occur (this was noted in Section 8.2.2, which is what makes multi-stage decision making with a continuous description of future scenarios difficult). However, by fitting one emulator model over a larger range, an approximation can be acquired to illustrate roughly how the estimate for optimal stage 2 decision would vary with the stage 2 scenario observed.

Figure 8.18 illustrates how estimated expected total costs vary with B6 reinforcement magnitude and value of $\boldsymbol{\psi}_2$ (i.e. the stage 2 scenario which details the estimate of expected year 16 peak demand level at the time the second decision is made at the beginning of year 11). All cost estimates come from a single emulation model fitted by considering a range of 0.85 to 1.15 for peak demand magnification (i.e. 85% to 115% of the year 16 peak demand level projected by [69], which is the entire range of peak demand that could be observed across any stage 2 scenario), 3360 MW to 8500 MW total B6 reinforcement (from the estimate of optimal stage 1 decision to an upper limit of 8500 MW) and 3130 MW to 5500 MW total B7a reinforcement (from the estimate of optimal stage 1 decision to an upper limit of 5500 MW), as well as the range of 0.55 to 0.85 nuclear availability probability and 0.8 to 0.95 CCGT availability probability

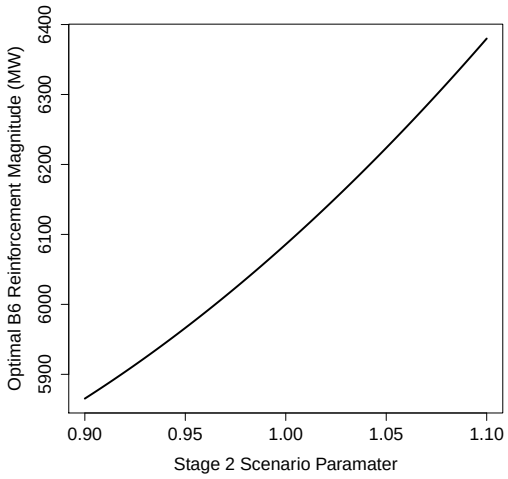

(a) Plot of how estimated optimal total B6 reinforcement magnitude varies with stage 2 scenario.

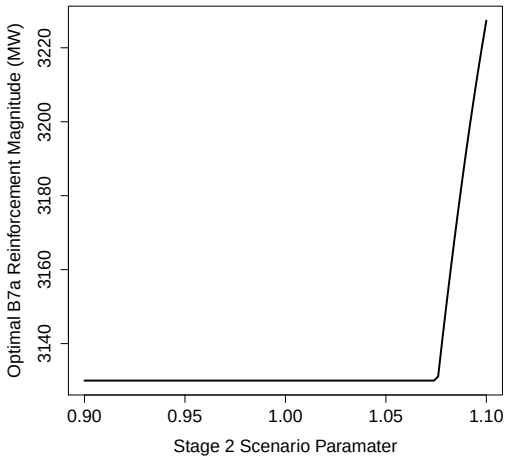

(b) Plot of how estimated optimal total B7a reinforcement magnitude varies with stage 2 scenario.

Figure 8.19: Plots to illustrate how estimates of optimal total reinforcement magnitude vary with $\boldsymbol{\psi}_2$ (stage 2 scenario).

used in all scenarios.

Figure 8.19 (a) shows how the estimated optimal total B6 reinforcement magnitude varies with the value of $\boldsymbol{\psi}_2$ (stage 2 scenario). Figure 8.19 (b) shows how the estimated optimal total B7a reinforcement magnitude varies with the value of $\boldsymbol{\psi}_2$ (stage 2 scenario). As can be seen, almost all values of $\boldsymbol{\psi}_2$ result in a total B7a reinforcement magnitude of 3130 MW after the second decision (i.e. no further B7a reinforcement in the second stage), though the larger values of $\boldsymbol{\psi}_2$ (which corresponds to larger values of potential year 16 peak demand level) do show some increases in B7a reinforcement in the second stage, with the largest being a 100 MW increase when the largest potential value of $\boldsymbol{\psi}_2$ is observed (i.e. $\boldsymbol{\psi}_2$=1.1). The total reinforcement of the B6 boundary is shown to be much more sensitive to the scenario observed in comparison, with total reinforcement ranging from 5860 MW to 6390 MW (increases of 2500 MW to 3030 MW from stage 1) depending on the stage 2 scenario observed.

However, all the estimated costs of Figure 8.18 and estimated optimal decisions of Figure 8.19 were acquired using a single emulation model fitted over a larger range of decisions and all possible stage 2 scenarios. In the previous sub-subsection, Figure 8.14 showed how the fitted emulator model is improved by fitting it over a smaller and

smaller range of possible decisions. Further, the emulator was fitted over all possible year 16 peak demand magnifications that could be considered by all potential stage 2 scenarios, but the accuracy of the emulator model would be improved further by only fitting it over the ranges of peak demand magnification deemed possible for the scenario actually observed.

Therefore, in practice, an emulator model must be fitted for the particular scenario actually observed, and then a wave process performed to eliminate decisions from consideration to improve the fit of the emulator model in order to make the best decision possible.

8.5.3 Estimating Optimal Decisions for a Range of Stage 2 Scenarios

The previous subsection noted how it is not feasible to acquire an accurate estimate of stage 2 decision for any stage 2 scenario that could possibly occur. In reality, this is not a problem, as an optimal decision only needs to be identified for the stage 2 scenario actually observed. However, it is of interest in this thesis to compare how the stage 2 decision would vary depending on what was learnt (i.e. the value of $\boldsymbol{\psi}_2$ observed) by the time the second decision is to be made.

Whilst a wave process cannot be performed for all values of $\boldsymbol{\psi}_2$ that could occur, it is feasible to perform the wave process for several values of $\boldsymbol{\psi}_2$, to compare how the decision made would vary with what was observed. This section will consider how results vary if $\boldsymbol{\psi}_2$ is observed to be 0.9, 1.1 or 1, i.e. the extreme low that could be observed, the extreme high that could be observed and the central value of what could be observed. These three scenarios are summarised in Table 8.3.

Recall, as detailed in Section 8.3.3, $\boldsymbol{\psi}_2$ is used to define the beliefs about the peak demand level in year 16 at the time the second decision is made, such that observing $\boldsymbol{\psi}_2 = 0.9$ would indicate that beliefs about stage 2 peak demand level would form a uniform distribution between 85% and 95% of the year 16 peak demand level projected by [69] (i.e. between $(100\boldsymbol{\psi}_2 - 5)\%$ and $(100\boldsymbol{\psi}_2 + 5)\%$ of the year 16 peak demand level projected by [69]), whereas observing $\boldsymbol{\psi}_2 = 1.1$ would indicate that beliefs about

stage 2 peak demand level would form a uniform distribution between 105% and 115% of the year 16 peak demand level projected by [69].

Stage 2 Scenario	$\boldsymbol{\psi}_2$
Stage 2 Scenario 1	0.9
Stage 2 Scenario 2	1
Stage 2 Scenario 3	1.1

Table 8.3: Table summarising the value of $\boldsymbol{\psi}_2$ observed for three scenarios considered.

Figure 8.20 compares how cost estimates vary with reinforcement decision for the three scenarios of Table 8.3 (after two waves of eliminating decisions with evidence against them being optimal as was illustrated in Section 8.5.1). As can be seen, estimated expected total costs increase as the value of $\boldsymbol{\psi}_2$ increases, which indicates mean constraint costs increase as peak demand level increases. Further, larger magnitudes of B6 reinforcement are considered in the third wave as the value of $\boldsymbol{\psi}_2$ is increased, as the greater constraint costs indicate a greater potential benefit from reinforcing the B6 boundary. Further, in the final wave all scenarios consider only decisions which make little to no further B7a reinforcement, indicating that the benefit from reinforcing the B7a boundary is small in comparison to reinforcing the B6 boundary, which is consistent with Sections 8.5.1 and 8.5.2.

Stage 2 Scenario	B6 Reinforcement Magnitude	B7a Reinforcement Magnitude
Stage 2 Scenario 1	5800 MW	3130 MW
Stage 2 Scenario 2	6140 MW	3150 MW
Stage 2 Scenario 3	6350 MW	3230 MW

Table 8.4: Table summarising how the estimated optimal total reinforcement after the second stage decision varies with stage 2 scenario.

Table 8.4 displays how the estimate for optimal stage 2 total reinforcement decision varies with the observed stage 2 scenario. As can be seen, the estimated optimal total B6 reinforcement magnitude increases as the observed value of $\boldsymbol{\psi}_2$ increases, with total B6 reinforcement after the second decision of 5800 MW, 6140 MW and 6350 MW (increases of 2440 MW, 2780 MW and 2990 MW from stage 1) estimated for scenarios 1, 2 and 3 respectively. In stage 2 scenario 1, no further B7a reinforcement would be made in the second stage, and stage 2 scenario 2 would only increase B7a reinforcement

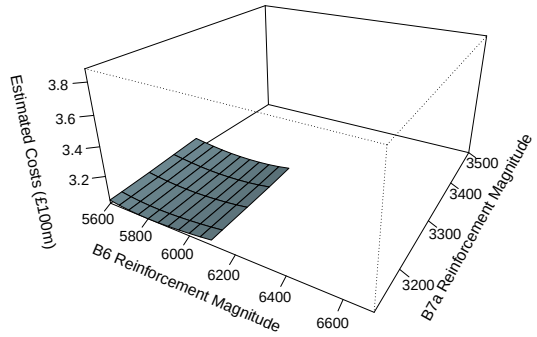

(a) Stage 2 Scenario 1.

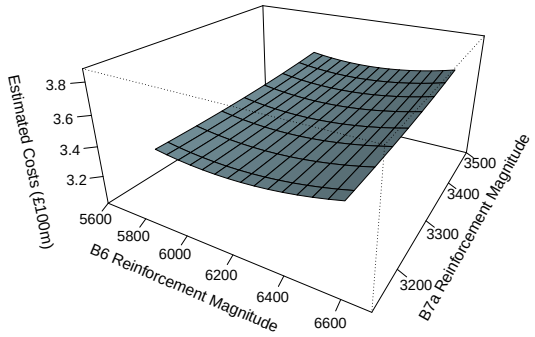

(b) Stage 2 Scenario 2.

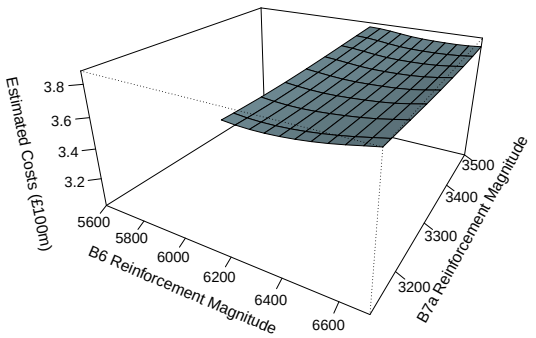

(c) Stage 2 Scenario 3.

Figure 8.20: Plots to show how estimated expected total costs vary with total B6 and B7a reinforcement decisions for each of the stage 2 scenarios considered in Table 8.3.

by a further 20 MW. However, a non-negligible increase of 100 MW was noted if the extreme of $\psi_2 = 1.1$ was observed.

This illustrates not only how the multi-stage methodology allows for a second large reinforcement to be made in a later year in comparison to having to build everything in year 1, but also how the second decision made depends on what was observed about the power system in the 10 years between decisions, allowing the transmission system to be better adapted to the observed power system, with a total of 650 MW difference between the largest reinforcement made and the smallest.

8.6 Comparison to Alternative Solution Methods

This chapter has presented a methodology and application for decision making across two stages. This allows for an initial reinforcement to be made, with a further reinforcement available when additional information has been learnt about the power system. This section will provide a comparison to results from two alternative solution methods.

The first will consider a problem where only a single reinforcement opportunity is available at the beginning of year 1, which becomes available at the beginning of year 6, i.e. solving the example detailed in Section 8.3 as a single stage decision problem. The second will consider a comparison to the case where two opportunities for reinforcement are available, at the beginning of year 1 and at the beginning of year 11 as outlined in Section 8.3.1. However, it will be assumed that at the time the second decision is made uncertainty has not been reduced about future peak demand level.

8.6.1 Solving the Problem Of Section 8.3 As a Single Stage Decision Problem

Cost Estimation of the Single Stage Problem

Section 8.3 outlined a particular two-stage decision problem to be considered. This subsection will consider the corresponding problem when only a single reinforcement

decision, $\mathbf{d}$, is to be made at the beginning of year 1, which will become available at the beginning year 6. All other aspects of the problem will remain as described in Section 8.3. The total costs of such a decision across both stages are calculated as

$$\tilde{F}_T(\mathbf{d}) = \int_{\mathbf{v}_1} \tilde{f}_{c,1}(\mathbf{v}_1, \mathbf{d}) \times p(\mathbf{v}_1) \mathrm{d}\mathbf{v}_1 + \int_{\mathbf{v}_2} \tilde{f}_{c,2}(\mathbf{v}_2, \mathbf{d}) \times p(\mathbf{v}_2) \mathrm{d}\mathbf{v}_2 + f_\rho(\mathbf{d}) \qquad (8.6.1)$$

where $\tilde{f}_{c,1}(\mathbf{v}_1, \mathbf{d})$ is the emulator approximation to the simulator for mean constraint costs between years 6 and 15 (stage 1 of the problem described in Section 8.3), $\tilde{f}_{c,2}(\mathbf{v}_2, \mathbf{d})$ is the emulator approximation to the simulator for mean constraint costs between years 16 and 25 (stage 2 of the problem described in Section 8.3), and $f_\rho(\mathbf{d})$ represents the reinforcement costs of making decision $\mathbf{d}$.

For the two stage decision problem a range of 0 to 4500 MW was initially considered for the B6 and B7a reinforcement in the first stage, with 0 to 8500 MW B6 and 0 to 5500 MW B7a total reinforcement initially considered for the stage 2 decision. For the single stage problem of this section there is no opportunity for a second reinforcement. Therefore, for the single stage problem the initial range of reinforcement decisions considered in year 1 will be 0 to 8500 MW B6 and 0 to 5500 MW B7a reinforcement.

For the methodology detailed in Section 8.2.4, the probability of variables containing uncertainty taking particular values in stage 2, $p(\mathbf{v}_2)$, did not need to be stated explicitly, only the conditional probability based on the particular stage 2 scenario observed, $p(\mathbf{v}_2|\boldsymbol{\psi}_2)$, was required. However, in order to calculate the costs of a single stage decision via Equation 8.6.1, an explicit formulation of $p(\mathbf{v}_2)$ is required. For the example detailed in Section 8.3.3, the prior beliefs about nuclear availability probability and CCGT availability probability in stage 2 were unaffected by the stage 2 scenario observed. Therefore

$$p(v_{2,1}) = p(v_{2,1}|\boldsymbol{\psi}_2)$$

i.e. the prior beliefs for nuclear availability probability in stage 2 is a uniform distribution between 0.55 and 0.85 and

$$p(v_{2,2}) = p(v_{2,2}|\boldsymbol{\psi}_2)$$

i.e. the prior beliefs for CCGT availability probability in stage 2 is a uniform distribution between 0.8 and 0.95.

For stage 2 peak demand magnification, $v_{2,3}$, the marginal distribution for $v_{2,3}$ must be calculated by integrating over $\boldsymbol{\psi}_2$ as

$$p(v_{2,3}) = \int_{\boldsymbol{\psi}_2} p(v_{2,3}|\boldsymbol{\psi}_2) p_{\boldsymbol{\psi}_{2|1}}(\boldsymbol{\psi}_2) \mathrm{d}\boldsymbol{\psi}_2 \tag{8.6.2}$$

where

$$p(v_{2,3}|\boldsymbol{\psi}_2) = \begin{cases} 10 & \text{for } \boldsymbol{\psi}_2 - 0.05 \leq v_{2,3} \leq \boldsymbol{\psi}_2 + 0.05 \\ 0 & \text{Otherwise} \end{cases}$$

(i.e. the density of a uniform distribution between $\boldsymbol{\psi}_2 - 0.05$ and $\boldsymbol{\psi}_2 + 0.05$) and

$$p_{\boldsymbol{\psi}_{2|1}}(\boldsymbol{\psi}_2) = \begin{cases} 5 & \text{for } 0.9 \leq \boldsymbol{\psi}_2 \leq 1.1 \\ 0 & \text{Otherwise} \end{cases}$$

(i.e. the density of a uniform distribution between 0.9 and 1.1).

The probability density function to describe prior beliefs about peak demand magnification in stage 2 can thus be calculated as

$$p(v_{2,3}) = \begin{cases} 50(v_{2,3} - 0.85) & \text{for } 0.85 \leq v_{2,3} < 0.95 \\ 5 & \text{for } 0.95 \leq v_{2,3} \leq 1.05 \\ 50(1.15 - v_{2,3}) & \text{for } 1.05 < v_{2,3} \leq 1.15 \\ 0 & \text{Otherwise} \end{cases}$$

which is illustrated in Figure 8.21.

Estimate of Optimal Decision

Figure 8.22 shows how estimates of expected total costs vary with B6 and B7a reinforcement magnitude for the example outlined in the previous subsection. By comparison to Figure 8.3 (the corresponding plot when a second reinforcement decision in year 11 is available) it can be seen that cost estimates are much greater in Figure 8.22 when little to no reinforcement is made. The reason for this is in the two stage problem it is assumed that the decision maker will act optimally in the second stage when estimates of expected total costs are estimated as a function of the first stage decision. This means that if a poor decision is made in year 1, a greater reinforcement can be made

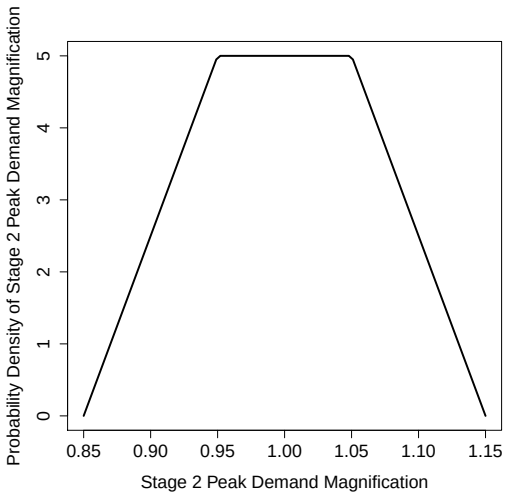

Figure 8.21: Plot to illustrate the prior beliefs about peak demand level in stage 2 at year 1.

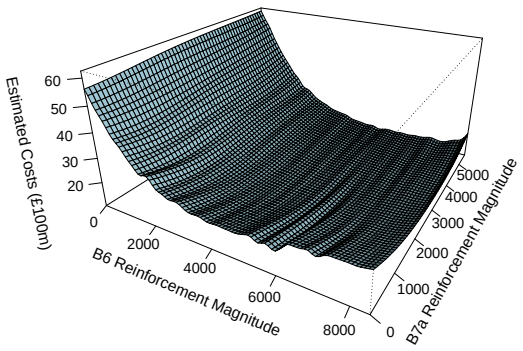

Figure 8.22: Plot to illustrate how expected total cost estimates vary with B6 reinforcement magnitude and B7a reinforcement magnitude in the first wave.

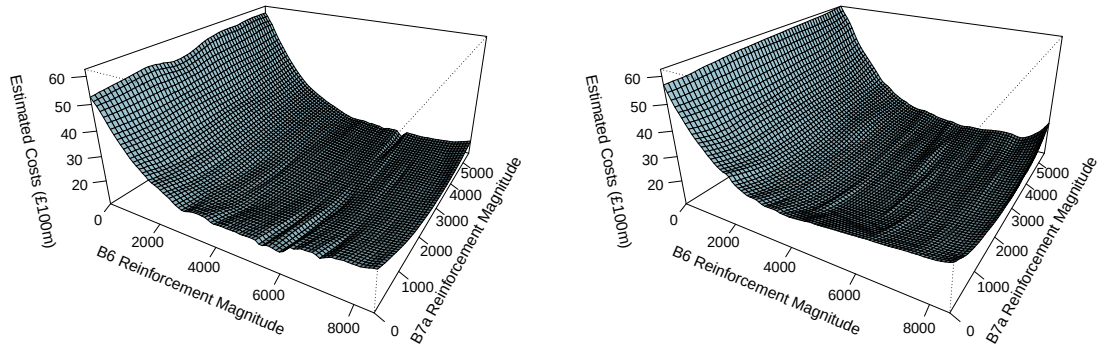

(a) Lower Bound. (b) Upper Bound.

Figure 8.23: Plots to show how credible bounds for the estimates of expected total costs vary with B6 and B7a reinforcement magnitude.

in year 11 to reduce constraint costs in year 16 onwards. However, for the single stage decision problem, if a poor decision is made in year 1 there is no opportunity for further reinforcement, so constraint costs will be much greater for year 16 onwards.

As was the case when considering the two stage problem, the emulator models used to estimate costs for the single stage problem are not perfect approximations to the simulator and contain error. Credible intervals for the estimates of expected total costs of Figure 8.22 are therefore illustrated in Figure 8.23.

The methodology of Section 6.2.1 can then use these credible intervals to eliminate decisions which have evidence against them being optimal, and the wave process described in Section 6.3 can then be used to iteratively eliminate decisions and fit a more accurate model using a new set of training runs over a smaller range of decisions. Figure 8.24 illustrates the decisions considered in the first and final waves after applying the wave process described in Section 6.3 to iteratively fit a more accurate emulator model over a smaller range of decisions. As can be seen, the range of decisions considered is much smaller in the final wave, with the values of B6 reinforcement considered in the final wave ranging from 5000 MW to 6000 MW, and B7a reinforcement magnitude considered in the final wave ranging from 2700 MW to 3400 MW.

Figure 8.25 compares how estimated expected total costs vary with B6 and B7a re-

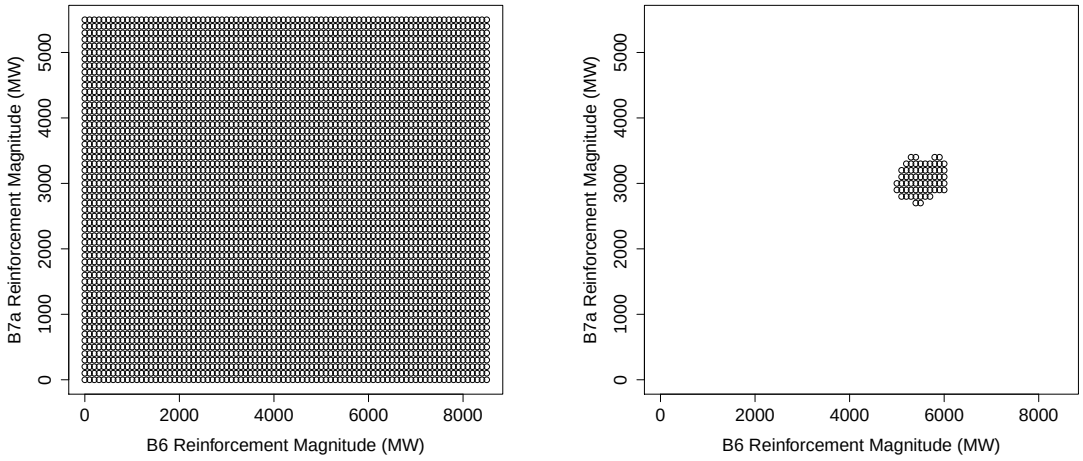

(a) First Wave. (b) Final Wave.

Figure 8.24: Plots to show values of decision variables considered in the first and final waves.

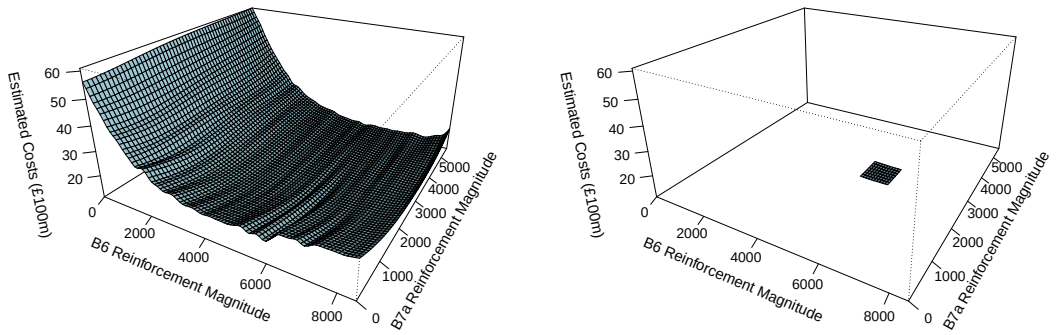

(a) Wave 1. (b) Wave 4.

Figure 8.25: Plots to show how estimated expected total costs vary with reinforcement decisions and fitted emulator model.

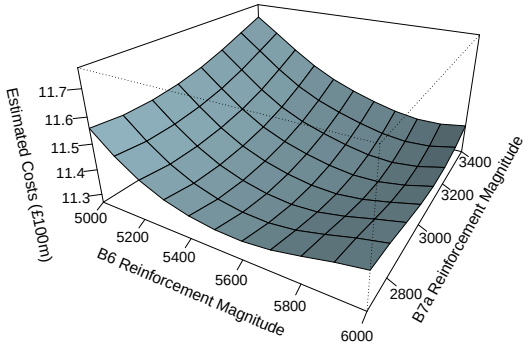

Figure 8.26: Plots to illustrate how estimates of expected total costs vary with B6 reinforcement magnitude and B7a reinforcement magnitude in the final wave.

inforcement magnitude in the first and final wave. As was the case for Figure 8.6 of Section 8.4 (the equivalent plot for the first stage of the 2 stage problem), the total costs estimated are much greater when little to no reinforcement has been made in comparison to when substantial reinforcement has been made, making the final fourth wave plot appear very flat in comparison. Therefore, Figure 8.26 gives a more detailed plot of the estimated expected total costs in wave 4, with this plot still showing very little variation in estimated costs as reinforcement decision is varied, indicating that in the final wave all reinforcement decisions considered give similar, relatively low estimates of expected total costs.

A decision which minimises the estimate of expected total costs based on the emulator model fitted in wave 4 (i.e. the estimate of optimal reinforcement) would make 5560 MW B6 and 3150 MW B7a reinforcement in year 1. By comparing this to the two stage results, this is what may have been expected. 3150 MW B7a reinforcement is very close to the estimated optimal 3130 MW B7a reinforcement from the first stage of the 2 stage problem. Further, Section 8.5 indicated that little to no further B7a reinforcement would be made in stage 2 regardless of which scenario is observed. Therefore, it is unsurprising that when making only a single reinforcement decision at the beginning of year 1, the B7a reinforcement is similar to what was observed for the first decision in the two stage problem.

However, the 5560 MW B6 reinforcement is 2200 MW larger than the estimated opti-

mal B6 reinforcement that was made in the first stage of the two stage problem, but slightly smaller than the estimated optimal second stage reinforcements (ranging from 5800 MW to 6350 MW) observed in Section 8.5.3. This is to be expected, as if a reinforcement similar to the 3360 MW made in the first stage of the 2 stage problem was made for the problem when only a single reinforcement is available, this would leave the power system insufficiently reinforced for all possible stage 2 scenarios. However, the fact that future costs are discounted at an assumed annual rate of 5% means that it is relatively more expensive to build a reinforcement in year 1 in comparison to year 11. This means that the benefits of reducing constraint costs in year 16 onwards are relatively smaller when a single decision is made in year 1, in comparison to when the second decision is made in year 11 of the 2 stage problem, resulting in a slightly smaller reinforcement being built in the single stage problem. This demonstrates another benefit of multi-stage planning, as in the two stage problem, even if the future scenario is known with certainty it can still be economically beneficial to postpone part of a reinforcement decision until it is necessary due to the discounting of future costs.

8.6.2 Solving the Problem Of Section 8.3 Without Reducing Uncertainty At Stage 2

Cost Estimation

It is also possible to consider solving the problem of Section 8.3 as a problem where two opportunities for reinforcement are available (in years 1 and 11 as outlined in Section 8.3.1), but where uncertainty in year 16 peak demand level is not reduced when the second decision is to be made in year 11. A real life interpretation of such a problem would be when there are two opportunities for reinforcement (in year 1 and year 11) but both decisions must be made at the beginning of year 1 for reasons such as budget allocation.

This could still be solved using the methodology of Section 8.2.4 to estimate expected total costs across both stages via backwards induction and emulation, with a couple of small changes to the methodology. First, as uncertainties are not reduced between the first and second decisions, the prior beliefs about variables containing uncertainty

in the second stage no longer depend on the stage 2 scenario, $\boldsymbol{\psi}_2$, i.e.

$$p(\mathbf{v}_2|\boldsymbol{\psi}_2) = p(\mathbf{v}_2)$$

for all values of $\boldsymbol{\psi}_2$.

Further, Section 8.2.4 details how an emulator model, $\tilde{G}_{T,2,\boldsymbol{\psi}_2}(\mathbf{d}_1, \boldsymbol{\psi}_2)$, is fitted to model expected total costs in stage 2 as a function of stage one decision and stage 2 scenario only. As uncertainty is no longer reduced before the second decision is made (i.e. estimates of expected total stage 2 costs do not depend on $\boldsymbol{\psi}_2$) the fitted model no longer depends on $\boldsymbol{\psi}_2$, so consequently a model is fitted to approximate how expected total stage 2 costs vary as a function of stage 1 decision only, i.e. the model $\tilde{G}_{T,2}(\mathbf{d}_1)$ is fitted instead of $\tilde{G}_{T,2,\boldsymbol{\psi}_2}(\mathbf{d}_1, \boldsymbol{\psi}_2)$.

For this example, the prior beliefs for nuclear and CCGT availability probabilities in stage 2, $p(v_{2,1})$ and $p(v_{2,2})$ respectively, are uniform distributions across the ranges 0.55 to 0.85 and 0.8 to 0.95 respectively as described in Section 8.3.3, as it was originally assumed uncertainty in these variables was not reduced between stage 1 and stage 2. However, the prior beliefs at the beginning of year 1 for stage 2 peak demand magnification would now be

$$p(v_{2,3}) = \begin{cases} 50(v_{2,3} - 0.85) & \text{for } 0.85 \leq v_{2,3} < 0.95 \\ 5 & \text{for } 0.95 \leq v_{2,3} \leq 1.05 \\ 50(1.15 - v_{2,3}) & \text{for } 1.05 < v_{2,3} \leq 1.15 \\ 0 & \text{Otherwise} \end{cases}$$

as was calculated in the Section 8.6.1 and illustrated in Figure 8.21.

First Stage Decision

Figure 8.27 (a) displays how estimated expected total costs vary with B6 and B7a reinforcement magnitude when using the methodology of Section 8.2.4 to estimate total costs across both stages and assuming both decisions are made at the beginning of stage 1. Credible bounds for these estimates are given in Figure 8.28.

Again, the emulator models used to estimate expected total costs for Figure 8.27 (a)

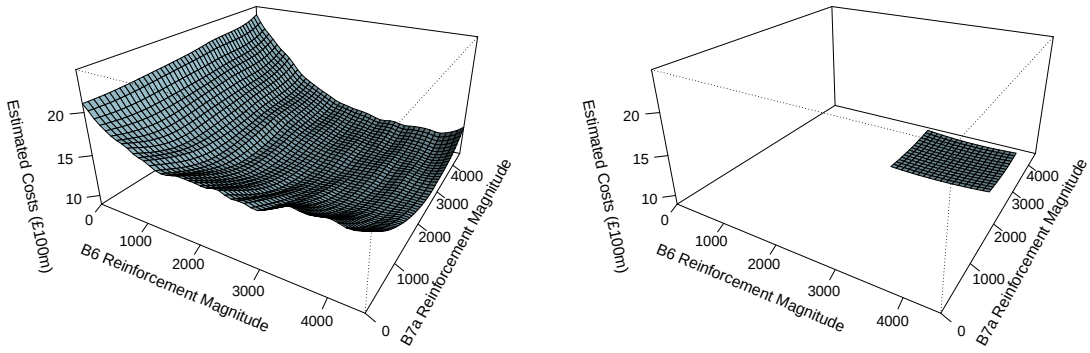

(a) Wave 1. (b) Wave 4.

Figure 8.27: Plots to show how estimates of expected total costs across both stages vary with stage 1 reinforcement decisions and fitted emulator model.

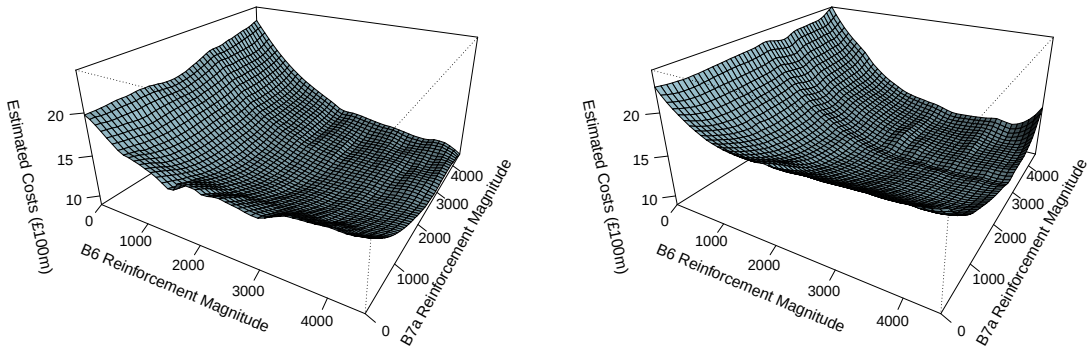

(a) Lower Bound. (b) Upper Bound.

Figure 8.28: Plots to show credible bounds for the estimates of expected total costs for the emulator models fitted in the first wave.

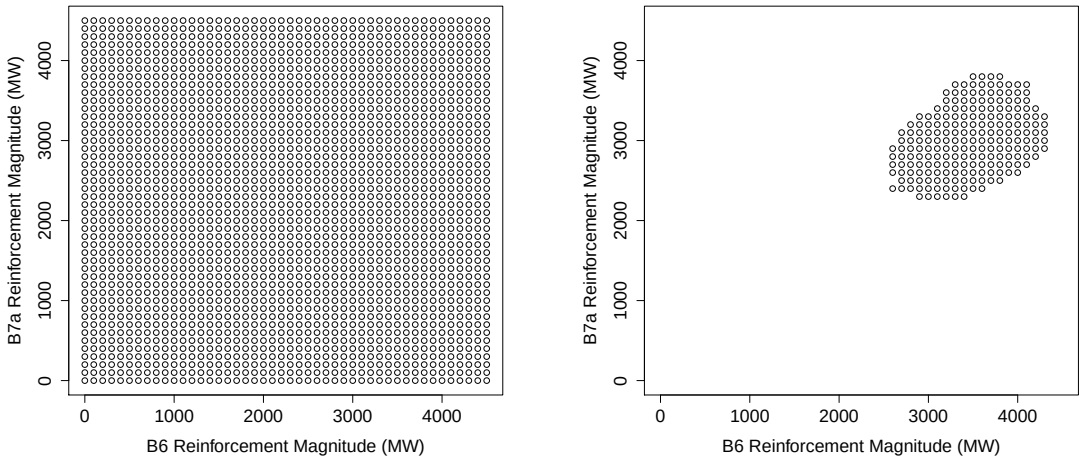

(a) Wave 1.

(b) Wave 4.

Figure 8.29: Plots to compare the values of decision variables considered in the first and fourth wave.

are not perfect approximations to the simulator and contain error. Therefore, the credible intervals of Figure 8.28 can be used to apply the wave process of Section 8.2.7 to eliminate decisions which have evidence against them being optimal in order to fit a more accurate emulator model over a smaller range of decisions. 60.1% of the decisions initially considered were eliminated in the first wave, with 46.4% eliminated in a further wave and a 54.6% being eliminated in a third wave. However, a fourth wave of elimination did not result in a further reduction of the decision space considered. Figure 8.29 compares the range of decisions initially considered in Figure 8.29 (a) to the decisions considered in the fourth wave illustrated in Figure 8.29 (b). As can be seen, the wave process has greatly reduced the decision space with 90.3% of the decisions initially considered eliminated by the fourth wave.

Figure 8.27 gives a comparison between how estimates of expected total costs vary with stage 1 B6 and B7a reinforcement magnitude in the first wave, displayed in Figure 8.27 (a), to the fourth wave, displayed in Figure 8.27 (b). As can be seen, the estimates of expected total costs are very flat over the range of decisions considered in the fourth wave, in the sense that estimates of expected total cost show little variation as B6 and B7a reinforcement magnitude are varied. Again, this suggests that there is little risk of making a poor decision by minimising the estimate of expected total costs

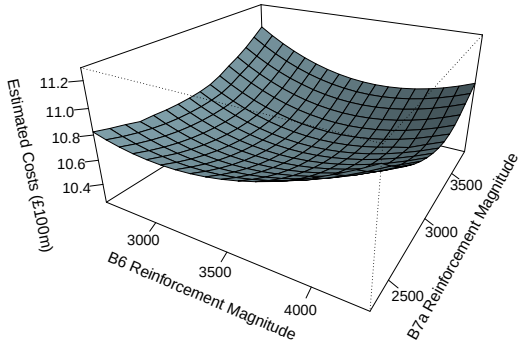

Figure 8.30: Plot to show how estimates of expected total costs across both stages vary with stage 1 B6 and B7a reinforcement magnitude for the emulator models fitted in the fourth wave.

based on the emulator models fitted in the fourth wave, as all decisions considered result in similar, relatively low estimates of expected total costs.

Figure 8.30 displays how estimates of expected total costs in wave 4 vary with stage 1 reinforcement decision, when only considering the estimates from the fourth wave model. An estimate of the optimal stage 1 decision from minimising the estimate of expected total costs based on the model fitted in the fourth wave would be to reinforce the B6 boundary by 3430 MW B6 and reinforce the B7a boundary by 3170 MW. This is slightly larger than the 3360 MW B6 and 3130 MW B7a that would be made when uncertainty is reduced about stage 2 peak demand level before the second decision is made, as identified in Section 8.4.

However, by comparing the ranges of decisions in Figure 8.5 (c) of Section 8.4 (the range of decisions considered in the final wave when uncertainty in stage 2 peak demand level is reduced before the second decision is to be made) to Figure 8.29 (b) (the range of decisions considered in the final wave when both decisions are made at the beginning of year 1) it can be seen that the final wave models are fitted over very similar ranges of decisions. In addition, as no further decisions were eliminated for either example it has not been definitively shown that there is a significant difference between the two decisions.

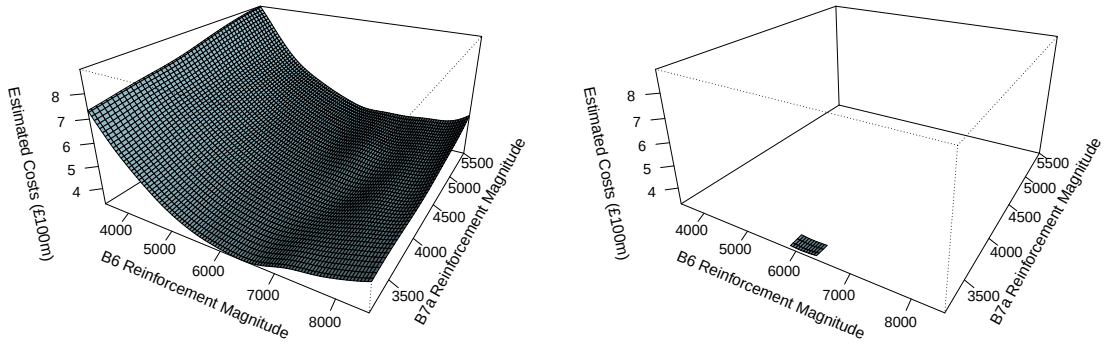

(a) Wave 1. (b) Wave 3.

Figure 8.31: Plots to show how estimated expected total costs vary with total reinforcement decisions and fitted emulator model in the second stage.

Second Stage Decision

For the example outlined in Section 8.3, Sections 8.5.2 and 8.5.3 illustrate how the estimates of expected total costs, and the resulting estimates of optimal decision, vary with stage 2 scenario. However, in this section it is assumed that both decisions are made at the beginning of year 1, i.e. without uncertainty being reduced when the second decision is made. This means there is only a single scenario to consider when making the second decision, with prior beliefs about stage 2 peak demand level, $p(v_{2,3})$, as described in Section 8.6.1 and illustrated in Figure 8.21.

Initially, a range of total reinforcement between 3430 MW (i.e. do nothing in stage 2) and 8500 MW B6 and 3170 MW (i.e. do nothing in stage 2) and 5500 MW B7a was considered for the stage 2 reinforcement decision. Figure 8.31 (a) illustrates how estimates of expected total costs vary with stage 2 total reinforcement decision over this range. As was previously noted in Sections 8.5.1 and 8.5.3, costs appear to rise quite linearly as B7a reinforcement magnitude is increased, indicating that little to no further B7a reinforcement is justified in the second stage. However, the B6 reinforcement magnitude is shown to have quite a large effect on the estimate of expected total costs.

Again, as was considered in Sections 8.5.1 and 8.5.3, the emulator model used is not a perfect approximation to the simulator, so the wave process of Section 6.2 was applied

to fit a more accurate emulator model over a smaller range of decisions. Figure 8.31 (b) illustrates how estimates of expected total costs vary over the range of decisions considered after two waves of elimination, with a negligible amount of decisions eliminated from further waves beyond this.

It can be seen that over this range the estimates of expected total costs are very flat, in the sense that there is little variation in the cost estimates as the reinforcement decision is varied. As all decisions result in similar, relatively low estimates of expected total costs this implies that there is little risk of making a poor decision when making the decision to minimise the estimate of expected total costs over this range. In particular, the very large estimates of expected total costs which arise when B6 reinforcement is low or B7a reinforcement is high have been eliminated from consideration.

The estimate of optimal stage 2 reinforcement was to increase total B6 reinforcement to 6100 MW (an increase of 2670 MW from stage 1) and make no further B7a reinforcement (i.e. total B7a reinforcement remains at 3170 MW). This is close to the estimated optimal reinforcement decision of 6140 MW total B6 and 3150 MW total B7a reinforcement that minimises the estimate of expected total costs when observing $\boldsymbol{\psi}_2 = 1$, which may have been expected.

By comparison to results from Table 8.4 of Section 8.5.3 (where uncertainty in year 16 peak demand level was reduced before the second decision, was to be made) it can be seen that if $\boldsymbol{\psi}_2 = 0.9$ was observed the B6 boundary would be over-reinforced by 300 MW (£30 million extra to build), whereas if $\boldsymbol{\psi}_2 = 1.1$ was observed the B6 boundary would be under-reinforced by 250 MW (and the B7a boundary under-reinforced by 60 MW). Things would be even worse in an example where a greater level of variation is observed in the estimate of optimal decision between scenarios.

8.6.3 Risk Profiles of Decisions

It is also of interest to compare the risk profiles of decision strategies depending on whether uncertainty is reduced about stage 2 peak demand level before the second decision is made (as in Section 8.5), uncertainty is not reduced about stage 2 peak demand level before the second decision is made (as in Section 8.6.2) or only a single

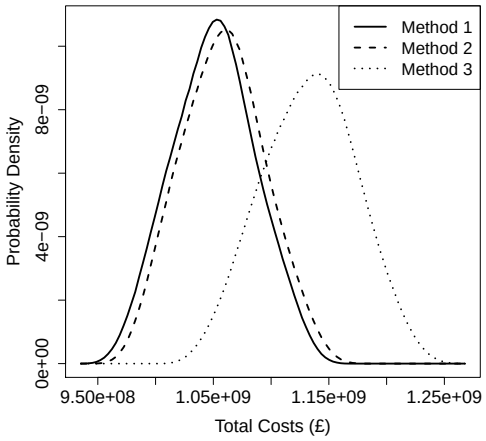

Figure 8.32: Plot to compare risk profiles for different methods of decision making.

opportunity for reinforcement is available (as in Section 8.6.1). These risk profiles are displayed in Figure 8.32 and summarised in Table 8.5.

Decision Method	Description	Estimated Expected of Total Costs
Method 1	Uncertainty is reduced about stage 2 peak demand before the second decision is made (as in Sections 8.4 and 8.5)	£1050 million
Method 2	Uncertainty is not reduced about stage 2 peak demand before the second decision is made (as in Section 8.6.2)	£1058 million
Method 3	Only a single opportunity for reinforcement is available (as in Section 8.6.1)	£1133 million

Table 8.5: Table summarising the risk profiles displayed in Figure 8.32.

As can be seen, when two opportunities for reinforcement are available, the risk profiles are very similar regardless of whether or not uncertainty in stage 2 peak demand level is reduced before the second decision is made. However, the risk profile when only a single reinforcement is available is quite different, with a larger mode and a larger range of potential costs. Table 8.5 also gives a summary of the expected total costs of each of the decisions.

When only a single opportunity for reinforcement is available at the beginning of year 1, expected total costs are £83 million greater in comparison to when two opportunities for reinforcement are available, with an opportunity to reduce uncertainty in peak

demand between decisions. This is unsurprising as the initial year 1 reinforcement is 2220 MW greater in comparison to when decisions are made across both stages and information is learnt between both decisions. Due to the effect of discounting, making such a reinforcement now is relatively more expensive in comparison to when part of the reinforcement can be postponed by 10 years, although this is partially offset due to a larger reinforcement being built earlier also reducing constraint costs in stage 1.

Despite there being quite a large benefit from making decisions over 2 stages instead of 1, the benefit from reducing uncertainty about stage 2 peak demand level before the second decision is made is quite small in comparison. This is because, for the particular example presented, although the stage 2 scenario observed does affect the decision made, the effect is not too great, with Table 8.4 of Section 8.5.3 showing how the estimated optimal total reinforcement varies by 650 MW depending on the stage 2 scenario observed. Further, as can be seen in Figure 8.20 of Section 8.5.3, the estimates of expected total costs are very flat near the optimal decision in the second stage. This means that if the second stage decision does not greatly differ from the optimal decision (and Section 8.6.2 showed the estimated optimal decision when uncertainty is not reduced about stage 2 peak demand level differs from the estimated optimal for any given scenario by less than 300 MW B6 reinforcement and less than 60 MW B7a reinforcement) then the increase in estimated expected total costs will be relatively small. If there was a greater variation in the optimal stage 2 decision with the observed scenario in stage 2 then there would be a greater benefit from reducing uncertainty between the first and second decisions.

8.7 Assessing the Accuracy of Estimated Optimal Stage 2 Decisions Used When Estimating Costs as a Function of the First Stage Decision

As part of the methodology of Section 8.2.4, a sample of N_θ stage 1 decisions (values of $\mathbf{d}_1$) and stage 2 scenarios (values of $\boldsymbol{\psi}_2$) are taken. For each, the optimal decision that would be made in the second stage is estimated as $\mathbf{d}_{2|\theta}$, and the corresponding estimate

of expected stage 2 total costs (reinforcement costs plus expected mean constraint costs) of the decision is calculated as $\tilde{F}_{T,2,\theta}$ using Equation 8.2.8. These estimates are then used to fit the model $\tilde{G}_{T,2,\boldsymbol{\psi}_2}(\mathbf{d}_1, \boldsymbol{\psi}_2)$, which estimates the expected total costs in stage 2 as a function of stage 1 decision and stage 2 scenario only.

Section 8.2.6 outlines how uncertainty in the estimate of expected total costs across both stages can be estimated for a particular stage 1 decision. Whilst error in the estimated stage 2 costs, $\tilde{F}_{T,2,\theta}$ (and therefore $\tilde{G}_{T,2,\boldsymbol{\psi}_2}(\mathbf{d}_1, \boldsymbol{\psi}_2)$) was considered, possible error in $\mathbf{d}_{2|\theta}$ was not considered, as it was noted that this would require N_θ separate stage 2 wave processes to be performed in each stage 1 wave, which is not feasible for the resources available to us in this thesis. Further, when generalising to M stages, this would require $\sum_{m=2}^{M} N_{\theta_m}$ total wave processes to be performed for each stage 1 wave.

However, performing a wave process for each θ to more accurately estimate $\mathbf{d}_{2|\theta}$ may have an effect on the total stage 2 costs estimated, $\tilde{F}_{T,2,\theta}$. Further, even if the estimate of the optimal stage 2 decision is unaffected for each θ, the wave process would mean that the model fitted to estimate constraint costs in the final wave of such a process would be fitted over a very small region of stage 2 decisions, which would reduce the uncertainty in the estimate of $\tilde{F}_{T,2,\theta}$. This increases the confidence in the estimates of expected total costs, resulting in narrower credible bounds being estimated using the methodology of Section 8.2.6, which would in turn mean more stage 1 decisions can be eliminated from consideration using the methodology of Section 8.2.7 and allow for a more accurate first stage decision to be made. This could make performing such a wave process an attractive option if sufficient computing resources are available.

8.7.1 Estimating Optimal Stage 2 Decisions

This section will consider how the estimated optimal stage 2 decisions, $\mathbf{d}_{2|\theta}$, vary depending on whether the stage 2 emulator fitted as part of the methodology of Section 8.2.4, $\tilde{f}_{c,2}(\mathbf{v}_2, \mathbf{d}_2|\mathbf{d}_1)$, is used to estimate $\mathbf{d}_{2|\theta}$ or whether $\mathbf{d}_{2|\theta}$ are estimated using a separate wave process to accurately estimate each of the optimal stage 2 decisions. Results are presented for a random sample of 5 of the 50 values of θ used to fit $\tilde{G}_{T,2,\boldsymbol{\psi}_2}(\mathbf{d}_1, \boldsymbol{\psi}_2)$ for the example presented in Section 8.3, with details of the stage 1 decisions and stage 2 scenarios considered given in Table 8.6.

Sampled Stage 1 Decision and Stage 2 Scenario	B6 Reinforcement Magnitude	B7a Reinforcement Magnitude	$\boldsymbol{\psi}_2$
θ_1	918.4 MW	3214 MW	0.9408
θ_2	1561 MW	3673 MW	0.9245
θ_3	3214 MW	3306 MW	1.096
θ_4	4316 MW	1837 MW	1.067
θ_5	3581 MW	2296 MW	1.035

Table 8.6: Table detailing the 5 sets of stage 1 decisions and stage 2 scenarios considered for estimating optimal stage 2 decisions in this section.

Sampled Stage 1 Decision and Stage 2 Scenario	B6 Reinforcement Magnitude	B7a Reinforcement Magnitude
θ_1	5630 MW	3214 MW
θ_2	5700 MW	3673 MW
θ_3	6730 MW	3510 MW
θ_4	6600 MW	3420 MW
θ_5	6490 MW	3310 MW

Table 8.7: Table of estimates of optimal stage 2 decisions for the scenarios detailed in Table 8.6 when using the emulator models fitted in the first wave when making the first stage decision.

Sampled Stage 1 Decision and Stage 2 Scenario	B6 Reinforcement Magnitude	B7a Reinforcement Magnitude
θ_1	5970 MW	3214 MW
θ_2	6220 MW	3673 MW
θ_3	6440 MW	3306 MW
θ_4	6280 MW	3190 MW
θ_5	6130 MW	3060 MW

Table 8.8: Table of estimates of optimal stage 2 decisions for the scenarios detailed in Table 8.6 when performing a stage 2 wave process for each scenario.

Estimates of the optimal stage 2 decision, $\mathbf{d}_{2|\theta}$, for each of the stage 1 decisions and stage 2 scenarios detailed in Table 8.6 when using the emulator model to estimate stage 2 mean constraint costs, $\tilde{f}_{c,2}(\mathbf{v}_2, \mathbf{d}_2|\mathbf{d}_1)$, fitted in the first wave are given in Table 8.7, whilst the estimated optimal stage 2 decisions when performing a separate wave process for each scenario are given in Table 8.8.

As can be seen, these estimates of optimal stage 2 decisions are not particularly accurate when not performing a separate wave process for each stage 2 scenario, with the optimal B6 reinforcement ranging from being under-estimated by 520 MW for θ_2 to being over-estimated by 360 MW for θ_5. Estimates of optimal stage 2 B7a reinforcement are more consistent, with both methods making no further B7a reinforcement for θ_1 and θ_2, and the biggest difference being 250 MW for θ_5.

It is important to also consider that even without performing a wave process to eliminate stage 2 decisions from consideration for each scenario, the range of stage 2 decisions that the stage 2 emulator model, $\tilde{f}_{c,2}(\mathbf{v}_2, \mathbf{d}_2|\mathbf{d}_1)$, is fitted over is reduced as stage 1 decisions are eliminated (as only total stage 2 reinforcements larger than the smallest stage 1 reinforcement need to be considered), as was illustrated in Figure 8.2 of Section 8.2.7. This means that estimates from the emulator model for stage 2 mean constraint costs will be more accurate in later waves than in the first, even without performing a separate stage 2 wave process, which in turn will mean the estimates for optimal stage 2 reinforcement will be more accurate.

Sampled Stage 1 Decision and Stage 2 Scenario	B6 Reinforcement Magnitude	B7a Reinforcement Magnitude
θ_1	6180 MW	3214 MW
θ_2	6220 MW	3673 MW
θ_3	6400 MW	3310 MW
θ_4	6250 MW	3200 MW
θ_5	6170 MW	3160 MW

Table 8.9: Table of estimates of optimal stage 2 decisions for the scenarios detailed in Table 8.6 when using the emulator models fitted in the fourth wave when making the first stage decision.

Table 8.9 details the estimates for optimal stage 2 reinforcement decisions, $\mathbf{d}_{2|\theta}$, for the scenarios of Table 8.6 when using the second stage emulator, $\tilde{f}_{c,2}(\mathbf{v}_2, \mathbf{d}_2|\mathbf{d}_1)$, fitted in the fourth wave of the example considered in Section 8.4.

Results now much more similar to those of Table 8.8, where a separate wave process was used to estimate the optimal stage 2 decision for each assumed stage 1 decision and stage 2 scenario detailed in Table 8.6. As can be seen, the estimate of optimal B7a reinforcement is very consistent with 4 of the 5 estimates differing by less than 10

MW, and the fifth by 100 MW. Estimates for the optimal level of B6 reinforcement also compare quite well to Table 8.8 with the largest difference being 210 MW for θ_1, though four of the differences are less than 50 MW. This indicates that even without performing a separate wave process for each θ, the estimate for optimal stage 2 decision is improved greatly as stage 1 decisions are eliminated and the models $\tilde{f}_{c,1}(\mathbf{v}_1, \mathbf{d}_1)$ and $\tilde{f}_{c,2}(\mathbf{v}_2, \mathbf{d}_2|\mathbf{d}_1)$ are fitted over a smaller range of decisions.

8.7.2 Comparison of Estimates of Expected Stage 2 Total Costs

It is important to also consider that $\tilde{G}_{T,2,\psi_2}(\mathbf{d}_1, \boldsymbol{\psi}_2)$ is used to model how estimates of expected total stage 2 costs vary as a function of stage 1 decision and stage 2 scenario (not how expected stage 2 decision varies as a function of stage 1 decision and stage 2 scenario). Further, in Section 8.5 it was shown how near the optimal stage 2 decision the estimate of expected total costs is relatively flat, in the sense that the estimate of expected total costs varies little as the stage 2 decision is varied. Therefore, it is of interest to not only compare how the estimate of optimal stage 2 decision varies depending on whether or not a separate wave process is used to estimate optimal stage 2 decisions for each sampled stage 1 decision and stage 2 scenario, but also how the resulting estimates of expected stage 2 total costs vary.

Sampled Stage 1 Decision and Stage 2 Scenario	Using Emulator Model fitted in Stage 1 Wave 1	Using Emulator Model fitted in Stage 1 Wave 4	Using a Stage 2 Wave Process for each θ
θ_1	£455,700,000	£461,800,000	£466,900,000
θ_2	£405,500,000	£403,200,000	£407,900,000
θ_3	£367,000,000	£373,100,000	£376,100,000
θ_4	£381,900,000	£383,500,000	£393,800,000
θ_5	£392,600,000	£387,800,000	£399,000,000

Table 8.10: Table of how estimated expected total stage 2 costs when making the estimated optimal stage 2 decision varies with the model used to estimate optimal decision and expected total costs for the scenarios detailed in Table 8.6.

Table 8.10 details how estimates of expected total costs in stage 2, $\tilde{F}_{T,2,\theta}$, vary with the method used to estimate the optimal stage two decisions, $\mathbf{d}_{2|\theta}$, for the five scenarios detailed in Table 8.6. The differences relative to the estimate when performing a stage 2 wave process for each scenario are given in Table 8.11.

Sampled Stage 1 Decision and Stage 2 Scenario	Using Emulator Model fitted in Stage 1 Wave 1	Using Emulator Model fitted in Stage 1 Wave 4
θ_1	-2.40%	-1.10%
θ_2	-0.59%	-1.16%
θ_3	-2.43%	-0.81%
θ_4	-3.02%	-2.59%
θ_5	-1.59%	-2.78%

Table 8.11: Table of how the estimated expected total stage 2 costs when making the estimated optimal stage 2 decision differ in comparison to using a separate stage 2 wave process for each of the stage 2 scenarios detailed in Table 8.6.

As can be seen, the differences are relatively quite small, with the largest being just over 3%. Further, despite the decisions from the emulators fitted in the fourth wave generally being closer to the decisions when performing a separate wave process for each scenario than estimates of decision from the first wave emulator models, estimates of expected total costs are similarly accurate for the first and fourth wave models. As was noted, this is due to the fact that the estimates of expected costs are very flat near the optimal decision in the sense that the estimates of expected total costs do not greatly vary as reinforcement decision is varied, resulting in the relatively small differences observed in Table 8.11.

However, it must also be noted that even when performing a wave process for each stage 2 decision, the emulator used is still not a perfect approximation to the simulator and contains a small amount of error. As part of the methodology of Section 8.2.6 to eliminate stage 1 decisions from consideration, this error is accounted for by forming credible intervals for $\tilde{F}_{T,2,\theta}$ by considering the how the emulator model currently fitted to estimate constraint costs in the second stage, $\tilde{f}_{c,2}(\mathbf{v}_2, \mathbf{d}_2|\mathbf{d}_1)$, varies as its parameters are varied. Performing an additional wave process for each stage 2 scenario would mean that N_θ models (i.e. N_θ separate models of $\tilde{f}_{c,2}(\mathbf{v}_2, \mathbf{d}_2|\mathbf{d}_1)$) are eventually fitted over small ranges of possible stage 2 decisions, leading to very narrow credible intervals for the resulting estimate of $\tilde{F}_{T,2,\theta}$, whereas the models for $\tilde{f}_{c,2}(\mathbf{v}_2, \mathbf{d}_2|\mathbf{d}_1)$ fitted in the first and fourth wave (without separate waves for each stage 2 scenario) are fitted over a much greater range of stage 2 decisions, leading to comparatively wider credible intervals for $\tilde{F}_{T,2,\theta}$.

This is illustrated in Figure 8.33 to 8.37 which show boxplots for 200 values of $\tilde{F}_{T,2,\theta,r}$ (values of $\tilde{F}_{T,2,\theta}$ calculated using random drawings of $\tilde{f}_{c,2}(\mathbf{v}_2, \mathbf{d}_2|\mathbf{d}_1)$ as detailed in Section 8.2.6) for the five scenarios detailed in Table 8.6, as well as credible intervals formed using the 200 randomly drawn values of $\tilde{F}_{T,2,\theta,r}$. As can be seen, for each of the stage 2 scenarios the credible intervals for the estimates of expected total stage 2 costs, $\tilde{F}_{T,2,\theta}$, are quite wide when using the stage 2 emulation model fitted in the first wave but very narrow credible intervals are acquired when performing a separate stage 2 wave process for each scenario. This indicates the increased level of confidence that arises in the estimate of $\tilde{F}_{T,2,\theta}$ when a separate wave process is performed for each stage 2 scenario. However, for the stage 2 emulator model fitted in the fourth wave when making the stage 1 decision, it can be seen that credible intervals are much narrower than those acquired from emulators in the first wave, indicating that the methodology of Section 8.2.6 does allow for an improvement to be made in the estimate of expected stage 2 costs even without performing a separate wave process for each stage 2 scenario used to fit $\tilde{G}_{T,2,\boldsymbol{\psi}_2}(\mathbf{d}_1, \boldsymbol{\psi}_2)$.

For each of the five scenarios, the estimate of expected total stage 2 costs, $\tilde{F}_{T,2,\theta}$, acquired from performing a separate wave process for each value of θ is included in all three sets credible intervals (i.e. included in the credible intervals when performing a separate wave process for each θ and the credible intervals from using $\tilde{f}_{c,2}(\mathbf{v}_2, \mathbf{d}_2|\mathbf{d}_1)$ from the stage 1 first or fourth wave without performing a separate wave process for each θ). Further, the credible intervals themselves when performing a separate wave process for each θ are included in the other two sets of credible intervals. This indicates that although the error in the estimate can be reduced by performing a separate wave process for each scenario, our method for modelling error is sufficient to account for the uncertainty in our estimates when eliminating stage 1 decisions, so there is little risk of wrongly eliminating a stage 1 decision. However, if sufficient computing resources were available to perform a separate wave process for each scenario, the narrower credible intervals would allow for a greater number of stage 1 decisions to be eliminated, improving the accuracy of the fitted emulator models and the resulting decision made.

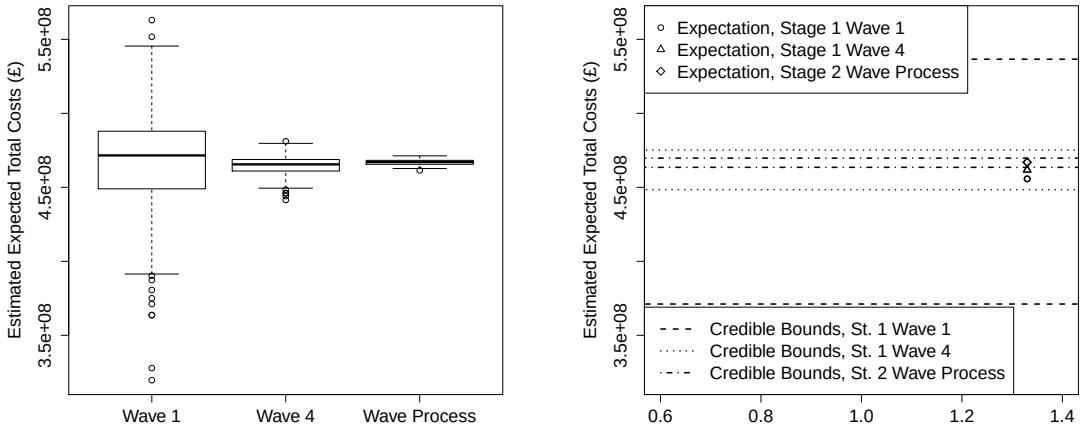

(a) Boxplots. (b) Credible Intervals.

Figure 8.33: Plots to compare the estimates of expected stage 2 costs for θ_1.

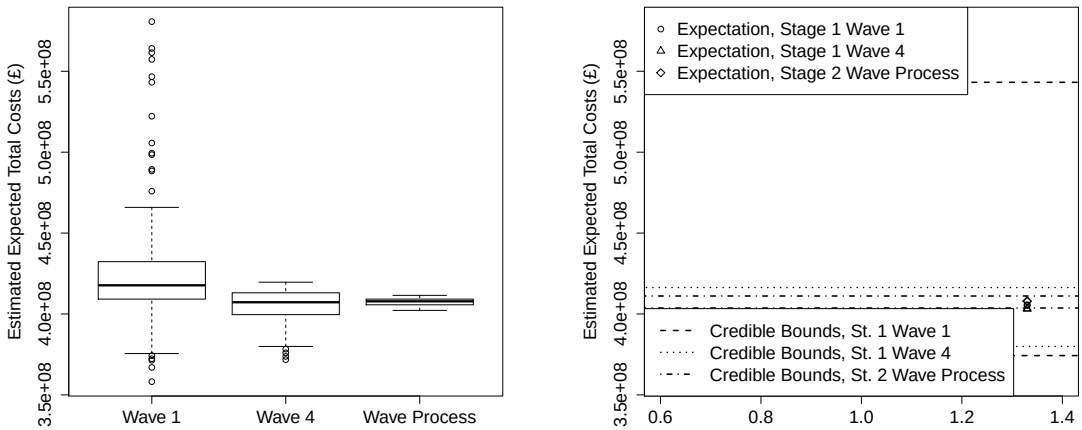

(a) Boxplots. (b) Credible Intervals.

Figure 8.34: Plots to compare the estimates of expected stage 2 costs for θ_2.

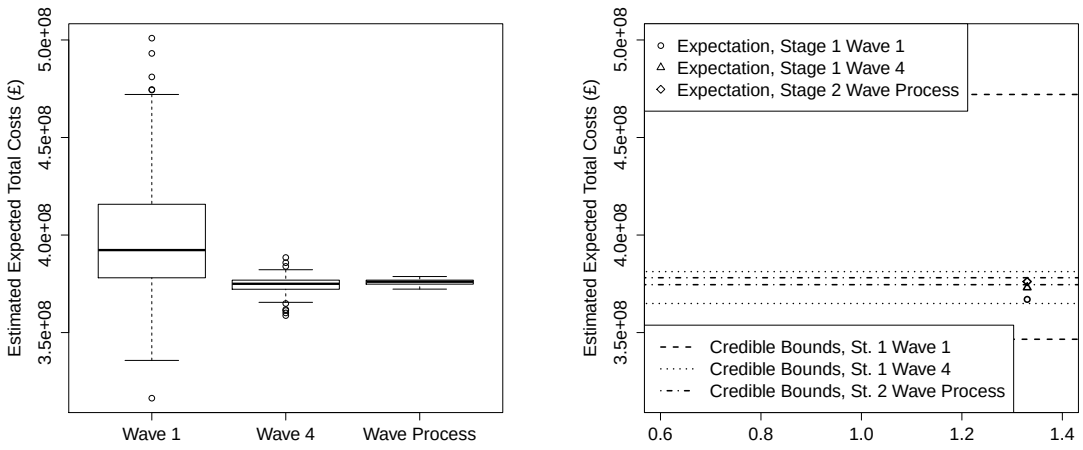

(a) Boxplots. (b) Credible Intervals.

Figure 8.35: Plots to compare the estimates of expected stage 2 costs for θ_3.

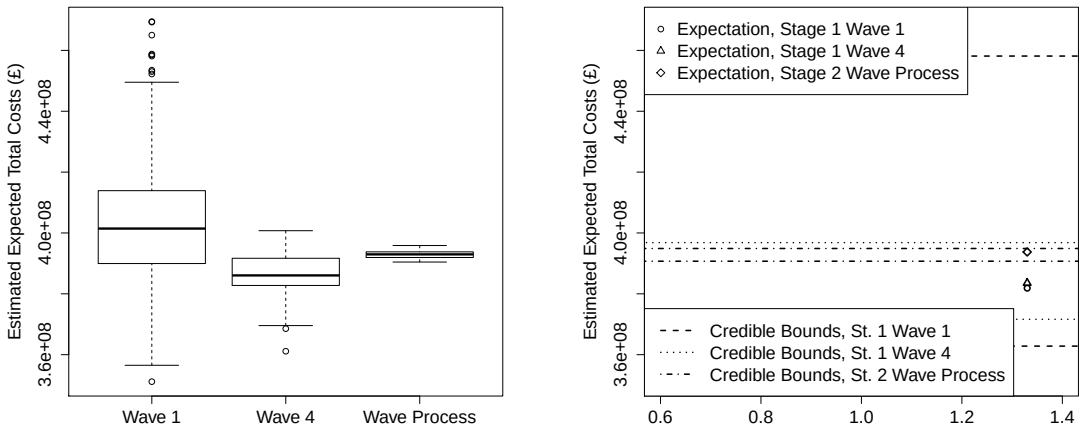

(a) Boxplots. (b) Credible Intervals.

Figure 8.36: Plots to compare the estimates of expected stage 2 costs for θ_4.

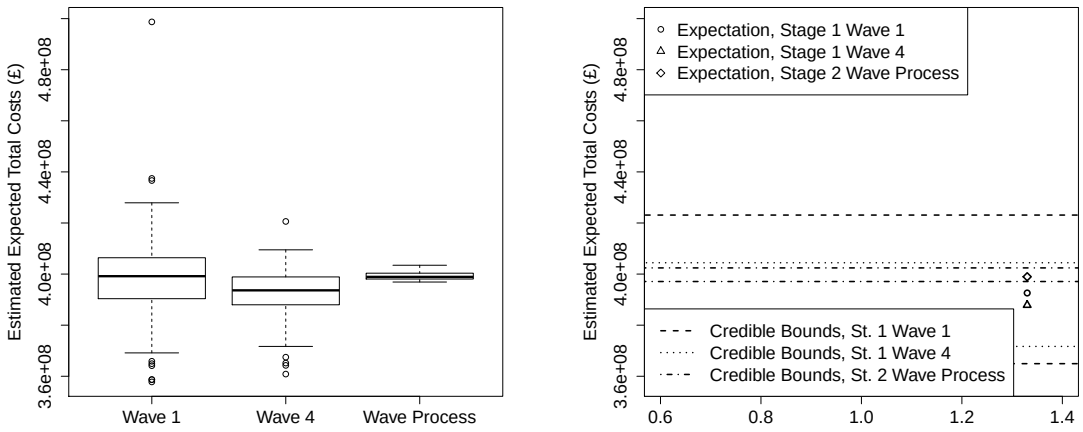

(a) Boxplots.

(b) Credible Intervals.

Figure 8.37: Plots to compare the estimates of expected stage 2 costs for θ_5.

Chapter 9

A General Methodology for M-Stage Decision Making, Using Emulation and Backwards Induction

The previous chapter considered how transmission expansion decisions are generally made over a number of consecutive stages. However, Section 8.2.2 noted the difficulty in calculating costs across all future stages as a function of the stage 1 decision only when using continuous variables to model the potential state of the future power system.

A solution to this when making decisions over 2 stages was presented in Section 8.2.4, using a combination of emulation and backwards induction. This chapter will consider expanding the methodology of Section 8.2.4 to provide a methodological framework for a general M-stage decision problem, and will present an application of this methodology to a three stage transmission expansion planning problem detailed in Section 9.2.

9.1 M-Stage Methodology

9.1.1 Preliminary Modelling Information

As in Section 8.2.4, $f_{c,1}(\mathbf{v}_1, \mathbf{d}_1)$ is the simulator which calculates mean constraint costs in stage 1 for variables containing uncertainty, $\mathbf{v}_1$, and decision variables, $\mathbf{d}_1$. For the M stage problem, the simulator $f_{c,m}(\mathbf{v}_m, \mathbf{d}_m|\mathbf{d}_{T_{m-1}})$ calculates mean constraint costs in stage m for variables which contain uncertainty, $\mathbf{v}_m$, and decision variables, $\mathbf{d}_m$, in stage m when total reinforcement $\mathbf{d}_{T_{m-1}}$ was made in the previous $m-1$ stages.

Emulator models are constructed to approximate the simulator in each stage as detailed in Section 5.2, such that $\tilde{f}_{c,1}(\mathbf{v}_1, \mathbf{d}_1)$ is the fitted emulator model which approximates $f_{c,1}(\mathbf{v}_1, \mathbf{d}_1)$, and $\tilde{f}_{c,m}(\mathbf{v}_m, \mathbf{d}_m|\mathbf{d}_{T_{m-1}})$ is the fitted emulator model which approximates $f_{c,m}(\mathbf{v}_m, \mathbf{d}_m|\mathbf{d}_{T_{m-1}})$.

Note, for the transmission expansion problem considered in this thesis, it is sufficient to work with $\mathbf{d}_{T_{m-1}}$ as the total reinforcement made before stage m, and the not the individual reinforcements of stages 1 to $m-1$, i.e. $\mathbf{d}_1, ..., \mathbf{d}_{m-1}$. This is quite a useful simplification, as it means the emulator models fitted in each stage, $\tilde{f}_{c,m}(\mathbf{v}_m, \mathbf{d}_m|\mathbf{d}_{T_{m-1}})$, are fitted over fewer variables. This should allow for more accurate emulator models to be fitted in each stage and also makes the problem more tractable when considering a large number of decision stages, as the number of variables used to fit the emulator model in each stage does not grow with the number of stages considered.

However, the methodology detailed in the next subsection is otherwise written in general terms and Section 9.1.3 will note how the methodology can be extended to multi-stage decision problems where the reinforcement in each of the previous stages, i.e. $\mathbf{d}_1, ..., \mathbf{d}_{m-1}$, must be considered and not just the total reinforcement in the previous $m-1$ stages, $\mathbf{d}_{T_{m-1}}$.

9.1.2 Estimating Expected Total Costs Across M Stages

Overview of the Methodology

As an overview of the methodology that will be presented, backwards induction will again be used as the basis for estimating expected total costs across all M stages as a

function of stage 1 decision only. Just as in Section 8.2.4, this requires first considering the expected costs in the final stage (stage M). To do this, optimal stage M decisions are estimated for a sample of total reinforcements in stages 1 to $M-1$, $\mathbf{d}_{T_{M-1}}$, and stage M scenarios, $\boldsymbol{\psi}_M$. The resulting estimates of expected total costs in stage M are then used as a set of training runs to fit an emulator model, $\tilde{G}_{T,M,\boldsymbol{\psi}_M}(\mathbf{d}_{T_{M-1}}, \boldsymbol{\psi}_M)$, to approximate how expected total costs in stage M vary as a function of total reinforcement in the previous $M-1$ stages and stage M scenario only.

An iterative approach is then taken, starting at stage $M-1$ and working backwards to stage 1, where at each stage (stage m) optimal decisions to be made in stage m are estimated for a sample of total reinforcements up to stage $m-1$, $\mathbf{d}_{T_{m-1}}$, and stage m scenarios, $\boldsymbol{\psi}_m$. The resulting estimates of expected total costs in stages m to M of such decisions are subsequently used as a set of training runs to fit an emulator model, $\tilde{G}_{T,m,\boldsymbol{\psi}_m}(\mathbf{d}_{T_{m-1}}, \boldsymbol{\psi}_m)$, to approximate how expected total costs in stage m onwards vary as a function of total reinforcement up to stage $m-1$ and stage m scenario.

Performing the iterative procedure eventually leads to expected total costs across all stages being estimated as a function of stage 1 decision and stage 1 scenario only. An estimate of the optimal stage 1 decision can then be identified as the decision which minimises such an estimate.

Estimating Expected Total Costs in Stage M

Expected mean constraint costs under uncertainty in stage M can be estimated by integrating the product of the emulator model of stage M mean constraint costs and the PDF which describes the beliefs about the variables which contain uncertainty in stage M as

$$\tilde{F}_{c,M}(\mathbf{d}_M|\mathbf{d}_{T_{M-1}}, \boldsymbol{\psi}_M) = \int_{\mathbf{v}_M} \tilde{f}_{c,M}(\mathbf{v}_M, \mathbf{d}_M|\mathbf{d}_{T_{M-1}}) \times p(\mathbf{v}_M|\boldsymbol{\psi}_M)\mathrm{d}\mathbf{v}_M \tag{9.1.1}$$

where $\tilde{f}_{c,M}(\mathbf{v}_M, \mathbf{d}_M|\mathbf{d}_{T_{M-1}})$ is the emulator model which approximates the simulator of stage M constraint costs and $p(\mathbf{v}_M|\boldsymbol{\psi}_M)$ represents beliefs about uncertainty in stage M for a given value of $\boldsymbol{\psi}_M$. As was noted in Section 8.2.1, $\boldsymbol{\psi}_M$ is a vector of variables which describe the stage M scenario (observed state of the power system background at the time the Mth decision is made) in some way by detailing what was

cumulatively observed about the power system in the previous $M-1$ stages in some way (for example, it could be the cumulative observed value of peak demand between stages 1 and $M-1$). The estimated expected total costs (expected mean constraint costs plus reinforcement costs) in stage M can then be calculated as

$$\tilde{F}_{T,M}(\mathbf{d}_M|\mathbf{d}_{T_{M-1}},\boldsymbol{\psi}_M) = \tilde{F}_{c,M}(\mathbf{d}_M|\mathbf{d}_{T_{M-1}},\boldsymbol{\psi}_M) + f_{\rho,M}(\mathbf{d}_M|\mathbf{d}_{T_{M-1}},\boldsymbol{\psi}_M) \qquad (9.1.2)$$

where $f_{\rho,M}(\mathbf{d}_M|\mathbf{d}_{T_{M-1}},\boldsymbol{\psi}_M)$ calculates the reinforcement costs of decision $\mathbf{d}_M$ given that the total reinforcement made in stages 1 to $M-1$ is $\mathbf{d}_{T_{M-1}}$ and scenario $\boldsymbol{\psi}_M$ is observed in stage M. As was the case for the two stage problem, $f_{\rho,M}(\mathbf{d}_M|\mathbf{d}_{T_{M-1}},\boldsymbol{\psi}_M)$ can be simplified to $f_{\rho,M}(\mathbf{d}_M|\mathbf{d}_{T_{M-1}})$ if the cost of reinforcement does not depend on the scenario observed.

Estimating Expected Total Costs in Stage M as a Function of Stage M Scenario and Total Reinforcement up to Stage $M-1$ Only

A model is then required to estimate how expected total costs in stage M vary as a function of stage M scenario and total reinforcement up to stage $M-1$ only, just as how the methodology of Section 8.2.4 fitted a model to estimate expected total stage 2 costs as a function of stage 1 decision only. This model is fitted by taking a random sample of N_{θ_M} total reinforcements by stage $M-1$ (values of $\mathbf{d}_{T_{M-1}}$) and stage M scenarios (values of $\boldsymbol{\psi}_M$) taken from all possible stage $M-1$ total reinforcement decisions being considered and all possible stage M scenarios that can occur. This gives a random sample of stage $M-1$ total reinforcement decisions as $\mathbf{d}_{T_{M-1},\theta_{i,M}}$ and stage M scenarios as $\boldsymbol{\psi}_{M,\theta_{i,M}}$ for $i = 1, ..., N_{\theta_M}$.

For each total reinforcement in stage $M-1$ and stage M scenario in the sample, the optimal decision to be made in stage M is then estimated by minimising Equation 9.1.2 (i.e. minimising the estimate of expected total costs in stage M for the given stage $M-1$ total reinforcement and stage M scenario), such that $\mathbf{d}_{M|\theta_{i,M}}$ is the estimated optimal decision to be made in stage M, when total reinforcement $\mathbf{d}_{T_{M-1},\theta_{i,M}}$ is made up to stage $M-1$ and scenario $\boldsymbol{\psi}_{M,\theta_{i,M}}$ is observed in stage M. The estimate of expected total stage M costs of such a decision can then be calculated as the resulting

evaluation of Equation 9.1.2, such that

$$\tilde{F}_{T,M,\theta_{i,M}} = \tilde{F}_{T,M}(\mathbf{d}_{M|\theta_{i,M}}|\mathbf{d}_{T_{M-1},\theta_{i,M}}, \boldsymbol{\psi}_{M,\theta_{i,M}}) \tag{9.1.3}$$

is the estimate of expected total costs that arise in stage M based on total reinforcement $\mathbf{d}_{T_{M-1},\theta_{i,M}}$ being made up until stage $M-1$; $\boldsymbol{\psi}_{M,\theta_{i,M}}$ being observed in stage M and the estimated optimal decision $\mathbf{d}_{M|\theta_{i,M}}$ being made in stage M.

The estimates of expected total costs in stage M, $\tilde{F}_{T,M,\theta_{i,M}}$, for the N_{θ_M} sampled values of total reinforcement made up to stage $M-1$, $\mathbf{d}_{T_{M-1},\theta_{i,M}}$, and stage M scenario, $\boldsymbol{\psi}_{M,\theta_{i,M}}$, can then be used as a set of N_{θ_M} training runs to fit an emulator model, $\tilde{G}_{T,M,\boldsymbol{\psi}_M}(\mathbf{d}_{T_{M-1}}, \boldsymbol{\psi}_M)$, which models how expected total costs in stage M vary as a function of total reinforcement in the previous $M-1$ stages, $\mathbf{d}_{T_{M-1}}$, and stage M scenario, $\boldsymbol{\psi}_M$, only.

For the two stage example of Section 8.2.4, the probability of observing a particular value of stage 2 scenario, $\boldsymbol{\psi}_2$, when the second decision was to be made was given by $p_{\boldsymbol{\psi}_{2|1}}(\boldsymbol{\psi}_2)$. However, for the M stage problem it is reasonable to assume that the probability of observing a particular stage m scenario (i.e. observing the values of $\boldsymbol{\psi}_m$) will depend on what was observed in the previous stage (i.e. the values of $\boldsymbol{\psi}_{m-1}$) for $1 < m \leq M$. This implies that the estimate of expected total costs of stage M in terms of stage $M-1$ scenario and decisions up to stage $M-1$ only can be acquired as

$$\tilde{G}_{T,M,\boldsymbol{\psi}_{M-1}}(\mathbf{d}_{T_{M-1}}, \boldsymbol{\psi}_{M-1}) = \int_{\boldsymbol{\psi}_M} \tilde{G}_{T,M,\boldsymbol{\psi}_M}(\mathbf{d}_{T_{M-1}}, \boldsymbol{\psi}_M) \times p_{\boldsymbol{\psi}_{M|M-1}}(\boldsymbol{\psi}_M|\boldsymbol{\psi}_{M-1}) \mathrm{d}\boldsymbol{\psi}_M \tag{9.1.4}$$

where $p_{\boldsymbol{\psi}_{M|M-1}}(\boldsymbol{\psi}_M|\boldsymbol{\psi}_{M-1})$ is the probability of observing scenario $\boldsymbol{\psi}_M$ in stage M given that scenario $\boldsymbol{\psi}_{M-1}$ was observed in stage $M-1$.

Estimating Expected Total Costs for a General Stage m Onwards

For a general stage m, where $1 < m < M$, expected mean constraint costs in stage m can be estimated as

$$\tilde{F}_{c,m}(\mathbf{d}_m|\mathbf{d}_{T_{m-1}}, \boldsymbol{\psi}_m) = \int_{\mathbf{v}_m} \tilde{f}_{c,m}(\mathbf{v}_m, \mathbf{d}_m|\mathbf{d}_{T_{m-1}}) \times p(\mathbf{v}_m|\boldsymbol{\psi}_m) \mathrm{d}\mathbf{v}_m \tag{9.1.5}$$

where $\tilde{f}_{c,m}(\mathbf{v}_m, \mathbf{d}_m|\mathbf{d}_{T_{m-1}})$ is the emulator model which approximates the simulator of constraint costs in stage m; $\boldsymbol{\psi}_m$ describes the scenario observed in the mth stage; $p(\mathbf{v}_m|\boldsymbol{\psi}_m)$ represents beliefs about variables containing uncertainty in stage m given that the scenario described by $\boldsymbol{\psi}_m$ was observed and that total reinforcement $\mathbf{d}_{T_{m-1}}$ was made in stages 1 to $m-1$.

Estimates for expected total costs beyond stage m (i.e. in stages $m+1$ to M) can be calculated as

$$\tilde{G}_{T,m+1,\boldsymbol{\psi}_m}(\mathbf{d}_{T_m}, \boldsymbol{\psi}_m) = \int_{\boldsymbol{\psi}_{m+1}} \tilde{G}_{T,m+1,\boldsymbol{\psi}_{m+1}}(\mathbf{d}_{T_m}, \boldsymbol{\psi}_{m+1}) \times p_{\boldsymbol{\psi}_{m+1|m}}(\boldsymbol{\psi}_{m+1}|\boldsymbol{\psi}_m)\mathrm{d}\boldsymbol{\psi}_{m+1} \tag{9.1.6}$$

where $p_{\boldsymbol{\psi}_{m+1|m}}(\boldsymbol{\psi}_{m+1}|\boldsymbol{\psi}_m)$ is the probability of observing scenario $\boldsymbol{\psi}_{m+1}$ in stage $m+1$ given that scenario $\boldsymbol{\psi}_m$ was observed in stage m, and $\mathbf{d}_{T_m}$ is calculated as the reinforcement made in stage m, $\mathbf{d}_m$, plus the reinforcement made in the previous $m-1$ stages, $\mathbf{d}_{T_{m-1}}$, i.e.

$$\mathbf{d}_{T_m} = \mathbf{d}_m + \mathbf{d}_{T_{m-1}}$$

An estimate for expected total costs for stage m onwards (i.e. stages m to M) can then be calculated as

$$\tilde{F}_{T,m}(\mathbf{d}_m|\mathbf{d}_{T_{m-1}}, \boldsymbol{\psi}_m) = \tilde{F}_{c,m}(\mathbf{d}_m|\mathbf{d}_{T_{m-1}}, \boldsymbol{\psi}_m) + f_{\rho,m}(\mathbf{d}_m|\mathbf{d}_{T_{m-1}}, \boldsymbol{\psi}_m) + \tilde{G}_{T,m+1,\boldsymbol{\psi}_m}(\mathbf{d}_{T_m}, \boldsymbol{\psi}_m) \tag{9.1.7}$$

where $f_{\rho,m}(\mathbf{d}_m|\mathbf{d}_{T_{m-1}}, \boldsymbol{\psi}_m)$ are the reinforcement costs of making decision $\mathbf{d}_m$ in stage m given that the total reinforcement in the previous stages was $\mathbf{d}_{T_{m-1}}$ and that $\boldsymbol{\psi}_m$ describes the observed scenario when the mth decision is made.

Estimating Expected Total Costs for a General Stage m Onwards as a Function of Stage m scenario and Total Reinforcement Up to Stage $m-1$ Only

An emulator model is then fitted to estimate expected total costs in stages m to M in terms of the total reinforcement by stage $m-1$ and stage m scenario only. This model is fitted by taking a random sample of N_{θ_m} total reinforcements by stage $m-1$ (values of $\mathbf{d}_{T_{m-1}}$) and stage m scenarios (values of $\boldsymbol{\psi}_m$) taken from all possible total reinforcement decisions being considered and all possible stage m scenarios that can

occur. This gives a random sample of total reinforcements up to and including stage $m-1$ as $\mathbf{d}_{T_{m-1},\theta_{i,m}}$ and stage m scenarios as $\boldsymbol{\psi}_{m,\theta_{i,m}}$ for $i = 1, ..., N_{\theta_m}$.

For each total reinforcement in stage $m-1$ and stage m scenario in the sample, the optimal decision to be made in stage m is then estimated by minimising Equation 9.1.7 (i.e. minimising the estimate of expected total costs in stage m onwards for the given stage $m-1$ total reinforcement and stage m scenario), such that $\mathbf{d}_{m|\theta_{i,m}}$ is the estimate of the optimal decision to be made in stage m, when total reinforcement decision $\mathbf{d}_{T_{m-1},\theta_{i,m}}$ is made up to stage $m-1$ and scenario $\boldsymbol{\psi}_{m,\theta_{i,m}}$ is observed in stage m. The estimate of expected total costs in stage m onwards of such a decision can then be calculated as the resulting evaluation of Equation 9.1.7, such that

$$\tilde{F}_{T,m,\theta_{i,m}} = \tilde{F}_{T,m}(\mathbf{d}_{m|\theta_{i,m}}|\mathbf{d}_{T_{m-1},\theta_{i,m}}, \boldsymbol{\psi}_{m,\theta_{i,m}}) \tag{9.1.8}$$

is the estimate of expected total costs that arise in stage m onwards based on total reinforcement $\mathbf{d}_{T_{m-1},\theta_{i,m}}$ being made up until stage $m-1$; $\boldsymbol{\psi}_{m,\theta_{i,m}}$ being observed in stage m and the estimated optimal decision $\mathbf{d}_{m|\theta_{i,m}}$ being made in stage m.

The estimates of expected total costs in stage m onwards, $\tilde{F}_{T,m,\theta_{i,m}}$, for the N_{θ_m} sampled values of total reinforcement made up to stage $m-1$, $\mathbf{d}_{T_{m-1},\theta_{i,m}}$, and stage m scenario, $\boldsymbol{\psi}_{m,\theta_{i,m}}$, can then be used as a set of N_{θ_m} training runs which are used to fit an emulator model, $\tilde{G}_{T,m,\boldsymbol{\psi}_m}(\mathbf{d}_{T_{m-1}}, \boldsymbol{\psi}_m)$, which models how expected total costs in stage m onwards vary as a function of total reinforcement in the previous $m-1$ stages, $\mathbf{d}_{T_{m-1}}$, and stage m scenario, $\boldsymbol{\psi}_m$, only.

This is performed for every stage beginning at stage $M-1$ and iteratively working backwards until eventually $\tilde{G}_{T,2,\boldsymbol{\psi}_2}(\mathbf{d}_1, \boldsymbol{\psi}_2)$ is fitted to model expected total costs in stage 2 onwards as a function of stage 1 decision, $\mathbf{d}_1$, and stage 2 scenario, $\boldsymbol{\psi}_2$, only.

Estimating Expected Total Costs Across All M Stages as a Function of Stage 1 Decision Only

Expected total costs for stage 2 onwards as a function of stage 1 decision, $\mathbf{d}_1$, and stage 1 scenario, $\boldsymbol{\psi}_1$, only can then be estimated as

$$\tilde{G}_{T,2,\boldsymbol{\psi}_1}(\mathbf{d}_1, \boldsymbol{\psi}_1) = \int_{\boldsymbol{\psi}_2} \tilde{G}_{T,2,\boldsymbol{\psi}_2}(\mathbf{d}_1, \boldsymbol{\psi}_2) \times p_{\boldsymbol{\psi}_{2|1}}(\boldsymbol{\psi}_2|\boldsymbol{\psi}_1)\mathrm{d}\boldsymbol{\psi}_2 \tag{9.1.9}$$

where $p_{\psi_{2|1}}(\boldsymbol{\psi}_2|\boldsymbol{\psi}_1)$ are the prior beliefs about observing scenario $\boldsymbol{\psi}_2$ in stage 2 given that $\boldsymbol{\psi}_1$ describes the stage 1 scenario (state of the power system in stage 1).

An estimate of expected mean constraint costs in the first stage can then be calculated as

$$\tilde{F}_{c,1}(\mathbf{d}_1|\boldsymbol{\psi}_1) = \int_{\mathbf{v}_1} \tilde{f}_{c,1}(\mathbf{v}_1, \mathbf{d}_1) \times p(\mathbf{v}_1|\boldsymbol{\psi}_1)\mathrm{d}\mathbf{v}_1 \tag{9.1.10}$$

where $\tilde{f}_{c,1}(\mathbf{v}_1, \mathbf{d}_1)$ is the emulator model which approximates the simulator of stage 1 constraint costs and $p(\mathbf{v}_1|\boldsymbol{\psi}_1)$ are the prior beliefs about the values of the uncertain variables in stage 1 for a given state of the stage 1 power system, $\boldsymbol{\psi}_1$.

Expected total cost across all stages as a function of stage 1 decision and stage 1 scenario only can then be estimated as

$$\tilde{G}_T(\mathbf{d}_1, \boldsymbol{\psi}_1) = \tilde{F}_{c,1}(\mathbf{d}_1|\boldsymbol{\psi}_1) + f_{\rho,1}(\mathbf{d}_1|\boldsymbol{\psi}_1) + \tilde{G}_{T,2,\boldsymbol{\psi}_1}(\mathbf{d}_1, \boldsymbol{\psi}_1) \tag{9.1.11}$$

where $f_{\rho,1}(\mathbf{d}_1|\boldsymbol{\psi}_1)$ represents the reinforcement costs of making decision $\mathbf{d}_1$ in stage 1 for a given observed state of the stage 1 power system, $\boldsymbol{\psi}_1$.

The decision, $\mathbf{d}_1$, which minimises Equation 9.1.11 is the estimate for the optimal decision to be made in stage 1, which minimises the estimate of expected total costs across stage 1 and all future stages. When the time comes to make the first decision, it is reasonable to assume that the stage 1 scenario, detailed by $\boldsymbol{\psi}_1$, is known. Therefore, it is not necessary to include such a parameter in Equation 9.1.11. However, the inclusion of $\boldsymbol{\psi}_1$ in Equation 9.1.11 allows the methodology of this section to generalise to estimating optimal decisions for stages 2 to M as follows.

After the first decision has been made, time will pass and eventually the second decision must be made for the state of the power system, $\boldsymbol{\psi}_2$, that has been observed when the second decision is to be made. The methodology of this section can be used to make such a decision, by treating the problem as an $M-1$ stage problem, where each stage m for $2 \leq m \leq M$ is treated as stage $m-1$ and solving the resulting $M-1$ stage problem. This can then be applied when the third decision is required, by treating stage m as stage $m-2$ for $3 \leq m \leq M$ and solving the resulting $M-2$ stage problem, and for every future stage by identifying the optimal mth decision via an $M-(m-1)$ stage problem.

9.1.3 Further Considerations Regarding the Methodology of Section 9.1.2

Generalising the Methodology to Problems Where it is Insufficient to Consider Only the Total Reinforcement of the Previous $M-1$ Stages

As was noted in Section 9.1.1, for the transmission expansion problem considered in this thesis, it is sufficient to work with $\mathbf{d}_{T_{m-1}}$ as the total reinforcement made before stage m, and the not the individual reinforcements of stages 1 to $m-1$. This means that the emulator models fitted to approximate the simulator in each stage, $\tilde{f}_{c,m}(\mathbf{v}_m, \mathbf{d}_m|\mathbf{d}_{T_{m-1}})$, and the emulators fitted to model expected total costs in stage m onwards as a function of total reinforcement up to stage $m-1$ and stage m scenario only, $\tilde{G}_{T,m,\boldsymbol{\psi}_m}(\mathbf{d}_{T_{m-1}}, \boldsymbol{\psi}_m)$, are fitted over fewer variables, which in turn should allow for more accurate models to be fitted.

For a more general problem, it may be necessary to model costs in stage m onwards as a function of the decisions in each of the previous $m-1$ stages, i.e. $\mathbf{d}_1, ..., \mathbf{d}_{m-1}$, and not the total reinforcement before stage m, $\mathbf{d}_{T_{m-1}}$. This would lead to the models $\tilde{f}_{c,m}(\mathbf{v}_m, \mathbf{d}_m|\mathbf{d}_1, ..., \mathbf{d}_{m-1})$ and $\tilde{G}_{T,m,\boldsymbol{\psi}_m}(\mathbf{d}_1, ..., \mathbf{d}_{m-1}, \boldsymbol{\psi}_m)$ being fitted in place of $\tilde{f}_{c,m}(\mathbf{v}_m, \mathbf{d}_m|\mathbf{d}_{T_{m-1}})$ and $\tilde{G}_{T,m,\boldsymbol{\psi}_m}(\mathbf{d}_{T_{m-1}}, \boldsymbol{\psi}_m)$ respectively. The methodology of the previous subsection would otherwise be unchanged. However, as was noted in Section 9.1.1, this may make the problem less tractable when considering problems with a large number of decision stages, with multiple decisions to be made in each stage, as the emulator models fitted in later stages will be fitted over a large number of variables, with it likely being the case that each of the decisions from each of the previous stages has a non-negligible effect on cost estimates.

Specification of the Decisions Considered in Each Stage

Another point of consideration is that for the transmission expansion problem considered in this thesis, the only constraint on the possible reinforcement decisions that can be made in stage m is that the total reinforcement of each boundary after the mth reinforcement decision must be at least as large as the total reinforcement made in the previous $m-1$ stages, i.e. the only constraint on the mth decision, $\mathbf{d}_m$, is that

$\mathbf{d}_m$ is non-negative. This means that it is sufficient to specify the initial ranges of decisions considered in each stage by specifying minimum and maximum values of the total reinforcement after the mth decision, $\mathbf{d}_{T_m}$, for $1 \leq m \leq M$.

However, in a more general problem it could be that the decisions made in the previous $m-1$ stages, i.e. $\mathbf{d}_1, ..., \mathbf{d}_{m-1}$, have a less trivial effect on the possible stage m decisions available, and making or not making certain decisions in the previous $m-1$ stages may restrict which decisions are available to be made in stage m. Such examples would therefore require a further specification of the decisions available to be made in stage m conditional on the previous $m-1$ decisions. As the methodology of Section 9.1.2 is written in general terms it could still be used for such problems, given a suitable specification of the decisions available in each stage.

Further Consideration Regarding the Specification of Prior Beliefs of Uncertainties in Each Stage

It is noted that as part of the methodology of Section 9.1.2, it is sufficient to express beliefs about the values of the variables which contain uncertainty in stage m, $\mathbf{v}_m$, conditional on the observed state of the power system at the time the mth decision is made, $\boldsymbol{\psi}_m$, i.e. it is sufficient to specify $p(\mathbf{v}_m|\boldsymbol{\psi}_m)$. It would be possible to calculate an explicit statement for $p(\mathbf{v}_m|\boldsymbol{\psi}_1)$, the prior beliefs about the uncertainty in stage m at the time the first decision is made, by calculating the marginal distribution across all possible future scenarios as

$$p(\mathbf{v}_m|\boldsymbol{\psi}_1) = \int_{\boldsymbol{\psi}_m} ... \int_{\boldsymbol{\psi}_3} \int_{\boldsymbol{\psi}_2} p(\mathbf{v}_m|\boldsymbol{\psi}_m) p_{\boldsymbol{\psi}_{m|m-1}}(\boldsymbol{\psi}_m|\boldsymbol{\psi}_{m-1}) ... p_{\boldsymbol{\psi}_{3|2}}(\boldsymbol{\psi}_3|\boldsymbol{\psi}_2) p_{\boldsymbol{\psi}_{2|1}}(\boldsymbol{\psi}_2|\boldsymbol{\psi}_1) \mathrm{d}\boldsymbol{\psi}_2 \mathrm{d}\boldsymbol{\psi}_3 ... \mathrm{d}\boldsymbol{\psi}_m \tag{9.1.12}$$

but the explicit calculation is never required.

Although this explicit calculation is never required for the multi-stage decision problem, Section 8.6 of Chapter 8 did explicitly calculate $p(\mathbf{v}_2|\boldsymbol{\psi}_1)$ for the two stage problem detailed in Section 8.3, in order to give a comparison of how reinforcement decisions would vary if only the first opportunity for reinforcement was available.

Calculating $p(\mathbf{v}_m|\boldsymbol{\psi}_1)$ explicitly for $m = 2, ..., M$ could also act as a preliminary diagnostic test to ensure that the specifications of $p(\mathbf{v}_m|\boldsymbol{\psi}_m)$ and $p_{\boldsymbol{\psi}_{2|1}}(\boldsymbol{\psi}_2|\boldsymbol{\psi}_1)$ to $p_{\boldsymbol{\psi}_{m|m-1}}(\boldsymbol{\psi}_m|\boldsymbol{\psi}_{m-1})$ accurately describe prior beliefs about uncertainties in each stage.

Further Consideration Regarding the Specification of Prior Beliefs of the Observed Scenario in Each Stage

Further, just as it is not necessary to explicitly specify $p(\mathbf{v}_m|\boldsymbol{\psi}_1)$, it is not necessary to explicitly state prior beliefs at the beginning of stage 1 for the scenario that will be observed in stage m, i.e. it is not necessary to explicitly state $p_{\boldsymbol{\psi}_{m|1}}(\boldsymbol{\psi}_m|\boldsymbol{\psi}_1)$, with the exception of $m = 2$. However, just as it would be possible to calculate $p(\mathbf{v}_m|\boldsymbol{\psi}_1)$ via Equation 9.1.12, it would be possible to calculate $p_{\boldsymbol{\psi}_{m|1}}(\boldsymbol{\psi}_m|\boldsymbol{\psi}_1)$ explicitly as

$$p_{\boldsymbol{\psi}_{m|1}}(\boldsymbol{\psi}_m|\boldsymbol{\psi}_1) = \int_{\boldsymbol{\psi}_{m-1}} ... \int_{\boldsymbol{\psi}_3} \int_{\boldsymbol{\psi}_2} p_{\boldsymbol{\psi}_{m|m-1}}(\boldsymbol{\psi}_m|\boldsymbol{\psi}_{m-1})...p_{\boldsymbol{\psi}_{3|2}}(\boldsymbol{\psi}_3|\boldsymbol{\psi}_2)p_{\boldsymbol{\psi}_{2|1}}(\boldsymbol{\psi}_2|\boldsymbol{\psi}_1)\mathrm{d}\boldsymbol{\psi}_2\mathrm{d}\boldsymbol{\psi}_3...\mathrm{d}\boldsymbol{\psi}_{m-1} \tag{9.1.13}$$

Similarly, for the methodology described in Section 9.1.2, a joint distribution for what will be observed in each stage (i.e. a joint distribution for $\boldsymbol{\psi}_1$ to $\boldsymbol{\psi}_M$) does not need to be explicitly specified, but one could easily be calculated as

$$p(\boldsymbol{\psi}_1, \boldsymbol{\psi}_2, ..., \boldsymbol{\psi}_{M-1}, \boldsymbol{\psi}_M) = p_{\boldsymbol{\psi}_1}(\boldsymbol{\psi}_1)p_{\boldsymbol{\psi}_{2|1}}(\boldsymbol{\psi}_2|\boldsymbol{\psi}_1)...p_{\boldsymbol{\psi}_{M-1|M-2}}(\boldsymbol{\psi}_{M-1}|\boldsymbol{\psi}_{M-2})p_{\boldsymbol{\psi}_{M|M-1}}(\boldsymbol{\psi}_M|\boldsymbol{\psi}_{M-1}) \tag{9.1.14}$$

9.1.4 The M-Stage Wave Process

Section 8.2.6 detailed how to estimate credible bounds for the estimate of expected total costs across both stages for the 2 stage problem, by first forming credible bounds $\tilde{G}_{T,2,\boldsymbol{\psi}_2,L}(\mathbf{d}_1, \boldsymbol{\psi}_2)$ and $\tilde{G}_{T,2,\boldsymbol{\psi}_2,U}(\mathbf{d}_1, \boldsymbol{\psi}_2)$ for the expected total costs in the second stage, then using these credible bounds to form credible bounds for the estimate of expected total costs across both stages as a function of the stage 1 decision only. This section will detail how this methodology can be adapted to estimate credible bounds for the estimates of expected total costs across all M stages of the M-Stage problem.

Forming Credible Bounds for Expected Total Costs in Stage M

As the estimate of expected total costs in stage m onwards is dependent on the expected total costs in stage $m+1$ onwards, to form credible intervals for the estimated expected total costs across all M stages it is necessary to first consider the error in the estimate of total costs in stage M and iteratively work backwards (just as when estimating an expectation for total costs across all M stages). This requires the methodology of Section 5.2.6 to be adapted to model variation in $\tilde{f}_{c,M}(\mathbf{v}_M, \mathbf{d}_M|\mathbf{d}_{T_{M-1}})$. A very brief recap of how this is applied (as was given in Section 8.2.6), model parameters for the polynomial portion of the emulator are modelled as following a normal distribution with mean $\hat{\boldsymbol{\beta}}$ and covariance matrix $cov(\hat{\boldsymbol{\beta}})$. Random variations of these model parameters, $\hat{\boldsymbol{\beta}}_r$, can be drawn from this normal distribution and a new Gaussian process model fitted to smooth the resulting residuals of the polynomial portion of the emulator when using $\hat{\boldsymbol{\beta}}_r$ instead of $\hat{\boldsymbol{\beta}}$. $\tilde{f}_{c,M,r}(\mathbf{v}_M, \mathbf{d}_M|\mathbf{d}_{T_{M-1}})$ can then be used as a randomly drawn variation of $\tilde{f}_{c,M}(\mathbf{v}_M, \mathbf{d}_M|\mathbf{d}_{T_{M-1}})$ when using $\hat{\boldsymbol{\beta}}_r$ as the parameters of the polynomial portion of the emulator and the resulting Gaussian process model. These randomly drawn models can then be used in Equation 9.1.2 to randomly draw estimates for $\tilde{F}_{T,M,\theta_{i,M}}$ (the estimate of expected total costs in stage M when making the estimated optimal stage M decision, $\mathbf{d}_{M|\theta_{i,M}}$, in stage M, given that total reinforcement $\mathbf{d}_{T_{M-1},\theta_{i,M}}$ was made in the previous $M-1$ stages and that scenario $\boldsymbol{\psi}_{M,\theta_{i,M}}$ is observed when the Mth decision is made) as

$$\tilde{F}_{T,M,\theta_{i,M},r} = \tilde{F}_{c,M,r}(\mathbf{d}_{M|\theta_{i,M}}|\mathbf{d}_{T_{M-1},\theta_{i,M}}, \boldsymbol{\psi}_{M,\theta_{i,M}}) + f_{\rho,M}(\mathbf{d}_{M|\theta_{i,M}}|\mathbf{d}_{T_{M-1},\theta_{i,M}}, \boldsymbol{\psi}_{M,\theta_{i,M}}) \tag{9.1.15}$$

where

$$\tilde{F}_{c,M,r}(\mathbf{d}_{M|\theta_{i,M}}|\mathbf{d}_{T_{M-1},\theta_{i,M}}, \boldsymbol{\psi}_{M,\theta_{i,M}}) = \int_{\mathbf{v}_M} \tilde{f}_{c,M,r}(\mathbf{v}_M, \mathbf{d}_{M|\theta_{i,M}}|\mathbf{d}_{T_{M-1},\theta_{i,M}}) \times p(\mathbf{v}_M|\boldsymbol{\psi}_{M,\theta_{i,M}}) \mathrm{d}\mathbf{v}_M \tag{9.1.16}$$

Credible intervals for $\tilde{F}_{T,M,\theta_{i,M}}$ can then be estimated using the methodology of Section 5.2.6, such that if an $\alpha\%$ credible interval is desired a lower bound is formed as the value which $\frac{100-\alpha}{2}\%$ of the $\tilde{F}_{T,M,\theta_{i,M},r}$ are smaller than, and the upper bound as the value which $\frac{100-\alpha}{2}\%$ of the $\tilde{F}_{T,M,\theta_{i,M},r}$ are greater than. These lower and upper bounds

are denoted by $\tilde{F}_{T,M,\theta_{i,M},L}$ and $\tilde{F}_{T,M,\theta_{i,M},U}$ respectively.

Recall that the methodology of Section 9.1.2 used the values of $\tilde{F}_{T,M,\theta_{i,M}}$ as a set of N_{θ_M} training runs in order to fit an emulator model, $\tilde{G}_{T,M,\boldsymbol{\psi}_M}(\mathbf{d}_{T_{M-1}}, \boldsymbol{\psi}_M)$, of how expected total stage M costs vary as a function of total reinforcement until stage $M-1$, $\mathbf{d}_{T_{M-1}}$, and stage M scenario, $\boldsymbol{\psi}_M$, only. Similarly, the values of $\tilde{F}_{T,M,\theta_{i,M},L}$ and $\tilde{F}_{T,M,\theta_{i,M},U}$ can be used as two sets of N_{θ_M} training runs which can be used to fit respective emulator models of how lower and upper bounds of the expected total costs in stage M vary as a function of $\mathbf{d}_{T_{M-1}}$ and $\boldsymbol{\psi}_M$ only, such that $\tilde{G}_{T,M,\boldsymbol{\psi}_M,L}(\mathbf{d}_{T_{M-1}}, \boldsymbol{\psi}_M)$ and $\tilde{G}_{T,M,\boldsymbol{\psi}_M,U}(\mathbf{d}_{T_{M-1}}, \boldsymbol{\psi}_M)$ represent the fitted emulator models which act as lower and upper bounds respectively for $\tilde{G}_{T,M,\boldsymbol{\psi}_M}(\mathbf{d}_{T_{M-1}}, \boldsymbol{\psi}_M)$.

Forming Credible Bounds for Expected Total Costs in a General Stage m Onwards

For a general stage m such that $2 \leq m \leq M-1$, credible bounds can be formed for the expected total costs in stage m onwards using the credible bounds for expected total costs in stage $m+1$ onwards (i.e. $\tilde{G}_{T,m+1,\boldsymbol{\psi}_{m+1},L}(\mathbf{d}_{T_m}, \boldsymbol{\psi}_{m+1})$ and $\tilde{G}_{T,m+1,\boldsymbol{\psi}_{m+1},U}(\mathbf{d}_{T_m}, \boldsymbol{\psi}_{m+1})$), and considering the error in the emulator used to approximate the simulator in stage m, $\tilde{f}_{c,m}(\mathbf{v}_m, \mathbf{d}_m|\mathbf{d}_{T_{m-1}})$. The methodology of Section 5.2.6 can again be used to randomly vary the model parameters of $\tilde{f}_{c,m}(\mathbf{v}_m, \mathbf{d}_m|\mathbf{d}_{T_{m-1}})$, with $\tilde{f}_{c,m,r}(\mathbf{v}_m, \mathbf{d}_m|\mathbf{d}_{T_{m-1}})$ representing such a random drawings of $\tilde{f}_{c,m}(\mathbf{v}_m, \mathbf{d}_m|\mathbf{d}_{T_{m-1}})$.

These random drawings can then be used in Equation 9.1.7 to calculate random drawings of $\tilde{F}_{T,m,\theta_{i,m}}$ (the estimate of expected total costs in stage m onwards when making the estimated optimal stage m decision, $\mathbf{d}_{m|\theta_{i,m}}$, in stage m given that total reinforcement $\mathbf{d}_{T_{m-1},\theta_{i,m}}$ was made in the previous $m-1$ stages and that scenario $\boldsymbol{\psi}_{m,\theta_{i,m}}$ is observed when the mth decision is made) such that a random drawing which uses the lower bound, $\tilde{G}_{T,m+1,\boldsymbol{\psi}_{m+1},L}(\mathbf{d}_{T_m}, \boldsymbol{\psi}_{m+1})$, to estimate expected total costs in stage $m+1$ onwards is calculated as

$$\tilde{F}_{T,m,\theta_{i,m},L,r}(\mathbf{d}_{m|\theta_{i,m}}|\mathbf{d}_{T_{m-1},\theta_{i,m}}, \boldsymbol{\psi}_{m,\theta_{i,m}}) = \tilde{G}_{T,m+1,\boldsymbol{\psi}_m,L}(\mathbf{d}_{T_m|\theta_{i,m}}, \boldsymbol{\psi}_{m,\theta_{i,m}}) + \tilde{F}_{c,m,r}(\mathbf{d}_{m|\theta_{i,m}}|\mathbf{d}_{T_{m-1},\theta_{i,m}}, \boldsymbol{\psi}_{m,\theta_{i,m}}) + f_{\rho,m}(\mathbf{d}_{m|\theta_{i,m}}|\mathbf{d}_{T_{m-1},\theta_{i,m}}, \boldsymbol{\psi}_{m,\theta_{i,m}}) \quad (9.1.17)$$

where

$$\tilde{F}_{c,m,r}(\mathbf{d}_{m|\theta_{i,m}}|\mathbf{d}_{T_{m-1},\theta_{i,m}},\boldsymbol{\psi}_{m,\theta_{i,m}}) = \int_{\mathbf{v}_m} \tilde{f}_{c,m,r}(\mathbf{v}_m,\mathbf{d}_{m|\theta_{i,m}}|\mathbf{d}_{T_{m-1},\theta_{i,m}}) \times p(\mathbf{v}_m|\boldsymbol{\psi}_{m,\theta_{i,m}})\mathrm{d}\mathbf{v}_m \quad (9.1.18)$$

and

$$\tilde{G}_{T,m+1,\boldsymbol{\psi}_m,L}(\mathbf{d}_{T_m|\theta_{i,m}},\boldsymbol{\psi}_{m,\theta_{i,m}}) = \int_{\boldsymbol{\psi}_{m+1}} \tilde{G}_{T,m+1,\boldsymbol{\psi}_{m+1},L}(\mathbf{d}_{T_m|\theta_{i,m}},\boldsymbol{\psi}_{m+1}) \times p_{\boldsymbol{\psi}_{m+1|m}}(\boldsymbol{\psi}_{m+1}|\boldsymbol{\psi}_{m,\theta_{i,m}})\mathrm{d}\boldsymbol{\psi}_{m+1} \quad (9.1.19)$$

and a random drawing which uses the upper bound, $\tilde{G}_{T,m+1,\boldsymbol{\psi}_{m+1},U}(\mathbf{d}_{T_m},\boldsymbol{\psi}_{m+1})$, to estimate expected total costs in stage $m+1$ onwards is calculated as

$$\tilde{F}_{T,m,\theta_{i,m},U,r}(\mathbf{d}_{m|\theta_{i,m}}|\mathbf{d}_{T_{m-1},\theta_{i,m}},\boldsymbol{\psi}_{m,\theta_{i,m}}) = \tilde{G}_{T,m+1,\boldsymbol{\psi}_m,U}(\mathbf{d}_{T_m|\theta_{i,m}},\boldsymbol{\psi}_{m,\theta_{i,m}}) + \tilde{F}_{c,m,r}(\mathbf{d}_{m|\theta_{i,m}}|\mathbf{d}_{T_{m-1},\theta_{i,m}},\boldsymbol{\psi}_{m,\theta_{i,m}}) + f_{\rho,m}(\mathbf{d}_{m|\theta_{i,m}}|\mathbf{d}_{T_{m-1},\theta_{i,m}},\boldsymbol{\psi}_{m,\theta_{i,m}}) \quad (9.1.20)$$

where

$$\tilde{F}_{c,m,r}(\mathbf{d}_{m|\theta_{i,m}}|\mathbf{d}_{T_{m-1},\theta_{i,m}},\boldsymbol{\psi}_{m,\theta_{i,m}}) = \int_{\mathbf{v}_m} \tilde{f}_{c,m,r}(\mathbf{v}_m,\mathbf{d}_{m|\theta_{i,m}}|\mathbf{d}_{T_{m-1},\theta_{i,m}}) \times p(\mathbf{v}_m|\boldsymbol{\psi}_{m,\theta_{i,m}})\mathrm{d}\mathbf{v}_m \quad (9.1.21)$$

and

$$\tilde{G}_{T,m+1,\boldsymbol{\psi}_m,U}(\mathbf{d}_{T_m|\theta_{i,m}},\boldsymbol{\psi}_{m,\theta_{i,m}}) = \int_{\boldsymbol{\psi}_{m+1}} \tilde{G}_{T,m+1,\boldsymbol{\psi}_{m+1},U}(\mathbf{d}_{T_m|\theta_{i,m}},\boldsymbol{\psi}_{m+1}) \times p_{\boldsymbol{\psi}_{m+1|m}}(\boldsymbol{\psi}_{m+1}|\boldsymbol{\psi}_{m,\theta_{i,m}})\mathrm{d}\boldsymbol{\psi}_{m+1} \quad (9.1.22)$$

Credible intervals can then be estimates for $\tilde{F}_{T,m,\theta_{i,m}}$ such that if an $\alpha\%$ credible interval is desired a lower bound, $\tilde{F}_{T,m,\theta_{i,m},L,L}$, is formed as the value which $\frac{100-\alpha}{2}\%$ of the $\tilde{F}_{T,m,\theta_{i,m},L,r}$ are smaller than, and the upper bound, $\tilde{F}_{T,m,\theta_{i,m},U,U}$, is formed as the value which $\frac{100-\alpha}{2}\%$ of the $\tilde{F}_{T,m,\theta_{i,m},U,r}$ are greater than.

The methodology of Section 9.1.2 used the values of $\tilde{F}_{T,m,\theta_{i,m}}$ as a set N_{θ_m} training runs in order to fit an emulator model, $\tilde{G}_{T,m,\boldsymbol{\psi}_m}(\mathbf{d}_{T_{m-1}},\boldsymbol{\psi}_m)$, of how expected total costs in stage m onwards vary as a function of stage m scenario, $\boldsymbol{\psi}_m$, and total reinforcement until stage $m-1$, $\mathbf{d}_{T_{m-1}}$, only. As was the case in the previous sub-subsection when

estimating credible bounds in stage M, the values of $\tilde{F}_{T,m,\theta_{i,m},L,L}$ and $\tilde{F}_{T,m,\theta_{i,m},U,U}$ can be used as two sets of N_{θ_m} training runs which can be used to fit respective emulator models of how lower and upper bounds of the estimates of expected total costs in stage m onwards vary as a function of $\boldsymbol{\psi}_m$ and $\mathbf{d}_{T_{m-1}}$ only, such that $\tilde{G}_{T,m,\boldsymbol{\psi}_m,L}(\mathbf{d}_{T_{m-1}}, \boldsymbol{\psi}_m)$ and $\tilde{G}_{T,m,\boldsymbol{\psi}_m,U}(\mathbf{d}_{T_{m-1}}, \boldsymbol{\psi}_m)$ represent the fitted emulator models which act as lower and upper bounds respectively for $\tilde{G}_{T,m,\boldsymbol{\psi}_m}(\mathbf{d}_{T_{m-1}}, \boldsymbol{\psi}_m)$.

Forming Credible Bounds for Expected Total Costs Across All M Stages as a Function of the First Stage Decision Only

This is repeated iteratively until eventually $\tilde{G}_{T,2,\boldsymbol{\psi}_2,L}(\mathbf{d}_1, \boldsymbol{\psi}_2)$ and $\tilde{G}_{T,2,\boldsymbol{\psi}_2,U}(\mathbf{d}_1, \boldsymbol{\psi}_2)$ are fitted which represent the fitted models which act as lower and upper bounds respectively for $\tilde{G}_{T,2,\boldsymbol{\psi}_2}(\mathbf{d}_1, \boldsymbol{\psi}_2)$. The methodology of Section 8.2.5 can then be used to form credible intervals for the estimates of expected total costs across all M stages as a function of stage 1 decision and scenario only, by first calculating lower and upper bounds for the estimates of expected total costs in stage 2 onwards as a function of stage 1 decision and scenario only as

$$\tilde{G}_{T,2,\boldsymbol{\psi}_1,L}(\mathbf{d}_1, \boldsymbol{\psi}_1) = \int_{\boldsymbol{\psi}_2} \tilde{G}_{T,2,\boldsymbol{\psi}_2,L}(\mathbf{d}_1, \boldsymbol{\psi}_2) \times p_{\boldsymbol{\psi}_{2|1}}(\boldsymbol{\psi}_2|\boldsymbol{\psi}_1)\mathrm{d}\boldsymbol{\psi}_2 \tag{9.1.23}$$

and

$$\tilde{G}_{T,2,\boldsymbol{\psi}_1,U}(\mathbf{d}_1, \boldsymbol{\psi}_1) = \int_{\boldsymbol{\psi}_2} \tilde{G}_{T,2,\boldsymbol{\psi}_2,U}(\mathbf{d}_1, \boldsymbol{\psi}_2) \times p_{\boldsymbol{\psi}_{2|1}}(\boldsymbol{\psi}_2|\boldsymbol{\psi}_1)\mathrm{d}\boldsymbol{\psi}_2 \tag{9.1.24}$$

As was noted in Section 8.2.5, the emulator used to approximate the simulator in stage 1, $\tilde{f}_{c,1}(\mathbf{v}_1, \mathbf{d}_1)$, also contains error and again, this is handled in the same manner as in Section 5.2.6, where the model parameters of $\tilde{f}_{c,1}(\mathbf{v}_1, \mathbf{d}_1)$ are randomly varied such that $\tilde{f}_{c,1,r}(\mathbf{v}_1, \mathbf{d}_1)$ represents a random drawing of $\tilde{f}_{c,1}(\mathbf{v}_1, \mathbf{d}_1)$. $\tilde{f}_{c,1,r}(\mathbf{v}_1, \mathbf{d}_1)$ can then be used to estimate expected mean constraint costs in stage 1 under uncertainty as

$$\tilde{F}_{c,1,r}(\mathbf{d}_1|\boldsymbol{\psi}_1) = \int_{\mathbf{v}_1} \tilde{f}_{c,1,r}(\mathbf{v}_1, \mathbf{d}_1) \times p(\mathbf{v}_1|\boldsymbol{\psi}_1)\mathrm{d}\mathbf{v}_1 \tag{9.1.25}$$

Random variations for the expected total costs that occur across all M stages, when fitting a lower bound for the estimated expected total costs in stage 2 onwards, can be

estimated as

$$\tilde{G}_{T,L,r}(\mathbf{d}_1, \boldsymbol{\psi}_1) = \tilde{G}_{T,2,\boldsymbol{\psi}_1,L}(\mathbf{d}_1, \boldsymbol{\psi}_1) + \tilde{F}_{c,1,r}(\mathbf{d}_1|\boldsymbol{\psi}_1) + f_{\rho,1}(\mathbf{d}_1|\boldsymbol{\psi}_1) \tag{9.1.26}$$

whilst random variations for the expected total costs that occur across all M stages, when fitting an upper bound for the estimated expected total costs in stage 2 onwards, can be estimated as

$$\tilde{G}_{T,U,r}(\mathbf{d}_1, \boldsymbol{\psi}_1) = \tilde{G}_{T,2,\boldsymbol{\psi}_1,U}(\mathbf{d}_1, \boldsymbol{\psi}_1) + \tilde{F}_{c,1,r}(\mathbf{d}_1|\boldsymbol{\psi}_1) + f_{\rho,1}(\mathbf{d}_1|\boldsymbol{\psi}_1) \tag{9.1.27}$$

Credible intervals can then be estimated for $\tilde{G}_{T,L,r}(\mathbf{d}_1, \boldsymbol{\psi}_1)$ such that if an $\alpha\%$ credible interval is desired a lower bound is formed as the value which $\frac{100-\alpha}{2}\%$ of the $\tilde{G}_{T,L,r}(\mathbf{d}_1, \boldsymbol{\psi}_1)$ are smaller than, and the upper bound as the value which $\frac{100-\alpha}{2}\%$ of the $\tilde{G}_{T,L,r}(\mathbf{d}_1, \boldsymbol{\psi}_1)$ are greater than (and similarly for credible bounds for $\tilde{G}_{T,U,r}(\mathbf{d}_1, \boldsymbol{\psi}_1)$). The lower and upper bounds for $\tilde{G}_{T,L,r}(\mathbf{d}_1, \boldsymbol{\psi}_1)$ are denoted as $\tilde{G}_{T,L,L}(\mathbf{d}_1, \boldsymbol{\psi}_1)$ and $\tilde{G}_{T,L,U}(\mathbf{d}_1, \boldsymbol{\psi}_1)$ respectively, with the lower and upper bounds for $\tilde{G}_{T,U,r}(\mathbf{d}_1, \boldsymbol{\psi}_1)$ similarly denoted as $\tilde{G}_{T,U,L}(\mathbf{d}_1, \boldsymbol{\psi}_1)$ and $\tilde{G}_{T,U,U}(\mathbf{d}_1, \boldsymbol{\psi}_1)$ respectively.

Finally, $\tilde{G}_{T,L,L}(\mathbf{d}_1, \boldsymbol{\psi}_1)$ and $\tilde{G}_{T,U,U}(\mathbf{d}_1, \boldsymbol{\psi}_1)$ can be used as credible bounds for $\tilde{G}_T(\mathbf{d}_1, \boldsymbol{\psi}_1)$, i.e. $\tilde{G}_{T,L,L}(\mathbf{d}_1, \boldsymbol{\psi}_1)$ and $\tilde{G}_{T,U,U}(\mathbf{d}_1, \boldsymbol{\psi}_1)$ represent the estimated credible bounds for the estimate of expected total costs across all M stages when making decision $\mathbf{d}_1$ in stage 1 for stage 1 scenario $\boldsymbol{\psi}_1$.

Using The Credible Bounds to Eliminate Decisions From Consideration

These credible bounds can then be used in the methodology outlined in Section 8.2.7 to iteratively eliminate stage 1 decisions (values of $\mathbf{d}_1$) from consideration in order to fit more accurate emulator models over a smaller range of decisions. Without repeating Section 8.2.7 in its entirety, a brief recap of this is the values of the decision variables which give the minimum value of $\tilde{G}_{T,U,U}(\mathbf{d}_1, \boldsymbol{\psi}_1)$ are then identified as $\mathbf{d}_1^o = d_{1,1}^o, ..., d_{1,N_d}^o$. The corresponding upper bound of the estimate of expected total costs across all stages of making decision $\mathbf{d}_1^o$ is then calculated as $\tilde{G}_{T,U,U}(\mathbf{d}_1^o, \boldsymbol{\psi}_1)$.

For any alternative set of decisions, $\mathbf{d}_1^a = d_{1,1}^a, ..., d_{1,N_d}^a$, such that $\tilde{G}_{T,L,L}(\mathbf{d}_1^a, \boldsymbol{\psi}_1) > \tilde{G}_{T,U,U}(\mathbf{d}_1^o, \boldsymbol{\psi}_1)$ it can be said that there is evidence against that

decision being optimal, as the lower bound of the estimate is not better than the least upper bound. That decision can thus be eliminated from the decision space.

A new set of training runs can then be taken which only considers values of decision variables not eliminated, and new emulator models fitted using these training runs. Credible intervals could again be formed for the new emulator models, and further decisions eliminated from consideration as outlined above. This is repeated iteratively until no further decisions are eliminated from consideration. An estimate of the optimal decision to be made in stage 1 can then be acquired as the values of $\mathbf{d}_1$ which minimise Equation 9.1.11 (i.e. minimise the estimate of expected total costs across all M stages) using the emulator models fitted in the final wave.

9.1.5 Further Consideration to the Credible Bounds Estimated in Section 9.1.4

Further Consideration to the Estimated Credible Intervals

It is noted that as part of the methodology of the previous subsection, whilst uncertainty is considered in $\tilde{F}_{T,m,\theta_{i,m}}$ (the estimate of expected total costs in stage m onwards when making the estimated optimal decision in stage m, $\mathbf{d}_{m|\theta_{i,m}}$, given that total reinforcement $\mathbf{d}_{T_{m-1},\theta_{i,m}}$ was made in the previous $m-1$ stages and that scenario $\boldsymbol{\psi}_{m,\theta_{i,m}}$ is observed in stage m), uncertainty is not considered in the estimate of optimal decision to be made in stage m, $\mathbf{d}_{m|\theta_{i,m}}$, itself.

Further thought to this for the two stage problem was given in Section 8.7, which considered using a wave process to estimate optimal stage 2 decisions, $\mathbf{d}_{2|\theta}$, for a subset of the sampled stage 1 decisions, $\mathbf{d}_{1,\theta}$, and stage 2 scenarios, $\boldsymbol{\psi}_{2,\theta}$. It was shown how this not only improved the accuracy of the resulting estimates of optimal stage 2 decision, but also how the resulting credible intervals for $\tilde{F}_{T,2,\theta}$ (the estimate of expected total costs in stage 2 when making decision the estimate of optimal decision $\mathbf{d}_{2|\theta}$ in stage 2, given that decision $\mathbf{d}_{1,\theta}$ was previously made and that scenario $\boldsymbol{\psi}_{2,\theta}$ was observed in stage 2) were much narrower, indicating the greater level of confidence in the estimate. The narrower credible intervals could subsequently allow for more stage 1 decisions to

be eliminated from consideration if a separate wave process was carried out for each of the N_θ samples.

However, it was also noted that in a general M stage problem this would require $\sum_{m=2}^{M} N_{\theta_m}$ separate wave processes to be carried out within each wave of eliminating stage 1 decisions, and carrying out just 1 wave process can be very expensive. Therefore, it is not feasible to carry out a such a wave process for each $\theta_{i,m}$ to more accurately estimate the "true" optimal decision for the resources available to us in this thesis.

It is therefore noted that the credible intervals estimated in Section 9.1.4 can be considered as a pragmatic approach which estimates credible intervals for expected total costs across all M stages as a function of the first stage decision only, when making the estimated optimal decision in stages 2 to M, rather the credible intervals for expected total costs across all M stages when making the "true" unknown optimal decision in stages 2 to M. This is quite a reasonable approach, as in practice the "true" optimal decision will be unknown, so it is therefore necessary to assume that instead of making the "true" unknown optimal decision the decision maker will instead make the best decision possible for the given emulator approximations in each stage, i.e. to minimise the estimate of expected total costs based on the available information by making the estimated optimal decision $\mathbf{d}_{m|\theta_{i,m}}$.

Alternative Credible Intervals

Even without performing a separate wave process for each of the $\sum_{m=2}^{M} N_{\theta_m}$ samples of total reinforcement in the previous $m-1$ stages, $\mathbf{d}_{T_{m-1},\theta_{i,m}}$, and stage m scenarios, $\boldsymbol{\psi}_{m,\theta_{i,m}}$, there are alternative methods of estimating credible intervals to the method proposed in Section 9.1.4.

As noted in the previous sub-subsection, the methodology proposed in Section 9.1.4 considers forming lower and upper bounds for the estimates of expected total costs in stage m onwards when making decision $\mathbf{d}_{m|\theta_{i,m}}$ in stage m (the decision which minimises the estimate of expected total costs in stage m onwards).

However, one could instead consider forming credible intervals for a decision making process where in each stage the decision maker acts to make the stage m decision which

minimises the upper bound of the estimate of expected total costs in stage m onwards, such that decision $\mathbf{d}_{m,a_U|\theta_{i,m}}$ is made to minimise the upper bound of the estimate of expected total costs in stage m onwards given that total reinforcement $\mathbf{d}_{T_{m-1},\theta_{i,m}}$ was made in the previous $m-1$ stages and that scenario $\boldsymbol{\psi}_{m,\theta_{i,m}}$ is observed in stage m. The methodology of Section 9.1.4 could then be applied to estimate $\tilde{F}_{T,m,\theta_{i,m},a_U,L}$ and $\tilde{F}_{T,m,\theta_{i,m},a_U,U}$ as the lower and upper bound respectively of expected total costs in stage m onwards when making decision $\mathbf{d}_{m,a_U|\theta_{i,m}}$ in stage m instead of $\mathbf{d}_{m|\theta_{i,m}}$.

Applying this for every stage would lead to fitting the models $\tilde{G}_{T,a_U,L,L}(\mathbf{d}_1,\psi_1)$ and $\tilde{G}_{T,a_U,U,U}(\mathbf{d}_1,\psi_1)$ which model lower and upper bounds for expected total costs across all M stages as a function of the stage 1 decision, $\mathbf{d}_1$, and stage 1 scenario, $\boldsymbol{\psi}_1$, only, whilst assuming the decision maker acts to minimise the upper bound of the estimates of expected total costs in stages 2 to M.

Acting to minimise the upper bound of the estimate of expected total costs in each stage, and not to minimise the estimate of expected total costs itself (i.e. making decisions $\mathbf{d}_{m,a_U|\theta_{i,m}}$ rather than $\mathbf{d}_{m|\theta_{i,m}}$) results in a greater expectation of total costs across all stages. However, the upper bound of the estimate, $\tilde{G}_{T,a_U,U,U}(\mathbf{d}_1,\psi_1)$, will be lower than $\tilde{G}_{T,U,U}(\mathbf{d}_1,\psi_1)$ (the upper bound when acting to minimise the expectation of costs in stages 2 to M) as a result of the more cautious approach. It must, however, be noted that this approach is not analogous to estimating credible bounds when making the unknown "true" optimal decision to minimise expected total costs across all M stages, so the credible bounds $\tilde{G}_{T,a_U,L,L}(\mathbf{d}_1,\psi_1)$ and $\tilde{G}_{T,a_U,U,U}(\mathbf{d}_1,\psi_1)$ can not be thought of as such.

More Conservative Credible Bounds

It could be considered that $\tilde{F}_{T,m,\theta_{i,m},U,U}$ (the upper bound of the estimate of expected total costs in stage m onwards when making the estimate of optimal decision, $\mathbf{d}_{m|\theta_{i,m}}$, given that total reinforcement $\mathbf{d}_{T_{m-1},\theta_{i,m}}$ was made in the previous $m-1$ stages and that scenario $\boldsymbol{\psi}_{m,\theta_{i,m}}$ is observed in stage m), is somewhat conservative. This is because, as noted, such an upper bound would represent an upper bound for costs when making the estimated optimal decision in stage m, $\mathbf{d}_{m|\theta_{i,m}}$, regardless of whether or not $\mathbf{d}_{m|\theta_{i,m}}$ is the "true" optimal decision. This in turn means that if an α% credible interval is

estimated, it is estimated that there is a $\frac{100+\alpha}{2}\%$ chance (e.g. if $\alpha = 95\%$, there is a 97.5% chance) that expected total costs are less than $\tilde{F}_{T,m,\theta_{i,m},U,U}$ when making decision $\mathbf{d}_{m|\theta_{i,m}}$.

If the expected total costs of making decision $\mathbf{d}_{m|\theta_{i,m}}$ are less than $\tilde{F}_{T,m,\theta_{i,m},U,U}$ (and as $\tilde{F}_{T,m,\theta_{i,m},U,U}$ is the estimated upper bound at the $\alpha\%$ level, it is estimated that there is a $\frac{100+\alpha}{2}\%$ chance this is the case), then the expected total costs of making the unknown "true" optimal decision are also less than $\tilde{F}_{T,m,\theta_{i,m},U,U}$ (otherwise the decision would not be optimal). However, even if the expected total costs of making decision $\mathbf{d}_{m|\theta_{i,m}}$ are greater than $\tilde{F}_{T,m,\theta_{i,m},U,U}$, it is possible that the expected total costs of making the unknown "true" optimal decision are less than $\tilde{F}_{T,m,\theta_{i,m},U,U}$, meaning the probability of expected total costs being less than $\tilde{F}_{T,m,\theta_{i,m},U,U}$ is greater than $\frac{100+\alpha}{2}\%$.

A more conservative lower bound for the estimate of expected total costs can be acquired by instead considering a decision making process where the decision maker acts to minimise the lower bound of the estimate of expected total costs in each stage, such that decision $\mathbf{d}_{m,a_L|\theta_{i,m}}$ is made in stage m given that total reinforcement $\mathbf{d}_{T_{m-1},\theta_{i,m}}$ was made in the previous $m-1$ stages and that scenario $\boldsymbol{\psi}_{m,\theta_{i,m}}$ is observed in stage m. The methodology of Section 9.1.4 could then be applied to estimate $\tilde{F}_{T,m,\theta_{i,m},a_L,L}$ and $\tilde{F}_{T,m,\theta_{i,m},a_L,U}$ as the lower and upper bounds of expected total costs in stage m onwards respectively when making decision $\mathbf{d}_{m,a_L|\theta_{i,m}}$ (the decision which minimises the lower bound of the estimate of expected total costs in stage m onwards) instead of $\mathbf{d}_{m|\theta_{i,m}}$ (the decision which minimises the estimate of expected total costs in stage m onwards).

Applying this for every stage would lead to fitting the models $\tilde{G}_{T,a_L,L,L}(\mathbf{d}_1, \psi_1)$ and $\tilde{G}_{T,a_L,U,U}(\mathbf{d}_1, \psi_1)$ which respectively model lower and upper bounds for expected total costs across all M stages as a function of the stage 1 decision, $\mathbf{d}_1$, and stage 1 scenario, $\boldsymbol{\psi}_1$, only, whilst assuming the decision maker acts to minimise the lower bound of expected total costs in stages 2 to M.

$\tilde{G}_{T,U,U}(\mathbf{d}_1, \psi_1)$ (the upper bound of the estimate of expected total costs across all M stages when assuming the decision maker acts to minimise the estimate of expected total costs in stages 2 to M) and $\tilde{G}_{T,a_L,L,L}(\mathbf{d}_1, \psi_1)$ (the lower bound of the estimate of expected total costs across all M stages when assuming the decision maker acts to minimise the lower bound of the estimate of expected total costs in stages 2 to M)

could therefore be used as conservative upper and lower bounds for the estimates of expected total costs across all M as a function of the first stage decision, $\mathbf{d}_1$, and scenario, $\boldsymbol{\psi}_1$, only.

Thought to Using More Conservative Credible Bounds When Eliminating Decisions

The methodology of Section 8.2.7 (which considers eliminating stage 1 reinforcement decisions from consideration which have evidence against them being optimal) first considers identifying the stage 1 decision which results in the minimum upper bound of the given estimated credible bounds, with the decision denoted $\mathbf{d}_1^o$ with corresponding minimum upper bound $\tilde{G}_{T,U}(\mathbf{d}_1^o, \boldsymbol{\psi}_1)$. For any alternative stage 1 decisions, $\mathbf{d}_1^a$, such that the lower bound of the estimate, $\tilde{G}_{T,L}(\mathbf{d}_1^a, \boldsymbol{\psi}_1)$, is greater than the minimum upper bound, i.e. $\tilde{G}_{T,L}(\mathbf{d}_1^a, \boldsymbol{\psi}_1) > \tilde{G}_{T,U}(\mathbf{d}_1^o, \boldsymbol{\psi}_1)$, it can be said that there is evidence against that decision being optimal and it can be eliminated from consideration.

This would mean that using the more conservative lower bound of the estimate of expected total costs, $\tilde{G}_{T,a_L,L,L}(\mathbf{d}_1, \psi_1)$, would represent a more cautious approach where there is a lower chance of incorrectly eliminating a decisions from consideration. However, this would come at the expense of a reduced level of power to eliminate sub-optimal decisions. Conversely, whilst it was noted that the use of $\tilde{G}_{T,L,L}(\mathbf{d}_1, \psi_1)$ (the lower bound of the estimate of expected total costs across all M stages when assuming the decision maker acts to minimise the estimate of expected total costs in stages 2 to M) represents a pragmatic approach to estimating credible bounds across all M stages, there will be a slightly increased chance of incorrectly eliminating an optimal decision from consideration in comparison to when the conservative lower bound, $\tilde{G}_{T,a_L,L,L}(\mathbf{d}_1, \psi_1)$, is used, though with a greater level of power to eliminate sub-optimal decisions from consideration.

It is noted that if the credible intervals are of similar widths for all decisions (which is generally true in the final waves for the transmission expansion problems considered in this thesis, though less true in the first wave) then there will be little difference between $\tilde{G}_{T,L,L}(\mathbf{d}_1, \psi_1)$ (the lower bound of the estimate of expected total costs across all M stages when assuming the decision maker acts to minimise the estimate of expected

total costs in stages 2 to M) and $\tilde{G}_{T,a_L,L,L}(\mathbf{d}_1, \psi_1)$ (the lower bound of the estimate of expected total costs across all M stages when assuming the decision maker acts to minimise the lower bound of the estimate of expected total costs in stages 2 to M).

For the example that will be detailed in Section 9.2, estimating credible bounds using the pragmatic approach detailed in Section 9.1.4 appears to be quite reasonable, as Section 9.3 will illustrate how this allows for range of decisions to be identified where the optimal decision could potentially lie, where all decisions result in similar, relatively low estimates of expected total costs, without the region appearing overly small. Further, the estimate of the optimal decision over the region identified lies around the centre of the range of decisions which were not eliminated in the final wave, as would be expected.

If estimating credible bounds using the pragmatic approach detailed in Section 9.1.4 results in an extremely large reduction in the decision space, or the resulting estimate of optimal stage 1 reinforcement decision in the final wave lies towards the extremes of the range of decisions considered in the final wave, this could be evidence that the approach is not cautious enough and the "true" unknown optimal stage 1 decision has been incorrectly eliminated from consideration.

Additional Consideration to the Credible Intervals Estimated in Section 9.1.4

It is also noted that as part of the methodology for Section 9.1.4, when estimating a lower bound (and similarly for an upper bound) for expected total costs in stage m onwards, for $1 \leq m \leq M-1$, the lower bound for the estimate of expected total costs in stage $m+1$ onwards is used. This means that $\tilde{G}_{T,L,L}(\mathbf{d}_1, \psi_1)$, the lower bound for estimated expected total costs across all M stages as a function of stage 1 decision, $\mathbf{d}_1$, and stage 1 scenario, $\boldsymbol{\psi}_1$, only, is effectively formed as the sum of the M lower bounds across each of the M stages (i.e. it assumes the lower bound of the estimate in each stage).

However, the probability that the actual expectation of total costs across all stages simultaneously takes the lower bound in each stage is less than the probability of the actual expectation of total costs taking the lower bound in any one particular stage. The resulting estimated credibility interval will therefore be wider than necessary for

an $\alpha\%$ credibility interval. As noted in the previous sub-subsection, this in turn means that there is less risk of incorrectly eliminating a decision which has evidence against it being optimal using the methodology of Section 8.2.7. However, this comes at the expense of a reduced level of power to eliminate sub-optimal decisions.

9.2 Details of a Three Stage Transmission Expansion Planning Problem

This chapter will consider an application of the methodology of Section 9.1 to a 3-stage decision problem. This problem will be the extension of the example outlined in Section 8.3 from 2 to 3 decision stages. As such, uncertainty will be considered in three variables (nuclear availability probability, CCGT availability probability and peak demand level) and two decision variables will be considered at each stage (increasing the transfer capacity of the B6 and B7a boundaries).

As in Section 8.3, the example will consider learning about peak demand level between each decision. Further, Section 9.6 will go on to consider how the estimates of expected total costs and resulting estimates of optimal decisions in each stage are sensitive to many assumptions made, such as the assumed cost of reinforcement and the assumed discount rate.

9.2.1 Time Frame of Problem

For the problem considered, the first decision will be made at the beginning of year 1 and the reinforcement made will be available at the beginning of year 6. The second decision will be made at the beginning of year 6 and the reinforcement made will be available at the beginning of year 11. The third decision will be made at the beginning of year 11 and the reinforcement made will be available at the beginning of year 16. This is summarised in Table 9.1.

The cost of the first reinforcement, the cost of the second reinforcement and the cost of the third reinforcement represent the reinforcement costs of the first, second and third stages respectively. Constraint costs for the first stage are the constraint costs

Decision	Time Decision is Made	Time Reinforcement is Available
First Decision	Beginning of Year 1	Beginning of Year 6
Second Decision	Beginning of Year 6	Beginning of Year 11
Third Decision	Beginning of Year 11	Beginning of Year 16

Table 9.1: Table of when decisions are made and when the reinforcement becomes available.

of the power system between years 6 and 10, constraint costs for the second stage are the constraint costs of the power system between the years 11 and 15 and constraint costs for the third stage are the constraint costs of the power system between the years 16 and 25 (as these are the years which are directly affected by the first, second and third decisions respectively). Just as in Section 8.3.1, constraint costs do not need to be calculated for years 1 to 5 as the they will be the same regardless of what decision was made in year 1 (as the reinforcement is not available until year 6). Again, in a real-world application the system would still be observed during this period in order to learn about the variables which contain uncertainty over this period, and reduce uncertainty as much as possible by the time the second decision is to be made.

At each decision stage, it is assumed that two decisions are to be made, the reinforcement magnitude (increase in transfer capacity) of the B6 and B7a boundaries. Therefore, $\mathbf{d}_1 = (d_{1,1}, d_{1,2})$, $\mathbf{d}_2 = (d_{2,1}, d_{2,2})$ and $\mathbf{d}_3 = (d_{3,1}, d_{3,2})$, where $d_{m,1}$ represents B6 reinforcement magnitude in stage m and $d_{m,2}$ represents B7a reinforcement magnitude in stage m.

Again, the methodology of [97, 66, 81] will be followed where the power system of year 6 (i.e. peak demand level, installed generators, availability probability of generators, etc) is assumed to be representative of the power system for the entirety of the first stage (i.e. the period between year 6 and year 10), the power system of year 11 is assumed to be representative of the power system for the entirety of the second stage (i.e. the period between year 11 and year 15) and the power system of year 16 is assumed to be representative of the power system for the entirety of the third stage (i.e. the period between year 16 and year 25).

9.2.2 Assumed Cost of Reinforcement

As was the case in Section 8.3.2, it will initially be assumed that it costs £1000 per MW per km to reinforce each boundary [78, 5]. As was also the case in Section 8.3.2, it is assumed that all reinforcement costs are incurred at the time each decision is made, which is consistent with how costs are modelled when assuming a fixed capital cost, such as £1000 per MW per km, to reinforce [78, 5, 70, 95]. That is, it is assumed that the reinforcement costs of the first decision are incurred at the beginning of year 1, the reinforcement costs of the second decision are incurred at the beginning of year 6 and the reinforcement costs of the third decision are incurred at the beginning of year 11.

Section 9.6.3 will consider how the assumed cost of reinforcement affects the estimates of optimal reinforcement decisions in each stage.

9.2.3 Uncertainties

Stage 1 Uncertainties

In all three stages, uncertainty will be considered in three variables: nuclear availability probability, CCGT availability probability and peak demand level. These three variables make up $\mathbf{v}_1$, $\mathbf{v}_2$ and $\mathbf{v}_3$, i.e. $\mathbf{v}_1 = (v_{1,1}, v_{1,2}, v_{1,3})$, $\mathbf{v}_2 = (v_{2,1}, v_{2,2}, v_{2,3})$ and $\mathbf{v}_3 = (v_{3,1}, v_{3,2}, v_{3,3})$, where $v_{m,1}$ represents nuclear availability probability in stage m, $v_{m,2}$ represents CCGT availability probability in stage m and $v_{m,3}$ represents peak demand level in stage m.

At year 1 there will be prior beliefs about the value these variables take. As in Section 8.3.3, nuclear availability probability is supposed to have a value between 0.55 and 0.85 in each stage and CCGT availability probability is supposed to have a value between 0.8 and 0.95 in each stage. Peak demand level in each stage will again be considered in terms of the projected peak demand level given by [69], National Grid's freely available online resource and the primary data reference for this thesis. Peak demand level in stage 1 is supposed to have a value between 95% and 105% of the year 6 peak demand level projected by [69], peak demand level in stage 2 is supposed to have a value between 90% and 110% of the year 11 peak demand level projected

by [69] and peak demand level in stage 3 is supposed to have a value between 85% and 115% of the year 16 peak demand level projected by [69]. As in Section 8.3.3, these limits for peak demand level are based on our interpretation of the expert judgement of Paul Plumptre, where an uncertainty of +/-1% in projections of peak demand level is used for each year into the future projections are made. These limits are summarised in Table 9.2.

Variable	Lower Limit of Beliefs	Upper Limit of Beliefs
Stage 1 CCGT Availability Probability	0.8	0.95
Stage 1 Nuclear Availability Probability	0.55	0.85
Stage 1 Peak Demand Level	95%	105%
Stage 2 CCGT Availability Probability	0.8	0.95
Stage 2 Nuclear Availability Probability	0.55	0.85
Stage 2 Peak Demand Level	90%	110%
Stage 3 CCGT Availability Probability	0.8	0.95
Stage 3 Nuclear Availability Probability	0.55	0.85
Stage 3 Peak Demand Level	85%	115%

Table 9.2: Table summarising the beliefs about the uncertain variables in year 1.

It is also necessary to specify a distribution to describe prior beliefs about the values the variables take across these ranges. As noted in Section 9.1.2, at the time the first decision is made it is assumed that the stage 1 scenario, described by $\boldsymbol{\psi}_1$, will be known (i.e. there is only a single scenario to consider in stage 1). As such, the distribution to describe prior beliefs about uncertainties in stage 1, $p(\mathbf{v}_1|\boldsymbol{\psi}_1)$, can be simplified to just $p(\mathbf{v}_1)$, where $p(\mathbf{v}_1)$ describes prior beliefs about uncertainties in stage 1 for the given state of the power system. An alternative could be to set $\boldsymbol{\psi}_1$ to take a specific value (such as $\boldsymbol{\psi}_1 = 1$) with certainty, then define $p(\mathbf{v}_1|\boldsymbol{\psi}_1 = 1)$.

As was the case for the two stage problem considered in Section 8.3.3, prior beliefs for variables containing uncertainty in stage 1, $\mathbf{v}_1$, will be based on the uncertainties used for the example of Section 6.1.1. That is, the distribution to describe prior beliefs about uncertainty, $p(\mathbf{v}_1) = p(\mathbf{v}_1|\boldsymbol{\psi}_1)$, is modelled as a uniform distribution between the lower and upper limits given in Table 9.2, such that prior beliefs about CCGT availability probability in stage 1 form a uniform distribution between 0.8 and 0.95; prior beliefs about nuclear availability probability in stage 1 form a uniform distribution

between 0.55 and 0.85; and prior beliefs for peak demand level in stage 1 form a uniform distribution between 95% and 105% of the year 6 peak demand level projected by [69].

Using the methodology of Section 9.1.2, at stage 1 it is not necessary to give an explicit specification for the beliefs about the values of the variables which contain in stage 2 or stage 3 (as was also the case for the two stage problem). Only prior beliefs about $\boldsymbol{\psi}_2$ (which describes the state of the power system at the time the second decision is made) are required, which can be used to estimate expected total costs in stage 2 onwards via Equation 9.1.9. It was noted in Section 9.1.3 that $p_{\psi_{2|1}}(\boldsymbol{\psi}_2|\boldsymbol{\psi}_1)$ and $p_{\psi_{3|2}}(\boldsymbol{\psi}_3|\boldsymbol{\psi}_2)$ (the specifications of the beliefs of observing a particular state of the power system in stage 2 and 3 respectively) could be used to calculate explicit expressions for $p(\mathbf{v}_2|\boldsymbol{\psi}_1)$ and $p(\mathbf{v}_3|\boldsymbol{\psi}_1)$ via Equation 9.1.12, but the explicit calculations are never required.

Further, as was noted for the two stage problem in Section 8.3.3, the methodology of Section 9.1.2 does not even require ranges to be explicitly specified for $\mathbf{v}_2$ and $\mathbf{v}_3$ at the time the first decision is made, though these are detailed in Table 9.2 to illustrate the level of uncertainty considered in the future power system. However, it is noted that the ranges detailed in Table 9.2 are consistent with those that arise from explicit calculations of $p(\mathbf{v}_2|\boldsymbol{\psi}_1)$ and $p(\mathbf{v}_3|\boldsymbol{\psi}_1)$ via Equation 9.1.12, for the specifications of $p(\mathbf{v}_2|\boldsymbol{\psi}_2)$, $p(\mathbf{v}_3|\boldsymbol{\psi}_3)$, $p_{\psi_{2|1}}(\boldsymbol{\psi}_2|\boldsymbol{\psi}_1)$ and $p_{\psi_{3|2}}(\boldsymbol{\psi}_3|\boldsymbol{\psi}_2)$ that will be given in the following two sub-subsections.

Stage 2 Uncertainties

It is assumed that between year 1 and year 6 (between making the first and second decision) that the state of the power system is observed and that information has been learnt about the variables which contain uncertainty. This information is quantified in $\boldsymbol{\psi}_2$.

Initially, it will be assumed that nothing is learnt about the nuclear and CCGT availability probabilities between years 1 and 6. This means that $p(v_{2,1}|\boldsymbol{\psi}_2)$ is a uniform distribution between 0.55 and 0.85 for all values of $\boldsymbol{\psi}_2$ and $p(v_{2,2}|\boldsymbol{\psi}_2)$ is a uniform distribution between 0.8 and 0.95 for all values of $\boldsymbol{\psi}_2$.

However, it will be assumed that information is learnt which affects beliefs about year 11 peak demand level between years 1 and 6. In the example presented, $\boldsymbol{\psi}_2$ will be used

to represent the estimated expected level of peak demand in year 11, as a proportion of the year 11 peak demand level projected by [69] based on what was observed about the power system between years 1 and 6. For example, $\boldsymbol{\psi}_2 = 1.03$ would mean that the estimate of expected year 11 peak demand level at year 6 is 103% of the year 11 peak demand projected by [69].

$\boldsymbol{\psi}_2$ is also used to specify the probability distribution which describes beliefs about the year 11 peak demand level based on what was observed by year 6 (i.e. to specify $p(v_{2,3}|\boldsymbol{\psi}_2)$). As was the case in Section 8.3.3, $p(v_{2,3}|\boldsymbol{\psi}_2)$ is modelled as a uniform distribution between $(100\boldsymbol{\psi}_2 - 5)\%$ and $(100\boldsymbol{\psi}_2 + 5)\%$ of the year 11 peak demand level projected by [69]. These beliefs are consistent with our earlier interpretation of the expert judgement of Paul Plumptre [78] from Section 6.1.1, as the second decision is made at the beginning of year 6 for the year 11 power system (5 years ahead) and $p(v_{2,3}|\boldsymbol{\psi}_2)$ is a uniform distribution across a +/-5% range.

For example, if at year 6 it is now believed that the expected peak demand level in year 11 will be 3% greater than the amount projected by [69] (i.e. $\boldsymbol{\psi}_2 = 1.03$), the beliefs about peak demand in year 11 at the time the second decision is made, $p(v_{2,3}|\boldsymbol{\psi}_2)$, would form a uniform distribution between 98% and 108% of the projected year 11 peak demand level given by [69].

A specification for the prior beliefs in year 1 for the particular value of $\boldsymbol{\psi}_2$ that will be observed in year 6 (i.e. $p_{\boldsymbol{\psi}_{2|1}}(\boldsymbol{\psi}_2|\boldsymbol{\psi}_1)$) is required to estimate expected total costs in stage 2 onwards at the time the first decision is made via Equation 9.1.9. As noted in the previous sub-subsection, it is assumed that there is only one scenario, $\boldsymbol{\psi}_1$, considered in stage 1, and as such $p_{\boldsymbol{\psi}_{2|1}}(\boldsymbol{\psi}_2|\boldsymbol{\psi}_1)$ can be simplified to $p_{\boldsymbol{\psi}_{2|1}}(\boldsymbol{\psi}_2)$. For this example, $p_{\boldsymbol{\psi}_{2|1}}(\boldsymbol{\psi}_2) = p_{\boldsymbol{\psi}_{2|1}}(\boldsymbol{\psi}_2|\boldsymbol{\psi}_1)$ is taken to be a uniform distribution between 0.95 and 1.05.

A practical interpretation of this could be that $\boldsymbol{\psi}_2$ is the observed peak demand level at the beginning of year 6 specified as a proportion of the projection of year 6 peak demand level from [69] (which is subsequently used to inform beliefs about peak demand level in year 11 as outlined above), i.e. $\boldsymbol{\psi}_2$ is the observed value of $v_{1,3}$. This again is consistent with our interpretation of the expert judgement of Paul Plumptre [78] as this would model the prior beliefs in year 1 for peak demand level in year 6 as a uniform

distribution over a +/-5% range. This is also consistent with the specification of prior beliefs about year 6 peak demand level, $p(v_{1,3}|\boldsymbol{\psi}_1)$, from the previous sub-subsection, which was specified as a uniform distribution between 0.95 and 1.05.

Stage 3 Uncertainties

It is assumed that the state of the power system is observed further between year 6 and year 11 (between making the second and third decision) and that further information has been learnt about the variables which contain uncertainty. This information is quantified in $\boldsymbol{\psi}_3$.

As was the case between years 1 and 6, it will initially be assumed that nothing is learnt about the nuclear and CCGT availability probabilities between years 6 and 11. This means that $p(v_{3,1}|\boldsymbol{\psi}_3)$ is a uniform distribution between 0.55 and 0.85 for all values of $\boldsymbol{\psi}_3$ and $p(v_{3,2}|\boldsymbol{\psi}_3)$ is a uniform distribution between 0.8 and 0.95 for all values of $\boldsymbol{\psi}_3$.

However, it will be assumed that information is learnt which affects beliefs about year 16 peak demand level between years 6 and 11. In the example presented, $\boldsymbol{\psi}_3$ will be used to represent the estimated expected level of peak demand in year 16, as a proportion of the year 16 peak demand level projected by [69] based on what was observed about the power system between years 6 and 11. For example, $\boldsymbol{\psi}_3 = 1.07$ would mean that the estimate of expected year 16 peak demand level in year 11 is 107% of the year 16 peak demand projected by [69].

Again, $\boldsymbol{\psi}_3$ is then used to specify a probability distribution to describe beliefs about the year 16 peak demand level based on what was observed by year 11 (i.e. to specify $p(v_{3,3}|\boldsymbol{\psi}_3)$). $p(v_{3,3}|\boldsymbol{\psi}_3)$ is modelled as a uniform distribution between $(100\boldsymbol{\psi}_3 - 5)\%$ and $(100\boldsymbol{\psi}_3 + 5)\%$ of the year 16 peak demand level projected by [69]. Again, this is consistent with our earlier interpretation of the expert judgement of Paul Plumptre [78] from Section 6.1.1, as the third decision is made at the beginning of year 11 for the year 16 power system (5 years ahead) and the beliefs for peak demand at the time the third decision is made, $p(v_{3,3}|\boldsymbol{\psi}_3)$, form a uniform distribution across a +/-5% range.

For example, if at year 11 it is now believed that the expected peak demand level in year 16 will be 7% greater than the amount projected by [69] (i.e. $\boldsymbol{\psi}_3 = 1.07$),

the beliefs about peak demand level in year 16 at the time the third decision is made, $p(v_{3,3}|\boldsymbol{\psi}_3)$, would form a uniform distribution between 102% and 112% of the projected peak demand level given by [69].

A specification for the beliefs in year 6 for the particular value of $\boldsymbol{\psi}_3$ that will be observed in year 11 (i.e. $p_{\psi_{3|2}}(\boldsymbol{\psi}_3|\boldsymbol{\psi}_2)$) is required to estimate expected total costs in stage 3 onwards at the time the second decision is made via Equation 9.1.6. For this example, $p_{\psi_{3|2}}(\boldsymbol{\psi}_3|\boldsymbol{\psi}_2)$ is taken to be a uniform distribution between $\boldsymbol{\psi}_2 - 0.05$ and $\boldsymbol{\psi}_2 + 0.05$.

A practical interpretation of this could be that $\boldsymbol{\psi}_3$ is the observed peak demand level at the beginning of year 11 specified as a proportion of the projection of year 11 peak demand from [69] (which is subsequently used to inform beliefs about peak demand level in year 16 as outlined above), i.e. $\boldsymbol{\psi}_3$ is the observed value of $v_{2,3}$. This again is consistent with our interpretation of the expert judgement of Paul Plumptre [78] as this would model the prior beliefs in year 6 for peak demand level in year 11 as a uniform distribution over a +/-5% range. This is also consistent with the specification of beliefs about year 11 peak demand level, $p(v_{2,3}|\boldsymbol{\psi}_2)$, from the previous sub-subsection, which was specified as a uniform distribution between $\boldsymbol{\psi}_2 - 0.05$ and $\boldsymbol{\psi}_2 + 0.05$.

Summary of Beliefs About Peak Demand Level

The previous sub-subsections detail a three stage decision problem where uncertainty about future peak demand levels is reduced between each decision. The information of the previous sub-subsections is summarised in Tables 9.3 to 9.5. Table 9.3 gives the ranges considered for peak demand level in years 6, 11 and 16 before any information has been observed (i.e. at the beginning of year 1), specified as a percentage of the projections of peak demand level given by [69]. Table 9.4 details ranges considered for peak demand level in years 6, 11 and 16 at the time the first, second and third decisions will be made respectively, also specified as a percentage of the projections of peak demand level given by [69]. Table 9.5 summarises the possible scenarios that could occur in stages 2 and 3 (i.e. values of $\boldsymbol{\psi}_2$ and $\boldsymbol{\psi}_3$ respectively).

Demand	Peak Demand Lower Bound	Peak Demand Upper Bound
Range for year 6 peak demand level considered at year 1	95%	105%
Range for year 11 peak demand level considered at year 1	90%	110%
Range for year 16 peak demand level considered at year 1	85%	115%

Table 9.3: Table detailing ranges of peak demand level considered for a year 6, 11 and 16 power system at the beginning of year 1, specified as a percentage of the projections of peak demand level given by [69].

Demand	Peak Demand Lower Bound	Peak Demand Upper Bound
Range for year 6 peak demand level considered at year 1	95%	105%
Range for year 11 peak demand level considered at year 6	$(100\boldsymbol{\psi}_2 - 5)\%$	$(100\boldsymbol{\psi}_2 + 5)\%$
Range for year 16 peak demand level considered at year 11	$(100\boldsymbol{\psi}_3 - 5)\%$	$(100\boldsymbol{\psi}_3 + 5)\%$

Table 9.4: Table detailing ranges of peak demand level considered for a year 6, 11 and 16 power system in terms of scenario observed, specified as a percentage of the projections of peak demand level given by [69].

	Lower Bound	Upper Bound
Beliefs about $\boldsymbol{\psi}_2$ at year 1	0.95	1.05
Beliefs about $\boldsymbol{\psi}_3$ at year 6	$\boldsymbol{\psi}_2 - 0.05$	$\boldsymbol{\psi}_2 + 0.05$

Table 9.5: Table detailing possible beliefs about the possible scenarios (values of $\boldsymbol{\psi}_2$ and $\boldsymbol{\psi}_3$) that could be observed in stages 2 and 3.

9.2.4 Assumed Discount Rate of Future Costs

Section 8.3.4 noted how the examples of Chapter 8 assumed a discount rate of 5%, which is a common figure within the multi-stage transmission expansion planning literature [2, 26, 3, 80]. A discount rate of 5% will also be initially assumed for the example detailed in this section.

However, Section 8.3.4 also noted that a discount rate of 10% (which increases the discounting effect) is also commonly assumed within the multi-stage transmission expansion planning literature [30, 85, 62]. Section 9.6.1 will therefore consider how cost

estimates and the resulting estimates of optimal decisions vary if the higher discount rate of 10% is assumed instead, as well as comparing results to an example which assumes a low discount rate of 1%.

9.3 Stage 1 Decision

9.3.1 Stage 1 Decision

Initial Ranges Considered for Decisions in Each Stage

Initially, it is considered that the first stage reinforcement will be between 0 and 4500 MW on both the B6 and B7a boundaries. The total reinforcement in the second stage will be between the reinforcement made in stage 1 (i.e. do nothing in stage 2) and 6500 MW B6 and 5500 MW B7a reinforcement. The total reinforcement in the third stage will be between the total reinforcement after the second stage (i.e. do nothing in stage 3) and 8500 MW B6 and 5500 MW B7a reinforcement.

Fitted Emulator Models

Emulator models are also required to approximate the simulator to estimate mean constraint costs in each of the three stages. As was detailed in Section 5.2, the emulators used in this thesis take a small number of training run evaluations from the simulator, then use a polynomial regression model with a Gaussian process smoother applied to the residuals of the polynomial regression model to approximate how input affects output of the simulator.

As was noted in Section 8.4, model selection was previously covered in quite a bit of detail in Sections 5.3.3 and 5.3.5 of Chapter 5 and Section 6.1.3 of Chapter 6. Therefore, to avoid substantial repetition and to concentrate on presenting an application of the methodology of Section 9.1 to the example detailed in Section 9.2, this section will give a brief overview of the emulator models fitted, with some further details on model selection given in Appendix D.1.

As a brief overview, the results of this model selection were that the emulator model which approximates the simulator calculation of mean constraint costs in the first stage, $\tilde{f}_{c,1}(\mathbf{v}_1, \mathbf{d}_1)$, is fitted using 300 training runs, and the polynomial portion of the emulator model takes the form

$$\beta_0 + \beta_1 v_{1,1} + \beta_2 v_{1,2} + \beta_3 v_{1,3} + \beta_4 d_{1,1} + \beta_5 d_{1,2} + \beta_6 v_{1,1}^2 + \beta_7 v_{1,2}^2 + \beta_8 v_{1,3}^2 + \beta_9 d_{1,1}^2 + \beta_{10} d_{1,2}^2 + \beta_{11} v_{1,1} d_{1,1} + \beta_{12} v_{1,1} d_{1,2} + \beta_{13} d_{1,1} d_{1,2} + \beta_{14} v_{1,1}^2 d_{1,1}^2 + \beta_{15} v_{1,1}^2 d_{1,2}^2 + \beta_{16} d_{1,1}^2 d_{1,2}^2 + \beta_{17} v_{1,1} d_{1,1} d_{1,2} + \beta_{18} v_{1,1}^2 d_{1,1}^2 d_{1,2}^2$$

The R^2 of the polynomial portion of the emulator model is 0.972. A Gaussian process model is then used to smooth the residuals of this polynomial regression model. The emulator model which approximates the simulator calculation of mean constraint costs in the second stage, $\tilde{f}_{c,2}(\mathbf{v}_2, \mathbf{d}_2|\mathbf{d}_1)$, is fitted using 300 training runs, and the polynomial potion of the emulator model takes the form

$$\beta_0 + \beta_1 v_{2,1} + \beta_2 v_{2,2} + \beta_3 v_{2,3} + \beta_4 d_{T_2,1} + \beta_5 d_{T_2,2} + \beta_6 v_{2,1}^2 + \beta_7 v_{2,2}^2 + \beta_8 v_{2,3}^2 + \beta_9 d_{T_2,1}^2 + \beta_{10} d_{T_2,2}^2$$

The R^2 of the polynomial portion of the emulator model is 0.912. A Gaussian process model is then used to smooth the residuals of this polynomial regression model. The emulator model which approximates the simulator calculation of mean constraint costs in the second stage, $\tilde{f}_{c,3}(\mathbf{v}_3, \mathbf{d}_3|\mathbf{d}_{T_2})$, is fitted using 300 training runs, and the polynomial potion of the emulator model takes the form

$$\beta_0 + \beta_1 v_{3,1} + \beta_2 v_{3,2} + \beta_3 v_{3,3} + \beta_4 d_{T_3,1} + \beta_5 d_{T_3,2} + \beta_6 v_{3,1}^2 + \beta_7 v_{3,2}^2 + \beta_8 v_{3,3}^2 + \beta_9 d_{T_3,1}^2 + \beta_{10} d_{T_3,2}^2$$

The R^2 of the polynomial portion of the emulator model is 0.968. A Gaussian process model is then used to smooth the residuals of this polynomial regression model. The model for expected total costs in stage 2 onwards as a function of stage 1 decision and stage 2 scenario only, $\tilde{G}_{T,2,\psi_2}(\mathbf{d}_1, \boldsymbol{\psi}_2)$, is fitted using 50 training runs, and the polynomial portion of the emulator model takes the form

$$\beta_0 + \beta_1 \boldsymbol{\psi}_2 + \beta_2 d_{1,1} + \beta_3 d_{1,2} + \beta_4 \boldsymbol{\psi}_2^2 + \beta_5 d_{1,1}^2 + \beta_6 d_{1,2}^2$$

The R^2 of the polynomial portion of the emulator model is 0.996. A Gaussian process model is then used to smooth the residuals of this polynomial regression model. The model for expected total costs in stage 3 as a function of stage 2 decision and stage 3 scenario only, $\tilde{G}_{T,3,\psi_3}(\mathbf{d}_{T_2}, \boldsymbol{\psi}_3)$, is fitted using 50 training runs, and the polynomial portion of the emulator model takes the form

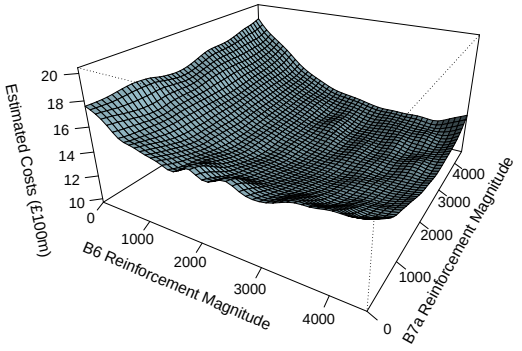

Figure 9.1: Plot to illustrate how estimates of expected total costs across all three stages vary with B6 reinforcement magnitude and B7a reinforcement magnitude in the first wave of stage 1.

$$\beta_0 + \beta_1 \boldsymbol{\psi}_3 + \beta_2 d_{T_2,1} + \beta_3 d_{T_2,2} + \beta_4 \boldsymbol{\psi}_3^2 + \beta_5 d_{T_2,1}^2 + \beta_6 d_{T_2,2}^2$$

The R^2 of the polynomial portion of the emulator model is 0.995. A Gaussian process model is then used to smooth the residuals of this polynomial regression model. Again, further details on how each of these emulator models were fitted are given in Appendix D.1.

Estimates of Expected Total Costs Across All Stages as a Function of Stage 1 Decision

Figure 9.1 shows how estimates of expected total costs across vary with stage 1 B6 and B7a reinforcement magnitude for the example outlined in Section 9.2, using the methodology of Section 9.1.2 to estimate expected total expected costs across all three stages. However, as was the case in the 2 stage examples of Chapter 8, the emulators used to estimate expected total costs are not perfect approximations to the simulator. Therefore, the methodology of Section 9.1.4 is used to estimate credible bounds for these estimates of expected total costs, which are displayed in Figure 9.2. These credible bounds can be used in turn to eliminate decisions from consideration which have evidence against them being optimal using the methodology of Section 8.2.7, which allows for a more accurate emulator model to be fitted over a smaller range of decisions.

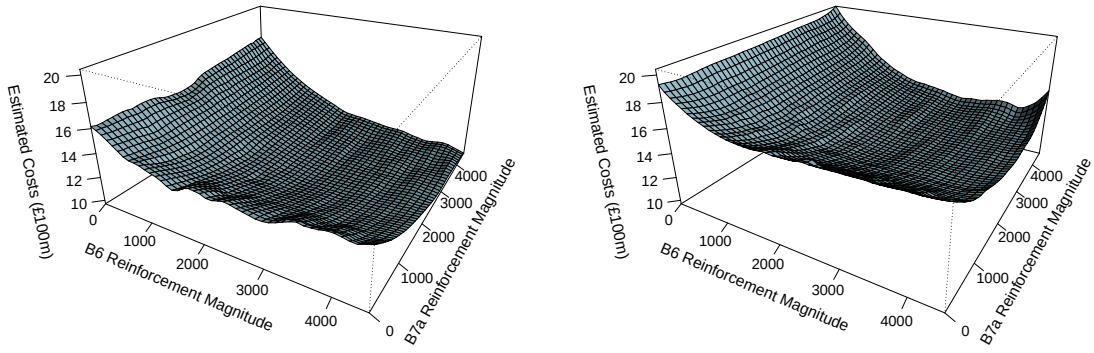

(a) Lower Bound. (b) Upper Bound.

Figure 9.2: Plots to show credible bounds for the estimates of expected total costs across all three stages from the emulator models fitted in the first wave of stage 1.

Figure 9.3 displays the decisions not eliminated from consideration in the second, third and fourth waves. After the first wave of elimination 30.3% of the decisions initially considered have been eliminated, whilst the second wave of elimination eliminated 30.1% of the decisions not eliminated after the first wave and the third eliminated 33.4% of what remained after the second wave, with 67.5% of the decisions initially considered eliminated after this third wave.

However, a negligible amount of decisions were eliminated in the fourth wave. As was the case for the first decision of the 2-stage example in Section 8.4, the reason a negligible number of decisions were eliminated beyond the fourth wave is because the estimates of expected total costs over the region displayed in Figure 9.3 (c) are relatively flat, in the sense that the estimates of expected total costs vary relatively little as B6 and B7a reinforcement magnitude are varied so very few decisions can be eliminated even with narrow credible intervals, as will be illustrated in the remainder of this section.

Figure 9.4 displays how estimates of expected total costs across all three stages vary as stage 1 B6 and B7a reinforcement magnitude are varied in each wave. As was the case when considering the 2 stage example in Section 8.4, costs are very large when the reinforcement magnitude of the B6 and B7a boundaries are small. As a result, the

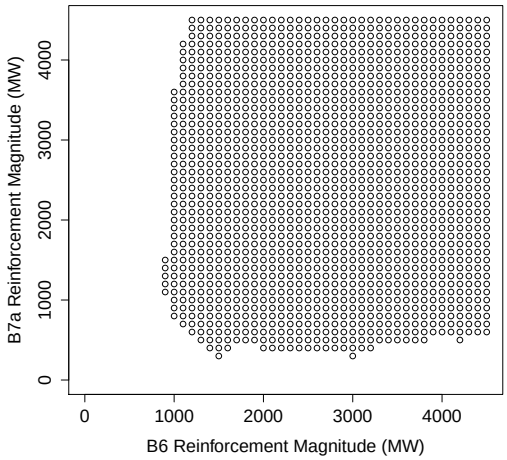

(a) Wave 2.

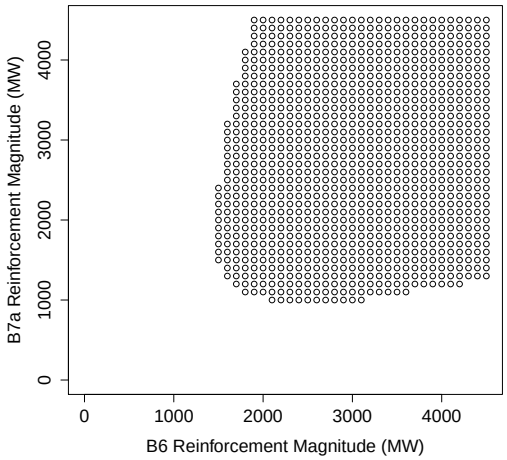

(b) Wave 3.

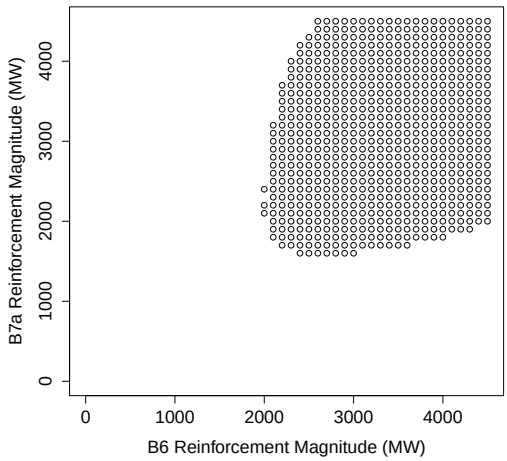

(c) Wave 4.

Figure 9.3: Plots to show decisions not eliminated from consideration in the second, third and fourth waves of Stage 1.

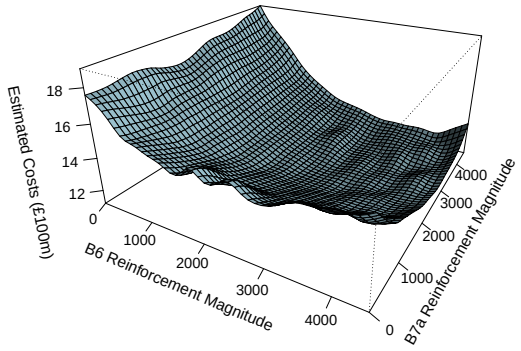

(a) Wave 1.

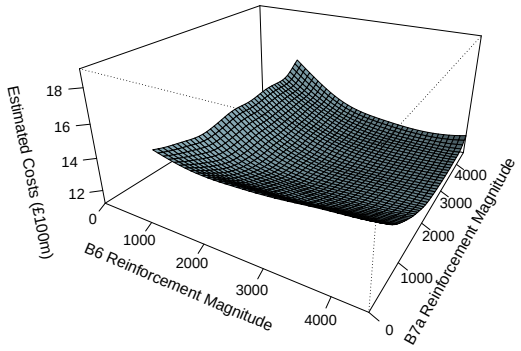

(b) Wave 2.

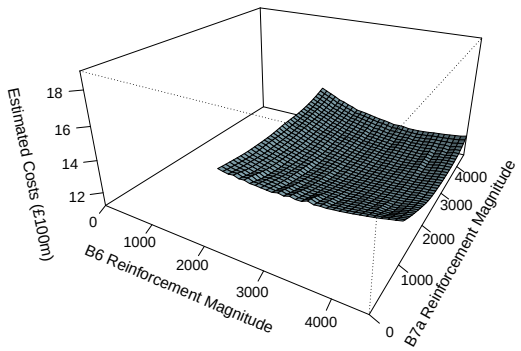

(c) Wave 3.

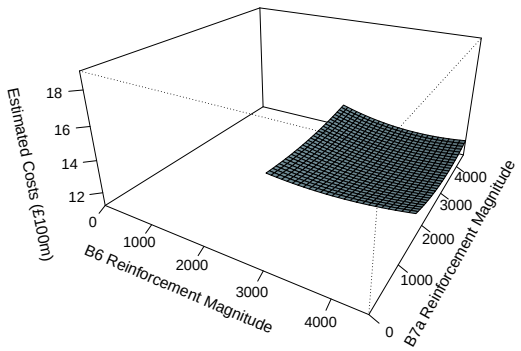

(d) Wave 4.

Figure 9.4: Plots to show how estimates of expected total costs across all three stages vary with reinforcement decisions and fitted emulator model.

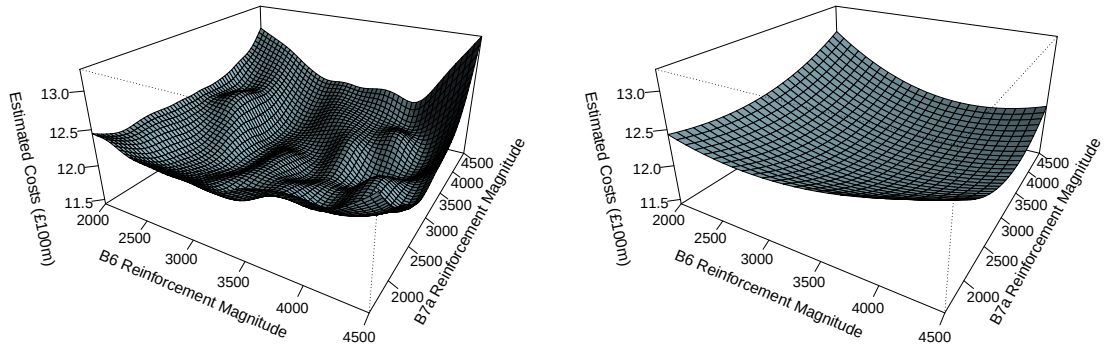

(a) Wave 1.

(b) Wave 4.

Figure 9.5: Plots to show how estimates of expected total costs across all three stages vary with stage 1 reinforcement decisions and fitted emulator model, over the range of decisions considered in the fourth wave.

variation in expected total costs as the decision is varied is much flatter over the range of decisions considered in the fourth wave in comparison to the first.

Therefore, Figure 9.5 was created which compares the estimates of expected total costs from the first and fourth waves over the range of decisions considered in the fourth wave. Again, the estimates of expected total costs from the emulator models fitted in the fourth wave show a smoother variation as B6 and B7a reinforcement magnitude are varied in comparison to estimates from the emulator models fitted in the first wave. This is due to the fact that models fitted in the fourth wave are fitted over a smaller range of values of the decision variables and can therefore fit a more accurate model over that smaller range.

Further evidence of this improvement can be seen by comparing Figure 9.6 to Figure 9.7, which compares credible intervals for the estimates of expected total costs for the first and fourth wave emulator models respectively over the range of B6 and B7a reinforcement magnitudes considered in the fourth wave. As can be seen, the credible intervals are much narrower in the fourth wave in comparison to the first (on average 4.17 times narrower) which indicates the improved level of confidence in the estimate from fitting the emulator model over a smaller range of decisions.

However, because the estimated expected total costs are relatively flat over this region

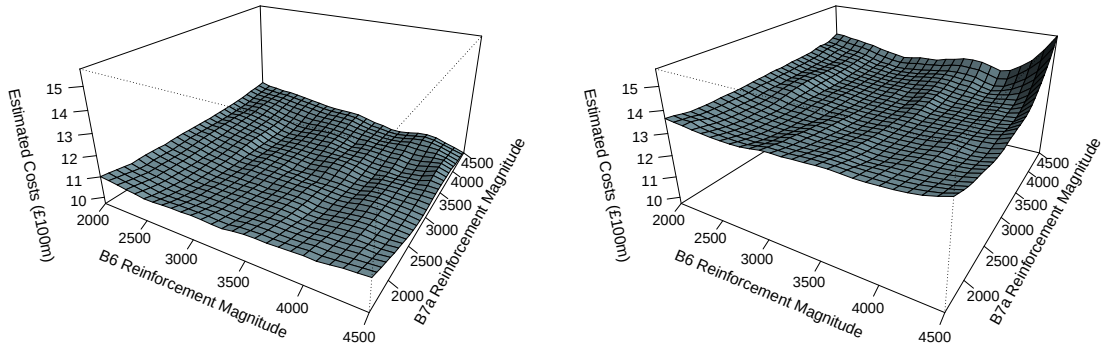

(a) Lower Bound. (b) Upper Bound.

Figure 9.6: Plots to show credible bounds for the estimates of expected total costs for the emulator models fitted in the first wave, over the range of decisions considered in the fourth wave.

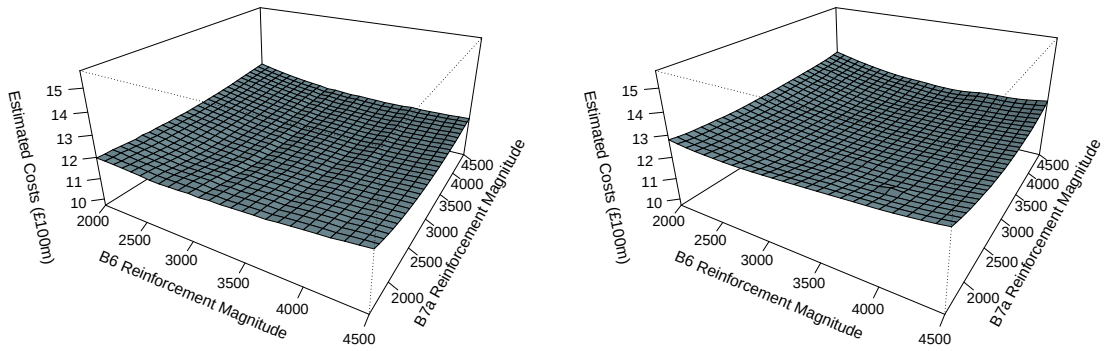

(a) Lower Bound. (b) Upper Bound.

Figure 9.7: Plots to show credible bounds for the estimates of expected total costs for the emulator models fitted in the fourth wave.

(i.e. there is relatively little variation in estimated expected total costs as reinforcement decision is varied) no further decisions can be eliminated from consideration. In particular, the decisions which result in costs of over £1.8 billion when little to no reinforcement is made have been eliminated from consideration and all decision still considered give similar, lower estimates of expected total costs, varying between £1.17 billion and £1.24 billion

However, even in the final wave the magnitudes of reinforcement vary considerably, with B6 reinforcement varying between 2000 MW and 4500 MW and B7a reinforcement varying between 1600 MW and 4500 MW, with this range considering 3.57 times as many decisions in comparison to the range of decisions considered in the final wave of stage 1 of the related two stage problem in Section 8.4. Further, despite eliminating the very large estimates of expected total costs when little to no reinforcement has been made, estimates of expected total costs in the final wave still vary by £70 million. Therefore, it would be desirable if the range of decisions considered could be reduced even further, to further improve the accuracy of the estimates and make an even better decision.

9.3.2 Stage 1 Decision Using Improved Emulator Models for Stage 2 and 3 Cost Estimates

Considering Alternative, Smaller Ranges for Possible Total Reinforcement After the Second and Third Decisions

In the previous subsection it was noted how relatively few stage 1 decisions are eliminated by the final stage 1 wave of the three stage problem of Section 9.2 in comparison to results from the final wave of stage 1 in the two stage problem considered in Section 8.4. This is due to the fact that the emulator models for stage 2 and stage 3 costs are fitted over quite a large range of decisions, so there exists quite a lot of uncertainty when estimating optimal reinforcement decisions for given stage 2 or 3 scenarios (values of $\boldsymbol{\psi}_{m,\theta_{i,m}}$) and stage 1 or 2 decision ($\mathbf{d}_{T_{m-1},\theta_{i,m}}$) using the methodology of Section 9.1.2.

This could be overcome by performing a separate wave process for each sampled decision and scenario, as was considered in Section 8.7, which was shown to greatly

reduce the error in the estimated expected total costs. However, as was noted in Sections 8.2.5 and 8.7, this would require $N_{\theta_2} + N_{\theta_3}$ (= 100 for the example presented) separate wave process to be carried out within each stage 1 wave which is not feasible for the resources available to us.

However, it is still possible that the error in the estimates of expected total costs in stages 2 and 3 can be reduced by more carefully considering the ranges of decision variables that these emulators are fitted over, instead of simply fitting each over the range 0 MW to some maximum values. For example, in Section 8.5.3 it was shown that all estimated optimal total B6 reinforcement magnitudes in the second stage of the 2-stage problem detailed in Section 8.3 (which is conditionally equivalent to the third stage of the 3-stage problem detailed in Section 9.2.3) are at least 5800 MW and no more than 6350 MW. This information could be used to fit the stage 3 emulator model over a smaller sensible range of decisions to improve the accuracy of the approximation to the simulator, and in turn increase confidence in the estimates that result from it.

This section will show that by fitting the stage 2 and 3 emulator models over a smaller range of values of decision variables (i.e. not considering unnecessarily small reinforcements), a greater range of stage 1 decisions can be eliminated from consideration, even when being quite conservative with the ranges of decisions considered in the second and third stages.

Therefore, when making the stage 1 reinforcement decision it will be considered that the total B6 reinforcement after the stage 2 decision will be between 3500 MW and 6500 MW; the total B6 reinforcement after the stage 3 decision will be between 5000 MW and 8000 MW; the total B7a reinforcement after the stage 2 decision will be between 2500 MW and 5500 MW and the total B7a reinforcement after the stage 3 decision will be between 2500 MW and 5500 MW. Sections 9.4 and 9.5 will verify that these are sensible (and still quite wide) initial ranges to consider for reinforcement decisions. These ranges are illustrated in Figure 9.9

By contrasting these to the ranges considered in Section 9.3.1, displayed in Figure 9.8, it can be seen that even though the ranges considered in Figure 9.9 are quite conservative they are much smaller than those of Section 9.3.1 with the stage 2 emulator now considering 74.8% fewer decisions and the stage 3 emulator now considering 80.7%

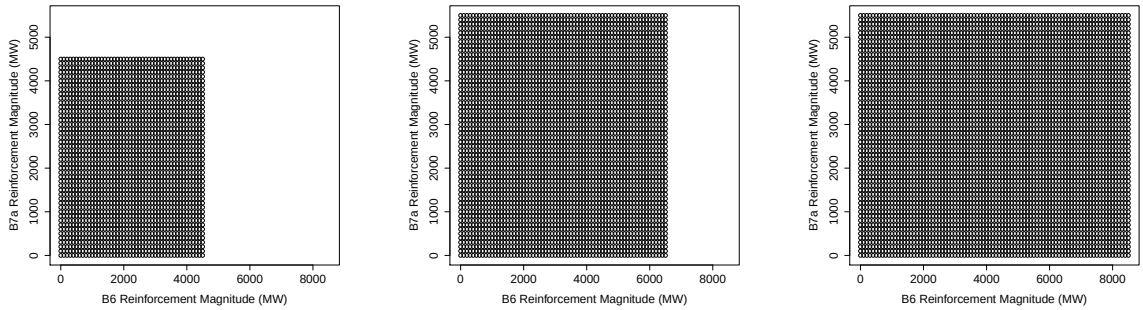

(a) Stage 1. (b) Stage 2. (c) Stage 3.

Figure 9.8: Plots to illustrate the ranges of possible total reinforcement considered in each stage in Section 9.3.1.

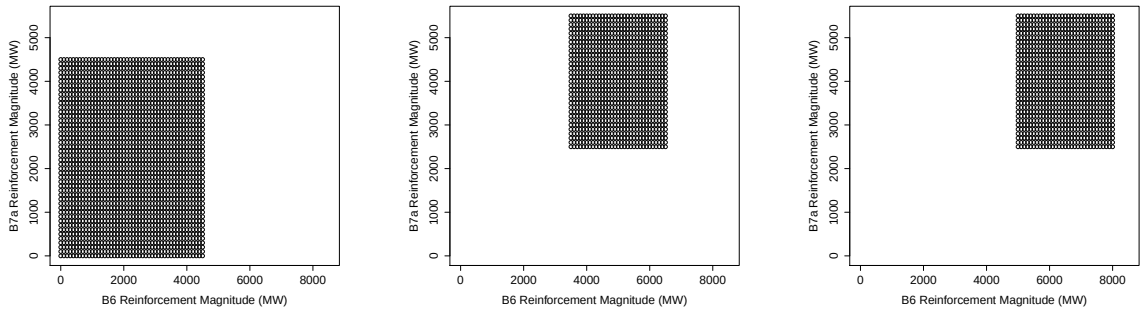

(a) Stage 1. (b) Stage 2. (c) Stage 3.

Figure 9.9: Plots to illustrate the smaller ranges of possible total reinforcement considered in each stage in this section.

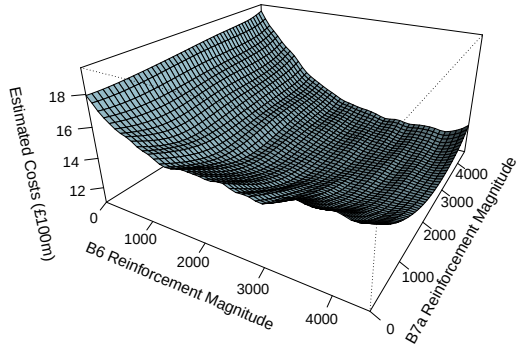

Figure 9.10: Plot to illustrate how estimates of expected total costs across all three stages vary with B6 reinforcement magnitude and B7a reinforcement magnitude in the first wave of stage 1.

fewer decisions. This will reduce the error in the estimates arising from these emulator models, which will allow more stage 1 decisions to be eliminated from consideration and allow for a more accurate stage 1 decision to be made.

Estimates of Expected Total Costs Across All Stages as a Function of Stage 1 Decision

Figure 9.10 displays how estimates of expected total costs vary with stage 1 B6 and B7a reinforcement magnitude when using the methodology of Section 9.1.2 to estimate expected total costs across all three stages. As was the case in the previous subsection, the emulators used are not perfect approximations to the simulators. Therefore, credible intervals for the estimates of Figure 9.10 were calculated using the methodology of Section 9.1.4 and are displayed in Figure 9.11.

By comparing the credible bounds of Figure 9.11 to those of Figure 9.2 (the equivalent plot of the previous subsection) it can be seen how the credible bounds of Figure 9.11 are much narrower, indicating the increased level of confidence in the estimates which arises from fitting the second and third wave emulators over a smaller range of values of decisions in these stages, which improves the accuracy and confidence in the estimates that arise from these emulators.

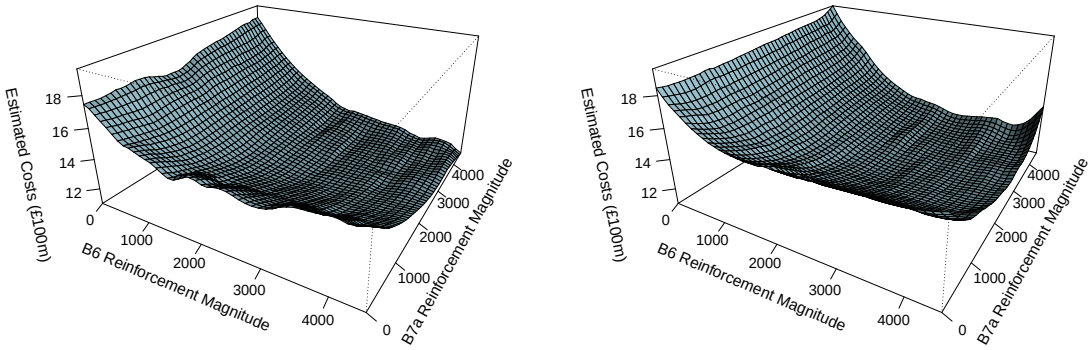

(a) Lower Bound. (b) Upper Bound.

Figure 9.11: Plots to show credible bounds for the estimates of expected total costs for the emulator models fitted in the first wave of stage 1.

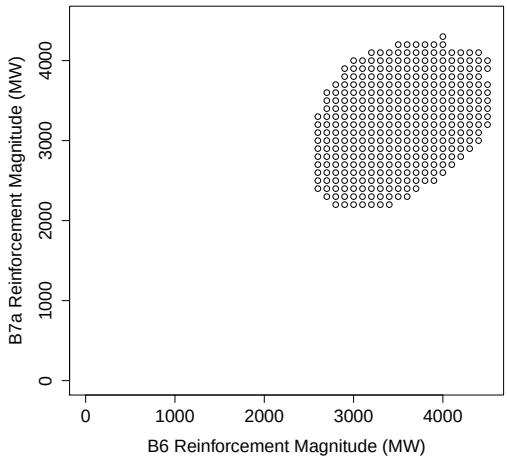

Figure 9.12: Plot to show decisions not eliminated from consideration in the fourth wave of stage 1.

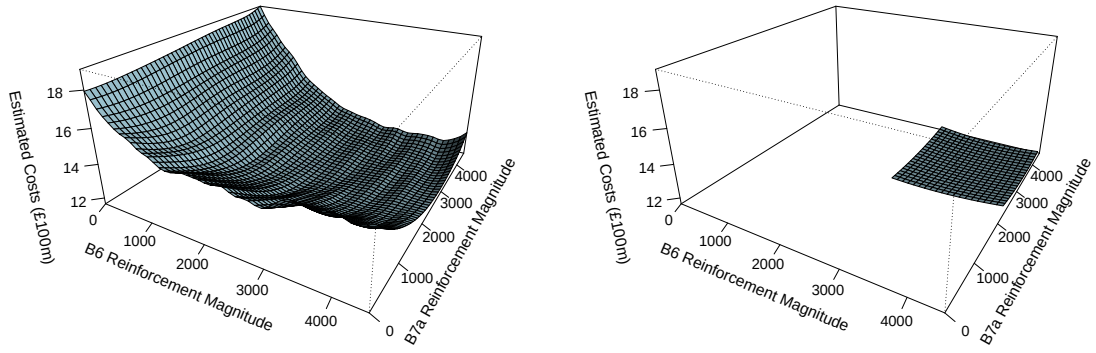

(a) Wave 1.

(b) Wave 4.

Figure 9.13: Plots to show how estimates of expected total costs across all three stages vary with reinforcement decisions and fitted emulator model.

The methodology of Section 8.2.7 can again be used to eliminate decisions from consideration which have evidence against them being optimal and fit a more accurate emulator model over a smaller range of decisions. Figure 9.12 displays the decisions which would merit consideration in a fourth wave (i.e. after three waves of elimination), which shows that 84.4% of the decisions initially considered have been eliminated. Further, the range of decisions considered in the fourth wave is 51.8% smaller than the that of the fourth wave displayed in Figure 9.3 (c) of Section 9.3.1. This highlights the increased level of power to eliminate decisions which have evidence against them being optimal from fitting the second and third stage emulator models over a smaller range of decisions.

Figure 9.13 displays how estimated expected total costs vary with B6 and B7a reinforcement magnitude in the first and fourth waves. As was the case in the previous subsection, it can be seen that due to estimated expected total costs being very high when little to no reinforcement is made (exceeding £1.8 billion when no B6 reinforcement is made) that estimates in fourth wave appear to be very flat in comparison to the first. This is even more true than in the previous subsection, as the final wave now considers less than half the decisions in comparison to the previous subsection, and there is even less variation in estimated expected total costs over this range. As a

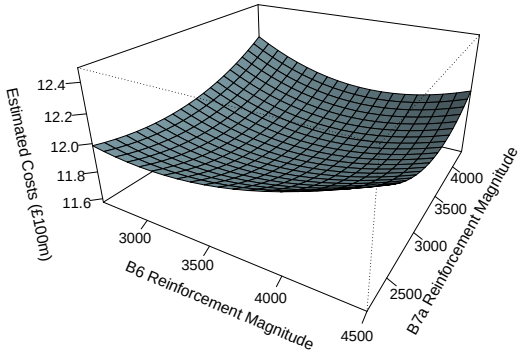

Figure 9.14: Plot to show how estimates of expected total costs across all three stages vary with reinforcement decisions in the fourth wave.

result, Figure 9.14 was created to illustrate how estimates of expected total costs vary with stage 1 B6 and B7a reinforcement magnitude in the fourth wave. As can be seen, estimates of expected total costs vary smoothly as reinforcement decisions are varied, with all decisions resulting in similar, relatively low estimates of expected total costs.

Estimate of Optimal Stage 1 Decision

A decision which minimises the estimate of expected total costs across all three stages based on the emulator models fitted in the fourth wave (i.e. the estimate of the optimal stage 1 decision) would make 3540 MW B6 and 3340 MW B7a reinforcement in stage 1. As all decisions considered in the final wave give similar, relatively low estimates of expected total costs there is little risk of making a poor decision when making such a decision which minimises the estimate of expected total costs. In particular, the estimates of expected total costs in excess of £1.8 billion which arise when little to no reinforcement is made have been eliminated from consideration.

9.4 Stage 2 Decisions

Estimating Optimal Decisions for a Range of Stage 2 Scenarios

In a real application, after the first decision has been made, a number of years will pass before a second decision must be made for the observed state of the power system (for the example outlined in Section 9.2, it is assumed that 5 years pass between making the first decision at the beginning of year 1 and making the second at the beginning of year 6 based on the observed value of $\boldsymbol{\psi}_2$). As was the case for the second stage of the 2 stage example, in a real life application it would only be necessary to estimate an optimal second stage decision for the stage 2 scenario actually observed. Section 8.5.1 demonstrated how to estimate an optimal decision for a given observation.

However, in this thesis it is also of interest to illustrate how the estimated expected total costs and the resulting estimates of optimal decisions vary depending on the scenario observed. Section 8.5.2 illustrated how the estimated optimal decision can be approximated as a function of stage 2 scenario, with Section 8.5.3 going on to accurately estimate optimal decisions for several scenarios to show how the estimated optimal decision varies with the stage 2 scenario observed.

Stage 2 Scenario	$\boldsymbol{\psi}_2$
Stage 2 Scenario 1	0.95
Stage 2 Scenario 2	1
Stage 2 Scenario 3	1.05

Table 9.6: Table summarising the value of $\boldsymbol{\psi}_2$ observed for three scenarios considered.

This section will consider how the estimated optimal stage 2 decision varies for three different stage 2 scenarios, detailed in Table 9.6. Recall from Section 9.2.3, for the example presented $\boldsymbol{\psi}_2$ is used to describe the beliefs about peak demand level in stage 2 at the time the second decision is made, such that stage 2 peak demand is believed to take a value between $(100\boldsymbol{\psi}_2 - 5)\%$ and $(100\boldsymbol{\psi}_2 + 5)\%$ of the year 11 peak demand level projected by [69]. This means that the greater the value of $\boldsymbol{\psi}_2$, the greater the expected stage 2 peak demand level. For each scenario it is assumed that 3540 MW B6 and 3340 MW B7a reinforcement was previously made in stage 1 (i.e. the reinforcement

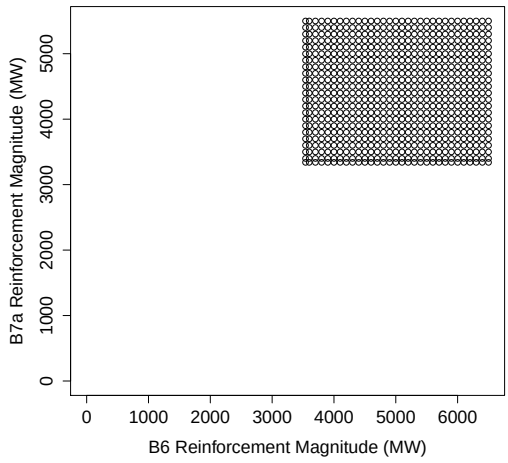

Figure 9.15: Plots to show initial range of decisions considered for all stage 2 scenarios, assuming 3540 MW B6 and 3340 MW B7a reinforcement was previously made in stage 1.

decision which minimises the estimate of expected total costs based on the emulator models fitted in the fourth wave of the first stage).

Again, it is noted that any value of $\boldsymbol{\psi}_2$ between 0.95 and 1.05 could be observed, and when total expected costs were estimated in stage 1 an expectation was taken across any stage 2 scenario that could be observed using the PDF of prior beliefs detailed in Section 9.2.3 and the methodology of Section 9.1.2.

Estimates of Expected Total Costs In Stage 2 Onwards as a Function of Stage 2 Decision

When the time comes to make the second reinforcement decision, it is assumed that the estimated optimal decision was previously made in stage 1 (i.e. reinforcing the B6 and B7a boundaries by 3540 MW and 3340 MW respectively). Initially it is considered that the total B6 reinforcement after the second reinforcement will be between 3540 MW (i.e. do nothing in stage 2) and 6500 MW, whereas the total B7a reinforcement after the second reinforcement will be between 3340 MW (i.e. do nothing in stage 2) and 5500 MW. This range of decisions is illustrated in Figure 9.15.

Figure 9.16 displays how estimates of expected total costs in stage 2 onwards vary with reinforcement decision for each of the three scenarios of Table 9.6. As can be seen,

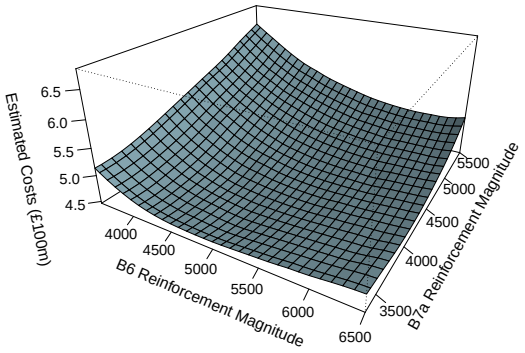

(a) Scenario 1.

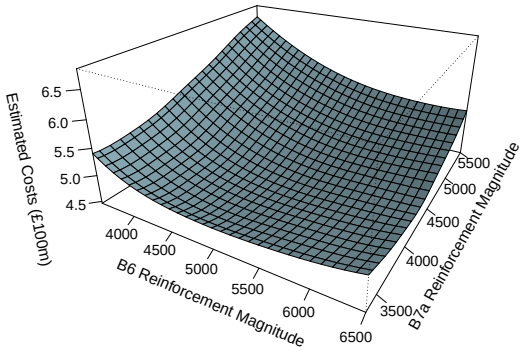

(b) Scenario 2.

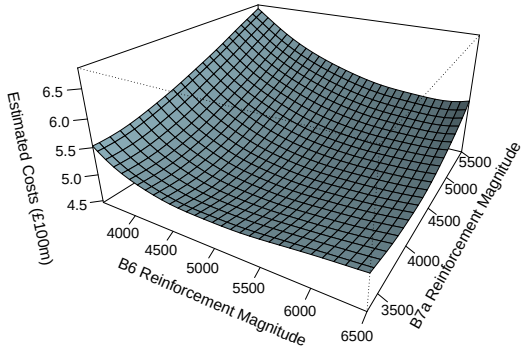

(c) Scenario 3.

Figure 9.16: Plots to show how estimates of expected total costs in stage 2 onwards vary with stage 2 total reinforcement decision and scenario.

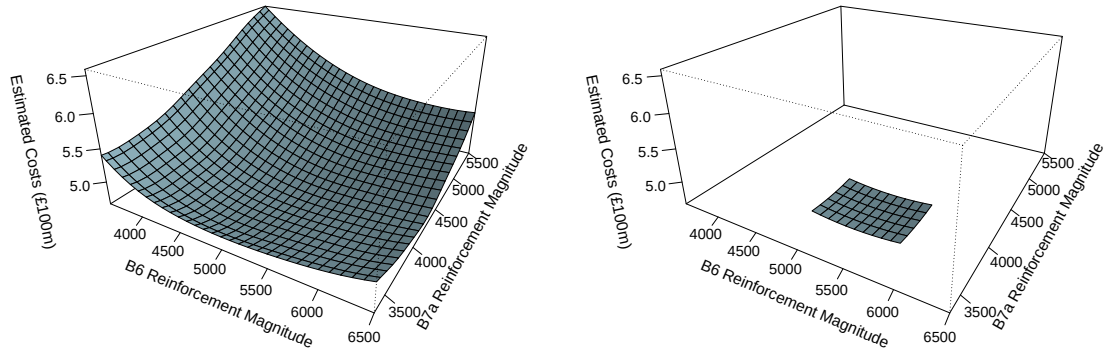

(a) Wave 1. (b) Wave 4.

Figure 9.17: Plots to show how estimates of expected total costs in stage 2 onwards vary with stage 2 total reinforcement decision in the first and final wave for scenario 2 ($\boldsymbol{\psi}_2 = 1$).

estimates of expected total costs are quite similar for each scenario, with estimates of expected total costs being greatest when little further B6 reinforcement is made or when a large further B7a reinforcement is made. Further, estimates of expected total costs appear to increase as $\boldsymbol{\psi}_2$ increases, with estimates being on average 3.78% (£19 million) greater in scenario 2 in comparison to scenario 1, and on average 6.40% (£31 million) greater in scenario 3 in comparison to scenario 1. This indicates that estimates of expected total costs increase as the expected future peak demand level increases.

Again, the emulator models used to estimate expected total costs are not perfect approximations to the simulators and contain error. Credible intervals for the estimates of expected total costs can be calculated using the methodology of Section 9.1.4, which can in turn be used in the methodology of Section 8.2.7 to eliminate decisions from consideration which have evidence against them being optimal in order to fit a more accurate model over a smaller range of decisions, which in turn allows for a more accurate decision to be made.

For example, Figure 9.17 compares how estimates of expected total costs vary with total B6 and B7a reinforcement in the first wave and in the fourth wave (i.e. after three waves of elimination have been performed), assuming scenario 2 was observed. As can be seen, decisions which result in large estimates of expected total costs (i.e.

when further B6 reinforcement is small or further B7a reinforcement is large) have been eliminated from consideration. Further, it can be seen that the estimates of expected total costs in wave 4 are very flat in comparison to those of wave 1, in the sense that there is little variation in the estimates of expected total costs as the reinforcement magnitudes of the B6 and B7a boundaries are varied.

Figure 9.18 displays how estimates of expected total costs in stage 2 onwards vary with total B6 and B7a reinforcement in the final wave for each scenario. For each scenario it can be seen that all estimates are quite flat in the sense that there is little variation in the estimates of expected total costs as the B6 and B7a reinforcement magnitudes are varied. This implies that in these regions there is little risk of making a poor decision (if the desire is to minimise the estimate of expected total costs), as all decisions result in similar, relatively low estimates of expected total costs. In particular, the large estimates of expected total costs from the first wave, displayed in Figure 9.16, which occur when B6 reinforcement magnitude is low or B7a reinforcement magnitude is high, have been avoided (i.e. eliminated from consideration).

In Figure 9.18 it can also be seen that as $\boldsymbol{\psi}_2$ increases (i.e. as expected future peak demand level increases) the estimates of expected total costs increase. Further, larger values of $\boldsymbol{\psi}_2$ generally consider slightly larger magnitudes of reinforcement in the fourth wave, suggesting that the optimal reinforcement magnitudes may increase as the observed value of $\boldsymbol{\psi}_2$ increases.

However, Figure 9.19 displays the decisions considered in the final wave for each of the scenarios. As can be seen all regions considered are quite similar, with many decisions appearing in the regions considered of all three scenarios. As further waves result in no further elimination of decisions, none of the decisions can be ruled out as potentially optimal, which in turn means it cannot definitively be said that a larger value of $\boldsymbol{\psi}_2$ necessarily results in a larger reinforcement magnitude.

Estimates of Optimal Stage 2 Total Reinforcement Decisions

Table 9.7 details how the estimated optimal stage 2 total reinforcement (i.e. reinforcement decisions which minimises the estimate of expected total costs in the final wave) varies with the scenario observed. All scenarios result in an increase in reinforcement

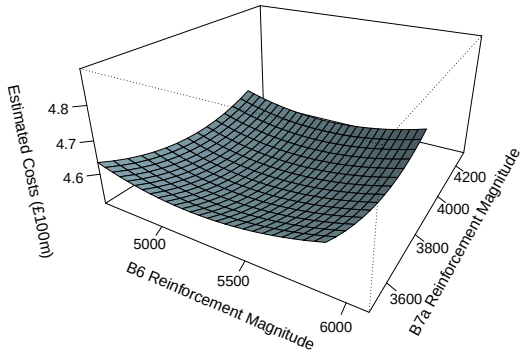

(a) Scenario 1.

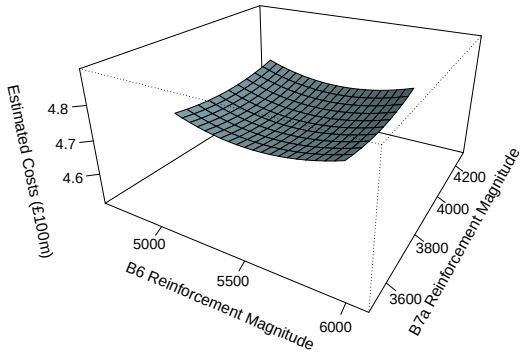

(b) Scenario 2.

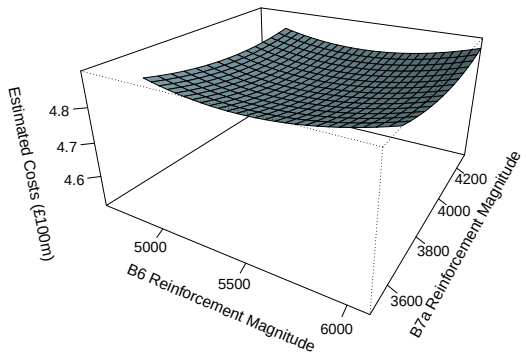

(c) Scenario 3.

Figure 9.18: Plots to show how estimates of expected total costs in stage 2 onwards vary with stage 2 total reinforcement decision and scenario in the final wave.

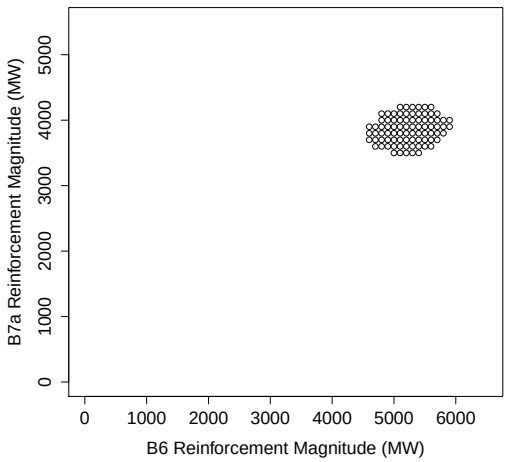

(a) Scenario 1.

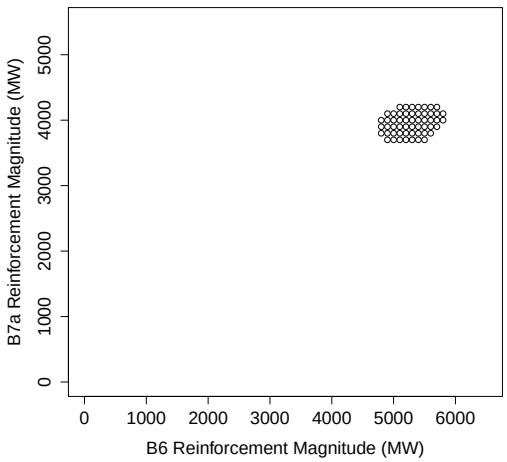

(b) Scenario 2.

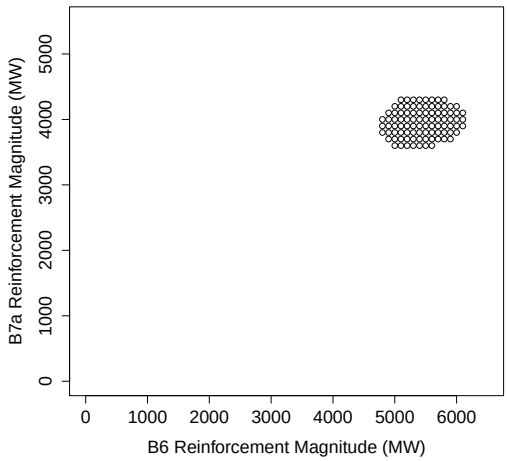

(c) Scenario 3.

Figure 9.19: Plots to show how the ranges of decisions considered in the final wave vary with stage 2 scenario.

Stage 2 Scenario	B6 Reinforcement Magnitude	B7a Reinforcement Magnitude
Stage 2 Scenario 1	5220 MW	3900 MW
Stage 2 Scenario 2	5300 MW	3920 MW
Stage 2 Scenario 3	5350 MW	4040 MW

Table 9.7: Table summarising how the estimated optimal stage 2 total reinforcement decision varies with stage 2 scenario.

of both boundaries from the first stage reinforcement. For example, the total reinforcement in scenario 2 is 5220 MW B6 and 3900 MW B7a, which is an increase of 1680 MW B6 and 560 MW B7a reinforcement from the first stage decision.

The estimated optimal B6 reinforcement varies by 130 MW (5220 MW in scenario 1 to 5350 in scenario 3) and the estimated optimal B7a reinforcement varies by 140 MW (3900 MW in scenario 1 to 4040 MW in scenario 3). These are quite small differences, which implies that for this example the scenario observed has relatively little effect on the decision made in the second stage. However, the next section will show how the observed stage 3 scenario has a large effect on decision made.

9.5 Stage 3 Decisions

Estimating Optimal Decisions for a Range of Stage 3 Scenarios

After the second decision has been made in year 6, the power system will continue to be observed until the third reinforcement decision is to be made in year 11. Again, it is noted that $\boldsymbol{\psi}_3$ (the parameter which describes the observed state of the power system in year 11) is modelled as a continuous variable and there are an infinite number of possible states of the power system that could be observed in year 11. For a real life application an estimate of the optimal reinforcement decision would only be required for the value of $\boldsymbol{\psi}_3$ actually observed. However, it is of interest in this thesis to compare how the estimated optimal decision to be made in year 11 varies with the observed state of the power system. Therefore, this section will provide results for 9 potential observations of $\boldsymbol{\psi}_3$ to show how the estimated optimal stage 3 decision varies depending on what was observed.

Recall, as detailed in Section 9.2.3, $\boldsymbol{\psi}_3$ represents the estimate in year 11 for the peak demand level in stage 3 as a proportion of the year 16 peak demand level projected by [69], such that beliefs about stage 3 peak demand level form a uniform distribution between $(100\boldsymbol{\psi}_3 - 0.05)\%$ and $(100\boldsymbol{\psi}_3 + 0.05)\%$ of the projected year 16 peak demand level given by [69].

Stage 3 Scenario	$\boldsymbol{\psi}_3$
Stage 3 Scenario 1.1	0.9
Stage 3 Scenario 1.2	0.95
Stage 3 Scenario 1.3	1
Stage 3 Scenario 2.1	0.95
Stage 3 Scenario 2.2	1
Stage 3 Scenario 2.3	1.05
Stage 3 Scenario 3.1	1
Stage 3 Scenario 3.2	1.05
Stage 3 Scenario 3.3	1.1

Table 9.8: Table summarising the value of $\boldsymbol{\psi}_3$ observed for nine scenarios considered.

Table 9.8 details the nine scenarios that will be considered in stage 3. For scenarios 1.1, 1.2 and 1.3, it is assumed that scenario 1 of Table 9.6 was previously observed in stage 2, and that the total reinforcement after the second decision was 5220 MW B6 and 3900 MW B7a (the corresponding estimate of optimal stage 2 decision for such a scenario as identified in Section 9.4). For scenarios 2.1, 2.2 and 2.3, it is assumed that scenario 2 of Table 9.6 was previously observed in stage 2, and that the total reinforcement after the second decision was 5300 MW B6 and 3920 MW B7a (the corresponding estimate of optimal stage 2 decision for such a scenario as identified in Section 9.4). For scenarios 3.1, 3.2 and 3.3, it is assumed that scenario 3 of Table 9.6 was previously observed in stage 2, and that the total reinforcement after the second decision was 5350 MW B6 and 4040 MW B7a (the corresponding estimate of optimal stage 2 decision for such a scenario as identified in Section 9.4).

This means that scenarios 1.3, 2.2 and 3.1 are not identical despite all having the same beliefs about stage 3 peak demand level, as all assume different reinforcement decisions were previously made as a result of the differing stage 2 observations. This will allow for the remainder of this section to illustrate how observations and the resulting decisions in previous stages can affect cost estimates and the resulting decisions in a later stage.

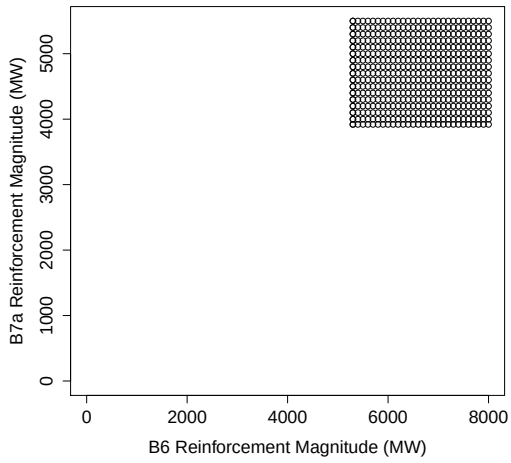

Figure 9.20: Plot to show ranges of stage 3 total reinforcement decisions initially considered for Scenarios 2.1, 2.2 and 2.3.

Estimates of Expected Total Costs In Stage 3

Initially it is considered that the total reinforcement after the third reinforcement will be between the reinforcement previously made after the second decision and 8000 MW B6 and 5500 MW B7a reinforcement. Figure 9.20 illustrates the range of decisions initially considered for scenarios 2.1, 2.2 and 2.3, where total B6 reinforcement ranges from 5300 MW (do nothing in stage 3) to 8000 MW and total B7a reinforcement ranges from 3920 MW (do nothing in stage 3) to 5500 MW.

Figure 9.21 illustrates how estimates of expected total costs vary with reinforcement decision for 3 of the 9 scenarios detailed in Table 9.8. The three scenarios illustrated are the two most extreme scenarios that could be observed (scenarios 1.1 and 3.3) with an intermediate scenario (scenario 2.2). Illustrations of how estimates of expected total costs vary with reinforcement decision for all nine scenarios are given in Appendix D.2. In all scenarios, estimates of expected total costs appear to rise quite linearly as B7a reinforcement magnitude is increased. This suggests that in the the third stage, reinforcement of the B6 boundary is more important than that of the B7a boundary. This is consistent with what was observed for the second stage of the two stage problem in Sections 8.5.1 and 8.5.3.

By comparing the three plots of Figures 9.21 it can be seen that estimated expected total costs increase as $\boldsymbol{\psi}_3$ increases (i.e. expected total costs increase as expected stage

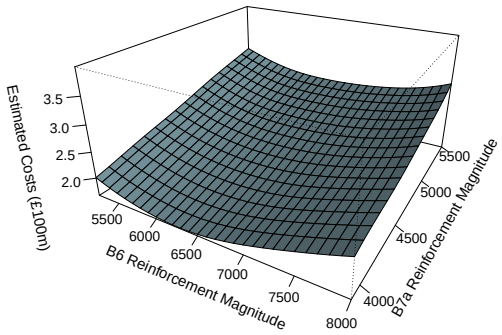

(a) Scenario 1.1.

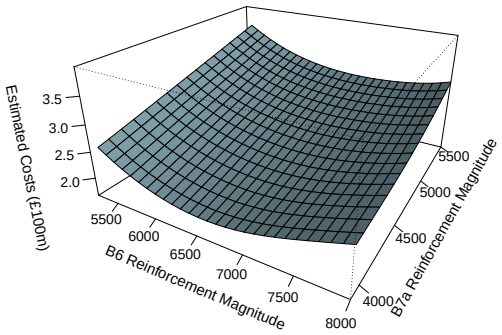

(b) Scenario 2.2.

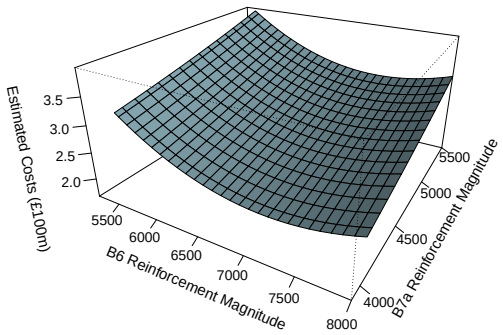

(c) Scenario 3.3.

Figure 9.21: Plots to show how estimates of expected total costs vary with stage 3 total reinforcement decision and scenario.

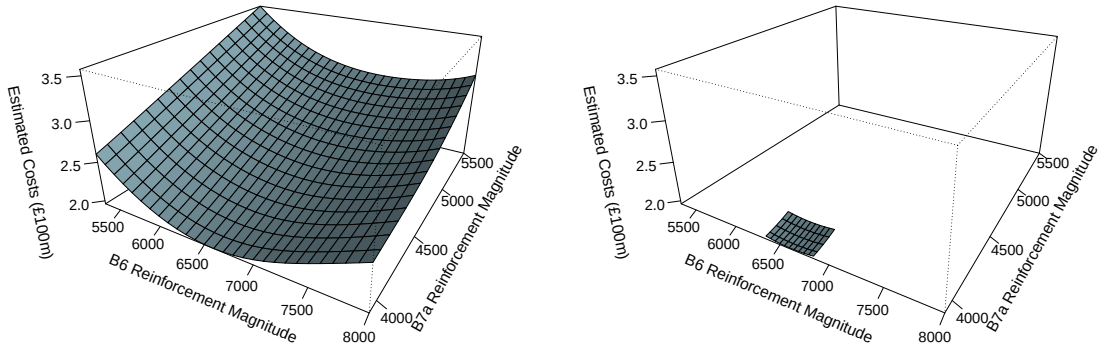

(a) Wave 1. (b) Wave 3.

Figure 9.22: Plots to show how estimates of expected total costs vary with total B6 and B7a reinforcement in first and final waves for stage 3 scenario 2.2.

3 peak demand level increases), with expected costs being on average around 11.2% (£26 million) greater in scenario 2.2 in comparison to scenario 1.1 and on average around 7.1% (£18 million) greater in scenario 3.3 in comparison to scenario 2.2.

Again, as the emulators models used to estimate costs are not perfect approximations to the simulators, the estimates of Figure 9.21 contain error. Credibility bounds for the estimates can therefore be calculated using the methodology of Section 5.2.6, which can in turn be used in the methodology of Section 6.2.1 to eliminate decisions from consideration which have evidence against them being optimal in order to fit a more accurate emulator model over a smaller range of decisions.

For example, Figure 9.22 compares how estimates of expected total costs vary with reinforcement decision for scenario 2.2 in the first wave (in Figure 9.22 (a)) and after two waves of eliminating reinforcement decisions which have evidence against them being optimal (in Figure 9.22 (b)). As can be seen, the estimates of expected total costs are very flat in the third wave (i.e. after two waves of elimination), in the sense that there is little variation in the estimates of expected total costs as B6 and B7a reinforcement magnitudes are varied, indicating that all decisions give similar, relatively low estimates of expected total costs. In particular, reinforcement decisions which result in large estimates of expected total costs (when B7a reinforcement is high

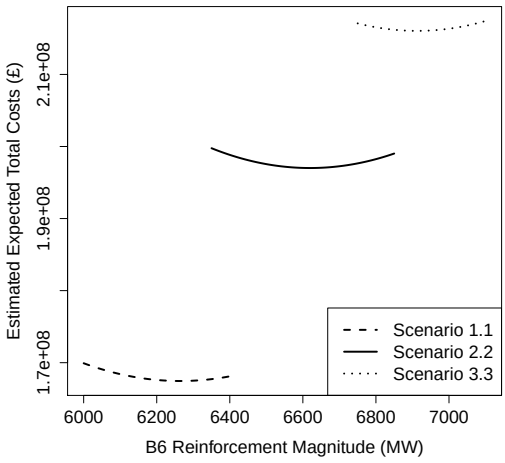

Figure 9.23: Plot to show how estimates of expected total costs vary with total B6 reinforcement magnitude in wave 3 for a range of stage 3 scenarios.

or B6 reinforcement is low) have been eliminated from consideration. An estimate of the optimal decision (i.e. a decision to minimise the estimate of expected costs based on the emulator model fitted in the third wave) would be to increase total B6 reinforcement to 6620 MW (an increase of 1320 MW from stage 2) and to make no further B7a reinforcement (i.e. keep total B7a reinforcement at 3920 MW).

Figure 9.23 displays how estimates of expected total costs vary with B6 reinforcement magnitude in wave 3 for a variety of stage 3 scenarios. The estimates of scenario 1.1 assume total B7a reinforcement was 3900 MW, the estimates of scenario 2.2 assume total B7a reinforcement was 3920 MW and the estimates of scenarios 3.3 assume total B7a reinforcement was 4040 MW. These B7a reinforcements will later be identified as the estimated optimal stage 3 total reinforcements in Table 9.9.

It can be seen that estimates of expected total costs are greater in scenario 2.2 in comparison to scenario 1.1, and greater in scenario 3.3 in comparison to scenario 2.2. This indicates that estimates of expected total costs increase as the observed value of $\boldsymbol{\psi}_3$ increases, i.e. that estimates of expected total costs increase as the expected stage 3 peak demand level increases. Further, it can be seen that the ranges of B6 reinforcement magnitude considered in the third wave also increase as $\boldsymbol{\psi}_3$ increases, indicating that the increase in the estimates of expected total costs justify a larger reinforcement of the B6 boundary.

Estimates of Optimal Stage 3 Total Reinforcement Decisions

Stage 3 Scenario	B6 Reinforcement Magnitude	B7a Reinforcement Magnitude
Stage 3 Scenario 1.1	6260 MW	3900 MW
Stage 3 Scenario 1.2	6430 MW	3900 MW
Stage 3 Scenario 1.3	6590 MW	3900 MW
Stage 3 Scenario 2.1	6460 MW	3920 MW
Stage 3 Scenario 2.2	6620 MW	3920 MW
Stage 3 Scenario 2.3	6760 MW	3920 MW
Stage 3 Scenario 3.1	6680 MW	4040 MW
Stage 3 Scenario 3.2	6820 MW	4040 MW
Stage 3 Scenario 3.3	6910 MW	4040 MW

Table 9.9: Table summarising how the estimated optimal stage 3 total reinforcement decision varies with stage 3 scenario.

Table 9.9 details how the estimated optimal stage 3 total reinforcement decision varies with stage 3 scenario observed. As can be seen, all potential stage 3 scenarios would make no further B7a reinforcement from stage 2. This is consistent with what has been observed throughout this section, with expected total costs increasing as B7a reinforcement magnitude is increased.

However, all scenarios show an increase in total B6 reinforcement magnitude after third stage decision, with total B6 reinforcement after the third stage varying from 6260 MW to 6910 MW (increases of 1040 MW to 1560 MW). The additional B6 reinforcement made in the third stage appears to increase as $\boldsymbol{\psi}_3$ (expected stage 3 peak demand level) increases. For example, scenarios 2.1, 2.2 and 2.3 all assume that 5300 MW B6 and 3920 MW B7a reinforcement was previously made in stage 2. However, observing $\boldsymbol{\psi}_3 = 0.95$ results in a further 1160 MW reinforcement being built in stage 3, whereas observing $\boldsymbol{\psi}_3 = 1.05$ results in a further 1460 MW reinforcement being built in stage 3.

It is also interesting to compare scenarios where equal values of $\boldsymbol{\psi}_3$ were observed, such as scenarios 3.2 and 2.3, both of which observe $\boldsymbol{\psi}_3 = 1.05$. In all cases a larger B7a reinforcement magnitude results in a larger estimated optimal B6 reinforcement (an additional 60 MW in scenario 3.2 in comparison to 2.3 for example). This implies that although no further B7a reinforcement would be made in any scenario, if a greater reinforcement was made in a previous stage this would justify a greater B6 reinforce-

ment in the third stage. This is consistent with what has been observed throughout this thesis, i.e. that an interaction exists between the B6 and B7a boundaries, which is what makes investigating an example which makes simultaneous reinforcement decisions about these boundaries interesting.

9.6 Sensitivities of the Problem of Section 9.2

Just as for the single stage problems considered in Chapters 5 and 6, the estimates of expected total costs and the resulting estimates of optimal reinforcement decisions to be made in each stage of the multi-stage problem are sensitive to many assumptions made about the power system, such as the assumed cost to reinforce. However, there are several other uncertainties that must be considered now which were not considered in the single stage example, such as the assumed discount rate of future costs, or how long of a future horizon is considered for future costs (for example, instead of stage 3 constraint costs being estimated between years 16 and 25, they could be estimated between years 16 and 20 or 16 and 30). This section will give consideration to how assumptions made about the power system affect the estimates of optimal reinforcement decisions to be made.

9.6.1 Discount Rate of Future Costs

In Section 8.3.4 it was stated that a discount rate of 5% was assumed for the examples of Chapters 8 and 9, as this was a common assumption in the existing multi-stage transmission expansion literature [2, 26, 3, 80]. However, it was also stated that 10% is also quite commonly assumed [30, 85, 62]. If a larger discount rate is assumed, costs in future years will be discounted at a greater rate (giving them a lower present value) which makes the cost of reinforcement relatively more expensive in comparison to the constraint costs in future years. This in turn may result in a smaller reinforcement being built. Conversely, if a lower discount rate is assumed, future costs are discounted at a lower rate, which makes the present value of future constraint costs greater in comparison to the cost of reinforcement, which may result in a larger reinforcement being built.

This subsection will present results for how the estimated optimal decisions made in each stage for the example detailed in Section 9.2 vary if the assumed discount rate was varied from 5% to a lower value of 1% or a higher value of 10%.

Estimates of Expected Total Costs Across All Stages as a Function of Stage 1 Decision

As was the case in Section 9.3, when assuming a discount rate of 5% or 10% a range of 0 to 4500 MW was initially considered for both the B6 and B7a reinforcement magnitudes in stage 1. However, when assuming a discount rate of 1%, future constraint costs are discounted at a lower rate, which makes the present value of constraint costs relatively larger in comparison to the costs of reinforcement, which in turn may justify a larger expenditure on reinforcement. Further, Sections 9.4 and 9.5 show how the decisions in stages 2 and 3 increase total reinforcement magnitude for every potential future scenario. When assuming a lower discount rate for future costs there is less benefit from postponing a reinforcement until nearer the time is needed, which may encourage a larger reinforcement to be built earlier. Therefore, it was necessary to consider a slightly larger initial range of 0 to 5500 MW reinforcement on both boundaries when assuming a discount rate of 1%.

Figure 9.24 displays how estimates of expected total costs vary as B6 and B7a reinforcement magnitude in the first stage are varied, using the methodology of Section 9.1.2 to estimate expected total costs across all three stages as a function of first stage decision only. As would be expected, expected total costs decrease as the assumed discount rate increases.

Further, by comparing Figure 9.24 (c) to Figure 9.24 (a) it can be seen that the variation in estimates of expected total costs as B6 and B7a reinforcement magnitudes are varied appears to be flatter when assuming a 10% discount rate (Figure 9.24 (c)) in comparison to assuming a 1% discount rate (Figure 9.24 (a)). This is because, for all assumed discount rates, estimated expected total costs are very large when little to no reinforcement is made. However, assuming a lower discount rate increases the present value of future constraint costs, making these costs even greater when assuming a 1% discount rate.

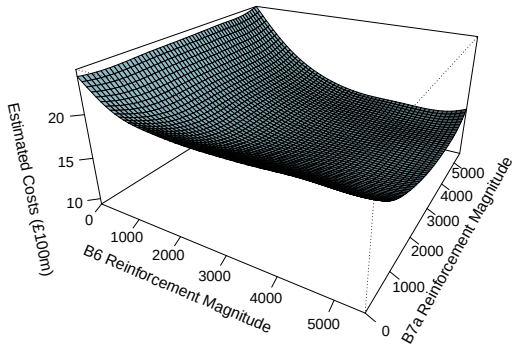

(a) 1% discount rate.

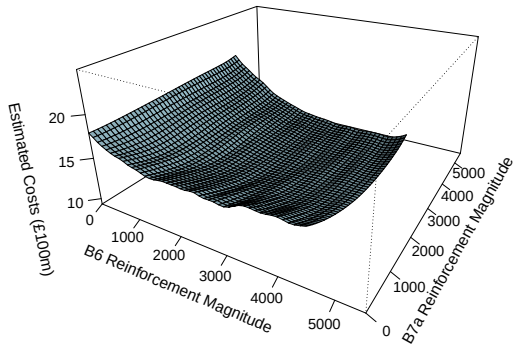

(b) 5% discount rate.

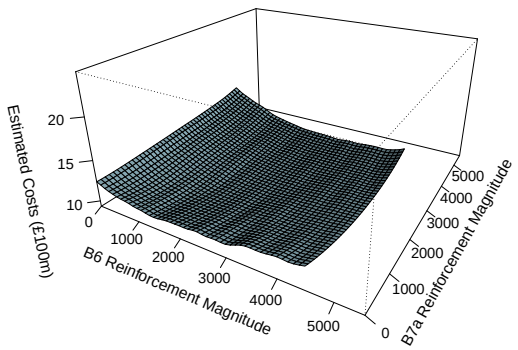

(c) 10% discount rate.

Figure 9.24: Plots to show estimates of expected total costs across all three stages vary with stage 1 B6 and B7a reinforcement magnitude and assumed discount rate in the first wave.

This means that there is a greater decrease in the present value of total costs when a near-optimal reinforcement is made when assuming a lower discount rate in comparison to a higher discount rate. For example, the difference between the greatest and lowest estimates of expected total costs is £1091 million when assuming a discount rate of 1%, in comparison to the £521 million difference when assuming a discount rate of 10%. However, the relative differences between the greatest and lowest estimates are more consistent as the assumed discount rate is varied, with the greatest estimate of expected total costs being 78.6% greater than the lowest when assuming a 1% discount rate, and the greatest estimate of expected total costs being 56.0% greater than the lowest when assuming a 10% discount rate, showing that the variation in cost estimates when assuming a 10% discount rate is far from negligible.

As was the case when a discount rate of 5% was assumed in Section 9.3, the fitted emulator models used to estimate costs in Figure 9.24 are not perfect approximations to the simulator and contain error. Credible bounds for the estimates can be calculated using the methodology of Section 9.1.4, which can in turn be used in the methodology of Section 8.2.7 to eliminate decisions which have evidence against them being optimal in order to fit more accurate emulator models over a smaller range of decisions.

For all three discount rates, three waves of elimination were performed, with negligible elimination of decisions occurring from further waves of elimination. As has been noted throughout this chapter, this is due to estimates of expected total costs being relatively flat near the optimal decision, in the sense that all decisions considered in the final wave result in similar, relatively low estimates of expected total costs. Therefore, optimal decisions were estimated as the decisions which minimise the estimate of expected total costs based on the emulator models fitted in the fourth wave.

Figure 9.25 illustrates how estimates of expected total costs in the final wave vary with stage 1 B6 and B7a reinforcement magnitude for an assumed discount rate of 1%, 5% and 10%. As can be seen, for all assumed discount rates the graphs are very flat, in the sense that there is little variation in the estimate of expected total costs as B6 and B7a reinforcement magnitude are varied, with cost estimates varying by less than 3.72%, 3.39% and 3.21% of the lowest estimate when assuming a 1%, 5% or 10% discount rate respectively.

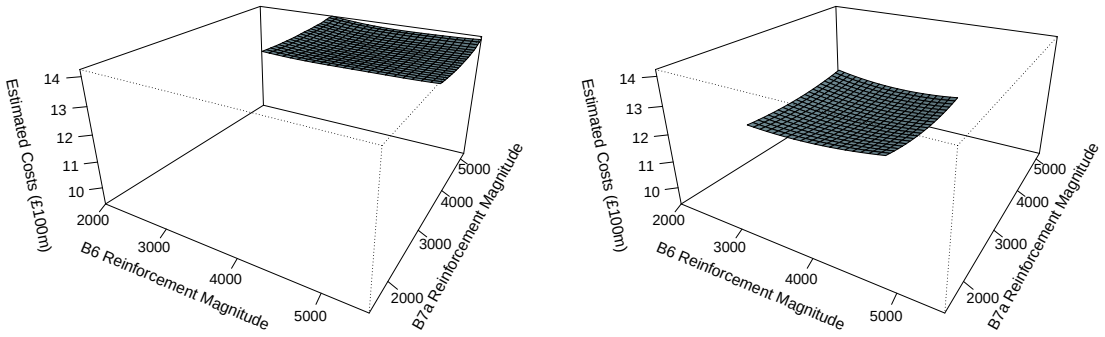

(a) 1% discount rate.

(b) 5% discount rate.

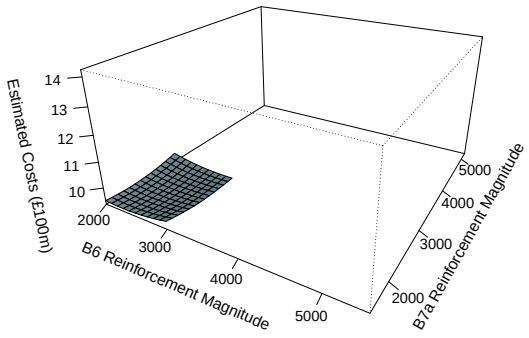

(c) 10% discount rate.

Figure 9.25: Plots to show how estimates of expected total costs across all three stages vary with stage 1 B6 and B7a reinforcement magnitude and assumed discount rate in the final wave.

This is consistent with what was observed in Figure 9.13 of Section 9.3.2. Again, this indicates that there is little risk of making a poor decision by minimising the estimate of expected total costs that arises when using the emulator models fitted in the final wave as all decisions result in similar, relatively low estimates of expected total costs.

It can also be seen that the values of reinforcement magnitude considered in the final wave tend to increase as the assumed discount rate decreases. This can be better seen in Figure 9.26, which illustrates the range of decisions considered in the final wave for each of the three discount rates. Again, this is to be expected, as a smaller discount rate increases the present value of future constraint costs, which justifies a larger expenditure on reinforcement. Further, it can be clearly seen that that the range of decisions considered in the final wave when assuming a discount rate of 1% does not overlap with the range of decisions considered in the final wave when assuming a discount rate of 10%, which is very strong evidence that the optimal reinforcement magnitudes increase as the assumed discount rate decreases.

Estimates of Optimal Stage 1 Decisions

Assumed Discount Rate	B6 Reinforcement Magnitude	B7a Reinforcement Magnitude
1%	4470 MW	4480 MW
5%	3540 MW	3340 MW
10%	2560 MW	2210 MW

Table 9.10: Table summarising how the estimated optimal stage 1 decision varies with the assumed discount rate of future costs.

Table 9.10 displays how estimates of optimal stage 1 decision vary with the assumed discount rate. When assuming a discount rate of 1%, B6 reinforcement magnitude is increased by 930 MW (26.3%) and B7a reinforcement magnitude is increased by 1140 MW (34.1%) in comparison to decisions made when a 5% discount rate was assumed, whereas assuming a discount rate of 10% decreases B6 reinforcement magnitude by 980 MW (27.7%) and B7a reinforcement magnitude by 1130 MW (33.8%) in comparison to decisions made when a 5% discount rate was assumed.

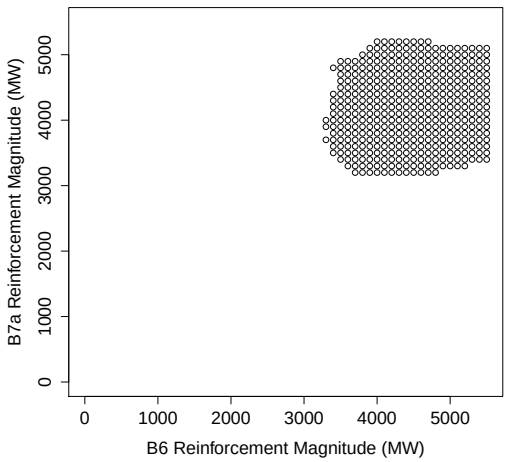

(a) 1% discount rate.

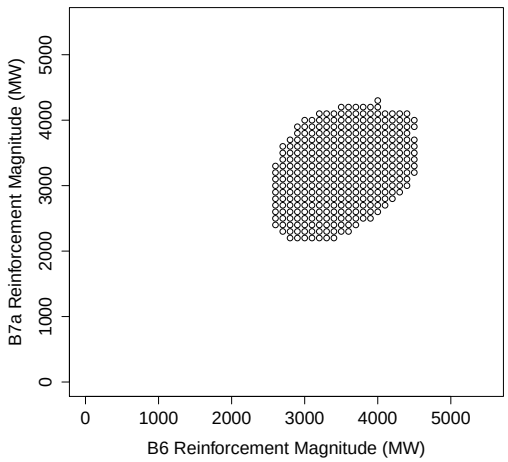

(b) 5% discount rate.

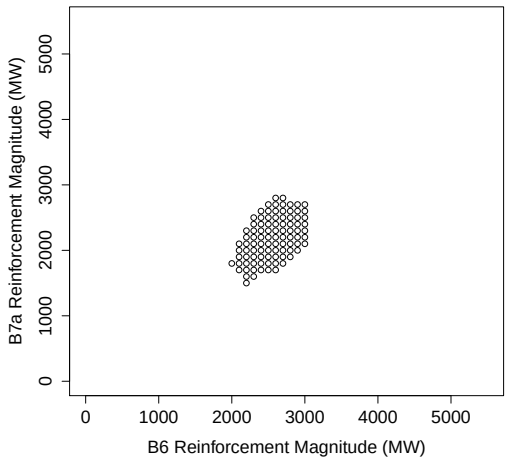

(c) 10% discount rate.

Figure 9.26: Plots to show how the range of decisions considered in the fourth wave varies with the assumed discount rate.

Stage 2 Scenarios and Reinforcement Decisions Considered

As was noted in Section 9.4, for a real life application it would only be necessary to identify an optimal stage 2 decision for the scenario actually observed when the time comes to make the second decision. However, to illustrate how estimates of expected total costs and the resulting estimates of optimal decision vary depending on what is observed, results will be presented for the three scenarios detailed in Table 9.6 of Section 9.4. All scenarios will assume that the decision maker acted optimally in stage 1, so for example, if a discount rate of 10% is assumed it is assumed that the estimated optimal reinforcement of 2560 MW B6 and 2210 MW B7a was previously made in the first stage.

As was the case in Section 9.4, when assuming a discount rate of 5% or 10% the initial range of values considered for total B6 reinforcement after the second decision was from the stage 1 reinforcement made (e.g. 2560 MW when assuming a discount rate of 10%) to 6500 MW, and a range of total B7a reinforcement after the second decision was from the stage 1 reinforcement made (e.g. 2210 MW when assuming a discount rate of 10%) to 5500 MW.

However, as was the case for the stage 1 decision, it was necessary to consider a slightly larger range for the decision variables when assuming a discount rate of 1%, as future constraint costs are discounted at a lower rate (resulting in a greater present value) which in turn may justify a larger reinforcement as there is a relatively greater benefit from building a larger reinforcement. Therefore, when assuming a 1% discount rate the range of total B6 reinforcement after the second decision initially considered was between 4470 MW (the estimate of stage 1 optimal) and 7500 MW and the range of total B7a reinforcement after the second decision initially considered was between 4480 MW (the estimate of stage 1 optimal) and 6000 MW.

Estimates of Expected Total Costs in Stage 2 Onwards

Figure 9.27 illustrates how estimates of expected total costs vary with stage 2 total reinforcement decision and assumed discount rate. All three graphs of Figure 9.27 assume that scenario 2 was observed in stage 2 (i.e. $\boldsymbol{\psi}_2 = 1$), which means that prior

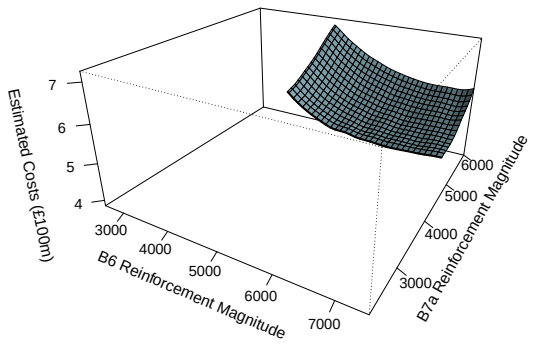

(a) 1% discount rate.

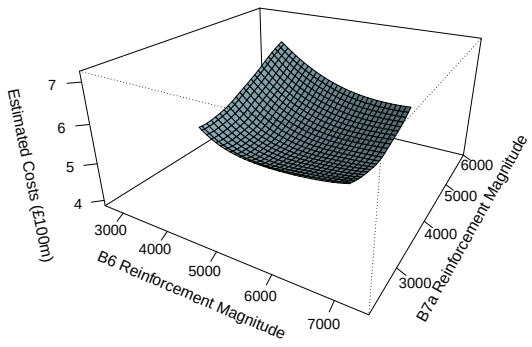

(b) 5% discount rate.

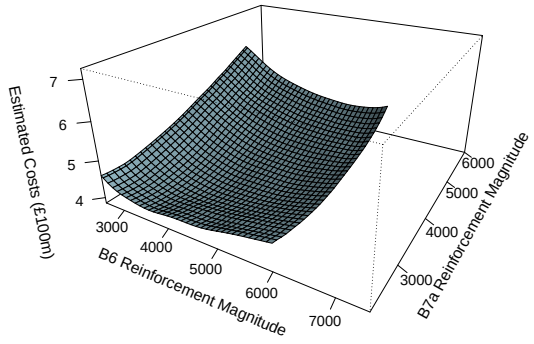

(c) 10% discount rate.

Figure 9.27: Plots to show how estimates of expected total costs in stage 2 onwards vary with stage 2 total reinforcement decision and assumed discount rate. Each plot assumes scenario 2 of Table 9.6 (i.e. $\boldsymbol{\psi}_2 = 1$) was observed at the time the second decision was made.

beliefs about stage 2 peak demand level form a uniform distribution between 95% and 105% of the year 11 peak demand level projected by [69]. As can be seen, estimates of expected total costs increase as the assumed discount rate decreases, which again is to be expected as a lower discount rate means future constraint costs have a greater present value.

For all discount rates it can be seen that expected total costs begin to rise if a large increase to B7a reinforcement is made, indicating that over-reinforcing the B7a boundary is a poor decision. Conversely, for any fixed value of B7a reinforcement, expected total costs are greatest when little to no further B6 reinforcement is made and total costs are not observed to increase greatly for large magnitudes of B6 reinforcement. This indicates that for the B6 boundary there is a greater financial penalty for under-reinforcing than for over-reinforcing.

A further comparison of how estimates of expected total cost vary with reinforcement decision, assumed discount rate and scenario observed is given in Appendix D.3.1. As an overview, in Appendix D.3.1 it is shown how, for a fixed discount rate, the observed scenario has little effect on the estimate of expected total costs, which is consistent with what was observed in Section 9.4. It is also shown that for any particular stage 2 scenario, the assumed discount rate has quite a large effect with cost estimates decreasing as assumed discount rate increases, indicating that in stage 2 the assumed discount rate has a much greater effect on the estimates of expected total costs than the scenario observed.

As was the case for when a 5% discount rate was assumed in Section 9.4, the emulator models are not perfect approximations to the simulator and therefore credible bounds for the estimates could be calculated using the methodology of Section 9.1.4, which in turn could be used to eliminate decisions which have evidence against them being optimal using the methodology of Section 8.2.7. A wave process was carried out for each scenario and each assumed discount rate, with generally 3 waves of elimination required before no further decisions can be eliminated (though for some scenarios, such as scenario 2 when a discount rate of 1% was assumed, just two waves of elimination were performed with negligible elimination in the third).

Figure 9.28 illustrates how estimates of expected total costs vary with stage 2 total

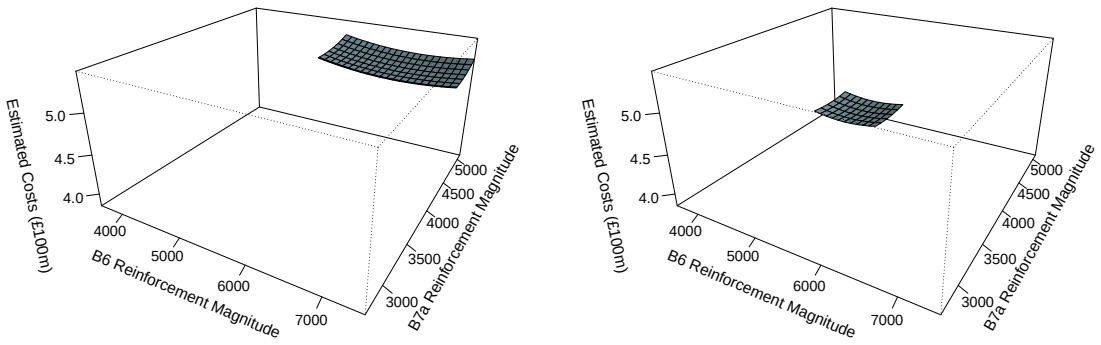

(a) 1% discount rate.

(b) 5% discount rate.

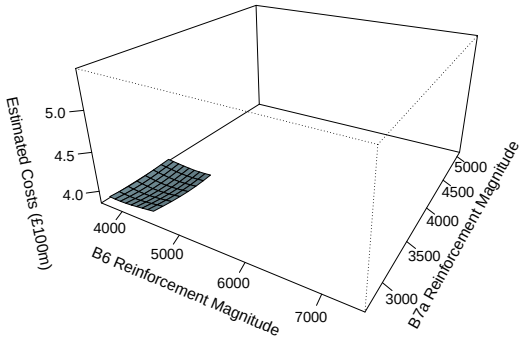

(c) 10% discount rate.

Figure 9.28: Plots to show how estimates of expected total costs in stage 2 onwards vary with stage 2 total reinforcement decision and assumed discount rate in the final wave. Each plot assumes scenario 2 of Table 9.6 (i.e. $\boldsymbol{\psi}_2 = 1$) was observed at the time the second decision was made.

reinforcement decision and assumed discount rate in the final wave. All three graphs of Figure 9.28 assume that scenario 2 was observed in stage 2 (i.e. $\psi_2 = 1$). As can be seen, for all discount rates all the plots are very flat, in the sense that there is little variation in the estimate of expected total costs as the B6 and B7a reinforcement magnitudes are varied. Again, this implies that there is little risk of making a poor decision when minimising the estimate of expected total costs in the final wave, as all decisions result in similar, relatively low estimates of expected total costs. In particular, decisions which resulted in comparatively large estimates of expected total costs, such as when a large B7a reinforcement is made, have been eliminated from consideration.

A further comparison of how final wave estimates of expected total cost vary with reinforcement decision, assumed discount rate and stage 2 scenario observed is given in Appendix D.3.1, where it is again shown that the assumed discount rate has a much greater effect on estimated costs than scenario observed, with estimates of expected total costs decreasing as assumed discount rate increases.

Estimates of Optimal Stage 2 Total Reinforcement Decisions

Stage 2 Scenario	B6 Reinforcement Magnitude	B7a Reinforcement Magnitude
Stage 2 Scenario 1	6590 MW	4640 MW
Stage 2 Scenario 2	6680 MW	4540 MW
Stage 2 Scenario 3	6700 MW	4690 MW

Table 9.11: Table summarising how the estimated optimal stage 2 total reinforcement decision varies with stage 2 scenario, when assuming a discount rate of 1%.

Stage 2 Scenario	B6 Reinforcement Magnitude	B7a Reinforcement Magnitude
Stage 2 Scenario 1	4150 MW	3060 MW
Stage 2 Scenario 2	4230 MW	3090 MW
Stage 2 Scenario 3	4220 MW	3080 MW

Table 9.12: Table summarising how the estimated optimal stage 2 total reinforcement decision varies with stage 2 scenario, when assuming a discount rate of 10%.

Tables 9.11 and 9.12 detail how estimates of optimal stage 2 total reinforcement decisions vary with stage 2 scenario when assuming a discount rate of 1% or 10% respec-

tively, and estimates of optimal stage 2 reinforcement when assuming a 5% discount rate were previously detailed in Table 9.7 of Section 9.4.

As can be seen, for any assumed discount rate, the estimated optimal reinforcement decision shows little variation with scenario observed, with estimated optimal B6 reinforcement varying by just 110 MW when assuming a discount rate of 1% and by 80 MW when assuming a discount rate of 10%, whereas the estimated optimal B7a reinforcement magnitude varies by 150 MW when assuming a discount rate of 1% and 30 MW when assuming a discount rate of 10%. Further, in Appendix D.3.1 Figures D.6 and D.7 show how different scenarios which assume the same discount rate consider very similar ranges of decisions in the final wave, meaning it cannot be conclusively said that any scenario gives a significantly different decision to any other when considering scenarios which assume the same discount rate.

However, all estimates of optimal total B6 reinforcement after the second decision were at least 2360 MW greater when assuming a discount rate of 1% in comparison to 10%, and all estimates of optimal total B7a reinforcement after the second decision were at least 1450 MW greater when assuming a discount rate of 1% in comparison to 10%. This indicates that when making the second decision, the discount rate assumed for future costs has a much larger impact on the estimate of optimal reinforcement decision than the scenario observed.

Stage 3 Scenarios and Reinforcement Decisions Considered

As was noted in Section 9.5, for a real life application it would only be necessary to estimate an optimal stage 3 decision for the scenario actually observed when the third decision is made at the beginning of year 11. However, as was the case for the second stage, this section will present results for a variety of stage 3 scenarios to illustrate how estimates of expected total costs and the resulting estimates of optimal decision vary with scenario observed and assumed discount rate.

The 9 scenarios detailed in Table 9.8 of Section 9.5 will be considered for all three assumed discount rates (1%, 5% and 10%). As was the case in Section 9.5, scenarios 1.1, 1.2 and 1.3 assume the estimated optimal stage 2 total reinforcement for scenario 1 was previously made (e.g. the estimated optimal stage 2 total reinforcement of 4150

MW B6 and 3060 MW B7a was made when scenario 1 is observed in stage 2 and a discount rate of 10% is assumed), scenarios 2.1, 2.2 and 2.3 assume the estimated optimal stage 2 reinforcement for scenario 2 was previously made and scenarios 3.1, 3.2 and 3.3 assume the estimated optimal stage 2 reinforcement for scenario 3 was previously made.

As was the case in Section 9.5, when a discount rate of 5% is assumed, it is assumed that the total reinforcement after the third decision will be between the assumed previous total reinforcement after the second decision (e.g. 5300 MW B6 and 3920 MW B7a when it is assumed scenario 2 was observed in stage 2 and a discount rate of 5% is assumed) and 8000 MW B6 and 5500 MW B7a total reinforcement.

However, when a 1% discount rate is assumed, future constraint costs are discounted at a lower rate which results in a greater present value of future constraint costs which in turn may justify a larger reinforcement. Therefore, it was necessary to consider a slightly larger range for total reinforcement, so the initial range of total reinforcement after the third decision was considered to between the assumed previous total reinforcement after the second decision (e.g. 6680 MW B6 and 4540 MW B7a when it is assumed scenario 2 was observed in stage 2 and a discount rate of 1% is assumed) and 8500 MW B6 and 6000 MW B7a total reinforcement.

Conversely, when a 10% discount rate was assumed a lower upper limit can be assumed, as a higher discount rate results in a lower present value of future constraint costs which justifies less reinforcement, so the initial range of total reinforcement after the third decision was considered to between the assumed previous total reinforcement after the second decision (e.g. 4230 MW B6 and 3090 MW B7a when it is assumed scenario 2 was observed in stage 2 and a discount rate of 10% is assumed) and 7500 MW B6 and 5500 MW B7a total reinforcement.

Estimates of Expected Total Costs in Stage 3

Figure 9.29 displays how estimates of expected total costs vary with total stage 3 reinforcement and assumed discount rate of future costs. All three graphs of Figure 9.29 assume that scenario 2.2 was observed in stage 3, i.e. $\boldsymbol{\psi}_3 = 1$ was observed which means that prior beliefs about stage 3 peak demand level form a uniform distribution

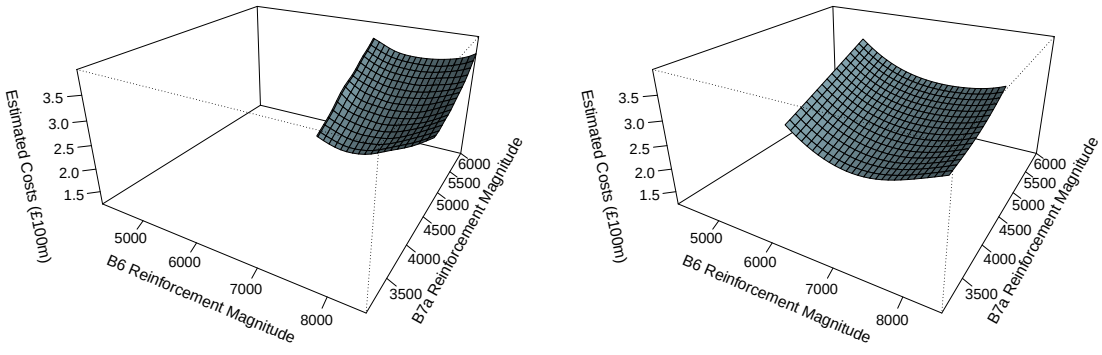

(a) 1% discount rate.

(b) 5% discount rate.

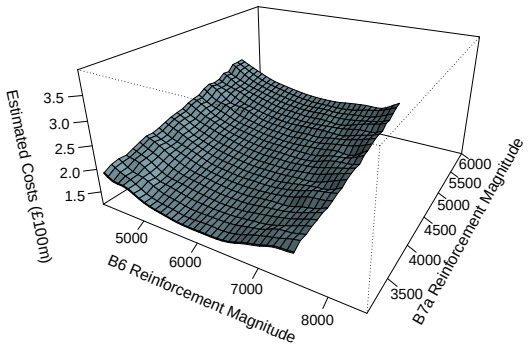

(c) 10% discount rate.

Figure 9.29: Plots to show how estimates of expected total costs vary with stage 3 total reinforcement decision and assumed discount rate. Each plot assumes Scenario 2.2 of Table 9.8 was observed at the time the third decision was made.

between 95% and 105% of the year 16 peak demand level projected by [69], and also that scenario 2 was previously observed in stage 2 and the corresponding estimate of optimal decision was previously made (e.g. 6680 MW B6 and 4540 MW B7a reinforcement when assuming a 1% discount rate). As was the case for the previous two stages, estimates of expected total costs increase as assumed discount rate decreases, as a lower discount rate means future constraint costs have a greater present value.

It can also be seen that for all assumed discount rates, costs appear to rise quite linearly as B7a reinforcement magnitude increases. This is consistent with what was observed in Section 9.5, and indicates that in the third stage little to no further B7a reinforcement is merited for all assumed discount rates.

A further consideration to how estimates of expected total costs vary with reinforcement decision, observed stage 3 scenario and assumed discount rate is given in Appendix D.3.2. As an overview of results, it is shown how in stage 3 both the observed scenario and assumed discount rate have quite a large effect on the estimates of expected total costs, with costs increasing as the observed value of $\boldsymbol{\psi}_3$ increases (i.e. estimates of expected total costs increase as expected stage 3 peak demand level increases) for each assumed discount rate, as well as showing how estimated expected total costs decrease as the assumed discount rate increases.

As was noted in Section 9.5, the emulators used to estimate expected total costs are not perfect approximations to the simulator. As such, credibility bounds for the estimates can be calculated using the methodology of Section 5.2.6, which can then be used in the methodology of Section 6.2.1 to eliminate decisions from consideration which have evidence against them being optimal in order to fit a more accurate emulator model over a smaller range of decisions. Generally, two waves of elimination for each observed scenario and assumed discount rate were performed before a negligible amount of further decisions could be eliminated from further waves.

Figure 9.30 illustrates how estimates of expected total costs vary with stage 3 decision and assumed discount rate in the final wave. All three graphs of Figure 9.30 assume that scenario 2.2 (i.e. $\boldsymbol{\psi}_3 = 1$) was observed in stage 3.

As can be seen, each scenario considers a very small range of decisions over this final wave, with estimates of expected total costs being very flat for all plots, in the sense

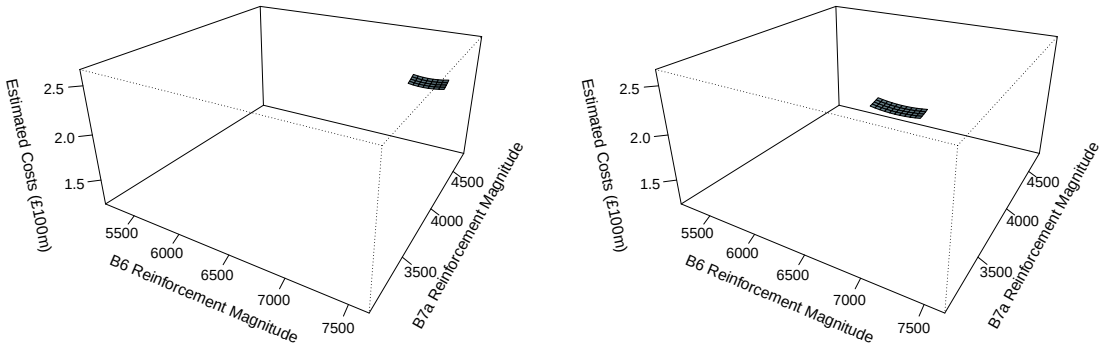

(a) 1% discount rate.

(b) 5% discount rate.

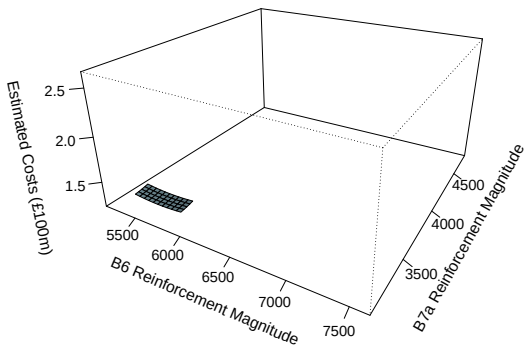

(c) 10% discount rate.

Figure 9.30: Plots to show how estimates of expected total costs vary with stage 3 total reinforcement decision and assumed discount rate in the final wave. Each plot assumes Scenario 2.2 of Table 9.8 was observed at the time the third decision was made.

that the estimates of expected total costs vary little as the B6 and B7a reinforcement magnitude are varied. Again, this implies that there is little risk of making a poor decision when making a decision to minimise the estimate of expected costs in the final wave, as all decisions result in similar, relatively low estimates of expected total costs. Further, it is again shown how estimates of expected total costs increase as assumed discount rate decreases, as well as showing how larger magnitudes of reinforcement are considered for lower discount rates.

Again, Appendix D.3.2 gives further consideration to how estimates of expected total costs in the final wave vary with reinforcement decision, observed stage 3 scenario and assumed discount rate. As a brief overview, it is again shown how both observed stage 3 scenario and assumed discount rate have quite a large effect on estimated expected total costs. As was the case in the first wave, expected costs appear to increase as the expected stage 3 peak demand level increases and decrease as the assumed discount rate increases. Further, it is shown how the ranges of decisions considered in the final wave differ depending on the scenario observed and assumed discount rate, implying these factors can have quite a large effect on the estimated optimal reinforcement decision.

Estimates of Optimal Stage 3 Total Reinforcement Decisions

Stage 3 Scenario	B6 Reinforcement Magnitude	B7a Reinforcement Magnitude
Stage 3 Scenario 1.1	6960 MW	4640 MW
Stage 3 Scenario 1.2	7150 MW	4640 MW
Stage 3 Scenario 1.3	7310 MW	4640 MW
Stage 3 Scenario 2.1	7100 MW	4540 MW
Stage 3 Scenario 2.2	7260 MW	4540 MW
Stage 3 Scenario 2.3	7390 MW	4540 MW
Stage 3 Scenario 3.1	7320 MW	4690 MW
Stage 3 Scenario 3.2	7450 MW	4690 MW
Stage 3 Scenario 3.3	7530 MW	4690 MW

Table 9.13: Table summarising how the estimated optimal stage 3 total reinforcement decision varies with stage 3 scenario, when assuming a discount rate of 1%.

Details of how estimated optimal stage 3 total reinforcement decisions vary with stage 3 scenario when assuming a 1% or 10% discount rate are detailed in Tables 9.13 and 9.14

Stage 3 Scenario	B6 Reinforcement Magnitude	B7a Reinforcement Magnitude
Stage 3 Scenario 1.1	5470 MW	3060 MW
Stage 3 Scenario 1.2	5630 MW	3060 MW
Stage 3 Scenario 1.3	5770 MW	3060 MW
Stage 3 Scenario 2.1	5640 MW	3090 MW
Stage 3 Scenario 2.2	5770 MW	3090 MW
Stage 3 Scenario 2.3	5890 MW	3090 MW
Stage 3 Scenario 3.1	5770 MW	3080 MW
Stage 3 Scenario 3.2	5890 MW	3080 MW
Stage 3 Scenario 3.3	5990 MW	3080 MW

Table 9.14: Table summarising how the estimated optimal stage 3 total reinforcement decision varies with stage 3 scenario, when assuming a discount rate of 10%.

respectively. The scenarios considered are the scenarios detailed in Table 9.8 of Section 9.5, with scenarios 1.1, 1.2 and 1.3 assuming the estimated optimal stage 2 reinforcement for scenario 1 was previously made (e.g. it is assumed 4150 MW B6 and 3060 MW B7a stage 2 total reinforcement was previously made when assuming a 10% discount rate), scenarios 2.1, 2.2 and 2.3 assuming the estimated optimal stage 2 reinforcement for scenario 2 was previously made and scenarios 3.1, 3.2 and 3.3 assuming the estimated optimal stage 2 reinforcement for scenario 3 was previously made. Results for a 5% discount rate were given previously in Table 9.9 of Section 9.5.

As can be seen, for all 9 scenarios considered and for all 3 discount rates considered, no further B7a reinforcement was made from stage 2. However, every scenario considered did result in an increase of B6 reinforcement from stage 2.

When assuming a 1% discount rate, total B6 reinforcement after the third decision ranges from 6960 MW (an increase of 370 MW from stage 2) to 7530 MW (an increase of 830 MW from stage 2). When assuming a 10% discount rate, total B6 reinforcement after the third decision ranges from 5470 MW (an increase of 1320 MW from stage 2) to 5990 MW (an increase in 1770 MW from stage 2). This means that when assuming a 1% discount rate, the total reinforcement after the third decision is greater in comparison to when a 10% discount rate is assumed, which would be expected as this gives future constraint costs a greater present value, which in turn justifies a greater reinforcement. However, the increase in reinforcement from stage 2 to stage 3 is greater when assuming a 10% discount rate. This is because when a lower discount

rate is assumed it is less beneficial to postpone part of a reinforcement until a time when it is required in comparison to when a higher discount rate is assumed.

Across all scenarios and discount rates, the estimated optimal total B6 reinforcement after the third decision ranges by 2060 MW (from 5470 MW to 7530 MW) whereas estimated optimal total B7a reinforcement ranges by 1630 MW (from 3060 MW to 4690 MW) showing how the scenario observed and assumed discount rate can have a large effect on the decisions made.

9.6.2 Time Period Considered

The example of Section 9.2 detailed a 3 stage decision problem over a 25 year planning horizon. Specifically, Section 9.2.1 detailed the time frame of the problem, with Table 9.1 detailing when decisions are made and when the resulting reinforcement becomes available. Within this time frame, there are many assumptions that have been made, such as when decisions are made, the difference between when a decision is made and when a reinforcement becomes available, how long between decisions and how long a horizon is considered.

When decisions are made and the length of time between decisions are variables controlled by the system planner, whilst the length of time between making a decision and the reinforcement becoming available is something it is reasonable to assume can be known quite accurately. However, the time horizon considered for the multi-stage problem is something set by the system planner but in reality future costs will continue over an indefinite horizon (though the effect of discounting would eventually make the present value of costs beyond a certain point in time negligible). If too short of a horizon is considered this may under-estimate future constraint costs which may lead to smaller transmission reinforcements being made, whilst a longer planning horizon may be infeasible if accurate projections about the future power system are unavailable beyond a certain point in the future.

This section will consider how the estimated optimal decisions vary if the planning horizon considered for the example detailed in Section 9.2 was increased to 30 years or decreased to 20 years.

Estimates of Optimal Stage 1 Reinforcement Decisions

Horizon Considered	B6 Reinforcement Magnitude	B7a Reinforcement Magnitude
20 Year	3420 MW	3380 MW
25 Year	3540 MW	3340 MW
30 Year	3550 MW	3370 MW

Table 9.15: Table summarising how the estimated optimal stage 1 decision varies with the planning horizon considered.

Table 9.15 details how the estimated optimal stage 1 reinforcement decisions vary with planning horizon considered. As can be seen, all estimated optimal decisions are very similar, with B7a reinforcement magnitude varying by just 40 MW and B6 reinforcement varying by 130 MW. This indicates that for the example of Section 9.2, the estimate of optimal stage 1 decision is insensitive to the planning horizon considered.

Estimates of Optimal Stage 2 Total Reinforcement Decisions

Stage 2 Scenario	B6 Reinforcement Magnitude	B7a Reinforcement Magnitude
Stage 2 Scenario 1	5220 MW	3770 MW
Stage 2 Scenario 2	5220 MW	3860 MW
Stage 2 Scenario 3	5370 MW	3900 MW

Table 9.16: Table summarising how the estimated optimal stage 2 total reinforcement decision varies with stage 2 scenario, when assuming a 20 year planning horizon.

Stage 2 Scenario	B6 Reinforcement Magnitude	B7a Reinforcement Magnitude
Stage 2 Scenario 1	5360 MW	4090 MW
Stage 2 Scenario 2	5420 MW	4170 MW
Stage 2 Scenario 3	5450 MW	4260 MW

Table 9.17: Table summarising how the estimated optimal stage 2 total reinforcement decision varies with stage 2 scenario, when assuming a 30 year planning horizon.

Table 9.16 details how the estimated optimal stage 2 total reinforcement decision varies with stage 2 scenario when assuming a 20 year planning horizon, with Table 9.17

detailing how the estimated optimal stage 2 total reinforcement decision varies with stage 2 scenario when assuming a 30 year planning horizon. The scenarios considered are the three scenarios detailed in Table 9.6 of Section 9.4. All scenarios assume the estimated optimal decision was previously made in stage 1 (for example all stage 2 scenarios when considering a 20 year planning horizon assume that 3420 MW B6 and 3380 MW B7a reinforcement was previously made in stage 1).

Scenarios within the same planning horizon do not show a great deal of variation between each scenario with estimated optimal B6 reinforcement varying by 150 MW when assuming a 20 year planning horizon and 90 MW when assuming a 30 year planning horizon; and estimated optimal B7a reinforcement varying by 130 MW when assuming a 20 year planning horizon and 170 MW when assuming a 30 year planning horizon. This is consistent with what was previously observed in Sections 9.4 and 9.6.1, where it was shown that estimates of expected total costs, and the ranges of decisions considered in the final wave, do not vary greatly with scenario observed.

However, it can be seen that reinforcement magnitudes are slightly greater when assuming 30 year planning horizon over a 20 year planning horizon, with the average B6 reinforcement across the 3 scenarios being 140 MW larger when assuming a 30 year horizon over a 20 year horizon and the average B7a reinforcement across the three scenarios being 330 MW larger when assuming a 30 year horizon over a 20 year horizon. Whilst these differences are not too great, it is some evidence that a longer planning horizon may justify a larger reinforcement in stage 2.

Estimates of Optimal Stage 3 Total Reinforcement Decisions

Stage 3 Scenario	$\boldsymbol{\psi}_3$
Stage 3 Scenario 1.1	0.9
Stage 3 Scenario 1.3	1
Stage 3 Scenario 3.1	1
Stage 3 Scenario 3.3	1.1

Table 9.18: Table summarising the value of $\boldsymbol{\psi}_3$ observed for four scenarios considered.

Tables 9.19 and 9.20 display how estimated optimal stage 3 total reinforcement decisions vary with stage 3 scenario when assuming a 20 or 30 year planning horizon

Stage 3 Scenario	B6 Reinforcement Magnitude	B7a Reinforcement Magnitude
Stage 3 Scenario 1.1	5530 MW	3770 MW
Stage 3 Scenario 1.3	5930 MW	3770 MW
Stage 3 Scenario 3.1	5950 MW	3900 MW
Stage 3 Scenario 3.3	6240 MW	3900 MW

Table 9.19: Table summarising how the estimated optimal stage 3 total reinforcement decision varies with stage 3 scenario, when assuming a 20 year planning horizon.

Stage 3 Scenario	B6 Reinforcement Magnitude	B7a Reinforcement Magnitude
Stage 3 Scenario 1.1	6610 MW	4090 MW
Stage 3 Scenario 1.3	6920 MW	4100 MW
Stage 3 Scenario 3.1	7030 MW	4260 MW
Stage 3 Scenario 3.3	7250 MW	4260 MW

Table 9.20: Table summarising how the estimated optimal stage 3 total reinforcement decision varies with stage 3 scenario, when assuming a 30 year planning horizon.

respectively. Results are presented for 4 scenarios, detailed in Table 9.18, which are a reduced subset of 4 of the 9 scenarios considered in Table 9.8 of Section 9.5. Scenarios 1.1 and 1.3 assume that the estimated optimal stage 2 reinforcement for scenario 1 was previously made (e.g. it is assumed 5220 MW B6 and 3770 MW B7a stage 2 total reinforcement was previously made when assuming a 20 year planning horizon) and scenarios 3.1 and 3.3 assume that the estimated optimal stage 2 reinforcement for scenario 3 was previously made.

The smallest estimate of optimal total reinforcement arises in scenario 1.1 when assuming a 20 year planning horizon (5530 MW B6 and 3770 MW B7a reinforcement) whereas the largest total reinforcement arises in scenario 3.3 when assuming a 30 year planning horizon (7250 MW B6 and 4260 MW B7a reinforcement), with the reinforcement decisions of these two scenarios differing by 1720 MW B6 and 490 MW B7a reinforcement.

Further, when comparing equivalent scenarios across different planning horizons (e.g. scenario 3.1 between the 20 year and 30 year planning horizon) a larger reinforcement is always made for a longer planning horizon (e.g. the estimated optimal total reinforcement for scenario 3.1 is 1080 MW B6 and 360 MW B7a greater when assuming a 30

year planning horizon over a 20 year planning horizon). This is what one would expect, as all planning horizons consider making the third reinforcement at the beginning of year 11 (so the cost of reinforcement of equal magnitude is the same for all planning horizons) but a longer planning horizon considers constraint costs over a longer period of time, which justifies a greater reinforcement being built to reduce constraint costs.

However, in earlier stages the estimates of optimal reinforcement decision show much less variation with the planning horizon considered. This is because, in the example considered, the stage 1 reinforcement decision is made at the beginning of year 1 and assumed to be available at the beginning of year 6, which directly affects the expected mean constraint costs in years 6 to 10 before the second reinforcement becomes available at the beginning of year 11. In this sense, the costs occurring as a direct result of the first decision are unaffected by how long of a horizon is considered.

The stage 2 decision on the other hand did show a small variation in decision made with horizon considered. This is because, as was seen in Figure 9.21 of Section 9.5, in stage 3 total costs appear to rise as B7a reinforcement magnitude is increased, indicating that the reduction in expected mean constraint costs from further B7a reinforcement does not outweigh the cost of further reinforcement.

However, as has been shown in Tables 9.9, 9.19 and 9.20 by comparing different scenarios with equivalent beliefs about stage 3 demand (such as scenarios 1.3 and 3.1 which both expect stage 3 peak demand level to be the year 16 peak demand level projected by [69]) that although little to no B7a reinforcement is merited in Stage 3 for all scenarios, if a larger B7a reinforcement was built in stage 2 this can justifying a larger B6 reinforcement in stage 3. If a longer planning horizon is considered this means that stage 3 constraint costs are considered over an even longer period of time, meaning there is greater benefit to reinforcing the B6 boundary in stage 3, which in turn justifies a greater B7a reinforcement in stage 2.

9.6.3 Cost to Reinforce

For the example of Section 9.2 it was initially assumed that in each stage the cost of reinforcement was £1000 per MW per km at the time the reinforcement decision

is made (i.e. at the beginning of years 1, 6 and 11 for the first, second and third reinforcements respectively). This was to remain consistent with the £1000 per MW per km [5, 78] initially assumed in Chapters 5 and 6.

When single stage decision problems were considered in Chapters 5 and 6,
Sections 5.4.1 and 6.4.2 showed that the assumed cost to reinforce can have a large effect on the estimates of expected total costs, which in turn had an effect on the estimates of optimal reinforcement decision to be made (with a rough trend of 100 MW less being built for every additional £100 per MW per km to reinforce). This section will consider how the assumed cost to reinforce affects decisions made in each stage for the example detailed in Section 9.2.

Estimates of Optimal Stage 1 Reinforcement Decisions

Assumed cost to reinforce	B6 Reinforcement Magnitude	B7a Reinforcement Magnitude
£500 per MW per km	3880 MW	3820 MW
£1000 per MW per km	3540 MW	3340 MW
£1500 per MW per km	3190 MW	2800 MW

Table 9.21: Table summarising how the estimated optimal stage 1 decision varies with the assumed cost to reinforce.

Table 9.21 shows how the estimated optimal stage 1 reinforcement decision varies with the assumed cost to reinforce. Assuming a cost of £500 per MW per km would increase the estimated optimal B6 reinforcement by 340 MW and B7a reinforcement by 480 MW in comparison to the estimated optimal decisions when assuming a cost of £1000 per MW per km to reinforce, whereas assuming a cost of £1500 per MW per km would decrease B6 reinforcement by 350 MW and B7a reinforcement by 540 MW in comparison to when assuming £1000 per MW per km to reinforce. This again shows how a larger reinforcement is justified when a smaller cost of reinforcement is assumed.

Estimates of Optimal Stage 2 Total Reinforcement Decisions

Table 9.22 details how the estimated optimal stage 2 total reinforcement decision varies with stage 2 scenario when assuming a cost of £500 per MW per km to reinforce,

Stage 2 Scenario	B6 Reinforcement Magnitude	B7a Reinforcement Magnitude
Stage 2 Scenario 1	6350 MW	4850 MW
Stage 2 Scenario 2	6350 MW	4930 MW
Stage 2 Scenario 3	6270 MW	4980 MW

Table 9.22: Table summarising how the estimated optimal stage 2 total reinforcement decision varies with stage 2 scenario, when assuming a cost of £500 per MW per km to reinforce.

Stage 2 Scenario	B6 Reinforcement Magnitude	B7a Reinforcement Magnitude
Stage 2 Scenario 1	4630 MW	3070 MW
Stage 2 Scenario 2	4630 MW	3260 MW
Stage 2 Scenario 3	4640 MW	3260 MW

Table 9.23: Table summarising how the estimated optimal stage 2 total reinforcement decision varies with stage 2 scenario, when assuming a cost of £1500 per MW per km to reinforce.

whereas Table 9.23 details how the estimated optimal stage 2 total reinforcement decision varies with stage 2 scenario when assuming a cost of £1500 per MW per km to reinforce. The scenarios considered are the three scenarios detailed in Table 9.6 of Section 9.4. All scenarios assume the estimated optimal decision was made in the previous stage (for example, all scenarios when assuming a cost of £500 per MW per km to reinforce assume that a reinforcement decision of 3880 MW B6 and 3820 MW B7a was made in the previous stage).

As can be seen, for a fixed cost to reinforce there is little difference between the estimated optimal decision as the observed stage 2 scenario is varied, with estimated optimal B6 reinforcement differing by just 80 MW and 10 MW when assuming a cost to reinforce of £500 or £1500 per MW per km respectively, whereas estimated optimal B7a reinforcement differs between scenario by just 130 MW and 190 MW when assuming a cost to reinforce of £500 or £1500 per MW per km respectively. This is consistent with what was observed in Section 9.4, where it was shown that the observed stage 2 scenario has little effect on the estimates of expected total costs (and the resulting estimates of optimal decisions) in stage 2.

However, the assumed cost to reinforce has a large effect on decision made, with the

estimated optimal B6 reinforcement being on average 1690 MW greater across the three scenarios when assuming a cost of £500 per MW per km in comparison to assuming £1500 per MW per km, whereas estimated optimal B7a reinforcement was 1723 MW greater on average across the three scenarios when assuming a cost to reinforce of £500 per MW per km in comparison to a cost of £1500 per MW per km.

Estimates of Optimal Stage 3 Total Reinforcement Decisions

Stage 3 Scenario	B6 Reinforcement Magnitude	B7a Reinforcement Magnitude
Stage 3 Scenario 1.1	7310 MW	4850 MW
Stage 3 Scenario 1.3	7630 MW	4850 MW
Stage 3 Scenario 3.1	7690 MW	4980 MW
Stage 3 Scenario 3.3	7900 MW	4980 MW

Table 9.24: Table summarising how the estimated optimal stage 3 total reinforcement decision varies with stage 3 scenario, when assuming a cost of £500 per MW per km to reinforce.

Stage 3 Scenario	B6 Reinforcement Magnitude	B7a Reinforcement Magnitude
Stage 3 Scenario 1.1	5520 MW	3000 MW
Stage 3 Scenario 1.3	5810 MW	3000 MW
Stage 3 Scenario 3.1	5920 MW	3260 MW
Stage 3 Scenario 3.3	6140 MW	3260 MW

Table 9.25: Table summarising how the estimated optimal stage 3 total reinforcement decision varies with stage 3 scenario, when assuming a cost of £1500 per MW per km to reinforce.

Tables 9.24 and 9.25 display how estimated optimal stage 3 total reinforcement decisions vary with stage 3 scenario when assuming a cost to reinforce of £500 or £1500 per MW per km respectively. Results are presented for 4 scenarios, detailed in Table 9.18 of Section 9.6.2, which are a reduced subset of 4 of the 9 scenarios considered in Table 9.8 of Section 9.5. Scenarios 1.1 and 1.3 assume that the estimated optimal stage 2 reinforcement for scenario 1 was previously made (e.g. it is assumed that 6350 MW B6 and 4850 MW B7a stage 2 total reinforcement was previously made when assuming a

cost to reinforce of £500 per MW per km) and scenarios 3.1 and 3.3 assume that the estimated optimal stage 2 reinforcement for scenario 3 was previously made.

As can be seen, no stage 3 scenario for either cost to reinforce results in any further reinforcement of the B7a boundary, which is consistent with what has been observed in Section 9.5 and throughout this chapter. As was also noted in Section 9.5 and throughout this chapter, total B6 reinforcement tends to increase as expected peak demand level increases for both assumed costs to reinforce, with total B6 reinforcement after the third decision ranging from 7310 MW (a 960 MW increase from stage 2) when observing scenario 1.1 to 7900 MW (a 1630 MW increase from stage 2) when observing scenario 3.3 when assuming a cost of £500 per MW per km to reinforce, and total B6 reinforcement after the third decision ranging from 5520 MW (an 890 MW increase from stage 2) when observing scenario 1.1 to 6140 MW (a 1500 MW increase from stage 2) when observing scenario 3.3 when assuming a cost of £1500 per MW per km to reinforce.

Further, it can be seen that the lowest reinforcement made when assuming a cost of £500 per MW per km to reinforce (7310 MW B6 and 4850 MW B7a) is 1170 MW B6 and 1590 MW B7a greater than the largest reinforcement made when assuming a cost of £1500 per MW per km to reinforce (6140 MW B6 and 3260 MW B7a), showing how the assumed cost to reinforce can have a large impact on the estimated optimal decision.

9.7 Discussion of the M-Stage Problem

This chapter considered expanding the two-stage decision problem considered in Chapter 8 to a general M-stage problem, where $M > 2$. To achieve this, Section 9.1 detailed a methodology for multi-stage decision making, where expected total costs across all M stages could be estimated as a function of stage 1 decision only.

An example where three sequential decisions were to be made was detailed in Section 9.2, where uncertainty was reduced about future peak demand level between each decision. Estimates of expected total costs as a function of the decision made in each stage, and the resulting estimates of optimal decision to be made in each stage, were

detailed Sections 9.3 to 9.5. It was detailed how the multi-stage decision making process allowed for an initial reinforcement of 3540 MW B6 and 3340 MW B7a to be built with further reinforcements being available as time progressed and more was learnt about the power system, with a total reinforcement of up to 6910 MW B6 and 4040 MW B7a being made in the third stage.

Section 9.4 showed how the estimate of optimal decision to be made in stage 2 was quite insensitive to the scenario observed, with Section 9.5 going on to show how the estimated optimal decision to be made in stage 3 was sensitive to the scenario observed, with total reinforcement varying by 790 MW depending on what was observed.

9.7.1 Discussion of Error Estimates

As mentioned, Section 9.2 detailed an initial three stage decision problem to be considered, with Section 9.3.1 detailing an initial application of the methodology of Section 9.1 to estimate an optimal stage 1 reinforcement decision to minimise the expected total costs across all three stages. Whilst this methodology did allow for the range of potentially optimal stage 1 decisions to be reduced to quite a small range, with all decisions in this range giving similar, relatively low estimates of expected total costs, it was noted that the final range considered was still quite large in comparison to that of the related two stage problem in Section 8.4, with 3.57 times as many stage 1 decisions considered in the final wave of the three stage problem in comparison to the related two stage problem.

Therefore, Section 9.3.2 considered how the error in the estimates of expected total costs could be reduced by fitting the stage 2 and 3 emulator approximations to the simulator, $\tilde{f}_{c,2}(\mathbf{v}_2, \mathbf{d}_2|\mathbf{d}_1)$ and $\tilde{f}_{c,3}(\mathbf{v}_3, \mathbf{d}_3|\mathbf{d}_{T_2})$ respectively, over smaller sensible ranges of stage 2 and stage 3 decisions (such as a range of 5000 MW to 8000 MW B6 and 2500 to 5500 MW B7a reinforcement in stage 3 instead of the larger 0 to 8500 MW B6 and 0 to 5500 MW B7a reinforcement initially considered). This allowed for more accurate emulator models to be fitted over a smaller range of decisions, without the need to perform N_{θ_m} separate wave processes when fitting $\tilde{G}_{T,m,\boldsymbol{\psi}_m}(\mathbf{d}_{T_{m-1}}, \boldsymbol{\psi}_m)$ (the emulator model to approximate total costs in stage m onwards), as was previously considered in Section 8.7.

It was shown in Section 9.3.2 how these smaller ranges resulted in the total number of stage 1 decisions considered in the final wave being reduced by 51.8% in comparison to when fitting $\tilde{f}_{c,2}(\mathbf{v}_2, \mathbf{d}_2|\mathbf{d}_1)$ and $\tilde{f}_{c,3}(\mathbf{v}_3, \mathbf{d}_3|\mathbf{d}_{T_2})$ over the larger ranges considered in Section 9.3.1. However, results from Section 9.5 showed that the estimated optimal total B6 reinforcement after the third decision varied between 6260 MW and 6910 MW and the estimated optimal total B7a reinforcement varied between 3900 MW and 4040 MW depending on the scenario observed. This would mean that $\tilde{f}_{c,3}(\mathbf{v}_3, \mathbf{d}_3|\mathbf{d}_{T_2})$ could have been fitted over an even smaller range of decisions, whilst still being cautious not to exclude the optimal decision, such as 5500 MW to 7500 MW total B6 reinforcement and 3600 to 4500 MW total B7a reinforcement. This in turn would result in the decision space $\tilde{f}_{c,3}(\mathbf{v}_3, \mathbf{d}_3|\mathbf{d}_{T_2})$ is fitted over being reduced by 80%, which would allow for even more accurate estimates of expected costs in stage 3, and thus lead to narrower credible intervals for the estimates of expected total costs across all stages as a function of stage 1 decision only.

This could give rise to an iterative procedure where emulator models which approximate the simulator in each stage, $\tilde{f}_{c,m}(\mathbf{v}_m, \mathbf{d}_m|\mathbf{d}_{T_{m-1}})$, are initially fitted over a large range of decisions. An estimate of optimal stage 1 decision could then be acquired using the methodology of Section 9.1, as was illustrated in Section 9.3, with estimates for optimal decisions to be made in future stages then estimated accurately for a small number of future stages, as illustrated in Sections 9.4 and 9.5.

After optimal decisions to be made in each stage have been estimated, the problem could be repeated fitting the emulator models in each stage, $\tilde{f}_{c,m}(\mathbf{v}_m, \mathbf{d}_m|\mathbf{d}_{T_{m-1}})$, over a smaller range of decisions based on the ranges of optimal decisions that were estimated in each stage. Optimal decisions to be made in each stage could then be re-estimated using the methodology of Section 9.1, giving a greater level of confidence in each decision due to the emulator models in each stage, $\tilde{f}_{c,m}(\mathbf{v}_m, \mathbf{d}_m|\mathbf{d}_{T_{m-1}})$, being fitted over a smaller range of decisions.

An even smaller range to fit the emulator models in each stage over could then be identified based on these optimals, and optimal decisions in turn estimated based on the emulator models fitted over this even smaller range, with the process being repeated iteratively. However, the practicality of such an iterative method could be quite limited,

as after several iterations it would become cheaper to simply perform a full wave process for each of the $\theta_{i,m}$ when fitting $\tilde{G}_{T,m,\boldsymbol{\psi}_m}(\mathbf{d}_{T_{m-1}}, \boldsymbol{\psi}_m)$, as considered in Section 8.7.

9.7.2 Discussion of Further Examples

In the example detailed in Section 9.2 many assumptions were made, such as the assumed cost of reinforcement in each stage. Section 9.6 considered how the estimates of optimal reinforcement decision in each stage varied if assumptions such as the assumed cost to reinforce was varied. In particular, it was shown that although the second stage decision was insensitive to the scenario observed, it was sensitive to the assumed cost of reinforcement.

The effect of the assumed cost to reinforce for single stage decision problems had previously been considered in Sections 5.4.1 and 6.4.2. For the single stage decision problem it was deemed sufficient to consider how the estimates of expected total costs and the resulting estimates of optimal decision to be made varied as the assumed cost to reinforce was varied as it is reasonable to believe the actual cost to reinforce will be known at the time the decision is made. Whilst this could also be considered to be the case for the first decision of a multi-stage decision problem, it is likely that when the first decision is made there will be some uncertainty as to what the cost to reinforce will be for future decisions.

Therefore, a natural extension to the example illustrated in this chapter would be to consider a problem which reduces uncertainty in the assumed cost to reinforce between each decision, as well as reducing uncertainty in the assumed peak demand level between each decision. Such an example could be considered using the methodology of Section 9.1 by simply defining $\boldsymbol{\psi}_m$ as $\boldsymbol{\psi}_m = (\psi_{m,1}, \psi_{m,2})$ where $\psi_{m,1}$ is the observed cost to reinforce in stage m and $\psi_{m,2}$ is the expected peak demand level in stage m. This would additionally require $p_{\boldsymbol{\psi}_{m|m-1}}(\boldsymbol{\psi}_m|\boldsymbol{\psi}_{m-1})$ to be extended to additionally quantify expert beliefs of the probability of observing cost to reinforce $\psi_{m,1}$ in stage m given that the cost to reinforce $\psi_{m-1,1}$ was observed in stage $m-1$, though the methodology of Section 9.1 would be otherwise unchanged.

A similar consideration could be given to the assumed discount rates for future costs, though this would additionally require an accurate model for how discount rates are

projected to vary the planning horizon considered (e.g. 25 years for the example detailed in Section 9.2). Further, Section 8.2.1 previously noted that uncertainty could be reduced in a general number of N_ψ variables between decisions by modelling $\boldsymbol{\psi}_m$ as $\boldsymbol{\psi}_m = (\boldsymbol{\psi}_{m,1}, ..., \boldsymbol{\psi}_{m,N_\psi})$, where $\boldsymbol{\psi}_{m,i}$ quantifies what was learnt about the ith uncertainty in an appropriate way. Such examples, where uncertainty is reduced in multiple variables between decisions, would be natural next areas to consider for further research.

Chapter 10

Discussion

10.1 Thesis Summary

The aim of this thesis was to provide a methodological framework for making good decisions under uncertainty when working with expensive simulators. Throughout the thesis the particular application of the transmission expansion problem applied to Britain's power system was considered, with the aim to minimise expected total costs (expected mean constraint costs plus reinforcement costs) of expansion decisions when there is uncertainty in the values of the variables used to describe Britain's power system.

Chapter 2 began by describing the constraint cost problem considered in the thesis. Constraint costs are the costs that occur due to bottlenecks in the transmission system, and Section 2.1.2 detailed how constraint costs can be calculated for a given power system. Section 2.2 then gave a simple example to show how mean constraint costs are sensitive to many assumptions made about the power system. In particular, it was shown how varying the value of certain variables alone (such as gas availability probability) has little effect on the mean constraint costs, yet interactions can exists (such as between gas availability probability and curtailment costs) which have a very large effect on the mean constraint costs.

Sections 3.1 to 3.6 of Chapter 3 defined the simulator used to estimate mean constraint costs throughout this thesis. Input data for this simulator was taken from [69], National

Grid's freely available online reference and dataset, which details projections about Britain's power system for the 20 year period between 2011 and 2030. An overview of this data is given in Section 3.6 and some further details are given in Appendix F. Section 3.7 then showed how mean constraint costs vary over the 20 year period using these projections, and went on to consider how these calculations of mean constraint costs are sensitive to some of the particular input values given by [69], such as the installed transmission capacity between zones or peak demand level.

Chapter 4 considered how importance sampling could be used as a method of reducing the computational work required to acquire an estimate of mean constraint costs in comparison to using the full simulator. Section 4.3.3 showed how importance sampling with weights based on the mean constraint costs of each half hour snapshot gave the best results. However, this required prior estimates of the mean constraint costs of each snapshot. Further, Section 4.3.4 showed how weights calculated for one power system background do not generalise well to other power system backgrounds. Therefore, Section 4.4.2 proposed a method which would take a small number of full simulator evaluations to estimate initial weights to be used for importance sampling, with these weights continually updated with information from subsequent simulator evaluations from importance sampling.

The primary aim of this thesis was to present a methodology for decision making under uncertainty. However, when working with expensive simulators it is infeasible to run the full simulator for any set of input values we would like. Section 5.2 detailed how this can be overcome by using a small number of training runs from the full simulator to construct a statistical emulator, to accurately approximate how input affects output of the simulator and provide an estimate of the expected response of the simulator for input values not simulated. Further, Equation 5.2.16 of Section 5.2.5 detailed how an estimate of expected response under uncertainty (i.e. an estimate of expected total costs under uncertainty for the examples considered) can be acquired by integrating the product of the estimated response from the emulator and a PDF which describes prior beliefs about the values the variables containing uncertainty can take.

The fitted emulator models are not perfect approximations to the simulator and contain error. Section 5.2.6 detailed how this error can be accounted for by considering how the

estimates of expected total costs under uncertainty from Equation 5.2.16 vary as the model parameters of the fitted emulator model are varied. Further, credible bounds for the estimated expected total costs could be calculated, such that if an $\alpha\%$ credible interval is desired, a lower credible bound could be formed as the value that $\frac{100-\alpha}{2}\%$ of the estimates of expected total costs using randomly drawn emulators are smaller than, and an upper credible bound could be formed as the value that $\frac{100-\alpha}{2}\%$ of the estimates of expected total costs using randomly drawn emulators are greater than.

Section 6.2 went on to detail a method in which the credible bounds can be used to eliminate values of decision variables from consideration which have evidence against them being optimal. This allows for a new set of training runs to be taken over the range of decisions not eliminated, in order to fit a more accurate emulator model over a smaller range of decisions, giving an increased level of confidence to the resulting estimates of expected total costs under uncertainty, allowing for a better decision to be made as a result. This gives rise to an iterative wave process where the decision space is reduced further and further in each wave, allowing for a more accurate emulation approximation to the simulator to be fitted in each wave.

An application to a simple example detailed in Section 5.3.1 of Chapter 5 was considered, where uncertainty was considered in a single variable and a single reinforcement decision was to be made, with the aim of estimating an optimal decision to minimise the estimate of expected total costs under uncertainty. Section 6.1.1 of Chapter 6 then extended this to a more complicated example akin to a real world transmission expansion planning problem where uncertainty is considered in three variables and two simultaneous decisions are to be made, with an interaction existing between the decision variables.

For both examples it was illustrated how the estimates of expected total costs, and the resulting estimates of optimal reinforcement decisions, were sensitive to many assumptions made, such as the attitude to risk of the decision maker or prior beliefs about uncertainty, in Section 5.4 and Section 6.4. Further, Chapter 7 considered how estimates of expected total costs and the resulting estimates of optimal reinforcement decisions were sensitive to various assumptions made about the underlying model and data for Britain's power system, such as the underlying seasonal model for Britain's

wind generation or the assumed distribution for annual demand.

In Section 8.2.4 we proposed a method for solving a general two-stage decision problem which modelled the future scenario as a set of continuous variables, which allows for an infinite number of possible future scenarios to be modelled. Estimates of expected total costs across both stages were then acquired via a combination of backwards induction and emulation to approximate how expected total costs across both stages vary as a function of the stage 1 decision only. This methodology was extended to a general M-stage problem in Section 9.1.

An initial application was considered in Section 8.3, which details a problem where two sequential reinforcement decisions are to be made, with uncertainty about future peak demand level reduced between each decision. Illustrations of how expected total costs vary with reinforcement decisions in the first and second stage (along with the resulting estimates of optimal decisions) were presented in Sections 8.4 and 8.5 respectively.

This example was extended to a 3 stage problem in Section 9.2, with estimates of expected total costs and the resulting estimates of optimal decisions detailed in Sections 9.3 to 9.5. The sensitivity of the estimates to various assumptions was considered in Section 9.6. In particular, the sensitivity of the estimates of expected total costs and the resulting decisions to the assumed discount rate of future costs and the planning horizon of the problem were considered, two factors which were not investigated when considering the single stage problems.

10.2 Discussion and Further Work

10.2.1 Discussion Regarding the Particular Examples Presented

Correlation Model Between Snapshots

Some areas of further work regarding the specific examples presented have already been discussed throughout this thesis. One of the bigger issues raised is that it is standard practice of National Grid, and broadly the case elsewhere, to work with mean constraint costs, without considering the distribution of constraint cost realisations in a year for a

given power system background. As such, the simulator defined in Chapter 3 simulates snapshots independently without considering correlation between snapshots to remain consistent with this practice.

However, in reality it is reasonable to think that certain elements of the power system will be correlated between snapshots, such as if a particular generator is unavailable in one snapshot it is reasonable to think that it will be more likely to be unavailable in the next snapshot. Therefore, if we were to consider a fresh approach to this problem it would be of interest to incorporate this correlation into the model in order to model how realisations of annual constraint costs vary for a given power system background, which may affect the decisions made.

Prior Beliefs About Uncertainties

One area of discussion regarding the specific examples considered which should also be considered in any further general examples are the choices of distributions used to represent prior information about uncertainties. For the examples of Chapter 5 and Chapter 6 our original interpretation of the information supplied by Paul Plumptre [78] was that a uniform distribution was suitable to express prior beliefs about variables containing uncertainty. Therefore, variations on these beliefs considered various uniform distributions which considered varying the windows and centres of the distribution. However, a uniform distribution is quite a limited distribution, as it assumes any value within a given window considered is equally likely to occur, and any value outside the window has a probability of 0 of occurring. One could make a strong case for instead using non-uniform distributions which give more weight to central values and less weight to extreme values.

A suitable alternative distribution for prior beliefs that could have been considered is a scaled beta distribution, where model parameters can be selected to give a desired expectation and variance of the distribution. In addition, for many choices of model parameters the scaled beta distribution has the attractive property that density given to values would smoothly go to zero at the limits of the windows considered for each variable.

The methodology of this thesis is written in general terms, and is sufficient handle such non-uniform distributions. For example, when estimating an expected response under uncertainty via Equation 5.2.16 of Section 5.2.5, $p(\mathbf{v})$ would simply have to be defined as the desired distribution which describes prior beliefs about uncertainties. While such variations were not considered for the examples of Chapter 5 and 6, non-uniform priors were used when considering multi-stage decision making in Section 8.6 of Chapter 8.

Further, in more general examples it could be that two or more of the variables of interest are not independent. For example, it could be that prior information suggests that if one variable, v_1, is observed to take a high value then a second variable, v_2, will be more likely to take a low value. This would mean it would be necessary to specify $p(\mathbf{v})$ as the joint distribution across all variables containing uncertainty, rather than a product of prior beliefs about each individual uncertainty. However, given that a suitable joint distribution is specified the methodology of this thesis would be unchanged, as $p(\mathbf{v})$ could still be used in Equation 5.2.16 to estimate expected costs by integrating over the product of the emulator fitted to estimate a response for given input, $\tilde{f}(\mathbf{v}, \mathbf{d})$, and the joint distribution of prior beliefs about variables which contain uncertainty, $p(\mathbf{v})$.

10.2.2 Discussion About the Application of the Methodology of This Thesis to Further Problems

Application of Methodology to Further Problems

As well as the issues discussed throughout this thesis regarding the specific examples considered, it is also important to consider any potential issues which may arise when applying the methodology considered in this thesis to more general examples. The methodology used throughout this thesis was detailed in quite general terms, so could easily be adapted to any other example which considered making a decision or decisions under uncertainty when using an expensive simulator or calculation with uncertainty in one or more aspects which affect the decision made. Natural areas to consider for further examples would be the closely related generation expansion planning problems and storage expansion planning problems applied to power systems.

For example, a generation planning problem could consider $f(\mathbf{v}, \mathbf{d})$ as being an expensive simulator which calculates generator profits for given input describing a power system background, with $\mathbf{v}$ being variables which contain uncertainties of interest to the generation expansion problem, such as variables related to demand level (which were of interest to the transmission expansion problem considered in this thesis) or variables related to the cost/profit of generation or generation emissions targets, and $\mathbf{d}$ describing decision variables for the generation expansion problem, which would be when and where to build new power stations.

Further, it would not be necessary to consider examples so closely related to the transmission expansion problem considered in this thesis. In the existing literature, quite a wide range of applications of emulation have been considered, such as galaxy formation [98], hydrocarbon reservoir modelling [23, 20] or tsunami free surface wave elevation [60] and as the methodology considered throughout this thesis is written in general terms it could also be applied to such areas.

Application of the Methodology to Problems With High Dimensional Input

Another point of consideration is that the majority of examples presented throughout this thesis considered uncertainty in three variables with two simultaneous decisions to be made. This meant that the emulator models were fitted over a total of 5 input variables of the simulator (though some of the examples of Chapter 7 consider 6). Whilst the methodology of Section 5.2, which details how to use a set of training runs from the full simulator to fit an emulation approximation to a simulator, was written in general terms for a general number of variables containing uncertainty, $\mathbf{v}$, and a general number of decision variables, $\mathbf{d}$, there are some additional considerations to make when fitting an emulator over a higher dimensional input space.

First, a more careful consideration of which terms are included in the polynomial regression portion of the emulator model is required, in particular which interactions between which input variables are included. In addition, as extra dimensions are considered in the input space, a set of training data of given size will give an increasingly sparse coverage to the input space. One potential solution could be to increase the number of training runs used to fit the emulator model, though as emulators are used

to approximate expensive simulators it will only be feasible to increase the number of training runs from the expensive simulator so far.

However, it is noted in [74] that often, when fitting an emulator model over a high dimensional input space, only a small subset of the input variables have a substantial effect on the simulator output. This is reflected when fitting the emulator model, as the resulting emulator model will be insensitive (and the Gaussian process portion of the emulator will be very smooth) to all variables except those which have a large impact on simulator output, which effectively projects the input space down to the smaller subset of inputs which have a large effect on simulator output. This is demonstrated in [72] which considers a 15 dimensional problem where 5 inputs have a larger effect on output than the other 10 and a second example where just 3 of 40 inputs have a large effect on simulator output.

This can be considered further, by separating the simulator input, $\mathbf{x} = (\mathbf{v}, \mathbf{d})$, into active inputs, $\mathbf{x}_{[A]}$, which are the input variables which the simulator output is sensitive to, and inactive inputs, which are the input variables which the output of the simulator is not sensitive to, as described in [98, 23, 22]. Then, instead of fitting an emulator model of the form

$$\tilde{f}_T(\mathbf{x}) = g(\mathbf{x})^{\mathrm{T}}\boldsymbol{\beta} + e(\mathbf{x})$$

as described in Section 5.2 (i.e. as the sum of a polynomial regression model, $g(\mathbf{x})^T\boldsymbol{\beta}$, and a Gaussian process model fitted to its residuals, $e(\mathbf{x})$), [98, 23, 22] consider fitting an emulator model of the form

$$\tilde{f}_T(\mathbf{x}) = g(\mathbf{x}_{[A]})^{\mathrm{T}}\boldsymbol{\beta} + e(\mathbf{x}_{[A]}) + v(\mathbf{x}) \tag{10.2.1}$$

where the polynomial regression and Gaussian process portions of the emulator model (or more generally a parametric form to model global trends and a stochastic process applied to its residuals) are now fitted as functions of the active inputs only. In Equation 10.2.1, the term $v(\mathbf{x})$ represents an uncorrelated nugget term with zero mean and constant variance to account for the residual variation of the response due to the inactive inputs.

There are many other methods which can be considered for fitting emulator models over high dimensional input. For example, [27] consider using additive functions (in-

cluding a Gaussian process model with an additive covariance function) to construct the emulator, whilst [60] consider using gradient-based kernel dimensionality reduction as a method of reducing the dimensionality of the input space (and [63] detail many further techniques such as generative topographic mapping and sliced inverse regression which could be used to reduce the dimension of the input space).

Application of the Methodology to Problems With High Dimensional Output

It should also be considered that all examples presented in this thesis consider simulators with a single output (the mean constraint costs). However, more general applications of the emulation methodology may consider simulators with multivariate output. Even for the examples considered in this thesis, it would have been possible to consider multivariate output. For example, as well as recording the mean constraint costs of each training run, a response relating to the reliability of the power system (such as expected energy not served (EENS), which is simply the expected amount of demand, in MW, that will not be satisfied for a given power system background) could also have been considered.

The simplest way to handle simulators with multivariate outputs would be to independently fit a separate emulator model to each output. However, [18, 32] note that this may not be the best course of action as it is possible (and in some cases likely) that outputs from the same simulator are related, and fitting separate emulator models would ignore correlations between outputs. Therefore, [18, 32, 23] and many others detail how the emulation methodology can be extended to model multivariate output, which [18] note is a simple extension to the univariate case when assuming a separable covariance function.

However, as is the case with a high dimensional input space, it may be necessary to give a more careful consideration when fitting emulator models with a high dimensional output space. [23, 22] note that it can be computationally intensive to fit an emulator to a simulator with a high dimensional output, so the method of principal variable selection, described in [24], is used to identify a subset of model outputs which capture the majority of the variation in all model outputs. For example, [23] consider

a hydrocarbon reservoir model which has 65 simulator outputs, and principal variable selection is used to identify a subset of 15 outputs to model, which capture at least 94.7% of the variation of the remaining 50 output variables.

[59] consider a possible alternative method for modelling high dimensional output when the simulator output forms a time series. For such cases, it is considered that instead of modelling a multi-variate output $\mathbf{y} = (y_1, ..., y_T)$ of a simulator $f(\mathbf{x})$, time could be modelled as an additional simulator input, which in turn could be used to model the simulator as if it had univariate output, i.e. $y = f(\mathbf{x}, t)$. Whilst [59] note this could possibly greatly increase the input dimension, they propose how a time varying auto regressive modelling can be used in addition to a Gaussian process model when fitting the emulator model, which can be thought of as an approximation to a Gaussian process emulator model which also includes time as an additional simulator input.

[32] note that similar approaches can also be taken when considering other examples when the multivariate output of a simulator describes how a response varies over continuous variables. For example, if the multivariate output of a simulator described how a response varied with location, variables describing location could be used as additional simulator input and a univariate response modelled.

Decision Making When Simulators Have Higher Dimensional Output

It is worth considering that the methodology of this thesis is primarily concerned with decision making under uncertainty. Therefore, if this methodology was extended to consider simulators with multi-variate output it would make sense to only model simulator outputs which affect the decisions made, which could act as a preliminary screening process of the output variables and reduce the dimension of the output space.

Further, it should also be considered that Section 5.2.5 considers how to estimate the expected response of the simulator under uncertainty by integrating the product of the estimated response from the emulator used to approximate the simulator, $\tilde{f}(\mathbf{v}, \mathbf{d})$, and a set of prior beliefs about variables containing uncertainty, $p(\mathbf{v})$, as

$$\tilde{F}(\mathbf{d}) = \int_{\mathbf{v}} \tilde{f}(\mathbf{v}, \mathbf{d}) \times p(\mathbf{v}) \mathrm{d}\mathbf{v} \tag{10.2.2}$$

with it being desirable to estimate an optimal decision to minimise (or maximise) $\tilde{F}(\mathbf{d})$, which is extended to an M-stage decision problem in Section 9.1.

However, when considering a simulator with multivariate output, it could be that there are Λ simulator outputs, $\mathbf{f}(\mathbf{v},\mathbf{d}) = (f_1(\mathbf{v},\mathbf{d}),...,f_\Lambda(\mathbf{v},\mathbf{d}))^{\mathrm{T}}$, which are affected by the decision made, which would be approximated by a multivariate emulator, $\tilde{\mathbf{f}}(\mathbf{v},\mathbf{d}) = (\tilde{f}_1(\mathbf{v},\mathbf{d}),...,\tilde{f}_\Lambda(\mathbf{v},\mathbf{d}))^{\mathrm{T}}$. This would require a utility function, $u(\tilde{f}_1(\mathbf{v},\mathbf{d}),...,\tilde{f}_\Lambda(\mathbf{v},\mathbf{d}))$, to be used to specify the decision maker's preference of outcomes across all Λ outputs, which would allow for an expected utility across all Λ outputs under uncertainty to be calculated as

$$\tilde{F}_u(\mathbf{d}) = \int_{\mathbf{v}} u(\tilde{f}_1(\mathbf{v},\mathbf{d}),...,\tilde{f}_\Lambda(\mathbf{v},\mathbf{d})) \times p(\mathbf{v})\mathrm{d}\mathbf{v} \tag{10.2.3}$$

with the objective of identifying optimal decisions to maximise utility.

For some specific examples it may be possible to simplify this slightly. For example, as mentioned earlier, the simulator considered in this thesis could be expanded to a simulator with bivariate output, $\mathbf{f}(\mathbf{v},\mathbf{d}) = (f_1(\mathbf{v},\mathbf{d}), f_2(\mathbf{v},\mathbf{d}))^{\mathrm{T}}$, where $f_1(\mathbf{v},\mathbf{d})$ is the total costs (mean constraint costs plus reinforcement costs) of the power system and $f_2(\mathbf{v},\mathbf{d})$ is the expected energy not served (EENS) of the power system. Instead of maximising the expected utility of this bivariate output using Equation 10.2.3, it may instead be desirable to minimise the estimate of expected total costs of the decision, calculated as

$$\tilde{F}(\mathbf{d}) = \int_{\mathbf{v}} \tilde{f}_1(\mathbf{v},\mathbf{d}) \times p(\mathbf{v})\mathrm{d}\mathbf{v} \tag{10.2.4}$$

subject to the upper bound for the EENS (which could be calculated using the methodology of Section 5.2.6 using $f_2(\mathbf{v},\mathbf{d})$ in place of $f_T(\mathbf{v},\mathbf{d})$) being below some specified threshold. This would equate to a transmission expansion planning problem with the goal of optimizing constraint costs under uncertainty, whilst also accounting for the security of the power system (which is measured as the EENS).

Potential Clustering of Decisions in the Wave Process

As part of the decision making methodology used throughout this thesis, a wave process is used to iteratively eliminate decisions from consideration which have evidence against

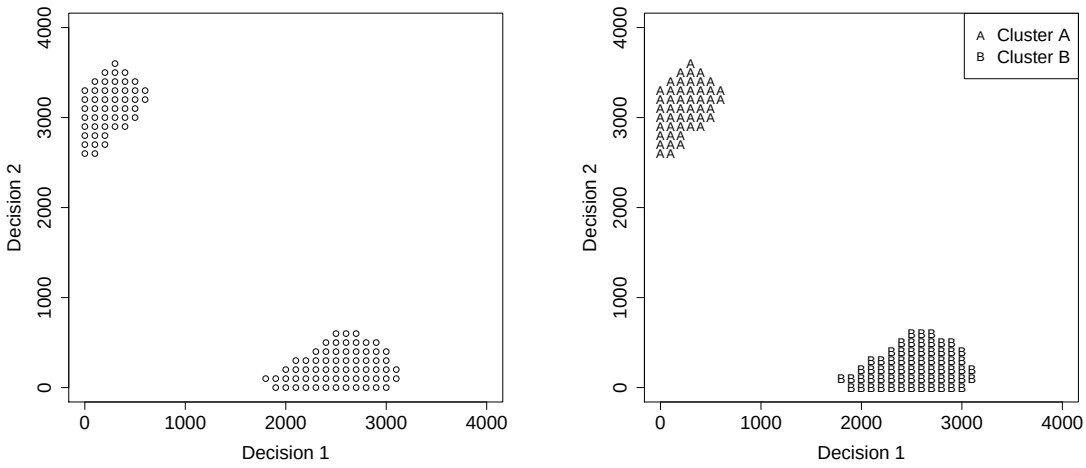

(a) Plot to illustrate decisions with two potential clusters.

(b) Plot to illustrate decisions with two potential clusters.

Figure 10.1: Plots to illustrate potential clustering of decisions beyond the first wave.

them being optimal, and fit a more accurate emulator model over a smaller and smaller range of decisions, as outlined in Section 6.2 for a single stage decision problem and in Section 9.1.4 for an M-stage decision problem.

In the examples presented throughout this thesis, the ranges of decisions considered in each wave form a single region, and a single emulator model was fitted across all decisions in that region. However, in a more general problem it could be that decisions to be considered beyond the first wave form multiple clusters. This is illustrated in Figure 10.1 (a), where the range of decisions considered clearly form two clusters, identified in Figure 10.1 (b) as Cluster A and Cluster B.

A practical interpretation of what could lead to the clusters illustrated in Figure 10.1 is if the cost of increasing the magnitude of a single decision gradually decreases as the magnitude of the decision increases, with no interaction between the two decisions on other costs/profits of the decision. This could possibly lead to it being economically beneficial to make a single decision of large magnitude, rather than two decisions of smaller magnitude. Further, if the benefits of either decision are of similar magnitude, due to uncertainty in the emulator model it may be difficult to identify which of the two decisions should be of large magnitude, leading to the observed clustering of Figure 10.1.

Whilst it would be possible to fit a single emulator model across both clusters, it

would be more accurate to take two sets of training runs from the simulator (one for each cluster) in order to fit a separate emulator model to each cluster. However, the computational requirements to estimate an expected response of the simulator would increase linearly as the number of clusters modelled is increased. Further, whilst it is quite easy to visually identify an appropriate number of clusters to use when making two simultaneous decisions, it could be much more difficult to identify an appropriate number of clusters to use when making 3 or more simultaneous decisions.

10.2.3 Further Discussion Regarding Multi-Stage Decision Problems

Chapter 9 considered a 3 stage decision problem detailed in Section 9.2, with the methodology of Section 9.1 used to estimate optimal decisions across all three stages. Further, the methodology detailed in Section 9.1 is written in general terms (again, making it suitable for problems other than the transmission expansion problem considered) for problems with a general number of M sequential decisions to be made. This means, in principle, it would also be possible to use this methodology to estimate optimal decisions for problems with more than 3 sequential decisions to be made. However, it is also important to consider how increasing the number of decision stages of a multi-stage decision problem affects the computational requirements to acquire an estimate of expected total costs (or profits/response for a general problem) across all M stages as well as the error of the resulting estimate.

Further Consideration to Multi-Stage Problems Where it is Insufficient to Consider Only the Total Reinforcement of the Previous $M-1$ Stages

One issue regarding the multi-stage decision problem that was given some previous consideration in Chapter 9 is that for the multi-stage transmission expansion problems considered, the emulator models fitted to approximate the simulator in each stage are of the form $\tilde{f}_{c,m}(\mathbf{v}_m, \mathbf{d}_m|\mathbf{d}_{T_{m-1}})$, i.e. the emulator model to approximate the simulator in stage m is only dependent on the total reinforcement made in the previous $m-1$ stages, $\mathbf{d}_{T_{m-1}}$, and not the individual reinforcements in stages 1 to $m-1$, i.e. $\mathbf{d}_1, ..., \mathbf{d}_{m-1}$.

However, it was noted that the methodology of Section 9.1.2 was otherwise written in general terms, with Section 9.1.3 going on to note how the methodology presented could be adapted to consider more general problems where the costs in stage m onwards are dependent on the individual decisions in the previous $m-1$ stages $(\mathbf{d}_1, ..., \mathbf{d}_{m-1})$ and not just the total reinforcement in the previous m stages $(\mathbf{d}_{T_{m-1}})$ by fitting emulator models of the form $\tilde{f}_{c,m}(\mathbf{v}_m, \mathbf{d}_m|\mathbf{d}_1, ..., \mathbf{d}_{m-1})$ and $\tilde{G}_{T,m,\boldsymbol{\psi}_m}(\mathbf{d}_1, ..., \mathbf{d}_{m-1}, \boldsymbol{\psi}_m)$ in place of $\tilde{f}_{c,m}(\mathbf{v}_m, \mathbf{d}_m|\mathbf{d}_{T_{m-1}})$ and $\tilde{G}_{T,m,\boldsymbol{\psi}_m}(\mathbf{d}_{T_{m-1}}, \boldsymbol{\psi}_m)$ respectively.

As was noted, the fact that the simulator in each stage depends only on the total reinforcement in the previous $m-1$ stages, $\mathbf{d}_{T_{m-1}}$, and not the individual reinforcements in the previous $m-1$ stages, i.e. $\mathbf{d}_1, ..., \mathbf{d}_{m-1}$, is quite a useful simplification as this means that the number of variables the emulator models are fitted over in each stage does not grow with the number of stages considered. As it is likely each decision in each previous stage has a non-negligible effect on costs in stage m onwards this could make the problem more tractable when considering a large number of decisions stages.

It is also noted that as part of the methodology of Section 9.1.2, a specification is required of how the decisions made in stages 1 to $m-1$ affect which decisions can be made in stage m (such as for when an optimal stage m decision to be made is estimated for a given total reinforcement in the previous $m-1$ stages and stage m scenario). For the transmission expansion planning problem considered in this thesis this is quite simple, as the only constraint is that the total reinforcement after the mth decision is at least as large as the total reinforcement made in the previous $m-1$ stages (i.e. that a non-negative reinforcement is made in stage m).

However, in a more general problem it is possible that the decisions made in stages 1 to $m-1$ $(\mathbf{d}_1, ..., \mathbf{d}_{m-1})$ have a less trivial effect on the decisions that can be made in stage m, such that making or not making decisions in each stage can have an effect on what decisions are available to be made in stage m. As was also noted in Section 9.1.3, the methodology of Section 9.1.2 is written quite generally and can still be applied to such examples given a suitable specification of how the decisions made in stages 1 to $m-1$ affect what decisions can be made in stage m. However, as the number of stages considered increases, this will require an increasingly complicated specification of how decisions made in stages 1 to $m-1$ affect what decisions are available to be made in

stage m, which could also make the problem less tractable when considering a large number of decision stages.

Computational Requirements of Problems With More Than Three Stages

As part of the M-stage decision methodology of Section 9.1, M emulator models are fitted to approximate the simulator in each stage, such that $\tilde{f}_{c,m}(\mathbf{v}_m, \mathbf{d}_m|\mathbf{d}_{T_{m-1}})$ is the emulator model which approximates the simulator in stage m. This in turn requires a total of $\sum_{m=1}^{M} N_{n_m}$ training runs from the simulator to be evaluated, where N_{n_m} is the number of training runs used to fit the the emulator model, $\tilde{f}_{c,m}(\mathbf{v}_m, \mathbf{d}_m|\mathbf{d}_{T_{m-1}})$, to approximate the simulator in stage m. This indicates that generally the number of simulator evaluations required (which will typically be the most computationally expensive part of the methodology of Section 9.1.2) increases linearly with the number of stages considered.

Further, as part of the methodology of Section 9.1, a sample of N_{θ_m} stage $m-1$ total reinforcement decisions (values of $\mathbf{d}_{T_{m-1}}$) and stage m scenarios (values of $\boldsymbol{\psi}_m$) are sampled to fit the emulator model $\tilde{G}_{T,m,\boldsymbol{\psi}_m}(\mathbf{d}_{T_{m-1}}, \boldsymbol{\psi}_m)$ which models how expected total costs in stage m onwards vary as a function of stage $m-1$ total reinforcement decision and stage m scenario only. For each of the N_{θ_m} values in the sample, optimal decisions were estimated to be made in stage m based on the stage m scenario that was observed and the decision that was made in the previous stage. In a general M-stage problem this would require a total of $\sum_{m=2}^{M} N_{\theta_m}$ estimates of optimal stage m decisions in order to model expected total costs across all stages as a function of stage 1 decision only, which also increases linearly with the number of decision stages considered.

This indicates that generally the work required to estimate expected total costs across all M stages of an M-stage decision problem increases linearly with the number of stages considered. This in turn means that computationally it is plausible to consider multi-stage decision problems with more than 3 stages using the methodology of Section 9.1. However, it should also be noted that a linear increase in work is by no means a negligible increase in computational requirements, so whilst more than three 3 stages could be considered, it won't be possible to increase the number of stages considered indefinitely.

Error Estimates for M-Stage Problems

As noted in the previous sub-subsection, as part of the methodology of Section 9.1 N_{θ_m} stage $m-1$ total reinforcement decisions (values of $\mathbf{d}_{T_{m-1}}$) and stage m scenarios (values of $\boldsymbol{\psi}_m$) are sampled to fit the emulator model $\tilde{G}_{T,m,\boldsymbol{\psi}_m}(\mathbf{d}_{T_{m-1}}, \boldsymbol{\psi}_m)$, which models how expected total costs in stage m onwards vary as a function of stage $m-1$ total reinforcement decision and stage m scenario only. For each of the N_{θ_m} values in the sample, optimal decisions to be made in stage m were estimated based on the stage m scenario that was observed and the total reinforcement decision that was made in the previous stage. These optimals were estimated using $\tilde{f}_{c,m}(\mathbf{v}_m, \mathbf{d}_m|\mathbf{d}_{T_{m-1}})$, the fitted emulator model to approximate the simulator in stage m.

However, as $\tilde{f}_{c,m}(\mathbf{v}_m, \mathbf{d}_m|\mathbf{d}_{T_{m-1}})$ is not a perfect approximation to the simulator in stage m there will be error in the estimates of optimal stage m decision and the resulting estimates of expected total costs across stages m to M. Section 9.1.4 detailed how this error can be accounted for to form credible intervals for the estimates of expected total costs across all M stages as a function of stage 1 decision only, which can in turn be used to eliminate stage 1 decisions from consideration which have evidence against them being optimal in order to fit a more accurate emulator model over a smaller range of decisions.

As error cascades through each stage, in the sense that if the stage M model is inaccurate the model of expected total costs across stages $M-1$ to M will also be inaccurate, which will in turn mean the model of expected total costs across stages $M-2$ to M will also be inaccurate and so on, this means that increasing the number of stages of the decision problem may increase the error in estimate of expected total costs across all M stages. This was actually noted Section 9.3.1, where it was shown that 3.57 times as many stage 1 decisions are considered in the final wave of the 3 stage problem in comparison to the range of stage 1 decisions considered in the final wave of the related 2 stage decision problem. Therefore, it may be necessary to consider potential methods of reducing error in the estimate of expected total costs across all M stages before considering problems with more than 3 stages.

This was already given some consideration throughout Chapters 8 and 9. For example, Section 8.7 showed how the error in the estimate could be greatly reduced if a separate

wave process was used for each of the N_{θ_m} samples when estimating optimal stage m decisions (and the resulting estimates of expected total costs in stage m onwards) used to fit $\tilde{G}_{T,m,\boldsymbol{\psi}_m}(\mathbf{d}_{T_{m-1}}, \boldsymbol{\psi}_m)$. However, it was also noted that performing such a wave process for each of the N_{θ_m} samples is a very expensive, and infeasible for the resources available to us in this thesis. Further, in a general M-stage problem this would require $\sum_{m=2}^{M} N_{\theta_m}$ separate wave processes to be carried out within each stage 1 wave when estimating the optimal decision to be made in stage 1, showing how the additional work required would grow as the number of decision stages considered is increased. However, as this work increases linearly with the number of stages considered and not exponentially, this means such a method may not be infeasible for an organisation with substantial computing resources, such as National Grid.

As an alternative, Section 9.3.2 showed how fitting the emulator models, $\tilde{f}_{c,m}(\mathbf{v}_m, \mathbf{d}_m|\mathbf{d}_{T_{m-1}})$, to approximate the simulator in stages 2 and 3 over smaller, sensible ranges of decisions could lead to the error in the estimated expected total costs across all stages being reduced. This in turn resulted in the total number of stage 1 decisions considered in the final wave to be reduced by 51.8% in comparison to when fitting $\tilde{f}_{c,2}(\mathbf{v}_2, \mathbf{d}_2|\mathbf{d}_1)$ and $\tilde{f}_{c,3}(\mathbf{v}_3, \mathbf{d}_3|\mathbf{d}_{T_2})$ over the larger ranges initially considered in Section 9.3.1.

This was then given some further consideration in Section 9.7.1, where it was noted that $\tilde{f}_{c,3}(\mathbf{v}_3, \mathbf{d}_3|\mathbf{d}_{T_2})$ could have been fitted over an even smaller range of decisions, which in turn would reduce the error in the estimated costs even further. A possible iterative procedure was therefore proposed which would iteratively estimate how optimal decisions across all stages vary depending on the scenario observed and use these estimates to reduce the range of decisions used to fit the emulator model to approximate the simulator in stage m, $\tilde{f}_{c,m}(\mathbf{v}_m, \mathbf{d}_m|\mathbf{d}_{T_{m-1}})$. However, it was also noted that such an iterative procedure may be of limited use as an alternative, as after several iterations it would become cheaper to simply perform a full wave process for each of the N_{θ_m} sampled stage $m-1$ total reinforcement decisions and stage m scenarios when fitting $\tilde{G}_{T,m,\boldsymbol{\psi}_m}(\mathbf{d}_{T_{m-1}}, \boldsymbol{\psi}_m)$ as described earlier.

A possible alternative method of reducing the error in the estimate of a general M-stage problem without substantially increasing the computational requirements could

be to treat the problem as a rolling M_2-stage problem where $M_2 < M$. For example, if a 7 stage decision problem is to be solved (i.e. $M = 7$), the problem could be initially treated as a 3 stage decision problem (i.e. $M_2 = 3$), with only the first 3 of the 7 decisions available. The methodology of Section 9.1 could then be used to estimate an optimal first stage decision for this reduced three stage problem. Then, when the time came to make the second decision, the problem could again be treated as a 3 stage decision problem, with the second to fourth decisions of the original seven stage problem available, and the methodology of Section 9.1 used to estimate an optimal stage 2 decision. This could be repeated with each subsequent decision, with optimal third to seventh decisions estimated using the methodology of Section 9.1 by treating the problem as at most a 3 stage decision problem.

Such a methodology could even be used in combination with the methodology which performs a separate wave process for each of the N_{θ_m} samples, or uses a smaller sensible range of decisions when fitting emulator models, $\tilde{f}_{c,m}(\mathbf{v}_m, \mathbf{d}_m | \mathbf{d}_{T_{m-1}})$, to approximate the simulator in stage m for even better results.

Reducing Uncertainty in Multiple Variables Between Decisions

Finally, the example detailed in Section 9.2 considers reducing uncertainty in a single variable (future peak demand level) between reinforcement decisions. However, in a more general M-stage problem it is possible that the example will consider reducing uncertainty in multiple variables between reinforcement decisions. This was previously considered in Section 9.7.2 as the next area of interest for the particular examples considered in this thesis, where it was noted the M-stage decision methodology of Section 9.1 is written in quite general terms and is sufficient to handle applications where uncertainty is reduced in multiple variables between stages.

As noted in Section 8.2.1, this would be achieved by defining $\boldsymbol{\psi}_m$ (the set of variables which define the stage m scenario observed) as $\boldsymbol{\psi}_m = (\boldsymbol{\psi}_{m,1}, ..., \boldsymbol{\psi}_{m,N_\psi})$ if uncertainty is reduced in N_ψ variables between decisions such that $\boldsymbol{\psi}_{m,i}$ quantifies what was learnt about the ith uncertainty in an appropriate way, with the methodology of Section 9.1 being otherwise unchanged.

Bibliography

[1] S.K. Abeygunawardane, P. Jirutitijaroen, and H. Xu. "Adaptive Maintenance Policies for Aging Devices Using a Markov Decision Process". In: *IEEE Transactions on Power Systems* 28 (3 2013), pp. 3194 –3203.

[2] T. Akbari, A. Rahimi-Kian, and M.T. Bina. "Security-constrained transmission expansion planning: A stochastic multi-objective approach". In: *International Journal of Electrical Power & Energy Systems* 43 (2012), pp. 444 –453.

[3] T. Akbari, A. Rahimikian, and A. Kazemi. "A multi-stage stochastic transmission expansion planning method". In: *Energy Conversion and Management* 52 (2011), pp. 2844 –2853.

[4] J.F. Alonso, A. Sáiz, L. Martín, G. Latorre, A. Ramos, and I.J. Pérez-Arriaga. "PERLA: An Optimization Model for Long Term Expansion Planning of Electric Power Transmission Networks". In: *IIT-91-009* (1991).

[5] *Amendment Report GSR009, Review of Required Boundary Transfer Capability with Significant Volumes of Intermittent Generation*. SQSS Review Group. 2011. URL: `http://www.nationalgrid.com/uk/Electricity/Codes/gbsqsscode/`.

[6] E.C. Anderson. *Monte Carlo Methods and Importance Sampling*. University of Berkeley. 1999. URL: `http://ib.berkeley.edu/labs/slatkin/eriq/classes/guest_lect/mc_lecture_notes.pdf`.

[7] I. Andrianakis, I.R. Vernon, N. McCreesh, T.J. McKinley, J.E. Oakley, R.N. Nsubuga, M. Goldstein, and R.G. White. "Bayesian History Matching of Complex Infectious Disease Models Using Emulation: A Tutorial and a Case Study on HIV in Uganda". In: *PLOS Computational Biology* 11 (1 2015), pp. 1 –18.

[8] E.N. Asada, E. Carreño, R. Romero, and A.V. Garcia. "A Branch-and-Bound Algorithm for the Multi-Stage Transmission Expansion Planning". In: *IEEE Power Engineering Society General Meeting*. 2005.

[9] A. Bassamboo and S. Jain. "Efficient Importance Sampling for Reduced Form Models in Credit Risk". In: *2006 Winter Simulation Conference*. 2006, pp. 741 –748.

[10] L.S. Bastos and A. O'Hagan. "Diagnostics for Gaussian Process Emulators". In: *Technometrics* 51 (2009), pp. 425 –438.

[11] S.J. Bates, J. Sienz, and V.V. Toropov. "Formulation of the Optimal Latin Hypercube Design of Experiments Using a Permutation Genetic Algorithm". In: *45th AIAA/ASME/ASCE/AHS/ASC Structures, Structural Dynamics & Materials Conference*. 2004.

[12] R. Billington, Y. Gao, and R. Karki. "Application of a Joint Deterministic-Probabilistic Criterion to Wind Integrated Bulk Power System Planning". In: *IEEE Transactions on Power Systems* 25 (2010), pp. 1384–1392.

[13] M. E. Boot-Handford, J. C. Abanades, E. J. Anthony, et al. "Carbon capture and storage update". In: *Energy & Environmental Science* 7 (2014), pp. 130 –189.

[14] *Carbon Capture & Storage Association. http : //www.ccsassociation.org/.*

[15] J. Choi, T.D. Mount, and R.J. Thomas. "Transmission Expansion Planning Using Contingency Criteria". In: *IEEE Transactions on Power Systems* 22 (2007), pp. 2249 –2261.

[16] L. Ciampolini, X. Jonsson, J. Nguyen, J-C. Lafont, F.T. Drissi, J-P. Morin, D. Turgis, and C. Desclèves. "Efficient Yield Estimation Through Generalized Importance Sampling with Application to NBL-Assisted SRAM Bitcells". In: *2016 IEEE/ACM International Conference on Computer-Aided Design (ICCAD)*. 2016.

[17] S. Conti, J.P. Gosling, J.E. Oakley, and A. O'Hagan. "Gaussian Process Emulation of Dynamic Computer Codes". In: *Biometrika* 96 (3 2009), pp. 663 – 676.

[18] S. Conti and A. O'Hagan. "Bayesian Emulation of Complex Multi-Output and Dynamic Computer Models". In: *Journal of Statistical Planning and Inference* 140 (3 2010), pp. 640 –651.

[19] J. Contreras and F.F. Wu. "A kernel-oriented algorithm for transmission expansion planning". In: *IEEE Transactions on Power Systems* 15 (2000), pp. 1434 –1440.

[20] P.S. Craig, M. Goldstein, J.C. Rougier, and A.H. Seheult. "Bayesian Forecasting for Complex Systems Using Computer Simulators". In: *Journal of the American Statistical Association* 96 (2001), pp. 717 –729.

[21] P.S. Craig, M. Goldstein A.H. Seheult, and J.A Smith. "Pressure Matching for Hydrocarbon Reservoirs: A Case Study in the Use of Bayes Linear Strategies for Large Computer Experiments". In: *Case Studies in Bayesian Statistics*. Ed. by C. Gatsonis, J.S. Hodges, R.E. Kass, R. McCulloch, P. Rossi, and N.D. Singpurwalla. Vol. 121. Springer, New York, NY, 1997, pp. 37 –93.

[22] J.A. Cumming and M. Goldstein. "Bayes Linear Uncertainty Analysis for Oil Reservoirs Based on Multiscale Computer Experiments". In: *The Oxford handbook of Applied Bayesian Analysis* (2010), pp. 241 –270.

[23] J.A. Cumming and M. Goldstein. "Small Sample Bayesian Designs for Complex High-Dimensional Models Based on Information Gained Using Fast Approximations". In: *Technometrics* 51 (4 2009), pp. 377 –388.

[24] J.A. Cumming and D.A. Wooff. "Dimension Reduction via Principal Variables". In: *Computational Statistics & Data Analysis* 52 (2007), pp. 550 –565.

[25] M.H. DeGroot. *Optimal Statistical Decisions*. McGraw-Hill, 1970.

[26] S. Dehghan, A. Kazemi, and N.Neyestani. "Multistage transmission expansion planning alleviating the level of transmission congestion". In: *IEEE Trondheim PowerTech*. 2011.

[27] N. Durrande, D. Ginsbourger, and O. Roustant. "Additive Covariance Kernels for High-Dimensional Gaussian Process Modeling". In: *Annales de la Faculté de Sciences de Toulouse* 21 (3 2012), pp. 481 –499.

[28] V. Elvira, L. Martino, D. Luengo, and M.F. Bugallo. "Heretical Multiple Importance Sampling". In: *IEEE Signal Processing Letter* 23 (10 2016), pp. 1474 –1478.

[29] S. Eriksson-Bique, M. Solbrig, M. Stefanelli, S. Warkentin, R. Abbey, and I. C. F. Ipsen. "Importance Sampling For a Monte Carlo Matrix Multiplication Algorithm, With Application To Information Retrieval". In: *SIAM Journal on Scientific Computing* 33 (2011), pp. 1689 –1706.

[30] A.H. Escobar, R. A. Gallego, and R. Romero. "Multistage and Coordinated Planning of the Expansion of Transmission Systems". In: *IEEE Transactions on Power Systems* 19 (2004), pp. 735 –744.

[31] S.L. Fogal, G. Biondini, and W.L. Kath. "Multiple Importance Sampling for First- and Second-Order Polarization-Mode Dispersion". In: *IEEE Photonics Technology Letters* 14 (2002), pp. 1273 –1275.

[32] T.E. Fricker, J.E. Oakley, and N.M. Urban. "Multivariate Gaussian Process Emulators With Nonseparable Covariance Structures". In: *Technometrics* 55 (2013), pp. 47 –56.

[33] D. Fudenberg and J. Tirole. *Game Theory*. MIT Press, 1991.

[34] J.K. Ghosh, M. Delampady, and T. Samanta. *An Introduction to Bayesian Analysis: Theory and Methods*. Springer, 2006.

[35] J. Gibbins and H. Chalmers. "Carbon capture and storage". In: *Energy Policy* 36 (2008), pp. 4317 –4322.

[36] P. Glasserman and J. Li. "Importance Sampling for Portfolio Credit Risk". In: *Management Science* 51 (11 2005), pp. 1643 –1656.

[37] M. Goldstein and N. Huntley. "Bayes Linear Emulation, History Matching, and Forecasting for Complex Computer Simulators". In: *Handbook of Uncertainty Quantification*. Ed. by R. Ghanem, D. Higdon, and H. Owhadi. Springer, Cham, 2015, pp. 1 –24.

[38] B.G. Gorenstin, N.M. Campodonico, J.P. Costa, and M.V.F. Pereira. "Power System Expansion Planning Under Uncertainty". In: *IEEE Transactions on Power Systems* 8 (1993), pp. 129 –136.

[39] M. R. Hesamzadeh, N. Hosseinzadeh, and P. J. Wolfs. "Economic Assessment of Transmission Expansion Projects in Competitive Electricity Markets - An Analytical Review". In: *43rd International Universities Power Engineering Conference*. 2008.

[40] M.R. Hesamzadeh, N. Hosseinzadeh, and P.J. Wolfs. "Security Constrained Augmentation for Transmission System Considering Preferences of Market Players on Expansion Options". In: *Australian Universities Power Engineering Conference*. 2007.

[41] J. Keirstead. *Gaussian process regression with R*. URL: `http://www.jameskeirstead.ca/`.

[42] S. Jaehnert, O. Wolfgang, H. Farahmand, S. Völler, and D. Huertas-Hernando. "Transmission Expansion Planning in Northern Europe in 2030 - Methodology and Analyses". In: *Energy Policy* 61 (2013), pp. 125 –139.

[43] H.W. Jensen. "Importance Driven Path Tracing Using the Photon Map". In: *Rendering Techniques*. 1995, pp. 326 –335.

[44] A.K. Kazerooni and J. Mutale. "Transmission Network Planning Under Security and Environmental Constraints". In: *IEEE Transactions on Power Systems* 25 (2 2010), pp. 1169 –1178.

[45] M.C. Kennedy and A. O'Hagan. "Bayesian Calibration of Computer Models". In: *Journal of the Royal Statistical Society: Series B (Statistical Methodology)* 63 (2001), pp. 425 –464.

[46] T. Kennedy. *Monte Carlo Methods - a Special Topics Course*. The University of Arizona. 2016. URL: `http://math.arizona.edu/~tgk/mc/book.pdf`.

[47] P.G. Kinas. "Bayesian Fishery Stock Assessment and Decision Making Using Adaptive Importance Sampling". In: *Canadian Journal of Fisheries and Aquatic Sciences* 53 (1996), pp. 414 –423.

[48] I. Konstantelos and G. Strbac. "Valuation of Flexible Transmission Investment Options Under Uncertainty". In: *IEEE Transactions on Power Systems* 30 (2015), pp. 1047 –1055.

[49] P.R.S. Kuruganty and D.A. Woodford. "A reliability cost-benefit analysis for HVDC transmission expansion planning". In: *IEEE Transactions on Power Delivery* 3 (1988), pp. 1241 –1248.

[50] A. L'Abbate, G. Migliavacca, G. Fulli, C. Vergine, and A. Sallati. "The European Research Project REALISEGRID: Transmission Planning Issues and Methodological Approach Towards the Optimal Development of the Pan-European System". In: *Power and Energy Society General Meeting*. 2012.

[51] *Large Combustion Plant Directive*. URL: `https://en.wikipedia.org/wiki/Large_Combustion_Plant_Directive`.

[52] A. Lawson, M. Goldstein, and C. Dent. "Bayesian Framework for Power Network Planning Under Uncertainty". In: *Sustainable Energy Grids and Networks* 7 (2016), pp. 47 –57.

[53] P. Lee. *Bayesian Statistics: an Introduction*. Arnold, 1997.

[54] A.M. Leite da Silva, L.S. Rezende, L.M. Honório, and L.A.F. Manso. "Performance Comparison of Metaheuristics to Solve the Multi-Stage Transmission Expansion Problem". In: *IET Generation, Transmission and Distribution* 5 (2011), pp. 360 –367.

[55] A.M. Leite da Silva, L.S. Rezende, L.A.F. Manso, and L.C. de Resende. "Reliability Worth Applied to Transmission Expansion Planning Based on Ant Colony System". In: *Electrical Power and Energy Systems* 32 (2010), pp. 1077 –1084.

[56] W. Li. *Probabilistic Transmission System Planning*. Wiley-Blackwell, 2011.

[57] W. Li. *Risk Assessment of Power Systems - Models, Methods, and Applications*. IEEE Press-Wiley, 2005.

[58] W. Li and P. Choudhury. "Probabilistic Transmission Planning". In: *IEEE Power and Energy Magazine* 5 (2007), pp. 46 –53.

[59] F. Liu and M. West. "A Dynamic Modelling Strategy for Bayesian Computer Model Emulation". In: *Bayesian Analysis* 4 (2009), pp. 393 –412.

[60] X. Liu and S. Guillas. "Dimension Reduction for Gaussian Process Emulation: An Application to the Influence of Bathymetry on Tsunami Heights". In: *SIAM/ASA Journal on Uncertainty Quantification* 5 (2017), pp. 787 –812.

[61] S. Lumbreras, A.Ramos, and S.Cerisola. "A Progressive Contingency Incorporation Approach for Stochastic Optimization Problems". In: *IEEE Transactions on Power Systems* 28 (2013), pp. 1452 –1460.

[62] P. Maghouli, S.H. Hosseini, M.O. Buygi, and M. Shahidehpour. "A Scenario-Based Multi-Objective Model for Multi-Stage Transmission Expansion Planning". In: *IEEE Transactions on Power Systems* 26 (2011), pp. 470 –478.

[63] D.M. Maniyar, D. Cornford, and A. Boukouvalas. *Dimensionality Reduction in the Emulator Setting*. Aston University. 2007. URL: `http://www.mucm.ac.uk/Pages/Downloads/Technical%20Reports/07-11.pdf`.

[64] E.A. Martínez Ceseña, T. Capuder, and P. Mancarella. "Flexible Distributed Multienergy Generation System Expansion Planning Under Uncertainty". In: *IEEE Transactions on Smart Grid* 7 (2016), pp. 348 –357.

[65] A. Mills, A. Phadke, and R. Wiser. "Exploration of Resource and Transmission Expansion Decisions in the Western Renewable Energy Zone Initiative". In: *Energy Policy* 39 (2011), pp. 1732 –1745.

[66] F.D. Munoz, B.F. Hobbs, J.L. Ho, and S. Kasina. "An Engineering-Economic Approach to Transmission Planning Under Market and Regulatroy Uncertainties: WECC Case Study". In: *IEEE Transactions on Power Systems* 29 (2014), pp. 307 –317.

[67] F.D. Munoz, E.E. Sauma, and B.F. Hobbs. "Approximations in Power Transmission Planning: Implications for the Cost and Performance of Renewable Portfolio Standards". In: *Journal of Regulatory Economics* 43 (3 2013), pp. 305 –338.

[68] D.Q. Naiman and C.E. Priebe. "Computing Scan Statistic p Values Using Importance Sampling, With Applications to Genetics and Medical Image Analysis". In: *Journal of Computational and Graphical Statistics* 10 (2 2001), pp. 296 –328.

[69] National Grid. *Electricity Scenarios Illustrator (ELSI)*. URL: `http://www.talkingnetworkstx.com`.

[70] National Grid. *GB Security and Quality of Supply Standard Review for Onshore Intermittent Generation. http : //www2.nationalgrid.com/uk/Industry-information/Electricitycodes/*. 2008.

[71] National Grid. *National Grid historical demand data.* URL: `http://www2.nationalgrid.com/UK/Industry-information/Electricity-transmission-operational-data/Data-Explorer/`.

[72] J.E. Oakley and A. O'Hagan. "Probabilistic Sensitivity Analysis of Complex Models: a Bayesian Approach". In: *The Journal of the Royal Statistical Society, Series B* 66 (3 2004), pp. 751 –769.

[73] Ofgem. *RIIO-T1: Initial Proposals for National Grid Electricity Transmission and National Grid Gas. https : //www.ofgem.gov.uk/ofgempublications/*. 2012.

[74] A. O'Hagan. "Bayesian Analysis of Computer Code Outputs: A Tutorial". In: *Reliability Engineering and System Safety* 91 (2006), pp. 1290 –1300.

[75] G.C. Oliveira, S. Binato, and M.V.F. Pereira. "Value-Based Transmission Expansion Planning of Hydrothermal Systems Under Uncertainty". In: *IEEE Transactions on Power Systems* 22 (2007), pp. 1429 –1435.

[76] A. Olsson, G. Sandberg, and O. Dahlblom. "On Latin Hypercube Sampling for structural Reliability Analysis". In: *Structural Safety* 25 (2003), pp. 47 –68.

[77] Art B. Owen. *Monte Carlo theory, methods and examples.* 2013.

[78] Paul Plumptre. *Correspondence with Paul Plumptre, formerly of National Grid.* Correspondence with Paul Plumptre, formerly of National Grid.

[79] J. Qiu, Z. Y. Dong, J. H. Zhao, Y. Xu, Y. Zheng, C. Li, and K. P. Wong. "Multi-Stage Flexible Expansion Co-Planning Under Uncertainties in a Combined Electricity and Gas Market". In: *IEEE Transactions on Power Systems* 30 (2015), pp. 2119 –2129.

[80] T. Qiu, B. Xu, Y. Wang, Y. Dvorkin, and D.S. Kirschen. "Stochastic Multi-Stage Co-Planning of Transmission Expansion and Energy Storage". In: *IEEE Transactions on Power Systems* 32 (2017), pp. 643 –651.

[81] M. Rahmani, G. Vinasco, M.J. Rider, R. Romero, and P.M. Pardalos. "Multistage Transmission Expansion Planning Considering Fixed Series Compensation Allocation". In: *IEEE Transactions on Power Systems* 28 (2013), pp. 3795 –3805.

[82] A. Rai, R.C. Valenzuela, B. Tuffin, G. Rubino, and P. Dersin. "Approximate Zero-Variance Importance Sampling for Static Network Reliability Estimation with Node Failures and Application to Rail Systems". In: *2016 Winter Simulation Conference (WSC)*. 2016, pp. 3201 –3212.

[83] P. Ranjan, R. Haynes, and R. Karsten. "A Computationally Stable Approach to Gaussian Process Interpolation of Deterministic Computer Simulation Data". In: *Technometrics* 53 (4 2011), pp. 366 –378.

[84] C.E. Rasmussen and C.K.I. Williams. *Gaussian Processes for Machine Learning*. MIT Press, 2006.

[85] L.S. Rezende, A.M. Leite da Silva, and L.M. Honório. "Artificial Immune Systems and Differential Evolution Based Approaches Applied to Multi-Stage Transmission Expansion Planning". In: *15th Internation Conference on Intelligent System Applications to Power Systems*. 2009.

[86] J-F. Richard and W. Zhang. "Efficient High-Dimensional Importance Sampling". In: *Journal of Econometrics* 141 (2007), pp. 1385 –1411.

[87] J.H. Roh, M. Shahidehpour, and L. Wu. "Market-Based Generation and Transmission Planning With Uncertainties". In: *IEEE Transactions on Power Systems* 24 (2009), pp. 1587 –1598.

[88] G. Romp. *Game Theory: Introduction and Applications*. Oxford University Press, 1997.

[89] J.C. Rougier. "Efficient Emulators for Multivariate Deterministic Functions". In: *Journal of Computational and Graphical Statistics* 17 (2008), pp. 827 –843.

[90] *Running hours during winter 2013/14 for plants opted-out of the Large Combustion Plant Directive (LCPD). https : //www.gov.uk*. 2014.

[91] P. Sánchez-Martín, A. Ramos, and J.F. Alonso. "Probabilistic Midterm Transmission Planning in a Liberalized Market". In: *IEEE Transactions on Power Systems* 20 (2005), pp. 2135 –2142.

[92] T.J. Santner, B.J. Williams, and W.I Notz. *The Design and Anaysis of Computer Experiments*. Springer, 2003.

[93] J.Q. Shi and Y. Cheng. *Gaussian Process Function Data Analysis R Package 'GPFDA'. https : //www.staff.ncl.ac.uk/j.q.shi/ps/gpfda.pdf*. 2014.

[94] S.N. Siddiqi and M.L. Baughman. "Value-based transmission planning and the effects of network models". In: *IEEE Transactions on Power Systems* 10 (1995), pp. 1835 –1842.

[95] G. Strbac, M. Aunedi, D. Pudjianto, P. Djapic, S. Gammons, and R. Druce. *Understanding the Balancing Challenge*. Imperial College London and NERA. 2012. URL: `http://www.nera.com/content/dam/nera/publications/archive2/PUB_DECC_0812.pdf`.

[96] E. Tómasson and L. Söder. "Improved Importance Sampling for Reliability Evaluation of Composite Power Systems". In: *IEEE Transactions on Power Systems* 32 (3 2017), pp. 2426 –2434.

[97] A.H. van der Weijde and B.F. Hobbs. "The Economics of Planning Electricity Transmission to Accommodate Renewables: Using Two-Stage Optimisation to Evaluate Flexibility and the Cost of Disregarding Uncertainty". In: *Energy Economics* 34 (6 2012), pp. 2089 –2101.

[98] I. Vernon, M. Goldstein, and R.G. Bower. "Galaxy Formation: a Bayesian Uncertainty Analysis". In: *Bayesian Analysis* 5 (2010), pp. 619 –670.

[99] Wikipedia. *http : //en.wikipedia.org/wiki/Latin_hypercube*.

[100] D. Williamson and M. Goldstein. "Bayesian Policy Support for Adaptive Strategies Using Computer Models for Complex Physical Systems". In: *Journal of the Operational Research Society* 63 (2012), pp. 1021 –1033.

[101] H. Yu, C.Y. Chung, K.P. Wong, and H.W. Lee. "Probabilistic Load Flow Evaluation With Hybrid Latin Hypercube Sampling and Cholesky Decomposition". In: *IEEE Transactions on Power Systems* 24 (2009), pp. 661 –667.

[102] S. Zachary. *Mathematical Methods to Support the Integration of Renewables into the Electricity Network*. Report for Scottish Funding Council as part of the SPIRIT scheme. 2013.

[103] A. Zaytsev. "Variable Fidelity Regression Using Low Fidelity Function Blackbox and Sparsification". In: *The 5TH Symposium on Conformal and Probabilistic Prediction with Applications (COPA 2016)*. 2016, pp. 147 –164.

[104] D. Zhao, H. Lam, H. Peng, S. Bao, D.J. LeBlanc, K. Nobukawa, and C.S. Pan. "Accelerated Evaluation of Automated Vehicles Safety in Lane-Change Scenarios Based on Importance Sampling Techniques". In: *IEEE Transactions on Intelligent Transportation Systems* 18 (3 2017), pp. 595 –607.

[105] J.H. Zhao, Z.Y. Dong, P. Lindsay, and K.P. Wong. "Flexible Transmission Expansion Planning With Uncertainties in an Electricty Market". In: *IEEE Transactions on Power Systems* 24 (2009), pp. 479 –488.

[106] Q. Zhao, G. Liu, and G. Gu. "Variance Reduction Techniques of Importance Sampling Monte Carlo Methods for Pricing Options". In: *Journal of Mathematical Finance* 3 (2013), pp. 431 –436.

Appendix A

Chapter 4 Additional Details

A.1 Variance Estimates

Section 4.2.2 gave details of how a selection of weights, $\boldsymbol{\omega}$, can be used to acquire an evaluation of annual constraint costs via Equation 4.2.5. It was then shown how this evaluation has the same mean as the full simulator, whilst evaluating fewer snapshots. However, it is important to also consider how the variance of the estimate of mean constraint costs is affected by the choice of weights, $\boldsymbol{\omega}$, in order to identify the most efficient importance sampling method.

If y is used to represent a single evaluation of constraint costs using the full simulator (i.e. evaluating each snapshot in each evaluation) and $y_{\boldsymbol{\omega}}$ is a single evaluation of constraint costs using importance sampling, the variance of the evaluations can be calculated naively as

$$\text{var}(y) = \text{var}\left(\sum_{\tau=1}^{17520} f_{c,\tau}(\tau)\right) = \sum_{\tau=1}^{17520} \text{var}(f_{c,\tau}(\tau)) \tag{A.1.1}$$

and

$$\text{var}(y_{\boldsymbol{\omega}}) = \text{var}\left(\sum_{\tau=1}^{17520} \frac{f_{c,\tau}(\tau)}{\omega_\tau} X(\tau)\right) = \sum_{\tau=1}^{17520} \frac{\text{var}(f_{c,\tau}(\tau)X(\tau))}{\omega_\tau^2} \tag{A.1.2}$$

when assuming the independence of snapshots (which is reasonable for the simulator defined in Chapter 3 which ignores correlation between snapshots and simulates snapshots independently). Using the result that if x_1 and x_2 are two independent random variables then $\text{var}(x_1x_2) = \text{var}(x_1)\text{var}(x_2) + \text{var}(x_1)(E(x_2))^2 + \text{var}(x_2)(E(x_1))^2$,

Equation A.1.2 can be expanded to

$$\begin{aligned}
&\sum_{\tau=1}^{17520} \frac{\text{var}(f_{c,\tau}(\tau)X(\tau))}{\omega_\tau^2} \\
&= \sum_{\tau=1}^{17520} \left(\frac{\text{var}(f_{c,\tau}(\tau))\text{var}(X(\tau))}{\omega_\tau^2} + \frac{\text{var}(f_{c,\tau}(\tau))(E(X(\tau)))^2}{\omega_\tau^2} + \frac{(E(f_{c,\tau}(\tau)))^2\text{var}(X(\tau))}{\omega_\tau^2} \right) \\
&= \sum_{\tau=1}^{17520} \left(\frac{\text{var}(f_{c,\tau}(\tau))\text{var}(X(\tau))}{\omega_\tau^2} + \text{var}(f_{c,\tau}(\tau)) + \frac{(E(f_{c,\tau}(\tau)))^2\text{var}(X(\tau))}{\omega_\tau^2} \right) \\
&\geq \sum_{\tau=1}^{17520} \text{var}(f_{c,\tau}(\tau))
\end{aligned} \tag{A.1.3}$$

with equality if and only if $\omega_\tau = 1$ for all τ (or more precisely, as noted in Section 4.2.2, with equality if and only if $\omega_\tau = 1$ for all τ except for snapshots where $E(f_{c,\tau}(\tau)) = 0$ with zero variance). This would seemingly indicate that any choice of weights other than $\omega_\tau = 1$ for all τ increases the variance of the estimate. This is because these equations simply calculate the variance in each simulation of constraint costs, without considering the amount of work that was required to evaluate the simulation.

The benefit from importance sampling comes from the fact that snapshots with more relevant information to the estimate of mean constraint costs are actually evaluated more frequently than snapshots with less relevance to the estimate of mean constraint costs. For example, it could be that a particular set of weights, $\boldsymbol{\omega}$, give a variance estimate such that $\text{var}(y_{\boldsymbol{\omega}})$ is twice as large as $\text{var}(y)$, but importance sampling using weights $\boldsymbol{\omega}$ expects to evaluate only 1 in 100 snapshots. This would mean that the resulting standard error of the estimate of mean constraint costs using importance sampling would be $\frac{\sqrt{2}}{10}$ of the standard error when evaluating each snapshot (not using importance sampling) when evaluating an equal number of snapshots. This makes the comparison of variance estimates from Equations A.1.1 and A.1.2 misleading when assessing the benefits of importance sampling, and instead an estimate which accounts for the work done (number of snapshots evaluated) of each evaluation should be considered when identifying a criterion on which to base the importance sampling weights, $\boldsymbol{\omega}$.

This can be achieved by considering an equivalent alternative to the methodology of Section 4.2.2 which treats the snapshot to be simulated as a random variable, as

opposed to treating whether or not the snapshot is simulated as a random variable. As was noted in Section 4.2.2, this would model τ as a discrete random variable which takes a value of the integers between 1 and 17520, with τ equally likely to take any value in this range (i.e. a discrete uniform distribution over the integers 1 to 17520), such that $p(\tau)$ describes the probability of τ taking a particular value as

$$p(\tau) = \begin{cases} \frac{1}{17520} & \text{for } \tau \text{ in 1,2,...,17520} \\ 0 & \text{Otherwise} \end{cases}$$

Under this model the simulator, $f_{c,\tau}(\tau)$, would simulate constraint costs for a single snapshot, τ, with the snapshot being modelled as a random variable with a distribution defined by $p(\tau)$. To estimate constraint costs for a year from this it would be necessary to multiply the output by 17520 (as there are 17520 half hour snapshots in a year), i.e. use the function

$$f_{c,\mathscr{T}}(\tau) = 17520 \times f_{c,\tau}(\tau) \tag{A.1.4}$$

If values of τ are sampled according to the distribution of $p(\tau)$, such that n values of τ are sampled and τ_i is the ith value of τ in the sample, an estimate of μ (the mean of the full simulator) can be acquired as

$$\hat{\mu}_p = \frac{1}{n} \sum_{i=1}^{n} f_{c,\mathscr{T}}(\tau_i) \tag{A.1.5}$$

It is trivial to show this has the same expectation as the simulator of Chapter 3, as the expectation of a function, f, of a discrete random variable, x, is

$$E_{p(x)}[f(x)] = \sum_{x} E(f(x = \mathbf{x}))p(x = \mathbf{x}) \tag{A.1.6}$$

where $p(x = \mathbf{x})$ is the the probability x takes the value $\mathbf{x}$. This means the expectation of $f_{c,\tau}(\tau)$ is the expectation of the constraint costs which occur in a single, random snapshot, which in turn means the expectation of $f_{c,\mathscr{T}}(\tau)$, is the expectation of constraint costs that occur in a single year, i.e. the mean annual constraint costs of the simulator, f_c, defined in Chapter 3.

Defining the simulator in this way means that the importance sampling methodology detailed in Section 4.2.1 can then be applied, where the density $p(\tau)$ is replaced by some alternative density $q(\tau)$. Importance sampling can then be applied by sampling

values of τ according to the distribution of $q(\tau)$ instead of $p(\tau)$. If values of τ are sampled according to the distribution of $q(\tau)$, such that n values of τ are sampled and τ_i is the ith value of τ in the sample, an estimate of μ (the mean of the full simulator) can be acquired as

$$\hat{\mu}_q = \frac{1}{n}\sum_{i=1}^{n}\frac{f_{c,\mathscr{T}}(\tau_i)p(\tau_i)}{q(\tau_i)} \tag{A.1.7}$$

Equation 4.2.4 of Section 4.2.1 shows how this gives the same expectation of the full simulator, μ.

As was noted in Section 4.2.2, if an appropriate distribution for weights, ω_τ, were calculated to apply importance sampling using Equation 4.2.5, these weights can then be used to calculate an equivalent $q(\tau)$ for use in Equation A.1.7 as

$$q(\tau) = \frac{\omega_\tau}{\sum_\tau \omega_\tau} \tag{A.1.8}$$

Alternatively, as was also noted in Section 4.2.2, if an appropriate specification of $q(\tau)$ for use in Equation A.1.7 was calculated, an equivalent set of weights, ω_τ, to apply importance sampling using Equation 4.2.5 could be calculated as

$$\omega_\tau = \frac{q(\tau)}{q^*} \tag{A.1.9}$$

where q^* is the maximum value of $q(\tau)$ across all snapshots.

[77, 46, 106] state that an optimal choice of $q(\tau)$ to minimise the variance of $\hat{\mu}_q$ from Equation A.1.7 is to select $q(\tau)$ in proportion to $f_{c,\mathscr{T}}(\tau)p(\tau)$, and this result will be verified in the remainder of this section. The variance from an importance sampling method using $q(\tau)$ as the alternative weights can then be calculated as

$$\begin{aligned}
\sigma^2_{q(\tau)} &= E_{q(\tau)}\left[\left(\frac{f_{c,\mathscr{T}}(\tau)p(\tau)}{q(\tau)} - \mu\right)^2\right] \\
&= \sum_\tau q(\tau)\left(\frac{f_{c,\mathscr{T}}(\tau)p(\tau)}{q(\tau)} - \mu\right)^2 \\
&= \sum_\tau q(\tau)\left(\frac{f_{c,\mathscr{T}}(\tau)^2p(\tau)^2}{q(\tau)^2} - 2\mu\frac{f_{c,\mathscr{T}}(\tau)p(\tau)}{q(\tau)} + \mu^2\right) \\
&= \sum_\tau \left(q(\tau)\frac{f_{c,\mathscr{T}}(\tau)^2p(\tau)^2}{q(\tau)^2} - 2q(\tau)\mu\frac{f_{c,\mathscr{T}}(\tau)p(\tau)}{q(\tau)} + q(\tau)\mu^2\right) \\
&= \sum_\tau \left(\frac{f_{c,\mathscr{T}}(\tau)^2p(\tau)^2}{q(\tau)} - 2\mu f_{c,\mathscr{T}}(\tau)p(\tau) + q(\tau)\mu^2\right)
\end{aligned} \tag{A.1.10}$$

The optimal choice of the values of $q(\tau)$ are the values of $q(\tau)$ which minimise the expected variance of the estimate of mean constraint costs, i.e. minimise $\sigma^2_{q(\tau)}$. This can be calculated by selecting the values $q(\tau)$ such that the derivative of $\sigma^2_{q(\tau)}$ with respect to $q(\tau)$ is zero, i.e. such that

$$\begin{aligned}\frac{\mathrm{d}\sigma^2_{q(\tau)}}{\mathrm{d}q(\tau)} &= \frac{\mathrm{d}\sum_\tau \left(\frac{f_{c,\mathscr{T}}(\tau)^2 p(\tau)^2}{q(\tau)} - 2\mu f_{c,\mathscr{T}}(\tau)p(\tau) + q(\tau)\mu^2\right)}{\mathrm{d}q(\tau)} \\ &= \sum_\tau \left(\mu^2 - \frac{f_{c,\mathscr{T}}(\tau)^2 p(\tau)^2}{q(\tau)^2}\right)\end{aligned} \tag{A.1.11}$$

is zero, i.e.

$$\sum_\tau \left(\mu^2 - \frac{f_{c,\mathscr{T}}(\tau)^2 p(\tau)^2}{q(\tau)^2}\right) = 0 \tag{A.1.12}$$

which implies the alternative density which minimises the variance of $\hat{\mu}_q$ is

$$q(\tau) = \frac{f_{c,\mathscr{T}}(\tau)p(\tau)}{\mu} \tag{A.1.13}$$

As μ is an unknown constant (it is what we are estimating) and $p(\tau)$ is constant for our example (recall, $p(\tau) = \frac{1}{17520}$ for all snapshots), this implies that the optimal values for $q(\tau)$ (and in turn for the weights ω_τ, which can be calculated via Equation A.1.9 for given values of $q(\tau)$) to minimise the variance of the estimate of mean constraint costs is to select the weight of each snapshot proportional to the mean constraint costs of that snapshot, i.e.

$$\omega_\tau \propto E(f_{c,\tau}(\tau)) \tag{A.1.14}$$

A.2 Accuracy of Estimates of Mean Constraint Costs from Importance Sampling

A.2.1 Accuracy of Estimates of Mean Constraint Costs from Importance Sampling

Section 4.2.2 gave details on how importance sampling can be used as a method for estimating mean annual constraint costs of a simulator by sampling certain snapshots

more frequently than others, with Section 4.3 going on to consider different selections of weights, $\boldsymbol{\omega}$, which could be used for importance sampling to acquire an estimate of mean constraint costs for a given power system background. Sections 4.3.3 and 4.3.4 considered estimating mean annual constraint costs such that the standard error of the estimate was less than 1% of the mean of the estimate, whereas Section 4.3.5 considered estimating mean constraint costs such that the error in the estimate was less than £100,000.

Whilst Equation 4.2.6 of Section 4.2.2 verifies that all estimates of mean annual constraint costs from importance sampling have the same mean as the full simulator, it was also noted that the simulator itself is random, so each estimate of mean annual constraint costs will differ slightly in comparison to the "true" mean of the simulator.

Section 4.3.6 gave an initial consideration to the accuracy of estimates of mean annual constraint costs for a year 6 power system background when importance sampling weights were based on the mean constraint costs for each snapshot. This section will give further consideration to the accuracy of the estimates of mean annual constraint costs for both a year 1 and year 6 power system background for all choices of importance sampling weights considered in Sections 4.3 and 4.4. However, the results of this section do not present anything greatly different to what was already shown in Section 4.3.6, other than for a year 1 power system background there is less improvement when estimating with a standard error of £100,000 in comparison to a standard error less than 1% of the mean of the estimate, due to the 1% of the mean of year 1 constraint costs being £126,000, which is close to £100,000.

A.2.2 Accuracy of Estimates With a Standard Error Less Than 1% of the Mean of Estimated Constraint Costs

Section 4.3.3 considered how much work, λ, was required to estimate mean annual constraint costs for a given power system background such that the standard error of the estimate is less than 1% of the mean of the estimate for a variety of methods of importance sampling. As the amount of work required to acquire an estimate is also random variable, this process was repeated 200 times to get an estimate of the

expected work required, giving 200 different estimates of mean annual constraint costs. This section gives consideration to how these estimates differ from $\hat{\mu}_1$ and $\hat{\mu}_6$, the highly accurate estimates of mean annual constraint costs calculated for a year 1 and year 6 power system background respectively from Section 4.3.6.

Year 1 Power System Background

Figure A.1 displays graphs to show how the 200 estimates of mean annual constraint costs vary for a year 1 power system background. These are the costs estimated in Section 4.3.3, where it was required that the standard error of the estimate was less than 1% of the mean of the estimate, and that a minimum of 175200 snapshots (the equivalent of 10 full simulator evaluations) had been evaluated. The estimates of mean annual constraint costs displayed in Figure A.1 based the weights used for importance sampling, $\boldsymbol{\omega}$, on the mean constraint costs of each snapshot.

Figure A.1 (a) shows a scatter plot for the final estimate of mean annual constraint costs for each of the 200 repetitions, with a horizontal line also shown to represent the $\hat{\mu}_1$, the very accurate estimate of mean annual constraint costs from the simulator estimated as the average of 100,000 full simulations in Section 4.3.6. As was the case for the year 6 power system background in Section 4.3.6, it appears that estimates of mean annual constraint costs are fairly evenly scattered around $\hat{\mu}_1$, with costs being over-estimated as often as they are under-estimated.

Figure A.1 (b) shows the difference between the estimates from each of the 200 repetitions and $\hat{\mu}_1$ ($\hat{\mu}_1$ minus the estimate of mean annual constraint costs acquired from importance sampling), with Figure A.1 (c) showing this difference as a percentage of $\hat{\mu}_1$. As can be seen, the vast majority of estimates are less than 2% away from $\hat{\mu}_1$, which is what would be expected for costs which are estimated such that the standard error of the estimate is less than 1% of the mean of the estimate. As mentioned, by the central limit theorem it is expected that cost estimates will be roughly normally distributed around the mean of the simulator with standard deviation of 1% of the mean of the simulator (meaning around 95% of estimates will fall within 2% of $\hat{\mu}_1$).

In comparison to the equivalent plots for a year 6 power system background, considered in Figure 4.8 (b) and (c) of Section 4.3.6, it is seen that the percentage difference

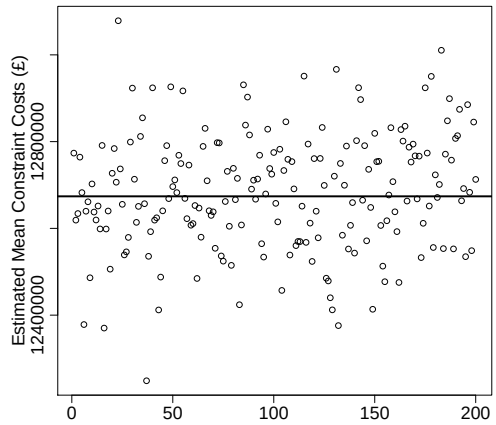

(a) Scatter plot of cost estimates.

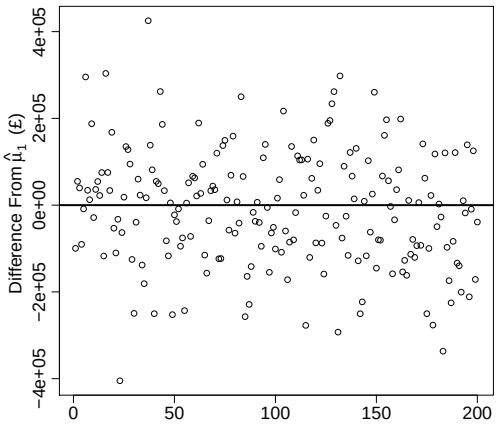

(b) Scatter plot of differences from $\hat{\mu}_1$.

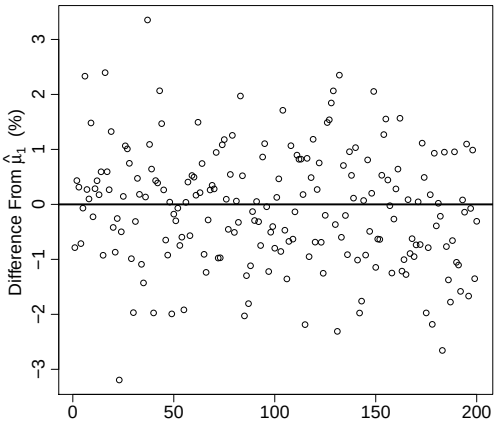

(c) Scatter plot of relative differences from $\hat{\mu}_1$.

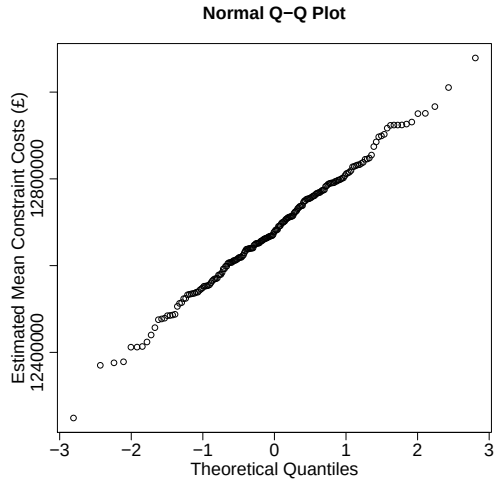

(d) Normal QQ plot.

Figure A.1: Plots to compare estimates of mean annual constraint costs from importance sampling to $\hat{\mu}_1$ for a year 1 power system background, when it is required that the standard error of the estimate is less than 1% of the mean of the estimate.

between the cost estimates and $\hat{\mu}_1$ or $\hat{\mu}_6$ is generally smaller for a year 6 power system background in comparison to a year 1 power system background. This is explained by the fact that these estimates require the standard error of the estimate to be less than 1% of the mean of the estimate, whilst also evaluating the equivalent of at least 10 full simulator evaluations. For a year 1 power system, it was shown in Section 4.3.3 that typically a much greater amount than 10 equivalent full simulator evaluations are required in order to acquire an estimate with a standard error of 1%, whereas for a year 6 power system background typically fewer than 10 equivalent full simulator evaluations are required for such an estimate. This means that requiring at least the equivalent of 10 full simulator evaluations for a year 6 power system background results in additional information being acquired after an error of 1% is reached, which reduces the error in the estimate even further.

As was the case for a year 6 power system background, the normal quantile plot of Figure A.1 (d) shows that the estimates approximately follow a normal distribution, which again is what should be expected by the central limit theorem.

Figure A.2 displays results for all four importance sampling methods considered in Section 4.3.3. As can be seen, all importance sampling methods behave similarly, with results being evenly distributed around $\hat{\mu}_1$, with most estimates lying within 2% of $\hat{\mu}_1$.

Importance Sample Basis	Mean Difference	Mean Absolute Difference	Mean Percentage Difference	Mean Absolute Percentage difference
All Snapshots	£1,240	£105,000	0.00977 %	0.825%
Demand	£16,500	£109,000	0.130%	0.861%
Snapshot Mean	-£9,010	£108,000	-0.0718%	0.849%
Snapshot Standard Deviation	£6,050	£100,000	0.0477%	0.787%

Table A.1: Table comparing estimated mean annual constraint costs from importance sampling to $\hat{\mu}_1$ for a year 1 power system background, when it is required that the standard error of the estimate is less than 1% of the mean of the estimate.

Table A.1 compares the estimates of mean annual constraint costs from importance sampling to $\hat{\mu}_1$. As can be seen, taking the mean of the 200 estimates for any importance

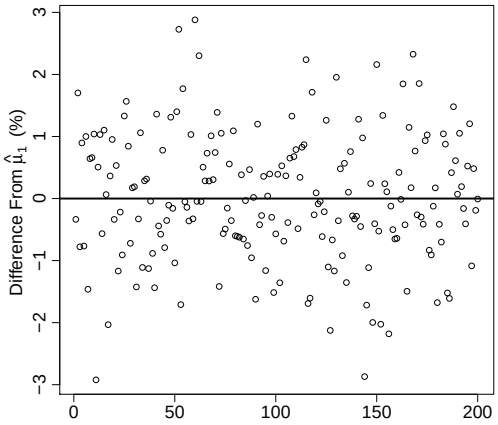

(a) Using all snapshots.

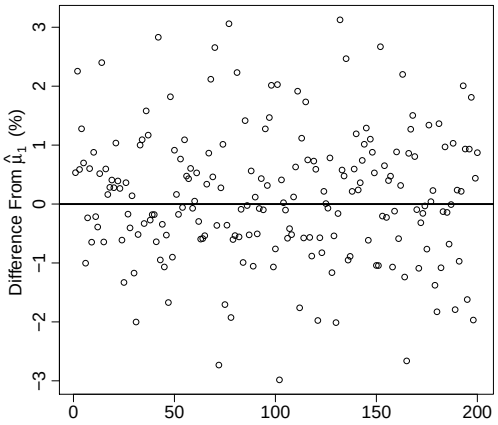

(b) Importance sampling based on snapshot demand.

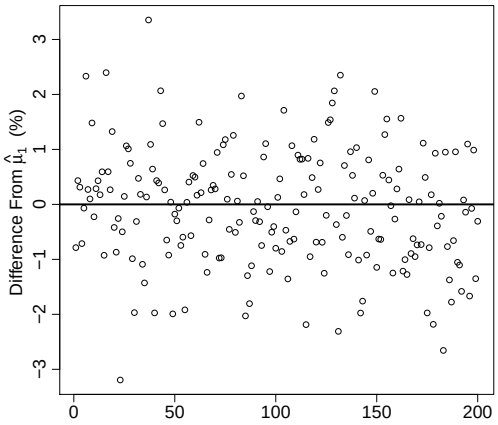

(c) Importance sampling based on snapshot mean.

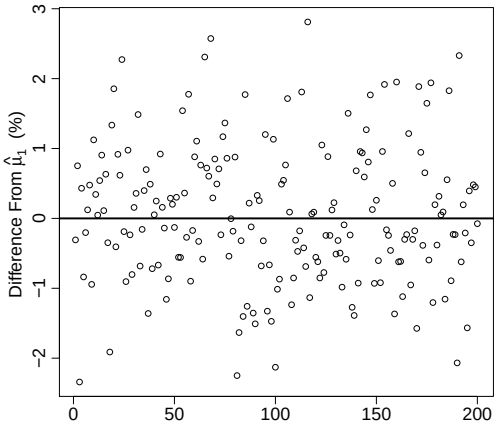

(d) Importance sampling based on snapshot standard deviation.

Figure A.2: Plots to compare estimates of mean annual constraint costs from importance sampling to $\hat{\mu}_1$ for a year 1 power system background, when it is required that the standard error of the estimate is less than 1% of the mean of the estimate.

sampling method gives a very small difference (0.13% or less for all conditions) in comparison to $\hat{\mu}_1$. As was the case for the year 6 power system background, this is to be expected, as estimates of constraint costs from importance sampling are unbiased (as shown in Equation 4.2.6) so the mean of all estimates is the same as the mean of the full simulator, which $\hat{\mu}_1$ is a very accurate estimate of.

Therefore, it is more useful to compare how the mean absolute difference compares to $\hat{\mu}_1$. This reveals how estimates typically vary from $\hat{\mu}_1$ by around £105,000 (between £100,000 to £109,000) for all choices of importance sampling weights (between 0.787% and 0.861% of $\hat{\mu}_1$). This is in line with what was noted earlier, where it is expected that cost estimates will be roughly normally distributed around $\hat{\mu}_1$ with a standard deviation of 1% of $\hat{\mu}_1$ (which would expect an absolute difference of 0.8% from $\hat{\mu}_1$).

Year 6 Power System Background

Results for a year 6 power system background were previously considered in Section 4.3.6, but only for when importance sampling weights were based on the mean constraint costs of each snapshot. Graphs to illustrate how estimates of mean constraint costs vary for all four importance sampling methods considered in Section 4.3.3 are displayed in Figure A.3. As can be seen, estimates from all importance sampling methods behave similarly, with estimates of mean annual constraint costs being fairly evenly distributed around $\hat{\mu}_6$, with almost all estimates lying within 2% of $\hat{\mu}_6$ and the majority lying within 1% of $\hat{\mu}_6$.

A.2.3 Accuracy of Estimates With a Standard Error of 1% of the Mean of the Estimate With No Minimum Work Level Required

Section 4.3.6 and Appendix A.2.2 consider how estimates of mean annual constraint costs vary when it is required that the standard error of the estimated costs is less than 1% of the mean of the estimate and a minimum of 175200 snapshots (the equivalent of 10 full simulator evaluations) have been evaluated. However, Section 4.3.3 initially considered estimating mean annual constraint costs without requiring a minimum of

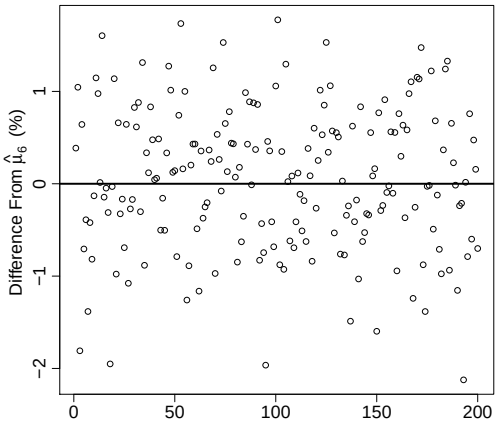

(a) Using all snapshots.

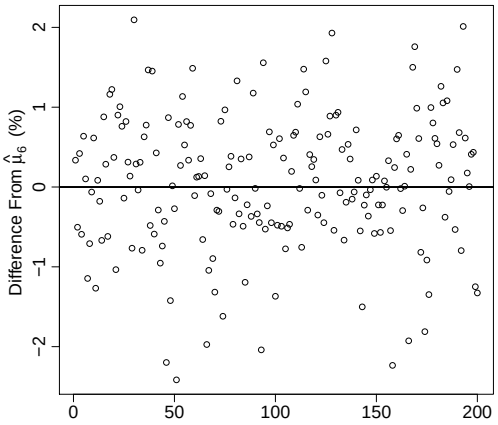

(b) Importance sampling based on snapshot demand.

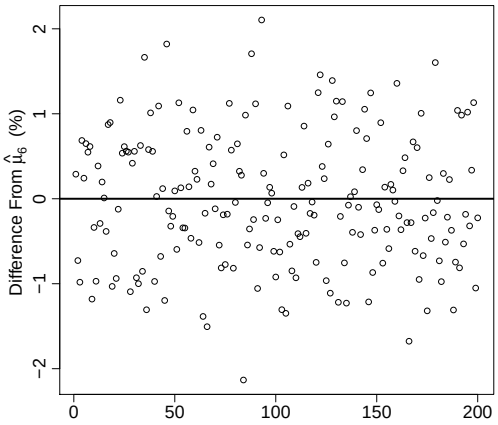

(c) Importance sampling based on snapshot mean.

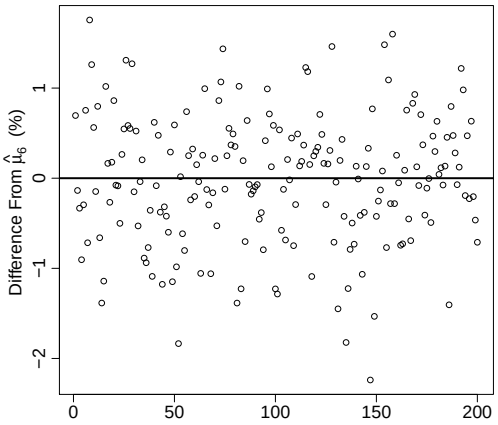

(d) Importance sampling based on snapshot standard deviation.

Figure A.3: Plots to compare estimates of mean annual constraint costs from importance sampling to $\hat{\mu}_6$ for a year 6 power system background, when it is required that the standard error of the estimate is less than 1% of the mean of the estimate.

175200 snapshots to be evaluated, which resulted in several estimates being acquired which evaluated very few snapshots. This section will consider how estimates of mean annual constraint costs compare to $\hat{\mu}_1$ and $\hat{\mu}_6$ (the accurate estimates of mean constraint costs of the simulator calculated in Section 4.3.6 using 100,000 full simulator evaluations) when no minimum work is required for the estimates.

Year 1 Power System Background

Figure A.4 displays graphs to consider the variation in the 200 estimates of mean annual constraint costs for a year 1 power system background. These are the costs estimated in Section 4.3.3, where it was required that the standard error of the estimate was less than 1% of the mean of the estimate, without any limitations on the minimum amount of snapshots that must be evaluated to achieve this. The estimates of mean annual constraint costs displayed in Figure A.4 based the weights used for importance sampling, $\boldsymbol{\omega}$, on the mean constraint costs of each snapshot.

Figure A.4 (a) shows a scatter plot for the final estimate of mean annual constraint costs for each of the 200 repetitions, with a horizontal line also shown to represent $\hat{\mu}_1$. Figure A.4 (b) shows the difference between these estimates and $\hat{\mu}_1$ ($\hat{\mu}_1$ minus the estimate of mean annual constraint costs acquired from importance sampling), with Figure A.4 (c) showing this difference as a percentage of $\hat{\mu}_1$. The majority of estimates of mean annual constraint costs lie close to $\hat{\mu}_1$. However, there 6 notable outliers, which under-estimate mean annual constraint costs by as much as 73% and over-estimate by as much as 35%.

Figure A.5 displays how the costs differ from $\hat{\mu}_1$ when also considering the amount of work, λ, used to acquire the estimates. As can be seen, the estimates which differ greatly from $\hat{\mu}_1$ are those which were acquired when the number of equivalent full simulator evaluations performed is low. In Section 4.3.3 it was noted that these estimates are acquired when a small number of yearly evaluations give similar values, which result in the standard error of the estimate being less than 1% of the estimate, regardless of whether the estimate of mean constraint costs is close to $\hat{\mu}_1$.

For this reason, it was then imposed that an equivalent of 10 full simulator evaluations must be performed before an estimate can be accepted, and such estimates were ex-

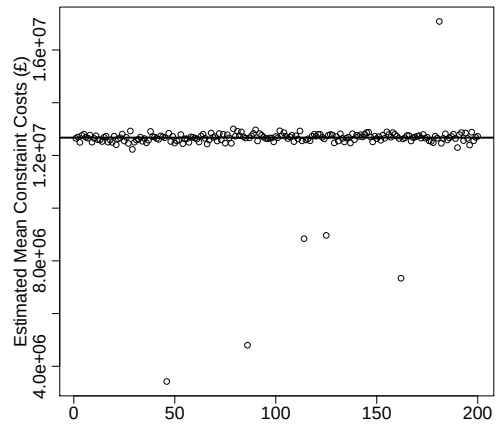

(a) Scatter plot of cost estimates.

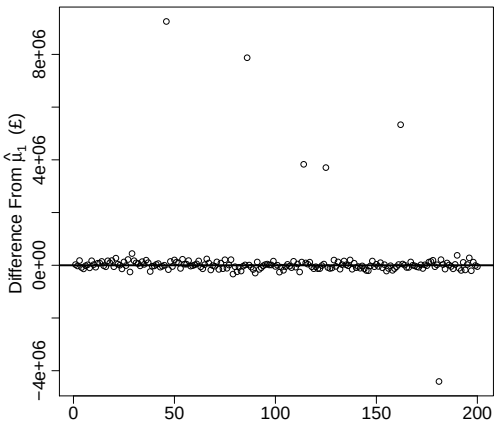

(b) Scatter plot of differences from $\hat{\mu}_1$.

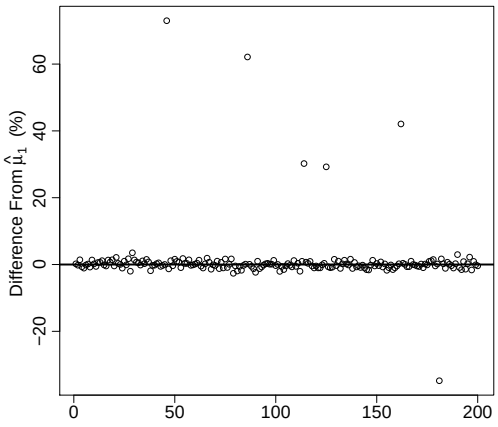

(c) Scatter plot of relative differences from $\hat{\mu}_1$.

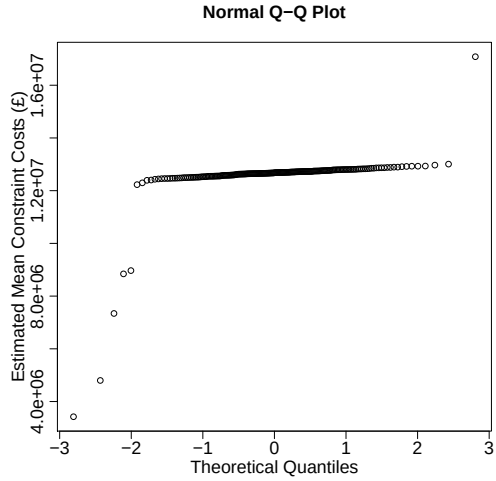

(d) Normal QQ plot.

Figure A.4: Plots to compare estimates of mean annual constraint costs from importance sampling to $\hat{\mu}_1$ for a year 1 power system background, when it is required that the standard error of the estimate is less than 1% of the mean of the estimate with no minimum amount of snapshots to be evaluated.

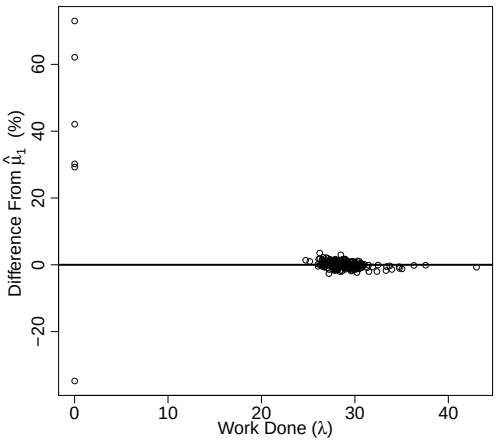

Figure A.5: Plot to compare estimates of mean annual constraint costs from importance sampling to $\hat{\mu}_1$ for a year 1 power system background, when it is required that the standard error of the estimate is less than 1% of the mean of the estimate with no minimum amount of snapshots to be evaluated.

plored in the previous subsection. This led to an improvement in the estimation of mean constraint costs, as the estimates of mean constraint costs detailed in Appendix A.2.2 all lie very close to $\hat{\mu}_1$ without any extreme outliers.

A QQ plot for the estimates of mean annual constraint costs is illustrated in Figure A.4 (d), which illustrates that with the outliers included, the estimates of mean annual constraint costs no longer form a normal distribution.

Figure A.6 displays results for all four importance sampling methods considered in Section 4.3.3. All four importance sampling methods show that the majority of estimates of mean annual constraint costs lie close to $\hat{\mu}_1$, though all have outliers which greatly over/under estimate costs. Basing the importance sample weights on the mean costs of each snapshot results in the largest under-estimations of these outliers (of up to 73% from $\hat{\mu}_1$) though outliers are much more frequent when basing results on snapshot demand or simply evaluating all snapshots (i.e. not using importance sampling). Further, it appears that these outliers greatly under-estimate mean constraint costs much more frequently than they greatly over-estimate mean constraint costs.

Table A.2 gives a comparison between the estimates of mean annual constraint costs from importance sampling to $\hat{\mu}_1$. Despite several estimates considerably under-estimating mean annual constraint cost, the mean difference between estimates of mean annual

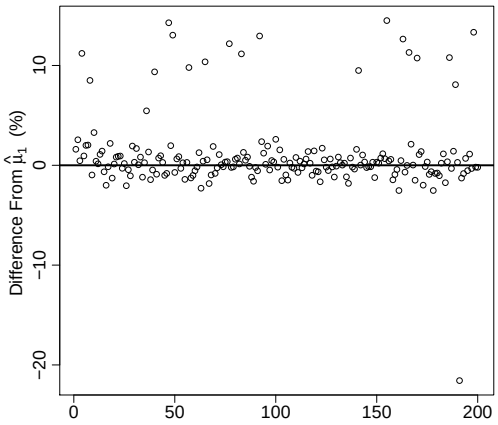

(a) Using all snapshots.

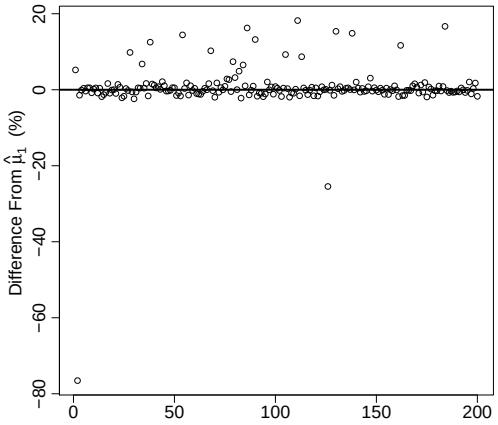

(b) Importance sampling based on snapshot demand.

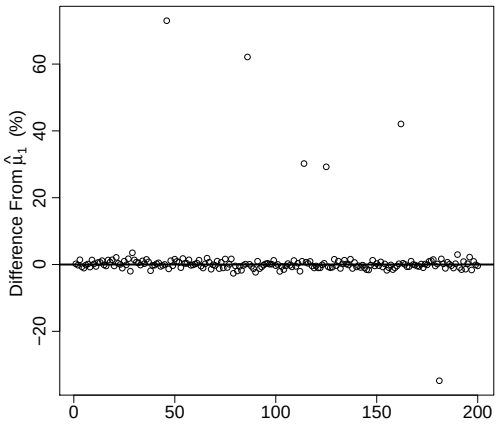

(c) Importance sampling based on snapshot mean.

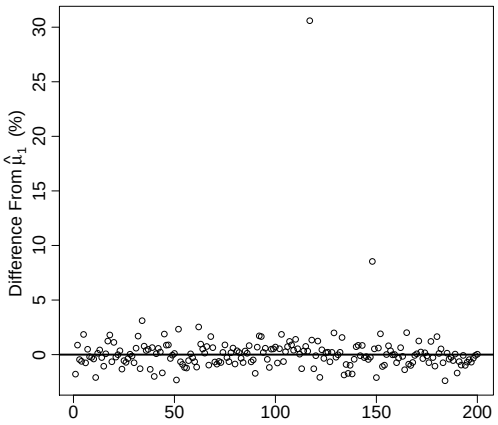

(d) Importance sampling based on snapshot standard deviation.

Figure A.6: Plots to compare estimates of mean annual constraint costs from importance sampling to $\hat{\mu}_1$ for a year 1 power system background, when it is required that the standard error of the estimate is less than 1% of the mean of the estimate with no minimum amount of snapshots to be evaluated.

Importance Sample Basis	Mean Difference	Mean Absolute Difference	Mean Percentage Difference	Mean Absolute Percentage difference
All Snapshots	£127,000	£243,000	1.00 %	1.92%
Demand	£56,300	£289,000	0.444%	2.28%
Snapshot Mean	£126,000	£270,000	0.998%	2.13%
Snapshot Standard Deviation	£20,600	£120,000	0.162%	0.948%

Table A.2: Table comparing estimated mean annual constraint costs from importance sampling to $\hat{\mu}_1$ for a year 1 power system background, when it is required that the standard error of the estimate is less than 1% of the mean of the estimate with no minimum amount of snapshots to be evaluated.

constraint costs and $\hat{\mu}_1$ is still 1% or less for all conditions. The mean absolute difference between the estimates of mean annual costs and $\hat{\mu}_1$ is a little greater, with mean absolute differences of up to 2.28%.

However, in Table A.1, where it was required that the equivalent of at least 10 full simulator evaluations were performed for an estimate, the mean difference between the estimates and $\hat{\mu}_1$ was less than 0.13% and the mean absolute difference from $\hat{\mu}_1$ was less than 0.861% for all importance sampling methods. This indicates an improvement in the accuracy of the estimates of mean annual constraint costs from imposing a minimum amount of snapshots to be evaluated, as this avoids acquiring an estimate which has a small standard error due to a small number of yearly simulations being acquired which happened to have similar estimates of constraint costs.

Year 6 Power System Background

Figure A.7 displays graphs to show the variation in the 200 estimates of mean annual constraint costs for a year 6 power system background. These costs are the estimated in Section 4.3.3, where it was required that the standard error of the estimate was less than 1% of the mean of the estimate, without any limitations on the minimum amount of snapshots that must be evaluated to achieve this. The estimates of mean annual constraint costs displayed in Figure A.7 based the weights used for importance sampling, $\boldsymbol{\omega}$, on the mean constraint costs of each snapshot.

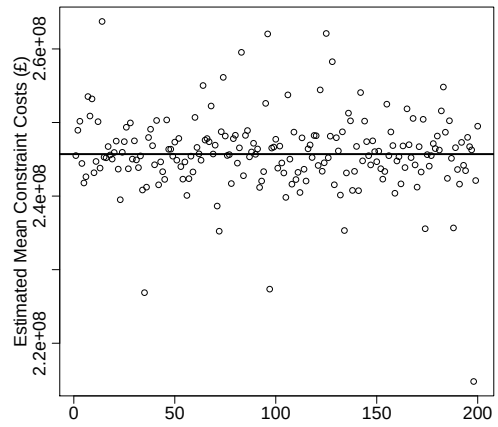

(a) Scatter plot of cost estimates.

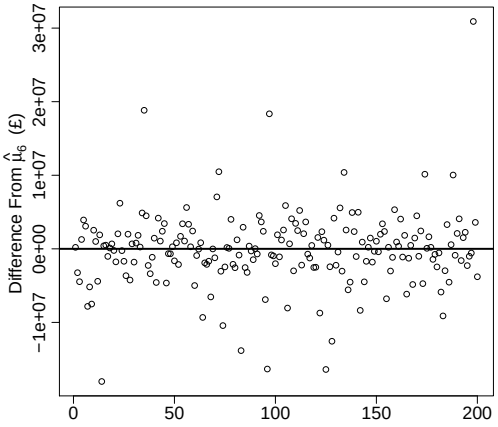

(b) Scatter plot of differences from $\hat{\mu}_6$.

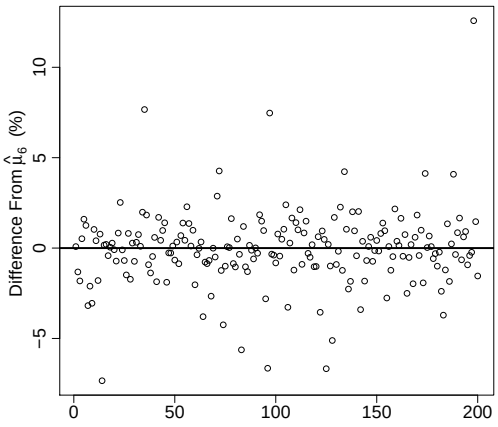

(c) Scatter plot of relative differences from $\hat{\mu}_6$.

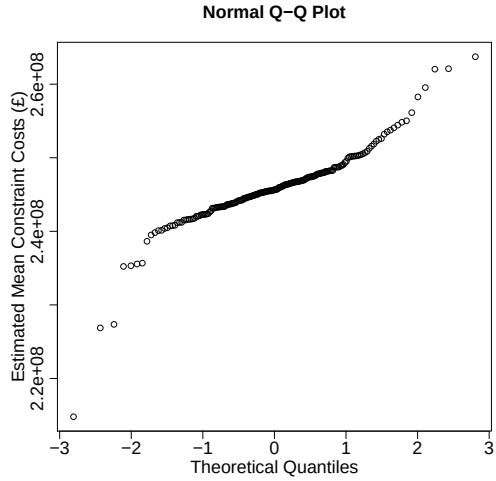

(d) Normal QQ plot.

Figure A.7: Plots to compare estimates of mean constraint costs from importance sampling to $\hat{\mu}_6$ for a year 6 power system background, when it is required that the standard error of the estimate is less than 1% of the mean of the estimate with no minimum amount of snapshots to be evaluated.

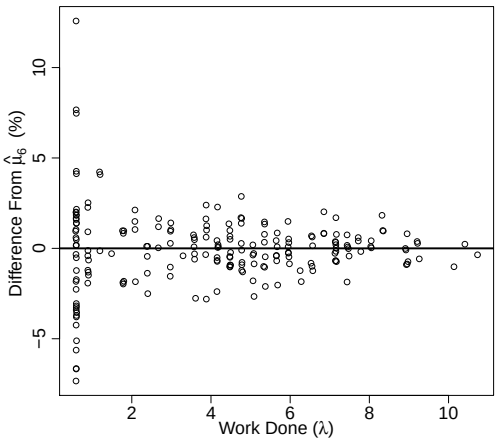

Figure A.8: Plot to compare estimates of mean annual constraint costs from importance sampling to $\hat{\mu}_6$ for a year 6 power system background, when it is required that the standard error of the estimate is less than 1% of the mean of the estimate with no minimum amount of snapshots to be evaluated.

Figure A.7 (a) shows a scatter plot for the final estimates of mean annual constraint costs for each of the 200 repetitions, with a horizontal line also shown to represent $\hat{\mu}_6$. Figure A.7 (b) shows the difference between these estimates and $\hat{\mu}_6$, with Figure A.7 (c) showing this difference as a percentage of $\hat{\mu}_6$.

By contrasting these graphs to Figure 4.8 of Section 4.3.6 (where a minimum of 175200 snapshot evaluations was imposed) it can be seen that generally there is a greater variation in the estimates of mean annual constraint costs when minimum amount of snapshot evaluations is imposed on an estimate. This is partially explained by the results of Section 4.3.3, where an estimate such that the standard error of the estimate is less than 1% of the mean of the estimate is often acquired by evaluating less than 175200 snapshots. Imposing a minimum number of evaluations that must be taken results in estimates of mean annual constraint costs that are on average based on a greater amount of information leading to more accurate estimates.

The normal quantile plot for the estimates of mean annual constraint costs is illustrated in Figure A.7 (d). As was the case for a year 1 power system background, when no minimum work is imposed the estimates of mean annual constraint costs do not appear to form a normal distribution.

Further, Figure A.8 displays how the costs differ from $\hat{\mu}_6$ when also considering the

amount of work done, λ, to acquire the estimates. As was the case for the year 1 power system background, it can be seen that the greatest variation in estimated mean annual constraint costs arises when very few evaluations have been performed. Again, this is due to the fact that if a small number of yearly evaluations happen to give similar results then an estimate of mean annual constraint costs will be acquired which has a low standard error despite not necessarily being an accurate estimate for the mean annual constraint costs of the power system.

Figure A.9 displays results for all four importance sampling methods considered in Section 4.3.3. By contrasting to the equivalent results for a year 1 power system background in Figure A.6, it can be seen that cost estimates for a year 6 power system background are less susceptible to estimates of mean constraint costs which are extremely different to the "true" mean constraint costs of the power system.

However, by contrasting to Figure A.3, which displays results for a year 6 power system background when a minimum of 175200 snapshot evaluations is imposed, it can be seen that estimates of mean annual constraint costs vary by a much greater amount when no minimum amount of work is imposed. In particular, when a minimum of 175200 snapshot evaluations is imposed, almost all estimates of mean annual constraint costs lie within 2% of $\hat{\mu}_6$, though when no minimum amount of work is imposed variations of up to 4% are observed infrequently, with differences of over 10% even being observed for importance sampling methods based on snapshot mean or standard deviation.

Importance Sample Basis	Mean Difference	Mean Absolute Difference	Mean Percentage Difference	Mean Absolute Percentage difference
All Snapshots	£119,000	£2,700,000	0.0485 %	1.10%
Demand	-£294,000	£2,550,000	-0.120%	1.04%
Snapshot Mean	-£132,000	£3,360,000	-0.0536%	1.37%
Snapshot Standard Deviation	-£200,000	£3,420,000	-0.0814%	1.39%

Table A.3: Table comparing estimated mean annual constraint costs from importance sampling to $\hat{\mu}_6$ for a year 6 power system background, when it is required that the standard error of the estimate is less than 1% of the mean of the estimate with no minimum amount of snapshots to be evaluated.

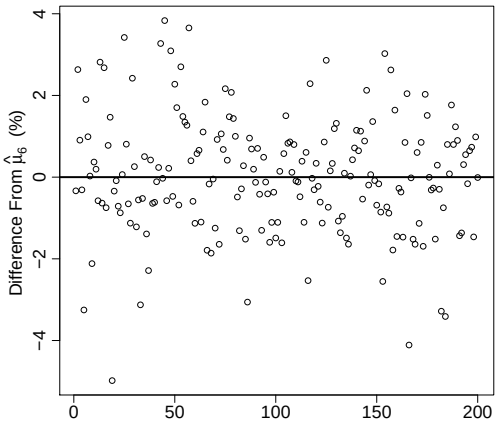

(a) Using all snapshots.

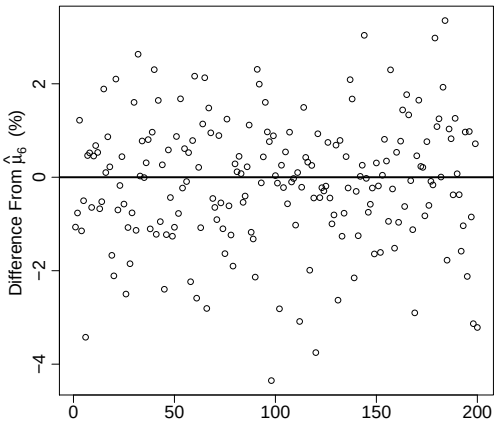

(b) Importance sampling based on snapshot demand.

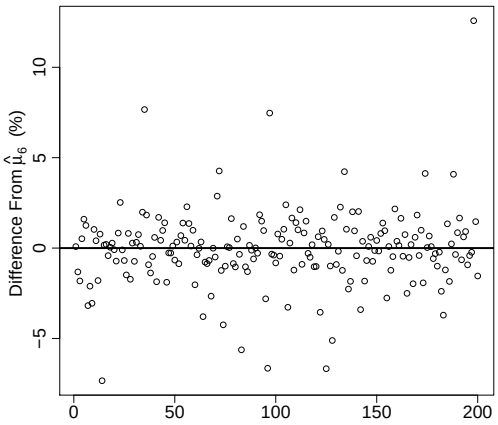

(c) Importance sampling based on snapshot mean.

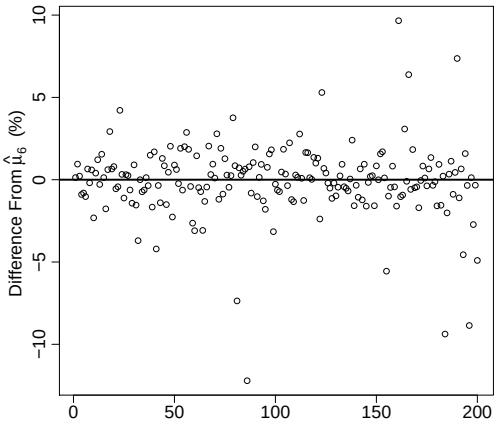

(d) Importance sampling based on snapshot standard deviation.

Figure A.9: Plots to compare estimates of mean annual constraint costs from importance sampling to $\hat{\mu}_6$ for a year 6 power system background, when it is required that the standard error of the estimate is less than 1% of the mean of the estimate with no minimum amount of snapshots to be evaluated.

Table A.3 gives a comparison between the estimates of mean annual constraint costs from importance sample to $\hat{\mu}_6$. By comparison to Table 4.8 of Section 4.3.6 (results when a minimum of 175200 snapshots were to be evaluated) it can be seen that results are somewhat comparable with the mean difference between estimates of mean annual constraint costs and $\hat{\mu}_6$ being less than 0.12% for all importance sampling methods. This indicates that although there is a greater level of variation in estimates of mean annual constraint costs when not imposing a minimum number of snapshots to be evaluated, costs appear to be under-estimated around as often as they are over-estimated and an average of many estimates is still very close to $\hat{\mu}_6$.

However, when considering the mean absolute difference from $\hat{\mu}_6$, it is now observed that the estimated mean annual constraint costs will differ from $\hat{\mu}_6$ by 1.04% to 1.39%, whereas when a minimum of 175200 snapshots were to be evaluated all the mean absolute difference was less than 0.66% for all importance sampling methods. This is a result of the greater level of variation in the estimates of mean annual constraint costs when no level of minimum work is required.

A.2.4 Accuracy of Estimates With a Standard Error of Less Than £100,000

Results presented in Sections 4.3.6, A.2.2 and A.2.3 consider how estimates of mean annual constraint costs vary when it is required that the standard error of the estimated costs is less than 1% of the mean of the estimate. However, Section 4.3.5 also considers how many equivalent full simulator evaluations were necessary to estimate constraint costs such that the standard error of the estimate was less than £100,000. Section 4.3.5 showed how this is a stricter convergence criterion which requires more snapshots to be evaluated in comparison to acquiring an estimate such that the error is less than 1% of the mean. Therefore, it would be expected that the resulting estimates of mean annual constraint costs will be more accurate, which will be shown in this subsection.

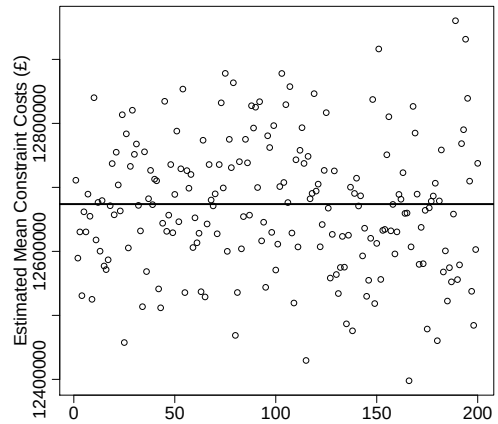

(a) Scatter plot of cost estimates.

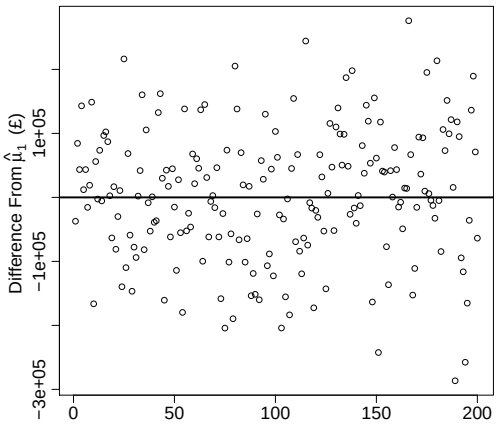

(b) Scatter plot of differences from $\hat{\mu}_1$.

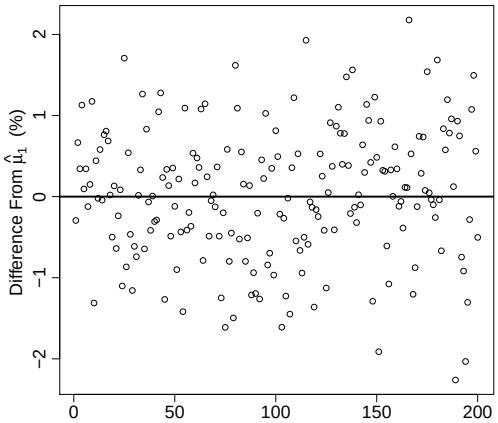

(c) Scatter plot of relative differences from $\hat{\mu}_1$.

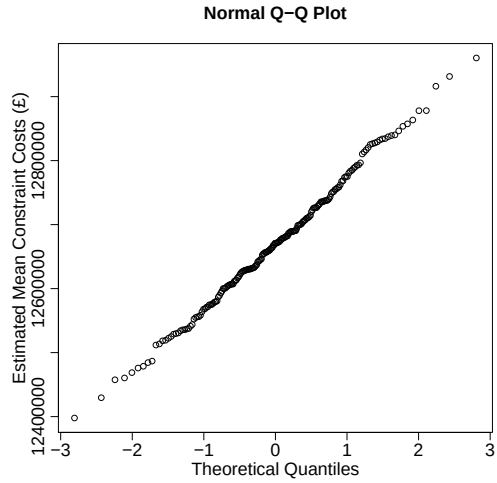

(d) Normal QQ plot.

Figure A.10: Plots to compare estimates of mean annual constraint costs from importance sampling to $\hat{\mu}_1$ for a year 1 power system background, when it is required that the standard error of the estimate is less than £100,000.

Year 1 Power System Background

Figure A.10 displays graphs to show how 200 estimates of mean annual constraint costs vary for a year 1 power system background. These are the costs estimated in Section 4.3.5, where it was required that the standard error of the estimate was less than £100,000, and that a minimum of 175200 snapshots (the equivalent of 10 full simulator evaluations) had been evaluated. The estimates of mean annual constraint costs displayed in Figure A.10 based the weights used for importance sampling, $\boldsymbol{\omega}$, on the mean constraint costs of each snapshot.

Figure A.10 (a) shows a scatter plot of the 200 estimates of mean annual constraint costs, with a horizontal line also shown to represent $\hat{\mu}_1$. Figure A.10 (b) shows the difference between these estimates and $\hat{\mu}_1$, with Figure A.10 (c) showing this difference as a percentage of $\hat{\mu}_1$. As can be seen, estimates are fairly evenly scattered around $\hat{\mu}_1$, with costs being over-estimated as often as they are under-estimated, as was the case in Figure A.1 of Appendix A.2.2 where costs were estimated such that the standard error of the estimate is less than 1% of the mean of the estimate. Further, almost all of the estimates of mean annual constraint costs differ from $\hat{\mu}_1$ by less than 2% of $\hat{\mu}_1$.

The normal quantile plot of Figure A.10 (d) shows that the estimates of mean annual constraint costs approximately form a normal distribution. Again, by the central limit theorem it is expected that estimates of mean annual constraint costs are normally distributed around $\hat{\mu}_1$.

Figure A.11 displays results for all four importance sampling methods considered in Section 4.3.5. As can be seen, all importance sampling methods result in similar behaviour, with results being distributed around $\hat{\mu}_1$, with almost all estimates of mean annual constraint lying within 2% of $\hat{\mu}_1$, and most within 1.5% of $\hat{\mu}_1$.

Table A.4 gives details on how the estimates of mean annual constraint costs differ from $\hat{\mu}_1$ on average. As can be seen, for any importance sampling method, the mean of the estimates of mean annual costs differs from $\hat{\mu}_1$ by less than £6,820 (0.054%), whereas the mean absolute difference between the estimates and $\hat{\mu}_1$ is less than £91,000 (0.72%) for all methods of importance sampling.

These figures indicate a greater level of accuracy in the estimates in comparison to

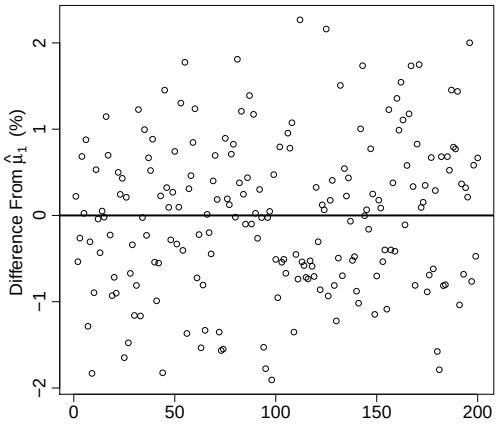

(a) Using all snapshots.

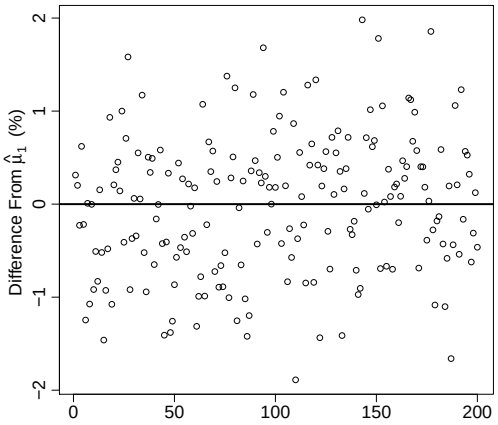

(b) Importance sampling based on snapshot demand.

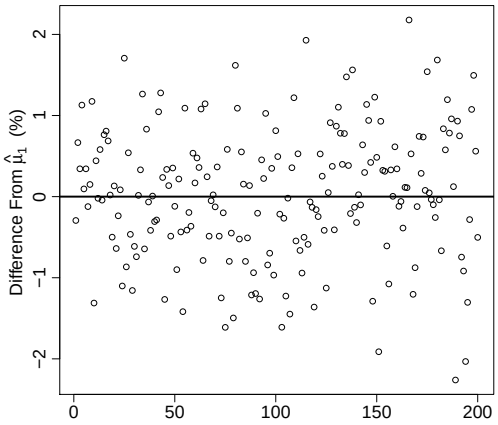

(c) Importance sampling based on snapshot mean.

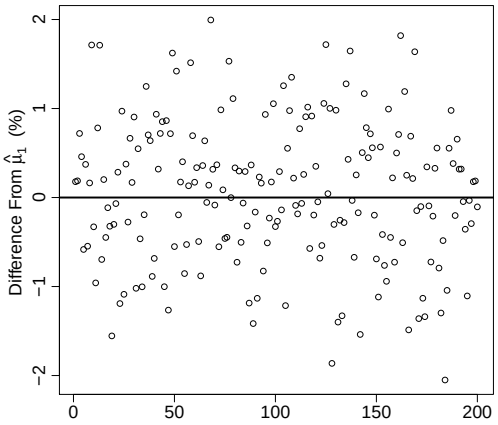

(d) Importance sampling based on snapshot standard deviation.

Figure A.11: Plots to compare estimates of mean annual constraint costs from importance sampling to $\hat{\mu}_1$ for a year 1 power system background, when it is required that the standard error of the estimate is less than £100,000.

Importance Sample Basis	Mean Difference	Mean Absolute Difference	Mean Percentage Difference	Mean Absolute Percentage difference
All Snapshots	-£284	£90,900	-0.00224 %	0.718%
Demand	-£1,370	£77,200	-0.0108%	0.609%
Snapshot Mean	£3,630	£82,000	0.0286%	0.647%
Snapshot Standard Deviation	£6,820	£82,300	0.0538%	0.649%

Table A.4: Table comparing estimated mean annual constraint costs from importance sampling to $\hat{\mu}_1$ for a year 1 power system background, when it is required that the standard error of the estimate is less than £100,000.

Table A.1, which considers estimating mean annual constraint costs such that the error in the estimate is less than 1% of the mean of the estimate. This is to be expected as £100,000 is less than £126,000 (1% of $\hat{\mu}_1$) which indicates that £100,000 is a stricter convergence criterion and hence gives more accurate estimates of mean annual constraint costs.

However, as was noted in Section 4.3.6, this improvement is small in comparison to the improvement noted for a year 6 power system background, where the error of the estimate was reduced by more than a factor of 18 by using the stricter convergence criterion. As was also noted in Section 4.3.6, this is because for a year 1 power system background when the standard error of the estimate is 1% of the mean of the estimate, the expected error will be around £126,000, whereas for a year 6 power system background the equivalent error is around £2,450,000. This means that requiring the standard error of the estimate to be less than £100,000 is relatively a much stricter convergence criterion for a year 6 power system background in comparison to a year 1 power system background, resulting in the observed larger reduction in the error of the estimate.

Year 6 Power System Background

As was the case when considering estimates with a standard error of less than 1%, results for a year 6 power system background were previously considered in Section 4.3.6,

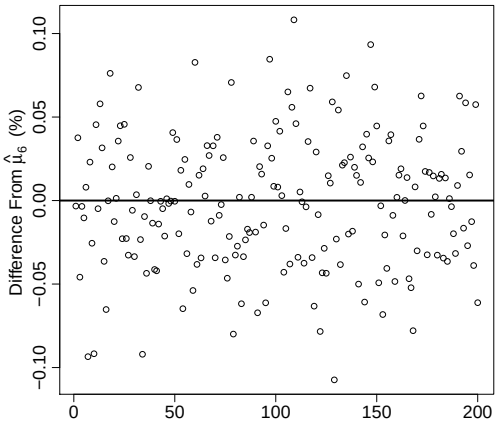

(a) Using all snapshots.

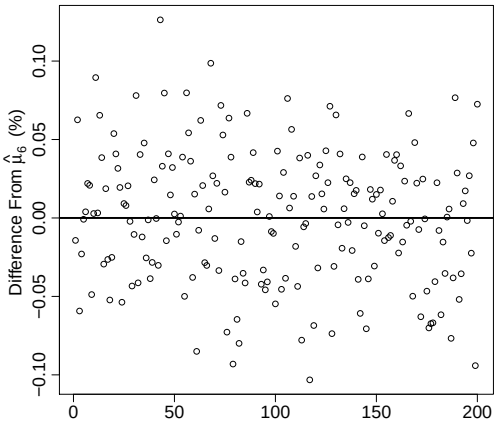

(b) Importance sampling based on snapshot demand.

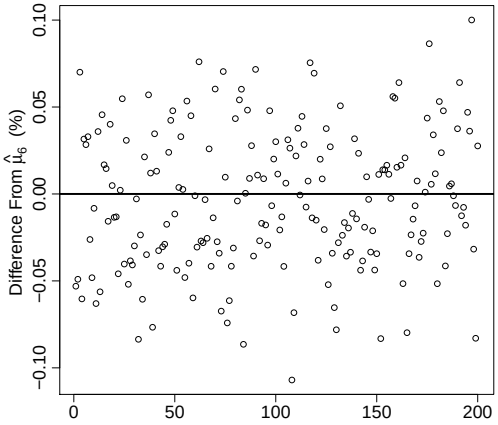

(c) Importance sampling based on snapshot mean.

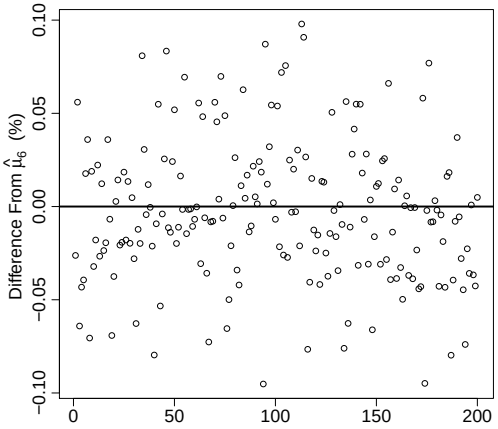

(d) Importance sampling based on snapshot standard deviation.

Figure A.12: Plots to compare estimates of mean annual constraint costs from importance sampling to $\hat{\mu}_6$ for a year 6 power system background, when it is required that the standard error of the estimate is less than £100,000.

but only for when importance sampling weights were based on the mean constraint costs of each snapshot. Plots to illustrate scatter plots of the relative differences between estimates of mean annual constraint costs and $\hat{\mu}_6$ for all four importance sampling methods considered in Section 4.3.5 are given in Figure A.12. As can be seen, all estimates of mean annual constraint costs give similarly good results, with almost all estimates differing from $\hat{\mu}_6$ by less than 0.1% of $\hat{\mu}_6$.

As was also mentioned in Section 4.3.6, these results can be contrasted with those where costs were estimated such that the standard error of the estimate was less than 1% of the mean of the estimate. These were displayed in Figure A.3 of Section A.2.2, where it was seen that estimates differed from $\hat{\mu}_6$ by up to 2%, which is 20 times greater than the typical difference seen in Figure A.12. Again, it is noted that this is due the fact that requiring the error to be less than £100,000 for a year 6 power system background is a much stricter convergence criterion, and due to the mean costs for a year 6 power system background being in excess of £245,000,000, the error is increased over 20-fold when the less strict criterion of the standard error being less than 1% of the mean is used.

A.2.5 Accuracy of Estimates When Updating Importance Sampling Weights as Outlined in Section 4.4.2

Section 4.4.2 detailed a methodology in which a small number of initial full simulations could be used to estimate weights to be used for importance sampling, and then allow for the weights to be updated after each subsequent yearly evaluation to account for the latest estimates of mean constraint costs in each snapshot. An application was then presented which considered how much work, λ, was required to estimate mean annual constraint costs for a given power system background such that the standard error of the estimate of constraint costs is less than 1% of the mean of the estimate. As part of this, 200 estimates of mean annual constraint costs were acquired when varying the initial number of yearly evaluations used to estimate importance sampling weights, $\boldsymbol{\omega}$. This subsection will compare how the estimates of constraint costs acquired for each repetition compare to $\hat{\mu}_1$, the highly accurate estimates of mean annual constraint costs for a year 1 power system background calculated in Section 4.3.6.

Year 1 Power System Background

Figure A.13 illustrates the variation in the estimates of mean annual constraint costs for each of the 200 repetitions for a year 1 power system background when using an initial 10 full simulator evaluations to estimate weights for importance sampling. These are the costs that were estimated in Section 4.4.2 where it was required that the standard error of the estimate was less than 1% of the mean of the estimate.

As can be seen, the estimates of mean annual constraint costs are fairly evenly scattered with cost being over-estimated as often as they are under-estimated. Further, the normal quantile plot of Figure A.13 (d) shows that the distribution of estimates of mean annual constraint costs is approximately normal, which again would be expected by the central limit theorem (though there are a couple of slight outliers towards the tail of the distribution).

Figure A.14 displays scatterplots to show how estimates of mean annual constraint costs differ from $\hat{\mu}_1$ (as a percentage of $\hat{\mu}_1$) for each of the 200 repetitions. Results are displayed for the four different numbers of initial full simulations used to estimate importance sampling weights considered in Section 4.4.2. Results do not appear to be affected by the number of initial simulations used, with all plots showing a random scatter around $\hat{\mu}_1$, with the vast majority of estimates of mean annual constraint costs lying within 2% of $\hat{\mu}_1$ for all conditions. This is to be expected, as Equation 4.2.6 of Section 4.2.2 shows that the importance sample is an unbiased estimate of constraint costs for all possible choices of values for importance sample weights, $\boldsymbol{\omega}$. Therefore, the expected value for all estimates is the mean of the full simulator, and by the central limit theorem estimates should be normally distributed around this mean.

Table A.5 gives details on a comparison between the estimates of mean annual constraint costs from importance sampling and the highly accurate estimate of mean constraint costs for a year 1 power system background, $\hat{\mu}_1$. For all importance sampling conditions, the mean difference of all 200 repetitions from $\hat{\mu}_1$ was less than £7200, which is a difference of less than 0.057%. Again, this to be expected, as all estimates have the same expectation as the full simulator, and Figure A.14 showed how they were evenly scattered around $\hat{\mu}_1$ with quite a small error, indicating their average should give a very accurate estimate of mean annual constraint costs.

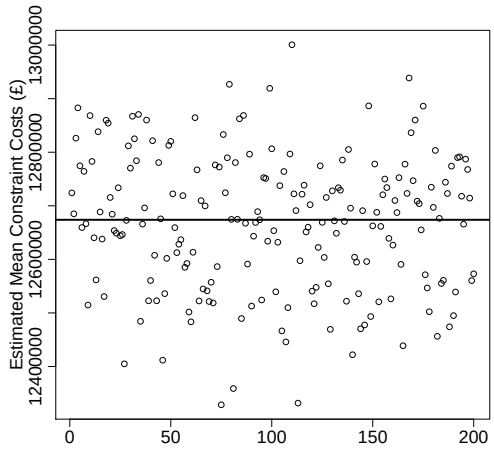

(a) Scatter plot of cost estimates.

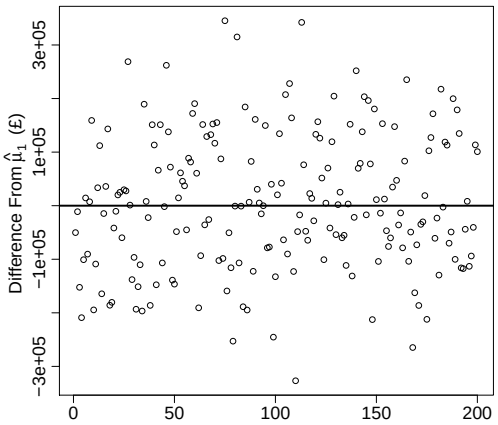

(b) Scatter plot of differences from $\hat{\mu}_1$.

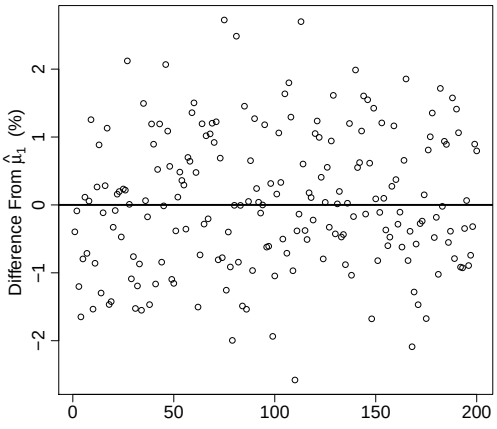

(c) Scatter plot of relative differences from $\hat{\mu}_1$.

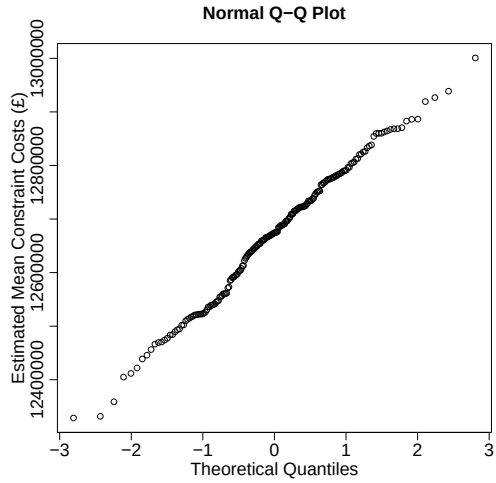

(d) Normal QQ plot.

Figure A.13: Plots to compare estimates of mean annual constraint costs from importance sampling to the $\hat{\mu}_1$ for a year 1 power system background, when it is required that the standard error of the estimate is less than 1% of the mean of the estimate.

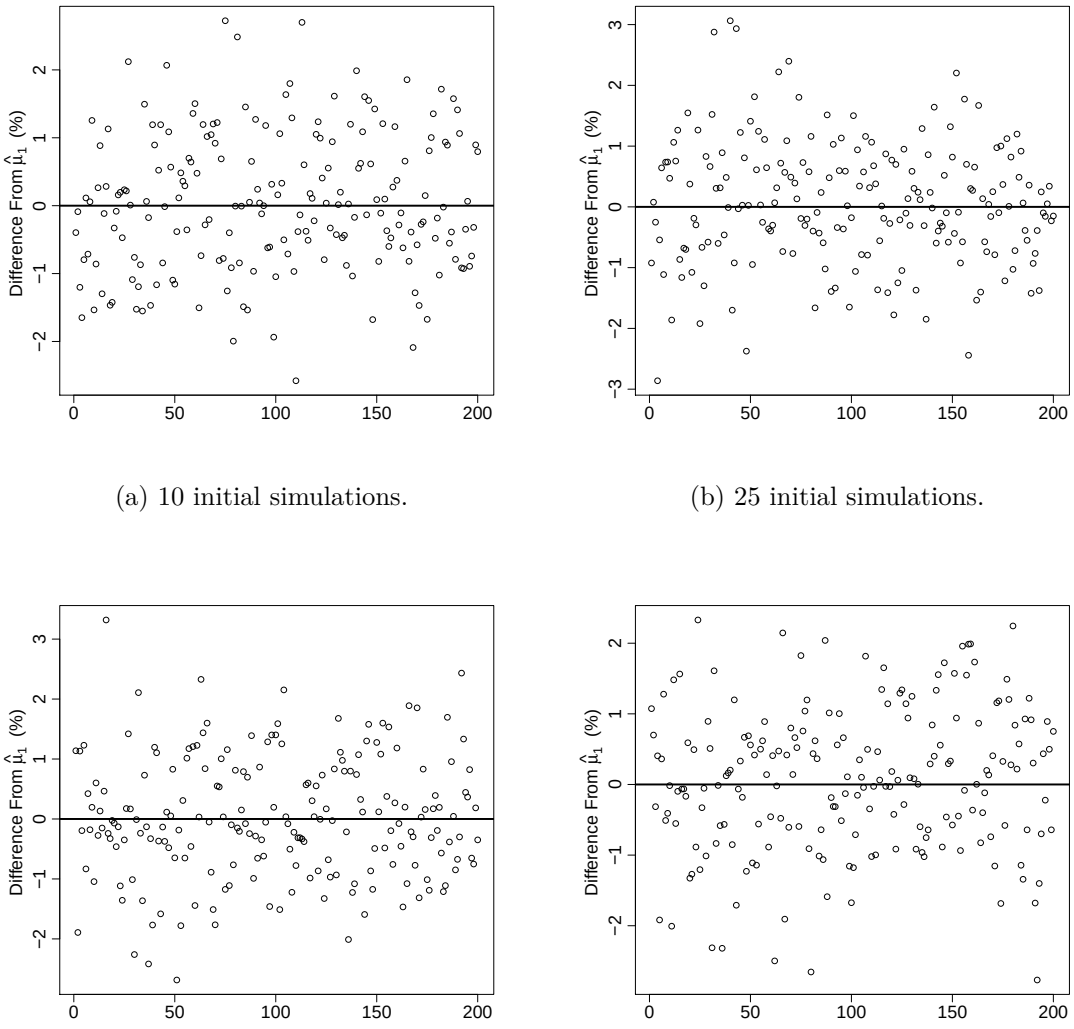

(a) 10 initial simulations.

(b) 25 initial simulations.

(c) 50 initial simulations.

(d) 100 initial simulations.

Figure A.14: Plots to compare estimates of mean annual constraint costs from importance sampling to $\hat{\mu}_1$ for a year 1 power system background, when it is required that the standard error of the estimate is less than 1% of the mean of the estimate.

Initial Number of Full Simulations	Mean Difference	Mean Absolute Difference	Mean Percentage Difference	Mean Absolute Percentage difference
10	£7,120	£105,000	0.0562 %	0.827%
25	£7,090	£99,800	0.0559%	0.787%
50	£1,630	£101,000	0.0129%	0.795%
100	£6,850	£103,000	0.0541%	0.815%

Table A.5: Table comparing estimated mean annual constraint costs from importance sampling to $\hat{\mu}_1$ for a year 1 power system background, when it is required that the standard error of the estimate is less than 1% of the mean of the estimate.

When considering the absolute difference, it appears on average estimates differ from $\hat{\mu}_1$ by 0.787% to 0.827% (by around £100,000). As was noted in Section A.2.2, this is what should be expected as estimates were acquired such that the standard error of the estimate was less than 1% of the mean of the estimate. Therefore, by the central limit theorem it should be expected that estimates of mean annual constraint costs are normally distributed with a standard deviation of £126,000 (1% of $\hat{\mu}_1$) and the expected absolute difference of such an estimate from $\hat{\mu}_1$ is 0.8%.

Appendix B

Chapter 6 Additional Details

B.1 Model Selection

Section 6.1.3 gave an overview of the model selection for the emulator model to approximate the simulator for the example of Section 6.1.1. This stated that the optimal form of the polynomial portion of the emulator model is

$$\beta_0 + \beta_1 v_1 + \beta_2 v_2 + \beta_3 v_3 + \beta_4 d_1 + \beta_5 d_2 + \beta_6 v_1^2 + \beta_7 v_2^2 + \beta_8 v_3^2 + \beta_9 d_1^2 + \beta_{10} d_2^2 + \beta_{11} v_1 d_1 + \beta_{12} v_1 d_2 + \beta_{13} d_1 d_2 + \beta_{14} v_1^2 d_1^2 + \beta_{15} v_1^2 d_2^2 + \beta_{16} d_1^2 d_2^2 + \beta_{17} v_1 d_1 d_2 + \beta_{18} v_1^2 d_1^2 d_2^2$$

Section 6.1.3 showed how the value of R^2 (a measure of how well the polynomial portion of the emulator fits the data used to fit the model) and P (a measure of how well the fitted emulator model, i.e. the sum of the polynomial regression model plus the Gaussian process model applied to its residuals, predicts a response for values not used to fit the emulator) vary with number of training runs used to fit the emulator model. However, it is also important to carefully consider which terms to include in the polynomial portion of the emulator model.

Table B.1 gives details of how values of R^2, P (defined in Equation 5.3.1 of Section 5.3.3 as the mean squared error when estimating a response for a second set of 50 training runs from the simulator not used to fit the model) and $\tilde{P}$ (defined in Equation 5.3.2 of Section 5.3.3 as the value of P normalised by the variance in the response in the second set of training data) vary as the form of the polynomial regression portion of the emulator model is varied. As was noted in Sections 5.3.3 and 6.1.3, R^2 is measure

Polynomial Model	Value of R^2	Value of P	Value of $\tilde{P}$
Polynomial 1	0.6481	2.097×10^{16}	0.07371
Polynomial 2	0.8743	1.109×10^{16}	0.03900
Polynomial 3	0.8886	1.318×10^{16}	0.04632
Polynomial 4	0.6853	1.884×10^{16}	0.06623
Polynomial 5	0.9346	4.662×10^{15}	0.01639
Polynomial 6	0.9547	6.853×10^{15}	0.02410
Polynomial 7	0.9714	2.177×10^{15}	0.007652
Polynomial 8	0.9393	4.060×10^{15}	0.01427
Polynomial 9	0.9419	3.965×10^{15}	0.01394

Table B.1: Table of how the model selection criteria vary with the form of polynomial used for the polynomial portion of the emulator.

of how well the fitted model fits the data used to construct it, whilst P and $\tilde{P}$ measure how well the fitted emulator predicts a response for input values not used to construct the model. Details of the terms included in each of the polynomial regression models are given in Table B.2.

As can be seen, only including first order terms and including no interactions gives a poor fit and poor predictive power, with the lowest R^2 value of any model and largest value of P. Including second order terms (polynomial 2) gives a large improvement in the fit of the model (with R^2 increasing from 0.65 to 0.87) and predictive power (with P decreasing from 2.097×10^{16} to 1.109×10^{16}). Including third order terms (polynomial 3) does slightly increase the value of R^2, though also slightly increases the value of P indicating that these terms may be unnecessary, and may result in over-fitting.

Including interaction terms between the two decision variables for terms of equal power (in polynomials 4, 5 and 6) appears to improve the fitted model for all orders of polynomial. Polynomial 5 (including first and second order terms for all variables as well as interactions between equal ordered terms for the decision variables) appears to give the best fit, as although the value of R^2 is slightly lower than when additionally including third order terms, the model has a greater predictive power (smaller value of P) in comparison to polynomial 6. This improvement when including interaction terms for the decision variables is consistent with what was observed in Figure 6.3 of Section 6.1.2.

Polynomials 7, 8 and 9 consider whether additional interaction terms should be included

in the model, with the best results acquired when additionally including interaction terms for nuclear availability probability (v_1). The inclusion of interactions between the decision variables and nuclear availability probability is consistent with what was observed in Figure 6.2 of Section 6.1.2.

Polynomial Model	Model Description
Polynomial 1	$\beta_0 + \beta_1 v_1 + \beta_2 v_2 + \beta_3 v_3 + \beta_4 d_1 + \beta_5 d_2$
Polynomial 2	$\beta_0 + \beta_1 v_1 + \beta_2 v_2 + \beta_3 v_3 + \beta_4 d_1 + \beta_5 d_2 + \beta_6 v_1^2 + \beta_7 v_2^2 + \beta_8 v_3^2 + \beta_9 d_1^2 + \beta_{10} d_2^2$
Polynomial 3	$\beta_0 + \beta_1 v_1 + \beta_2 v_2 + \beta_3 v_3 + \beta_4 d_1 + \beta_5 d_2 + \beta_6 v_1^2 + \beta_7 v_2^2 + \beta_8 v_3^2 + \beta_9 d_1^2 + \beta_{10} d_2^2 + \beta_{11} v_1^3 + \beta_{12} v_2^3 + \beta_{13} v_3^3 + \beta_{14} d_1^3 + \beta_{15} d_2^3$
Polynomial 4	$\beta_0 + \beta_1 v_1 + \beta_2 v_2 + \beta_3 v_3 + \beta_4 d_1 + \beta_5 d_2 + \beta_6 d_1 d_2$
Polynomial 5	$\beta_0 + \beta_1 v_1 + \beta_2 v_2 + \beta_3 v_3 + \beta_4 d_1 + \beta_5 d_2 + \beta_6 v_1^2 + \beta_7 v_2^2 + \beta_8 v_3^2 + \beta_9 d_1^2 + \beta_{10} d_2^2 + \beta_{11} d_1 d_2 + \beta_{12} d_1^2 d_2^2$
Polynomial 6	$\beta_0 + \beta_1 v_1 + \beta_2 v_2 + \beta_3 v_3 + \beta_4 d_1 + \beta_5 d_2 + \beta_6 v_1^2 + \beta_7 v_2^2 + \beta_8 v_3^2 + \beta_9 d_1^2 + \beta_{10} d_2^2 + \beta_{11} v_1^3 + \beta_{12} v_2^3 + \beta_{13} v_3^3 + \beta_{14} d_1^3 + \beta_{15} d_2^3 + \beta_{16} d_1 d_2 + \beta_{17} d_1^2 d_2^2 + \beta_{18} d_1^3 d_2^3$
Polynomial 7	$\beta_0 + \beta_1 v_1 + \beta_2 v_2 + \beta_3 v_3 + \beta_4 d_1 + \beta_5 d_2 + \beta_6 v_1^2 + \beta_7 v_2^2 + \beta_8 v_3^2 + \beta_9 d_1^2 + \beta_{10} d_2^2 + \beta_{11} v_1 d_1 + \beta_{12} v_1 d_2 + \beta_{13} d_1 d_2 + \beta_{14} v_1^2 d_1^2 + \beta_{15} v_1^2 d_2^2 + \beta_{16} d_1^2 d_2^2 + \beta_{17} v_1 d_1 d_2 + \beta_{18} v_1^2 d_1^2 d_2^2$
Polynomial 8	$\beta_0 + \beta_1 v_1 + \beta_2 v_2 + \beta_3 v_3 + \beta_4 d_1 + \beta_5 d_2 + \beta_6 v_1^2 + \beta_7 v_2^2 + \beta_8 v_3^2 + \beta_9 d_1^2 + \beta_{10} d_2^2 + \beta_{11} v_2 d_1 + \beta_{12} v_2 d_2 + \beta_{13} d_1 d_2 + \beta_{14} v_2^2 d_1^2 + \beta_{15} v_2^2 d_2^2 + \beta_{16} d_1^2 d_2^2 + \beta_{17} v_2 d_1 d_2 + \beta_{18} v_2^2 d_1^2 d_2^2$
Polynomial 9	$\beta_0 + \beta_1 v_1 + \beta_2 v_2 + \beta_3 v_3 + \beta_4 d_1 + \beta_5 d_2 + \beta_6 v_1^2 + \beta_7 v_2^2 + \beta_8 v_3^2 + \beta_9 d_1^2 + \beta_{10} d_2^2 + \beta_{11} v_3 d_1 + \beta_{12} v_3 d_2 + \beta_{13} d_1 d_2 + \beta_{14} v_3^2 d_1^2 + \beta_{15} v_3^2 d_2^2 + \beta_{16} d_1^2 d_2^2 + \beta_{17} v_3 d_1 d_2 + \beta_{18} v_3^2 d_1^2 d_2^2$

Table B.2: Table which describes the terms included in the polynomial portion of the emulator model.

B.2 Credible Bound Diagnostics

B.2.1 Wave 1

Just as in Section 5.3.5, it is necessary to check that the credible bounds calculated give an accurate model for the error in the estimated response from the fitted emulator model. Again, to do this the full simulator was used to calculate total costs for a new sample of 500 values of simulator input. Then, credible bounds at various credibility

levels were calculated using the methodology of Section 5.2.6. If these credible bounds are a good model for error in the estimation from emulation, it is expected that at the 99% credibility level approximately 495 (99%) of the simulated values will fall within the credible bounds, at the 95% credibility level 475 (95%) of the simulated values will fall within the credible bounds and at the 90% credibility level 450 (90%) of the simulated values will fall within the credible bounds.

Credible Level	Expected Simulations Falling Into Credible Intervals	Observed Simulations Falling Into Credible Intervals
99%	495	498
95%	475	492
90%	450	483

Table B.3: Table detailing how many of the simulated values lie in the credibility intervals of the estimate from the emulator model fitted in the first wave for the example detailed in Section 6.1.1.

Table B.3 details how many evaluations of total costs from the simulator lie within the credibility bounds for the estimate from the emulator in comparison to how many would be expected if the credibility bounds are an accurate model for the error in the estimated response from the emulator fitted in the first wave for the example of Section 6.1.1. As can be seen, it appears that the credible bounds over-estimate error in the response as fewer simulated responses are falsely rejected than would be expected for a given credibility level. For example, at the 90% credibility level only 17 of the simulations fell outside of the credible bounds, in comparison to the 50 that would be expected.

As the widths of the credible bounds are wider and falsely exclude fewer calculations than would be expected for a given credibility level, this means that the chance of falsely eliminating a decision from consideration using the methodology of Section 6.2.1 is lower than the 5% used in Section 6.3.1. If the credible bounds were narrower, such that the number of simulations that lie inside them is closer to the number that would be expected, more decisions could be eliminated in the first wave.

B.2.2 Wave 3

As was noted in Section 6.3.2, the credible intervals are much narrower for the emulator model fitted in the third wave in comparison to the emulator model fitted in the first wave. Therefore, a new sample of 500 simulator inputs was taken (over only the range of decisions considered by the third wave model) and credible intervals for total costs estimates from the emulator at these inputs were compared to calculations from simulation, to check whether this decreased width in credible intervals is due to an increased level of confidence in the estimate, or represents error being under-estimated in the emulator model fitted in the third wave.

Credible Level	Expected Simulations Falling Into Credible Intervals	Observed Simulations Falling Into Credible Intervals
99%	495	498
95%	475	491
90%	450	477

Table B.4: Table detailing how many of the simulated values lie in the credibility intervals of the estimate from the emulator model fitted in the third wave for the example detailed in Section 6.1.1.

Table B.4 details how many evaluations of the simulator lie in the credibility bounds for the estimate from the emulator in comparison to how many would be expected if the credibility bounds are an accurate model for the error in the estimated response from the emulator model fitted in the third wave for the example of Section 6.1.1. As can be seen, the credible intervals falsely exclude estimates from simulation at a similar rate to what was observed in Table B.3. This indicates that despite the credible bounds being narrower in the third wave, this does not come at the expense of under-estimating error in the expected response.

However, it is noted that, as was the case for the first wave model, a greater number of simulated costs are included in the credible intervals than would be expected for a given level of credibility, indicating that the credible intervals may be slightly too wide. Further, it was also noted that no further decisions were eliminated from consideration based on the third wave model, as the credible intervals for the estimates of expected costs were wide in comparison to the variation in expected costs as the reinforcement

decision was varied. If the credible intervals were narrower, this may allow for a further reduction in the decision space.

B.3 Further Graphical Illustrations of the Emulation Approximation

B.3.1 Further Consideration of the Emulation Approximation When Varying Nuclear and CCGT availability Probabilities

Figure 6.9 of Section 6.1.3 illustrated how estimates of mean constraint costs from the fitted emulator model vary as nuclear availability probability and CCGT availability probability are varied for the example of Section 6.1.1, when assuming that no B6 or B7a reinforcement had been made. These graphs were compared to the equivalent calculations from the simulator in Figure 6.1 of Section 6.1.2. This subsection gives further thought to this comparison, by considering the plot of differences and relative differences between the two values, as well as credible intervals for the estimates from emulation. Further, Section 6.1.3 noted how the emulation estimate was slightly hindered as extreme values for 4 of the 5 variables were considered, so it is illustrated how the estimates from the emulator improve when even a small amount of B6 and B7a reinforcement is considered.

Figure B.1 displays the difference between the calculations from the simulator and estimates from the emulator as nuclear availability probability and CCGT availability probability are varied, when assuming a peak demand magnification of 0.95 and that no reinforcement of either boundary has been made, with Figure B.2 displaying an equivalent plot when assuming a peak demand magnification of 1.05. These plots verify what was noted in Section 6.1.3, that the emulator generally under-estimates costs over the ranges considered, especially when considering a peak demand magnification of 0.95.

When considering a peak demand magnification of 0.95, all costs are under-estimated by the emulator by at least 4% with differences of over 14% being noted when nuclear

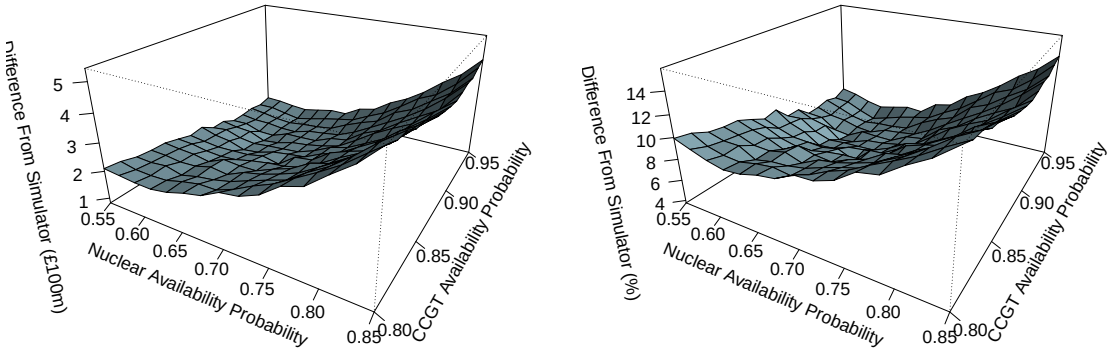

(a) Difference.

(b) Relative difference.

Figure B.1: Plots to show how the difference between mean constraint cost calculations from the simulator and estimates from the emulator vary with nuclear and CCGT availability probabilities, when assuming a peak demand magnification of 0.95.

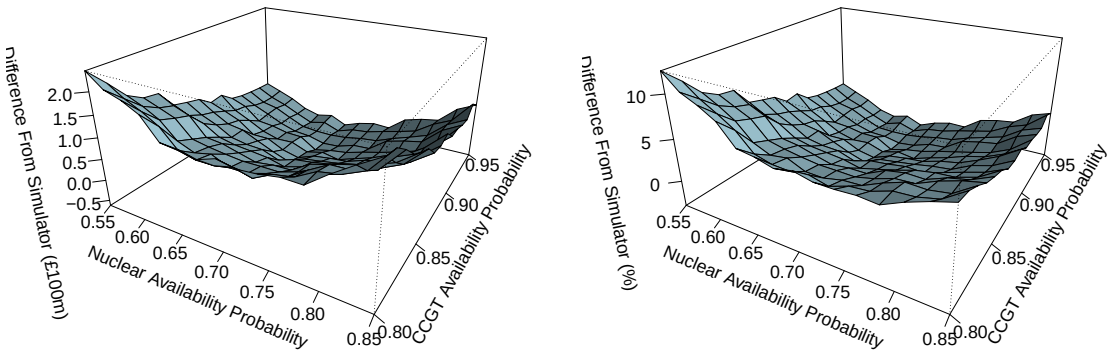

(a) Difference.

(b) Relative difference.

Figure B.2: Plots to show how the difference between mean constraint cost calculations from the simulator and estimates from the emulator vary with nuclear and CCGT availability probabilities, when assuming a peak demand magnification of 1.05.

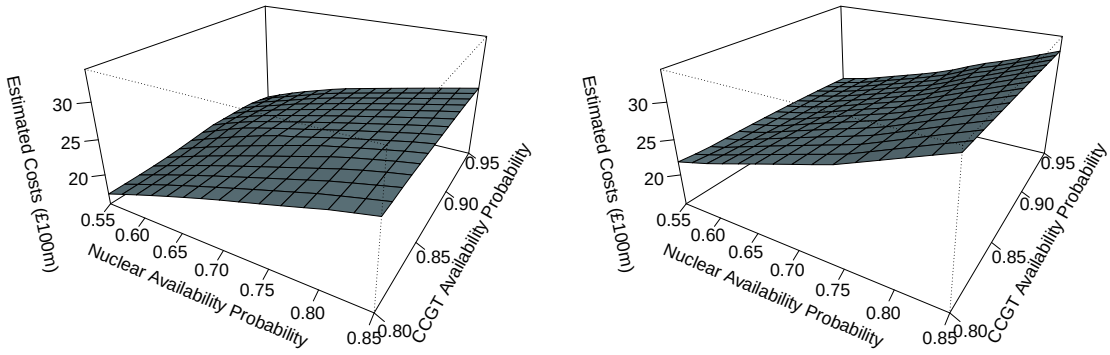

(a) Lower bound.

(b) Upper bound.

Figure B.3: Plots to show how credible bounds of the estimates of mean constraint costs from the emulator vary with nuclear and CCGT availability probabilities, when assuming a peak demand magnification of 0.95 and no B6 or B7a reinforcement.

availability probability is assumed to be 0.85. There is less difference between calculations from simulation and estimates from the fitted emulator when assuming a peak demand magnification of 1.05, with costs even being over-estimated by the emulator when CCGT availability is high, and all differences being less than 12.4%.

Figures B.3 and B.4 display credible intervals for the estimates of mean constraint costs when varying nuclear availability probability and CCGT availability when assuming no reinforcement has been made. These plots make a better comparison to the calculations from simulation displayed in Figure 6.1 of Section 6.1.2, though cost estimates still appear to be slightly under estimated when peak demand magnification is assumed to be 0.95 and nuclear availability probability is assumed to be 0.85.

74.7% of the simulated values of Figure 6.1 (a) fell within the credible bounds of Figure B.3, in comparison to the 95% that would be expected, indicating that the credible intervals when assuming no reinforcement, 0.95 peak demand magnification and high nuclear availability are too narrow and under-estimate the error in the estimate. However, when assuming a peak demand magnification of 1.05, 97.4% of the simulated values of Figure 6.1 (b) fell within the credible bounds of Figure B.4, which is close to what would be expected, indicating that the credible bounds are adequate over this range (possibly even a little wide).

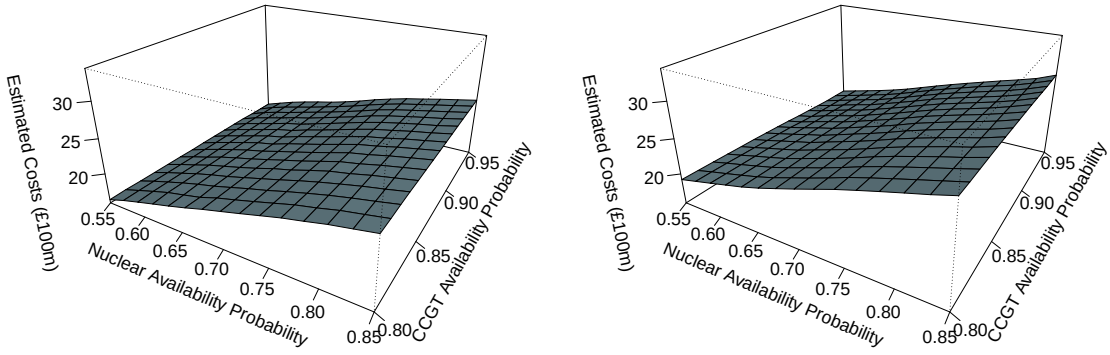

(a) Lower bound.

(b) Upper bound.

Figure B.4: Plots to show how credible bounds of the estimates of mean constraint costs from the emulator vary with nuclear and CCGT availability probabilities, when assuming a peak demand magnification of 1.05 and no B6 or B7a reinforcement.

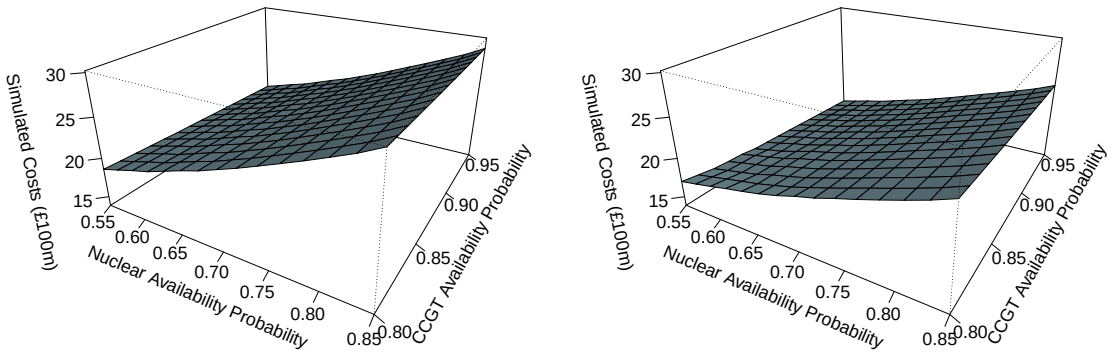

(a) 0.95 peak demand magnification assumed.

(b) 1.05 peak demand magnification assumed.

Figure B.5: Plots to show how calculations of total costs from the simulator vary with nuclear and CCGT availability probabilities, assuming 200 MW B6 and 200 MW B7a reinforcement has been made.

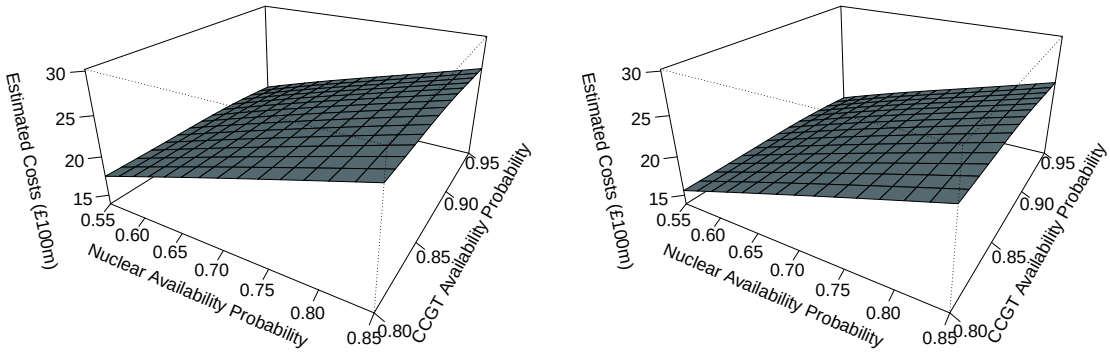

(a) 0.95 peak demand magnification assumed. (b) 1.05 peak demand magnification assumed.

Figure B.6: Plots to show how estimates of total costs from the emulator vary with nuclear and CCGT availability probabilities, assuming 200 MW B6 and 200 MW B7a reinforcement has been made.

Figure B.5 illustrates how calculations of total costs from the simulator vary with nuclear and CCGT availability probabilities for two peak demand levels when assuming 200 MW B6 and 200 MW B7a reinforcement has been made, with Figure B.6 displaying the corresponding plot when estimating from the fitted emulator model. When assuming this small amount of reinforcement, the emulator model compares better to the simulator in comparison to when assuming no reinforcement in Figures 6.1 and 6.9. However, there is still some evidence of under-estimating total costs when assuming a peak demand magnification of 0.95 and a nuclear availability probability of 0.85.

Figure B.7 displays the differences between the emulator and simulator when varying nuclear and CCGT availability probabilities and assuming 200 MW reinforcement of each boundary has been made, when assuming a peak demand magnification of 0.95, with Figure B.8 displaying the corresponding plot when assuming a peak demand magnification of 1.05.

As can be seen, the emulator still under-estimates total costs when assuming a peak demand magnification of 0.95, though to a lesser extent in comparison to when no reinforcement was assumed. However, when assuming a peak demand magnification of 1.05, the emulator under-estimates the calculation from simulation as often as it over-estimates. Further, the relative differences between the emulator and simulator are

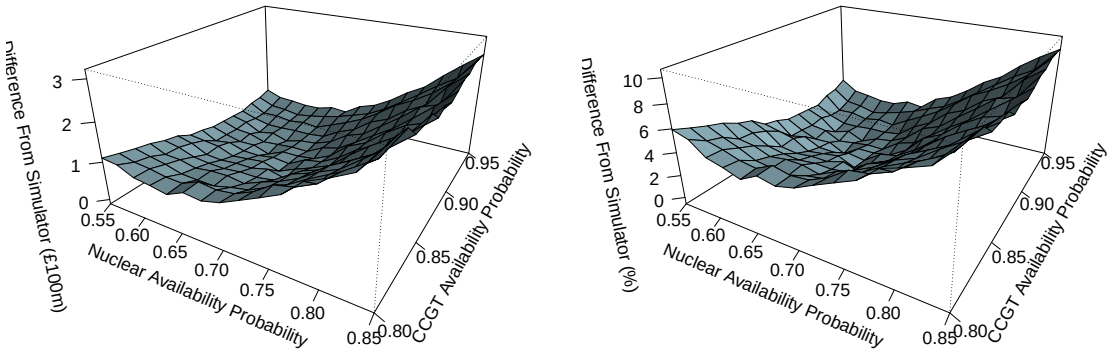

(a) Difference.

(b) Relative difference.

Figure B.7: Plots to show how the difference between total cost calculations from the simulator and estimates from the emulator vary with nuclear and CCGT availability probabilities, assuming a peak demand magnification of 0.95 and that 200 MW B6 and 200 MW B7a reinforcement has been made.

much smaller when assuming each boundary has been reinforced by 200 MW (as the vast majority of differences are now less than 10% or 5% when assuming a peak demand magnification of 0.95 or 1.05 respectively) in comparison to when no reinforcement was assumed (where differences of 10% or 5% were not uncommon when assuming a peak demand magnification of 0.95 or 1.05 respectively).

Figures B.9 and B.10 display credible intervals for the estimates of Figure B.6. As can be seen, when assuming a peak demand magnification of 0.95 (credible bounds displayed in Figure B.9), the upper bound of the credible bounds shows much less evidence of under-estimating calculations from simulation in comparison to when no reinforcement was assumed. This is supported by the fact that 93.3% of the values from simulation are now contained within the 95% credible interval (though this would still suggest that the intervals may be slightly too narrow in this range) when assuming 200 MW reinforcement of each boundary has been made, in comparison to the 74.7% that was noted when assuming no reinforcement was made.

When assuming a peak demand magnification of 1.05 (with credible bounds displayed in Figure B.10), 98.7% of all calculations from simulation were contained in the 95% credible bounds for the estimate from emulation. This suggests that the error at this

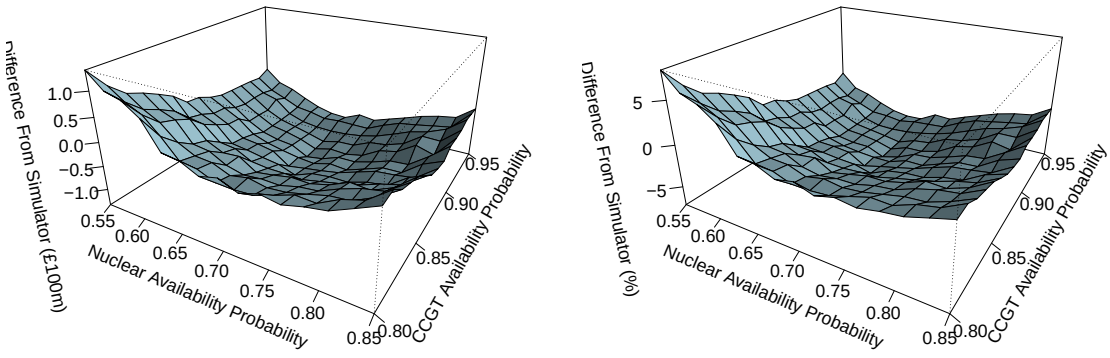

(a) Difference.

(b) Relative difference.

Figure B.8: Plots to show how the difference between total cost calculations from the simulator and estimates from the emulator vary with nuclear and CCGT availability probabilities, assuming a peak demand magnification of 1.05 and that 200 MW B6 and 200 MW B7a reinforcement has been made.

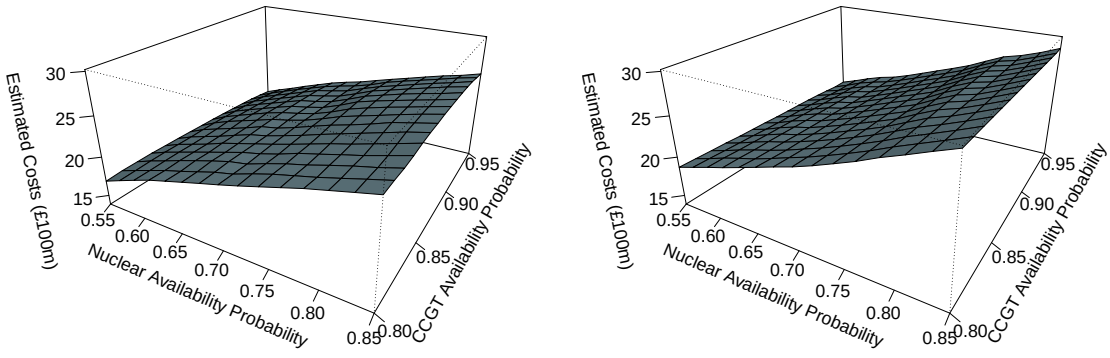

(a) Lower bound.

(b) Upper bound.

Figure B.9: Plots to show how credible bounds of the estimates of total costs from the emulator vary with nuclear and CCGT availability probabilities, when assuming a peak demand magnification of 0.95 and that 200 MW B6 and 200 MW B7a reinforcement has been made.

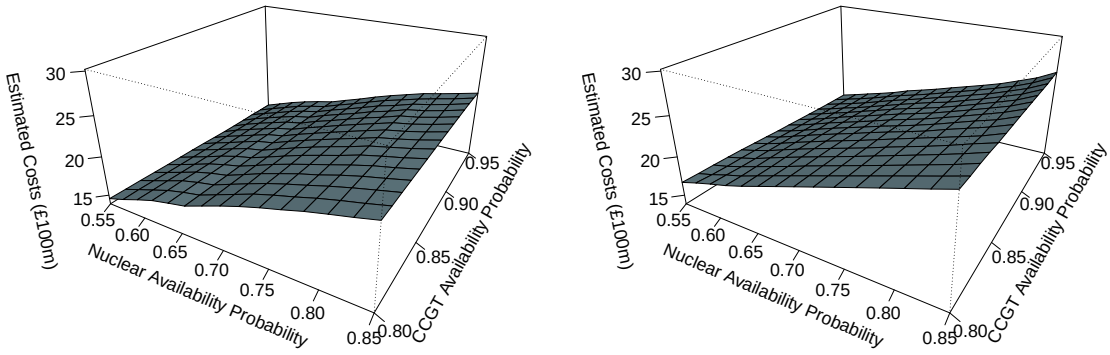

(a) Lower bound.

(b) Upper bound.

Figure B.10: Plots to show how credible bounds of the estimates of total costs from the emulator vary with nuclear and CCGT availability probabilities, when assuming a peak demand magnification of 1.05 and that 200 MW B6 and 200 MW B7a reinforcement has been made.

larger peak demand level is slightly over-estimated and the credible intervals are slightly too wide.

B.3.2 Further Consideration of the Emulation Approximation When Varying B6 and B7a Reinforcement Magnitude

Figure 6.10 of Section 6.1.3 considered how estimates from the fitted emulator model compare to calculations from the simulator displayed in Figure 6.2 of Section 6.1.2, i.e. a comparison of the emulator to the simulator when varying the B6 and B7a reinforcement magnitude for two different assumed values of nuclear availability probability. This subsection gives further thought to this comparison, by considering the plot of differences and relative differences between the two values, as well as credible intervals for the estimates from emulation.

Figure B.11 displays the differences between total costs calculated via simulation and estimated total costs from the fitted emulator, as B6 and B7a reinforcement magnitude are varied when assuming a nuclear availability probability of 0.55, with Figure B.12 showing the corresponding plots when assuming a nuclear availability probability of

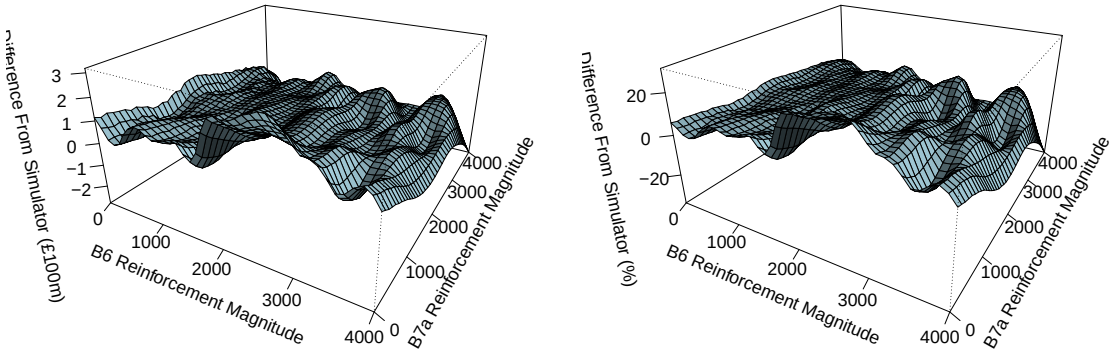

(a) Difference.

(b) Relative Difference.

Figure B.11: Plots to show the difference between calculations from the simulator and estimates from the fitted emulator as B6 and B7a reinforcement magnitude are varied, assuming a nuclear availability probability of 0.55.

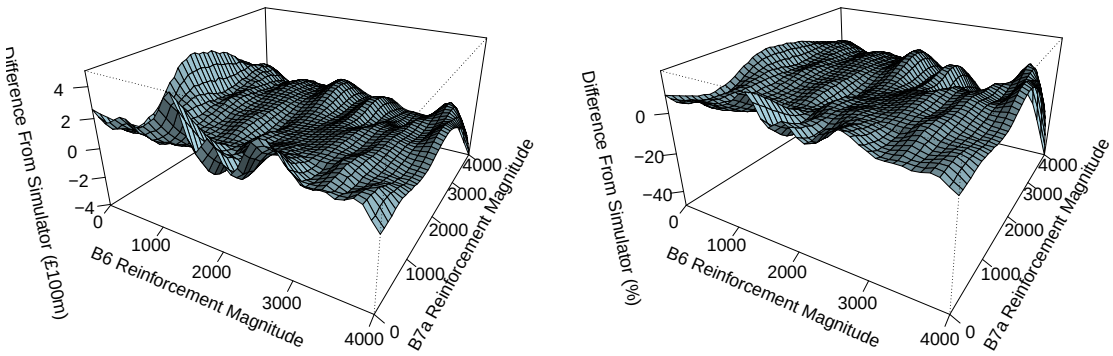

(a) Difference.

(b) Relative Difference.

Figure B.12: Plots to show the difference between calculations from the simulator and estimates from the fitted emulator as B6 and B7a reinforcement magnitude are varied, assuming a nuclear availability probability of 0.85.

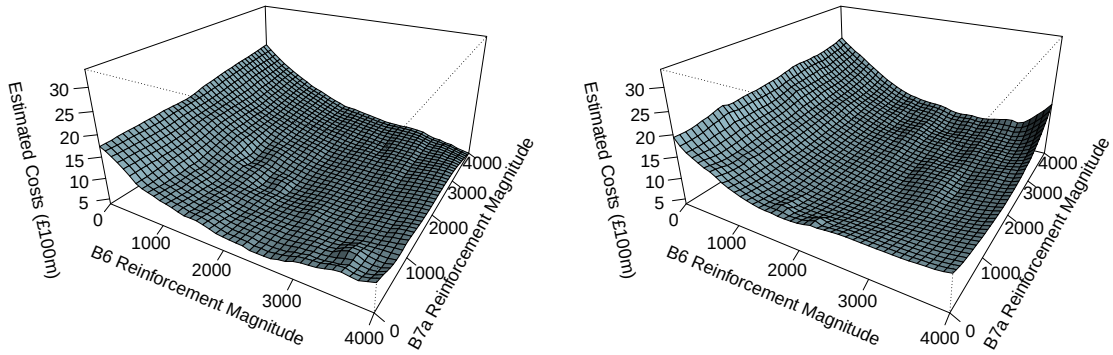

(a) Lower Bound.

(b) Upper Bound.

Figure B.13: Plots to show how credible bounds for the estimated total costs from the emulator vary as B6 and B7a reinforcement magnitude are varied, assuming a nuclear availability probability of 0.55.

0.85 (with both figures assuming CCGT availability probability to be 0.875 and peak demand level to be the level projected by [69]).

As can be seen, whilst the difference between the emulator and simulator can be quite large in real terms (up to several hundreds of millions of pounds at the extremes) the difference relative to the simulator calculation is generally quite small, except where both B6 and B7a reinforcement magnitudes are very large and the emulator over-estimates total costs.

Figure B.13 displays 95% credible bounds for the estimates of total costs from the emulator as B6 and B7a reinforcement magnitude are varied when assuming a nuclear availability probability of 0.55, with Figure B.14 displaying the corresponding plot when assuming a nuclear availability probability of 0.85. As has been noted for similar plots in Section 6.1.3, the credible intervals are particular wide when B6 and B7a reinforcement magnitudes are large with the simulated values lying between the two bounds, indicating that although the emulator over-estimates costs considerably in this range, this is accounted for when assessing the error in the estimate.

When assuming a peak demand magnification of 0.55, 98.6% of the simulated values fell within the 95% credible bounds, whereas 97.0% of the simulated values fell within the 95% credible bounds when assuming a peak demand magnification of 0.85. These

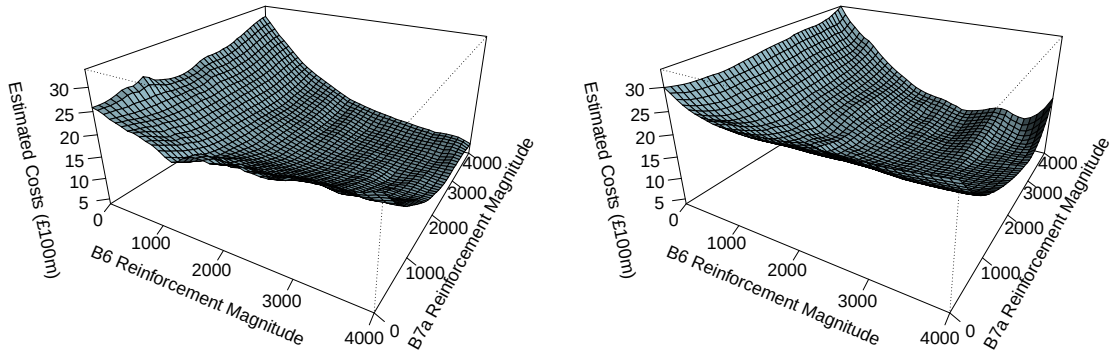

(a) Lower Bound.

(b) Upper Bound.

Figure B.14: Plots to show how credible bounds for the estimated total costs from the emulator vary as B6 and B7a reinforcement magnitude are varied, assuming a nuclear availability probability of 0.85.

are greater than the 95% that would be expected, indicating that error in the estimate is slightly over-estimated.

Further, Figures 6.11 and 6.12 of Section 6.1.3 also considered comparing calculations of total costs from the simulator to estimates from the emulator as B6 and B7a reinforcement magnitude are varied when at least 2000 MW reinforcement has been made on both boundaries (i.e. over the range where the optimal reinforcement would lie). Therefore, Figure B.15 displays 95% credible intervals for estimated total costs from the fitted emulator as B6 and B7a reinforcement magnitudes are varied (for reinforcement magnitudes greater than 2000 MW on both boundaries) when assuming a nuclear availability probability of 0.55, CCGT availability probability of 0.875 and peak demand magnification of 1 (i.e. credible intervals for the estimates displayed in Figure 6.12 (a) of Section 6.1.3) and Figure B.16 displays 95% credible intervals for estimated total costs from the fitted emulator as B6 and B7a reinforcement magnitudes are varied (for reinforcement magnitudes greater than 2000 MW on both boundaries) when assuming a nuclear availability probability of 0.85, CCGT availability probability of 0.875 and peak demand magnification of 1 (i.e. credible intervals for the estimates displayed in Figure 6.12 (b) of Section 6.1.3).

These plots are very similar in shape to the estimates of total costs, with the lower

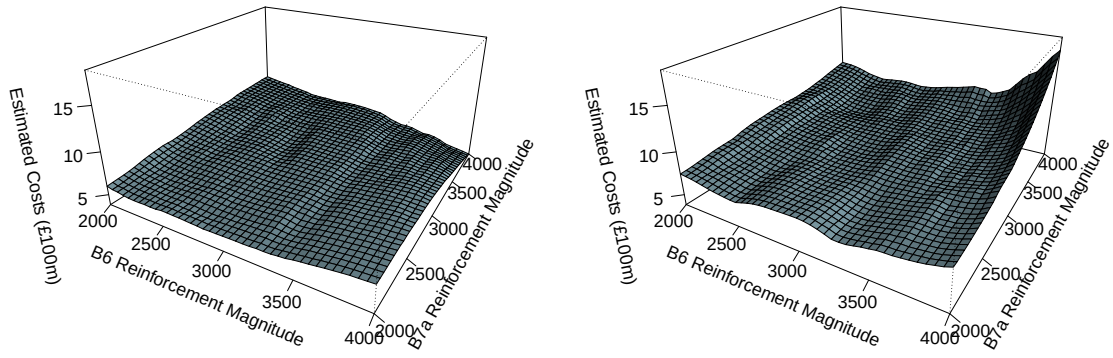

(a) Lower Bound.

(b) Upper Bound.

Figure B.15: Plots to show how credible bounds for the estimated total costs from the emulator vary as B6 and B7a reinforcement magnitude are varied for reinforcement magnitudes greater than 2000 MW on both boundaries, assuming a nuclear availability probability of 0.55.

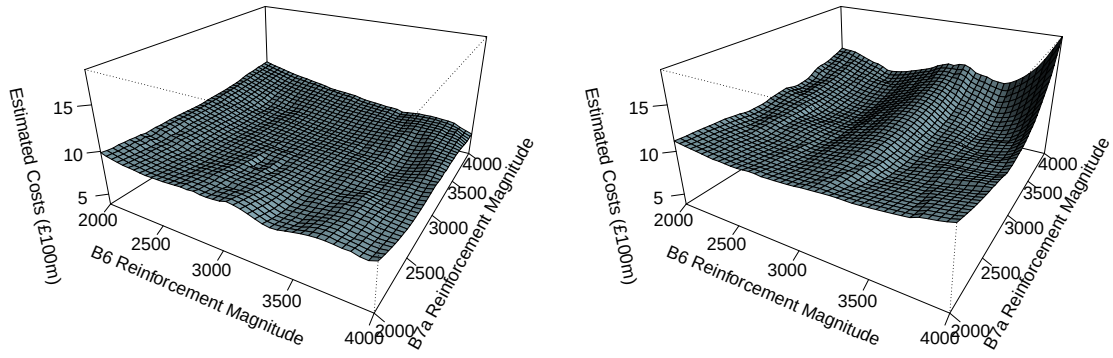

(a) Lower Bound.

(b) Upper Bound.

Figure B.16: Plots to show how credible bounds for the estimated total costs from the emulator vary as B6 and B7a reinforcement magnitude are varied for reinforcement magnitudes greater than 2000 MW on both boundaries, assuming a nuclear availability probability of 0.85.

bound giving a lower estimate of total costs and the upper bound giving a greater estimate of total costs (again, as should be expected). As was the case in Figure 6.6 of Section 6.1.3, the credible intervals are noticeably wider when a large reinforcement is made on both boundaries, indicating the increased level of uncertainty in the estimate.

All calculations from the simulator displayed in Figure 6.11 are contained with credible intervals of Figure B.15 and B.16 (unlike what was previously noted for the credible bounds over the larger ranges of reinforcement considered in Figures B.13 and B.14). This indicates that when a simulated value does not fall in the credible intervals, at least one boundary's reinforcement magnitude is below 2000 MW.

As total costs are lowest when the reinforcement of both boundaries is greater than 2000 MW, this means that the credible intervals over-estimate error in the estimate in the region where the optimal reinforcement decisions lies. This in turn means that there is less chance of falsely eliminating a decision from consideration when applying the methodology of Section 6.2.1 to fit a more accurate emulator model over a smaller range of values of the decision variables.

Appendix C

Chapter 8 Additional Details

C.1 Fitting a Beta Distribution For Given Observations

Section 8.2.1 noted that it would be possible to specify a (scaled) beta distribution to represent beliefs about the availability probability of a particular generating capacity based on the observed availability by the time the mth decision is to be made in the M-stage decision problem. This section gives details on how such a distribution can be fitted based on an observation $\psi_{m,1}$ with weight $\psi_{m,2}$ given to the observation.

C.1.1 Fitting a Beta Distribution

A beta distribution, $Be(x|\alpha, \beta)$, is a function which specifies a probability density function of a random variable, x, between 0 and 1 for given model parameters a and b. Typically, model parameters can be selected such that the expectation of x can be calculated as

$$E(x) = \frac{a}{a+b} \tag{C.1.1}$$

and the variance of x can be calculated as

$$\text{var}(x) = \frac{ab}{(a+b)^2(a+b+1)} \tag{C.1.2}$$

However, [53] offers an alternative view of these model parameters, which is used in this thesis, such that model parameters can be selected such that the expectation of x can be calculated, as in Equation C.1.1, as

$$E(x) = \frac{a}{a+b}$$

and a and b are selected such that $a+b$ is the number of observations the belief about expectation is said to be worth.

Relating this to Section 8.2.1, it was noted that if uncertainty is considered in nuclear availability probability, $\boldsymbol{\psi}_m = (\psi_{m,1}, \psi_{m,2})$ could be used to quantify what has been observed about nuclear availability probability by the time the mth decision is to be made, where $\psi_{m,1}$ denotes the average observed nuclear availability probability in stages 1 to $m-1$ and $\psi_{m,2}$ denotes how much weight is given to these observations. Based on the interpretation of [53], $\psi_{m,1}$ and $\psi_{m,2}$ could be used to specify a beta distribution with model parameters

$$a_\psi = \psi_{m,1}\psi_{m,2} \tag{C.1.3}$$

and

$$b_\psi = \psi_{m,2} - \psi_{m,1}\psi_{m,2} \tag{C.1.4}$$

to represent beliefs about nuclear availability probability in stage m. It can be verified that this gives $\psi_{m,1} = \frac{a_\psi}{a_\psi + b_\psi}$, and $\psi_{m,2} = a_\psi + b_\psi$.

C.1.2 Fitting A Scaled Beta Distribution

The beta distribution is used to specify a probability density function over the range 0 to 1. However, often it is required that a distribution is specified over some alternative range between a lower limit L_l and an upper limit L_u. This can be achieved by using a scaled beta distribution, where a beta distribution is first fitted over the range 0 to 1, then this distribution is shifted and scaled appropriately such that the density occurs over the range L_l to L_u.

If a scaled beta distribution is to be fitted to a variable x over the range L_l to L_u, first

a beta distribution is fitted to the transformed variable $\tilde{x}$ over the range 0 to 1, where

$$\tilde{x} = \frac{x - L_l}{L_u - L_l} \tag{C.1.5}$$

If the expectation of x was $\psi_{m,1}$ with the weight of $\psi_{m,2}$ observations given to this expectation, a transformed expectation can be calculated as

$$\tilde{\psi}_{m,1} = \frac{\psi_{m,1} - L_l}{L_u - L_l} \tag{C.1.6}$$

Model parameters to fit a beta distribution for $\tilde{x}$ can then be calculated as

$$a_\psi = \tilde{\psi}_{m,1}\psi_{m,2} \tag{C.1.7}$$

and

$$b_\psi = \psi_{m,2} - \tilde{\psi}_{m,1}\psi_{m,2} \tag{C.1.8}$$

such that $Be(\tilde{x}|a_\psi, b_\psi)$ is the resulting beta distribution.

This beta distribution can then be shifted and scaled to specify a scaled beta distribution for x over the range L_l to L_u, such that

$$SBe(x|a_\psi, b_\psi, L_l, L_u) = \frac{1}{L_u - L_l} Be(\tilde{x}|a_\psi, b_\psi) \tag{C.1.9}$$

where $SBe(x|a_\psi, b_\psi, L_l, L_u)$ is the resulting scaled beta distribution, the relationship between x and $\tilde{x}$ is defined as in Equation C.1.5 and the factor $\frac{1}{L_u - L_l}$ is used to scale the density of the beta distribution such that the resulting density of the scaled beta distribution integrates to one over the range L_l to L_u, i.e. so that a probability density function is formed over the range L_l to L_u.

C.1.3 Using Observations to Update a Prior Distribution

It is also possible that a given observation in stage m would not be used in isolation to fit a scaled beta distribution to represent beliefs about a variable of interest, but rather to update an initial set of prior beliefs about the variable. Suppose the initial prior beliefs about the variable x (e.g. nuclear availability probability) at the time the

first decision was made are defined by the scaled beta distribution

$$SBe(x|a_0, b_0, L_l, L_u) = \frac{1}{L_u - L_l} Be(\tilde{x}|a_0, b_0) \tag{C.1.10}$$

An observation of the variable of $\psi_{m,1}$ with weight $\psi_{m,2}$ given to this observation could subsequently be used to update the initial prior beliefs.

To do this, first the observation is transformed to the range 0 to 1 as

$$\tilde{\psi}_{m,1} = \frac{\psi_{m,1} - L_l}{L_u - L_l} \tag{C.1.11}$$

An updated scaled beta distribution based on this observation could then be calculated as

$$SBe(x|a_0, b_0, L_l, L_u, \tilde{\psi}_{m,1}, \tilde{\psi}_{m,2}) = \frac{1}{L_u - L_l} Be(x|a_m, b_m) \tag{C.1.12}$$

where

$$a_m = a_0 + \psi_{m,2}\tilde{\psi}_{m,1} \tag{C.1.13}$$

and

$$b_m = b_0 + \psi_{m,2}(1 - \tilde{\psi}_{m,1}) \tag{C.1.14}$$

In doing this, the total weight of these beliefs is equal to the initial weight plus the weight of the observations, and the expectation will be a weighted expectation of the prior beliefs and the observation. This is the same way one would use a beta distribution as a conjugate prior to update beliefs about p, the parameter representing the probability of success in a binomial distribution.

C.2 Backwards Induction

C.2.1 General Backwards Induction Methodology

Section 8.2.2 stated that the multi-stage methodology used in this thesis adapts the methodology of backwards induction to estimate total costs across all M stages as a function of the stage 1 decision only. This section will give details of the general backwards induction methodology for an unfamiliar reader, with a subsequent example to illustrate this methodology being given in Appendix C.2.2.

As noted in Section 8.2.2, backwards induction is a methodology for identifying an optimal decision strategy for a multi-stage decision problem, by first identifying optimal decisions for the final stage which maximise expected profits (or alternatively minimise expected losses) conditional on the current state in the final stage and decisions made in previous stages. Then, optimal decisions are identified for the previous stage to maximise expected profits for stages $M-1$ and M, assuming the decision maker acts optimally in stage M. This is done for each stage, until eventually the optimal stage 1 decision is identified to maximise expected profits across all M stages, assuming the decision maker will act in an optimal manner in stages 2 to M.

For a typical M stage decision problem solved by backwards induction, it is assumed that in each stage there are N_{S^m} possible states to be in, labelled S_j^m for $j = 1, ..., N_{S^m}$, and a decision d_m (with a finite set of values) to be made. If the system is in state S_j^m in stage m and decisions $d_1, ..., d_{m-1}$ have previously been made, then the profit of making decision d_m is a random variable $r(d_m|S_j^m, d_1, ..., d_{m-1})$, with $N_{r_{d_m}|S_j^m,d_1,...,d_{m-1}}$ possible profits labelled $r_{i,d_m|S_j^m,d_1,...,d_{m-1}}$ for $i = 1, ..., N_{r_{d_m}|S_j^m,d_1,...,d_{m-1}}$. If the probability of acquiring profit $r_{i,d_m|S_j^m,d_1,...,d_{m-1}}$ is $p_{i,d_m|S_j^m,d_1,...,d_{m-1}}$ the expected profit of decision d_m can then be calculated as

$$R_m(d_m|S_j^m, d_1, ..., d_{m-1}) = \sum_i r_{i,d_m|S_j^m,d_1,...,d_{m-1}} \times p_{i,d_m|S_j^m,d_1,...,d_{m-1}} \tag{C.2.1}$$

At each stage a decision is to be made to maximise the sum of expected profits between the current and final stage. Backwards induction solves this by first identifying optimal decisions to maximise profits in the final Mth stage, and iteratively working backwards to identify optimal decisions to be made in each previous stage until an optimal strategy is identified for the decision to make in every stage for every possible scenario that could be observed.

In stage M, given that decisions $d_1, ..., d_{M-1}$ were previously made and given that the system is in state S_j^M, the expected profits for making decision d_M are
$R_M(d_M|S_j^M, d_1, ..., d_{M-1})$. The optimal Mth stage decision to be made is represented as $d_M^o(S_j^M, d_1, ..., d_{M-1})$ such that $d_M^o(S_j^M, d_1, ..., d_{M-1})$ maximises
$R_M(d_M|S_j^M, d_1, ..., d_{M-1})$. Optimal decisions are calculated for every possible combination of stage M state and previous stage 1 to stage $M-1$ decisions.

Expected profits in stages $M-1$ to M can then be calculated as a function of the stage $M-1$ decision, d_{M-1}, assuming the decision maker will act optimally in stage M as

$$R_{T,M-1}(d_{M-1}|S_j^{M-1}, d_1, ..., d_{M-2}) = R_{M-1}(d_{M-1}|S_j^{M-1}, d_1, ..., d_{M-2}) + \sum_k R_M(d_M^o(S_k^M, d_1, ..., d_{M-1})|S_k^M, d_1, ..., d_{M-1}) p(S_k^M|S_j^{M-1}) \quad \text{(C.2.2)}$$

where $p(S_k^M|S_j^{M-1})$ is the probability of observing state S_k^M in stage M given that the state is S_j^{M-1} in stage $M-1$. The optimal stage $M-1$ decision, $d_{M-1}^o(S_j^{M-1}, d_1, ..., d_{M-2})$, can then be calculated such that $d_{M-1}^o(S_j^{M-1}, d_1, ..., d_{M-2})$ maximises $R_{T,M-1}(d_{M-1}|S_j^{M-1}, d_1, ..., d_{M-2})$ for the given state in stage $M-1$, S_j^{M-1}, and given that decisions $d_1, ..., d_{M-2}$ were made in the previous $M-2$ stages. Such optimal decisions are identified for all combinations of stage $M-1$ state and stage 1 to $M-2$ decisions.

For a general stage m, expected profits in stages m to M can then be calculated as a function of d_m assuming the decision maker will act optimally in stage $m+1$ to M as

$$R_{T,m}(d_m|S_j^m, d_1, ..., d_{m-1}) = R_m(d_m|S_j^m, d_1, ..., d_{m-1}) + \sum_k R_{T,m+1}(d_{m+1}^o(S_k^{m+1}, d_1, ..., d_m)|S_k^{m+1}, d_1, ..., d_m) p(S_k^{m+1}|S_j^m) \quad \text{(C.2.3)}$$

where $p(S_k^{m+1}|S_j^m)$ is the probability of observing state S_k^{m+1} in stage $m+1$ given that the state is S_j^m in stage m. The optimal stage m decision, $d_m^o(S_j^m, d_1, ..., d_{m-1})$, can then be calculated such that $d_m^o(S_j^m, d_1, ..., d_{m-1})$ maximises $R_{T,m}(d_m|S_j^m, d_1, ..., d_{m-1})$ for the given state in stage m, S_j^m, and given that decisions $d_1, ..., d_{m-1}$ were made in the previous $m-1$ stages. Such optimal decisions are identified for all combinations of state m state and stage 1 to $m-1$ decisions.

This recursion is iteratively solved backwards until eventually the optimal decisions are identified for all M stages for all possible states that can arise in each stage. An example to illustrate this methodology is given in the next subsection.

C.2.2 Backwards Induction Example

Sections 8.2.2 and C.2.1 gave details of how backwards induction can be used as a method for decision making over multiple stages. This section gives a supplementary

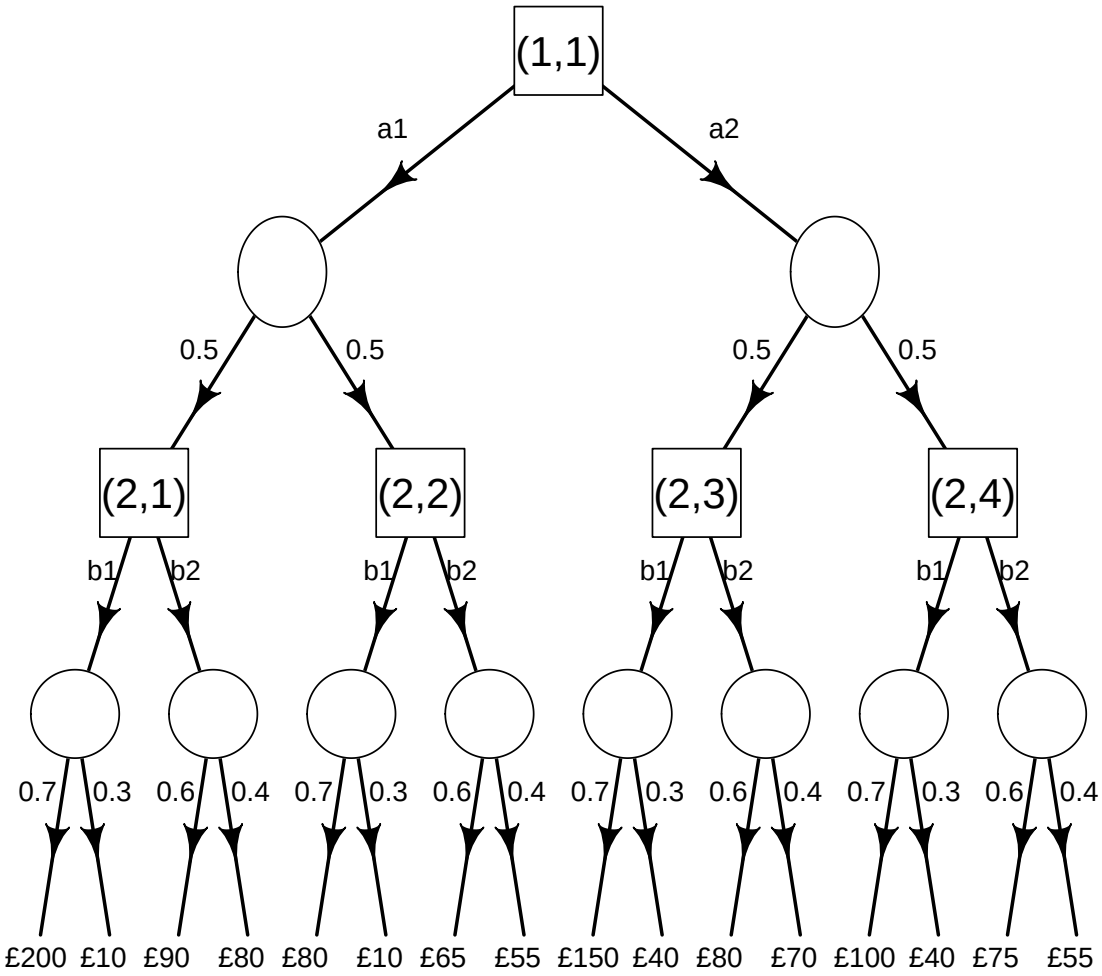

Figure C.1: Tree diagram to illustrate an example 2 stage decision problem.

example to illustrate how this methodology works.

To illustrate the backwards induction methodology, Figure C.1 illustrates an example where 2 sequential decisions are to be made with the objective of maximising expected profit. The profits given in Figure C.1 represent the net present value of profits across both stages. In each decision stage, one of two decisions must be made, with each decision node followed by a chance node which has two potential outcomes. For example, if at decision node $(1, 1)$ decision a1 is made, there is a 0.5 chance of ending up at decision node $(2, 1)$ and a 0.5 chance of ending up at decision node $(2, 2)$. If the decision maker finds themselves at decision node $(2, 2)$, there are again two possible

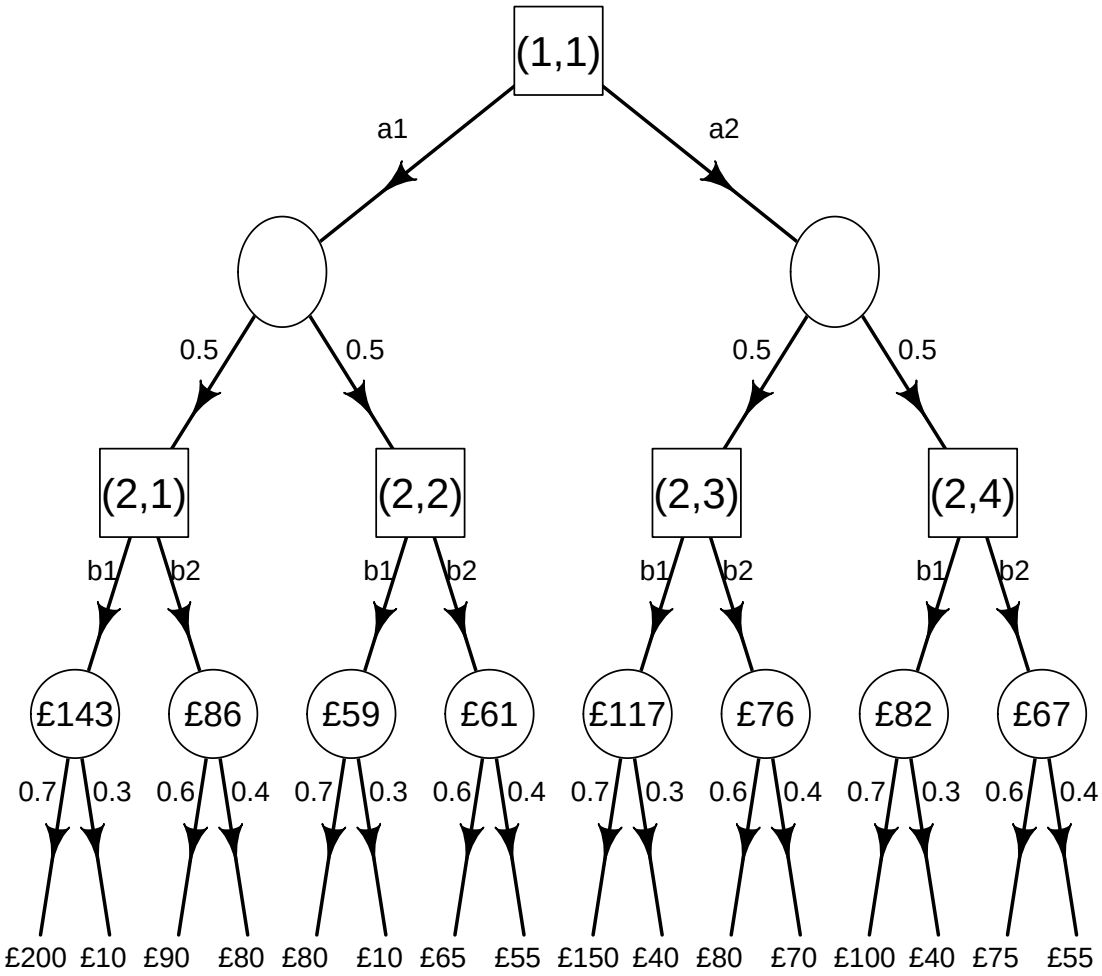

Figure C.2: Tree diagram to illustrate an example 2 stage decision problem, with the final expectations calculated.

decisions that can be made, each followed by a chance node. For example, if decision b1 is made at decision node $(2, 2)$, this will result in a profit of £80 with probability 0.7 and a profit of £10 with probability 0.3.

To identify the optimal decisions to be made, first, expectations at the chance nodes of the final stage are calculated. For example, if decision b1 is made at decision node $(2, 2)$, the expected profits are $£80 \times 0.7 + £10 \times 0.3 = £59$. Figure C.2 displays the expected profits for each of the potential chance nodes after the stage 2 decisions.

These expectations are then used to identify the optimal decisions to be made at each

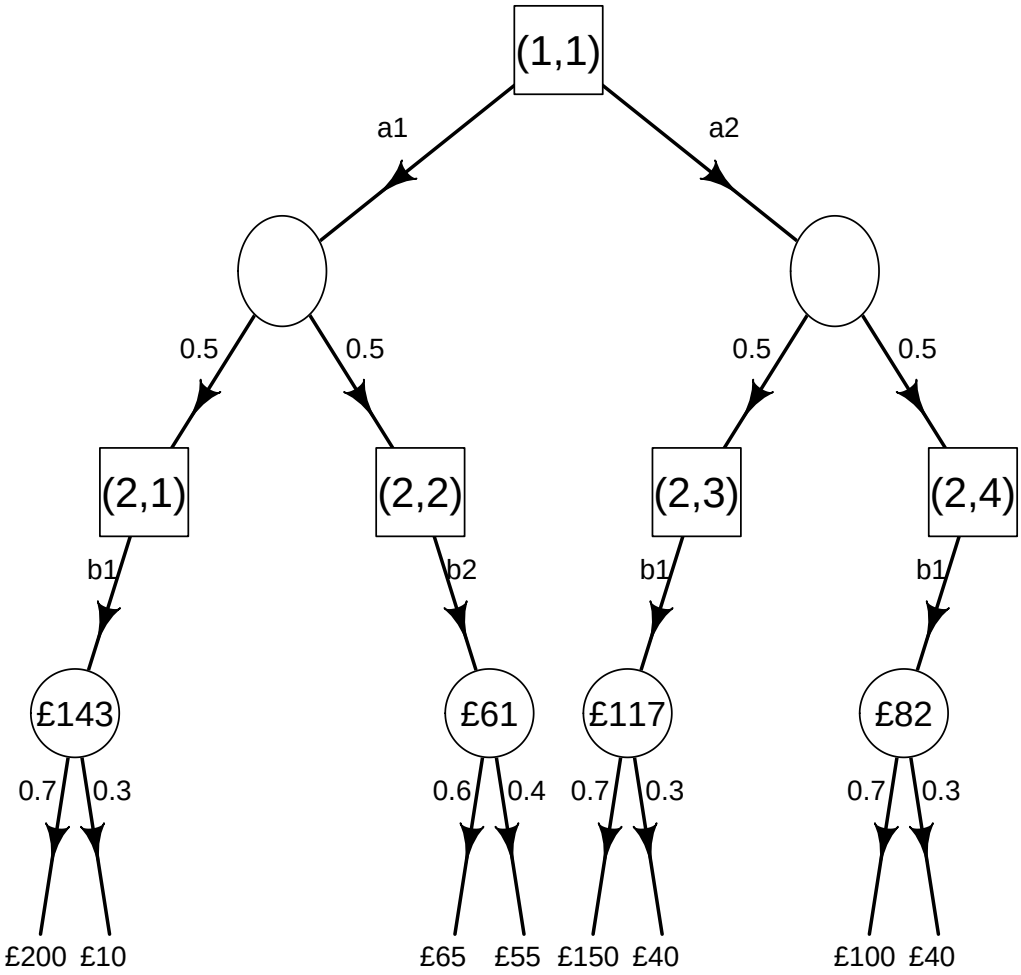

Figure C.3: Tree diagram to illustrate an example 2 stage decision problem, illustrating the decisions that would be made in the second stage.

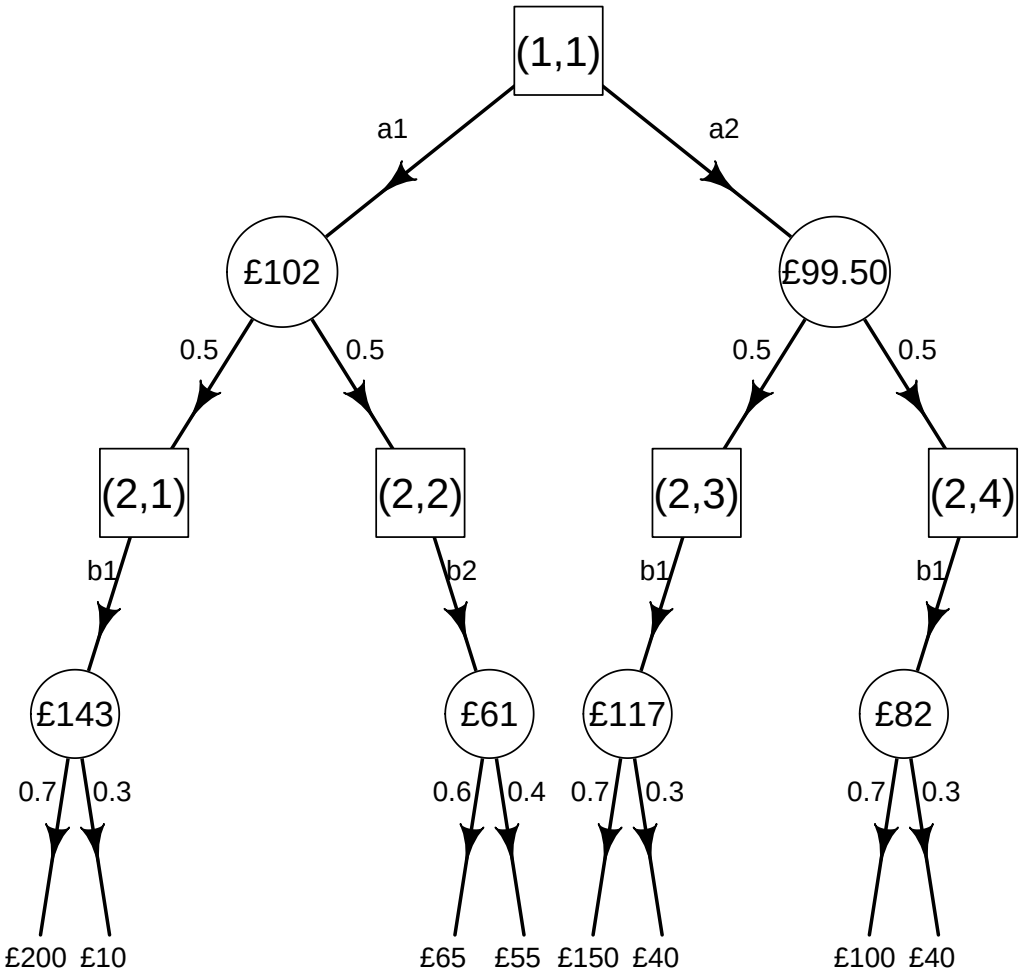

Figure C.4: Tree diagram to illustrate an example 2 stage decision problem, calculating the expected profits as a function of the first decision only.

of the second stage decision nodes to maximise the expected profits. For example, at decision node $(2, 2)$ making decision b1 results in an expected profit of £59, whereas decision b2 results in an expected profit of £61. Therefore, at decision node $(2, 2)$ the optimal decision would be b2. Figure C.3 displays the decision tree, assuming the optimal decision is made at each decision node of the second stage.

Expected profits are then calculated for each of the first stage decisions. For example, if decision a1 is made there is 0.5 chance of being at node $(2, 1)$ in stage 2 and a 0.5 chance of being at node $(2, 2)$ at stage 2. If the decision maker is at node $(2, 1)$ in stage 2, it is assumed they will act optimally and make decision b1, which results in

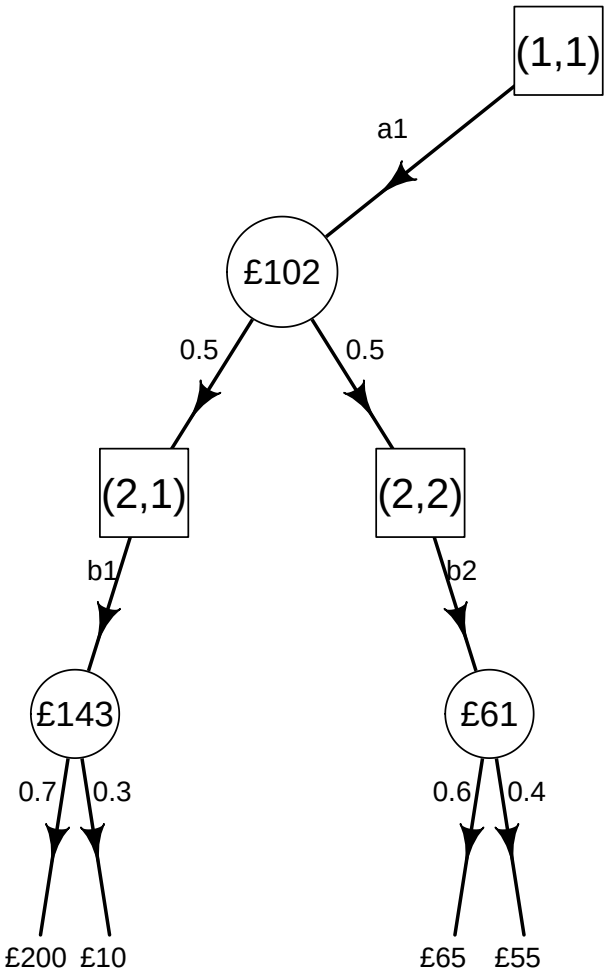

Figure C.5: Tree diagram to illustrate an example 2 stage decision problem, illustrating the optimal decision strategy.

an expected profit of £143 whereas if the decision maker is at node $(2, 2)$ in stage 2, it is assumed they will act optimally and make decision b2, which results in an expected profit of £61. The expected profit of decision a1 at node $(1, 1)$ is therefore $£143 \times 0.5 + £61 \times 0.5 = £102$.

Figure C.4 displays the expected profits of each stage 1 decision. If decision a1 is made, the expected profits are £102, whereas the expected profits of decision a2 are £99.50. Therefore, decision a1 would be made to maximise expected profits.

Figure C.5 displays the optimal decision strategy to be made across both stages. Ini-

tially decision a1 is made. If at stage 2 the decision maker is at node $(2, 1)$, decision b1 would be made whereas if at stage 2 the decision maker is at node $(2, 2)$, decision b2 would be made.

C.3 Fitting Emulator Models for the Example of Section 8.3

Previously, Section 5.3.3 considered model selection for the emulator model fitted to approximate the simulator of total costs for the example presented in Chapter 5, whilst Section 6.1.3 and Appendix B.1 considered model selection for the emulator model fitted to approximate the simulator of total costs for the example presented in Chapter 6. For the two stage problem of Section 8.3 it is also necessary to consider the number of training runs and terms to be included in the polynomial portion of the emulator models for mean constraint costs in stage 1, $\tilde{f}_{c,1}(\mathbf{v}_1, \mathbf{d}_1)$, mean constraint costs in stage 2, $\tilde{f}_{c,2}(\mathbf{v}_2, \mathbf{d}_2|\mathbf{d}_1)$, and expected total costs in stage 2 as a function of stage 1 decision and stage 2 scenario only, $\tilde{G}_{T,2,\boldsymbol{\psi}_2}(\mathbf{d}_1, \boldsymbol{\psi}_2)$.

As mean constraint costs for stage 1 are estimated based on a year 6 power system background (the power system background assumed for the example of Section 6.1.1); consider uncertainty in nuclear availability probability, CCGT availability probability and peak demand level (the same three variables, as well as the same ranges for uncertainty, as considered for the example detailed in Section 6.1.1); and consider decision variables as the reinforcement magnitudes of the B6 and B7a boundaries (the same two decision variables as for the example detailed in Section 6.1.1), this would suggest that the emulator for stage 1 mean constraint costs should be fitted using 300 training runs and using a polynomial of the form

$$\beta_0 + \beta_1 v_{1,1} + \beta_2 v_{1,2} + \beta_3 v_{1,3} + \beta_4 d_{1,1} + \beta_5 d_{1,2} + \beta_6 v_{1,1}^2 + \beta_7 v_{1,2}^2 + \beta_8 v_{1,3}^2 + \beta_9 d_{1,1}^2 + \beta_{10} d_{1,2}^2 + \beta_{11} v_{1,1} d_{1,1} + \beta_{12} v_{1,1} d_{1,2} + \beta_{13} d_{1,1} d_{1,2} + \beta_{14} v_{1,1}^2 d_{1,1}^2 + \beta_{15} v_{1,1}^2 d_{1,2}^2 + \beta_{16} d_{1,1}^2 d_{1,2}^2 + \beta_{17} v_{1,1} d_{1,1} d_{1,2} + \beta_{18} v_{1,1}^2 d_{1,1}^2 d_{1,2}^2$$

for the polynomial portion of the emulator, as was identified in Section 6.1.3 and Appendix B.1. This was verified to also be a suitable design for $\tilde{f}_{c,1}(\mathbf{v}_1, \mathbf{d}_1)$.

The remainder of this section will identify an appropriate number of training runs and appropriate forms for the polynomial portion of the emulator models $\tilde{f}_{c,2}(\mathbf{v}_2, \mathbf{d}_2|\mathbf{d}_1)$ and $\tilde{G}_{T,2,\psi_2}(\mathbf{d}_1, \boldsymbol{\psi}_2)$.

C.3.1 Model Selection for $\tilde{f}_{c,2}$

As was noted in Section 8.2.7, the output of the simulator of mean constraint costs in stage 2, $f_{c,2}(\mathbf{v}_2, \mathbf{d}_2|\mathbf{d}_1)$, is dependent on the total reinforcement after the second decision, i.e. $\mathbf{d}_{T_2} = \mathbf{d}_1 + \mathbf{d}_2$, and not the individual reinforcements in stages 1 and 2. For example, if 6500 MW of total B6 reinforcement is built after the second decision, the simulator would not distinguish between 2500 MW being built in stage 1 and 4000 MW in stage 2 or 4000 MW in stage 1 and 2500 MW in stage 2 (or any other combination of reinforcements which result in a total of 6500 MW after the second decision).

This allows for a simplification to be made when fitting an emulator model to approximate $f_{c,2}(\mathbf{v}_2, \mathbf{d}_2|\mathbf{d}_1)$, as it is sufficient to fit the emulator in terms of the total reinforcement after the second decision, $\mathbf{d}_{T_2} = \mathbf{d}_1 + \mathbf{d}_2$, and not the individual reinforcements in stages 1 and 2, $\mathbf{d}_1$ and $\mathbf{d}_2$, i.e. it is sufficient to fit an emulator of the form $\tilde{f}_{c,2}(\mathbf{v}_2, \mathbf{d}_{T_2})$ and not $\tilde{f}_{c,2}(\mathbf{v}_2, \mathbf{d}_2|\mathbf{d}_1)$.

Number of Training Runs	Value of R^2	Value of P	Value of $\tilde{P}$
50	0.9715	3.898×10^{16}	0.03189
100	0.9694	1.516×10^{16}	0.01240
200	0.9662	4.275×10^{15}	0.003498
300	0.9680	2.668×10^{15}	0.002184
400	0.9647	2.915×10^{15}	0.002386
500	0.9639	2.244×10^{15}	0.001837

Table C.1: Table of how the model selection criteria vary with the number of training runs used when fitting the emulator model for mean constraint costs in stage 2, $\tilde{f}_{c,2}$.

Table C.1 considers how the R^2 value of the polynomial portion of the emulator model of stage 2 mean constraint costs, $\tilde{f}_{c,2}(\mathbf{v}_2, \mathbf{d}_{T_2})$, for the example of Section 8.3 varies with the number of training runs used to fit the model. Values of P and $\tilde{P}$ are also given when the fitted emulator model (polynomial plus Gaussian process applied to

its residuals) is used to estimate a response for a second set of 50 training runs which were not used to fit the model.

Recall, P was defined in Equation 5.3.1 of Section 5.3.3 as the mean squared error of the fitted emulator when used to estimate the response of a second set of n_2 evaluations from the simulator which were not used to fit the emulator model. As such P represents a measure of predictive power of the fitted emulator model, with a smaller value of P indicating a greater level of predictive power. $\tilde{P}$ was subsequently defined in Equation 5.3.2 of Section 5.3.3 as the value of P normalised by the variance in the response in the second set of training data, with smaller values of $\tilde{P}$ indicating a greater level of predictive power of the fitted emulator model.

Values in Table C.1 are based on using a polynomial of the form

$$\beta_0+\beta_1 v_{2,1}+\beta_2 v_{2,2}+\beta_3 v_{2,3}+\beta_4 d_{T_2,1}+\beta_5 d_{T_2,2}+\beta_6 v_{2,1}^2+\beta_7 v_{2,2}^2+\beta_8 v_{2,3}^2+\beta_9 d_{T_2,1}^2+\beta_{10} d_{T_2,2}^2$$

in the polynomial portion of the emulator model. This will later be identified as the optimal form of the polynomial portion of the emulator model based on Table C.2.

As can be seen, for all sample sizes the value of R^2 of the fitted emulator model is greater than 0.96, which indicates that a very good fit is given. However, as has previously been noted, this is a measure of how well the model fits the training data and not necessarily how well it predicts a response outside of the training data. P, a measure of how well the model predicts a response for data not used to fit the emulator, shows considerable improvement when using 100 training runs over 50 and further improvement when using 200 training runs over 100. There is a slight improvement in increasing the sample size further to 300 training runs, though little improvement beyond this. This implies it may be optimal to use 300 training runs to fit the emulator, though a good fit could also be acquired using just 200 training runs.

Table C.2 details how the values of R^2, P and $\tilde{P}$ vary with the polynomial model fitted in the polynomial portion of the emulator model, assuming 300 training runs were used to fit the emulator model. Details of the terms included in each of the polynomial portions of the emulator models are given in Table C.3.

As can be seen, including only first order terms with no interactions (polynomial 1 of Table C.3) gives the lowest value of R^2 and the largest value of P indicating this model

Polynomial Model	Value of R^2	Value of P	Value of $\tilde{P}$
Polynomial 1	0.7289	8.455×10^{15}	0.006918
Polynomial 2	0.9680	2.668×10^{15}	0.002184
Polynomial 3	0.9786	3.201×10^{15}	0.002619
Polynomial 4	0.7500	8.031×10^{15}	0.006572
Polynomial 5	0.9738	3.233×10^{15}	0.002646
Polynomial 6	0.9823	4.188×10^{15}	0.003427

Table C.2: Table of how the model selection criteria vary with the form of the polynomial portion of the emulator model used to estimate mean constraint costs in stage 2, $\tilde{f}_{c,2}$.

Polynomial Model	Model Description
Polynomial 1	$\beta_0 + \beta_1 v_{2,1} + \beta_2 v_{2,2} + \beta_3 v_{2,3} + \beta_4 d_{T_2,1} + \beta_5 d_{T_2,2}$
Polynomial 2	$\beta_0 + \beta_1 v_{2,1} + \beta_2 v_{2,2} + \beta_3 v_{2,3} + \beta_4 d_{T_2,1} + \beta_5 d_{T_2,2} + \beta_6 v_{2,1}^2 + \beta_7 v_{2,2}^2 + \beta_8 v_{2,3}^2 + \beta_9 d_{T_2,1}^2 + \beta_{10} d_{T_2,2}^2$
Polynomial 3	$\beta_0 + \beta_1 v_{2,1} + \beta_2 v_{2,2} + \beta_3 v_{2,3} + \beta_4 d_{T_2,1} + \beta_5 d_{T_2,2} + \beta_6 v_{2,1}^2 + \beta_7 v_{2,2}^2 + \beta_8 v_{2,3}^2 + \beta_9 d_{T_2,1}^2 + \beta_{10} d_{T_2,2}^2 + \beta_{11} v_{2,1}^3 + \beta_{12} v_{2,2}^3 + \beta_{13} v_{2,3}^3 + \beta_{14} d_{T_2,1}^3 + \beta_{15} d_{T_2,2}^3$
Polynomial 4	$\beta_0 + \beta_1 v_{2,1} + \beta_2 v_{2,2} + \beta_3 v_{2,3} + \beta_4 d_{T_2,1} + \beta_5 d_{T_2,2} + \beta_6 d_{T_2,1} d_{T_2,2}$
Polynomial 5	$\beta_0 + \beta_1 v_{2,1} + \beta_2 v_{2,2} + \beta_3 v_{2,3} + \beta_4 d_{T_2,1} + \beta_5 d_{T_2,2} + \beta_6 v_{2,1}^2 + \beta_7 v_{2,2}^2 + \beta_8 v_{2,3}^2 + \beta_9 d_{T_2,1}^2 + \beta_{10} d_{T_2,2}^2 + \beta_{11} d_{T_2,1} d_{T_2,2} + \beta_{12} d_{T_2,1}^2 d_{T_2,2}^2$
Polynomial 6	$\beta_0 + \beta_1 v_{2,1} + \beta_2 v_{2,2} + \beta_3 v_{2,3} + \beta_4 d_{T_2,1} + \beta_5 d_{T_2,2} + \beta_6 v_{2,1}^2 + \beta_7 v_{2,2}^2 + \beta_8 v_{2,3}^2 + \beta_9 d_{T_2,1}^2 + \beta_{10} d_{T_2,2}^2 + \beta_{11} v_{2,1}^3 + \beta_{12} v_{2,2}^3 + \beta_{13} v_{2,3}^3 + \beta_{14} d_{T_2,1}^3 + \beta_{15} d_{T_2,2}^3 + \beta_{16} d_{T_2,1} d_{T_2,2} + \beta_{17} d_{T_2,1}^2 d_{T_2,2}^2 + \beta_{18} d_{T_2,1}^3 d_{T_2,2}^3$

Table C.3: Table which describes the terms included in the polynomial portion of the emulator model for mean constraint costs in stage 2, $\tilde{f}_{c,2}$.

gives the poorest fit to the training data as well as giving the poorest predictive power when estimating a response away from the training data. Polynomials 2 and 3 (which include up to 2nd and 3rd order terms of each variable respectively) greatly improve the models, with both having an R^2 value greater than 0.96. However, it appears that third order terms may be unnecessary as only including second order terms gives a slightly lower value of P indicating a greater level of predictive power.

The inclusion of interaction terms does not seem necessary, as for all models they give little improvement in the values R^2 or P in comparison to including no interaction terms. Therefore, it appears that the optimal form of the polynomial model used in $\tilde{f}_{c,2}(\mathbf{v}_2, \mathbf{d}_{T_2})$ is a second order polynomial with no interaction terms (polynomial 2 in

Table C.3).

C.3.2 Model Selection for $\tilde{G}_{T,2,\boldsymbol{\psi}_2}$

Further to identifying an appropriate numbers of training runs and forms for the polynomial portions of $\tilde{f}_{c,1}$ and $\tilde{f}_{c,2}$ (the emulator models to approximate the simulator of mean constraint costs in stages 1 and 2 respectively), an appropriate number of training runs and form of the polynomial portion of the emulator model must be identified for $\tilde{G}_{T,2,\boldsymbol{\psi}_2}(\mathbf{d}_1, \boldsymbol{\psi}_2)$, the emulator which models expected total costs in stage 2 as a function of stage 1 decision and stage 2 scenario only. For the example detailed in Section 8.3, $\boldsymbol{\psi}_2$ is a single variable which informs the beliefs about peak demand level in the second stage.

Number of Training Runs	Value of R^2	Value of P	Value of $\tilde{P}$
25	0.9968	7.794×10^{13}	0.006992
50	0.9953	6.211×10^{13}	0.005572
100	0.9947	7.081×10^{13}	0.006353
200	0.9950	6.576×10^{13}	0.005899
300	0.9942	6.834×10^{13}	0.006130
400	0.9935	6.649×10^{13}	0.005965

Table C.4: Table of how the model selection criteria vary with the number of training runs used when fitting $\tilde{G}_{T,2,\boldsymbol{\psi}_2}$.

Table C.4 displays how the values of R^2, P and $\tilde{P}$ vary with the number of training runs used to fit the emulation model. The values in this table assumed the form of the polynomial portion of the emulator model used was

$$\beta_0 + \beta_1\boldsymbol{\psi}_2 + \beta_2 d_{1,1} + \beta_3 d_{1,2} + \beta_4\boldsymbol{\psi}_2^2 + \beta_5 d_{1,1}^2 + \beta_6 d_{1,2}^2$$

which will later be identified as the optimal form of the polynomial portion of the emulator model based on Table C.5.

As can be seen, sample size has very little effect on the fitted model, with all samples giving a value of R^2 greater than 0.99 and a similar predictive power (similar values of P). There is some weak evidence that the predictive power is improved slightly when using a sample of size 50 over 25, but no need to use a sample size greater than 50.

Polynomial Model	Value of R^2	Value of P	Value of $\tilde{P}$
Polynomial 1	0.9842	1.356×10^{14}	0.01216
Polynomial 2	0.9953	6.211×10^{13}	0.005572
Polynomial 3	0.9964	7.929×10^{13}	0.007114
Polynomial 4	0.9900	9.905×10^{13}	0.008886
Polynomial 5	0.9961	6.703×10^{13}	0.006013
Polynomial 6	0.9973	8.959×10^{13}	0.008035
Polynomial 7	0.9930	1.303×10^{14}	0.01169
Polynomial 8	0.9979	7.950×10^{13}	0.007131
Polynomial 9	0.9992	1.035×10^{14}	0.009286

Table C.5: Table of how the model selection criteria vary with the form of the polynomial portion of the emulator model used when fitting $\tilde{G}_{T,2,\boldsymbol{\psi}_2}$.

Polynomial Model	Model Description
Polynomial 1	$\beta_0 + \beta_1\boldsymbol{\psi}_2 + \beta_2 d_{1,1} + \beta_3 d_{1,2}$
Polynomial 2	$\beta_0 + \beta_1\boldsymbol{\psi}_2 + \beta_2 d_{1,1} + \beta_3 d_{1,2} + \beta_4\boldsymbol{\psi}_2^2 + \beta_5 d_{1,1}^2 + \beta_6 d_{1,2}^2$
Polynomial 3	$\beta_0 + \beta_1\boldsymbol{\psi}_2 + \beta_2 d_{1,1} + \beta_3 d_{1,2} + \beta_4\boldsymbol{\psi}_2^2 + \beta_5 d_{1,1}^2 + \beta_6 d_{1,2}^2 + \beta_7\boldsymbol{\psi}_2^3 + \beta_8 d_{1,1}^3 + \beta_9 d_{1,2}^3$
Polynomial 4	$\beta_0 + \beta_1\boldsymbol{\psi}_2 + \beta_2 d_{1,1} + \beta_3 d_{1,2} + \beta_4 d_{1,1} d_{1,2}$
Polynomial 5	$\beta_0 + \beta_1\boldsymbol{\psi}_2 + \beta_2 d_{1,1} + \beta_3 d_{1,2} + \beta_4\boldsymbol{\psi}_2^2 + \beta_5 d_{1,1}^2 + \beta_6 d_{1,2}^2 + \beta_7 d_{1,1} d_{1,2} + \beta_8 d_{1,1}^2 d_{1,2}^2$
Polynomial 6	$\beta_0 + \beta_1\boldsymbol{\psi}_2 + \beta_2 d_{1,1} + \beta_3 d_{1,2} + \beta_4\boldsymbol{\psi}_2^2 + \beta_5 d_{1,1}^2 + \beta_6 d_{1,2}^2 + \beta_7\boldsymbol{\psi}_2^3 + \beta_8 d_{1,1}^3 + \beta_9 d_{1,2}^3 + \beta_{10} d_{1,1} d_{1,2} + \beta_{11} d_{1,1}^2 d_{1,2}^2 + \beta_{12} d_{1,1}^3 d_{1,2}^3$
Polynomial 7	$\beta_0 + \beta_1\boldsymbol{\psi}_2 + \beta_2 d_{1,1} + \beta_3 d_{1,2} + \beta_4\boldsymbol{\psi}_2 d_{1,1} + \beta_5\boldsymbol{\psi}_2 d_{1,2} + \beta_6 d_{1,1} d_{1,2} + \beta_7\boldsymbol{\psi}_2 d_{1,1} d_{1,2}$
Polynomial 8	$\beta_0 + \beta_1\boldsymbol{\psi}_2 + \beta_2 d_{1,1} + \beta_3 d_{1,2} + \beta_4\boldsymbol{\psi}_2^2 + \beta_5 d_{1,1}^2 + \beta_6 d_{1,2}^2 + \beta_7\boldsymbol{\psi}_2 d_{1,1} + \beta_8\boldsymbol{\psi}_2 d_{1,2} + \beta_9 d_{1,1} d_{1,2} + \beta_{10}\boldsymbol{\psi}_2^2 d_{1,1}^2 + \beta_{11}\boldsymbol{\psi}_2^2 d_{1,2}^2 + \beta_{12} d_{1,1}^2 d_{1,2}^2 + \beta_{13}\boldsymbol{\psi}_2 d_{1,1} d_{1,2} + \beta_{14}\boldsymbol{\psi}_2^2 d_{1,1}^2 d_{1,2}^2$
Polynomial 9	$\beta_0 + \beta_1\boldsymbol{\psi}_2 + \beta_2 d_{1,1} + \beta_3 d_{1,2} + \beta_4\boldsymbol{\psi}_2^2 + \beta_5 d_{1,1}^2 + \beta_6 d_{1,2}^2 + \beta_7\boldsymbol{\psi}_2^3 + \beta_8 d_{1,1}^3 + \beta_9 d_{1,2}^3 + \beta_{10}\boldsymbol{\psi}_2 d_{1,1} + \beta_{11}\boldsymbol{\psi}_2 d_{1,2} + \beta_{12} d_{1,1} d_{1,2} + \beta_{13}\boldsymbol{\psi}_2^2 d_{1,1}^2 + \beta_{14}\boldsymbol{\psi}_2^2 d_{1,2}^2 + \beta_{15} d_{1,1}^2 d_{1,2}^2 + \beta_{16}\boldsymbol{\psi}_2^3 d_{1,1}^3 + \beta_{17}\boldsymbol{\psi}_2^3 d_{1,2}^3 + \beta_{18} d_{1,1}^3 d_{1,2}^3 + \beta_{19}\boldsymbol{\psi}_2 d_{1,1} d_{1,2} + \beta_{20}\boldsymbol{\psi}_2^2 d_{1,1}^2 d_{1,2}^2 + \beta_{21}\boldsymbol{\psi}_2^3 d_{1,1}^3 d_{1,2}^3$

Table C.6: Table which describes the terms included in the polynomial portion of the emulator models considered for $\tilde{G}_{T,2,\boldsymbol{\psi}_2}$.

Table C.5 gives details of how the model selection criteria (values of R^2, P and $\tilde{P}$) vary with the form of the polynomial portion of the fitted emulator model, with details of the terms included in the polynomial model given in Table C.6.

As can be seen, a polynomial model which uses only first order terms and no interaction terms still has a high value of R^2 (over 0.98). This can be slightly improved by including second order terms with no interactions (R^2 in excess of 0.995) though the improvement in including additional terms beyond this is minimal.

The measure of the models predictive power, value of P (with a smaller value indicating a better fit), is improved when including second order terms in addition to first order terms. However, including any further terms in the model does not improve the models predictive power.

Therefore, the example of Section 8.3 will use 50 training runs (i.e. $N_\theta = 50$) and use a polynomial regression model including up to second order terms with no interactions (polynomial 2 from Table C.6) to fit the model $\tilde{G}_{T,2,\boldsymbol{\psi}_2}(\mathbf{d}_1, \boldsymbol{\psi}_2)$.

Appendix D

Chapter 9 Additional Details

D.1 Fitting Emulator Models for the Example of Section 9.2

The selection of an appropriate number of training runs used to fit an emulator, as well as an appropriate form for the polynomial portion of the emulator model, was previously considered in Section 5.3.3 for the example presented in Chapter 5, Section 6.1.3 and Appendix B.1 for the example presented in Chapter 6 and Appendix C.3 for the two stage decision problem detailed in Section 8.3.

This section will give consideration to the number of training runs to be used and terms to be included in the polynomial portion of the emulator models for the example detailed in Section 9.2, i.e. for the emulator models to approximate the simulator for mean constraint costs in stage 1 ($\tilde{f}_{c,1}(\mathbf{v}_1, \mathbf{d}_1)$), mean constraint costs in stage 2 ($\tilde{f}_{c,2}(\mathbf{v}_2, \mathbf{d}_2|\mathbf{d}_1)$), mean constraint costs in stage 3 ($\tilde{f}_{c,3}(\mathbf{v}_3, \mathbf{d}_3|\mathbf{d}_{T_2})$), expected total costs in stage 3 as a function of stage 2 total reinforcement and stage 3 scenario only ($\tilde{G}_{T,3,\boldsymbol{\psi}_3}(\mathbf{d}_{T_2}, \boldsymbol{\psi}_3)$) and expected total costs in stage 2 onwards as a function of stage 1 decision and stage 2 scenario only ($\tilde{G}_{T,2,\boldsymbol{\psi}_2}(\mathbf{d}_1, \boldsymbol{\psi}_2)$).

However, the third stage of the example of Section 9.2 is equivalent to the second stage of Section 8.3 (i.e. both estimate costs based on a year 16 power system background, consider the same two decision variables and consider uncertainties in the same 3 variables). Therefore, the model selections detailed in Appendix C.3.1 and Appendix C.3.2

are valid for selecting an appropriate number of training runs and terms to be included in the polynomial portion of the emulator models for mean constraint costs in stage 3 ($\tilde{f}_{c,3}(\mathbf{v}_3, \mathbf{d}_3|\mathbf{d}_{T_2})$) and expected total costs in stage 3 as a function of stage 2 total reinforcement and stage 3 scenario only ($\tilde{G}_{T,3,\psi_3}(\mathbf{d}_{T_2}, \boldsymbol{\psi}_3)$) respectively. This means that the emulator model which approximates the simulator of mean constraint costs in the third stage, $\tilde{f}_{c,3}(\mathbf{v}_3, \mathbf{d}_3|\mathbf{d}_{T_2})$, is fitted using 300 training runs, and the polynomial potion of the emulator model takes the form

$$\beta_0 + \beta_1 v_{3,1} + \beta_2 v_{3,2} + \beta_3 v_{3,3} + \beta_4 d_{T_3,1} + \beta_5 d_{T_3,2} + \beta_6 v_{3,1}^2 + \beta_7 v_{3,2}^2 + \beta_8 v_{3,3}^2 + \beta_9 d_{T_3,1}^2 + \beta_{10} d_{T_3,2}^2$$

A Gaussian process model is then used to smooth the residuals of this polynomial regression model.

The emulator model for expected total costs in stage 3 as a function of stage 2 total reinforcement and stage 3 scenario only, $\tilde{G}_{T,3,\psi_3}(\mathbf{d}_{T_2}, \boldsymbol{\psi}_3)$, is fitted using 50 training runs and the polynomial portion of the emulator model takes the form

$$\beta_0 + \beta_1 \boldsymbol{\psi}_3 + \beta_2 d_{T_2,1} + \beta_3 d_{T_2,2} + \beta_4 \boldsymbol{\psi}_3^2 + \beta_5 d_{T_2,1}^2 + \beta_6 d_{T_2,2}^2$$

A Gaussian process model is then used to smooth the residuals of this polynomial regression model.

Further, the first stages of the examples of both Section 8.3 and Section 9.2 consider estimating costs based on a year 6 power system background, consider decision variables of reinforcing the B6 and B7a boundaries and consider the same uncertainty ranges for nuclear availability probability, CCGT availability probability and peak demand level. As was noted in Appendix C.3, this is equivalent to the example of Section 6.1.1 which would suggest, based on the results of Section 6.1.3 and Appendix B.1, that an appropriate emulator model to approximate the simulator of mean constraint costs in the first stage, $\tilde{f}_{c,1}(\mathbf{v}_1, \mathbf{d}_1)$, is to be fitted using 300 training runs, with a polynomial portion of the emulator model of the form

$$\beta_0 + \beta_1 v_{1,1} + \beta_2 v_{1,2} + \beta_3 v_{1,3} + \beta_4 d_{1,1} + \beta_5 d_{1,2} + \beta_6 v_{1,1}^2 + \beta_7 v_{1,2}^2 + \beta_8 v_{1,3}^2 + \beta_9 d_{1,1}^2 + \beta_{10} d_{1,2}^2 + \beta_{11} v_{1,1} d_{1,1} + \beta_{12} v_{1,1} d_{1,2} + \beta_{13} d_{1,1} d_{1,2} + \beta_{14} v_{1,1}^2 d_{1,1}^2 + \beta_{15} v_{1,1}^2 d_{1,2}^2 + \beta_{16} d_{1,1}^2 d_{1,2}^2 + \beta_{17} v_{1,1} d_{1,1} d_{1,2} + \beta_{18} v_{1,1}^2 d_{1,1}^2 d_{1,2}^2$$

with a Gaussian process model then used to smooth the residuals of this polynomial regression model, which was again verified to also be appropriate for $\tilde{f}_{c,1}(\mathbf{v}_1, \mathbf{d}_1)$.

However, for the example of Section 9.2, an optimal number of training runs and terms to be included in polynomial portion of the emulator model must still be identified for the emulator model which approximates the simulator for mean constraint costs in stage 2 ($\tilde{f}_{c,2}(\mathbf{v}_2, \mathbf{d}_2|\mathbf{d}_1)$) and the emulator model which models expected total costs in stage 2 onwards as a function of stage 1 decision and stage 2 scenario only ($\tilde{G}_{T,2,\boldsymbol{\psi}_2}(\mathbf{d}_1, \boldsymbol{\psi}_2)$). This will be detailed in the remainder of this section.

D.1.1 Model Selection for $\tilde{f}_{c,2}$

As was noted in Appendix C.3.1, the simulator of mean constraint costs in stage 2, $f_{c,2}(\mathbf{v}_2, \mathbf{d}_2|\mathbf{d}_1)$, is dependent on the total reinforcement after the second decision, i.e. $\mathbf{d}_{T_2} = \mathbf{d}_1 + \mathbf{d}_2$, and not the individual reinforcements in stages 1 and 2. This means it is sufficient to fit an emulator approximation of the form $\tilde{f}_{c,2}(\mathbf{v}_2, \mathbf{d}_{T_2})$ and not $\tilde{f}_{c,2}(\mathbf{v}_2, \mathbf{d}_2|\mathbf{d}_1)$.

Number of Training Runs	Value of R^2	Value of P	Value of $\tilde{P}$
50	0.9476	1.171×10^{16}	0.07022
100	0.9269	8.229×10^{15}	0.04935
200	0.9158	1.765×10^{15}	0.01059
300	0.9120	3.876×10^{14}	0.002324
400	0.9087	3.818×10^{14}	0.002289
500	0.9106	4.091×10^{14}	0.002453

Table D.1: Table of how the model selection criteria vary with the number of training runs used when fitting the emulator model for mean constraint costs in stage 2, $\tilde{f}_{c,2}$.

Table D.1 considers how the values of model selection criteria (R^2, P and $\tilde{P}$) vary with the number of training runs used to fit the emulator model $\tilde{f}_{c,2}(\mathbf{v}_2, \mathbf{d}_{T_2})$ for the example of Section 9.2. All values of Table D.1 assume that the polynomial portion of the emulator model was of the form

$$\beta_0 + \beta_1 v_{2,1} + \beta_2 v_{2,2} + \beta_3 v_{2,3} + \beta_4 d_{T_2,1} + \beta_5 d_{T_2,2} + \beta_6 v_{2,1}^2 + \beta_7 v_{2,2}^2 + \beta_8 v_{2,3}^2 + \beta_9 d_{T_2,1}^2 + \beta_{10} d_{T_2,2}^2$$

which will later be identified as the optimal form of the polynomial portion of the emulator model based on Table D.2.

All sample sizes give a value of R^2 of at least 0.9, which indicates all models give quite a good fit to the training data. However, it is also necessary to consider how

well the fitted emulator models estimate a response for simulator input not used to fit the emulator model. Therefore, Table D.1 also details how values of P and $\tilde{P}$ vary when using the fitted emulator models (polynomial plus Gaussian process applied to its residuals) to estimate a response for a second set of 50 training runs which were not used to fit the model. Recall, P was defined in Equation 5.3.1 of Section 5.3.3 as the mean squared error of the fitted emulator when used to predict the response of a second set of n_2 evaluations from the simulator which were not used to fit the emulator model. As such, P represents a measure of predictive power of the fitted emulator model, with a smaller value of P indicating a greater level of predictive power. $\tilde{P}$ was subsequently defined in Equation 5.3.2 of Section 5.3.3 as the value of P normalised by the variance in the response in the second set of training data, with smaller values of $\tilde{P}$ indicating a greater level of predictive power of the fitted emulator model.

As can be seen, the values of P and $\tilde{P}$ decrease as additional training runs are used to construct the emulator model until 300 training runs are used, indicating a greater level of predictive power of the emulator from using a greater number of training runs to fit it. However, there appears to be little benefit in using more than 300 training runs to construct the emulator model.

Polynomial Model	Value of R^2	Value of P	Value of $\tilde{P}$
Polynomial 1	0.6982	9.297×10^{14}	0.005575
Polynomial 2	0.9120	3.876×10^{14}	0.002324
Polynomial 3	0.9283	4.605×10^{14}	0.002761
Polynomial 4	0.7725	7.522×10^{14}	0.004611
Polynomial 5	0.9638	4.857×10^{14}	0.002912
Polynomial 6	0.9802	5.883×10^{14}	0.003528

Table D.2: Table of how the model selection criteria vary with the form of the polynomial portion of the emulator model used to estimate mean constraint costs in stage 2, $\tilde{f}_{c,2}$.

Table D.2 details how the values of R^2, P and $\tilde{P}$ vary with polynomial model fitted in the polynomial portion of the emulator model. Details of the terms included in each of the polynomial models are given in Table D.3.

As can be seen, including only first order terms with no interactions gives the lowest value of R^2 at 0.70, as well as the largest value of P, which indicates that such a model

results in the poorest fit to the training data used to fit the emulator model, as well as giving the poorest predictive power when estimating a response for input values not used to fit the emulator model.

Including second order terms in the polynomial model results in a considerable improvement in the fit of the training data, with an R^2 value greater than 0.91, with a slight further improvement when including third order terms. Further, including interaction terms does appear to improve the fit to the training data, with polynomial 6 giving an R^2 value greater than 0.98. However, this may be the result of over-fitting as opposed to genuinely improving the model, as the predictive power of the model (detailed by value of P) is slightly worse when including interaction terms. Selecting a model to maximise the predictive power of the resulting emulator (polynomial model plus Gaussian process applied to its residuals) by minimising the value of P of the resulting model would suggest using polynomial 2 from Table D.3 as the form of the polynomial portion of the emulator model, i.e. the polynomial portion of the emulator model is a second order polynomial with no interaction terms.

Polynomial Model	Model Description
Polynomial 1	$\beta_0 + \beta_1 v_{2,1} + \beta_2 v_{2,2} + \beta_3 v_{2,3} + \beta_4 d_{T_2,1} + \beta_5 d_{T_2,2}$
Polynomial 2	$\beta_0 + \beta_1 v_{2,1} + \beta_2 v_{2,2} + \beta_3 v_{2,3} + \beta_4 d_{T_2,1} + \beta_5 d_{T_2,2} + \beta_6 v_{2,1}^2 + \beta_7 v_{2,2}^2 + \beta_8 v_{2,3}^2 + \beta_9 d_{T_2,1}^2 + \beta_{10} d_{T_2,2}^2$
Polynomial 3	$\beta_0 + \beta_1 v_{2,1} + \beta_2 v_{2,2} + \beta_3 v_{2,3} + \beta_4 d_{T_2,1} + \beta_5 d_{T_2,2} + \beta_6 v_{2,1}^2 + \beta_7 v_{2,2}^2 + \beta_8 v_{2,3}^2 + \beta_9 d_{T_2,1}^2 + \beta_{10} d_{T_2,2}^2 + \beta_{11} v_{2,1}^3 + \beta_{12} v_{2,2}^3 + \beta_{13} v_{2,3}^3 + \beta_{14} d_{T_2,1}^3 + \beta_{15} d_{T_2,2}^3$
Polynomial 4	$\beta_0 + \beta_1 v_{2,1} + \beta_2 v_{2,2} + \beta_3 v_{2,3} + \beta_4 d_{T_2,1} + \beta_5 d_{T_2,2} + \beta_6 d_{T_2,1} d_{T_2,2}$
Polynomial 5	$\beta_0 + \beta_1 v_{2,1} + \beta_2 v_{2,2} + \beta_3 v_{2,3} + \beta_4 d_{T_2,1} + \beta_5 d_{T_2,2} + \beta_6 v_{2,1}^2 + \beta_7 v_{2,2}^2 + \beta_8 v_{2,3}^2 + \beta_9 d_{T_2,1}^2 + \beta_{10} d_{T_2,2}^2 + \beta_{11} d_{T_2,1} d_{T_2,2} + \beta_{12} d_{T_2,1}^2 d_{T_2,2}^2$
Polynomial 6	$\beta_0 + \beta_1 v_{2,1} + \beta_2 v_{2,2} + \beta_3 v_{2,3} + \beta_4 d_{T_2,1} + \beta_5 d_{T_2,2} + \beta_6 v_{2,1}^2 + \beta_7 v_{2,2}^2 + \beta_8 v_{2,3}^2 + \beta_9 d_{T_2,1}^2 + \beta_{10} d_{T_2,2}^2 + \beta_{11} v_{2,1}^3 + \beta_{12} v_{2,2}^3 + \beta_{13} v_{2,3}^3 + \beta_{14} d_{T_2,1}^3 + \beta_{15} d_{T_2,2}^3 + \beta_{16} d_{T_2,1} d_{T_2,2} + \beta_{17} d_{T_2,1}^2 d_{T_2,2}^2 + \beta_{18} d_{T_2,1}^3 d_{T_2,2}^3$

Table D.3: Table which describes the terms included in the polynomial portion of the emulator model for mean constraint costs in stage 2, $\tilde{f}_{c,2}$.

D.1.2 Model Selection for $\tilde{G}_{T,2,\boldsymbol{\psi}_2}$

An appropriate number of training runs and form of the polynomial portion of the emulator model must also be identified for $\tilde{G}_{T,2,\boldsymbol{\psi}_2}(\mathbf{d}_1, \boldsymbol{\psi}_2)$, the emulator which models expected total costs in stage 2 onwards as a function of stage 2 scenario and stage 1 decision only. For the example of Section 9.2, $\boldsymbol{\psi}_2$ is a single variable which informs the beliefs about peak demand level in the second stage.

Number of Training Runs	Value of R^2	Value of P	Value of $\tilde{P}$
25	0.9922	2.735×10^{13}	0.001392
50	0.9957	2.594×10^{13}	0.001320
100	0.9968	2.781×10^{13}	0.001415
200	0.9945	2.704×10^{13}	0.001376
300	0.9952	2.653×10^{13}	0.001350
400	0.9938	2.572×10^{13}	0.001309

Table D.4: Table of how the model selection criteria vary with the number of training runs used when fitting $\tilde{G}_{T,2,\boldsymbol{\psi}_2}$.

Details of how the values of R^2, P and $\tilde{P}$ vary with the number of training runs used to fit the emulation model are given in Table D.4. The values in this table assumed the form of the polynomial portion of the emulator model used was

$$\beta_0 + \beta_1\boldsymbol{\psi}_2 + \beta_2 d_{1,1} + \beta_3 d_{1,2} + \beta_4\boldsymbol{\psi}_2^2 + \beta_5 d_{1,1}^2 + \beta_6 d_{1,2}^2$$

which will later be identified as the optimal form of the polynomial portion of the emulator model based on Table D.5.

All sample sizes give a similarly good to fit to the training data, with all values of R^2 exceeding 0.99. Further, all fitted models result in similar values of P and $\tilde{P}$ when predicting a response for an additional 50 training runs not used to fit the emulator, indicating a similar level of predictive power for all sample sizes. There is some weak evidence (slight increase in R^2 from 0.9922 to 0.9957 and slight decrease in P from 2.735×10^{13} to 2.594×10^{13}) in favour of using 50 training runs over 25, but no need to use more than 50 training runs to fit the emulator model for $\tilde{G}_{T,2,\boldsymbol{\psi}_2}$.

Details of how values of R^2, P and $\tilde{P}$ vary with the form of the polynomial used for the polynomial portion of the emulator model are given in Table D.5. Details of the terms included in the polynomial portion of the emulator model are given in Table D.6.

Polynomial Model	Value of R^2	Value of P	Value of $\tilde{P}$
Polynomial 1	0.9904	3.581×10^{13}	0.001823
Polynomial 2	0.9957	2.594×10^{13}	0.001320
Polynomial 3	0.9976	2.925×10^{13}	0.001489
Polynomial 4	0.9942	3.062×10^{13}	0.001558
Polynomial 5	0.9962	2.774×10^{13}	0.001412
Polynomial 6	0.9980	3.041×10^{13}	0.001548
Polynomial 7	0.9944	3.557×10^{13}	0.001810
Polynomial 8	0.9971	3.195×10^{13}	0.001627
Polynomial 9	0.9987	3.456×10^{13}	0.001759

Table D.5: Table of how the model selection criteria vary with the form of the polynomial portion of the emulator model used when fitting $\tilde{G}_{T,2,\boldsymbol{\psi}_2}$.

Polynomial Model	Model Description
Polynomial 1	$\beta_0 + \beta_1\boldsymbol{\psi}_2 + \beta_2 d_{1,1} + \beta_3 d_{1,2}$
Polynomial 2	$\beta_0 + \beta_1\boldsymbol{\psi}_2 + \beta_2 d_{1,1} + \beta_3 d_{1,2} + \beta_4\boldsymbol{\psi}_2^2 + \beta_5 d_{1,1}^2 + \beta_6 d_{1,2}^2$
Polynomial 3	$\beta_0 + \beta_1\boldsymbol{\psi}_2 + \beta_2 d_{1,1} + \beta_3 d_{1,2} + \beta_4\boldsymbol{\psi}_2^2 + \beta_5 d_{1,1}^2 + \beta_6 d_{1,2}^2 + \beta_7\boldsymbol{\psi}_2^3 + \beta_8 d_{1,1}^3 + \beta_9 d_{1,2}^3$
Polynomial 4	$\beta_0 + \beta_1\boldsymbol{\psi}_2 + \beta_2 d_{1,1} + \beta_3 d_{1,2} + \beta_4 d_{1,1} d_{1,2}$
Polynomial 5	$\beta_0 + \beta_1\boldsymbol{\psi}_2 + \beta_2 d_{1,1} + \beta_3 d_{1,2} + \beta_4\boldsymbol{\psi}_2^2 + \beta_5 d_{1,1}^2 + \beta_6 d_{1,2}^2 + \beta_7 d_{1,1} d_{1,2} + \beta_8 d_{1,1}^2 d_{1,2}^2$
Polynomial 6	$\beta_0 + \beta_1\boldsymbol{\psi}_2 + \beta_2 d_{1,1} + \beta_3 d_{1,2} + \beta_4\boldsymbol{\psi}_2^2 + \beta_5 d_{1,1}^2 + \beta_6 d_{1,2}^2 + \beta_7\boldsymbol{\psi}_2^3 + \beta_8 d_{1,1}^3 + \beta_9 d_{1,2}^3 + \beta_{10} d_{1,1} d_{1,2} + \beta_{11} d_{1,1}^2 d_{1,2}^2 + \beta_{12} d_{1,1}^3 d_{1,2}^3$
Polynomial 7	$\beta_0 + \beta_1\boldsymbol{\psi}_2 + \beta_2 d_{1,1} + \beta_3 d_{1,2} + \beta_4\boldsymbol{\psi}_2 d_{1,1} + \beta_5\boldsymbol{\psi}_2 d_{1,2} + \beta_6 d_{1,1} d_{1,2} + \beta_7\boldsymbol{\psi}_2 d_{1,1} d_{1,2}$
Polynomial 8	$\beta_0 + \beta_1\boldsymbol{\psi}_2 + \beta_2 d_{1,1} + \beta_3 d_{1,2} + \beta_4\boldsymbol{\psi}_2^2 + \beta_5 d_{1,1}^2 + \beta_6 d_{1,2}^2 + \beta_7\boldsymbol{\psi}_2 d_{1,1} + \beta_8\boldsymbol{\psi}_2 d_{1,2} + \beta_9 d_{1,1} d_{1,2} + \beta_{10}\boldsymbol{\psi}_2^2 d_{1,1}^2 + \beta_{11}\boldsymbol{\psi}_2^2 d_{1,2}^2 + \beta_{12} d_{1,1}^2 d_{1,2}^2 + \beta_{13}\boldsymbol{\psi}_2 d_{1,1} d_{1,2} + \beta_{14}\boldsymbol{\psi}_2^2 d_{1,1}^2 d_{1,2}^2$
Polynomial 9	$\beta_0 + \beta_1\boldsymbol{\psi}_2 + \beta_2 d_{1,1} + \beta_3 d_{1,2} + \beta_4\boldsymbol{\psi}_2^2 + \beta_5 d_{1,1}^2 + \beta_6 d_{1,2}^2 + \beta_7\boldsymbol{\psi}_2^3 + \beta_8 d_{1,1}^3 + \beta_9 d_{1,2}^3 + \beta_{10}\boldsymbol{\psi}_2 d_{1,1} + \beta_{11}\boldsymbol{\psi}_2 d_{1,2} + \beta_{12} d_{1,1} d_{1,2} + \beta_{13}\boldsymbol{\psi}_2^2 d_{1,1}^2 + \beta_{14}\boldsymbol{\psi}_2^2 d_{1,2}^2 + \beta_{15} d_{1,1}^2 d_{1,2}^2 + \beta_{16}\boldsymbol{\psi}_2^3 d_{1,1}^3 + \beta_{17}\boldsymbol{\psi}_2^3 d_{1,2}^3 + \beta_{18} d_{1,1}^3 d_{1,2}^3 + \beta_{19}\boldsymbol{\psi}_2 d_{1,1} d_{1,2} + \beta_{20}\boldsymbol{\psi}_2^2 d_{1,1}^2 d_{1,2}^2 + \beta_{21}\boldsymbol{\psi}_2^3 d_{1,1}^3 d_{1,2}^3$

Table D.6: Table which describes the terms included in the polynomial portion of the emulator models considered for $\tilde{G}_{T,2,\boldsymbol{\psi}_2}$.

As can be seen, all choices of polynomial give similarly good fits, with all values of R^2 exceeding 0.99. The lowest value of R^2 arises from using polynomial 1, which uses only first order terms with no interactions, which is slightly improved when additionally

including second order terms, with an R^2 in excess of 0.995, though there is minimal improvement from including further terms beyond this.

The values of P and $\tilde{P}$, i.e. the measure of the models power to predict a response for data not used to fit the emulator, also shows little variation with polynomial model used, with P minimised (i.e. predictive power maximised) when second order terms with no interaction terms are included.

Therefore, for the example of Section 9.2, $\tilde{G}_{T,2,\boldsymbol{\psi}_2}(\mathbf{d}_1, \boldsymbol{\psi}_2)$ will be fitted using 50 training runs (i.e. $N_{\theta_2} = 50$) and use a polynomial of the form of polynomial 2 from Table D.6, i.e. a second order polynomial term with no interactions.

D.2 Additional Graphs for the Problem of Section 9.2

Section 9.2 detailed a three stage decision problem, with Sections 9.3 to 9.5 illustrating how the methodology of Section 9.1 can be applied to estimate optimal decisions to be made in each stage. Throughout Sections 9.3 to 9.5 many graphs were included to illustrate how estimated expected total costs vary in each stage with reinforcement decision and scenario observed.

In particular, Section 9.5 considered how the estimated optimal reinforcement decision varies with observed scenario for 9 potential stage 3 scenarios, with Figure 9.21 illustrating how estimated expected total costs vary with stage 3 reinforcement decision for a subset of 3 of the 9 scenarios considered. Illustrations of how estimated expected total costs vary with reinforcement decision for all 9 scenarios detailed in Table 9.8 of Section 9.5 are given in Figures D.1 to D.3.

As was noted in Section 9.5, the estimates of expected total costs appear to rise linearly as B7a reinforcement magnitude is increased for all scenarios. This suggests that for all stage 3 scenarios, reinforcement of the B6 boundary is more important than the reinforcement of the B7a boundary, and little to no further B7a reinforcement will be made in any stage 3 scenario. As was also noted in Section 9.5, estimates of expected

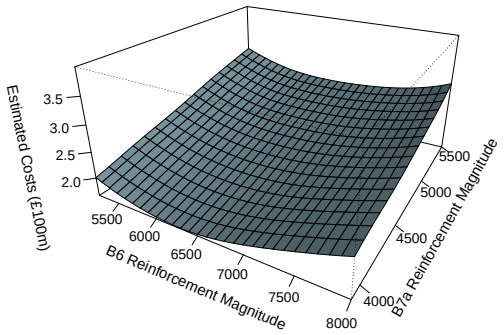

(a) Scenario 1.1 ($\psi_3 = 0.9$).

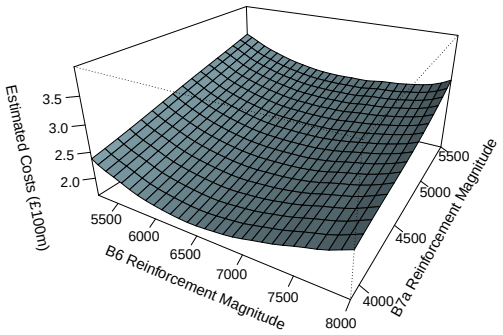

(b) Scenario 1.2 ($\psi_3 = 0.95$).

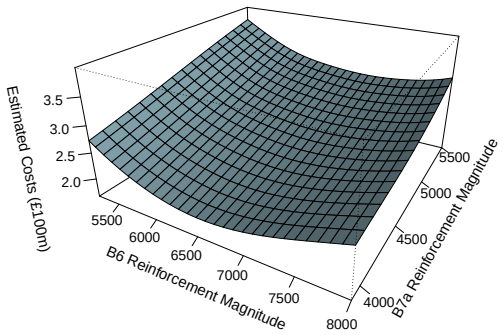

(c) Scenario 1.3 ($\psi_3 = 1$).

Figure D.1: Plots to show how estimates of expected total costs vary with stage 3 total reinforcement decision and scenario.

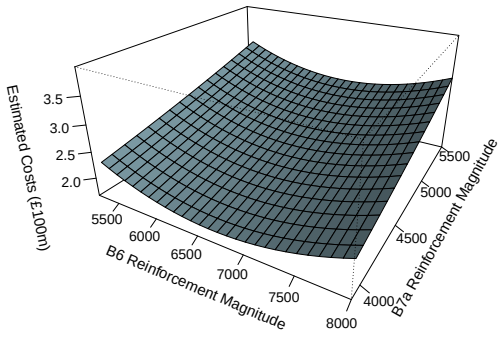

(a) Scenario 2.1 ($\boldsymbol{\psi}_3 = 0.95$).

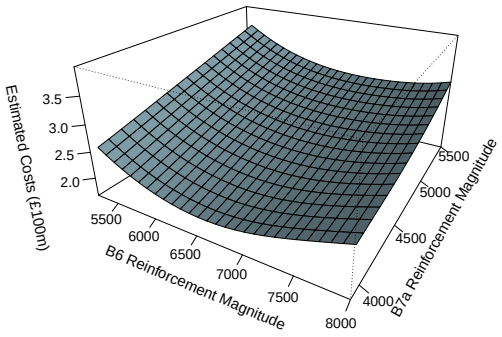

(b) Scenario 2.2 ($\boldsymbol{\psi}_3 = 1$).

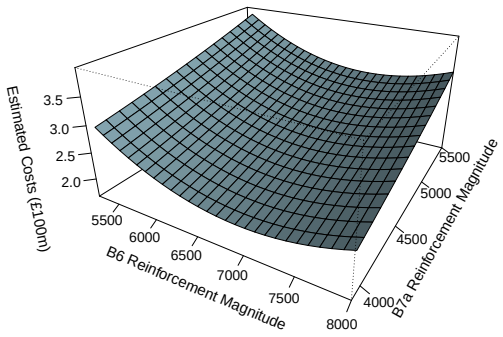

(c) Scenario 2.3 ($\boldsymbol{\psi}_3 = 1.05$).

Figure D.2: Plots to show how estimates of expected total costs vary with stage 3 total reinforcement decision and scenario.

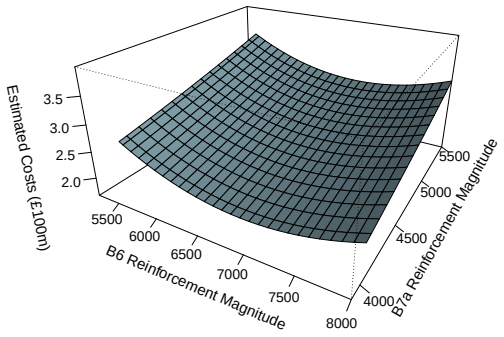

(a) Scenario 3.1 ($\boldsymbol{\psi}_3 = 1$).

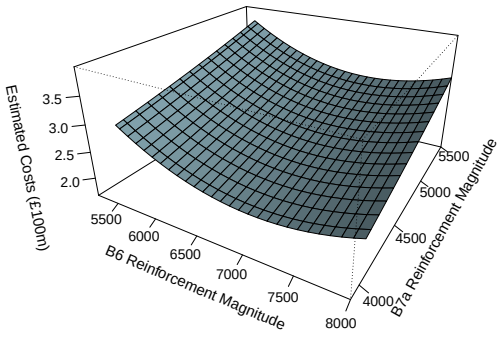

(b) Scenario 3.2 ($\boldsymbol{\psi}_3 = 1.05$).

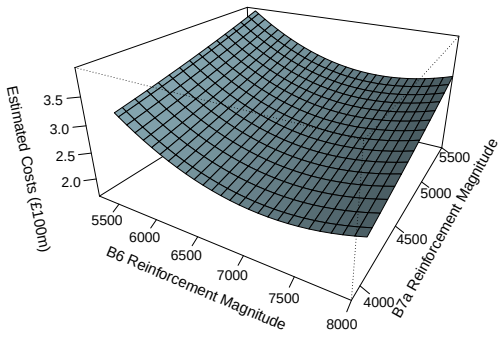

(c) Scenario 3.3 ($\boldsymbol{\psi}_3 = 1.1$).

Figure D.3: Plots to show how estimates of expected total costs vary with stage 3 total reinforcement decision and scenario.

total costs appear to increase as the observed value of $\boldsymbol{\psi}_3$ increases (i.e. as expected stage 3 peak demand level increases).

Estimates of expected total costs for scenarios 1.3, 2.2 and 3.1, which are displayed in Figure D.1 (c), Figure D.2 (b) and Figure D.3 (a) respectively, are very similar, which is what may have been expected as all assumed $\boldsymbol{\psi}_3 = 1$ is observed when the third reinforcement decision is to be made (though, recall from Section 9.5, each assume a different reinforcement decision was previously made in stage 2). However, estimates of expected total costs are slightly greater on average in scenario 1.3 than scenario 2.2, and slightly greater in scenario 2.2 than in scenario 3.1. This is to be expected as scenario 3.1 assumes a larger stage 2 reinforcement was previously made on both boundaries in comparison to scenarios 2.2 and 1.3, which reduces expected total cost in stage 3 as less reinforcement costs are incurred to reach the same level of total reinforcement after the third decision. Similar observations can also be made about other scenarios which share the same beliefs about stage 3 demand level, such as scenarios 1.2 and 2.1.

D.3 Additional Graphs For the Results of Section 9.6.1

Section 9.6.1 considered how estimates of optimal decision vary with the assumed discount rate of future costs for the three stage problem detailed in Section 9.2. As part of this, Section 9.6.1 included many graphs to compare how estimated expected costs vary with reinforcement decision, scenario observed and assumed discount rate across each stage.

However, due to the range of scenarios that could possibly be observed in the second and third stages it was impractical to include a large number of graphs to compare every possible combination of discount rate and observed scenario in the main body of this thesis. Therefore, this appendix gives additional details of how the observed future scenario and assumed discount rate affect the estimates of expected total costs in stages 2 and 3 of the problem detailed in Section 9.2.

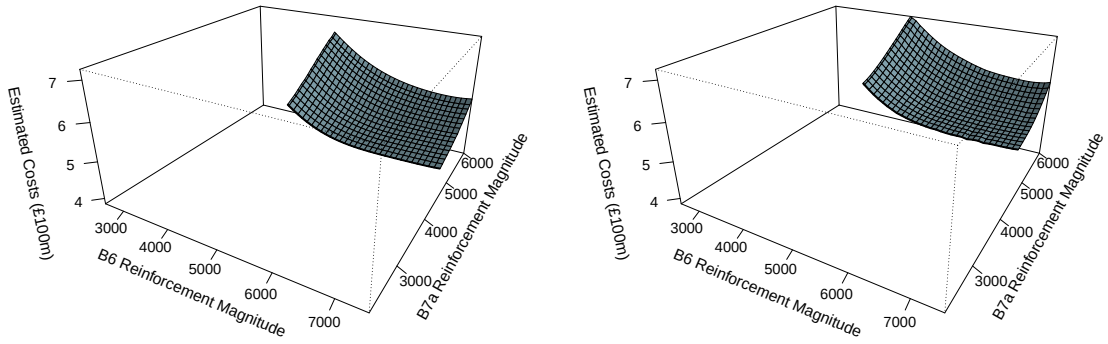

(a) Scenario 1.

(b) Scenario 3.

Figure D.4: Plots to show how estimates of expected total costs in stage 2 onwards vary with stage 2 total reinforcement decision and scenario in the first wave, when assuming a discount rate of 1%.

D.3.1 Additional Stage 2 Graphs

Figures D.4 and D.5 display how estimates of expected total costs vary with B6 and B7a reinforcement magnitude for two stage 2 scenarios (detailed in Table 9.6 of Section 9.4) when assuming a 1% or 10% discount rate respectively. As can be seen, for a fixed discount rate the plot for observing scenario 1 (i.e. $\boldsymbol{\psi}_2 = 0.95$) is very similar to the plot when observing scenario 3 (i.e. $\boldsymbol{\psi}_2 = 1.05$). However, comparing Figure D.4 to Figure D.5 shows that the estimates of expected total costs differ greatly depending on the assumed discount rate of future costs. This implies that in stage 2 the assumed discount rate has a much larger effect on the estimate of expected total costs and the resulting estimate of optimal decision than the scenario observed.

Figures D.6 and D.7 display how estimates of expected total costs vary with B6 and B7a reinforcement magnitude for two stage 2 scenarios when assuming a 1% or 10% discount rate respectively for the emulator models fitted in the final wave. Again, it can be seen that Figure D.6 (a), which assumes scenario 1 was observed when a discount rate of 1% is assumed, is much more similar to Figure D.6 (b), which assumes scenario 3 was observed when a discount rate of 1% is assumed, than Figure D.7 (a), which assumes scenario 1 was observed when a discount rate of 10% is assumed.

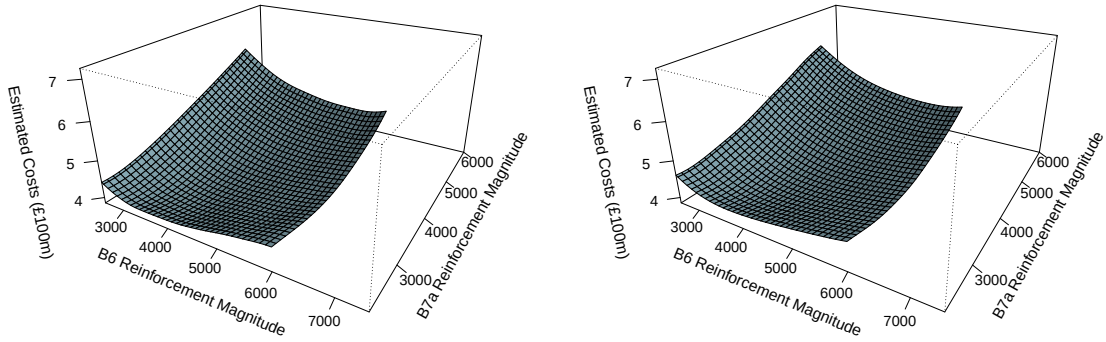

(a) Scenario 1. (b) Scenario 3.

Figure D.5: Plots to show how estimates of expected total costs in stage 2 onwards vary with stage 2 total reinforcement decision and scenario in the first wave, when assuming a discount rate of 10%.

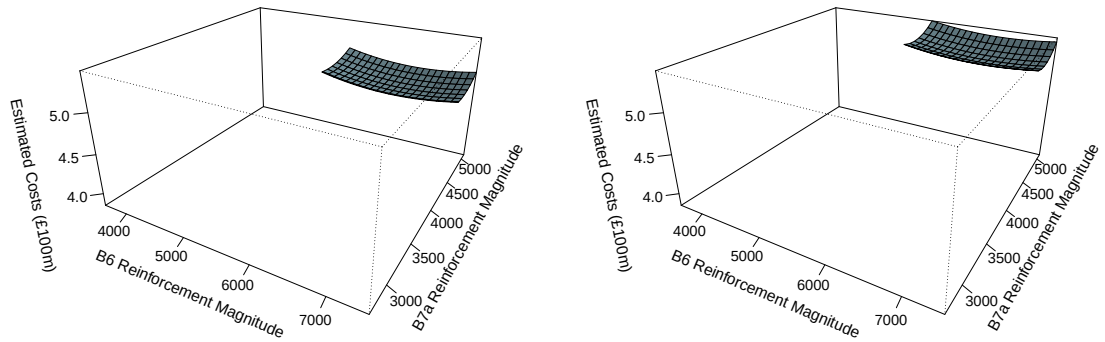

(a) Scenario 1. (b) Scenario 3.

Figure D.6: Plots to show how estimates of expected total costs in stage 2 onwards vary with stage 2 total reinforcement decision and scenario in the final wave, when assuming a discount rate of 1%.

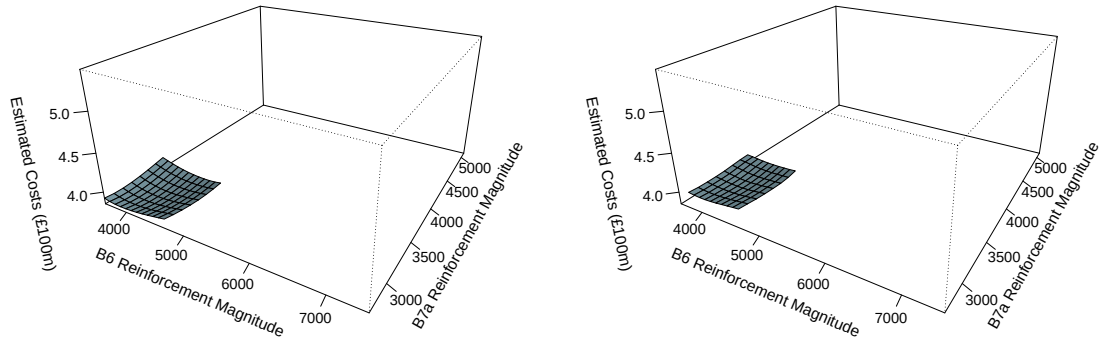

(a) Scenario 1.

(b) Scenario 3.

Figure D.7: Plots to show how estimates of expected total costs in stage 2 onwards vary with stage 2 total reinforcement decision and scenario in the final wave, when assuming a discount rate of 10%.

This is further evidence that in the second stage the assumed discount rate has a considerably larger effect on the estimates of expected total costs than the scenario observed. In particular, when a discount rate of 1% is assumed the average of the expected total costs across all stage 2 decisions considered is £33 million (6.79%) greater when scenario 3 is observed in comparison to scenario 1. By comparison, when scenario 3 is observed when the second decision is made, the average of the expected total costs across all stage 2 decisions considered is £122 million (30.3%) greater when a discount rate of 1% is assumed in comparison to when a discount rate of 10% is assumed.

It can also be seen that the reinforcement magnitudes considered in the final wave are much larger when a 1% discount rate is assumed in comparison to when a 10% discount rate is assumed, implying the estimated optimal reinforcement will be greater when assuming a discount rate of 1% in comparison to 10%. This is to be expected as a smaller discount rate results in a greater present value of future constraint costs, which in turn justifies a larger reinforcement being built.

However, the range of decisions considered for scenarios 1 and 3 are very similar for a fixed discount rate. As no further decisions could be eliminated this means that for a fixed discount rate it cannot be said that one particular scenario definitively results

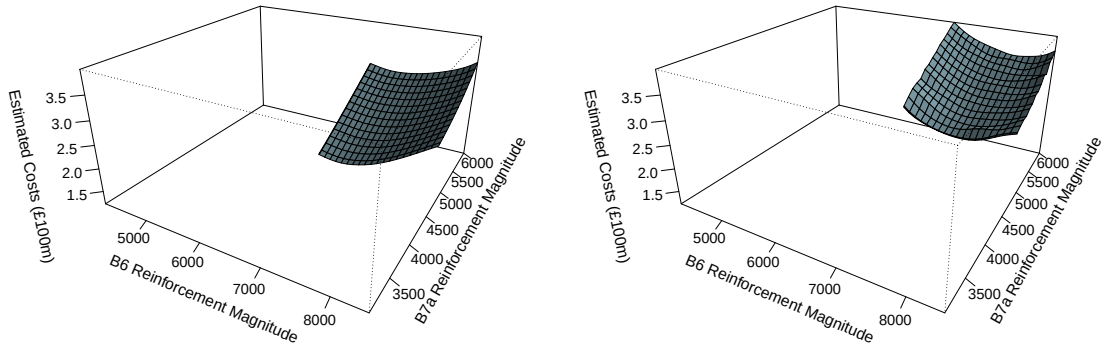

(a) Scenario 1.1.

(b) Scenario 3.3.

Figure D.8: Plots to show how estimates of expected total costs vary with stage 3 total reinforcement decision and scenario in the first wave, when assuming a discount rate of 1%.

in a larger optimal reinforcement than any other, which is consistent with what was observed in Section 9.4.

D.3.2 Additional Stage 3 Graphs

Figures D.8 and D.9 display how estimates of expected total costs vary with B6 and B7a reinforcement magnitude in the first wave for two stage 3 scenarios when assuming a 1% or 10% discount rate respectively. The two stage 3 scenarios considered are scenario 1.1 and scenario 3.3, which were detailed in Section 9.5 as observing $\boldsymbol{\psi}_3 = 0.9$ (which in turn means beliefs about stage 3 peak demand form a uniform distribution between 85% and 95% of the projection of year 16 peak demand level from [69]) and $\boldsymbol{\psi}_3 = 1.1$ (which in turn means beliefs about stage 3 peak demand form a uniform distribution between 105% and 115% of the projection of year 16 peak demand level from [69]) respectively.

For both a 1% and a 10% discount rate, estimates of expected total costs are greater for scenario 3.3 in comparison to scenario 1.1. This indicates that expected total costs increase as expected peak demand level increases, which is consistent with what was previously observed in Section 9.5. It is also observed that the assumed discount rate

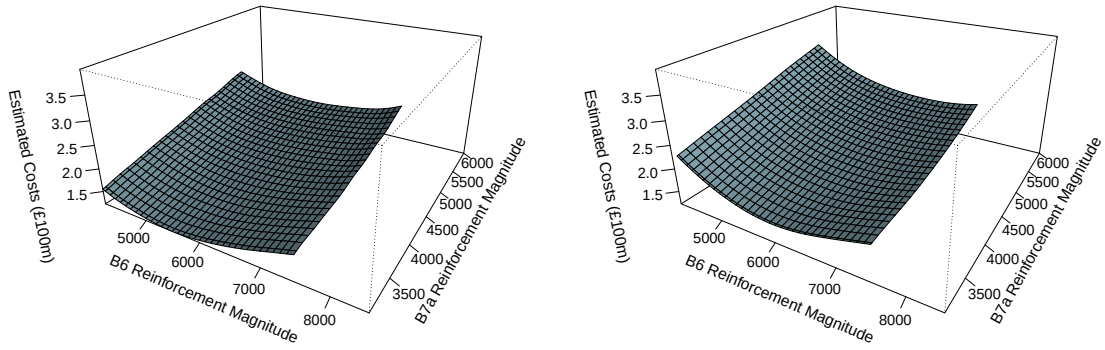

(a) Scenario 1.1.

(b) Scenario 3.3.

Figure D.9: Plots to show how estimates of expected total costs vary with stage 3 total reinforcement decision and scenario in the first wave, when assuming a discount rate of 10%.

still has a large effect on the cost estimates, with estimates of expected total costs being greater for scenario 1.1 (the scenario with the lowest estimates of expected total costs for a fixed discount rate) when assuming a 1% discount rate than estimates of expected total costs for scenario 3.3 (the scenario with the greatest estimates of expected total costs for a fixed discount rate) when assuming a 10% discount rate.

Figures D.10 and D.11 display how estimates of expected total costs in the final wave vary with reinforcement decision for two stage 3 scenarios when assuming a 1% or 10% discount rate respectively. As was the case for Figures D.8 and D.9, the two stage 3 scenarios considered are scenario 1.1 ($\boldsymbol{\psi}_3 = 0.9$) and scenario 3.3 ($\boldsymbol{\psi}_3 = 1.1$).

As can be seen, for both assumed discount rates the estimates of expected total costs are greater in scenario 3.3 in comparison to scenario 1.1, giving further evidence that expected total costs increase as expected peak demand level increases. Further, the ranges of decisions considered for B6 reinforcement magnitude differ between the scenarios, with scenario 3.3 considering larger magnitudes of B6 reinforcement, giving strong evidence that the optimal B6 reinforcement magnitude increases as expected peak demand level increases.

Comparing Figure D.10 to Figure D.11 shows again that estimates of expected total costs are greater when assuming a 1% discount rate in comparison to a 10% discount

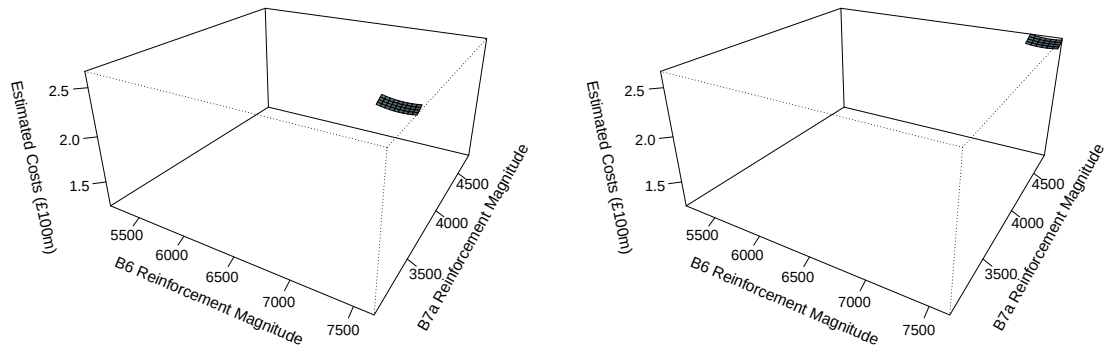

(a) Scenario 1.1. (b) Scenario 3.3.

Figure D.10: Plots to show how estimates of expected total costs vary with stage 3 total reinforcement decision and scenario in the final wave, when assuming a discount rate of 1%.

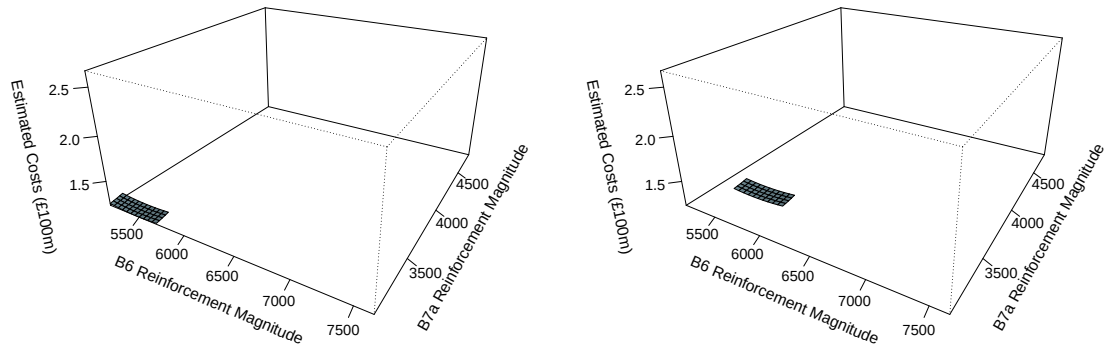

(a) Scenario 1.1. (b) Scenario 3.3.

Figure D.11: Plots to show how estimates of expected total costs vary with stage 3 total reinforcement decision and scenario in the final wave, when assuming a discount rate of 10%.

rate, with reinforcement magnitudes considered in the final wave also being greater when a 1% discount rate is assumed implying that the optimal reinforcement magnitude increases as the assumed discount rate decreases.

Appendix E

Notation

E.1 Notation

Symbol	Description	Introduced In
$\mathfrak{T}$	Total number of generating technologies in the power system	Section 3.2
$\mathfrak{t}$	Subscript used to denote generating technology type (such as coal or gas)	Section 2.1
$\mathfrak{c}_{\mathfrak{t}}^{+}$	Offer Price of generating technology type $\mathfrak{t}$	Section 2.1
$\mathfrak{c}_{\mathfrak{t}}^{-}$	Bid Price of generating technology type $\mathfrak{t}$	Section 2.1
$\mathfrak{g}_{\mathfrak{t}}^{+}$	Volume (in MW) of generating technology $\mathfrak{t}$ constrained on	Section 2.1
$\mathfrak{g}_{\mathfrak{t}}^{-}$	Volume (in MW) of generating technology $\mathfrak{t}$ constrained off	Section 2.1
$\mathfrak{R}$	Total number of zones in the power system	Section 3.1
$\mathfrak{r}$	Subscript used to index zones in the power system	Section 3.1
$\mathscr{T}$	Total number of snapshots in a year	Section 3.2
τ	Subscript used to index snapshots	Section 3.1
$\mathfrak{d}^{y}$	Peak demand level of year y	Section 3.1
$\mathfrak{d}^{\tau}$	Proportion of peak demand in the system in snapshot τ	Section 3.1
$\mathfrak{d}^{\mathfrak{r}}$	Proportion of snapshot demand in the zone $\mathfrak{r}$	Section 3.1
$\mathfrak{d}_{y,\tau,\mathfrak{r}}$	Demand in zone $\mathfrak{r}$ in snapshot τ in year y	Section 3.1
$\mathfrak{g}_{\mathfrak{r}\mathfrak{t}}^{\mathfrak{M}}$	Installed capacity of technology $\mathfrak{t}$ in zone $\mathfrak{r}$	Section 3.1
$x_{\mathfrak{r}\mathfrak{t}}$	Available capacity of technology $\mathfrak{t}$ in zone $\mathfrak{r}$	Section 3.3
$\mathfrak{g}_{\mathfrak{r}\mathfrak{t}}^{0}$	Generation level (MW) of technology $\mathfrak{t}$ in zone $\mathfrak{r}$ in the unconstrained schedule	Section 3.1
$\mathfrak{f}_{\mathfrak{r},\mathfrak{s}}^{\mathfrak{M}}$	Boundary transmission capacity between zones $\mathfrak{r}$ and $\mathfrak{s}$	Section 3.1
$\mathfrak{f}_{\mathfrak{r},\mathfrak{s}}$	Power flow from zone $\mathfrak{r}$ to $\mathfrak{s}$	Section 3.1
$\mathfrak{g}_{\mathfrak{r}\mathfrak{t}}^{+}$	Volume of accepted offers from technology $\mathfrak{t}$ in zone $\mathfrak{r}$	Section 3.1
$\mathfrak{g}_{\mathfrak{r}\mathfrak{t}}^{-}$	Volume of accepted bids from technology $\mathfrak{t}$ in zone $\mathfrak{r}$	Section 3.1

Symbol	Description	Introduced In
$a_{\mathfrak{t}}$	Availability probability of technology $\mathfrak{t}$	Section 3.5
$\mathfrak{X}$	Set of all information required to simulate constraint costs for a power system across all snapshots	Section 3.4
$f_c(\mathfrak{X})$	Simulator which calculates mean annual constraint costs for a given power system	Section 3.4.3
$\boldsymbol{\omega}$	Vector of weights to be used in importance sampling	Section 4.2.2
ω_τ	The value of the τth element of $\boldsymbol{\omega}$, i.e. the probability that snapshot τ is actually sampled when utilising importance sampling	Section 4.2.2
$X(\tau)$	Indicator function used when taking an importance sample, takes the value 1 if the snapshot was actually simulated and zero otherwise	Section 4.2.2
λ	A measure of the amount of work required to acquire an estimate of mean constraint costs expressed as a proportion of snapshot evaluations in comparison to the 17520 half hour snapshots in a year	Section 4.3.2
ϕ_τ	Value of a measurement (e.g. demand in snapshot) in snapshot τ which is used to fit weights, $\boldsymbol{\omega}$, for importance sampling	Section 4.3.1
Φ	Maximum value of ϕ_τ across all snapshots	Section 4.3.1
$\mathbf{v}$	Elements of $\mathfrak{X}$ which contain uncertainty which is modelled explicitly	Section 5.1
$\mathbf{a}$	Elements of $\mathfrak{X}$ which are either known with certainty or in which uncertainties are not of interest	Section 5.1
$\mathbf{d}$	Elements of $\mathfrak{X}$ which are decision variables	Section 5.1
N_v	The number of variables with uncertainty of interest, i.e. the length of $\mathbf{v}$	Section 5.2.1
N_d	The number of decision variables, i.e. the length of $\mathbf{d}$	Section 5.1
$f_\rho(\mathbf{d})$	Function which calculates reinforcement costs for a given decision	Section 5.1
$f_T(\mathfrak{X})$	Simulator which calculates total costs (the sum of mean constraint costs plus reinforcement costs) for a given power system background	Section 5.1
$\tilde{f}_T(\mathbf{v},\mathbf{d})$	Emulator approximation to the simulator	Section 5.2.1
$\tilde{f}_{T_1}(\mathbf{v},\mathbf{d})$	Polynomial regression portion of the emulator model	Section 5.2.1
$\tilde{f}_{T_2}(\mathbf{v},\mathbf{d})$	Gaussian process portion of the emulator model	Section 5.2.1
$\hat{\boldsymbol{\beta}}$	Fitted model parameters of $\tilde{f}_{T_1}(\mathbf{v},\mathbf{d})$	Section 5.2.2
$cov(\hat{\boldsymbol{\beta}})$	Covariance matrix of fitted model parameters of $\tilde{f}_{T_1}(\mathbf{v},\mathbf{d})$	Section 5.2.2
$\boldsymbol{\gamma}$	Parameters of the fitted Gaussian process model, $\tilde{f}_{T_2}(\mathbf{v},\mathbf{d})$	Section 5.2.3

Symbol	Description	Introduced In
$\boldsymbol{\varepsilon}$	Residuals of the polynomial regression model	Section 5.2.1
X_{dp}	Design matrix of the polynomial regression portion of the emulator model	Section 5.2.2
X_{dg}	Design matrix of the Gaussian process portion of the emulator model	Section 5.2.3
$m(\mathbf{x})$	Mean function used in Gaussian process modelling	Section 5.2.3
$\kappa(\mathbf{x}_a, \mathbf{x}_b)$	Covariance function used in Gaussian process modelling	Section 5.2.3
$\text{cor}(\mathbf{x}_a, \mathbf{x}_b)$	Correlation function used in Gaussian process modelling	Section 5.2.3
K_{X_a,X_b}	Correlation matrix describing the correlation between matrices X_a and X_b used in Gaussian process modelling	Section 5.2.3
$p(\mathbf{v})$	Specification of prior beliefs about the values the variables containing uncertainty, $\mathbf{v}$, can take	Section 5.2.5
$\tilde{F}_T(\mathbf{d})$	Estimate of expected total costs under uncertainty using the emulator, $\tilde{f}_T(\mathbf{v}, \mathbf{d})$, and the prior beliefs about uncertainty, $p(\mathbf{v})$	Section 5.2.5
$\tilde{f}_{T,r}(\mathbf{v}, \mathbf{d})$	Random variation of the fitted emulator model	Section 5.2.6
$\tilde{F}_{T,r}(\mathbf{d})$	Estimate of expected total costs under uncertainty using the random variation of the emulator, $\tilde{f}_{T,r}(\mathbf{v}, \mathbf{d})$, and the prior beliefs about uncertainty, $p(\mathbf{v})$	Section 5.2.6
$\tilde{F}_{T,L}(\mathbf{d})$	Lower bound for the estimate of $\tilde{F}_T(\mathbf{d})$	Section 5.2.6
$\tilde{F}_{T,U}(\mathbf{d})$	Upper bound for the estimate of $\tilde{F}_T(\mathbf{d})$	Section 5.2.6
P	Mean square error of a fitted emulator when estimating the response of a second set of training data not used to fit the emulator model	Section 5.3.3
$\tilde{P}$	P normalised by the variance of the response of the second set of training data	Section 5.3.3
l	Loss function	Section 5.4.3
$\tilde{F}_{T,l}(\mathbf{d})$	Estimate of expected losses under uncertainty using the emulator, $\tilde{f}_T(\mathbf{v}, \mathbf{d})$, and the prior beliefs about uncertainty, $p(\mathbf{v})$	Section 5.4.3
$\tilde{f}_b(\mathbf{v}, \mathbf{d})$	Relative difference between the costs of making decision $\mathbf{d}$ when uncertain variables take values $\mathbf{v}$ in comparison to the expected costs of the estimated risk neutral optimal decision	Section 6.5.2
$\tilde{F}_{b,l}(\mathbf{d})$	Estimate of expected value of a loss of function applied to $\tilde{f}_b(\mathbf{v}, \mathbf{d})$, when taking an expectation over variables containing uncertainty, $\mathbf{v}$, with $p(\mathbf{v})$ describing prior beliefs about the values the variables containing uncertainty take	Section 6.5.2

Symbol	Description	Introduced In
M	Total number of decision stages in the multi-stage problem	Section 8.1.4
m	Symbol for a generic stage $1 \leq m \leq M$	Section 8.1.4
$\mathbf{v}_m$	Variables containing uncertainty in stage m	Section 8.2.1
$\mathbf{d}_m$	Decision variables in stage m	Section 8.2.1
$\boldsymbol{\psi}_m$	Parameters which describe the state of the power system (scenario) in stage m	Section 8.2.1
$f_{c,1}(\mathbf{v}_1, \mathbf{d}_1)$	Simulator to calculate mean constraint costs in stage 1 for given values of decision and uncertain variables	Section 8.2.4
$\tilde{f}_{c,1}(\mathbf{v}_1, \mathbf{d}_1)$	Emulator to approximate the simulator (i.e. $f_{c,1}(\mathbf{v}_1, \mathbf{d}_1)$) in Stage 1	Section 8.2.4
$f_{c,m}(\mathbf{v}_m, \mathbf{d}_m \vert \mathbf{d}_1, ..., \mathbf{d}_{m-1})$	Simulator to calculate mean constraint costs for values of uncertain variables and decisions in stage m for given decisions in the previous $m-1$ stages	Section 8.2.1
$\tilde{f}_{c,m}(\mathbf{v}_m, \mathbf{d}_m \vert \mathbf{d}_1, ..., \mathbf{d}_{m-1})$	Emulator to approximate the simulator (i.e. $f_{c,m}(\mathbf{v}_m, \mathbf{d}_m \vert \mathbf{d}_1, ..., \mathbf{d}_{m-1})$) in stage m	Section 8.2.4
$\tilde{F}_{c,m}(\mathbf{d}_m \vert \mathbf{d}_1, ..., \mathbf{d}_{m-1}, \boldsymbol{\psi}_m)$	Estimate of expected mean constraint costs when integrating over uncertainties, when decision $\mathbf{d}_m$ is made in stage m given that decisions $\mathbf{d}_1, ..., \mathbf{d}_{m-1}$ were previously made and that the scenario described by $\boldsymbol{\psi}_m$ is observed in stage m	Section 8.2.4
$f_{\rho,1}(\mathbf{d}_1)$	Calculation of reinforcement costs for a stage 1 decision	Section 8.2.4
$f_{\rho,m}(\mathbf{d}_m \vert \mathbf{d}_1, ..., \mathbf{d}_{m-1}, \boldsymbol{\psi}_m)$	Calculation of reinforcement costs for a stage m decision, for given decisions in the previous $m-1$ stages and that scenario $\boldsymbol{\psi}_m$ is observed in stage m	Section 8.2.2
$\tilde{F}_{T,m}(\mathbf{d}_m \vert \mathbf{d}_1, ..., \mathbf{d}_{m-1}, \boldsymbol{\psi}_m)$	Estimate of expected total costs in stage m onwards (expected mean constraint plus reinforcement costs in stage m plus expected total costs from stage $m+1$ to stage M) from making decision $\mathbf{d}_m$ in stage m given that decisions $\mathbf{d}_1, ..., \mathbf{d}_{m-1}$ were previously made and that the scenario described by $\boldsymbol{\psi}_m$ is observed in stage m	Section 8.2.4

Symbol	Description	Introduced In
$\tilde{G}_{T,2,\boldsymbol{\psi}_2}(\mathbf{d}_1, \boldsymbol{\psi}_2)$	Emulator fitted to approximate how expected total costs in stage 2 vary with stage 1 decision made and stage 2 scenario	Section 8.2.4
N_θ	Number of randomly sampled stage 1 decisions and stage 2 scenarios used to fit $\tilde{G}_{T,2,\boldsymbol{\psi}_2}(\mathbf{d}_1, \boldsymbol{\psi}_2)$	Section 8.2.4
θ	Symbol used to denote a particular one of the N_θ samples	Section 8.2.4
$\mathbf{d}_{1,\theta}$	Values of the stage 1 decision variables for the θth sample of the N_θ samples used to fit $\tilde{G}_{T,2,\boldsymbol{\psi}_2}(\mathbf{d}_1, \boldsymbol{\psi}_2)$	Section 8.2.4
$\boldsymbol{\psi}_{2,\theta}$	Values of the stage 2 scenario for the θth sample of the N_θ samples used to fit $\tilde{G}_{T,2,\boldsymbol{\psi}_2}(\mathbf{d}_1, \boldsymbol{\psi}_2)$	Section 8.2.4
$\mathbf{d}_{2\|\theta}$	The estimated optimal decision that would be made in the second stage for the θth element of the N_θ samples of stage 2 scenarios and stage 1 decisions	Section 8.2.4
$\tilde{F}_{T,2,\theta}$	Estimated expected total costs in stage 2 onwards when making decision $\mathbf{d}_{2\|\theta}$ in stage 2 when decision $\mathbf{d}_{1,\theta}$ was made in stage 1 and scenario $\boldsymbol{\psi}_{2,\theta}$ is observed in stage 2	Section 8.2.4
$p(\mathbf{v}_2\|\boldsymbol{\psi}_2)$	Prior beliefs about variables containing uncertainty in stage 2, $\mathbf{v}_2$, given that scenario $\boldsymbol{\psi}_2$ is observed in stage 2	Section 8.2.4
$p_{\boldsymbol{\psi}_{2\|1}}(\boldsymbol{\psi}_2)$	Prior beliefs in stage 1 of observing scenario $\boldsymbol{\psi}_2$ in stage 2	Section 8.2.4
$\tilde{G}_{T,2}(\mathbf{d}_1)$	The estimate of expected total costs in stage 2 as a function of stage 1 decision only in the two stage problem	Section 8.2.4
$\tilde{G}_T(\mathbf{d}_1)$	The estimate of expected total costs across both stages of the 2 stage problem as a function of stage 1 decision only	Section 8.2.4

Symbol	Description	Introduced In
$\tilde{f}_{c,2,r}(\mathbf{v}_2, \mathbf{d}_2 \vert \mathbf{d}_1)$	Randomly drawn variation of the stage 2 emulator model, $\tilde{f}_{c,2}(\mathbf{v}_2, \mathbf{d}_2 \vert \mathbf{d}_1)$	Section 8.2.6
$\tilde{F}_{T,2,\theta,r}$	Randomly drawn variation of $\tilde{F}_{T,2,\theta}$ that arises when using $\tilde{f}_{c,2,r}(\mathbf{v}_2, \mathbf{d}_2 \vert \mathbf{d}_1)$, the randomly drawn variation of $\tilde{f}_{c,2}(\mathbf{v}_2, \mathbf{d}_2 \vert \mathbf{d}_1)$, to estimate expected costs in stage 2	Section 8.2.6
$\tilde{F}_{T,2,\theta,L}$	Lower bound for the estimate of $\tilde{F}_{T,2,\theta}$	Section 8.2.6
$\tilde{F}_{T,2,\theta,U}$	Upper bound for the estimate of $\tilde{F}_{T,2,\theta}$	Section 8.2.6
$\tilde{G}_{T,2,L}(\mathbf{d}_1)$	Lower bound for $\tilde{G}_{T,2}(\mathbf{d}_1)$, the estimate of expected total stage 2 costs as a function of stage 1 decision only	Section 8.2.6
$\tilde{G}_{T,2,U}(\mathbf{d}_1)$	Upper bound for $\tilde{G}_{T,2}(\mathbf{d}_1)$, the estimate of expected total stage 2 costs as a function of stage 1 decision only	Section 8.2.6
$\tilde{f}_{c,1,r}(\mathbf{v}_1, \mathbf{d}_1)$	Randomly drawn variation of the stage 1 emulator model, $\tilde{f}_{c,1}(\mathbf{v}_1, \mathbf{d}_1)$	Section 8.2.6
$\tilde{G}_{T,L,r}(\mathbf{d}_1)$	Randomly drawn variation of an estimate of expected total costs across both stages, $\tilde{G}_T(\mathbf{d}_1)$, using a random variation of the emulator for stage 1 mean constraint costs, $\tilde{f}_{c,1,r}(\mathbf{v}_1, \mathbf{d}_1)$, and the lower bound for stage 2 total costs, $\tilde{G}_{T,2,L}(\mathbf{d}_1)$	Section 8.2.6
$\tilde{G}_{T,U,r}(\mathbf{d}_1)$	Randomly drawn variation of an estimate of expected total costs across both stages, $\tilde{G}_T(\mathbf{d}_1)$, using a random variation of the emulator for stage 1 mean constraint costs, $\tilde{f}_{c,1,r}(\mathbf{v}_1, \mathbf{d}_1)$, and the upper bound for stage 2 total costs, $\tilde{G}_{T,2,U}(\mathbf{d}_1)$	Section 8.2.6
$\tilde{G}_{T,L,L}(\mathbf{d}_1)$	Lower bound for $\tilde{G}_T(\mathbf{d}_1)$, the estimate of expected total costs across both stages of the two stage problem as a function of stage 1 decision only	Section 8.2.6
$\tilde{G}_{T,U,U}(\mathbf{d}_1)$	Upper bound for $\tilde{G}_T(\mathbf{d}_1)$, the estimate of expected total costs across both stages of the two stage problem as a function of stage 1 decision only	Section 8.2.6

Symbol	Description	Introduced In
$\mathbf{d}_{T_m}$	Total reinforcement built up to and including stage m	Section 9.1.2
$f_{c,m}(\mathbf{v}_m, \mathbf{d}_m \vert \mathbf{d}_{T_{m-1}})$	Simulator to calculate mean constraint costs for values of uncertain variables and decisions in stage m, for given total reinforcement decisions in the previous stages	Section 9.1.2
$\tilde{f}_{c,m}(\mathbf{v}_m, \mathbf{d}_m \vert \mathbf{d}_{T_{m-1}})$	Emulator to approximate simulator (i.e. $f_{c,m}(\mathbf{v}_m, \mathbf{d}_m \vert \mathbf{d}_{T_{m-1}})$) in stage m	Section 9.1.2
$f_{\rho,m}(\mathbf{d}_m \vert \mathbf{d}_{T_{m-1}}, \boldsymbol{\psi}_m)$	Calculation of reinforcement costs for stage m decision, for given total reinforcement decisions in the previous $m-1$ stages and that scenario $\boldsymbol{\psi}_m$ is observed in stage m	Section 9.1.2
$\tilde{F}_{T,m}(\mathbf{d}_m \vert \mathbf{d}_{T_{m-1}}, \boldsymbol{\psi}_m)$	Estimate of expected total costs in stage m onwards (expected mean constraint costs plus reinforcement costs in stage m plus expected total costs from stage $m+1$ to stage M) from making decision $\mathbf{d}_m$ in stage m given that total reinforcement $\mathbf{d}_{T_{m-1}}$ was previously made and that the scenario described by $\boldsymbol{\psi}_m$ is observed in stage m	Section 9.1.2
$\tilde{G}_{T,m,\boldsymbol{\psi}_m}(\mathbf{d}_{T_{m-1}}, \boldsymbol{\psi}_m)$	Emulator fitted to approximate how expected total costs in stage m onwards vary with total reinforcement up to and including stage $m-1$, $\mathbf{d}_{T_{m-1}}$, and stage m scenario, $\boldsymbol{\psi}_m$	Section 9.1.2
N_{θ_m}	Number of randomly sampled stage $m-1$ total reinforcements and stage m scenarios used to fit $\tilde{G}_{T,m,\boldsymbol{\psi}_m}(\mathbf{d}_{T_{m-1}}, \boldsymbol{\psi}_m)$	Section 9.1.2
$\theta_{i,m}$	Symbol used to denote a particular one of the N_{θ_m} samples	Section 9.1.2
$\mathbf{d}_{T_{m-1},\theta_{i,m}}$	Values of the total stage $m-1$ reinforcement for the $\theta_{i,m}$th sample of the N_{θ_m} samples used to fit $\tilde{G}_{T,m,\boldsymbol{\psi}_m}(\mathbf{d}_{T_{m-1}}, \boldsymbol{\psi}_m)$	Section 9.1.2
$\boldsymbol{\psi}_{m,\theta_{i,m}}$	Values of the stage m scenario for the $\theta_{i,m}$th sample of the N_{θ_m} samples used to fit $\tilde{G}_{T,m,\boldsymbol{\psi}_m}(\mathbf{d}_{T_{m-1}}, \boldsymbol{\psi}_m)$	Section 9.1.2
$\mathbf{d}_{m\vert\theta_{i,m}}$	The estimated optimal decision that would be made in the mth stage for the $\theta_{i,m}$th element of the N_{θ_m} samples of stage m scenarios, $\boldsymbol{\psi}_{m,\theta_{i,m}}$, and stage $m-1$ total reinforcement decisions, $\mathbf{d}_{T_{m-1},\theta_{i,m}}$	Section 9.1.2
$\tilde{F}_{T,m,\theta_{i,m}}$	Estimated expected total costs in stage m onwards when making decision $\mathbf{d}_{m\vert\theta_{i,m}}$ in stage m, given that total reinforcement $\mathbf{d}_{T_{m-1},\theta_{i,m}}$ was made up to stage $m-1$ and scenario $\boldsymbol{\psi}_{m,\theta_{i,m}}$ is observed in stage m	Section 9.1.2

Symbol	Description	Introduced In
$p(\mathbf{v}_m\|\boldsymbol{\psi}_m)$	Beliefs about variables containing uncertainty in stage m, $\mathbf{v}_m$, given that scenario $\boldsymbol{\psi}_m$ is observed in stage m	Section 9.1.2
$p_{\boldsymbol{\psi}_{m\|m-1}}(\boldsymbol{\psi}_m\|\boldsymbol{\psi}_{m-1})$	Beliefs about observing scenario $\boldsymbol{\psi}_m$ in stage m given that scenario $\boldsymbol{\psi}_{m-1}$ was observed in stage $m-1$	Section 9.1.2
$\tilde{G}_{T,m+1,\boldsymbol{\psi}_m}(\mathbf{d}_{T_m}, \boldsymbol{\psi}_m)$	The estimate of expected total costs in stages $m+1$ to M as a function of total reinforcement up until stage m, $\mathbf{d}_{T_m}$, and stage m scenario, $\boldsymbol{\psi}_m$, only	Section 9.1.2
$\tilde{G}_T(\mathbf{d}_1, \boldsymbol{\psi}_1)$	The estimate of expected total costs across all M stages of the M stage problem as a function of the stage 1 decision (and stage 1 scenario, $\boldsymbol{\psi}_1$, for generalisation) only	Section 9.1.2
$\tilde{f}_{c,m,r}(\mathbf{v}_m, \mathbf{d}_m\|\mathbf{d}_{T_{m-1}})$	Randomly drawn variation of the stage m emulator model, $\tilde{f}_{c,m}(\mathbf{v}_m, \mathbf{d}_m\|\mathbf{d}_{T_{m-1}})$	Section 9.1.4
$\tilde{F}_{T,M,\theta_{i,M},r}$	Randomly drawn variation of $\tilde{F}_{T,M,\theta_{i,M}}$ that arises when using $\tilde{f}_{c,M,r}(\mathbf{v}_M, \mathbf{d}_M\|\mathbf{d}_{T_{M-1}})$ (the randomly drawn variation of $\tilde{f}_{c,M}(\mathbf{v}_M, \mathbf{d}_M\|\mathbf{d}_{T_{M-1}})$) to estimate expected costs in stage M	Section 9.1.4
$\tilde{F}_{T,M,\theta_{i,M},L}$	Lower bound for the estimate of $\tilde{F}_{T,M,\theta_{i,M}}$	Section 9.1.4
$\tilde{F}_{T,M,\theta_{i,M},U}$	Upper bound for the estimate of $\tilde{F}_{T,M,\theta_{i,M}}$	Section 9.1.4
$\tilde{G}_{T,m,\boldsymbol{\psi}_m,L}(\mathbf{d}_{T_{m-1}}, \boldsymbol{\psi}_m)$	Lower bound for $\tilde{G}_{T,m,\boldsymbol{\psi}_m}(\mathbf{d}_{T_{m-1}}, \boldsymbol{\psi}_m)$, the estimate of expected total costs in stage m onwards as a function of total reinforcement until stage $m-1$, $\mathbf{d}_{T_{m-1}}$, and stage m scenario, $\boldsymbol{\psi}_m$, only	Section 9.1.4
$\tilde{G}_{T,m,\boldsymbol{\psi}_m,U}(\mathbf{d}_{T_{m-1}}, \boldsymbol{\psi}_m)$	Upper bound for $\tilde{G}_{T,m,\boldsymbol{\psi}_m}(\mathbf{d}_{T_{m-1}}, \boldsymbol{\psi}_m)$, the estimate of expected total costs in stage m onwards as a function of total reinforcement until stage $m-1$, $\mathbf{d}_{T_{m-1}}$, and stage m scenario, $\boldsymbol{\psi}_m$, only	Section 9.1.4
$\tilde{G}_{T,m+1,\boldsymbol{\psi}_m,L}(\mathbf{d}_{T_m}, \boldsymbol{\psi}_m)$	Lower bound for $\tilde{G}_{T,m+1,\boldsymbol{\psi}_m}(\mathbf{d}_{T_m}, \boldsymbol{\psi}_m)$, the estimate of expected total costs in stage $m+1$ onwards as a function of stage m scenario, $\boldsymbol{\psi}_m$, and total reinforcement until stage m, $\mathbf{d}_{T_m}$, only	Section 9.1.4
$\tilde{G}_{T,m+1,\boldsymbol{\psi}_m,U}(\mathbf{d}_{T_m}, \boldsymbol{\psi}_m)$	Upper bound for $\tilde{G}_{T,m+1,\boldsymbol{\psi}_m}(\mathbf{d}_{T_m}, \boldsymbol{\psi}_m)$, the estimate of expected total costs in stage $m+1$ onwards as a function of stage m scenario, $\boldsymbol{\psi}_m$, and total reinforcement until stage m, $\mathbf{d}_{T_m}$, only	Section 9.1.4

Symbol	Description	Introduced In
$\tilde{F}_{T,m,\theta_{i,m},L,r}$	Randomly drawn variation of $\tilde{F}_{T,m,\theta_{i,m}}$ that arises when using $\tilde{f}_{c,m,r}(\mathbf{v}_m, \mathbf{d}_m \vert \mathbf{d}_{T_{m-1}})$ (the randomly drawn variation of $\tilde{f}_{c,m}(\mathbf{v}_m, \mathbf{d}_m \vert \mathbf{d}_{T_{m-1}})$) and the lower bound to estimate expected total costs for stage $m+1$ onwards, $\tilde{G}_{T,m+1,\boldsymbol{\psi}_m,L}(\mathbf{d}_{T_m}, \boldsymbol{\psi}_m)$	Section 9.1.4
$\tilde{F}_{T,m,\theta_{i,m},U,r}$	Randomly drawn variation of $\tilde{F}_{T,m,\theta_{i,m}}$ that arises when using $\tilde{f}_{c,m,r}(\mathbf{v}_m, \mathbf{d}_m \vert \mathbf{d}_{T_{m-1}})$ (the randomly drawn variation of $\tilde{f}_{c,m}(\mathbf{v}_m, \mathbf{d}_m \vert \mathbf{d}_{T_{m-1}})$) and the upper bound to estimate expected total costs for stage $m+1$ onwards, $\tilde{G}_{T,m+1,\boldsymbol{\psi}_m,U}(\mathbf{d}_{T_m}, \boldsymbol{\psi}_m)$	Section 9.1.4
$\tilde{F}_{T,m,\theta_{i,m},L,L}$	Lower bound for the estimate of $\tilde{F}_{T,m,\theta_{i,m}}$	Section 9.1.4
$\tilde{F}_{T,m,\theta_{i,m},U,U}$	Upper bound for the estimate of $\tilde{F}_{T,m,\theta_{i,m}}$	Section 9.1.4
$\tilde{G}_{T,L,L}(\mathbf{d}_1, \boldsymbol{\psi}_1)$	Lower bound for, $\tilde{G}_T(\mathbf{d}_1, \boldsymbol{\psi}_1)$, the estimate of expected total costs across all M stages of the M stage problem as a function of stage 1 decision, $\mathbf{d}_1$, and stage 1 scenario, $\boldsymbol{\psi}_1$, only	Section 9.1.4
$\tilde{G}_{T,U,U}(\mathbf{d}_1, \boldsymbol{\psi}_1)$	Upper bound for, $\tilde{G}_T(\mathbf{d}_1, \boldsymbol{\psi}_1)$, the estimate of expected total costs across all M stages of the M stage problem as a function of stage 1 decision, $\mathbf{d}_1$, and stage 1 scenario, $\boldsymbol{\psi}_1$, only	Section 9.1.4

Appendix F

Data Appendix

This appendix gives an overview of the data used as simulator input throughout this thesis, with the vast majority of this data taken from [69], National Grid's freely available online reference.

F.1 Zone Structure

F.1.1 Zone Structure

The zone structure used to model Britain's power system in this thesis was previously detailed in Section 3.1. This is repeated in this appendix for completion, with Figure F.1 illustrating the linear structure of the power system, with 7 zones separated by 6 boundaries where each zone is connected to only the zone(s) directly North and/or South of itself.

These zones are labelled zone 1 to zone 7 from North to South, and Table F.1 gives a description of each zone for use later in this chapter when detailing other aspects of the power system (such as zonal demand). For interest, approximate geographical interpretations of these zones are: zones 1 and 2 together represent Scotland, zone 3 represents Northern England (from Northumberland to North Yorkshire), zone 4 represents the remainder of Northern England and parts of Northern Wales, zone 5 represents The Midlands, zone 6 represents the majority of Southern England (including London) and

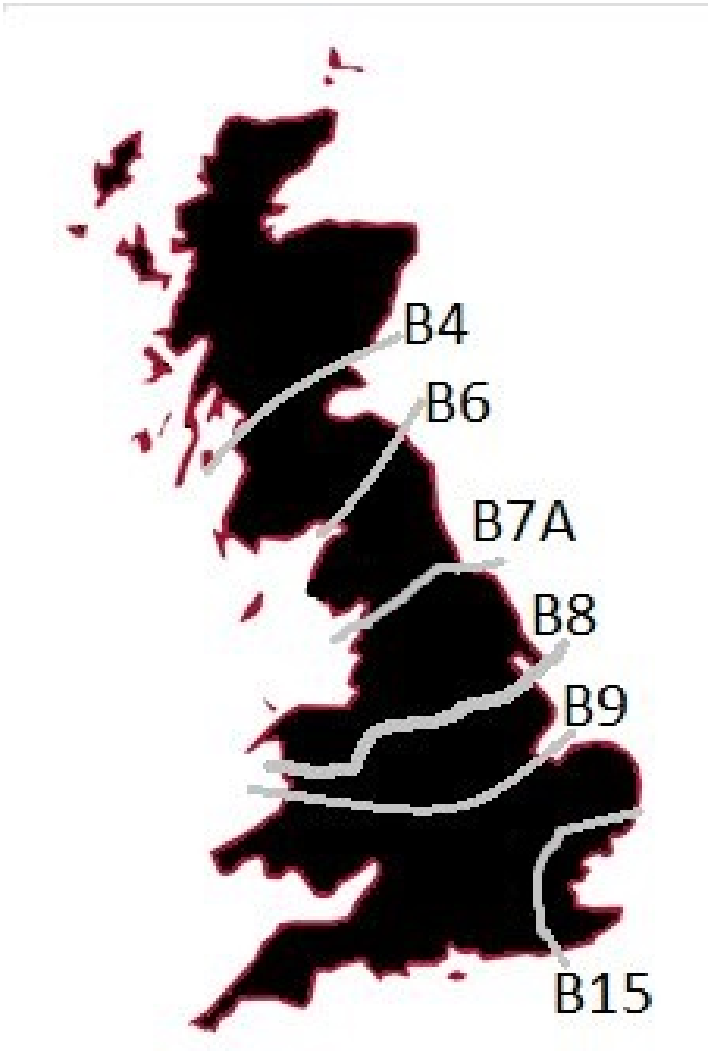

Figure F.1: Graph displaying the structure of zones and boundaries of the power system used in this thesis.

Southern Wales and zone 7 represents a small zone of the most South Eastern parts of England.

Zone	Zone Description
Zone 1	North of B4
Zone 2	Between B4 and B6
Zone 3	Between B6 and B7a
Zone 4	Between B7a and B8
Zone 5	Between B8 and B9
Zone 6	Between B9 and B15
Zone 7	South of B15

Table F.1: Table detailing the seven zones used in this thesis.

F.1.2 Boundary Transfer Capacity

Year	B4	B6	B7a	B8	B9	B15
1	2205	3300	5400	11300	12600	6400
2	2205	3300	5400	11300	12600	6400
3	2205	3300	5400	11300	12600	6400
4	3155	4300	5800	10700	12600	6400
5	3155	6400	7900	11900	12000	6400
6	4705	6400	7900	11900	12000	6400
7	4705	6400	7900	11300	12500	6400
8	6805	8500	8600	11300	12500	6400
9	6805	8500	8600	11300	12500	6400
10	6805	8500	8600	14000	13900	6500
11	6805	8500	8600	14000	13900	6500
12	6805	8500	8600	13700	13900	6400
13	6805	8500	8600	13700	13900	6400
14	6805	8500	8600	13700	13900	6400
15	6805	8500	8600	13700	13900	6400
16	6805	8500	8600	13700	13900	6400
17	6805	8500	8600	13700	13900	6400
18	6805	8500	8600	13700	13900	6400
19	6805	8500	8600	13700	13900	6400
20	6805	8500	8600	13700	13900	6400

Table F.2: Table detailing the projected boundary transfer capacity of each boundary in each year.

Details of the projected boundary transfer capacities from [69] over a 20 year period are

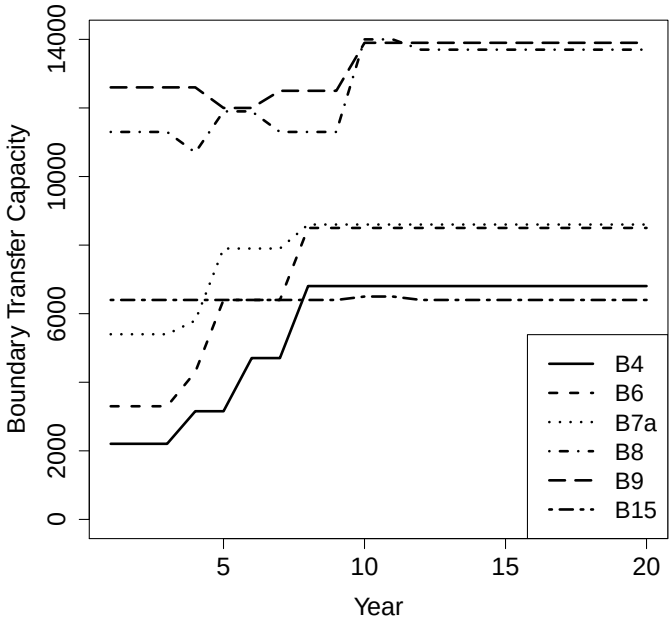

Figure F.2: Graph to illustrate how the projected transfer capacity of each boundary varies over the 20 year period.

given in Table F.2, with Figure F.2 illustrating these projections of boundary transfer capacity. As can be seen, the projected installed boundary transfer capacity generally increases with time, as further reinforcements are built on each boundary.

However, there are a couple of exceptions, such as a decrease of 600 MW in B8 transfer capacity in year 4. This reason for this is explained in [73] as the result of phased investment in these instances. Phased investments are where one element of boundary capability is improved (such as thermal, voltage or stability) at one point in time, before a later investment can be made to improve the other elements and increase the transfer capacity of the boundary.

There are no such decreases projected for the B6 and B7a boundaries, which are the boundaries of interest for the examples of Chapters 6 to 9. Further, in the examples of Chapters 6 to 9, as was mentioned in Section 6.1.1 of Chapter 6, it was assumed that the transfer capacity of the B6 and B7a boundary were the projected capacities in year 1 (3300 MW B6 and 5400 MW B7a) plus the reinforcement magnitude of our decision variables as these examples were meant to represent real world transmission expansion problem with the decision variables representing the reinforcements made by a real world transmission expansion planner.

F.2 Demand

As was detailed in Section 3.1.3, the demand level in a particular zone in a particular snapshot is calculated as the product of the peak demand level of the power system background, $\mathfrak{d}^y$, the snapshot demand level specified as a proportion of the peak demand level, $\mathfrak{d}^\tau$, and the proportion of snapshot demand in that particular zone, $\mathfrak{d}^\mathfrak{r}$, i.e.

$$\mathfrak{d}_{y,\tau,\mathfrak{r}} = \mathfrak{d}^y \times \mathfrak{d}^\mathfrak{r} \times \mathfrak{d}^\tau$$

This section will give details of the data used for $\mathfrak{d}^y$, $\mathfrak{d}^\mathfrak{r}$ and $\mathfrak{d}^\tau$.

F.2.1 Peak Demand Level

[69] give projections of peak demand level for 20 consecutive years between 2011 and 2030 (referred to as years 1 to 20 throughout this thesis). These projections are detailed in Table F.3 and illustrated in Figure F.3. As can be seen, there is relatively little variation in the projections of peak demand level between years 1 and 5, with projections varying by less than 0.13% (71 MW) of the 58130 MW projected in year 1. This observation was discussed with Paul Plumptre, formerly of National Grid [78], and our interpretation of these discussions is that the reason there is little variation in projections in these years is that when these projections were made it was believed that the increase in demand in the near future would be offset by improvement in the efficiency of technology.

The smallest projection of peak demand level is 57073 MW in year 10 (a 1.82% decrease from the projection in year 1) and the greatest projection of peak demand level is 60218 MW in year 20 (a 3.59% increase from the projection in year 1), with a difference of 3145 MW between the greatest and lowest projections.

Figure F.4 illustrates the projected peak demand level, as well as bounds to indicate uncertainty of these projections based on discussions with Paul Plumptre [78], where our interpretations of discussions is that an appropriate level of uncertainty is +/-x% when predicting x years into the future. As can be seen, the variation in the projected peak demand level is small in comparison to the uncertainty in these projections, with this even more evident in later years. In particular, the projected peak demand level

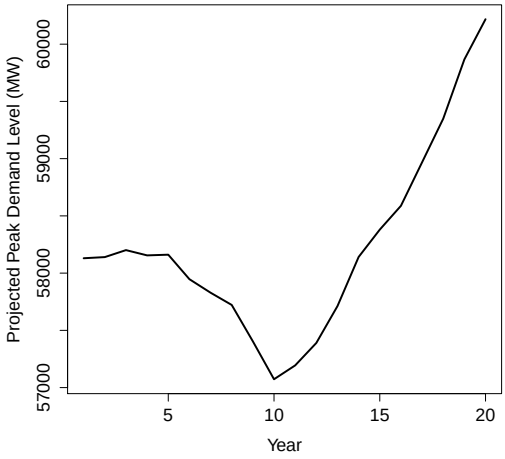

Figure F.3: Graph to illustrate the projected peak demand level over the 20 year period considered by [69].

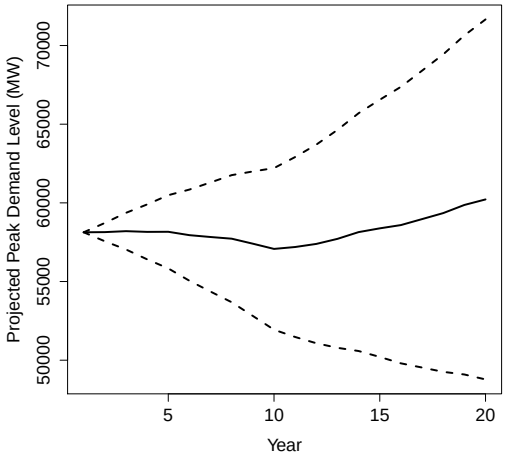

Figure F.4: Graph to illustrate the projected peak demand level over the 20 year period considered by [69], with credible intervals for these projections based on discussions with Paul Plumptre [78].

Year	Projected Peak Demand Level
Year 1	58130 MW
Year 2	58140 MW
Year 3	58201 MW
Year 4	58155 MW
Year 5	58161 MW
Year 6	57947 MW
Year 7	57829 MW
Year 8	57722 MW
Year 9	57404 MW
Year 10	57073 MW
Year 11	57194 MW
Year 12	57390 MW
Year 13	57712 MW
Year 14	58141 MW
Year 15	58380 MW
Year 16	58588 MW
Year 17	58968 MW
Year 18	59349 MW
Year 19	59867 MW
Year 20	60218 MW

Table F.3: Table detailing the projected peak demand level over the 20 year horizon from [69].

in year 20 is 2088 MW greater than the projected peak demand level in year 1, but the uncertainty of this projection is +/- 12043.6 MW.

F.2.2 Zonal Demand

Zone	Zone Demand
Zone 1	0.028
Zone 2	0.070
Zone 3	0.061
Zone 4	0.211
Zone 5	0.185
Zone 6	0.410
Zone 7	0.035

Table F.4: Table detailing the breakdown of $\mathfrak{d}^{\mathfrak{r}}$ by zone (i.e. the proportion of snapshot demand in each zone).

Table F.4 details the proportion of snapshot demand in each zone described in Ta-

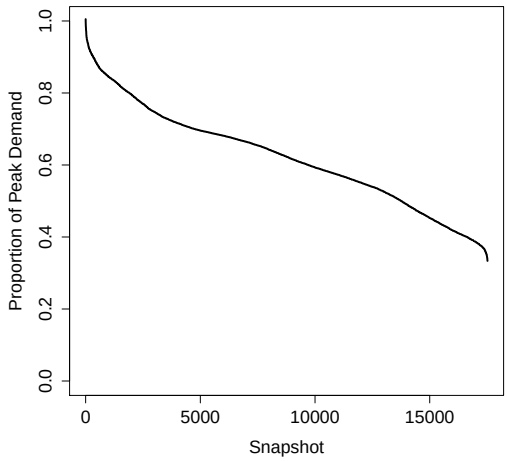

Figure F.5: Graph to illustrate the load duration curve used in this thesis.

ble F.1. These descriptions are inline with what may have been expected based on the zone descriptions given in Section F.1.1. In particular, zone 6 has the largest proportion of demand (0.41) which makes sense as it is quite a large zone which includes London; and zones 1 and 2 together have a proportion of demand of 0.098, which is very close to 10% of snapshot demand that Scotland was assumed to have in the initial example in Section 2.2.1.

F.2.3 Snapshot Demand

Section 4.1.2 of Chapter 4 detailed how the demand level in each snapshot is specified via a load duration curve, which specifies distribution for demand throughout a year by specifying a proportion of peak demand to be used in each snapshot for simulation. Exact details are omitted from this thesis (as it would require giving figures for 17520 individual snapshots) but full details of the demand in each snapshot are given in [69], National Grid's freely available online resource and the primary data reference of this thesis.

Figure F.5 repeats the illustration of an LDC from Section 4.1.2, and illustrates the distribution of demand throughout the year by showing how many snapshots exceed a particular proportion of peak demand. As was noted in Section 4.1.2, it can be seen that a very small number of snapshots are modelled as having a demand level in excess of 80% of peak demand (1906 out of 17520 snapshots, or 10.8% of snapshots) whilst an

even smaller number of snapshots are modelled as having a demand level greater than 90% of peak demand (328 of 17520 snapshots, or 1.8% of snapshots) whereas the vast majority of snapshots are modelled as having a demand level which is between 40% and 80% of peak demand.

F.3 Generation Technologies

[69] gives details of 30 different generation technologies across 7 zones for 20 consecutive years. However, certain technologies such as "CHP New" or "Gas Other" are not projected to have any installed capacity across all 20 years. Therefore, in this section details will only be given for the 20 technologies which have any installed capacity projected over the 20 year period.

F.3.1 Generating Capacity Availability Models

Table F.5 gives details about the 20 types of installed generating capacity considered in this thesis, with details included about the models used to randomly simulator available generating capacity as described in Section 3.5 of Chapter 3.

Of the acronyms used in the table, CCGT stands for combined cycle gas turbine, whereas OCGT stands for open cycle gas turbine, two forms of generating technology which use natural gas as a fuel. CCS stands for carbon capture and storage, a technology which is being developed to reduce carbon dioxide emissions from non-renewable generation (gas and coal) [14, 35, 13]. To achieve this, carbon dioxide produced as part of electricity generation is absorbed by a solvent before it would be emitted into the atmosphere, then stored underground. From the projections given in [69], Clean Coal CCS is first projected to be installed in year 8 (2018), and CCGT CCS is first projected to be installed in year 13 (2023).

LCPD stands for Large Combustion Plant Directive, which is a European directive which applies to a "dirty" form of coal and oil generation from large combustion plants with high emissions of sulphur dioxide, nitrogen oxides, and dust [90, 51]. Plants built after 1987 (and plants built before 1987 which opt in) must meet new emission

Technology Name	Random Generation Model	Mean Availability (a_t or μ_t)	Availability Standard Deviation (σ_t)	Unit size (u_t)
Hydro	Gaussian	0.75	0.04	N/A
Offshore Wind	National Grid's Onshore Wind model	N/A	N/A	N/A
Onshore Wind	National Grid's Offshore Wind model	N/A	N/A	N/A
Wave and Tidal	Binomial	1	N/A	100 MW
Nuclear	Binomial	0.7	N/A	600 MW
New Nuclear	Binomial	0.8	N/A	600 MW
Biomass	Binomial	0.8	N/A	500 MW
CHP	Binomial	0.8	N/A	500 MW
CCGT CCS	Binomial	0.8	N/A	500 MW
Clean Coal CCS	Binomial	0.8	N/A	500 MW
CCGT New	Binomial	0.8	N/A	500 MW
CCGT	Binomial	0.8	N/A	500 MW
Europe Interconnection	Binomial	0.95	N/A	500 MW
Coal LCPD	Binomial	0.8	N/A	500 MW
Coal LCPD (opt out)	Binomial	0.8	N/A	500 MW
Ireland Interconnection	Binomial	0.95	N/A	500 MW
Pumped Storage	Binomial	0.95	N/A	100 MW
Oil	Binomial	0.9	N/A	600 MW
OCGT	Binomial	1	N/A	500 MW
Curtailment	Available With Certainty	N/A	N/A	N/A

Table F.5: Table detailing the models used for the random availabilities of generating technologies.

standards, whereas those built before 1987 can opt out, which would require them to close by the end of 2015 with a maximum of 20,000 hours of operation in that time. [69] project that all Coal LCPD (opt out) generation will have closed by the end of year 4 (the end of 2014).

Technology Name	Offer Price	Bid Price
Hydro	£0 per MW	£-50 per MW
Offshore Wind	£0 per MW	£-100 per MW
Onshore Wind	£0 per MW	£-50 per MW
Wave	£0 per MW	£-50 per MW
Nuclear	£10.40 per MW	£0 per MW
New Nuclear	£10.40 per MW	£0 per MW
Biomass	£40 per MW	£15 per MW
CHP	£44.34 per MW	£16.63 per MW
CCGT CCS	£63.98 per MW	£23.99 per MW
Clean Coal CCS	£60.20 per MW	£22.58 per MW
CCGT New	£68.81 per MW	£25.80 per MW
CCGT	£72.56 per MW	£27.21 per MW
Europe Interconnection	£74.38 per MW	£27.89 per MW
Coal LCPD	£89.68 per MW	£33.63 per MW
Coal LCPD (opt out)	£89.68 per MW	£33.63 per MW
Ireland Interconnection	£91.92 per MW	£34.47 per MW
Pumped Storage	£90.58 per MW	£33.97 per MW
Oil	£208.22 per MW	£78.08 per MW
OCGT	£273.88 per MW	£102.70 per MW
Curtailment	£4000 per MW	£4000 per MW

Table F.6: Table detailing the bid and offer prices of generating technologies.

F.3.2 Generation Bid and Offer Prices

Table F.6 gives details of the bid and offer prices of each of the installed generating technology types. As was noted in Section 2.2.1, the bid price for renewable generating capacities (such as hydro, wind and wave) is negative, which indicates that if these generation types are included in the unconstrained schedule (some of which always will be due to these having the lowest offer prices) and that generating capacity cannot be used due to transmission constraints, these generating capacities would then be paid to do nothing.

Also, there is a very high price of curtailment of £4000, which is over 14 times greater than the next highest offer price. However, as was also noted in Section 2.2.1, curtailment can be included in the unconstrained schedule, and if no further curtailment was included in the constrained schedule, constraint costs would not increase as this would indicate an insufficient generation system, not necessarily an insufficient transmission system.

F.3.3 Installed Generating Capacities

A full detail of generating capacities installed in all 20 generating capacities across all 7 zones and all 20 years are omitted from this thesis, due to the space required to give such details, and there not being any particularly remarkable features about the data. However, full details are available at [69], the primary reference of this thesis. Some minor points of interest have already been mentioned, such as all large combustion plants closing by the end of year 4, and there are other smaller trends to note that would reasonably be expected, such as more renewable generating capacity (such as wind) being installed in later years (due to future emissions targets) and less non-renewable generating capacity (such as CCGT and coal without CCS) being installed in later years (also due to future emissions targets).

Appendix G

A Selection of R Code

G.1 R Code of the Simulator for the Example of Section 2.2

Section 2.2 of Chapter 2 detailed a simple example to illustrate how to randomly simulate constraint cost for a given power system. This section will give details of the R code used to simulate constraint costs for the simple example.

Function Input	Input Description
GenDataInst	Vector detailing installed generating capacities (in MW)
GenDataAvail	Vector detailing availability probabilities of generating capacities
GenDataUnits	Vector detailing the unit sizes (in MW) of generating capacities
DemData	Vector detailing the demand (in MW) in each of the two zones
CPlus	Vector detailing the offer prices (in pounds per MW) of the generating capacities
CMinus	Vector detailing the bid prices (in pounds per MW) of the generating capacities
TransferCapacity	Single value detailing the transfer capacity between the two zones

Table G.1: Table giving details of the input variables for the simulator used in the simple example of Section 2.2.

Table G.1 gives details of the input variables of the simulator, as well as a brief description of each. It is assumed that GenDataInst, GenDataAvail, GenDataUnits, CPlus and CMinus are four elements long each with these four elements giving details for wind, coal, gas and curtailment respectively (i.e. in order of offer price for the example of Section 2.2). Appendix G.2 will go on to define a more general simulator, where the order of such variables is unimportant, so long as all simulator inputs have the same relative order (e.g. if the ith element of CPlus is the offer price of coal, then the ith element of all other vectors should also relate to coal). DemData is a vector with two entries, of which the first element of DemData is Scottish demand in MW and the second element is English demand in MW.

The R code for the simulator used in the simple example of Section 2.2 is given below. Some annotations are given to help the reader follow the code, with a further overview given after the R code.

```
SimpleTwoZoneFunction<-function(GenDataInst,GenDataAvail,GenDataUnits,
    DemData,CPlus,CMinus,TransferCapacity){


  InstalledUnits<-round(GenDataInst/GenDataUnits)
  #Calculates the number of installed units based on input data

  AvailableUnits<-c(0,0,0,0)
  for(i in 1:4){
    AvailableUnits[i]<-(rbinom(1,InstalledUnits[i],GenDataAvail[i])
        /InstalledUnits[i])*GenDataInst[i]
  }

  #The above randomly simulates available generating capacities using
    a binomial distribution based on the simulator input

  UnconstrainedSchedule<-c(0,0,0,0)
  TotalDemand<-sum(DemData)
```

```
RemainingDemand<-TotalDemand

i<-1
while(RemainingDemand>0){
  UnconstrainedSchedule[i]<-min(RemainingDemand,AvailableUnits[i])
  RemainingDemand<-RemainingDemand-UnconstrainedSchedule[i]
  i<-i+1
}

#The above creates an unconstrained schedule where capacity is scheduled
  in order of offer price until scheduled capacity equals total demand

UnusedCapacity<-AvailableUnits-UnconstrainedSchedule
#Calculates the available generating units not used in the
  unconstrained schedule


ScottishGen<-UnconstrainedSchedule[1]+UnconstrainedSchedule[2]
EnglishGen<-UnconstrainedSchedule[3]
ConstrainedSchedule<-UnconstrainedSchedule
ConstrainedOn<-c(0,0,0,0)
ConstrainedOff<-c(0,0,0,0)

#The above creates the necessary vectors to calculate the
  constrained schedule


if(ScottishGen>DemData[1]){

  ScottishSurplus<-ScottishGen-DemData[1]
  if(ScottishSurplus>TransferCapacity){
    CoalOff<-ScottishSurplus-TransferCapacity
    ConstrainedSchedule[2]<-ConstrainedSchedule[2]-CoalOff
    ConstrainedOff[2]<-CoalOff
```

```
    i<-3
    while(CoalOff>0){
      ConstrainedOn[i]<-min(CoalOff,UnusedCapacity[i])
      ConstrainedSchedule[i]<-ConstrainedSchedule[i]+ConstrainedOn[i]
      CoalOff<-CoalOff-ConstrainedOn[i]
      i<-i+1
    }
  }
}

#The above calculates the constrained schedule when scheduled
  Scottish generation exceeds Scottish Demand in the unconstrained
  schedule.
#First, ScottishSurplus is calculated as the difference between
  Scottish demand and the generating capacity scheduled in Scotland.
#If this exceeds the transfer capacity, coal capacity is constrained off,
 with gas and curtailment are constrained on its place, such that all
 demand is satisfied and the transfer capacity is not exceeded.

if(ScottishGen<DemData[1]){

  EnglishSurplus<-EnglishGen-DemData[2]
  if(EnglishSurplus>TransferCapacity){
    ConstrainedOff[3]<-EnglishSurplus-TransferCapacity
    ConstrainedOn[4]<-EnglishSurplus-TransferCapacity
    ConstrainedSchedule[3]<-ConstrainedSchedule[3]-ConstrainedOff[3]
    ConstrainedSchedule[4]<-ConstrainedSchedule[4]+ConstrainedOn[4]
  }
}
#The above calculates the constrained schedule when scheduled
  Scottish demand exceeds Scottish generation in the
  unconstrained schedule.
#First EnglishSurplus is calculated as the difference between
  English demand and the generating capacity scheduled in England.
```

```
  #If this exceeds the transfer capacity, gas capacity is constrained off
    and curtailment is constrained on its place such that all demand
    is satisfied and the transfer capacity is not exceeded.

  ##Note, the case of Scottish demand being equal to Scottish generation
    is ignored as in this case no capacity is transferred between zones,
    so the unconstrained schedule is equal to the constrained schedule

  ConstraintCosts<-ConstrainedOn%*%CPlus-ConstrainedOff%*%CMinus

  #Constraint costs are calculated as the difference between offer prices
    of capacity constrained on and bid prices of capacity constrained off

  out.list<-list("UnconstrainedSchedule"=UnconstrainedSchedule,
    "ConstrainedSchedule"=ConstrainedSchedule,
    "ConstraintCosts"=ConstraintCosts)
  #The constraint costs (as well as constrained and unconstrained schedule)
    are returned as simulator output
  return(out.list)
}
```

As an overview, the above function first simulates the available generating capacity of all four types of generating capacity (i.e. wind, coal, gas and curtailment) based on the simulator input using a binomial distribution. As described in Section 2.1.2, an unconstrained schedule is then created based on the available generating capacities simulated, with capacity scheduled in order of offer price (lowest to highest) until all demand is satisfied, whilst ignoring the limits on what can be traded between zones.

Then, a constrained schedule is calculated as the cheapest way to constrain off (not use) some capacity which was initially included in the unconstrained schedule and constrain on (use instead) some alternative generating capacity such that all demand is satisfied whilst the limitation on the amount of generating capacity that can be traded between zones is also obeyed. Note, the R code for calculating the constrained schedule is not very general and only suitable for the example described in Section 2.2. However, the

R code for a much more general simulator is described in Appendix G.2, which uses a linear program to calculate the constrained schedule.

Finally, constraint costs are calculated as the difference between the offer prices of generating capacity constrained on and the bid prices of generating capacity constrained off (as described in Equation 2.1.1 of Section 2.1.2).

As was noted at the beginning of this section, the above function is only suitable when the merit order (order of offer price in ascending order) is wind, coal, gas then curtailment, as was the case for the example of Section 2.2. This will not necessarily be the case for a general problem, and the full simulator, which will be detailed in Appendix G.2, accounts for this by reordering all input depending on the input offer prices.

A brief R code to illustrate how constraint costs are simulated when assuming values for simulator input as those detailed in Table 2.1 and Figure 2.4 of Section 2.2.1 is given below.

```
AssumedGenInst<-c(2000,6000,54000,100000)
AssumedGenAvail<-c(1,0.85,0.9,1)
AssumedDataUnits<-c(2000,500,500,100000)
AssumedDemData<-c(5000,45000)
AssumedCPlus<-c(0,50,120,120)
AssumedCMinus<-c(-50,25,80,120)
AssumedTransferCapacity<-1000

SimpleTwoZoneFunction(AssumedGenInst,AssumedGenAvail,AssumedDataUnits,
  AssumedDemData,AssumedCPlus,AssumedCMinus,AssumedTransferCapacity)
```

G.2 R Code for the Simulator Defined in Chapter 3

Chapter 3 detailed the simulator used throughout this thesis, with Chapter 4 going on to detail how this simulator could be improved by using importance sampling within the simulator to actually simulate snapshots more relevant to the estimate of mean annual constraint costs more frequently than others. This section will give the R code

Input Variable	Description
in.peak.demand	The peak demand level (in MW) of the year to be simulated, i.e. $\mathfrak{d}^y$
in.loaddurc	The load duration curve to be used in simulation (where each entry is the proportion of peak demand to be used in simulation for each half hour snapshot, $\mathfrak{d}^\tau$)
in.fmax	A vector of length 6, detailing the transfer capacity of the B4 to B15 boundaries (in MW)
in.cminus	A vector where the tth entry is the bid price of technology t
in.cplus	A vector where the tth entry is the offer price of technology t
in.instCap	A matrix where the the tth entry of the rth row is the installed generating capacity of technology t in zone r
in.meanAvail	A vector where the tth entry is the availability probability of technology t (if the availability of technology t is assumed to follow a binomial distribution) or the tth entry is the mean availability of technology t (if the availability of technology t is assumed to follow a normal distribution)
in.sdAvail	A vector where the tth entry is the standard deviation of the availability of technology t (if the availability of technology t is assumed to follow a normal distribution)
in.UnitSize	A vector where the tth entry is the unit size of technology t (if the availability of technology t is assumed to follow a binomial distribution)
in.propDemand	A vector of length 7 where the rth entry is the proportion of snapshot demand in zone r, $\mathfrak{d}^{\mathfrak{r}}$
in.distType	A vector where the tth entry is the distribution type of technology t (i.e. the model used for random simulation of generation). In the code 1 denotes a binomial distribution, 2 denotes a normal distribution, 5 denotes available with certainty, 6 denotes on-shore wind and 7 denotes off-shore wind
in.techName	A vector where the tth entry is the name of technology t (e.g. nuclear, gas, wind, etc)
in.importanceprobabilities	A vector where the ith entry is the probability that snapshot i is actually sampled when applying importance sampling

Table G.2: Table giving details of the input variables of the function fullsimulatorIStrack, the simulator used in this thesis.

for the the simulator which uses importance sampling, with details then given of how the code could be modified if importance sampling is not being used.

Table G.2 details the input variables used for the simulator, with a brief description of each. Note, the order of elements of in.cminus, in.cplus, in.instCap, in.meanAvail, in.sdAvail, in.UnitSize, in.distType, and in.techName is unimportant, so long as they all use the same order (e.g. if the ith element of in.cminus relates to the bid price of nuclear generating capacity, then the ith element of all other vectors should relate to nuclear generating capacity) as the R code is written quite generally, and will reorder input data by offer price before simulating.

The following details the R code for the simulator used in this thesis, with quite a few annotations added to help the reader follow. Further to these annotations, a summary of how the code works will be given after the code.

```
fullsimulatorIStrack<-function(in.peak.demand,in.loaddurc,in.fmax,in.cminus,
  in.cplus,in.instCap,in.meanAvail,in.sdAvail,in.UnitSize,in.propDemand,
  in.distType,in.techName,in.importanceprobabilities){

  #Create the main code for simulating annual constraint costs
  oneyearfull<-function(instCap,the.ldc,peakDemand,fmax,nUnits,
    meanAvail,sdAvail,cminus,cplus,distType,propDemand,
    importanceprobabilities){

    TotalSnapshots<-length(the.ldc)
    #The number of snapshots in a year are noted
    workingobs<-c(rep(0,TotalSnapshots))
    #Create a vector to store the simulated constraint costs in each
      snapshot
    SimTrack<-c(rep(0,TotalSnapshots))
    #Create a vector to keep track of whether a snapshot was actually
      simulated or not when using importance sampling
    for(f in 1:TotalSnapshots){#Beginning of a loop where snapshots
    are simulated sequentially

      ###############################################################
```

```
ISSimCheckerT<-runif(1)
if(importanceprobabilities[f]>=ISSimCheckerT){
#The above randomly simulates whether or not constraint costs
  will be simulated for snapshot f
#If importanceprobabilities[f]>=ISSimCheckerT constraint costs
  are simulated, otherwise they are not

  puDemand<-the.ldc[f]
  #The proportion of peak demand assumed for the current snapshot

  demvec<-propDemand*peakDemand*puDemand
  #Creates the demand vector (the rth entry is the demand in
   zone r) for the current snapshot

  ntype<-30  #Number of technologies (note, specific to our data)
  ntech<-30    #Number of technologies (note, specific to our data)
  nregion<-7   #Number of regions (note, specific to our data)
  nvar<-(6 + 2*nregion*ntype)
  #Number of variables that will be later used in the linear
    program (note, specific to our data)

  propAvail<-matrix(c(rep(0)),nrow=7,ncol=30)
  #Creates a blank matrix to store simulated generation data

  #Now simulate the proportions of generation available for each
    technology by randomly drawing from binomial/normal
    distributions as appropriate

  for(t in 1:ntech){
    for(r in 1:nregion){
      if(distType[t]==1){
        if(nUnits[r,t]>0){
          propAvail[r,t]<-(rbinom(1,nUnits[r,t],meanAvail[t])
            /nUnits[r,t])
```

```
      }
    }
    else if(distType[t]==2){
      if(nUnits[r,t]>0){
        propAvail[r,t]<-rnorm(1,meanAvail[t],sdAvail[t])
      }
      if(propAvail[r,t]<0){
        propAvail[r,t]<-0
      }
      if(propAvail[r,t]>1){
        propAvail[r,t]<-1
      }
    }
    else if(distType[t]==5){
      propAvail[r,t]<-1
    }
    else if(distType[t]==3){
      propAvail[r,t]<-0
    }
  }
}
#Multiply these proportions by installed generation capacity
  to simulate the available generating capacity

gmax<-matrix(c(rep(0)),nrow=nregion,ncol=ntech)
for(r in 1:nregion){
  for(t in 1:ntech){
    gmax[r,t]<-instCap[r,t]*propAvail[r,t]
  }
}

#Now simulate wind availabilities using
  National Grid's model and data
#Note, there are 2 different loops to account for National
```

```
  Grid's seasonal model, which classifies each snapshot as a summer
  or winter snapshot
#Further, within each zone both on-shore and off-shore
  wind availability is simulated

if(f>4321){ #For a summer snapshot
  simdat1<-mvrnorm(1,c(rep(0,16)),WindSigma)
  #simdat1 is a random drawing from the multivariate normal
   distribution used to simulate available wind generating
   capacity, using WindSigma, National Grid's account for
   covariance between wind speeds and geographical zone

  simdat1<-pnorm(simdat1)
  #Transform the data to [0,1] using the normal CDF

  #Below re-adjusts the data to allow for one of the zones
   being split into 2 by the National Grid AFTER simulation
  #(For interest the difference is the wind correlation model
   accounts for the B1, B4, B6, B7a, B8, B9 and B15 boundaries,
   whereas the CDFs include sufficient data for the
   B1, B4, B5, B6, B7a, B8, B9 and B15 boundaries)


  simdat1<-c(simdat1,0,0)
  j<-16
  while(j>4){
    simdat1[j+2]<-simdat1[j]
    j<-j-1
  }

  windpropvec<-c(rep(0,18))


  #The below transforms our previous transformation using
```

```
  National Grid's wind load CDFs to give a proportion of wind
  generation capacity available

windpropvec[1]<-NGWindTransformSummerZ1(simdat1[1])
windpropvec[2]<-NGWindTransformSummerZ1(simdat1[2])
windpropvec[3]<-NGWindTransformSummerZ2(simdat1[3])
windpropvec[4]<-NGWindTransformSummerZ2(simdat1[4])
windpropvec[5]<-NGWindTransformSummerZ3(simdat1[5])
windpropvec[6]<-NGWindTransformSummerZ3(simdat1[6])
windpropvec[7]<-NGWindTransformSummerZ4(simdat1[7])
windpropvec[8]<-NGWindTransformSummerZ4(simdat1[8])
windpropvec[9]<-NGWindTransformSummerZ5(simdat1[9])
windpropvec[10]<-NGWindTransformSummerZ5(simdat1[10])
windpropvec[11]<-NGWindTransformSummerZ6(simdat1[11])
windpropvec[12]<-NGWindTransformSummerZ6(simdat1[12])
windpropvec[13]<-NGWindTransformSummerZ7(simdat1[13])
windpropvec[14]<-NGWindTransformSummerZ7(simdat1[14])
windpropvec[15]<-NGWindTransformSummerZ8(simdat1[15])
windpropvec[16]<-NGWindTransformSummerZ8(simdat1[16])
windpropvec[17]<-NGWindTransformSummerZ9(simdat1[17])
windpropvec[18]<-NGWindTransformSummerZ9(simdat1[18])

#Now create vectors for offshore and
 onshore wind generation in each zone

windonprops<-c(rep(0,7))
windoffprops<-c(rep(0,7))

#Input proportions into the above, averaging where necessary
 due to the boundaries differing slightly between the
 CDFs and installed capacity data
#This is due to the CDFs accounting for the B1, B4, B5, B6, B7a,
 B8, B9 and B15 boundaries, whereas the installed capacity data
 accounts for the B4, B6, B7a, B8, B9 and B15 boundaries
```

```
windonprops[1]<-(windpropvec[1]+windpropvec[3])/2
windoffprops[1]<-(windpropvec[2]+windpropvec[4])/2
windonprops[2]<-(windpropvec[5]+windpropvec[7])/2
windoffprops[2]<-(windpropvec[6]+windpropvec[8])/2
windonprops[3]<-windpropvec[9]
windonprops[4]<-windpropvec[11]
windonprops[5]<-windpropvec[13]
windonprops[6]<-windpropvec[15]
windonprops[7]<-windpropvec[17]
windoffprops[3]<-windpropvec[10]
windoffprops[4]<-windpropvec[12]
windoffprops[5]<-windpropvec[14]
windoffprops[6]<-windpropvec[16]
windoffprops[7]<-windpropvec[18]

#Now use the above proportions to simulate the
  available wind generating capacity in each zone
for(t in 1:ntech){

  if(distType[t]==6){
    for(r in 1:nregion){
      gmax[r,t]<-instCap[r,t]*windonprops[r]
    }
  }
  else if(distType[t]==7){
    for(r in 1:nregion){
      gmax[r,t]<-instCap[r,t]*windoffprops[r]
    }
  }
  else{
  }

}
```

```
}


####Repeat above loop for winter snapshots
else{
  simdat1<-mvrnorm(1,c(rep(0,16)),WindSigma)
  simdat1<-pnorm(simdat1)

  simdat1<-c(simdat1,0,0)
  j<-16
  while(j>4){
    simdat1[j+2]<-simdat1[j]
    j<-j-1
  }

  windpropvec<-c(rep(0,18))

  windpropvec[1]<-NGWindTransformWinterZ1(simdat1[1])
  windpropvec[2]<-NGWindTransformWinterZ1(simdat1[2])
  windpropvec[3]<-NGWindTransformWinterZ2(simdat1[3])
  windpropvec[4]<-NGWindTransformWinterZ2(simdat1[4])
  windpropvec[5]<-NGWindTransformWinterZ3(simdat1[5])
  windpropvec[6]<-NGWindTransformWinterZ3(simdat1[6])
  windpropvec[7]<-NGWindTransformWinterZ4(simdat1[7])
  windpropvec[8]<-NGWindTransformWinterZ4(simdat1[8])
  windpropvec[9]<-NGWindTransformWinterZ5(simdat1[9])
  windpropvec[10]<-NGWindTransformWinterZ5(simdat1[10])
  windpropvec[11]<-NGWindTransformWinterZ6(simdat1[11])
  windpropvec[12]<-NGWindTransformWinterZ6(simdat1[12])
  windpropvec[13]<-NGWindTransformWinterZ7(simdat1[13])
  windpropvec[14]<-NGWindTransformWinterZ7(simdat1[14])
  windpropvec[15]<-NGWindTransformWinterZ8(simdat1[15])
  windpropvec[16]<-NGWindTransformWinterZ8(simdat1[16])
  windpropvec[17]<-NGWindTransformWinterZ9(simdat1[17])
```

```
windpropvec[18]<-NGWindTransformWinterZ9(simdat1[18])



windonprops<-c(rep(0,7))
windoffprops<-c(rep(0,7))

windonprops[1]<-(windpropvec[1]+windpropvec[3])/2
windoffprops[1]<-(windpropvec[2]+windpropvec[4])/2
windonprops[2]<-(windpropvec[5]+windpropvec[7])/2
windoffprops[2]<-(windpropvec[6]+windpropvec[8])/2
windonprops[3]<-windpropvec[9]
windonprops[4]<-windpropvec[11]
windonprops[5]<-windpropvec[13]
windonprops[6]<-windpropvec[15]
windonprops[7]<-windpropvec[17]
windoffprops[3]<-windpropvec[10]
windoffprops[4]<-windpropvec[12]
windoffprops[5]<-windpropvec[14]
windoffprops[6]<-windpropvec[16]
windoffprops[7]<-windpropvec[18]

for(t in 1:ntech){

  if(distType[t]==6){
    for(r in 1:nregion){
      gmax[r,t]<-instCap[r,t]*windonprops[r]
    }
  }
  else if(distType[t]==7){
    for(r in 1:nregion){
      gmax[r,t]<-instCap[r,t]*windoffprops[r]
    }
  }
  else{
```

```
    }

  }
}
#####End of simulating wind

sysAvail<-colSums(gmax)
#Total available generating capacity in the power system such
 that the t th entry of sysAvail is the total available
 generating capacity of technology t across all zones
 in the system
g0<-matrix(c(rep(0)),nrow=nregion,ncol=ntech)
#Blank matrix to be used to detail the unconstrained schedule

remDem<-peakDemand*puDemand*sum(propDemand)
#Total demand in the power system

#The below loop creates an unconstrained schedule, where generating
  capacity is scheduled to be used, in order of lowest offer price,
  until all demand is met
#It is assumed data is ordered in order of offer price where
  appropriate (as will be detailed later after this function
  is defined)

t<-1
repeat{
  if(remDem>sysAvail[t]){

    g0[,t]<-gmax[,t]
    remDem<-remDem-sysAvail[t]
    t<-t+1
  }
  else{
    g0[,t]<-gmax[,t]*remDem/sysAvail[t]
```

```
    break
  }
}
#g0 is now what generating capacity is included in the
  unconstrained schedule

gpmax<-gmax-g0
#gpmax is the remaining generating capacity not contained in the
  unconstrained schedule (i.e. the generating capacity that can be
  constrained on if necessary)

cccs<-c(-cminus,cplus)
#A vector of bid and offer prices to be used for linear programming
#Negative bid prices are used as constraint costs are the sum of
  offer prices of capacity constrained on minus the sum of bid prices
  of capacity constrained off

nvar<-(6+2*7*30)
#The number of variables used in our linear programme

#The following will define a linear program of (6+2*7*30) variables

#The variables are ordered as:
#The flow across the 6 boundaries from North (B4) to South (B15)
#Then 30 variables for generating capacity constrained off
  in a zone followed by 30 variables for generating capacity
  constrained on in a zone
#These 60 variables are included for all 7 zones from the northmost
  (north of boundary B4) to the southmost (south of B15) zones

gmaxvec<-c(rep(0,nvar))
#A vector to define the maximum values variables can take
  in the linear program
```

```
for(i in 1:6){
  gmaxvec[i]<-fmax[i]
}
#The above defines the first 6 elements of gmaxvec as the
  boundary transfer capacities

for(i in 1:7){
  for(j in 1:30){
    gmaxvec[6+(i-1)*30*2+j]<-g0[i,j]
    #These entries are what capacity is available to be
      constrained off
    gmaxvec[6+(i-1)*30*2+30+j]<-gmax[i,j]-g0[i,j]
    #These entries are what capacity is available to be
      constrained on
  }
}
#The above ensures that no more can be constrained on than is
  available (and not included in the unconstrained schedule),
  and no more can be constrained off than is included
  in the unconstrained schedule



gminvec<-c(-fmax,rep(0,2*30*7))
#Creates a vector for the minimum values variables can take
#The first 6 entries define the transfer capacity of each boundary
#Note, we treat positive flow as flow from north to south
  and negative flow as flow from south to north
#The remaining entries are zero, as there is no obligation
  to constrain on/off any capacity if boundary transfer capacity
  constraints are satisfied

#Now create linear programme
#The objective is to minimise the sum of offer prices of generating
  capacity constrained on minus the sum of bid prices of generating
```

```
  capacity constrained off
#(lpSolve minimises by default, making the following sufficient
 for us)
#For each constraint we balance flow into zone - flow out of zone
  - constrained off in zone  + constrained on in zone >=
  demand in zone -generation schedule in zone
#As capcity is balanced in each zone, a global power balance
  is not necessary
#Then we use gminvec and gmaxvec to ensure we cannot
  constrain off more than is scheduled, constrain on more
  than is available or exceed flow capacity

mymodobj<-make.lp(0,nvar)
set.objfn(mymodobj,c(rep(0,6),rep(cccs,7)))
add.constraint(mymodobj,c(-1,0,0,0,0,0,rep(-1,30),rep(1,30),
  rep(0,6*30*2)),">=",demvec[1]-sum(g0[1,]))
add.constraint(mymodobj,c(1,-1,0,0,0,0,rep(0,1*30*2),rep(-1,30),
  rep(1,30),rep(0,5*30*2)),">=",demvec[2]-sum(g0[2,]))
add.constraint(mymodobj,c(0,1,-1,0,0,0,rep(0,2*30*2),rep(-1,30),
  rep(1,30),rep(0,4*30*2)),">=",demvec[3]-sum(g0[3,]))
add.constraint(mymodobj,c(0,0,1,-1,0,0,rep(0,3*30*2),rep(-1,30),
  rep(1,30),rep(0,3*30*2)),">=",demvec[4]-sum(g0[4,]))
add.constraint(mymodobj,c(0,0,0,1,-1,0,rep(0,4*30*2),rep(-1,30),
  rep(1,30),rep(0,2*30*2)),">=",demvec[5]-sum(g0[5,]))
add.constraint(mymodobj,c(0,0,0,0,1,-1,rep(0,5*30*2),rep(-1,30),
  rep(1,30),rep(0,30*2)),">=",demvec[6]-sum(g0[6,]))
add.constraint(mymodobj,c(0,0,0,0,0,1,rep(0,6*30*2),rep(-1,30),
  rep(1,30)),">=",demvec[7]-sum(g0[7,]))
set.bounds(mymodobj, lower = gminvec)
set.bounds(mymodobj, upper = gmaxvec)
solve(mymodobj)
get.objective(mymodobj)

workingobs[f]<-get.objective(mymodobj)
```

```
      #The above stores the objective function of the solution as
        the snapshot constraint costs simulated

      SimTrack[f]<-1  #Indicate that this snapshot was actually simulated

    }
    else{#For when the snapshot was not simulated in importance sampling
      workingobs[f]<-0
      SimTrack[f]<-0 #Note that the snapshot was not simulated
    }
  }
  Out.List.T<-list("workingobs"=workingobs,"SimTrack"=SimTrack)
  return(Out.List.T)
  #Return the simulated constraint costs plus a vector indicating
    whether the snapshot was simulated
}

#The following sets up data to be used for simulation, by ordering
  the input data by offer price from lowest to highest

orderingvec<-order(in.cplus)#order data by offer price

new.cminus<-in.cminus[orderingvec]
new.cplus<-in.cplus[orderingvec]
new.sdAvail<-in.sdAvail[orderingvec]

new.meanAvail<-in.meanAvail[orderingvec]

new.distType<-in.distType[orderingvec]
new.techName<-in.techName[orderingvec]

blankmat<-matrix(rep(0),nrow=7,ncol=30)
for(i in 1:7){
  blankmat[i,]<-in.UnitSize
```

```
}
UnitSizes<-blankmat

temp.nUnits<-in.instCap/UnitSizes
temp.nUnits<-round(temp.nUnits)
#Calculate the number of units of each generating technology
 in each zone (rounding to give an integer where necessary)

new.nUnits<-temp.nUnits
for(i in 1:7){
 new.nUnits[i,]<-new.nUnits[i,][orderingvec]
}

new.instCap<-in.instCap
for(i in 1:7){
  new.instCap[i,]<-new.instCap[i,][orderingvec]
}

#The above reorders all necessary data by offer price

#Rename remaining inputs for completion
new.fmax<-in.fmax
new.peakDemand<-in.peak.demand
new.ldc<-in.loaddurc
new.propDemand<-in.propDemand
new.importanceprobabilities<-in.importanceprobabilities

#Now randomly simulate constraint costs for the year
workingcosts<-oneyearfull(new.instCap,new.ldc,new.peakDemand,
  new.fmax,new.nUnits,new.meanAvail,new.sdAvail,new.cminus,new.cplus,
  new.distType,new.propDemand,new.importanceprobabilities)


#Record information from the simulation
```

```
  SnapCostsT<-workingcosts$workingobs
  SimTrackOut<-workingcosts$SimTrack



  WeightedSnapCosts<-SnapCostsT/new.importanceprobabilities
  #Weight the simulated constraint costs based on the importance
    sampling weights used

  YearCostEst<-sum(WeightedSnapCosts)
  #The estimate of annual constraint costs from importance sampling

  ##########################################################################

  #Finally, return the results
  outlist<-list("YearCostEst"=YearCostEst,
    "WeightedSnapCosts"=WeightedSnapCosts,"SnapCostsT"=SnapCostsT,
    "SimTrackOut"=SimTrackOut)
  return(outlist)
}
```

The above function details how to simulate constraint costs whilst using importance sampling. As a summary to how the code works, first the input data is reorganized to order the data by offer price (lowest first) to be used for calculating constraint costs.

Then, snapshots are considered sequentially, beginning at midnight on the 1st of December and ending at 23:30 on the 30th of November. First, importance sampling is applied by randomly simulating whether or not a snapshot will be simulated using the input snapshot weights in in.importanceprobabilities.

If a snapshot is to be simulated, first a vector detailing the demand in each snapshot is calculated via Equation 3.1.1 of Chapter 3, where the demand in each zone is a product of the peak demand level, the proportion of peak demand level in the current snapshot from the LDC and proportion of total snapshot demand in that zone. Then, availabilities of generating capacities are then randomly simulated by the appropriate distribution (such as binomial for CCGT), as was described in Section 3.5.

Then, an unconstrained schedule is created, where available generating capacity is scheduled for use (ignoring boundary transfer constraints) until the total capacity scheduled across the system is equal to the total demand across the system. The linear program described in Section 3.3.2 is then used to calculate constraint costs for the state of the system (given the randomly simulated available generating capacity), and these constraint costs are recorded, as well as recording that this snapshot was actually simulated. If the snapshot was not actually simulated, this is also noted.

This is repeated for each snapshot sequentially, and eventually two vectors are acquired, one which gives the constraint costs simulated in each snapshot and another which details whether a snapshot was actually simulated or not. An estimate of constraint costs for the entire year can then be acquired via Equation 4.2.5 of Section 4.2.2 using these two vectors. Finally, the simulation of constraint costs for the entire year is returned, as well as vectors detailing the simulated constraint costs in each snapshot and whether each snapshot was actually simulated or not, which can be used to update the importance sampling weights, as will be detailed in the next section.

To acquire full simulator evaluations from the above function (i.e. evaluations which do not use importance sampling), there are two possibilities. The simplest is to enter in.importanceprobabilities as a vector of length 17520 (i.e. 17520 snapshots) where each entry is 1 (i.e. each snapshot is actually simulated with probability 1 when using importance sampling as defined in Section 4.2.2). However, this would be slightly inefficient, as this would still randomly simulate from a uniform distribution between 0 and 1 and verify that the simulation was not greater than 1.

An alternative method would be to remove the following portion of the R code

```
ISSimCheckerT<-runif(1)
if(importanceprobabilities[f]>=ISSimCheckerT){
  ###Simulation details from above
  }
else{
    workingobs[f]<-0
    SimTrack[f]<-0 ##Note that the snapshot was not simulated
}
```

which would also result in all snapshots being simulated, and be slightly more efficient as there are no longer 17520 needless random draws from a uniform distribution.

G.3 The Importance Sampling Algorithm of Section 4.4.2

G.3.1 Importance Sampling Weight Updating Function

This section will give details on the R code for the function used to update importance sampling weights, as described in steps 8 and 9 of the algorithm detailed in Section 4.4.2.

Function Input	Input Description
inMeanVec	Vector detailing the mean constraint costs simulated for each snapshot before the additional simulations were taken
inTimesSimmed	Vector detailing the number of times each snapshot was simulated before the additional simulations were taken
nuMeanVec	Vector detailing the mean constraint costs simulated for each snapshot in the additional simulations
nuTimesSimmed	Vector detailing the number of times each snapshot was simulated in the additional simulations

Table G.3: Table giving details of the input variables for UpdateISMethodFuncTracking, the function used to updated importance sampling weights.

The R code for this function is given below, with Table G.3 giving some brief details of the input variables of this simulator. The function contains some annotations to aid understanding, and further details will be given after the function is defined.

```
UpdateISMethodFuncTracking<-function(inMeanVec,inTimesSimmed,nuMeanVec,
  nuTimesSimmed){

  snapnum<-length(inMeanVec) #Number of snapshots in a year

  next.MeanVec<-c(rep(0,snapnum))
```

```
  next.TimesSimmed<-c(rep(0,snapnum))

  for(i in 1:snapnum){#create a loop to repeat calculations for all snapshots
    next.TimesSimmed[i]<-inTimesSimmed[i]+nuTimesSimmed[i]
    #Calculates the total number of times snapshot i has been simulated
    next.MeanVec[i]<-(inMeanVec[i]*inTimesSimmed[i]+
      nuMeanVec[i]*nuTimesSimmed[i])/next.TimesSimmed[i]
    #Calculates the mean of those simulations
  }

  daMax<-max(next.MeanVec)
  next.WeightVec<-next.MeanVec/daMax
  #Calculates the updated importance sampling weights

  for(i in 1:snapnum){
    next.WeightVec[i]<-max(c(next.WeightVec[i],0.01))
  }
  #As importance sampling weights must be strictly positive, each snapshot
   is given minimum weight of 0.01

  out.list<-list("next.WeightVec"=next.WeightVec,
  "next.MeanVec"=next.MeanVec,"next.TimesSimmed"=next.TimesSimmed)

  return(out.list)

}
```

As detailed in Table G.3, inMeanVec represents the estimated snapshot means before additional simulations are taken (i.e. a vector detailing the values of $\hat{\phi}_\tau$); inTimesSimmed represents the number of times each snapshot has been before the additional simulations are taken (i.e. a vector detailing the values of N_τ); nuMeanVec represents the estimated snapshot means from the additional simulations (i.e. a vector detailing the values of $\hat{\phi}_{\tau,+}$) and nuTimesSimmed represents the number of times each snapshot has been in the additional simulations (i.e. a vector detailing the values of $N_{\tau,+}$).

First, the function performs step 8 of the algorithm detailed in Section 4.4.2, i.e. updates the mean simulated constraint costs from all simulations and the number of times each snapshot was simulated as

$$\hat{\phi}_\tau \leftarrow \frac{\hat{\phi}_\tau N_\tau + \hat{\phi}_{\tau,+} N_{\tau,+}}{N_\tau + N_{\tau,+}}$$

and

$$N_\tau \leftarrow (N_\tau + N_{\tau,+})$$

Then, the function calculates updated weights to be used for importance sampling, $\boldsymbol{\omega}$, via Equation 4.3.1 using the updated estimates of the snapshot means, $\hat{\phi}_\tau$.

In the above function a minimum weight of 0.01 is set for each snapshot, as Equation 4.2.5 requires each snapshot to have non-zero weight. However, it would be simple to change this to some alternative minimum, for example by using an additional input, in.Min.Snap.Weight, in the function.

G.3.2 Estimating Mean Constraint Costs

This subsection will detail how the importance sampling method detailed in Section 4.4.2 can be applied to estimate mean annual constraint costs for a given power system background by using the simulator defined in Appendix G.2 and the function to update importance sampling weights defined in Appendix G.3.1.

Below details an annotated R code required to take an initial number (in this case 10) full simulator evaluations, and then uses these evaluations to calculate some initial weights to be used for importance sampling, i.e. steps 2 to 4 of the algorithm specified in Section 4.4.2. For this application it is assumed that mean constraint costs are being estimated for a year 1 power system background, with the data defined as such. However, by changing the data appropriately (such as PeakDemandYear1 to the peak demand level of the desired power system) the following code can be applied for any power system.

```
#In the following R code the following input data will be used to simulate
 constraint costs for a year 1 power system background
```

```
#PeakDemandYear1 #The peak demand in the year to be simulated
#LDCToUse #The LDC to be used
#BoundaryCapacitiesYear1 #The boundary transfer capacities
#cminusToUse #The bid prices to be used
#cplusToUse #The offer prices to be used
#InstalledCapacityYear1 #The installed generating capacities
#meanAvailsToUse #The assumed availability probabilities
#sdAvailToUse #The assumed standard deviation of availabilities
#UnitSizesToUse #The assumed unit sizes of generation
#RegionalDemandProportionsToUse #The assumed regional demand
#DistributionTypeToUse #Vector detailing the models used for
  each generating capacity
#TechnologyNameToUse #Names of the generating technologies
impvec.all<-c(rep(1,17520)) #Importance sampling weights for the initial
  full evaluations (which ensure each snapshot is evaluated
  in each simulation)

NumberOfInitialSims<-10
#Set a number of initial full simulations to be taken

InitialSampleMatrix<-matrix(ncol=length(LDCToUse),nrow=NumberOfInitialSims)
#Create a matrix to store the snapshot evaluations of this initial sample
  such that the ith evaluation of the jth snapshot is stored in row i of
  column j
Initial.SimC<-c(rep(0,NumberOfInitialSims))
#Create a vector to store the initial yearly simulations of constraint costs



for(i in 1:NumberOfInitialSims){
  TempR<-fullsimulatorIStrack(PeakDemandYear1,LDCToUse,
    BoundaryCapacitiesYear1,cminusToUse,cplusToUse,InstalledCapacityYear1,
    meanAvailsToUse,sdAvailToUse,UnitSizesToUse,
    RegionalDemandProportionsToUse,DistributionTypeToUse,TechnologyNameToUse,
    impvec.all)
```

```
  InitialSampleMatrix[i,]<-TempR$SnapCostsT
  Initial.SimC[i]<-TempR$YearCostEst
}
#The above loop takes the required number of full simulator evaluations
  and stores the output

################################################


InitialMeans<-c(rep(0,17520))
for(i in 1:length(LDCToUse)){
  InitialMeans[i]<-mean(InitialSampleMatrix[,i])
}
#The above estimates the mean constraint costs of each snapshot from the
  initial simulations


InitialMax<-max(InitialMeans)
InitialWeights<-InitialMeans/InitialMax
#The above calculates the initial importance sampling weights as the
  proportion of the mean constraint constraint costs in each
  snapshot to the greatest mean constraint costs in any snapshot



for(i in 1:length(LDCToUse)){
  InitialWeights[i]<-max(c(InitialWeights[i],0.01))
}
#As it is required that each snapshot has non-zero weight, a minimum
 weight of 0.01 is given to snapshots where necessary


InitialSampled<-c(rep(NumberOfInitialSims,length(LDCToUse)))
#The above notes that in the initial simulator evaluations, each snapshot
```

```
  was evaluated NumberOfInitialSims times
```

The above code defines the how to take an initial number of full simulations and use these to estimate importance sampling weights. First, the data which defines the power system (such as installed generating capacities) is defined. Then, the specified number of full simulator evaluations are taken using the simulator defined in Appendix G.2. The means of the simulated constraint in each snapshot are calculated, which are subsequently used to calculate importance sampling weights via Equation 4.3.1 of Section 4.3.1.

The following annotated R code can then be used to take further simulator evaluations which apply importance sampling using these weights via Equation 4.2.5 of Section 4.2.2. After each further simulation, the weights are updated using the function UpdateISMethodFuncTracking, defined in Section G.3.1, until the estimate of mean constraint costs reaches convergence, i.e. steps 5 to 10 of the algorithm defined in Section 4.4.2.

```
CurrentMeans<-InitialMeans
CurrentWeights<-InitialWeights
CurrentSampled<-InitialSampled
#Set the current data for importance sampling weights to those from the
  initial simulations

##############################################################################

MinimumWorkToDo<-10
SERatioCriterion<-0.01
#Set some criteria required for convergence
#These can be changed as required

RunningWorkDone<-0
RunningIndividualEstimates<-0
#Prepare to take further simulations
```

```
ISAnnual.SimC<-NULL
#A vector which stores evaluations of yearly constraint costs

RunningMean<-NULL
RunningSD<-NULL
RunningSEFull<-NULL
RunningSERatio<-NULL
#Statistics about the evaluations of yearly constraint costs (such as their
  mean or standard deviation)

while(RunningWorkDone<MinimumWorkToDo){ #Create a loop to take additional
  simulations, until some minimum amount of work (in terms of EFSE)
  has been done

  TempR<-fullsimulatorIStrack(PeakDemandYear1,LDCToUse,
    BoundaryCapacitiesYear1,cminusToUse,cplusToUse,InstalledCapacityYear1,
    meanAvailsToUse,sdAvailToUse,UnitSizesToUse,
    RegionalDemandProportionsToUse,DistributionTypeToUse,
    TechnologyNameToUse,CurrentWeights)
  TempU<-UpdateISMethodFuncTracking(CurrentMeans,CurrentSampled,
    TempR$SnapCostsT,TempR$SimTrackOut)
  #The above takes one further yearly simulator evaluation (using
   importance sampling), then updates the importance sampling weights
   based on this simulation

  CurrentWeights<-TempU$next.WeightVec
  #Update the importance sampling weights
  CurrentMeans<-TempU$next.MeanVec
  #Update the estimates of snapshot mean
  CurrentSampled<-TempU$next.TimesSimmed
  #Update the number of times each snapshot has been sampled

  #The above updates vectors which store information used to update
    importance sampling weights (such as the mean of all snapshot
```

```
    evaluations and the number of times each snapshot has been evaluated)

  RunningIndividualEstimates<-RunningIndividualEstimates+1
  #Update the number of yearly simulator evaluations taken in total



  ISAnnual.SimC[RunningIndividualEstimates]<-TempR$YearCostEst
  #Update ISAnnual.SimC such that it stores all evaluations of yearly
    constraint costs

  RunningMean<-mean(ISAnnual.SimC)
  RunningSD<-sd(ISAnnual.SimC)
  RunningSE<-RunningSD/sqrt(RunningIndividualEstimates)
  RunningSERatio<-RunningSE/RunningMean
  #The above then calculates statistics of the yearly evaluations (such as
    the mean of all yearly evaluations or the standard error of the
    evaluations)

  RunningWorkDone<-RunningWorkDone+(sum(TempR$SimTrackOut)/17520)
  #The total work done (in terms of equivalent full simulator
   evaluations, EFSE) is then noted
}
#The above loop ensures that a specified minimum of equivalent full
  simulator evaluations have been carried out

#The below loop then repeats the above loop until the standard error
  of the estimate falls below the specified value
while(RunningSERatio>SERatioCriterion){

  TempR<-fullsimulatorIStrack(PeakDemandYear1,LDCToUse,
    BoundaryCapacitiesYear1,cminusToUse,cplusToUse,InstalledCapacityYear1,
    meanAvailsToUse,sdAvailToUse,UnitSizesToUse,
    RegionalDemandProportionsToUse,DistributionTypeToUse,
    TechnologyNameToUse,CurrentWeights)
```

```
  TempU<-UpdateISMethodFuncTracking(CurrentMeans,CurrentSampled,
    TempR$SnapCostsT,TempR$SimTrackOut)



  CurrentMeans<-TempU$next.MeanVec
  CurrentWeights<-TempU$next.WeightVec
  CurrentSampled<-TempU$next.TimesSimmed



  RunningIndividualEstimates<-RunningIndividualEstimates+1



  ISAnnual.SimC[RunningIndividualEstimates]<-TempR$YearCostEst
  RunningMean<-mean(ISAnnual.SimC)
  RunningSD<-sd(ISAnnual.SimC)
  RunningSE<-RunningSD/sqrt(RunningIndividualEstimates)
  RunningWorkDone<-RunningWorkDone+(sum(TempR$SimTrackOut)/17520)
  RunningSERatio<-RunningSE/RunningMean



}



FinaleMean<-mean(ISAnnual.SimC)
#The final estimate of mean constraint costs after convergence has
  been reached is noted.

##############################################################################
```

In the above R code, the importance sampling weights to be used (and the means and number of times each snapshot has been simulated) calculated from the initial simulations are noted. Then, the criteria that must be met for convergence of the estimate of mean annual constraint costs (i.e. minimum amount of work in terms of equivalent full simulator evaluations, EFSE, and a maximum value for the standard

error of the estimate) are set.

Subsequent simulator evaluations using the latest estimates of importance sampling weights are then taken, with the weights updated after each simulator evaluation using the function UpdateISMethodFuncTracking, defined in Appendix G.3.1, until the specified minimum work criterion has been met. Then, further simulator evaluations are taken (with again the importance sampling weights updated after each simulator evaluation) until the criterion relating to the standard error of the estimate is met. After the convergence criteria have been met, an estimate of mean annual constraint costs is calculated as the mean of all simulator evaluations of annual constraint costs.

In the above R code the initial full simulator evaluations were used only to calculate initial importance sampling weights, and not used in the estimate of mean annual constraint costs (and as a result the work done for these evaluations was not counted towards the total work done). However, it would be possible to include the evaluations of yearly constraint costs from the initial evaluations in the estimate of mean annual constraint costs by changing the first 25 lines of the above code to those below, with the remainder of the code being otherwise unchanged.

```
CurrentMeans<-InitialMeans
CurrentWeights<-InitialWeights
CurrentSampled<-InitialSampled
#Set the current data for importance sampling weights to those from the
  initial simulations

##############################################################################

MinimumWorkToDo<-10
SERatioCriterion<-0.01
#Set some criteria required for conversion

RunningWorkDone<-NumberOfInitialSims
RunningIndividualEstimates<-NumberOfInitialSims
#Prepare to take further simulations
```

```
ISAnnual.SimC<-Initial.SimC
#A vector which store evaluations of yearly constraint costs

RunningMean<-mean(ISAnnual.SimC)
RunningSD<-sd(ISAnnual.SimC)
RunningSE<-RunningSD/sqrt(RunningIndividualEstimates)
RunningSERatio<-RunningSE/RunningMean
#Statistics about the evaluations of yearly constraint costs (such as their
  mean or standard deviation)
```

The above simply defines the current evaluations of yearly constraint costs as those acquired from the initial simulator evaluations, and calculates the resulting estimate of mean constraint costs and standard error of the estimate. The work done to acquire these evaluations is also noted.

G.4 A Selection of R Code for Chapters 5 and 6

G.4.1 Preliminary R Code Details

This section will give detail a selection of the R code used to consider the transmission expansion planning problems outlined in Sections 5.3.1 and 6.1.1.

As may aspects of the full R code (such as Latin hypercube sampling or fitting an emulator model) are fairly standard procedures, a line by line breakdown of such functions is not given. Instead, instead a description of input and output of the functions used is given in a manner that is sufficient to understand the remainder of the details for the problems outlined in Sections 5.3.1 and 6.1.1.

Latin Hypercube Sampling

The function used to sample input values for training runs is represented by the function

```
LHC.Sample.Function(Sample.Size,in.lower.bounds,in.upper.bounds)
```

Where Sample.Size represents the number of training runs required, in.lower.bounds details the lower bounds of the variables to be sampled and in.upper.bounds details the upper bounds of the variables to be sampled.

in.lower.bounds and in.upper.bounds are defined as vectors of length $N_v + N_d$, such that the ith value of in.lower.bounds is the lower bound for the ith variable containing uncertainty and the $N_v + j$th entry of in.lower.bounds is the lower bound of the range considered for the jth decision variable (and equivalently for the in.upper.bounds). Recall, N_v is the number of variables considered containing uncertainty and N_d is the number of decision variables considered, e.g. the example detailed in Section 6.1.1 considers uncertainty in 3 variables of interest (i.e. $N_v = 3$) and considers making two decisions (i.e. $N_d = 2$).

For example, a sample of 300 training runs for the problem detailed in Section 6.1.1 could be acquired using the following code

```
SamSize<-300
SamLB<-c(0.55,0.8,0.95,0,0)
SamUB<-c(0.85,0.95,1.05,4000,4000)

SampledTrainingInput<-LHC.Sample.Function(SamSize,SamLB,SamUB)
```

The output of LHC.Sample.Function is a matrix with Sample.Size rows and $N_v + N_d$ columns, such that the ith row of the matrix describes values of input variables for the ith sample, with column j detailing values for the jth variable containing uncertainty and column $N_v + l$ detailing values for the lth decision variable.

It can be useful to separate the elements of the training runs into the elements which correspond to variables containing uncertainty, $\mathbf{v}$, and the elements corresponding to decision variables, $\mathbf{d}$. The below R code illustrates how to do this for the example detailed in Section 6.1.1

```
SampledTrainingInput.v<-SampledTrainingInput[,c(1,2,3)]
SampledTrainingInput.d<-SampledTrainingInput[,c(4,5)]
```

In the above R code, SampledTrainingInput.v is a matrix of 300 rows and 3 columns such that the ith row details the values of the variables containing uncertainty for the ith training run, such that the first column details values of nuclear availability probability, the second column details values of CCGT availability probability and the third column details values of peak demand magnification. SampledTrainingInput.d is a matrix of 300 rows and 2 columns such that the ith row details the values of the decision variables for the ith training run, such that the first column details values of B6 reinforcement magnitude and the second column details values of B7a reinforcement magnitude.

Simulating Training Runs

Appendix G.3.2 details the R code to simulate mean constraint costs for given simulator input. In practice, parallel computing is used to simulate mean constraint costs for each training run. This means that instead of having to simulate hundreds of training runs on a single computer (which may take days to run), many smaller jobs can be submitted to be completed on several computers in parallel where each job simulates mean constraint costs for a small number of training runs.

For the simplicity of the code that will be presented, the process of using parallel computing to simulate mean constraint costs as outlined in Appendix G.3.2 for given input data is represented as

```
TrainingRunSimulator(in.TrainingRun.Matrix)
```

where in.TrainingRun.Matrix is the matrix acquired from LHC.Sample.Function, i.e. such that the ith row of in.TrainingRun.Matrix details the input values (values of variables containing uncertainties and decision variables to be used as simulator input) for the ith training run.

The output of TrainingRunSimulator is a vector such that the ith entry in the vector is the simulated mean constraint costs for the ith training run (i.e. simulated mean constraint costs using simulator inputs detailed by the ith row of in.TrainingRun.Matrix).

For simplicity, it is assumed that TrainingRunSimulator correctly defines other aspects of the power system (e.g. variables which are not decisions and are not modelled

as containing uncertainties, such as installed generating capacities) when simulating constraint costs as outlined in Appendix G.3.2 (e.g. when simulating mean constraint costs for training runs for the example outlined in Section 6.1.1, a year 6 power system background is assumed for variables not containing uncertainty of interest such as installed generating capacities).

Fitting an Emulator Model to Training Data

The fitting of an emulator model to a set of training data is also standard, so details given will be very brief. However, a brief outline of the model fitting is given, as this will be required to randomly draw an estimated response from the emulator model, and subsequently form credible intervals as outlined in Section 5.2.6. The R code for forming credible intervals as outlined in Section 5.2.6 will later be given in Appendix G.4.4.

Input Variable	Description
in.Training.Input.Mat.v	A matrix which defines the training data for variables containing uncertainty such that the ith row of in.Training.Input.Mat.v defines the input values for variables containing uncertainty for the ith training run
in.Training.Input.Mat.d	A matrix which defines the training data for the decision variables such that the ith row of in.Training.Input.Mat.d defines the input values for the decision variables for the ith training run
in.SimulatedResponse	A vector of simulated responses from the training data, such that the ith entry of in.SimulatedResponse defines the simulated response when using the inputs defined in the ith rows of in.Training.Input.Mat.v and in.Training.Input.Mat.d

Table G.4: Table detailing the inputs used for Em.Fitter, which fits an emulator model to a given set of training data.

An outline of a function which could be used to fit an emulator model to a given set of training data is given below, with the details of the inputs of this function given in Table G.4.

```
Em.Fitter<-function(in.Training.Input.Mat.v,in.Training.Input.Mat.d,
  in.SimulatedResponse){
```

```
lm.part<-lm.fitter(in.Training.Input.Mat.v,in.Training.Input.Mat.d,
  in.SimulatedResponse)
#Fit the polynomial portion of the emulator model

lm.part.beta<-lm.part$beta
lm.part.betacov<-lm.part$betacov
#Record the model parameters and the corresponding covariance matrix
 of this fitted polynomial model
#These will be required later when estimating credible bounds

lm.part.func<-lm.part$func
#Define lm.part.func as the polynomial portion of the emulator model
#lm.part.func returns an estimate of costs for given input variables

lm.resids<-in.SimulatedResponse-lm.part.func(in.Training.Input.Mat.v,
  in.Training.Input.Mat.d)
#Calculate the residuals of the polynomial portion of the emulator model

gp.part.func<-gp.fitter(in.Training.Input.Mat.v,in.Training.Input.Mat.d,
  lm.resids)
#Fit a Gaussian process model to the resulting residuals

Fitted.Emulator<-Total.Fitter(lm.part.func,gp.part.func)
#Create a single function which returns the sum of the estimated
 responses of the polynomial regression model, lm.part.func,
 and the Gaussian process model, gp.part.func, for given input

out.list<-list("Fitted.Emulator"=Fitted.Emulator,
  "lm.part.beta"=lm.part.beta,"lm.part.betacov"=lm.part.betacov)
return(out.list)
#Return the fitted emulator model, as well as the parameters of the
 polynomial portion of the emulator model and the corresponding
 covariance matrix of the model parameters
```

```
}
```

The above function is summarised in the following algorithm

1. Fit a polynomial regression model to a given set of training data using lm.fitter. Also, record the model parameters and corresponding covariance matrix of the model parameters of the fitted polynomial model.
2. Calculate residuals of this polynomial model.
3. Fit a Gaussian process model to these residuals using the function gp.fitter.
4. Combine the polynomial model and the Gaussian process model fitted to its residuals using the function Total.Fitter.

The function Total.Fitter combines the fitted polynomial and Gaussian process model to create a single function. The function returned as output is the fitted emulator model, which estimates a response of the simulator for given values of variables containing uncertainty, $\mathbf{v}$, and given values of decision variables, $\mathbf{d}$, as the sum of the estimated response from the polynomial regression model plus the estimated response of the Gaussian process model fitted to its residuals, i.e.

```
Total.Fitter<-function(in.lm,in.gp){
  out.func<-function(in.v,in.d){
    return(in.lm(in.v,in.d)+in.gp(in.v,in.d))
  }
  return(out.func)
}
```

Note, it is not necessary to combine the polynomial regression model and the Gaussian process applied to its residuals using the function Total.Fitter, as estimates could simply be acquired from evaluating the two separately and taking the resulting sum. However, for the simplicity of the code presented for throughout this appendix it will be assumed that the polynomial regression model and Gaussian process applied to its residuals have been combined using Total.Fitter, to create a single function which

returns the estimated response of the fitted emulator model (polynomial regression model plus Gaussian process model applied to its residuals) for given input.

For the simplicity of the code detailed, it will be assumed that lm.fitter automatically fits a polynomial model of the required form. However, most functions (such as the function lm which was used in this thesis) require the polynomial form of the polynomial regression model to be specified as an input.

For example, the application in Chapter 5 used an emulator model where the polynomial portion of the emulator model takes the form

$$\beta_0 + \beta_1 v + \beta_2 d + \beta_3 v^2 + \beta_4 d^2 + \beta_5 vd + \beta_6 v^2 d^2$$

The function lm.fitter could then be defined as

```
lm.fitter<-function(in.Training.Input.Mat.v,in.Training.Input.Mat.d,
  in.SimulatedResponse){

  Temp.lm.Mat<-cbind(in.Training.Input.Mat.v[,1],
    in.Training.Input.Mat.d[,1],in.SimulatedResponse)

  outmod<-lm(V3~V1+V2+I(V1^2)+I(V2^2)+V1*V2+I(V1^2)*I(V2^2),
    data = as.data.frame(Temp.lm.Mat))

  beta<-outmod$beta
  betacov<-vcov(outmod)
  func<-function(in.v,in.d){
    return(outmod$beta[1]+in.v*outmod$beta[2]+in.d*outmod$beta[3]+
      in.v^2*outmod$beta[4]+in.d^2*outmod$beta[5]+
      in.v*in.d*outmod$beta[6]+in.v^2*in.d^2*outmod$beta[7])
  }
  lm.out.list<-list("beta"=beta,"betacov"=betacov,"func"=func)
  return(lm.out.list)
}
```

It is also noted that gp.part.func represents a function which takes specific values of

v and **d** as input, and returns the estimated response of the fitted Gaussian process model.

Initial Application of Code in Chapter 5

This sub-subsection will give a brief overview of how the methodology of the previous sub-subsections of this subsection can be used to fit an emulator model for the problem detailed in Section 5.3 of Chapter 5.

First, values must be set for parameters used during the emulation process, i.e. the assumed cost of reinforcement, the number of training runs to use and lower/upper bounds for the variables to be sampled (i.e. peak demand magnification and B15 reinforcement magnitude).

```
FixedSamSize<-200
#Set the number of training runs to 200
AssumedCTR<-1000
#Set the assumed cost of reinforcement to 1000 (in pounds/MW/km)
SamLB<-c(0.95,0)
#Set lower bounds for the variables to be sampled
SamUB<-c(1.05,1500)
#Set lower bounds for the variables to be sampled
```

The above sets the lower and upper bounds for peak demand magnification to 0.95 and 1.05 respectively, and lower and upper bounds for B15 reinforcement magnitude to 0 MW and 1500 MW respectively, as outlined in Section 5.3.

Then, an emulator model for the problem outlined Section 5.3 can be fitted using the following R code

```
SampledTrainingInputWave1<-LHC.Sample.Function(FixedSamSize,SamLB,SamUB)
#Sample inputs based on the given sample size, lower bounds for variables
 and upper bounds for the variables
#SampledTrainingInputWave1 will be a matrix of 200 rows and 2 columns
#The ith row details input for the ith training run
#Column 1 details values of peak demand magnification
```

```
#Column 2 details values of B15 reinforcement magnitude

SampledTrainingInputWave1.v<-SampledTrainingInputWave1[,1]
SampledTrainingInputWave1.d<-SampledTrainingInputWave1[,2]
#Create separate matrices detailing the input for training runs for
 variables containing uncertainty (i.e. peak demand magnification)
 and decision variables (i.e. B15 reinforcement magnitude)

SampleSimulatedConstraintsWave1<-TrainingRunSimulator(
  SampledTrainingInputWave1)
#Simulate mean constraint costs for the given training run inputs
#The ith entry of SampleSimulatedConstraintsWave1 details the
 simulated constraint costs of the ith training run

SampleReinforcementCostsWave1<-(as.vector(SampledTrainingInputWave1[,2])*
  100*AssumedCTR)
#Calculate reinforcement costs for each sampled decision as the reinforcement
 magnitude of each sample multiplied by 100*AssumedCTR (the cost in
 pounds/MW/km multiplied by 100 to account for 100km boundary thickness)

SampleTotalCostsWave1<-(SimulatedConstraintsWave1*10+
  SampleReinforcementCostsWave1)
#Calculate simulated total costs for each training run as the sum of
 reinforcement costs plus mean constraint costs
#As noted, initially an extrapolation of constraint costs from a single
 power system background is used, so an estimate of constraint costs
 over a 10 year period is calculated by multiplying the simulated
 constraint costs by 10

Chap5EmWave1List<-Em.Fitter(SampledTrainingInputWave1.v,
  SampledTrainingInputWave1.d,SampleTotalCostsWave1)
#Fit an emulator model using these training runs

Chap5EmWave1<-Chap5EmWave1List$Fitted.Emulator
```

```
Chap5PolyBeta<-Chap5EmWave1List$lm.part.beta
Chap5PolyBetaCov<-Chap5EmWave1List$lm.part.betacov
#Store the elements of Chap5EmWave1List separately for convenience
```

The above R code first takes Latin hypercube sample using the specified information to acquire inputs to use for training runs. Mean constraint costs are then simulated based on these sampled inputs, which are subsequently used to calculate total costs (mean constraint costs plus reinforcement costs) for the sampled inputs. Finally, an emulator model is fitted to these training runs using Em.Fitter.

Initial Application of Code in Chapter 6

This sub-subsection will give a brief overview of how the methodology of the previous sub-subsections of this subsection can be used to fit an emulator model for the problem detailed in Section 6.1.1 of Chapter 6.

As in the previous sub-subsection, values must be set for parameters used during the emulation process as follows:

```
FixedSamSize<-300
#Set the number of training runs
AssumedCTR<-1000
#Set the assumed cost of reinforcement to 1000 (in pounds/MW/km)
SamLB<-c(0.55,0.8,0.95,0,0)
#Set lower bounds for the variables to be sampled
SamUB<-c(0.85,0.95,1.05,4000,4000)
#Set upper bounds for the variables to be sampled
```

The above sets lower and upper bounds for nuclear availability probability to 0.55 and 0.85 respectively, CCGT availability probability to 0.8 and 0.95 respectively, peak demand magnification to 0.95 and 1.05 respectively, B6 reinforcement magnitude to 0 and 4000 MW respectively and B7a reinforcement magnitude to 0 and 4000 MW respectively.

As in the previous sub-subsection, an emulator model for the problem outlined Section 6.1.1 can be fitted using the following R code

```
SampledTrainingInputWave1<-LHC.Sample.Function(FixedSamSize,SamLB,SamUB)
#Sample inputs based on the given sample size, lower bounds for variables
 and upper bounds for the variables
#SampledTrainingInputWave1 will be a matrix of 300 rows and 5 columns
#The ith row details input for the ith training run
#Column 1 details values of nuclear availability probability
#Column 2 details values of CCGT availability probability
#Column 3 details values of peak demand magnification
#Column 4 details values of B6 reinforcement magnitude
#Column 5 details values of B7a reinforcement magnitude

SampledTrainingInputWave1.v<-SampledTrainingInputWave1[,c(1,2,3)]
SampledTrainingInputWave1.d<-SampledTrainingInputWave1[,c(4,5)]
#Create separate matrices detailing the input for training runs for
 variables containing uncertainty (i.e. nuclear availability probability,
 CCGT availability probability and peak demand magnification)
 and decision variables (i.e. B6 reinforcement magnitude and
 B7a reinforcement magnitude)

SimulatedConstraintsWave1<-TrainingRunSimulator(SampledTrainingInputWave1)
#Simulate mean constraint costs for the training runs
#The ith entry of SampleSimulatedConstraintsWave1 details the
 simulated constraint costs of the ith training run

SampleReinforcementCostsWave1<-(as.vector(SampledTrainingInputWave1[,4]+
  SampledTrainingInputWave1[,5])*100*AssumedCTR)
#Calculate reinforcement costs for each of the sampled sets of decisions
 as the total reinforcement of both the B6 and B7a boundaries of each
 sample multiplied by 100*AssumedCTR (the cost in pounds/MW/km
 multiplied by 100 to account for 100km boundary thickness)

SampleTotalCostsWave1<-(SimulatedConstraintsWave1*10+
  SampleReinforcementCostsWave1)
#Calculate simulated total costs for each training run as the sum of
```

```
 reinforcement costs plus mean constraint costs
#As in the previous sub-subsection, initially an extrapolation of
 constraint costs from a single power system background is used,
 so an estimate of constraint costs over a 10 year period is
 calculated by multiplying the simulated constraint costs by 10

Chap6EmWave1List<-Em.Fitter(SampledTrainingInputWave1.v,
  SampledTrainingInputWave1.d,SampleTotalCostsWave1)
#Fit an emulator model using these training runs

Chap6EmWave1<-Chap6EmWave1List$Fitted.Emulator
Chap6PolyBeta<-Chap6EmWave1List$lm.part.beta
Chap6PolyBetaCov<-Chap6EmWave1List$lm.part.betacov
#Store the elements of Chap6EmWave1List separately for convenience
```

G.4.2 Estimating an Expected Response Under Uncertainty

Estimating an Expected Response Under Uncertainty

Section 5.2.5 details how an estimate of expected costs under uncertainty for a given decision can be acquired using Equation 5.2.16, by integrating the product of the fitted emulator model and a set of prior beliefs about uncertainties. The R code for a function to evaluate Equation 5.2.16 is given below, with details of the inputs to this function given in Table G.5.

```
ExpectationUnderUncertainty<-function(Em.Mod,Low.B.Bounds,Up.B.Bounds,
  In.Decisions,Prior.Beliefs,ATR.fun){

  f2<-function(x){
    return(ATR.fun(Em.Mod(x,In.Decisions))*Prior.Beliefs(x,Low.B.Bounds,
      Up.B.Bounds))
  }
  #Define f2 as a function to return the product of an attitude to risk
   applied to the emulator, and the density of the PDF to describe
```

Input Variable	Description
Em.Mod	$\tilde{f}(\mathbf{v}, \mathbf{d})$, i.e. the fitted emulator to estimate costs for given values of variables containing uncertainty, $\mathbf{v}$, and decision variables, $\mathbf{d}$. $\tilde{f}(\mathbf{v}, \mathbf{d})$ can be an emulator model for the total costs from the simulator (as is considered in Chapters 5 and 6) or an emulator model for constraint costs only (as considered in Chapters 8 and 9)
Low.B.Bounds	A vector detailing the lower bounds for the variables containing uncertainty, such that the ith element of Low.B.Bounds is the lower bound for the ith variable containing uncertainty
Up.B.Bounds	A vector detailing the upper bounds for the variables containing uncertainty, such that the ith element of Up.B.Bounds is the upper bound for the ith variable containing uncertainty
In.Decisions	$\mathbf{d}^*$, i.e. a vector detailing specific values of the decision variables such that the ith element of In.Decisions details the specific value considered for the ith decision variable
Prior.Beliefs	$p(\mathbf{v})$, i.e. a function to describe the prior beliefs about the variables containing uncertainty
ATR.fun	A function to define the decision maker's attitude to risk (i.e. a loss or utility function)

Table G.5: Table giving details of the inputs for ExpectationUnderUncertainty, the function to estimate an expected response under uncertainty of a given decision for a given emulator model.

```
   prior beliefs for given input


  outvals<-adaptIntegrate(f2, lowerLimit = c(Low.B.Bounds),
    upperLimit = c(Up.B.Bounds))$integral
  #Use the function adaptIntegrate from the package cubature
   to integrate f2 over the specified limits


  return((outvals))
  #Return the resulting integral as output
}
```

In the above code, the function f2 would calculate

$$l(\tilde{f}(\mathbf{v}, \mathbf{d}^*))p(\mathbf{v})$$

i.e. the product of an attitude to risk (described by the function $l(\cdot)$) applied to the emulator model, and the density of the PDF to describe prior beliefs for given input.

The function adaptIntegrate from the package cubature is then used to calculate an expected response under uncertainty, i.e. to calculate

$$\tilde{F}_l(\mathbf{d}^*) = \int_{\mathbf{v}} l(\tilde{f}(\mathbf{v}, \mathbf{d}^*))p(\mathbf{v})\mathrm{d}\mathbf{v}$$

with $\tilde{F}_l(\mathbf{d}^*)$ returned as the output of ExpectationUnderUncertainty.

Application of This Function

Input Variable	Description
in.v	A vector detailing the specific values of variables containing uncertainty, $\mathbf{v}$, that a density is to be calculated for
in.lowers	A vector detailing the lower bounds for the variables containing uncertainty, such that the ith element of in.lowers is the lower bound for the ith variable containing uncertainty
in.uppers	A vector detailing the upper bounds for the variables containing uncertainty, such that the ith element of in.uppers is the upper bound for the ith variable containing uncertainty

Table G.6: Table giving details of the inputs for Gen.U.Prior, the function to calculate the density of a uniform distribution.

Before detailing an application of the function ExpectationUnderUncertainty, a function to describe prior beliefs must be specified. The R code to describe a uniform distribution between given lower and upper bounds is given below, with details of the function input given in Table G.6.

```
Gen.U.Prior<-function(in.v,in.lowers,in.uppers){
  Bound.Dif<-in.uppers-in.lowers
  UniformFactor<-1/(prod(Bound.Dif))
  #Calculate the constant density of the uniform distribution
   between the given lower and upper bounds
```

```
  return(UniformFactor)
  #Return the calculated density
}
```

Gen.U.Prior simply calculates the density of the uniform distribution for given lower and upper bounds, and returns the density calculated. As the function ExpectationUnderUncertainty integrates between given lower and upper bounds, the density defined by Gen.U.Prior is sufficient. However, Gen.U.Prior could be made more general by returning the value UniformFactor if in.v falls between the specified lower and upper bounds, and 0 otherwise. An alternative function which would achieve this is given below.

```
Gen.U.PriorAlt<-function(in.v,in.lowers,in.uppers){
  Bound.Dif<-in.uppers-in.lowers
  UniformFactor<-1/(prod(Bound.Dif))
  #Calculate the constant density of the uniform distribution
   between the given lower and upper bounds

  Test.v<-c(rep(1,length(in.lowers)))
  #Create a vector to check if in.v lies between the lower and
   upper credible bounds

  Test.lowers<-Test.v[in.v<in.lowers]
  #Note if any elements of in.v lie below in.lowers
  Test.uppers<-Test.v[in.v>in.uppers]
  #Note if any elements of in.v lie above in.uppers
  Test.x2<-0+sum(Test.lowers)+sum(Test.uppers)
  #Note the total number of elements of in.v that lie outside
   the lower and upper bounds

  if(Test.x2>0){
    Out.Density<-0
  }
  #If any elements of in.v lie outside the input
```

```
   lower and upper bounds, the density of the uniform distribution
   at in.v is zero

  else{
    Out.Density<-UniformFactor
  }
  #Else the density is the constant density calculated ealier

  return(Out.Density)
}
```

The above function calculates the density of a uniform distribution between in.lowers and in.uppers (as in the function Gen.U.Prior) but additionally checks if in.v lies between the given lower and upper bounds. If in.v does not lie between the lower and upper bounds a density of zero is returned, otherwise the density calculated as UniformFactor is returned.

A function to describe the decision maker's attitude to risk must also be defined. A function to describe a risk neutral attitude can be defined as

```
RN.Att<-function(in.x){
return(in.x)
}
```

which simply returns the input as output.

Gen.U.Prior and RN.Att can then be used to estimate an expected repose under uncertainty for a given emulator model for the example of chapter 6 using the following R code:

```
Chap6EmWave1 #The emulator model fitted for the example of chapter 6

Chap6LB<-c(0.55,0.8,0.95)
#Lower bounds of variables containing uncertainty
Chpa6UB<-c(0.85,0.95,1.05)
#Upper bounds of variables containing uncertainty
```

```
SpecificDecision<-c(500,1800)
#A specific decision of 500 MW B6 reinforcement
 and 1800 MW B7a reinforcement

ExpectationUnderUncertainty(Chap6EmWave1,Chap6LB,Chpa6UB,SpecificDecision,
  Gen.U.Prior,RN.Att)
```

The above estimates expected total costs under uncertainty using the emulator model fitted for the example of chapter 6 when assuming a risk neutral attitude and making a decision of 500 MW B6 and 1800 MW B7a reinforcement.

The lower bounds define a lower bound of 0.55, 0.8 and 0.95 for nuclear availability probability, CCGT availability probability and peak demand magnification respectively, with the respective upper bounds defined as 0.85, 0.95 and 1.05 respectively.

A Possible Simplification of This Function

As most applications in Chapters 5 and 6 consider using a risk neutral attitude, with a uniform distribution used to represent prior beliefs about the variables containing uncertainty, it is possible to make the function used to estimate expected costs under uncertainty simpler, and slightly more efficient to evaluate. Such a function is detailed below

```
ExpectationUnderUncertaintyAlt<-function(Em.Mod,Low.B.Bounds,Up.B.Bounds,
  In.Decisions){

  BoundDif<-(Up.B.Bounds-Low.B.Bounds)
  UniformFactor<-1/(prod(BoundDif))

  f2<-function(x){
    return(Em.Mod(x,In.Decisions))
  }
  temp.outvals<-adaptIntegrate(f2, lowerLimit = c(Low.B.Bounds),
    upperLimit = c(Up.B.Bounds))$integral
```

```
  outvals<-temp.outvals*UniformFactor
  return((outvals))
}
```

ExpectationUnderUncertaintyAlt is a reduced version of ExpectationUnderUncertainty, where an attitude to risk is no longer required as input (as a risk neutral attitude is assumed) so it is no longer applied in the integration process. Further, as a uniform distribution has a constant density over a given range, this constant density can be calculated outside of the integration.

G.4.3 Estimating an Optimal Reinforcement Decision

Throughout this thesis, estimates of optimal reinforcement decisions which arise from fitted emulator models have been given. This subsection will briefly outline R code which could be used to estimate optimal reinforcement decisions for a given emulator model for the examples detailed in Sections 5.3.1 and 6.1.1.

Estimating an Optimal Reinforcement Decision for the Example Detailed in Section 5.3.1

For the example detailed in Section 5.3.1, only a single reinforcement decision is to be made (reinforcement of the B15 boundary) with uncertainty considered in a single variable (peak demand magnification). As only a single reinforcement decision is to be made, and decisions are identified to the nearest 10 MW, it is feasible to estimate an optimal decision using an exhaustive search of all decisions in the range 0 MW to 1500 MW as described in the following code

```
Chap5EmWave1
#Chap5EmWave1 represents the fitted emulator model for total costs for the
 example of chapter 5

Rvec1<-seq(0,1500,by=10)
#Create a vector of all decisions in the range 0 MW to 1500 MW
```

```
Chap5LB<-0.95
Chpa5UB<-1.05
#Define the lower and upper bounds for peak demand magnification


Est.Exp.Resp<-c(rep(0,length(Rvec1)))
#Create a vector to store estimated expected total costs for each decision

for(i in 1:length(Rvec1)){
  Est.Exp.Resp[i]<-ExpectationUnderUncertainty(Chap5EmWave1,Chap5LB,Chpa5UB,
    Rvec1[i],Gen.U.Prior,RN.Att)
}
#Create a loop to estimate the expected total costs under uncertainty for
 each decision
#The ith entry of Est.Exp.Resp is the estimate of expected total costs when
 making the decision defined by the ith entry of Rvec1

Opt.Dec<-Rvec1[order(Est.Exp.Resp)][1]
#Estimate the optimal decision as the decision which minimises the estimate
 of expected total costs
```

The above code simply defines Rvec1 as a vector of each possible reinforcement decision (to the nearest 10 MW) of the B15 boundary. Then, for each decision in turn the function ExpectationUnderUncertainty, defined in Appendix G.4.2, is used to estimate expected total costs under uncertainty, such that the ith entry of Est.Exp.Resp is the estimate of expected total costs under uncertainty when making the decision described by the ith entry of Rvec1. An optimal decision is then estimated as the decision which results in the minimum estimate of expected total costs under uncertainty.

Estimating an Optimal Reinforcement Decision for the Example Detailed in Section 6.1.1

For the example outlined in Section 6.1.1, two simultaneous decisions are to be made, with a range of 0 to 4000 MW initially considered for each decision (Appendix G.4.4 will later show how this range can be reduced using the methodology of Section 6.2 to eliminate decisions which have evidence against them being optimal). This would mean that in the first wave a total of 160,801 decisions to the nearest 10 MW would be considered, meaning an exhaustive search would be very expensive (and if a higher number of simultaneous decisions were to be made this number would grow exponentially making such an exhaustive process infeasible). Therefore, numerical methods must be used to estimate an optimal reinforcement decision for a given emulator model.

For the constraint cost problem considered in this thesis, mean constraint costs decrease monotonically as reinforcement magnitude is increased and reinforcement costs increase linearly as reinforcement magnitude is increased. This means that total cost calculations using the simulator would have a single global optimum, and not several local optima. This can be seen in Figure 6.21 (c), though it is noted in early waves several local minima may occur due to the emulator models being imperfect approximations to the simulator.

This means a quite simple iterative procedure can be used to estimate an optimal reinforcement decision, where an optimal reinforcement decision is initially estimated to the nearest 100 MW. Then, the region around this initial estimate can be considered to estimate a more precise optimal reinforcement decision to the nearest 10 MW.

To perform this iterative procedure, first, two vectors are created to represent every possible combination of B6 and B7a reinforcement decisions (to the nearest 100 MW) as follows:

```
Rvec1Temp<-seq(0,4000,by=100)
Rvec2Temp<-seq(0,4000,by=100)
#Create vectors describing the decisions that could be made on either
 boundary to the nearest 100 MW
```

```
#These vectors are then used to define two matrices to describe every
 possible combination of B6 and B7a reinforcement
WorkingRvec1Mat<-matrix(nrow=length(Rvec1Temp),ncol=length(Rvec2Temp))
WorkingRvec2Mat<-matrix(nrow=length(Rvec1Temp),ncol=length(Rvec2Temp))
#WorkingRvec1Mat will describe reinforcement of the B6 boundary
#WorkingRvec2Mat will describe reinforcement of the B7a boundary

for(i in 1:length(Rvec1Temp)){
  WorkingRvec1Mat[i,]<-c(rep(Rvec1Temp[i],length(Rvec2Temp)))
}
for(j in 1:length(Rvec2Temp)){
  WorkingRvec2Mat[,j]<-c(rep(Rvec2Temp[j],length(Rvec1Temp)))
}
#The above defines WorkingRvec1Mat such that the jth entry of the ith row is
 the B6 reinforcement made when making reinforcement decisions Rvec1Temp[i]
 and Rvec2Temp[j]
#Similarly, WorkingRvec2Mat is defined such that the jth entry of the ith row
 is the B7a reinforcement made when making reinforcement decisions
 Rvec1Temp[i] and Rvec2Temp[j]

Rvec1<-as.vector(WorkingRvec1Mat)
Rvec2<-as.vector(WorkingRvec2Mat)
#Create vectors from these two matrices
```

The above code creates two vectors detailing every possible combination of B6 and B7a reinforcement magnitude to the nearest 100 MW, such that the ith element of Rvec1 represents the ith B6 reinforcement decision and the ith element of Rvec2 represents the ith B7a reinforcement. Figure G.1 (a) plots Rvec2 against Rvec1 to show how all combinations of B6 and B7a reinforcement to the nearest 100 MW are considered.

Estimates of expected total costs under uncertainty for each of the reinforcement decisions detailed in Rvec1 and Rvec2 are then acquired using the following code

```
Chap6EmWave1
#Chap6EmWave1 represents the fitted emulator model for total costs for the
```

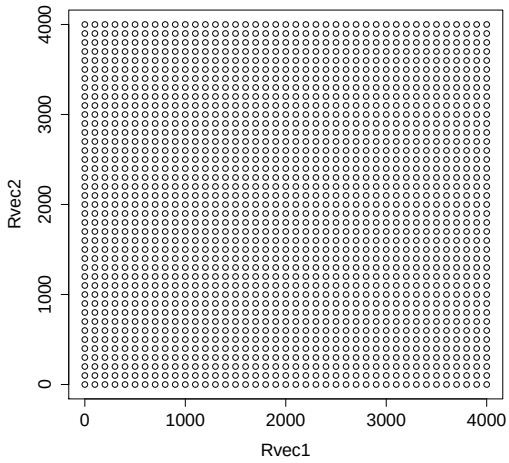

(a) Plot illustrating the reinforcement combinations initially considered.

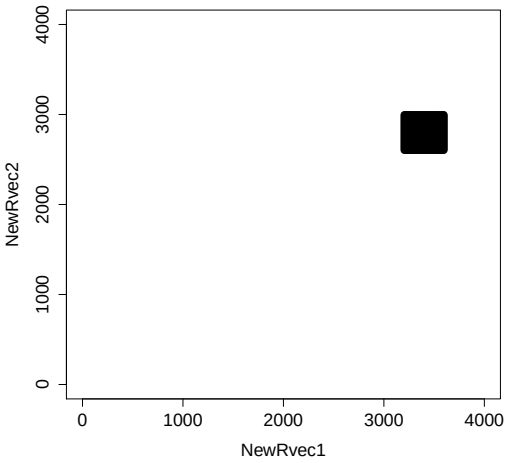

(b) Plot illustrating the reinforcement combinations considered in the second part of the numerical procedure.

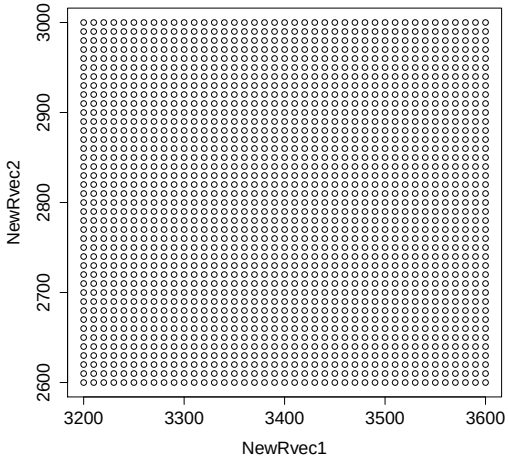

(c) Plot illustrating the reinforcement combinations considered in the second part of the numerical procedure.

Figure G.1: Plots to illustrate the decision vectors.

```
 example of chapter 6

Chap6LB<-c(0.55,0.8,0.95)
#Vector of lower bounds of variables containing uncertainty
Chpa6UB<-c(0.85,0.95,1.05)
#Vector of upper bounds of variables containing uncertainty

Wave1.Rvec.Length<-length(Rvec1)
#Wave1.Rvec.Length notes the number of decisions an estimate of expected
 total costs is required for

Est.Exp.Resp<-c(rep(0,length(Wave1.Rvec.Length)))
#Create a vector to store the estimates of expected total costs

for(i in 1:length(Wave1.Rvec.Length)){
 Est.Exp.Resp[i]<-ExpectationUnderUncertainty(Chap6EmWave1,Chap6LB,Chap6UB,
   c(Rvec1[i],Rvec2[i]),Gen.U.Prior,RN.Att)
}
#Create a loop to estimate the expected total costs under uncertainty for
 each decision
#The ith entry of Est.Exp.Resp is the estimate of expected total costs
 when making the decisions defined by the ith entry of Rvec1 and Rvec2
```

The above estimates expected total costs for each reinforcement decisions detailed in Rvec1 and Rvec2, as was outlined in Appendix G.4.2, simply by creating a loop to evaluate the estimate of expected total costs using the function ExpectationUnderUncertainty (defined in Appendix G.4.2) for each element of Rvec1 and Rvec2 in turn.

An initial estimate of optimal reinforcement decision can then be acquired as the initial decision considered which results in the minimum estimate of expected total costs under uncertainty, i.e. the decision detailed by Rvec1 and Rvec2 which results in the minimum value of Est.Exp.Resp. A function which can be used to calculate this initial estimate of optimal decision is detailed below, with details of the input to this function given in

Input Variable	Description
in.cost.ests	A vector of estimates of expected total costs under uncertainty
in.rvec1	A vector detailing the B6 reinforcement magnitudes, such that the ith element of in.rvec1 is the B6 reinforcement used when estimating the expected total costs for the ith element of in.cost.ests
in.rvec2	A vector detailing the B7a reinforcement magnitudes, such that the ith element of in.rvec2 is the B7a reinforcement used when estimating the expected total costs for the ith element of in.cost.ests

Table G.7: Table giving details of the inputs for optimal.estimator, the function used to estimate an optimal decision for given vectors of estimates of expected total costs, B6 reinforcement magnitudes and B7a reinforcement magnitudes.

Table G.7.

```
optimal.estimator<-function(in.cost.ests,in.rvec1,in.rvec2){
  rvec1.opt.est<-in.rvec1[order(in.cost.ests)][1]
  #The estimated optimal B6 reinforcement magnitude

  rvec2.opt.est<-in.rvec2[order(in.cost.ests)][1]
  #The estimated optimal B7a reinforcement magnitude

  cost.opt.est<-in.cost.ests[order(in.cost.ests)][1]
  #The minimum estimate of expected total costs

  out.list<-list("rvec1.opt.est"=rvec1.opt.est,"rvec2.opt.est"=rvec2.opt.est,
    "cost.opt.est"=cost.opt.est)
  return(out.list)
  #Return the estimated optimal decisions, and resulting minimum estimate of
   expected total costs
}
```

The above function is straightforward, and simply returns the elements of in.rvec1 and in.rvec2 which results in the minimum value of in.cost.ests (as well as the minimum value of in.cost.ests itself).

Based on the estimates of expected total costs contained in Est.Exp.Resp, new vectors of more precise decisions (to the nearest 10 MW) are then created over a range of decisions near the initially estimated optimal decision using the following R code:

```
TempOpt<-optimal.estimator(Est.Exp.Resp,Rvec1,Rvec2)
#Use optimal.estimator to estimate the optimal reinforcement decision to
 the nearest 100 MW

#Use this estimated optimal decision to form a vector of more precise
 decisions (to the nearest 10 MW) near this estimated optimal
#The below creates a vector of precise decisions over the +/-200 MW range
 of the estimated optimal to be slightly cautious, though a +/-100 MW range
 should suffice
TTempRvec1<-seq(TempOpt$rvec1.opt.est-200,TempOpt$rvec1.opt.est+200,by=10)
TTempRvec2<-seq(TempOpt$rvec2.opt.est-200,TempOpt$rvec2.opt.est+200,by=10)

for(i in 1:length(TTempRvec1)){
  TTempRvec1[i]<-max(TTempRvec1[i],0)
}
for(i in 1:length(TTempRvec2)){
  TTempRvec2[i]<-max(TTempRvec2[i],0)
}
#Ensure that all reinforcements are non-negative

TempRvec1<-unique(TTempRvec1)
TempRvec2<-unique(TTempRvec2)

WorkingR1Mat<-matrix(nrow=length(TempRvec1),ncol=length(TempRvec2))
WorkingR2Mat<-matrix(nrow=length(TempRvec1),ncol=length(TempRvec2))
for(i in 1:length(TempRvec1)){
  WorkingR1Mat[i,]<-c(rep(TempRvec1[i],length(TempRvec2)))
}
for(j in 1:length(TempRvec2)){
  WorkingR2Mat[,j]<-c(rep(TempRvec2[j],length(TempRvec1)))
```

```
}

NewRvec1<-as.vector(WorkingR1Mat)
NewRvec2<-as.vector(WorkingR2Mat)
```

The above R code first estimates an optimal reinforcement decision to the nearest 100 MW (based on the estimates of expected total costs previously acquired). For the example of Section 6.1.1, this estimate of optimal decision based on the emulator model fitted in the first wave was 3400 MW B6 and 2800 MW B7a reinforcement. This estimated optimal decision is then used to create two new vectors of more precise decisions (to the nearest 10 MW) over the range of +/-200 MW from the estimated optimal decision, such that ith element of NewRvec1 represents the ith B6 reinforcement decision and the ith element of NewRvec2 represents the ith B7a reinforcement over this range. The decisions considered by NewRvec1 and NewRvec2 are illustrated in Figure G.1 (b) and (c).

It is noted that considering a range of +/-200 MW is slightly cautious to avoid inadvertently excluding the optimal decision (to a precision of 10 MW) from this range, and that a +/-100 MW from the initial estimate of the optimal should suffice.

Estimates of expected total costs can then be acquired for each of the more precise decisions detailed in NewRvec1 and NewRvec2, and an optimal decisions can be estimated to minimise the resulting estimates of expected total costs using the following R code:

```
New.Est.Exp.Resp<-c(rep(0,length(NewRvec1)))

for(i in 1:length(NewRvec1)){
 New.Est.Exp.Resp[i]<-ExpectationUnderUncertainty(Chap6EmWave1,Chap6LB,
   Chpa6UB,c(NewRvec1[i],NewRvec2[i]),Gen.U.Prior,RN.Att)
}
#Create a loop to estimate the expected total costs under uncertainty for
 each of the more precise decisions
#The ith entry of New.Est.Exp.Resp is the estimate of expected total costs
 when making the decisions defined by the ith entry of NewRvec1 and NewRvec2
```

```
Est.to.Nearest.10<-optimal.estimator(New.Est.Exp.Resp,NewRvec1,NewRvec2)
#Estimate the optimal reinforcement decision based on these estimates of
 expected total costs.
```

The above code estimates expected total costs for each of the reinforcement decisions detailed in NewRvec1 and NewRvec2, as was outlined in Appendix G.4.2, again by creating a loop to evaluate the estimate of expected total costs using the function ExpectationUnderUncertainty (defined in Appendix G.4.2) for each element of NewRvec1 and NewRvec2 in turn. An estimate of optimal reinforcement decision to the nearest 10 MW is then acquired as the decision which results in the lowest estimate of expected total costs.

This iterative procedure can be summarised in the following algorithm:

1. Create vectors to describe the reinforcement decisions considered to the nearest 100 MW.

2. Estimate expected total costs for each of these decisions as outlined in Appendix G.4.2.

3. Identify the decision which results in the minimum estimate of expected total costs.

4. Use this estimated optimal decision to define more precise vectors of reinforcement decisions (to the nearest 10 MW) over an appropriate range.

5. Estimate expected total costs for each of the more precise decisions.

6. Identify the decision which results in the minimum estimate of expected total costs for the more precise decisions. This is the estimated optimal decision using the currently fitted emulator model.

As was noted in Section 6.3.3, real life transmission reinforcements are often discrete and "lumpy", meaning that such a precise decision may not be implemented in practise. This could actually make it much easier to estimate an optimal reinforcement decision.

For example, if in practice a transmission system planner considered reinforcement decisions in terms of how many 500 MW lines to add to each boundary, every combination of B6 and B7a reinforcement (to the precision of 500 MW) when making between 0 and 4000 MW reinforcement on each boundary could be considered by 81 different decisions. An exhaustive search could therefore be very feasible, by simply estimating expected total costs under uncertainty for each of the 81 decisions and identifying the decision which results in the lowest estimate of expected total costs.

Similarly, if it is preferable to reinforce one boundary over another (for example, suppose it is easier to reinforce the B6 boundary over the B7a boundary in practise so the transmission system planner would prefer a larger B6 reinforcement in comparison to B7a, even if this slightly increases expected total costs) an optimal B6 reinforcement could be estimated for varying levels of B7a reinforcement. For example, optimal B6 reinforcement magnitudes could be estimated for the 9 B7a reinforcement magnitudes to a precision of 500 MW between 0 MW and 4000 MW. The transmission planner could then be shown the estimated optimal B6 reinforcement decision for each of the B7a reinforcement decisions, as well as the resulting estimates of expected total costs. This would offer decision support to the transmission system planner, as they would be able to use the information presented to balance their preferences of making a decision to minimise the estimate of expected total costs and making a decision with a reduced B7a reinforcement.

G.4.4 R Code for Estimating Credible Bounds

The previous subsection detailed how an estimate of optimal reinforcement decisions can be acquired for a fitted emulator model. However, it is noted that the fitted emulator model is an imperfect approximation to the simulator, which is why Section 6.2 detailed how decisions can be eliminated from consideration in order to fit a more accurate emulator model over a smaller range of decisions.

This subsection will detail the R code for calculating credible bounds for estimated expected total costs under uncertainty, and go on to detail the R code for using these credible bounds to eliminate decisions from consideration.

Randomly Drawing an Emulator Model

Input Variable	Description
in.Training.Input.Mat.v	A matrix which defines the training data for variables containing uncertainty such that the ith row of in.Training.Input.Mat.v defines the input values for variables containing uncertainty for the ith training run
in.Training.Input.Mat.d	A matrix which defines the training data for the decision variables such that the ith row of in.Training.Input.Mat.d defines the input values for the decision variables for the ith training run
in.SimulatedResponse	A vector of simulated responses from the training data, such that the ith entry of in.SimulatedResponse defines the simulated response when using the inputs defined in the ith rows of in.Training.Input.Mat.v and in.Training.Input.Mat.d
in.Random.Beta	A vector of randomly drawn parameters for the polynomial portion of the emulator model

Table G.8: Table detailing the inputs used for Random.Em.Fitter, which fits a random variation of the fitted emulator model to a given set of training data, for a given set of randomly drawn parameters of the polynomial portion of the emulator model.

Appendix G.4.1 described how the function Em.Fitter is used to represent fitting an emulator model to a given set of training data. This subsection will detail a function, Random.Em.Fitter, which is used to represent fitting a random variation of the emulator model as described in Section 5.2.6, using the same set of training data and a random drawing of the parameters of the polynomial portion of the emulator model (details on how these parameters are randomly drawn are given in the next sub-subsection). A summary of the inputs of this function are given in Table G.8, with the code for Random.Em.Fitter as follows:

```
Random.Em.Fitter<-function(in.Training.Input.Mat.v,in.Training.Input.Mat.d,
  in.SimulatedResponse,in.Random.Beta){

  Random.lm.func<-Random.lm.fitter(in.Random.Beta)
  #Fit the polynomial portion of the emulator model using the randomly
   drawn parameters
```

```
  Random.lm.resids<-(in.SimulatedResponse-Random.lm.func(
    in.Training.Input.Mat.v,in.Training.Input.Mat.d))
  #Calculate the residuals when using the randomly drawn variation of the
   polynomial model

  Random.gp.func<-gp.fitter(in.Training.Input.Mat.v,in.Training.Input.Mat.d,
    Random.lm.resids)
  #Fit a Gaussian process model to the resulting residuals

  Fitted.Random.Emulator<-Total.Fitter(Random.lm.func,Random.gp.func)
  #Create a single function which returns the sum of the estimated responses
   of the polynomial regression model, Random.lm.func, and the Gaussian
   process model, Random.gp.func, for given input

  return(Fitted.Random.Emulator)
  #Return the resulting randomly drawn variation of the emulator model
}
```

The above function is very similar to Em.Fittter, described in Appendix G.4.1, with the exception of parameters for the polynomial portion of the emulator model being given as an input, rather than estimated as part of the model fitting process.

As was the case in Appendix G.4.1, for simplicity in the above code it will be assumed that Random.lm.fitter automatically fits a polynomial model of the required form. However, most functions (such as the function lm which was used in this thesis) require the polynomial form of the linear model to be specified as an input.

For example, the application in Chapter 5 used an emulator model where the polynomial portion of the emulator model takes the form

$$\beta_0 + \beta_1 v + \beta_2 d + \beta_3 v^2 + \beta_4 d^2 + \beta_5 vd + \beta_6 v^2 d^2$$

The function Random.lm.fitter could then be defined as

```
Random.lm.fitter<-function(in.Random.Beta){
```

```
  Random.Out.lm<-function(in.v,in.d){
    return(in.Random.Beta[1]+in.v*in.Random.Beta[2]+in.d*in.Random.Beta[3]+
      in.v^2*in.Random.Beta[4]+in.d^2*in.Random.Beta[5]+
      in.v*in.d*in.Random.Beta[6]+in.v^2*in.d^2*in.Random.Beta[7])
  }

  return(Random.Out.lm)
}
```

Estimating Credible Bounds for a Set of Decisions

The following code details how to take 200 random drawings of the emulator model for the problem described in Section 6.1.1 of Chapter 6, then how these random drawings can be used to estimate an expected response under uncertainty for a set of decisions. Some annotations are given throughout, and a summary will be given after the code. For the following code Rvec1 and Rvec2 are as described in Appendix G.4.3 and depicted in Figure G.1 (a), i.e. vectors which describe all possible combinations of reinforcement of the B6 and B7a boundaries to a precision of 100 MW.

```
RandomDrawSize<-200
#Set a number of randomly drawn emulator models to use

RandomBetasChap6<-mvrnorm(RandomDrawSize,Chap6PolyBeta,Chap6PolyBetaCov)
#Randomly draw parameters for the polynomial regression portion
 of the emulator model from the multivariate normal distribution

#RandomBetasChap6 is matrix with RandomDrawSize rows,
 such that the ith row gives the parameters for the polynomial
 portion of the ith randomly drawn model

RandomlyDrawnCostEstimates<-matrix(nrow=RandomDrawSize,ncol=length(Rvec1))
#Create a matrix to store random draws of expected cost estimates for a
 set of decisions
```

```
#The ith row of the jth column will detail estimate for
 the ith random draw of the jth decision

for(i in 1:RandomDrawSize){

  Temp.Random.Em<-Random.Em.Fitter(SampledTrainingInputWave1.v,
    SampledTrainingInputWave1.d,SampleTotalCostsWave1,RandomBetasChap6[i,])
  #Fit a randomly drawn emulator model for the ith sample of parameters

  for(j in 1:length(Rvec1)){
    RandomlyDrawnCostEstimates[i,j]<-ExpectationUnderUncertainty(
      Temp.Random.Em,Chap6LB,Chap6UB,c(Rvec1[j],Rvec2[j]),Gen.U.Prior,RN.Att)
  }
  #Estimate expected total costs for each decision, when using the randomly
   drawn emulator model
}
```

The above code first randomly draws 200 sets of parameters from the polynomial portion of the emulator model from a multivariate normal distribution, as Section 5.2.2 describes how beliefs about these variables are represented by a multivariate normal distribution with mean $\hat{\boldsymbol{\beta}}$ described in Equation 5.2.5 and covariance $cov(\hat{\boldsymbol{\beta}})$ described in Equation 5.2.7.

For each of these random drawings, a randomly drawn emulator model is then fitted using the function Random.Em.Fitter as described in the previous sub-subsection. These randomly drawn emulator models are then used to estimate expected total costs for each decision detailed by Rvec1 and Rvec2. These randomly drawn estimates of expected total costs are stored in the matrix RandomlyDrawnCostEstimates, such that the ith entry of the jth column details the estimate of expected total costs under uncertainty when using the ith randomly drawn emulator model and making the reinforcement decision detailed by the jth entry of Rvec1 and Rvec2 (i.e. Rvec1[j] and Rvec2[j]).

It is again noted that these random drawings can be acquired using parallel computing, where instead of estimating an expected response for all 200 of the random drawings on

a single computer, several jobs can be submitted to be completed on several computers in parallel (such as 20 batches each evaluating estimates of expected total costs for 5 of the randomly drawn models).

These random drawings can subsequently be used to form credible intervals using the following function

```
CredibleBoundCreator200RD<-function(inmat){
  #inmat is a matrix of 200 random drawings of a general number of decisions,
   such that the ith row of the jth column of inmat (i.e. inmat[i,j])
   is the ith random drawing for the jth decision

  in.decs<-length(inmat[1,])
  #Note the number of decisions credible bounds are to be estimated for

  outmat<-matrix(nrow=6,ncol=in.decs)
  #Create a matrix to store the credible bounds at different levels
  #Credible intervals are estimated at 3 levels (90%, 95% and 99%
   as detailed below)
  #Each column details credible bounds for a particular decision
   (such that the ith column of outmat details credible bounds for
   the ith decision used for inmat)
  #Each row details credible bounds for all decisions at a
   particular credibility level

  for(i in 1:in.decs){

    outmat[1,i]<-(sort(inmat[,i])[1]+sort(inmat[,i])[2])/2
    #Lower bound of the 99% credible interval
    outmat[2,i]<-(sort(inmat[,i])[199]+sort(inmat[,i])[200])/2
    #Upper bound of the 99% credible interval
    outmat[3,i]<-(sort(inmat[,i])[5]+sort(inmat[,i])[6])/2
    #Lower bound of the 95% credible interval
    outmat[4,i]<-(sort(inmat[,i])[195]+sort(inmat[,i])[196])/2
    #Upper bound of the 95% credible interval
```

```
    outmat[5,i]<-(sort(inmat[,i])[10]+sort(inmat[,i])[11])/2
    #Lower bound of the 90% credible interval
    outmat[6,i]<-(sort(inmat[,i])[190]+sort(inmat[,i])[191])/2
    #Upper bound of the 90% credible interval
  }
  #The above loop estimates credible bounds for the
   90%, 95% and 99% credible intervals

  return(outmat)

}
```

The above function has a single input, inmat, which should be entered as a matrix of 200 random drawings of estimates of expected total costs for a general number of decision variables, such that the ith row for the jth column of inmat (i.e. inmat[i,j]) is the ith random drawing of the jth decision. For each decision, credible intervals are estimated at the 90%, 95% and 99% level for each decision in turn such that at the α% level, $\frac{100-\alpha}{2}$% of the random drawings of estimates of expected total costs are smaller than the lower bound and $\frac{100-\alpha}{2}$% of the random drawings of estimates of expected total costs are greater than the upper bound.

For example, for the 90% credible interval the lower bound is calculated as the mid-point between the 10th and 11th smallest randomly drawn estimates, such that 10 (5%) of the randomly drawn estimates are smaller than the lower bound and 190 (95%) of the randomly drawn estimates are greater. Similarly, the upper bound of the 90% credible interval is calculated as the mid-point between the 190th and 191st smallest values (i.e. the 11th and 10th greatest), such that 10 (5%) of the randomly drawn estimates are greater than the upper bound and 190 (95%) of the randomly drawn estimates are smaller. Together, 180 (90%) of the randomly drawn estimates are contained within the credible bounds, whilst 20 (10%) are excluded.

However, any value between the 10th smallest and 11th smallest randomly drawn values would also mean that 10 (5%) of the randomly drawn estimates are smaller than the lower bound and 190 (95%) of the randomly drawn estimates are greater. Therefore, a

more cautious approach could be to instead use the 10th smallest and 191st smallest randomly drawn estimates as lower and upper bounds respectively for the 90% credible intervals (with a similar approach taken for the 95% and 99% credible intervals), which would result in wider credible intervals.

As the number of random draws used increases, the difference between the two becomes very small, e.g. if 2 million random draws were used there would be very little difference between the 100,000th smallest randomly drawn estimate and the 100,001th smallest randomly drawn estimate.

An application of using CredibleBoundCreator200RD to estimate credible bounds for the random drawings of RandomlyDrawnCostEstimates detailed earlier in this subsubsection is simply

```
Chap6CredBounds<-CredibleBoundCreator200RD(RandomlyDrawnCostEstimates)
```

It is noted that the function CredibleBoundCreator200RD is specific to estimating credible bounds when using 200 random drawings of the emulator model, though it would be easy to generalise to a general number of random drawings such that the lower bound at the α% level is defined as the value which $\frac{100-\alpha}{2}$% of the random draws are smaller than, and the upper bound as the value which $\frac{100-\alpha}{2}$% of the random draws are greater than.

Eliminating Decisions From Consideration

Section 6.2.1 noted how decisions can be eliminated from consideration by first identifying decisions which result in the minimum upper bound of the estimate of expected total costs, with such a decision denoted $\mathbf{d}^o$ with corresponding upper bound $F_{T,U}(\mathbf{d}^o)$. For any alternative decision, $\mathbf{d}^a$, where the lower bound of the estimate of expected total costs, $F_{T,L}(\mathbf{d}^a)$, is greater than the minimum upper bound, i.e. $F_{T,L}(\mathbf{d}^a) > F_{T,U}(\mathbf{d}^o)$, it can be said there is evidence against that decision being optimal, and it can thus be eliminated from consideration.

The R code for eliminating decisions from consideration for the example detailed in Section 6.1.1 is as follows:

```
#Eliminating Decisions Part 1

Rvec1Temp<-seq(0,4000,by=100)
Rvec2Temp<-seq(0,4000,by=100)

WorkingRvec1Mat<-matrix(nrow=length(Rvec1Temp),ncol=length(Rvec2Temp))
WorkingRvec2Mat<-matrix(nrow=length(Rvec1Temp),ncol=length(Rvec2Temp))
for(i in 1:length(Rvec1Temp)){
  WorkingRvec1Mat[i,]<-c(rep(Rvec1Temp[i],length(Rvec2Temp)))
}
for(j in 1:length(Rvec2Temp)){
  WorkingRvec2Mat[,j]<-c(rep(Rvec2Temp[j],length(Rvec1Temp)))
}

Rvec1<-as.vector(WorkingRvec1Mat)
Rvec2<-as.vector(WorkingRvec2Mat)

############################################################

#Eliminating Decisions Part 2

RandomDrawSize<-200
RandomBetasChap6<-mvrnorm(RandomDrawSize,Chap6PolyBeta,Chap6PolyBetaCov)

RandomlyDrawnCostEstimates<-matrix(nrow=RandomDrawSize,ncol=length(Rvec1))

for(i in 1:RandomDrawSize){
  Temp.Random.Em<-Random.Em.Fitter(SampledTrainingInputWave1.v,
    SampledTrainingInputWave1.d,SampleTotalCostsWave1,RandomBetasChap6[i,])
  for(j in 1:length(Rvec1)){
    RandomlyDrawnCostEstimates[i,j]<-ExpectationUnderUncertainty(
      Temp.Random.Em,Chap6LB,Chap6UB,c(Rvec1[j],Rvec2[j]),Gen.U.Prior,RN.Att)
  }
}
```

```
Chap6CredBounds<-CredibleBoundCreator200RD(RandomlyDrawnCostEstimates)

############################################################

#Eliminating Decisions Part 3

Chap6CredBounds95pLB<-Chap6CredBounds[3,]
#Note the lower credible bound of the 95% credible intervals
Chap6CredBounds95pUB<-Chap6CredBounds[4,]
#Note the upper credible bound of the 95% credible intervals

min.UB.DetailsWave1<-optimal.estimator(Chap6CredBounds95pUB,Rvec1,Rvec2)
#Identify the minimum upper bound

Rvec1Wave2<-Rvec1[Chap6CredBounds95pLB <= min.UB.DetailsWave1$cost.opt.est]
#Identify elements of Rvec1 where the lower bound of expected total costs is
 smaller than the estimated minimum upper bound

Rvec2Wave2<-Rvec2[Chap6CredBounds95pLB <= min.UB.DetailsWave1$cost.opt.est]
#Identify elements of Rvec2 where the lower bound of expected total costs is
 smaller than the estimated minimum upper bound
```

The portion of the code denoted Eliminating Decisions Part 1 creates vectors of initial decisions to be considered (i.e. all combinations of B6 and B7a reinforcement to a precision of 100 MW) as outlined in Appendix G.4.3. The portion of the code denoted Eliminating Decisions Part 2 calculates lower and upper bounds for Rvec1 and Rvec2 as detailed in the previous sub-subsection. The portion of the code denoted Eliminating Decisions Part 3 details how elements of Rvec1 and Rvec2 are eliminated as outlined in Section 6.2.1. First, the decision which results in the minimum upper bound of the estimate of expected total costs is identified (though only the cost estimate itself is of interest). This minimum upper bound is then used to create Rvec1Wave2 and Rvec2Wave2, which respectively denote the elements of Rvec1 and Rvec2 where the lower bound of the resulting cost estimate is lower than the estimated minimum upper

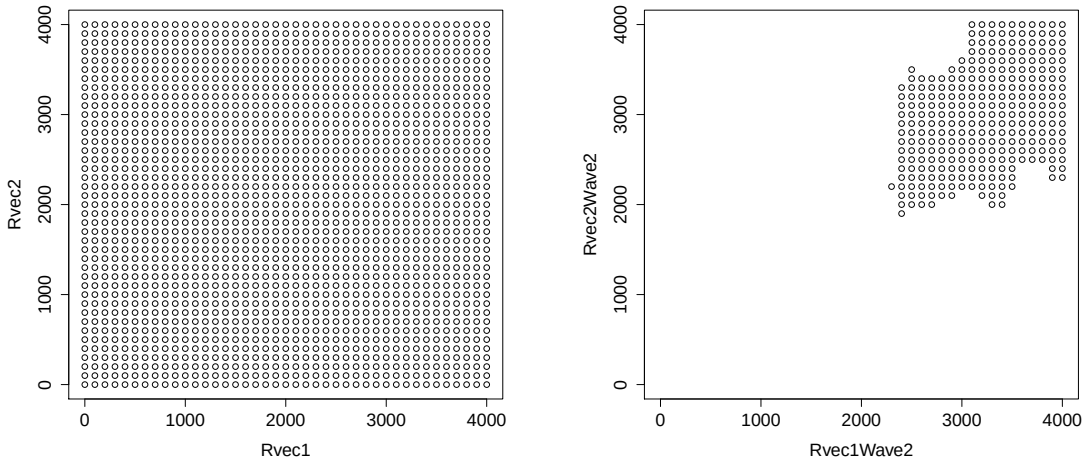

(a) Plot illustrating the reinforcement combinations initially considered.

(b) Plot illustrating the reinforcement combinations which would be considered in the second wave.

Figure G.2: Plots to illustrate the decision vectors.

bound.

The function optimal.estimator used in the portion of the code denoted Eliminating Decisions Part 3 was defined in Appendix G.4.3. Although optimal.estimator is used to identify the decision which minimises the estimate of expected total costs in Appendix G.4.3, it can equivalently be used to identify the decision which minimises the upper bound of the estimate (as well as detail the minimum upper bound itself).

Figure G.2 (a) plots the decisions initially considered (i.e. a plot of Rvec2 against Rvec1), whilst Figure G.2 (b) illustrates the decisions which would not be eliminated from consideration in the second wave (i.e. a plot of Rvec2Wave2 against Rvec1Wave2).

It is noted that as part of the code, a minimum upper bound is only estimated for a decision to the precision of the nearest 100 MW. It would be possible to carry out the iterative procedure outlined in Appendix G.4.3 to estimate a more precise upper bound (e.g. to the nearest 10 MW). However, credible bounds can be expensive to calculate, which in turn make such an iterative procedure expensive.

It is noted that the decision which minimises the upper bound of the estimate to the nearest 100 MW (as is acquired in the code detailed) results in an upper bound of the cost estimate at least as large as the upper bound of a more precise estimate to the nearest 10 MW (i.e. it represents a conservative estimate of the minimum upper

bound). As decisions are eliminated when the lower bound of a decisions is greater than the minimum upper bound, this means that not carrying out this iterative procedure does not result in an increased risk of incorrectly eliminating the optimal decision.

However, it is noted that as estimating a more precise decision (e.g. to the nearest 10 MW) which minimises the upper bound would result in a lower estimate of minimum upper bound, there is a slightly reduced level of power to eliminate decisions from consideration when only estimating to a precision of 100 MW. As estimates of expected total costs (and the corresponding bounds) are flat near the optimal decision (as can be seen in Figure 6.21 (c) of Section 6.3.2) the relatively small changes of a few tens of MW will have little effect on the estimate of the minimum upper bound, meaning the reduced power to eliminate the optimal decision is small.

It is noted that the example detailed in Section 6.1.1 considers making a reinforcement between 0 and 4000 MW on the B6 and B7a boundaries, and Rvec1Wave2 and Rvec2Wave2 have simply identified which decisions to a precision of 100 MW which would merit further consideration in the second wave. As was noted in Section 6.2.2, this is sufficient for sampling training runs to fit an emulator model over the range of decisions which merit further consideration (i.e. over the range of decisions considered in Figure G.2 (b)), and this will be demonstrated in the next sub-subsection.

Sampling Training Runs for the Next Wave

As can be seen in Figure G.2 (b), the range of decisions to be considered in the second wave does not form a hypercube (i.e. a rectangle in two dimensions). Therefore, the methodology detailed in Section 6.2.2 is used to sample input values for decision variables in waves 2 onwards. The R code for this will be presented in this sub-subsection.

Below details the R code for a function to sample potential values for B6 and B7a reinforcement for given vectors of B6 and B7a reinforcement which have not been eliminated from consideration (i.e. using Rvec1Wave2 and Rvec2Wave2 as input, as were identified in the previous sub-subsection).

```
Further.Wave.d.Sampler<-function(in.rvec1,in.rvec2){
```

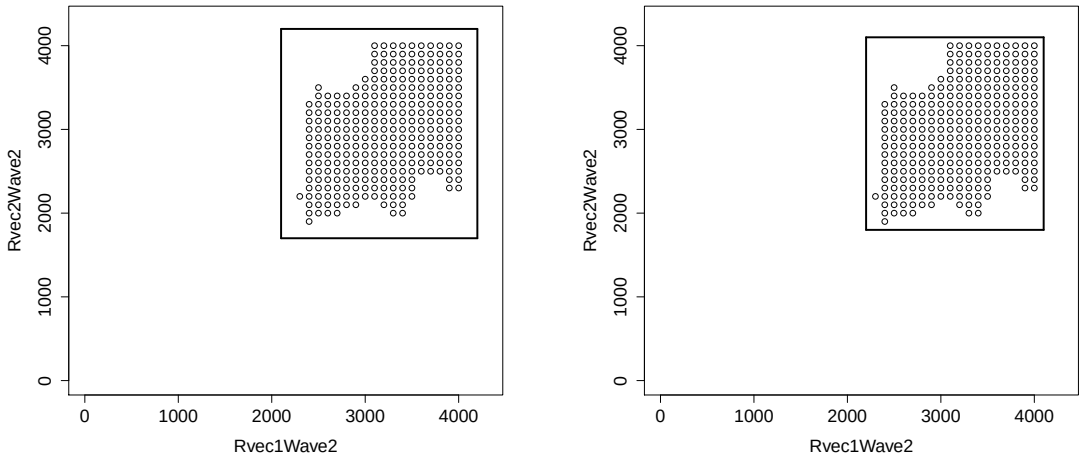

(a) Plot to illustrate the region sampled from using Further.Wave.d.Sampler.

(b) Plot to illustrate a potential alternative region to sample from.

Figure G.3: Plots to illustrate possible regions to uniformly sample potential values of decision variables for input for training runs in wave 2.

```
  out.r1<-runif(1,min(in.rvec1)-200,max(in.rvec1)+200)
  out.r2<-runif(1,min(in.rvec2)-200,max(in.rvec2)+200)
  out.dec<-c(out.r1,out.r2)
  return(out.dec)

}
```

The function Further.Wave.d.Sampler would sample decisions over the region illustrated in Figure G.3 (a), i.e. uniformly sampling over the Latin hypercube from 200 MW below the smallest values of Rvec1Wave2 and Rvec2Wave2 to 200 MW above the greatest values of Rvec1Wave2 and Rvec2Wave2.

However, Rvec1Wave2 and Rvec2Wave2 are the reinforcement decisions to the precision of 100 MW which would not be eliminated using the methodology of Section 6.2.1. Therefore, the function Further.Wave.d.Sampler is slightly overly cautious, and it could be more efficient to uniformly sample decisions over the Latin hypercube from 100 MW below the smallest values of Rvec1Wave2 and Rvec2Wave2 to 100 MW above the greatest values of Rvec1Wave2 and Rvec2Wave2. Such a region is illustrated in Figure G.3 (b).

After values of decision variables, $\mathbf{d}^a$, have been sampled using Further.Wave.d.Sampler,

the methodology of Section 6.2.2 notes how if the lower bound of the estimate of expected total costs of such a decision, $F_{T,L}(\mathbf{d}^a)$, is not greater the the minimum upper bound, $F_{T,U}(\mathbf{d}^o)$, then $\mathbf{d}^a$ can be used as input values of decision variables for training runs in the second wave.

Input Variable	Description
sam.size.d	Sample size required for values of B6 and B7a reinforcement to be used as training data in the next wave
in.rvec1	Vector of values of B6 reinforcement which were not eliminated from consideration in the next wave, to a precision of 100 MW (i.e. Rvec1Wave2 identified in the previous subsection for wave 2)
in.rvec2	Vector of values of B7a reinforcement which were not eliminated from consideration in the next wave, to a precision of 100 MW (i.e. Rvec2Wave2 identified in the previous subsection for wave 2)
in.RD.betas	A matrix of randomly drawn parameters for the polynomial portion of the current emulator model, such that the rth row details parameters for the polynomial portion of the rth randomly drawn model
in.Training.Input.Mat.v	A matrix which defines the training data for variables containing uncertainty for the current emulator model, such that the ith row of in.Training.Input.Mat.v defines the input values for variables containing uncertainty for the ith training run
in.Training.Input.Mat.d	A matrix which defines the training data for the decision variables for the current emulator model, such that the ith row of in.Training.Input.Mat.d defines the input values for the decision variables for the ith training run
in.SimulatedResponse	A vector of simulated responses from the training data for the current emulator model, such that the ith entry of in.SimulatedResponse defines the simulated response when using the inputs defined in the ith rows of in.Training.Input.Mat.v and in.Training.Input.Mat.d
in.v.LBs	A vector describing the lower bounds of the beliefs about the variables containing uncertainty
in.v.UBs	A vector describing the upper bounds of the beliefs about the variables containing uncertainty
in.min.UB	Minimum upper bound for the estimate of expected total costs, $F_{T,U}(\mathbf{d}^o)$, based on the currently fitted emulator model, i.e. min.UB.DetailsWave1$cost.opt.est as identified in the previous sub-subsection

Table G.9: Table detailing the inputs used for Further.Wave.d.set.Sampler, which samples values of the decision variables for inputs of training data in wave 2 onwards.

The R code for sampling values of decision variables for training run input in stage 2 onwards is given below, with details of the function input given in Table G.9. Some annotations are given throughout the code and a summary of the code will be given after the code has been detailed.

```
Further.Wave.d.set.Sampler<-function(sam.size.d,in.rvec1,in.rvec2,
  in.RD.betas,In.Training.Input.Mat.v,In.Training.Input.Mat.d,
  In.SimulatedResponse,in.v.LBs,in.v.UBs,in.min.UB){

  out.rvec.sam<-matrix(nrow=sam.size.d,ncol=2)
  #Create a matrix to store the sampled decisions
  in.RD.size<-length(in.RD.betas[,1])
  #Note the number of random emulator draws used

  Sample.Counter<-0
  #Set the counter of wave 2 decisions acquired to zero

  while(Sample.Counter<sam.size.d){
  #Create a loop to sample wave 2 decisions until the desired sample
   size is achieved

    temp.d<-Further.Wave.d.Sampler(in.rvec1,in.rvec2)
    #Randomly sample a potential wave 2 decision
    temp.RDs<-matrix(nrow=in.RD.size,ncol=1)
    #Create a matrix to store randomly drawn estimates of expected
     total costs for this decision

    for(j in 1:in.RD.size){
    #Create a loop to take random draws of estimates of expected
     total costs for the sampled decision

      Temp.Random.Em<-Random.Em.Fitter(In.Training.Input.Mat.v,
        In.Training.Input.Mat.d,In.SimulatedResponse,in.RD.betas[j,])
      temp.RDs[j,1]<-ExpectationUnderUncertainty(Temp.Random.Em,in.v.LBs,
```

```
        in.v.UBs,temp.d,Gen.U.Prior,RN.Att)
      #Randomly draw an emulator model and note the resulting estimate
       of expected total costs for the sampled decision
    }
    Temp.LB<-CredibleBoundCreator200RD(temp.RDs)[3,1]
    #Estimate a lower bound for the sampled decision using the randomly
     drawn estimates of expected total costs
    #For this function the lower bound of a 95% credible interval is taken,
     though this can be changed as necessary
    if(Temp.LB<=in.min.UB){
      out.rvec.sam[Sample.Counter+1,]<-temp.d
      Sample.Counter<-Sample.Counter+1
      #If the lower bound is less than the minimum upper bound (i.e. the
       decision would not have been eliminated from consideration) store
       the decision, otherwise do not
    }
  }

  return(out.rvec.sam)
  #Return the sample of decisions
}

PotentialWave2Sample<-Further.Wave.d.set.Sampler(300,Rvec1Wave2,Rvec2Wave2,
  RandomBetasChap6,SampledTrainingInputWave1.v,SampledTrainingInputWave1.d,
  SampleTotalCostsWave1,Chap6LB,Chap6UB,min.UB.DetailsWave1$cost.opt.est)
#An application of the above function to sample 300 values of B6 and B7a
 reinforcement magnitude in wave 2
```

The above R code details a function for sampling decisions beyond the current wave. Within the code, the function Further.Wave.d.Sampler is used to iteratively sample potential stage 2 decisions, i.e. sample values of $\mathbf{d}^a$. For each sampled decision, a lower bound for the estimate of expected total costs when making the sampled decision, $F_{T,L}(\mathbf{d}^a)$, is estimated as outlined in the previous sub-subsection.

If this lower bound is not greater than the minimum upper bound, i.e. if

$F_{T,L}(\mathbf{d}^a) \leq F_{T,U}(\mathbf{d}^o)$, this decision would not be eliminated from consideration using the methodology of Section 6.2.1. Therefore, the sampled decision can be used as input for training runs in the second wave, so the decision is recorded. If the lower bound is greater than the minimum upper bound, i.e. if $F_{T,L}(\mathbf{d}^a) > F_{T,U}(\mathbf{d}^o)$, then the decision would have been eliminated from consideration using the methodology of Section 6.2.1, so the decision is discarded and a new decision sampled.

As noted in Section 5.2.4, in practice many different samples of the specified size for values of decision variables to use as training run input in wave 2, (as well as many Latin hypercube samples of values for the variables containing uncertainty, $\mathbf{v}$, to use as training run input in wave 2) would be acquired. Then, the sample which resulted in the maximum minimum distance between points would be selected, as is common practice to ensure that the training runs give a dense coverage to the input space of the simulator [74, 98, 23].

G.5 A Selection of R Code for Chapter 9

G.5.1 Preliminary Code for Multi-Stage Decision Problems

Specifying Initial Data

For the multi-stage decision problem, quite a lot of initial assumptions must be specified, such as the assumed discount rate at each stage, the assumed cost of reinforcement, when decisions are made, etc. The R code for detailing the initial assumptions outlined in Section 9.2 is given below:

```
AssumedCTR<-1000
#The assumed cost of reinforcement (pounds/MW/km)

DiscountRate<-0.05
#The assumed discount rate (5%)
DiscountFactor<-1/(1+DiscountRate)
#The assumed discount factor from the assumed discount rate
```

```
Stage1.v.lowers<-c(0.55,0.8,0.95)
Stage2.v.lowers<-c(0.55,0.8,0.9)
Stage3.v.lowers<-c(0.55,0.8,0.85)
#Lower bounds for variables containing uncertainty in each stage
#The first element is the lower bound for nuclear availability probability,
 the second is the lower bound for CCGT availability probability,
 the third is the lower bound for peak demand magnification

Stage2.v.lowers.ND<-c(0.55,0.8)
Stage3.v.lowers.ND<-c(0.55,0.8)
#Lower bounds excluding peak demand magnification

Stage1.v.uppers<-c(0.85,0.95,1.05)
Stage2.v.uppers<-c(0.85,0.95,1.1)
Stage3.v.uppers<-c(0.85,0.95,1.15)
#Upper bounds for variables containing uncertainty in each stage
#The first element is the upper bound for nuclear availability probability,
 the second is the upper bound for CCGT availability probability,
 the third is the upper bound for peak demand magnification

Stage2.v.uppers.ND<-c(0.85,0.95)
Stage3.v.uppers.ND<-c(0.85,0.95)
#Upper bounds excluding peak demand magnification

Psi.2.lower<-0.95
Psi.2.upper<-1.05
#Set minimum and maximum values for the value of psi_2 that will be
 observed when the second decision is to be made

Psi.3.lower<-0.9
Psi.3.upper<-1.1
#Set minimum and maximum values for the value of psi_3 that will be
 observed when the third decision is to be made
```

```
Min.Stage1.B6.Val<-0
Min.Stage2.B6.Val<-0
Min.Stage3.B6.Val<-0
#Set values for the minimum values of total B6 reinforcement after
 the first, second and third decision

Max.Stage1.B6.Val<-4500
Max.Stage2.B6.Val<-6500
Max.Stage3.B6.Val<-8500
#Set values for the maximum values of total B6 reinforcement after
 the first, second and third decision

Min.Stage1.B7.Val<-0
Min.Stage2.B7.Val<-0
Min.Stage3.B7.Val<-0
#Set values for the minimum values of total B7a reinforcement after
 the first, second and third decision

Max.Stage1.B7.Val<-4500
Max.Stage2.B7.Val<-5500
Max.Stage3.B7.Val<-5500
#Set values for the maximum values of total B7a reinforcement after
 the first, second and third decision

Stage1RStart<-0
Stage2RStart<-5
Stage3RStart<-10
#Times the first, second and third reinforcement decisions are made

Stage1CStart<-6
Stage1CEnd<-10
Stage2CStart<-11
Stage2CEnd<-15
Stage3CStart<-16
```

```
Stage3CEnd<-25
#Note the first and final years that constraint costs are considered for
 in each stage
```

It is noted that Min.Stage2.B6.Val and Max.Stage2.B6.Val specify minimum and maximum values for the total reinforcement of the B6 boundary after the second stage (i.e. values of $d_{T_2,1}$), and similarly Min.Stage2.B7.Val and Max.Stage2.B7.Val specify minimum and maximum values for the total reinforcement of the B7a boundary after the second stage (i.e. values of $d_{T_2,2}$), and similarly for stage 3. As was noted in Section 8.2.7 and Appendices C.3 and D.1, this is sufficient as the simulator for constraint costs in the second and third stages is dependent only on the total reinforcement after the second and third stages only respectively, and not the individual in stages 1, 2 and 3.

In particular, Section 8.2.7 notes that for the simulator of constraint costs in stage 2, if a total reinforcement of 4000 MW B6 reinforcement is built after the second decision, the simulator would not distinguish between 1000 MW being built in stage 1 and 3000 MW in stage 2 or 3000 MW in stage 1 and 1000 MW in stage 2 (or any other combination of reinforcements which result in a total of 4000 MW B6 reinforcement after the second decision). Therefore, when fitting the emulator model for mean constraint costs in the second and third stages it is sufficient to specify values of total reinforcement after the second and third stages respectively.

It is also noted that the vectors Stage2.v.lower.ND and Stage2.v.uppers.ND are created to specify lower and upper bounds for beliefs about nuclear and CCGT availability in stage 2, without limits for peak demand level (and similarly for Stage3.v.lower.ND and Stage3.v.uppers.ND in stage 3). This is because the beliefs about peak demand level in stages 2 and 3 at the time the second and third decisions are made are dependent on the stage 2 and 3 scenario observed. Therefore, Stage2.v.lower.ND and Stage2.v.uppers.ND are useful to be specified, then extended appropriately to also specify beliefs about stage 2 peak demand level depending on the observed stage 2 scenario (and similarly for stage 3), as will be noted when appropriate in what follows.

Section 9.2.1 noted that for the problem detailed in Section 9.2; the first, second and third reinforcement decisions are made at the beginning of year 1, year 6 and

year 11 respectively. This is represented in the above code by setting Stage1RStart, Stage2RStart and Stage3RStart (which are variables which represent when the first, second and third decisions are made respectively) to 0, 5 and 10 respectively. This is so reinforcement costs are correctly discounted later. For example, the first decision is made at the beginning of year 1 (i.e. now), and it is assumed all costs are paid up front, hence it is appropriate to apply discounting of 0 years. On the other hand, the third decision is made at the beginning of year 11 (i.e. 10 years from now) and it is assumed the reinforcement costs of such a decision are incurred when the decision is made, hence it is appropriate to apply 10 years of discounting to the reinforcement costs of the third decision.

Section 9.2.1 also noted that constraint costs for the first stage are considered between years 6 and 10, as these are the years directly affected by the first stage decision, and these are noted as Stage1CStart and Stage1CEnd respectively in the above code (with similar specifications for stages 2 and 3 made in the above code based on the time frame detailed in Section 9.2.1). These values can subsequently be used to simulate mean constraint costs, as will be detailed in the next sub-subsection.

Fitting Initial Emulator Models For Each Stage

This subsection will detail the R code for fitting the emulator models for mean constraint costs in the first, second and third stages, i.e. $\tilde{f}_{c,1}(\mathbf{v}_1, \mathbf{d}_1)$, $\tilde{f}_{c,2}(\mathbf{v}_2, \mathbf{d}_2|\mathbf{d}_1) = \tilde{f}_{c,2}(\mathbf{v}_2, \mathbf{d}_{T_2})$ and $\tilde{f}_{c,3}(\mathbf{v}_3, \mathbf{d}_3|\mathbf{d}_{T_2}) = \tilde{f}_{c,3}(\mathbf{v}_3, \mathbf{d}_{T_3})$ respectively. First, a number of training runs used to fit each emulator model must be specified, using the following code

```
Stage1.C.Em.Sam.Size<-300
Stage2.C.Em.Sam.Size<-300
Stage3.C.Em.Sam.Size<-300
Stage2.G.Em.Sam.Size<-50
Stage3.G.Em.Sam.Size<-50
#Set a number of training runs to fit each emulator model
```

such that Stage1.C.Em.Sam.Size, Stage2.C.Em.Sam.Size and Stage3.C.Em.Sam.Size are the number of training runs used to fit $\tilde{f}_{c,1}(\mathbf{v}_1, \mathbf{d}_1)$, $\tilde{f}_{c,2}(\mathbf{v}_2, \mathbf{d}_{T_2})$ and $\tilde{f}_{c,3}(\mathbf{v}_3, \mathbf{d}_{T_3})$ respectively.

Stage2.G.Em.Sam.Size and Stage3.G.Em.Sam.Size are the number of training runs used to fit the emulator models $\tilde{G}_{T,2,\psi_2}(\mathbf{d}_1, \boldsymbol{\psi}_2)$ and $\tilde{G}_{T,3,\psi_3}(\mathbf{d}_{T_2}, \boldsymbol{\psi}_3)$ (i.e. emulator models for total costs in stage 2 onwards and total costs in stage 3 respectively). Details on the R code used to fit $\tilde{G}_{T,2,\psi_2}(\mathbf{d}_1, \boldsymbol{\psi}_2)$ and $\tilde{G}_{T,3,\psi_3}(\mathbf{d}_{T_2}, \boldsymbol{\psi}_3)$ will later be given in Appendices G.5.3 and G.5.4

The R code for simulating mean constraint costs in each stage is given below

```
SampledTrainingInput.Stage1.Wave1<-LHC.Sample.Function(Stage1.C.Em.Sam.Size,
  c(Stage1.v.lowers,Min.Stage1.B6.Val,Min.Stage1.B7.Val),
  c(Stage1.v.uppers,Max.Stage1.B6.Val,Max.Stage1.B7.Val))
SampledTrainingInput.Stage2.Wave1<-LHC.Sample.Function(Stage2.C.Em.Sam.Size,
  c(Stage2.v.lowers,Min.Stage2.B6.Val,Min.Stage2.B7.Val),
  c(Stage2.v.uppers,Max.Stage2.B6.Val,Max.Stage2.B7.Val))
SampledTrainingInput.Stage3.Wave1<-LHC.Sample.Function(Stage3.C.Em.Sam.Size,
  c(Stage3.v.lowers,Min.Stage3.B6.Val,Min.Stage3.B7.Val),
  c(Stage3.v.uppers,Max.Stage3.B6.Val,Max.Stage3.B7.Val))
#Sample inputs based on the given sample size, lower bounds for variables
 and upper bounds for the variables in each stage
#SampledTrainingInput.Stage1.Wave1, SampledTrainingInput.Stage2.Wave1 and
 SampledTrainingInput.Stage3.Wave1 will be a matrices of 300 rows
 and 5 columns
#The ith row details input for the ith training run
#Column 1 details values of nuclear availability probability
#Column 2 details values of CCGT availability probability
#Column 3 details values of peak demand magnification
#Column 4 details values of total B6 reinforcement magnitude
 after the respective stage
 e.g. the fourth column of SampledTrainingInput.Stage2.Wave1
 details value of total B6 reinforcement magnitude after
 the second decision
#Column 5 details values of total B7a reinforcement magnitude
 after the respective stage decision

SampledTrainingInput.Stage1.Wave1.v<-SampledTrainingInput.Stage1.Wave1[,
```

```
  c(1,2,3)]
SampledTrainingInput.Stage1.Wave1.d<-SampledTrainingInput.Stage1.Wave1[,
  c(4,5)]
SampledTrainingInput.Stage2.Wave1.v<-SampledTrainingInput.Stage2.Wave1[,
  c(1,2,3)]
SampledTrainingInput.Stage2.Wave1.d<-SampledTrainingInput.Stage2.Wave1[,
  c(4,5)]
SampledTrainingInput.Stage3.Wave1.v<-SampledTrainingInput.Stage3.Wave1[,
  c(1,2,3)]
SampledTrainingInput.Stage3.Wave1.d<-SampledTrainingInput.Stage3.Wave1[,
  c(4,5)]
#Create separate matrices detailing the input for training runs for
 variables containing uncertainty (i.e. nuclear availability
 probability, CCGT availability probability and peak demand
 magnification) and decision variables (i.e. total B6 reinforcement
 magnitude and total B7a reinforcement magnitude) in each stage

SimulatedConstraints.Stage1.Wave1<-TrainingRunSimulatorStage1(
  SampledTrainingInput.Stage1.Wave1)
#Simulate mean constraint costs for the given training data input for
 stage 1
SimulatedConstraints.Stage2.Wave1<-TrainingRunSimulatorStage2(
  SampledTrainingInput.Stage2.Wave1)
#Simulate mean constraint costs for the given training data input for
 stage 2
SimulatedConstraints.Stage3.Wave1<-TrainingRunSimulatorStage3(
  SampledTrainingInput.Stage3.Wave1)
#Simulate mean constraint costs for the given training data input for
 stage 3

#Each of the above are vectors of length 300 (as 300 training runs are used
 to fit each emulator model), such that the ith entry of each vector
 represents the simulated constraint costs for the ith training run of the
 respective stage
```

As was noted in Appendix G.4.1, TrainingRunSimulatorStage1, TrainingRunSimulatorStage2 and TrainingRunSimulatorStage3 are used to represent the simulation process as outlined in Appendix G.3.2. As was also noted in Appendix G.4.1, in practice parallel computing can be used as part of the simulation process such that several jobs can be submitted where each simulates mean constraint costs for a small number of training runs, rather than performing hundreds of simulations on a single computer.

Section 9.2.1 notes that constraint costs for each stage are simulated by simulating mean constraint costs for a particular power system background which is assumed to be representative of the power system for the entirety of each stage, as is common practice in the existing literature. Therefore, TrainingRunSimulatorStage1 simulates mean constraint costs based on a year 6 power system background, TrainingRunSimulatorStage2 simulates mean constraint costs based on a year 11 power system background and TrainingRunSimulatorStage3 simulates mean constraint costs based on a year 16 power system background as Section 9.2.1 noted years 6, 11 and 16 are assumed to be representative of the power system in stages 1, 2 and 3 respectively.

These simulations can then be used to extrapolate constraint costs for the entirety of each stage using the following R code:

```
SimulatedFullConstraints.Stage1.Wave1<-c(rep(0,Stage1.C.Em.Sam.Size))
for(i in 1:Stage1.C.Em.Sam.Size){
  for(j in Stage1CStart:Stage1CEnd){
    SimulatedFullConstraints.Stage1.Wave1[i]<-(
      SimulatedFullConstraints.Stage1.Wave1[i]+
      SimulatedConstraints.Stage1.Wave1[i]*DiscountFactor^j)
  }
}

SimulatedFullConstraints.Stage2.Wave1<-c(rep(0,Stage2.C.Em.Sam.Size))
for(i in 1:Stage2.C.Em.Sam.Size){
  for(j in Stage2CStart:Stage2CEnd){
    SimulatedFullConstraints.Stage2.Wave1[i]<-(
      SimulatedFullConstraints.Stage2.Wave1[i]+
      SimulatedConstraints.Stage2.Wave1[i]*DiscountFactor^j)
```

```
  }
}

SimulatedFullConstraints.Stage3.Wave1<-c(rep(0,Stage3.C.Em.Sam.Size))
for(i in 1:Stage3.C.Em.Sam.Size){
  for(j in Stage3CStart:Stage3CEnd){
    SimulatedFullConstraints.Stage3.Wave1[i]<-(
      SimulatedFullConstraints.Stage3.Wave1[i]+
      SimulatedConstraints.Stage3.Wave1[i]*DiscountFactor^j)
  }
}
#Use the simulated mean constraint costs to extrapolate mean constraint costs
 for each stage
```

The above R code extrapolates mean constraint costs for an entire stage, as follows. If $c_{m,R}$ represents the mean constraint costs of the power system background year which is supposed to be representative of the power system background for the entirety of stage m, the above R code would work by extrapolating mean constraint costs for the entirety of stage m, $C_{m,R}$, as

$$C_{m,R} = \sum_{y=Y_B}^{y=Y_E} c_{m,R} \frac{1}{(1.05)^y} \tag{G.5.1}$$

where Y_B is the first year constraint costs are considered for in stage m (e.g. $Y_B = 6$ in stage 1) and Y_E is the final year constraint costs are considered for in stage m (e.g. $Y_E = 10$ in stage 1). This effectively assumes $c_{m,R}$ represents constraint costs in each year of stage m, and takes the resulting discounted sum.

It is noted that the above code results in mean constraint costs being discounted as if all constraint costs are incurred at the end of the year. It would have been desirable to use the discount rate within the simulator, so that each snapshot is discounted appropriately (such that costs in January are discounted less than those in December). This would have been very easy to implement within the simulator described in Appendix G.2 (the costs simulated in each snapshot would be simulated as described in Appendix G.2, with an appropriate effect of discounting then applied to them). However, we decided against doing this, as this would ignore the fact that a stochastic

element is not used within our simulator (to remain consistent with National Grid), and the specified distribution of demand used throughout the year (i.e. the LDC which details snapshot demand) is more correctly thought of as the distribution of demand throughout the year, rather than prescribing specific demand levels to specific snapshots. Further, within the existing literature it is common to discount the sum of annual operating costs (constraint costs for our example) as if they were all acquired at the end of the year [30, 62, 66, 97], and estimate the total costs over a given period of time as outlined in Equation G.5.1.

These simulations of constraint costs are then used to fit emulator models for constraint costs in each stage as outlined in Appendix G.4.1 using the following R code

```
Stage1.C.Em.Wave1.List<-Em.FitterStage1(SampledTrainingInput.Stage1.Wave1.v,
  SampledTrainingInput.Stage1.Wave1.d,SimulatedFullConstraints.Stage1.Wave1)
Stage2.C.Em.Wave1.List<-Em.FitterStage2(SampledTrainingInput.Stage2.Wave1.v,
  SampledTrainingInput.Stage2.Wave1.d,SimulatedFullConstraints.Stage2.Wave1)
Stage3.C.Em.Wave1.List<-Em.FitterStage3(SampledTrainingInput.Stage3.Wave1.v,
  SampledTrainingInput.Stage3.Wave1.d,SimulatedFullConstraints.Stage3.Wave1)
#Fit emulator models for mean constraint costs in each stage using the
 training runs

Stage1.C.Em.Wave1<-Stage1.C.Em.Wave1.List$Fitted.Emulator
Stage1.C.Em.Wave1.PolyBeta<-Stage1.C.Em.Wave1.List$lm.part.beta
Stage1.C.Em.Wave1.PolyBetaCov<-Stage1.C.Em.Wave1.List$lm.part.betacov

Stage2.C.Em.Wave1<-Stage2.C.Em.Wave1.List$Fitted.Emulator
Stage2.C.Em.Wave1.PolyBeta<-Stage2.C.Em.Wave1.List$lm.part.beta
Stage2.C.Em.Wave1.PolyBetaCov<-Stage2.C.Em.Wave1.List$lm.part.betacov

Stage3.C.Em.Wave1<-Stage3.C.Em.Wave1.List$Fitted.Emulator
Stage3.C.Em.Wave1.PolyBeta<-Stage3.C.Em.Wave1.List$lm.part.beta
Stage3.C.Em.Wave1.PolyBetaCov<-Stage3.C.Em.Wave1.List$lm.part.betacov

#Store the elements of Stage1.C.Em.Wave1, Stage2.C.Em.Wave1 and
 Stage3.C.Em.Wave1 separately for convenience
```

The functions Em.FitterStage1, Em.FitterStage2 and Em.FitterStage3 behave as Em.Fitter detailed in Appendix G.4.1, which is used to fit an emulator model to a set of training data. It is assumed that Em.FitterStage1, Em.FitterStage2 and Em.FitterStage3 fit appropriate polynomial regression portions of the emulator models for the emulators fitted in stages 1, 2 and 3 respectively. For example, when fitting the emulator model for stage 1 constraint costs it is assumed that the polynomial portion of the emulator model fitted using Em.FitterStage1 takes the form

$$\beta_0+\beta_1 v_{1,1}+\beta_2 v_{1,2}+\beta_3 v_{1,3}+\beta_4 d_{1,1}+\beta_5 d_{1,2}+\beta_6 v_{1,1}^2+\beta_7 v_{1,2}^2+\beta_8 v_{1,3}^2+\beta_9 d_{1,1}^2+\beta_{10} d_{1,2}^2+\beta_{11} v_{1,1} d_{1,1}+\beta_{12} v_{1,1} d_{1,2}+\beta_{13} d_{1,1} d_{1,2}+\beta_{14} v_{1,1}^2 d_{1,1}^2+\beta_{15} v_{1,1}^2 d_{1,2}^2+\beta_{16} d_{1,1}^2 d_{1,2}^2+\beta_{17} v_{1,1} d_{1,1} d_{1,2}+\beta_{18} v_{1,1}^2 d_{1,1}^2 d_{1,2}^2$$

as Section 8.4 noted that this was the form of the polynomial portion of the emulator model for stage 1 constraint costs, $\tilde{f}_{c,1}(\mathbf{v}_1, \mathbf{d}_1)$.

G.5.2 R Code For Functions Used to Estimate Expected Mean Constraint Costs Under Uncertainty in Each Stage and Expected Total Costs Under Uncertainty in Stage m Onwards

Functions to Estimate Expected Mean Constraint Costs Under Uncertainty in Stages 2 and 3

The function ExpectationUnderUncertainty detailed in Appendix G.4.2 can be used to estimate expected mean constraint costs under uncertainty in stage 1 for a given emulator model.

However, in stages 2 and 3 the prior beliefs about variables containing uncertainty may depend on the scenario observed. Therefore, a slightly different function is required to estimate expected mean constraint costs under uncertainty in stages 2 and 3. This function is detailed below, with details about the function input given in Table G.10.

```
ExpectationUnderUncertainty.Psi.m<-function(Em.Mod,Low.B.Bounds,Up.B.Bounds,
  In.Decisions,Prior.Beliefs,ATR.fun,in.psi.m){
```

Input Variable	Description
Em.Mod	$\tilde{f}_{c,m}(\mathbf{v}_m, \mathbf{d}_{T_m})$, i.e. the fitted emulator to estimate mean constraint costs in stage m for given values of variables containing uncertainty, $\mathbf{v}_m$, and decision variables, $\mathbf{d}_{T_m}$
Low.B.Bounds	A vector detailing the lower bounds for the variables containing uncertainty, such that the ith element of Low.B.Bounds is the lower bound for the ith variable containing uncertainty
Up.B.Bounds	A vector detailing the upper bounds for the variables containing uncertainty, such that the ith element of Up.B.Bounds is the upper bound for the ith variable containing uncertainty
In.Decisions	$\mathbf{d}^*_{T_m}$, i.e. specific values of the decision variables in stage m (in terms of total reinforcement after the mth decision)
Prior.Beliefs	$p(\mathbf{v}_m\|\boldsymbol{\psi}_m)$, i.e. a function to describe the prior beliefs about the variables containing uncertainty given the observed stage m scenario
ATR.fun	A function to define the decision maker's attitude to risk (i.e. a loss or utility function)
in.psi.m	$\boldsymbol{\psi}^*_m$, a specific observed scenario in stage m, i.e. a specific value of $\boldsymbol{\psi}_m$

Table G.10: Table giving details of the inputs for ExpectationUnderUncertainty.Psi.m, the function used to estimate expected mean constraint costs under uncertainty in stage m for a given emulator.

```
  f2<-function(x){
    return(ATR.fun(Em.Mod(x,In.Decisions))*Prior.Beliefs(x,Low.B.Bounds,
      Up.B.Bounds,in.psi.m))
  }
  outvals<-adaptIntegrate(f2, lowerLimit = c(Low.B.Bounds),
    upperLimit = c(Up.B.Bounds))$integral

  return((outvals))
}
```

This function is the same as ExpectationUnderUncertainty detailed in Appendix G.4.2, except it allows the prior beliefs to account for the observed scenario, $\boldsymbol{\psi}_m$, if necessary.

For the three stage problem outlined in Section 9.2, the beliefs about uncertainties

in each stage form a uniform distribution across a given range. Beliefs about nuclear and CCGT availability are unaffected by the scenario observed, with beliefs about peak demand magnification forming a uniform distribution over the range $\boldsymbol{\psi}_m - 0.05$ to $\boldsymbol{\psi}_m + 0.05$. Therefore, an appropriate function is simply to specify beliefs about uncertainties in stage m is simply to adapt the function Gen.U.Prior specified in Appendix G.4.2 as follows:

```
Gen.U.Prior.Psi.m<-function(in.v,in.lowers,in.uppers,in.psi.m){
  Bound.Dif<-in.uppers-in.lowers
  UniformFactor<-1/(prod(Bound.Dif))
  return(UniformFactor)
}
```

with details of the input to this function given in Table G.11. The function Gen.U.Prior.Psi.m does not depend on $\boldsymbol{\psi}_m$, given that the lower and upper bounds used as input are specified appropriately (i.e. so that lower and upper bounds given as input specify lower and upper bounds for peak demand magnification as $\boldsymbol{\psi}_m - 0.05$ and $\boldsymbol{\psi}_m + 0.05$ respectively).

Input Variable	Description
in.v	A vector detailing the specific values of variables containing uncertainty, $\mathbf{v}_m$, that a density is to be calculated for
in.lowers	A vector detailing the lower bounds for the variables containing uncertainty, such that the ith element of in.lowers is the lower bound for the ith variable containing uncertainty
in.uppers	A vector detailing the upper bounds for the variables containing uncertainty, such that the ith element of in.uppers is the upper bound for the ith variable containing uncertainty
in.psi.m	$\boldsymbol{\psi}_m^*$, a specific observed scenario in stage m, i.e. a specific value of $\boldsymbol{\psi}_m$

Table G.11: Table giving details of the inputs for Gen.U.Prior.Psi.m, the function to calculate the density of a uniform distribution for a given stage m scenario.

A Possible Alternative Function to Estimate Expected Mean Constraint Costs Under Uncertainty in Stages 2 and 3

For the function specified in the previous subsection to estimate expected mean constraint costs under uncertainty in stage m (ExpectationUnderUncertainty.Psi.m) appropriate lower and upper bounds for the scenario observed, $\boldsymbol{\psi}_m$, need to be specified as input. However, it would be possible to incorporate this into the function itself. For the example detailed in Section 9.2 an appropriate alternative function would be:

```
ExpectationUnderUncertainty.Psi.m.Alternative<-function(Em.Mod,Low.B.Bounds,
  Up.B.Bounds,In.Decisions,Prior.Beliefs,ATR.fun,in.psi.m){

  Complete.Low.B.Bounds<-c(Low.B.Bounds,in.psi.m-0.05)
  Complete.Up.B.Bounds<-c(Low.B.Bounds,in.psi.m+0.05)

  f2<-function(x){
    return(ATR.fun(Em.Mod(x,In.Decisions))*Prior.Beliefs(x,Low.B.Bounds,
      Up.B.Bounds,in.psi.m))
  }
  outvals<-adaptIntegrate(f2, lowerLimit = c(Complete.Low.B.Bounds),
    upperLimit = c(Complete.Up.B.Bounds))$integral

  return((outvals))
}
```

ExpectationUnderUncertainty.Psi.m.Alternative is the same as ExpectationUnderUncertainty.Psi.m, expect Low.B.Bounds and Up.B.Bounds now only specify lower and upper bounds respectively for nuclear and CCGT availability probability. These are then extended to specify lower and upper bounds for peak demand magnification as $\boldsymbol{\psi}_m - 0.05$ and $\boldsymbol{\psi}_m + 0.05$ respectively, as outlined in Section 9.2.

In ExpectationUnderUncertainty.Psi.m.Alternative as detailed above, the function detailing prior beliefs is specified in terms of Low.B.Bounds, Up.B.Bounds and in.psi.m, though this could be changed to Complete.Low.B.Bounds, Complete.Up.B.Bounds and in.psi.m if necessary.

Function to Estimate Expected Total Costs in Stage 2 or 3 Onwards

As well as a function to estimate expected mean constraint costs under uncertainty in stages 2 and 3, a function is required to estimate expected total costs under uncertainty in stages 2 (or 3) onwards a function of the previous stage decision and scenario only, i.e. to evaluate

$$\tilde{G}_{T,2,\boldsymbol{\psi}_1}(\mathbf{d}_1, \boldsymbol{\psi}_1) = \int_{\boldsymbol{\psi}_2} \tilde{G}_{T,2,\boldsymbol{\psi}_2}(\mathbf{d}_1, \boldsymbol{\psi}_2) \times p_{\boldsymbol{\psi}_{2|1}}(\boldsymbol{\psi}_2|\boldsymbol{\psi}_1)\mathrm{d}\boldsymbol{\psi}_2 \tag{G.5.2}$$

and

$$\tilde{G}_{T,3,\boldsymbol{\psi}_2}(\mathbf{d}_{T_2}, \boldsymbol{\psi}_2) = \int_{\boldsymbol{\psi}_3} \tilde{G}_{T,3,\boldsymbol{\psi}_3}(\mathbf{d}_{T_2}, \boldsymbol{\psi}_3) \times p_{\boldsymbol{\psi}_{3|2}}(\boldsymbol{\psi}_3|\boldsymbol{\psi}_2)\mathrm{d}\boldsymbol{\psi}_3 \tag{G.5.3}$$

as outlined in Section 9.1.2.

Input Variable	Description
G.Em.Mod	$\tilde{G}_{T,m,\boldsymbol{\psi}_m}(\mathbf{d}_{T_{m-1}}, \boldsymbol{\psi}_m)$, i.e. the fitted emulator to estimate expected total costs in stage m onwards as a function of total reinforcement by stage $m-1$, $\mathbf{d}_{T_{m-1}}$, and stage m scenario, $\boldsymbol{\psi}_m$
In.Decisions	$\mathbf{d}^*_{T_{m-1}}$, i.e. specific values of the total reinforcement made by stage $m-1$
Prior.Beliefs	$p(\boldsymbol{\psi}_{m+1}\|\boldsymbol{\psi}_m)$, i.e. a function to describe the prior beliefs about observing scenario $\boldsymbol{\psi}_{m+1}$ in stage $m+1$ given that scenario $\boldsymbol{\psi}_m$ is observed in stage m
ATR.fun	A function to define the decision maker's attitude to risk (i.e. a loss or utility function)
in.psi.mless1	$\boldsymbol{\psi}^*_{m-1}$, i.e. a specific observed scenario in stage $m-1$

Table G.12: Table giving details of the inputs for ExpectationUnderUncertainty.Stage.m.G, the function to used to estimate expected total costs in stage m onwards given the stage $m-1$ decision and stage $m-1$ scenario.

For the example detailed in Section 9.2, an appropriate adaptation of the function ExpectationUnderUncertainty from Appendix G.4.2 to evaluate Equations G.5.3 and G.5.2 is detailed below, with a summary of the inputs of the function, ExpectationUnderUncertainty.Stage.m.G, detailed in Table G.12.

```
ExpectationUnderUncertainty.Stage.m.G<-function(G.Em.Mod,In.Decisions,
  Prior.Beliefs,ATR.fun,in.psi.mless1){
```

```
  Psi.Low.B.Bounds<-in.psi.mless1-0.05
  Psi.Up.B.Bounds<-in.psi.mless1+0.05
  #Lower and upper bounds for the value of psi_m (the stage m scenario)
   that will be observed when the mth decision is to be made
   given that scenario in.psi.mless1 is observed in stage m-1

  f2<-function(x){
    return(ATR.fun(G.Em.Mod(x,In.Decisions))*Prior.Beliefs(x,
      Psi.Low.B.Bounds,Psi.Up.B.Bounds,in.psi.mless1))
  }
  outvals<-adaptIntegrate(f2, lowerLimit = c(Psi.Low.B.Bounds),
    upperLimit = c(Psi.Up.B.Bounds))$integral

  return((outvals))
}
```

In the above code, the function f2 would calculate

$$l(\tilde{G}_{T,m,\boldsymbol{\psi}_m}(\mathbf{d}^*_{T_{m-1}},\boldsymbol{\psi}_m))p_{\boldsymbol{\psi}_{m|m-1}}(\boldsymbol{\psi}_m|\boldsymbol{\psi}^*_{m-1})$$

i.e. the product of an attitude to risk applied to the emulator, $\tilde{G}_{T,m,\boldsymbol{\psi}_m}(\mathbf{d}^*_{T_{m-1}},\boldsymbol{\psi}_m)$, and the density of the PDF to describe prior beliefs about observing scenario $\boldsymbol{\psi}_m$ in stage m given that scenario $\boldsymbol{\psi}^*_{m-1}$ is observed in stage $m-1$, $p_{\boldsymbol{\psi}_{m|m-1}}(\boldsymbol{\psi}_m|\boldsymbol{\psi}^*_{m-1})$.

The function adaptIntegrate from the package cubature is then used to calculate an expected response under uncertainty, i.e. to calculate

$$\tilde{G}_{T,m,\boldsymbol{\psi}_{m-1},l}(\mathbf{d}^*_{T_{m-1}},\boldsymbol{\psi}^*_{m-1})=\int_{\boldsymbol{\psi}_m} l(\tilde{G}_{T,m,\boldsymbol{\psi}_m}(\mathbf{d}^*_{T_{m-1}},\boldsymbol{\psi}_m))p_{\boldsymbol{\psi}_{m|m-1}}(\boldsymbol{\psi}_m|\boldsymbol{\psi}^*_{m-1})\mathrm{d}\boldsymbol{\psi}_m$$

with $\tilde{G}_{T,m,\boldsymbol{\psi}_{m-1},l}(\mathbf{d}^*_{T_{m-1}},\boldsymbol{\psi}^*_{m-1})$ returned as the output of ExpectationUnderUncertainty.Stage.m.G.

Entering ATR.fun to describe a risk neutral attitude (i.e. RN.Att from Appendix G.4.2) would mean ExpectationUnderUncertainty.Stage.m.G calculates

$$\tilde{G}_{T,m,\boldsymbol{\psi}_{m-1}}(\mathbf{d}^*_{T_{m-1}},\boldsymbol{\psi}^*_{m-1})=\int_{\boldsymbol{\psi}_m} \tilde{G}_{T,m,\boldsymbol{\psi}_m}(\mathbf{d}^*_{T_{m-1}},\boldsymbol{\psi}_m)p_{\boldsymbol{\psi}_{m|m-1}}(\boldsymbol{\psi}_m|\boldsymbol{\psi}^*_{m-1})\mathrm{d}\boldsymbol{\psi}_m$$

as is required for the methodology of Section 9.1.2. However, the ability to use an attitude to risk in the function ExpectationUnderUncertainty.Stage.m.G is retained for generality.

In ExpectationUnderUncertainty.Stage.m.G lower and upper bounds (denoted Psi.Low.B.Bounds and Psi.Up.B.Bounds respectively in the R code) for the scenario that will be observed in stage m, $\boldsymbol{\psi}_m$, for the given input scenario, $\boldsymbol{\psi}_{m-1}$, are set at $\boldsymbol{\psi}_{m-1} - 0.05$ and $\boldsymbol{\psi}_{m-1} + 0.05$ respectively, which is consistent with the beliefs detailed in Section 9.2.3. However, this can be changed as required for a more general problem.

G.5.3 Estimating Optimal Stage 3 Total Reinforcement Decisions for a Sample of Stage 2 Total Reinforcements and Stage 3 Scenarios

As part of the methodology detailed in Section 9.1.2, an emulator model, $\tilde{G}_{T,3,\boldsymbol{\psi}_3}(\mathbf{d}_{T_2}, \boldsymbol{\psi}_3)$, is fitted to model how expected total costs in stage 3 vary as a function of total reinforcement in stage 2, $\mathbf{d}_{T_2}$, and stage 3 scenario, $\boldsymbol{\psi}_3$, only.

In order to fit $\tilde{G}_{T,3,\boldsymbol{\psi}_3}(\mathbf{d}_{T_2}, \boldsymbol{\psi}_3)$, optimal stage 3 decisions are estimated for a sample of N_{θ_3} stage 2 total reinforcements (with the ith sampled total stage 2 reinforcement denoted as $\mathbf{d}_{T_2,\theta_{i,3}}$) and stage 3 scenarios (with the ith sampled stage 3 scenario denoted as $\boldsymbol{\psi}_{3,\theta_{i,3}}$). The resulting estimates of expected total costs in stage 3 of such a decision, $\tilde{F}_{T,3,\theta_{i,3}}$, can then be used as a set of training data (alongside $\mathbf{d}_{T_2,\theta_{i,3}}$ and $\boldsymbol{\psi}_{3,\theta_{i,3}}$) to fit $\tilde{G}_{T,3,\boldsymbol{\psi}_3}(\mathbf{d}_{T_2}, \boldsymbol{\psi}_3)$.

This subsection will detail the R code for estimating the optimal stage 3 decision (stated as the total reinforcement made after the third decision) for a given stage 2 total reinforcement and stage 3 scenario, and subsequently detail the R code for how these estimates are used to fit $\tilde{G}_{T,3,\boldsymbol{\psi}_3}(\mathbf{d}_{T_2}, \boldsymbol{\psi}_3)$, which models how expected total costs in stage 3 vary as a function of total reinforcement after the second decision and the stage 3 scenario only.

Input Variable	Description
in.Stage3.Em	$\tilde{f}_{c,3}(\mathbf{v}_3, \mathbf{d}_{T_3})$, i.e. the fitted emulator model used to estimate mean constraint costs in stage 3 for given values of variables containing uncertainty, $\mathbf{v}_3$, and stage 3 total reinforcement decision variables, $\mathbf{d}_{T_3}$
in.sam.r1	$d_{T_2,\theta_{i,3},1}$, i.e. a sampled value of total B6 reinforcement magnitude after the second decision
in.sam.r2	$d_{T_2,\theta_{i,3},2}$, i.e. a sampled value of total B7a reinforcement magnitude after the second decision
in.sam.psi3	$\boldsymbol{\psi}_{3,\theta_{i,3}}$, i.e. a sampled stage 3 scenario

Table G.13: Table giving details of the inputs for Sampled.Stage3.Estimator, the function which estimates an optimal stage 3 total reinforcement decision for a given stage 2 total reinforcement and stage 3 scenario.

Function to Estimate an Optimal Stage 3 Total Reinforcement Decision for a Given Stage 2 Total Reinforcement and Stage 3 Scenario

The below R code defines a function, Sampled.Stage3.Estimator, which estimates an optimal stage 3 total reinforcement decision for given values of previous total reinforcement after stage 2, $\mathbf{d}_{T_2,\theta_{i,3}}$, and stage 3 scenario, $\boldsymbol{\psi}_{3,\theta_{i,3}}$. Details of the input to Sampled.Stage3.Estimator are given in Table G.13. Some annotations are given throughout, and a summary will be given after the code has been detailed.

```
Sampled.Stage3.Estimator<-function(in.Stage3.Em,in.sam.r1,in.sam.r2,
  in.sam.psi3){


  TTempSampledRvec1<-c(max(in.sam.r1,Min.Stage3.B6.Val),
    seq(max(round_any(in.sam.r1, 100, f = ceiling),Min.Stage3.B6.Val),
    Max.Stage3.B6.Val,by=100))
  #Create an initial vector of total B6 reinforcements after the
   stage 3 reinforcement to be considered
  #Each B6 reinforcement is at least as large as the input stage 2 B6
   reinforcement or the minimum total B6 reinforcement the emulator
   is fitted over (whichever is largest)
  #A sequence is then created to a precision of 100 MW to the maximum
   total B6 reinforcement the emulator is fitted over
```

```
  TTempSampledRvec2<-c(max(in.sam.r2,Min.Stage3.B7.Val),
    seq(max(round_any(in.sam.r2, 100, f = ceiling),Min.Stage3.B7.Val),
    Max.Stage3.B7.Val,by=100))
  #Similarly, a vector is created for total B7a reinforcements after the
   stage 3 reinforcement to be considered

  TempSampledRvec1<-unique(TTempSampledRvec1)
  TempSampledRvec2<-unique(TTempSampledRvec2)
  #Extract the unique elements of each vector (as it is possible the first
   two elements of TTempSampledRvec1 are both Min.Stage3.B6.Val, and
   similarly for TTempSampledRvec2)

##############################################################################

  WorkingR1Mat<-matrix(nrow=length(TempSampledRvec1),
    ncol=length(TempSampledRvec2))
  WorkingR2Mat<-matrix(nrow=length(TempSampledRvec1),
    ncol=length(TempSampledRvec2))
  for(k in 1:length(TempSampledRvec1)){
    WorkingR1Mat[k,]<-c(rep(TempSampledRvec1[k],length(TempSampledRvec2)))
  }
  for(k in 1:length(TempSampledRvec2)){
    WorkingR2Mat[,k]<-c(rep(TempSampledRvec2[k],length(TempSampledRvec1)))
  }

  SampledRvec1<-as.vector(WorkingR1Mat)
  SampledRvec2<-as.vector(WorkingR2Mat)

  #Create vectors which consider every combination of total B6 and B7a
   reinforcement after the third decision to the precision of 100 MW

##############################################################################

  Temp.R.Length<-length(SampledRvec1)
```

```
#Note the number of decisions initially considered

sampled.psi3<-in.sam.psi3
sampled.Stage3.lowers<-c(Stage3.v.lowers.ND,sampled.psi3-0.05)
sampled.Stage3.uppers<-c(Stage3.v.uppers.ND,sampled.psi3+0.05)
#Create vectors of lower and upper bounds for the variables
 containing uncertainty
#The first element details bounds for nuclear availability probability
#The second element details bounds for CCGT availability probability
#The third element details bounds for stage 3 peak demand magnification

Temp.Expected.Costs.Part1<-c(rep(0,Temp.R.Length))
#A vector to store estimates of expected mean constraint costs in stage 3
Temp.Expected.Costs.Part2<-c(rep(0,Temp.R.Length))
#A vector to store calculations of reinforcement costs in stage 3

for(j in 1:(Temp.R.Length)){

  Temp.Expected.Costs.Part1[j]<-ExpectationUnderUncertainty.Psi.m(
    in.Stage3.Em,sampled.Stage3.lowers,sampled.Stage3.uppers,
    c(SampledRvec1[j],SampledRvec2[j]),Gen.U.Prior.Psi.m,RN.Att,
    sampled.psi3)
  #The estimate of expected mean constraint costs in stage 3 of the
   jth stage 3 total reinforcement decision for the sampled
   stage 3 scenario

  Temp.Expected.Costs.Part2[j]<-(SampledRvec1[j]+SampledRvec2[j]-
  in.sam.r1-in.sam.r2)*100*AssumedCTR*DiscountFactor^Stage3RStart
  #The reinforcement costs in stage 3 of the jth stage 3 total
   reinforcement decision, given that the sampled stage 2 total
   reinforcement decision was previously made
}

Temp.Expected.Costs<-Temp.Expected.Costs.Part1+Temp.Expected.Costs.Part2
```

```
  #Create a vector of estimates of expected total costs (expected
   mean constraint costs plus reinforcement costs) for each of the
   stage 3 decisions given the sampled stage 2 decision and stage 3 scenario

##############################################################################

  TempOptEstimate<-optimal.estimator(Temp.Expected.Costs,SampledRvec1,
    SampledRvec2)
  #Use the estimates of expected stage 3 total costs to estimate an optimal
   stage 3 reinforcement decision to a precision of 100 MW, for the
   sampled stage 2 decision and stage 3 scenario

  New.TTempSampledRvec1<-seq(TempOptEstimate$rvec1.opt.est-200,
    TempOptEstimate$rvec1.opt.est+200,10)
  New.TTempSampledRvec2<-seq(TempOptEstimate$rvec2.opt.est-200,
    TempOptEstimate$rvec2.opt.est+200,10)
  #Create new vectors of total stage 3 B6 and B7a reinforcement to a
   precision of 10 MW around this estimated optimal

  for(j in 1:length(New.TTempSampledRvec1)){
    New.TTempSampledRvec1[j]<-max(New.TTempSampledRvec1[j],in.sam.r1)
  }
  for(j in 1:length(New.TTempSampledRvec2)){
    New.TTempSampledRvec2[j]<-max(New.TTempSampledRvec2[j],in.sam.r2)
  }
  #Ensure that each of the total reinforcements after stage 3 is at least
   as large as the reinforcement previously made in stage 2 (i.e. so that
   the increase in reinforcement in stage 3 is non-negative)

  New.TempSampledRvec1<-unique(New.TTempSampledRvec1)
  New.TempSampledRvec2<-unique(New.TTempSampledRvec2)
  #Extract the unique elements of each vector (as many may be in.sam.r1 or
   in.sam.r2 if the estimated optimal stage 3 decision is around the
   input stage 2 decision)
```

```
  New.WorkingR1Mat<-matrix(nrow=length(New.TempSampledRvec1),
    ncol=length(New.TempSampledRvec2))
  New.WorkingR2Mat<-matrix(nrow=length(New.TempSampledRvec1),
    ncol=length(New.TempSampledRvec2))
  for(k in 1:length(New.TempSampledRvec1)){
    New.WorkingR1Mat[k,]<-c(rep(New.TempSampledRvec1[k],
      length(New.TempSampledRvec2)))
  }
  for(k in 1:length(New.TempSampledRvec2)){
    New.WorkingR2Mat[,k]<-c(rep(New.TempSampledRvec2[k],
      length(New.TempSampledRvec1)))
  }

  New.SampledRvec1<-as.vector(New.WorkingR1Mat)
  New.SampledRvec2<-as.vector(New.WorkingR2Mat)
  #Create vectors which considers combinations of total B6 and B7a
   reinforcement after the third decision around the optimal decision
   to the precision of 10 MW

##########################################################################

  New.Temp.R.Length<-length(New.SampledRvec1)
  #Note the number of decisions considered using these more precise
   decision vectors

  New.Temp.Expected.Costs.Part1<-c(rep(0,New.Temp.R.Length))
  #A vector to store estimates of expected mean constraint costs in
   stage 3 when using the more precise decision vectors
  New.Temp.Expected.Costs.Part2<-c(rep(0,New.Temp.R.Length))
  #A vector to store calculations of reinforcement costs in stage 3 when
   using the more precise decision vectors

  for(j in 1:New.Temp.R.Length){
```

```
  New.Temp.Expected.Costs.Part1[j]<-ExpectationUnderUncertainty.Psi.m(
    in.Stage3.Em,sampled.Stage3.lowers,sampled.Stage3.uppers,
    c(New.SampledRvec1[j],New.SampledRvec2[j]),Gen.U.Prior.Psi.m,
    RN.Att,sampled.psi3)
  #The estimate of expected mean constraint costs in stage 3 of the
   jth decision for the sampled stage 3 scenario

  New.Temp.Expected.Costs.Part2[j]<-((New.SampledRvec1[j]+
    New.SampledRvec2[j]-in.sam.r1-in.sam.r2)*100*AssumedCTR*
    DiscountFactor^Stage3RStart)
  #The reinforcement costs in stage 3 of the jth decision, given that
   the sampled stage 2 reinforcement decision was previously made
}

New.Temp.Expected.Costs<-(New.Temp.Expected.Costs.Part1+
  New.Temp.Expected.Costs.Part2)
#Create a vector of estimates of expected total costs (expected mean
 constraint costs plus reinforcement costs) for each of the precise
 stage 3 decisions given the sampled stage 2 decision
 and stage 3 scenario

Sampled.Optimal<-optimal.estimator(New.Temp.Expected.Costs,
  New.SampledRvec1,New.SampledRvec2)
#Use the estimates of expected stage 3 total costs to estimate an
 optimal stage 3 reinforcement decision to a precision of 10 MW,
 for the sampled stage 2 decision and stage 3 scenario

Sampled.Optimal2<-c(Sampled.Optimal$rvec1.opt.est,
Sampled.Optimal$rvec2.opt.est)
#Note the estimated optimal reinforcement decision

Sampled.Optimal.Cost<-Sampled.Optimal$cost.opt.est
#Note the estimate of expected total costs in stage 3
```

```
   of such a decision


  out.list<-list("Sampled.Optimal2"=Sampled.Optimal2,
    "Sampled.Optimal.Cost"=Sampled.Optimal.Cost)
  #Return the estimate of optimal stage 3 total reinforcement decision
   and the resulting estimate of expected total costs in stage 3

}
```

The above code starts by defining initial vectors of stage 3 total reinforcement decisions to consider. These vectors are formed such that each total stage 3 reinforcement decision considered is at least as large as the total reinforcement previously made after the second decision (i.e. such that a non-negative increase to reinforcement is made in the third stage). As in Appendix G.4.3, initial vectors of B6 and B7a reinforcement (SampledRvec1 and SampledRvec2 respectively) are created to consider every combination of B6 and B7a reinforcement to a precision of 100 MW.

For each of these stage 3 total reinforcements, estimates of expected total costs in stage 3 for the given stage 2 total reinforcement, $\mathbf{d}_{T_2,\theta_{i,3}}$, and stage 3 scenario, $\boldsymbol{\psi}_{3,\theta_{i,3}}$, are then acquired. Estimates of expected mean constraint costs in stage 3 are stored in the vector Temp.Expected.Costs.Part1, such that jth element of Temp.Expected.Costs.Part1 is

$$\tilde{F}_{c,3}(\mathbf{d}_{T_3,j}|\mathbf{d}_{T_2,\theta_{i,3}},\boldsymbol{\psi}_{3,\theta_{i,3}}) = \int_{\mathbf{v}_3} \tilde{f}_{c,3}(\mathbf{v}_3,\mathbf{d}_{T_3,j}) \times p(\mathbf{v}_3|\boldsymbol{\psi}_{3,\theta_{i,3}})\mathrm{d}\mathbf{v}_3 \tag{G.5.4}$$

where $\mathbf{d}_{T_3,j}$ represents the stage 3 total reinforcement decision defined by the jth elements of SampledRvec1 and SampledRvec2.

The reinforcement costs in stage 3 are stored in the vector Temp.Expected.Costs.Part2, such that the jth element of Temp.Expected.Costs.Part2 is $f_{\rho,3}(\mathbf{d}_{T_3,j}|\mathbf{d}_{T_2,\theta_{i,3}},\boldsymbol{\psi}_{3,\theta_{i,3}})$.

Estimates of expected total costs in stage 3 for each decision are then stored in the vector Temp.Expected.Costs, such that the jth element of Temp.Expected.Costs is

$$\tilde{F}_{T,3}(\mathbf{d}_{T_3,j}|\mathbf{d}_{T_2,\theta_{i,3}},\boldsymbol{\psi}_{3,\theta_{i,3}}) = \tilde{F}_{c,3}(\mathbf{d}_{T_3,j}|\mathbf{d}_{T_2,\theta_{i,3}},\boldsymbol{\psi}_{3,\theta_{i,3}}) + f_{\rho,3}(\mathbf{d}_{T_3,j}|\mathbf{d}_{T_2,\theta_{i,3}},\boldsymbol{\psi}_{3,\theta_{i,3}}) \tag{G.5.5}$$

An initial estimate of optimal stage 3 total reinforcement is then acquired as the stage 3 total reinforcement decision (value of $\mathbf{d}_{T_3,j}$ detailed by SampledRvec1 and Sample-

dRvec2) which minimises the estimate of expected total costs in stage 3 ($\tilde{F}_{T,3}(\mathbf{d}_{T_3,j}|\mathbf{d}_{2,\theta_{i,3}}, \boldsymbol{\psi}_{3,\theta_{i,3}})$ detailed in Temp.Expected.Costs). The function optimal.estimator which is used to calculate this initial estimate of optimal decision was previously defined in Appendix G.4.3.

An iterative procedure is then carried out, as detailed in Appendix G.4.3, to increase the precision of the estimate of optimal stage 3 reinforcement decision to the nearest 10 MW.

Finally, the estimate of optimal stage 3 total reinforcement, $\mathbf{d}_{3|\theta_{i,3}}$ denoted by Sampled.Optimal2, is returned, as well as the resulting estimate of expected total costs in stage 3,

$$\tilde{F}_{T,3,\theta_{i,3}} = \tilde{F}_{T,3}(\mathbf{d}_{3|\theta_{i,3}}|\mathbf{d}_{T_2,\theta_{i,3}}, \boldsymbol{\psi}_{3,\theta_{i,3}}) \tag{G.5.6}$$

denoted by Sampled.Optimal.Cost.

It is again noted that parallel computing can be used, where several jobs are submitted to be completed on separate computers in parallel, each of which estimates optimal stage 3 decisions for a small number of the sampled stage 2 total reinforcements and stage 3 scenarios.

Estimating Optimal Stage 3 Total Reinforcement Decisions for a Sample of Stage 2 Total Reinforcements and Stage 3 Scenarios

Input Variable	Description
in.Stage3.Em	$\tilde{f}_{c,3}(\mathbf{v}_3, \mathbf{d}_{T_3})$, i.e. the fitted emulator model used to estimate mean constraint costs in stage 3 for given values of variables containing uncertainty, $\mathbf{v}_3$, and stage 3 total reinforcement decision variables, $\mathbf{d}_{T_3}$
in.sam.dec.mat	A matrix of N_{θ_3} rows and 2 columns, such that the ith row details the ith sampled stage 2 total reinforcement, $\mathbf{d}_{T_2,\theta_{i,3}}$
in.sam.psi3s	A vector of length N_{θ_3}, such that the ith entry details the ith sampled stage 3 scenario, $\boldsymbol{\psi}_{3,\theta_{i,3}}$

Table G.14: Table giving details of the inputs for Multi.Stage3.Estimator, the function which estimates optimal stage 3 total reinforcement decisions for a given set of stage 2 total reinforcement decisions and stage 3 scenarios.

Below details the R code for Multi.Stage3.Estimator, which is a function which estimates an optimal stage 3 total reinforcement decision for a set of sampled stage 3 scenarios and stage 2 total reinforcement decisions. Details of the input to Multi.Stage3.Estimator are given in Table G.14. The code contains some annotations, but it is straightforward, using the function Sampled.Stage3.Estimator, defined in the previous sub-subsection, to estimate optimal stage 3 total reinforcement decisions for each sampled stage 2 total reinforcement and stage 3 scenario in turn.

```
Multi.Stage3.Estimator<-function(in.Stage3.Em,in.sam.dec.mat,in.sam.psi3s){

  in.sample.size<-length(in.sam.psi3s)
  #Note the number of sampled stage 3 scenarios given as input
  out.dec.mat<-matrix(nrow=in.sample.size,ncol=2)
  #Create a matrix to store estimates of optimal stage 3 total
   reinforcement decisions
  out.dec.cost<-c(rep(0,in.sample.size))
  #Create a vector to store the resulting estimates of expected total
   costs in stage 3

  for(i in 1:in.sample.size){
    Temp.r1<-in.sam.dec.mat[i,1]
    Temp.r2<-in.sam.dec.mat[i,2]
    Temp.psi<-in.sam.psi3s[i]
    Temp.Est<-Sampled.Stage3.Estimator(in.Stage3.Em,Temp.r1,Temp.r2,Temp.psi)
    out.dec.mat[i,]<-Temp.Est$Sampled.Optimal2
    out.dec.cost[i]<-Temp.Est$Sampled.Optimal.Cost
  }
  #The above creates a loop to estimate an optimal stage 3 decision, using
  the function Sampled.Stage3.Estimator defined in the previous
  sub-subsection, for each stage 2 total reinforcement and stage 3
  scenario given as input

  out.list<-list("out.dec.mat"=out.dec.mat,"out.dec.cost"=out.dec.cost)
  return(out.list)
```

```
  #The estimates of optimal stage 3 total reinforcement decision,
   and resulting estimates of expected total costs in stage 3,
   are returned as output
}
```

An R code to illustrate an application of Multi.Stage3.Estimator is given below:

```
Stage3.G.Lowers<-c(Psi.3.lower,Min.Stage2.B6.Val,Min.Stage2.B7.Val)
Stage3.G.Uppers<-c(Psi.3.upper,Max.Stage2.B6.Val,Max.Stage2.B7.Val)
#Create vectors of lower and upper bounds for psi_3, total B6 reinforcement
 after stage 2 and total B7a reinforcement after stage 2

Sample.For.Stage3.G.em<-LHC.Sample.Function(Stage3.G.Em.Sam.Size,
  Stage3.G.Lowers,Stage3.G.Uppers)
#Take a sample of stage 3 scenarios and stage 2 total
 reinforcements based on these bounds

Sample.For.Stage3.G.em.decs<-Sample.For.Stage3.G.em[,c(2,3)]
Sample.For.Stage3.G.em.psis<-as.vector(Sample.For.Stage3.G.em[,1])
#Separate the sample into stage 2 total reinforcements and stage 3 scenarios
#Sample.For.Stage3.G.em.decs denotes the stage 2 total reinforcements
#Sample.For.Stage3.G.em.psis denotes the stage 3 scenarios

Sample.Stage3.G.Opt.Est.List<-Multi.Stage3.Estimator(Stage3.C.Em.Wave1,
  Sample.For.Stage3.G.em.decs,Sample.For.Stage3.G.em.psis)
#Use Multi.Stage3.Estimator to estimate optimal stage 3 total reinforcement
 for each of the samples

Sample.Stage3.G.Opt.Est.decs<-Sample.Stage3.G.Opt.Est.List$out.dec.mat
Sample.Stage3.G.Opt.Est.costs<-Sample.Stage3.G.Opt.Est.List$out.dec.cost
#Record the estimated optimal stage 3 total reinforcement decisions and
 the resulting estimates of expected total stage 3 costs
```

```
Stage3.G.Em.Wave1.List<-Em.FitterStage3.G(Sample.For.Stage3.G.em.psis,
  Sample.For.Stage3.G.em.decs,Sample.Stage3.G.Opt.Est.costs)
#Use the estimates of expected total stage 3 costs to fit an emulator model
 for how estimates of expected total stage 3 costs vary as a function of
 total stage 2 reinforcement decisions and stage 3 scenario

Stage3.G.Em.Wave1<-Stage3.G.Em.Wave1.List$Fitted.Emulator
Stage3.G.Em.Wave1.PolyBeta<-Stage3.G.Em.Wave1.List$lm.part.beta
Stage3.G.Em.Wave1.PolyBetaCov<-Stage3.G.Em.Wave1.List$lm.part.betacov
#Store the elements of Stage3.G.Em.Wave1.List separately for convenience
```

In the above code Em.FitterStage3.G represents the variation of Em.Fitter, defined in Appendix G.4.1, which is a function which is used to fit the emulator model $\tilde{G}_{T,3,\boldsymbol{\psi}_3}(\mathbf{d}_{T_2}, \boldsymbol{\psi}_3)$ to the set of N_{θ_3} samples of stage 2 total reinforcement decisions, $\mathbf{d}_{T_2,\theta_{i,3}}$ (Sample.For.Stage3.G.em.decs in the above code), stage 3 scenarios, $\boldsymbol{\psi}_{3,\theta_{i,3}}$ (Sample.For.Stage3.G.em.psis in the above code), and the resulting estimates of expected total costs in stage 3, $\tilde{F}_{T,3,\theta_{i,3}}$ (Sample.Stage3.G.Opt.Est.costs in the above code).

G.5.4 Estimating Optimal Stage 2 Total Reinforcement Decisions for a Sample of Stage 1 Reinforcements and Stage 2 Scenarios

As part of the methodology detailed in Section 9.1.2, an emulator model, $\tilde{G}_{T,2,\boldsymbol{\psi}_2}(\mathbf{d}_1, \boldsymbol{\psi}_2)$, is fitted to model how expected total costs in stage 2 onwards vary as a function of stage 1 reinforcement, $\mathbf{d}_1$, and stage 2 scenario, $\boldsymbol{\psi}_2$, only.

In order to fit $\tilde{G}_{T,2,\boldsymbol{\psi}_2}(\mathbf{d}_1, \boldsymbol{\psi}_2)$, optimal stage 2 decisions are estimated for a sample of N_{θ_2} stage 1 reinforcements (with the ith sampled stage 1 reinforcement denoted as $\mathbf{d}_{1,\theta_{i,2}}$) and stage 2 scenarios (with the ith sampled stage 2 scenario denoted as $\boldsymbol{\psi}_{2,\theta_{i,2}}$). The resulting estimates of expected total costs in stage 2 onwards of such a decision, $\tilde{F}_{T,2,\theta_{i,2}}$, can then be used as a set of training data (alongside $\mathbf{d}_{1,\theta_{i,2}}$ and $\boldsymbol{\psi}_{2,\theta_{i,2}}$) to fit $\tilde{G}_{T,2,\boldsymbol{\psi}_2}(\mathbf{d}_1, \boldsymbol{\psi}_2)$.

This subsection will detail the R code for estimating the optimal stage 2 decision for a given stage 1 reinforcement and stage 2 scenario, and subsequently detail the R code for how these estimates are used to fit $\tilde{G}_{T,2,\boldsymbol{\psi}_2}(\mathbf{d}_1, \boldsymbol{\psi}_2)$, which models how expected total costs in stage 2 onwards vary as a function of first reinforcement decision and the stage 2 scenario only.

Function to Estimate an Optimal Stage 2 Total Reinforcement Decision for a Given Stage 1 Reinforcement and Stage 2 Scenario

Input Variable	Description
in.Stage2.Em	$\tilde{f}_{c,2}(\mathbf{v}_2, \mathbf{d}_{T_2})$, i.e. the fitted emulator model used to estimate mean constraint costs in stage 2 for given values of variables containing uncertainty, $\mathbf{v}_2$, and stage 2 total reinforcement decision variables, $\mathbf{d}_{T_2}$
in.Stage3.G.Em	$\tilde{G}_{T,3,\boldsymbol{\psi}_3}(\mathbf{d}_{T_2}, \boldsymbol{\psi}_3)$, i.e. the fitted emulator model used to estimate expected total costs in stage 3 as a function of total reinforcement in stage 2, $\mathbf{d}_{T_2}$, and stage 3 scenario, $\boldsymbol{\psi}_3$
in.sam.r1	$d_{1,\theta_{i,2},1}$, i.e. the sampled stage 1 B6 reinforcement magnitude
in.sam.r2	$d_{1,\theta_{i,2},2}$, i.e. the sampled stage 1 B7a reinforcement magnitude
in.sam.psi3	$\boldsymbol{\psi}_{2,\theta_{i,2}}$, i.e. the sampled stage 2 scenario

Table G.15: Table giving details of the inputs for Sampled.Stage2.Estimator, the function which estimates an optimal stage 2 total reinforcement decision for a given stage 1 reinforcement and stage 2 scenario.

The below R code defines a function, Sampled.Stage2.Estimator, which estimates an optimal stage 2 total reinforcement decision for given values of previous reinforcement in stage 1, $\mathbf{d}_{1,\theta_{i,2}}$, and stage 2 scenario, $\boldsymbol{\psi}_{2,\theta_{i,2}}$. Details of the input to Sampled.Stage2.Estimator are given in Table G.15. Some annotations are given throughout, and a summary will be given after the code has been detailed.

```
Sampled.Stage2.Estimator<-function(in.Stage2.Em,in.Stage3.G.Em,in.sam.r1,
  in.sam.r2,in.sam.psi2){

  TTempSampledRvec1<-c(max(in.sam.r1,Min.Stage2.B6.Val),
```

```
    seq(max(round_any(in.sam.r1, 100, f = ceiling),Min.Stage2.B6.Val),
    Max.Stage2.B6.Val,by=100))
  #Create an initial vector of total B6 reinforcements after stage 2
   to be considered
  #Each B6 reinforcement is at least as large as the input stage 1
   B6 reinforcement or the minimum total B6 reinforcement the emulator
   is fitted over (whichever is largest)
  #A sequence is then created to a precision of 100 MW to the maximum total
   B6 reinforcement the emulator is fitted over

  TTempSampledRvec2<-c(max(in.sam.r2,Min.Stage2.B7.Val),
  seq(max(round_any(in.sam.r2, 100, f = ceiling),Min.Stage2.B7.Val),
  Max.Stage2.B7.Val,by=100))
  #Similarly, a vector is created for total B7a reinforcements after
   stage 2 to be considered

  TempSampledRvec1<-unique(TTempSampledRvec1)
  TempSampledRvec2<-unique(TTempSampledRvec2)
  #Extract the unique elements of each vector (as it is possible the first
   two elements of TTempSampledRvec1 are both Min.Stage2.B6.Val,
   and similarly for TTempSampledRvec2)
##########################################################################

  WorkingR1Mat<-matrix(nrow=length(TempSampledRvec1),
    ncol=length(TempSampledRvec2))
  WorkingR2Mat<-matrix(nrow=length(TempSampledRvec1),
    ncol=length(TempSampledRvec2))
  for(k in 1:length(TempSampledRvec1)){
    WorkingR1Mat[k,]<-c(rep(TempSampledRvec1[k],length(TempSampledRvec2)))
  }
  for(k in 1:length(TempSampledRvec2)){
    WorkingR2Mat[,k]<-c(rep(TempSampledRvec2[k],length(TempSampledRvec1)))
  }
```

```
  SampledRvec1<-as.vector(WorkingR1Mat)
  SampledRvec2<-as.vector(WorkingR2Mat)

  #Create vectors which consider every combination of total B6 and B7a
   reinforcement after the second decision to the precision of 100 MW

##########################################################################

  Temp.R.Length<-length(SampledRvec1)
  #Note the number of decisions initially considered

  sampled.psi2<-in.sam.psi2
  sampled.Stage2.lowers<-c(Stage2.v.lowers.ND,sampled.psi2-0.05)
  sampled.Stage2.uppers<-c(Stage2.v.uppers.ND,sampled.psi2+0.05)
  #Create vectors of lower and upper bounds for the variables
   containing uncertainty
  #The first element details bounds for nuclear availability probability
  #The second element details bounds for CCGT availability probability
  #The third element details bounds for stage 2 peak demand magnification

  Temp.Expected.Costs.Part1<-c(rep(0,Temp.R.Length))
  #A vector to store estimates of expected mean constraint costs in stage 2
  Temp.Expected.Costs.Part2<-c(rep(0,Temp.R.Length))
  #A vector to store calculations of reinforcement costs in stage 2
  Temp.Expected.Costs.Part3<-c(rep(0,Temp.R.Length))
  #A vector to store estimates of expected total costs in stage 3

  for(j in 1:(Temp.R.Length)){

    Temp.Expected.Costs.Part1[j]<-ExpectationUnderUncertainty.Psi.m(
      in.Stage2.Em,sampled.Stage2.lowers,sampled.Stage2.uppers,
      c(SampledRvec1[j],SampledRvec2[j]),Gen.U.Prior.Psi.m,
      RN.Att,sampled.psi2)
    #The estimate of expected mean constraint costs in stage 2 for the
```

```
     jth total stage 2 reinforcement decision for the sampled
     stage 2 scenario

    Temp.Expected.Costs.Part2[j]<-((SampledRvec1[j]+SampledRvec2[j]-
      in.sam.r1-in.sam.r2)*100*AssumedCTR*DiscountFactor^Stage2RStart)
    #The reinforcement costs in stage 2 of the jth total stage 2
     reinforcement decision, given that the sampled stage 1 reinforcement
     decision was previously made

    Temp.Expected.Costs.Part3[j]<-ExpectationUnderUncertainty.Stage.m.G(
      in.Stage3.G.Em,c(SampledRvec1[j],SampledRvec2[j]),Gen.U.Prior.Psi.m,
      RN.Att,sampled.psi2)
    #The estimate of expected total costs in stage 3 of the jth total
     stage 2 reinforcement decision for the sampled stage 2 scenario

  }

  Temp.Expected.Costs<-(Temp.Expected.Costs.Part1+
    Temp.Expected.Costs.Part2+Temp.Expected.Costs.Part3)
  #Create a vector for the estimates of expected total costs in stage 2
   onwards  (expected mean constraint costs plus reinforcement costs in
   stage 2 plus expected total costs in stage 3) for each of the stage 2
   total reinforcement decisions for the sampled stage 1 reinforcement
   decision and stage 2 scenario

##########################################################################

  TempOptEstimate<-optimal.estimator(Temp.Expected.Costs,SampledRvec1,
    SampledRvec2)
  #Use the estimates of expected total costs in stage 2 onwards to estimate
    an optimal stage 2 total reinforcement decision to a precision of 100 MW,
    for the sampled stage 1 decision and stage 2 scenario

  New.TTempSampledRvec1<-seq(TempOptEstimate$rvec1.opt.est-200,
```

```
  TempOptEstimate$rvec1.opt.est+200,10)
New.TTempSampledRvec2<-seq(TempOptEstimate$rvec2.opt.est-200,
  TempOptEstimate$rvec2.opt.est+200,10)
#Create new vectors of B6 and B7a reinforcement to a precision of 10 MW
 around this estimated optimal

for(j in 1:length(New.TTempSampledRvec1)){
  New.TTempSampledRvec1[j]<-max(New.TTempSampledRvec1[j],in.sam.r1)
}
for(j in 1:length(New.TTempSampledRvec2)){
  New.TTempSampledRvec2[j]<-max(New.TTempSampledRvec2[j],in.sam.r2)
}
#Ensure that each of the total reinforcements after stage 2 are at least
 as large as the reinforcement previously made in stage 1 (i.e. so that
 the increase in reinforcement in stage 2 is non-negative)

New.TempSampledRvec1<-unique(New.TTempSampledRvec1)
New.TempSampledRvec2<-unique(New.TTempSampledRvec2)
#Extract the unique elements of each vector (as many may be in.sam.r1 or
 in.sam.r2 if the estimated optimal stage 2 decision is around the
 input stage 1 decision)

New.WorkingR1Mat<-matrix(nrow=length(New.TempSampledRvec1),
  ncol=length(New.TempSampledRvec2))
New.WorkingR2Mat<-matrix(nrow=length(New.TempSampledRvec1),
  ncol=length(New.TempSampledRvec2))
for(k in 1:length(New.TempSampledRvec1)){
  New.WorkingR1Mat[k,]<-c(rep(New.TempSampledRvec1[k],
    length(New.TempSampledRvec2)))
}
for(k in 1:length(New.TempSampledRvec2)){
  New.WorkingR2Mat[,k]<-c(rep(New.TempSampledRvec2[k],
    length(New.TempSampledRvec1)))
}
```

```
  New.SampledRvec1<-as.vector(New.WorkingR1Mat)
  New.SampledRvec2<-as.vector(New.WorkingR2Mat)
  #Create vectors which considers combinations of total B6 and B7a
   reinforcement after the second decision to the precision of 10 MW
   around the estimate of the optimal stage 2 total reinforcement decision

##############################################################################

  New.Temp.R.Length<-length(New.SampledRvec1)
  #Note the number of decisions considered using these more
   precise decision vectors

  New.Temp.Expected.Costs.Part1<-c(rep(0,New.Temp.R.Length))
  #A vector to store estimates of expected mean constraint costs in stage 2
   using the more precise decision vectors
  New.Temp.Expected.Costs.Part2<-c(rep(0,New.Temp.R.Length))
  #A vector to store calculations of reinforcement costs in stage 2 using
   the more precise decision vectors
  New.Temp.Expected.Costs.Part3<-c(rep(0,New.Temp.R.Length))
  #A vector to store estimates of expected total costs in stage 3 using
   the more precise decision vectors

  for(j in 1:New.Temp.R.Length){

    New.Temp.Expected.Costs.Part1[j]<-ExpectationUnderUncertainty.Psi.m(
      in.Stage2.Em,sampled.Stage2.lowers,sampled.Stage2.uppers,
      c(New.SampledRvec1[j],New.SampledRvec2[j]),Gen.U.Prior.Psi.m,
      RN.Att,sampled.psi2)
    #The estimate of expected mean constraint costs in stage 2 for the
     jth stage 2 total reinforcement decision for the sampled
     stage 2 scenario

    New.Temp.Expected.Costs.Part2[j]<-((New.SampledRvec1[j]+
```

```
    New.SampledRvec2[j]-in.sam.r1-in.sam.r2)*100*AssumedCTR*
    DiscountFactor^Stage2RStart)
  #The reinforcement costs in stage 2 of the jth stage 2 total
   reinforcement decision, given that the sampled stage 1
   reinforcement decision was previously made

  New.Temp.Expected.Costs.Part3[j]<-(
    ExpectationUnderUncertainty.Stage.m.G(in.Stage3.G.Em,
    c(New.SampledRvec1[j],New.SampledRvec2[j]),Gen.U.Prior.Psi.m,
    RN.Att,sampled.psi2))
  #The estimate of expected total costs in stage 3 of the jth stage 2
   total reinforcement decision for the sampled stage 2 scenario

}

New.Temp.Expected.Costs<-(New.Temp.Expected.Costs.Part1+
  New.Temp.Expected.Costs.Part2+New.Temp.Expected.Costs.Part3)
#Create a vector for the estimates of expected total costs in
 stage 2 onwards (expected mean constraint costs plus reinforcement
 costs in stage 2 plus expected total costs in stage 3)
 for each of the precise stage 2 total reinforcement decisions for
 the sampled stage 1 decisions and stage 2 scenario

Sampled.Optimal<-optimal.estimator(New.Temp.Expected.Costs,
  New.SampledRvec1,New.SampledRvec2)
#Use the estimates of expected total costs in stage 2 onwards to estimate
 an optimal stage 2 reinforcement decision to a precision of 10 MW,
 for the sampled stage 1 decision and stage 2 scenario

Sampled.Optimal2<-c(Sampled.Optimal$rvec1.opt.est,
  Sampled.Optimal$rvec2.opt.est)
#Note the estimated optimal stage 2 total reinforcement decision
 Sampled.Optimal.Cost<-Sampled.Optimal$cost.opt.est
#Note the estimate of expected total costs in stage 2 onwards of
```

```
   such a decision


  out.list<-list("Sampled.Optimal2"=Sampled.Optimal2,
    "Sampled.Optimal.Cost"=Sampled.Optimal.Cost)
  #Return the estimate of optimal stage 2 total reinforcement decision and
   the resulting estimate of expected total costs in stage 2 onwards

}
```

The above code starts by defining initial vectors of stage 2 total reinforcement decisions to consider. These vectors are formed such that each total stage 2 reinforcement decision considered is at least as large as the reinforcement previously made in the first stage (i.e. such that a non-negative increase to reinforcement is made in the second stage). As in Section G.4.3, initial vectors of B6 and B7a reinforcement (SampledRvec1 and SampledRvec2 respectively) are created to consider every combination of stage 2 total B6 and B7a reinforcement to a precision of 100 MW.

For each of these stage 2 total reinforcements, estimates of expected total costs in stage 2 onwards for the given stage 1 reinforcement, $\mathbf{d}_{1,\theta_{i,2}}$, and stage 2 scenario, $\boldsymbol{\psi}_{2,\theta_{i,2}}$, are then acquired. Estimates of expected mean constraint costs in stage 2 are stored in the vector Temp.Expected.Costs.Part1, such that jth element of Temp.Expected.Costs.Part1 is

$$\tilde{F}_{c,2}(\mathbf{d}_{T_2,j}|\mathbf{d}_{1,\theta_{i,2}},\boldsymbol{\psi}_{2,\theta_{i,2}}) = \int_{\mathbf{v}_2} \tilde{f}_{c,2}(\mathbf{v}_2,\mathbf{d}_{T_2,j}) \times p(\mathbf{v}_2|\boldsymbol{\psi}_{2,\theta_{i,2}})\mathrm{d}\mathbf{v}_2 \tag{G.5.7}$$

where $\mathbf{d}_{T_2,j}$ represents the stage 2 total reinforcement decision defined by the jth elements of SampledRvec1 and SampledRvec2.

The reinforcement costs in stage 2 are stored in the vector Temp.Expected.Costs.Part2, such that the jth element of Temp.Expected.Costs.Part2 is $f_{\rho,2}(\mathbf{d}_{T_2,j}|\mathbf{d}_{1,\theta_{i,2}},\boldsymbol{\psi}_{2,\theta_{i,2}})$.

Estimates of expected total costs in stage 3 are stored in the vector Temp.Expected.Costs.Part3, such that jth element of Temp.Expected.Costs.Part3 is

$$\tilde{G}_{T,3,\psi_2}(\mathbf{d}_{T_2,j},\boldsymbol{\psi}_{2,\theta_{i,2}}) = \int_{\boldsymbol{\psi}_3} \tilde{G}_{T,3,\boldsymbol{\psi}_3}(\mathbf{d}_{T_2,j},\boldsymbol{\psi}_3) \times p_{\boldsymbol{\psi}_{3|2}}(\boldsymbol{\psi}_3|\boldsymbol{\psi}_{2,\theta_{i,2}})\mathrm{d}\boldsymbol{\psi}_3 \tag{G.5.8}$$

Estimates of expected total costs in stage 2 onwards for each decision are then stored

in the vector Temp.Expected.Costs, such that the jth element of Temp.Expected.Costs is

$$\tilde{F}_{T,2}(\mathbf{d}_{T_2,j}|\mathbf{d}_{1,\theta_{i,2}},\boldsymbol{\psi}_{2,\theta_{i,2}}) = \tilde{F}_{c,2}(\mathbf{d}_{T_2,j}|\mathbf{d}_{1,\theta_{i,2}},\boldsymbol{\psi}_{2,\theta_{i,2}}) + f_{\rho,2}(\mathbf{d}_{T_2,j}|\mathbf{d}_{1,\theta_{i,2}},\boldsymbol{\psi}_{2,\theta_{i,2}}) + \tilde{G}_{T,3,\psi_2}(\mathbf{d}_{T_2,j},\boldsymbol{\psi}_{2,\theta_{i,2}}) \quad \text{(G.5.9)}$$

An initial estimate of optimal stage 2 total reinforcement is then acquired as the stage 2 total reinforcement decision (value of $\mathbf{d}_{T_2,j}$ detailed by SampledRvec1 and SampledRvec2) which minimises the estimate of expected total costs in stage 2 onwards ($\tilde{F}_{T,2}(\mathbf{d}_{T_2,j}|\mathbf{d}_{1,\theta_{i,2}},\boldsymbol{\psi}_{2,\theta_{i,2}})$ detailed in Temp.Expected.Costs). The function optimal.estimator, which is used to calculate this initial estimate of optimal decision, was previously defined in Appendix G.4.3.

An iterative procedure is then carried out, as detailed in Appendix G.4.3, to increase the precision of the estimate of optimal total stage 2 reinforcement decision to the nearest 10 MW.

Finally, the estimate of optimal stage 2 total reinforcement, $\mathbf{d}_{2|\theta_{i,2}}$ denoted by Sampled.Optimal2, is returned, as well as the resulting estimate of expected total costs in stage 2 onwards,

$$\tilde{F}_{T,2,\theta_{i,2}} = \tilde{F}_{T,2}(\mathbf{d}_{2|\theta_{i,2}}|\mathbf{d}_{1,\theta_{i,2}},\boldsymbol{\psi}_{2,\theta_{i,2}}) \quad \text{(G.5.10)}$$

denoted by Sampled.Optimal.Cost.

It is again noted that parallel computing can be used, to submit several jobs which each estimate optimal stage 3 decisions for a small number of the sampled stage 2 total reinforcements and stage 3 scenarios.

Estimating Optimal Stage 2 Total Reinforcement Decisions for a Sample of Stage 1 Reinforcements and Stage 2 Scenarios

Below details the R code for Multi.Stage2.Estimator, which is a function which estimates an optimal stage 2 total reinforcement decision for a set of sampled stage 2 scenarios and stage 1 reinforcement decisions. Details of the input to Multi.Stage2.Estimator are given in Table G.16. The code contains some annotations, but it is straightforward, using the function Sampled.Stage2.Estimator, defined in the

Input Variable	Description
in.Stage2.Em	$\tilde{f}_{c,2}(\mathbf{v}_2, \mathbf{d}_{T_2})$, i.e. the fitted emulator model used to estimate mean constraint costs in stage 2 for given values of variables containing uncertainty, $\mathbf{v}_2$, and stage 2 total reinforcement decision variables, $\mathbf{d}_{T_2}$
in.Stage3.G.Em	$\tilde{G}_{T,3,\boldsymbol{\psi}_3}(\mathbf{d}_{T_2}, \boldsymbol{\psi}_3)$, i.e. the fitted emulator model used to estimate expected total costs in stage 3 as a function of total reinforcement in stage 2, $\mathbf{d}_{T_2}$, and stage 3 scenario, $\boldsymbol{\psi}_3$
in.sam.dec.mat	A matrix of N_{θ_2} rows and 2 columns, such that the ith row details the ith sampled stage 1 reinforcement, $\mathbf{d}_{1,\theta_{i,2}}$
in.sam.psi2s	A vector of length N_{θ_2}, such that the ith entry details the ith sampled stage 2 scenario, $\boldsymbol{\psi}_{2,\theta_{i,2}}$

Table G.16: Table giving details of the inputs for Multi.Stage2.Estimator, the function which estimates optimal stage 2 total reinforcement decisions for a given set of stage 1 reinforcement decisions and stage 2 scenarios.

previous sub-subsection, to estimate optimal stage 2 total reinforcement decisions for each sampled stage 1 reinforcement and stage 2 scenario in turn.

```
Multi.Stage2.Estimator<-function(in.Stage2.Em,in.Stage3.G.Em,in.sam.dec.mat,
  in.sam.psi2s){

  in.sample.size<-length(in.sam.psi2s)
  #Note the number of sampled stage 2 scenarios given as input
  out.dec.mat<-matrix(nrow=in.sample.size,ncol=2)
  #Create a matrix to store estimates of optimal stage 2 total
   reinforcement decisions
  out.dec.cost<-c(rep(0,in.sample.size))
  #Create a vector to store the resulting estimates of expected total costs
   in stage 2 onwards

  for(i in 1:in.sample.size){
    Temp.r1<-in.sam.dec.mat[i,1]
    Temp.r2<-in.sam.dec.mat[i,2]
    Temp.psi<-in.sam.psi2s[i]
    Temp.Est<-Sampled.Stage2.Estimator(in.Stage2.Em,in.Stage3.G.Em,Temp.r1,
      Temp.r2,Temp.psi)
```

```
    out.dec.mat[i,]<-Temp.Est$Sampled.Optimal2
    out.dec.cost[i]<-Temp.Est$Sampled.Optimal.Cost
  }
  #The above creates a loop to estimate an optimal stage 2 total reinforcement
   decision, using the function Sampled.Stage2.Estimator defined
   in the previous sub-subsection, for each stage 1 reinforcement and
   stage 2 scenario given as input

  out.list<-list("out.dec.mat"=out.dec.mat,"out.dec.cost"=out.dec.cost)
  return(out.list)
  #The estimates of optimal stage 2 total reinforcement decision, and
  resulting estimates of expected total costs in stage 2 onwards,
  are returned as output
}
```

An R code to illustrate an application of Multi.Stage2.Estimator is given below

```
Stage2.G.Lowers<-c(Psi.2.lower,Min.Stage1.B6.Val,Min.Stage1.B7.Val)
Stage2.G.Uppers<-c(Psi.2.upper,Max.Stage1.B6.Val,Max.Stage1.B7.Val)
#Create vectors of lower and upper bounds for psi_2, stage 1 B6
  reinforcement magnitude and stage 1 B7a reinforcement magnitude

Sample.For.Stage2.G.em<-LHC.Sample.Function(Stage2.G.Em.Sam.Size,
  Stage2.G.Lowers,Stage2.G.Uppers)
#Take a sample of stage 2 scenarios and stage 1 reinforcement decisions
 based on these bounds

Sample.For.Stage2.G.em.decs<-Sample.For.Stage2.G.em[,c(2,3)]
Sample.For.Stage2.G.em.psis<-as.vector(Sample.For.Stage2.G.em[,1])
#Separate the sample into stage 1 reinforcements and stage 2 scenarios
#Sample.For.Stage2.G.em.decs denotes the sampled stage 1 reinforcements
#Sample.For.Stage2.G.em.psis denotes the sampled stage 2 scenarios

Sample.Stage2.G.Opt.Est.List<-Multi.Stage2.Estimator(Stage2.C.Em.Wave1,
```

```
  Stage3.G.Em.Wave1,Sample.For.Stage2.G.em.decs,
  Sample.For.Stage2.G.em.psis)
#Use Multi.Stage2.Estimator to estimate optimal stage 2 total reinforcement
 for each of the samples

Sample.Stage2.G.Opt.Est.decs<-Sample.Stage2.G.Opt.Est.List$out.dec.mat
Sample.Stage2.G.Opt.Est.costs<-Sample.Stage2.G.Opt.Est.List$out.dec.cost
#Record the estimated optimal stage 2 total reinforcement decisions and
 the resulting estimates of expected total costs in stage 2 onwards

Stage2.G.Em.Wave1.List<-Em.FitterStage2.G(Sample.For.Stage2.G.em.psis,
  Sample.For.Stage2.G.em.decs,Sample.Stage2.G.Opt.Est.costs)
#Use the estimates of expected total costs in stage 2 onwards to fit an
 emulator model for how estimates of expected total costs in stage 2
 onwards vary as a function of stage 1 decisions and stage 2 scenario

Stage2.G.Em.Wave1<-Stage2.G.Em.Wave1.List$Fitted.Emulator
Stage2.G.Em.Wave1.PolyBeta<-Stage2.G.Em.Wave1.List$lm.part.beta
Stage2.G.Em.Wave1.PolyBetaCov<-Stage2.G.Em.Wave1.List$lm.part.betacov
#Store the elements of Stage2.G.Em.Wave1.List separately for convenience
```

In the above code Em.FitterStage2.G represents the variation of Em.Fitter, defined in Appendix G.4.1, which is a function which is used to fit the emulator model $\tilde{G}_{T,2,\boldsymbol{\psi}_2}(\mathbf{d}_1, \boldsymbol{\psi}_2)$ to the set of N_{θ_2} samples of stage 1 reinforcement decisions, $\mathbf{d}_{1,\theta_{i,2}}$ (Sample.For.Stage2.G.em.decs in the above code), stage 2 scenarios, $\boldsymbol{\psi}_{2,\theta_{i,2}}$ (Sample.For.Stage2.G.em.psis in the above code), and the resulting estimates of expected total costs in stage 2 onwards, $\tilde{F}_{T,2,\theta_{i,2}}$ (Sample.Stage2.G.Opt.Est.costs in the above code).

G.5.5 Estimating Expected Total Costs Across All Stages as a Function of the First Stage Decision Only

Below details the R code for Expected.Total.Costs.In.Stage1.Onwards, which is a function which estimates expected total costs across all 3 stages for a given first stage

Input Variable	Description
in.Stage1.Em	$\tilde{f}_{c,1}(\mathbf{v}_1, \mathbf{d}_1)$, i.e. the fitted emulator model used to estimate mean constraint costs in stage 1 for given values of variables containing uncertainty, $\mathbf{v}_1$, and decision variables, $\mathbf{d}_1$
in.Stage2.G.Em	$\tilde{G}_{T,2,\boldsymbol{\psi}_2}(\mathbf{d}_1, \boldsymbol{\psi}_2)$, i.e. the fitted emulator model used to estimate expected total costs in stage 2 onwards as a function of reinforcement in stage 1, $\mathbf{d}_1$, and stage 2 scenario, $\boldsymbol{\psi}_2$
in.stage1.lowers	A vector detailing the lower bounds for the variables containing uncertainty in stage 1, such that the ith element of in.stage1.lowers is the lower bound for the ith variable containing uncertainty
in.stage1.uppers	A vector detailing the upper bounds for the variables containing uncertainty in stage 1, such that the ith element of in.stage1.uppers is the lower bound for the ith variable containing uncertainty
in.r1	$d^*_{1,1}$, i.e. a particular stage 1 B6 reinforcement magnitude
in.r2	$d^*_{1,2}$, i.e. a particular stage 1 B7a reinforcement magnitude
in.psi.1	$\boldsymbol{\psi}^*_1$, i.e. a particular stage 1 scenario

Table G.17: Table giving details of the inputs for Expected.Total.Costs.In.Stage1.Onwards, the function used to estimate expected total costs across all three stages as a function of the first stage decision and scenario only.

decision and scenario. Details of the input to Expected.Total.Costs.In.Stage1.Onwards are given in Table G.17. The code contains some annotations and a summary will be given after the code has been detailed.

```
Expected.Total.Costs.In.Stage1.Onwards<-function(in.Stage1.Em,in.Stage2.G.Em,
  in.stage1.lowers,in.stage1.uppers,in.r1,in.r2,in.psi.1){

  Temp.Expected.Costs.Part1<-ExpectationUnderUncertainty(in.Stage1.Em,
    in.stage1.lowers,in.stage1.uppers,c(in.r1,in.r2),Gen.U.Prior,RN.Att)
  #The estimate of expected mean constraint costs in stage 1 of the
   decision given as input (i.e. when making in.r1 B6 reinforcement and
   in.r2 B7a reinforcement in stage 1)
```

```
  Temp.Expected.Costs.Part2<-((in.r1+in.r2)*
    100*AssumedCTR*DiscountFactor^Stage1RStart)
  #The reinforcement costs in stage 1 of the decision given as input

  Temp.Expected.Costs.Part3<-ExpectationUnderUncertainty.Stage.m.G(
    in.Stage2.G.Em,c(in.r1,in.r2),Gen.U.Prior.Psi.m,RN.Att,in.psi.1)
  #The estimate of expected total costs in stage 2 onwards of the
   stage 1 decision given as input

  Total.Expected.Costs<-(Temp.Expected.Costs.Part1+
    Temp.Expected.Costs.Part2+Temp.Expected.Costs.Part3)
  #Estimate of expected total costs across all 3 stages

  return(Total.Expected.Costs)

}
```

Temp.Expected.Costs.Part1 represents the estimate of expected mean constraint costs in stage 1 for the given decision, i.e. Temp.Expected.Costs.Part1 represents

$$\tilde{F}_{c,1}(\mathbf{d}_1^*|\boldsymbol{\psi}_1^*) = \int_{\mathbf{v}_1} \tilde{f}_{c,1}(\mathbf{v}_1, \mathbf{d}_1^*) \times p(\mathbf{v}_1|\boldsymbol{\psi}_1^*) \mathrm{d}\mathbf{v}_1 \tag{G.5.11}$$

where $\mathbf{d}_1^*$ is the stage 1 decision defined by in.r1 (stage 1 B6 reinforcement magnitude) and in.r2 (stage 1 B7a reinforcement magnitude).

Temp.Expected.Costs.Part2 represents the reinforcement costs of the particular stage 1 decision, i.e. $f_{\rho,1}(\mathbf{d}_1^*|\boldsymbol{\psi}_1^*)$.

Temp.Expected.Costs.Part3 represents the estimate of expected total costs in stage 2 onwards of the particular stage 1 decision, i.e. Temp.Expected.Costs.Part3 represents

$$\tilde{G}_{T,2,\boldsymbol{\psi}_1}(\mathbf{d}_1^*, \boldsymbol{\psi}_1^*) = \int_{\boldsymbol{\psi}_2} \tilde{G}_{T,2,\boldsymbol{\psi}_2}(\mathbf{d}_1^*, \boldsymbol{\psi}_2) \times p_{\boldsymbol{\psi}_{2|1}}(\boldsymbol{\psi}_2|\boldsymbol{\psi}_1^*) \mathrm{d}\boldsymbol{\psi}_2 \tag{G.5.12}$$

Total.Expected.Costs then uses Temp.Expected.Costs.Part1, Temp.Expected.Costs.Part2 and Temp.Expected.Costs.Part3 to estimate expected to-

tal costs across all three stages, i.e. Temp.Expected.Costs represents

$$\tilde{G}_T(\mathbf{d}_1^*, \boldsymbol{\psi}_1^*) = \tilde{F}_{c,1}(\mathbf{d}_1^*|\boldsymbol{\psi}_1^*) + f_{\rho,1}(\mathbf{d}_1^*|\boldsymbol{\psi}_1^*) + \tilde{G}_{T,2,\boldsymbol{\psi}_1}(\mathbf{d}_1^*, \boldsymbol{\psi}_1^*) \tag{G.5.13}$$

An application of the R code to estimate expected total costs across all three stages when a reinforcement decision of 3000 MW B6 and 2000 MW B7a is made in stage 1 is given below.

```
Psi.1<-1
#Define the stage 1 scenario


Expected.Total.Costs.In.Stage1.Onwards(Stage1.C.Em.Wave1,
  Stage2.G.Em.Wave1,Stage1.v.lowers,Stage1.v.uppers,3000,2000,Psi.1)
#An estimate of expected total costs across all 3 stages when making
 a 3000 MW B6 and 2000 MW B7a reinforcement in stage 1
```

Note, there is only one stage 1 scenario to be considered (i.e. where $\boldsymbol{\psi}_1 = 1$) as it is reasonable to assume the stage 1 scenario can be known precisely. Defining the stage 1 scenario as $\boldsymbol{\psi}_1 = 1$ defines uncertainties in stage 1 as described in Section 9.2.3, i.e. such that beliefs about nuclear availability probability in stage 1 form a uniform distribution between 0.55 and 0.85, beliefs about stage 1 CCGT availability probability form a uniform distribution between 0.8 and 0.95, beliefs about stage 1 peak demand magnification form a uniform distribution between 0.95 and 1.05 and so that beliefs about the the scenario that will be observed when the second stage decision is to be made ($p_{\boldsymbol{\psi}_{2|1}}(\boldsymbol{\psi}_2|\boldsymbol{\psi}_1)$) form a uniform distribution between 0.95 and 1.05.

An estimate of optimal stage 1 decision for the fitted emulator models can be acquired using Expected.Total.Costs.In.Stage1.Onwards within the iterative procedure detailed in Section G.4.3.

G.5.6 R Code for Estimating Credible Bounds for the Estimates of Expected Total Costs

Section 9.1.4 described how credible bounds for the estimates of expected total costs across all M stages of the M stage problem can be estimated as a function of the first

stage decision only. This process will present a selection of R code to show how to estimate $\tilde{G}_{T,L,L}(\mathbf{d}_1, \boldsymbol{\psi}_1)$ and $\tilde{G}_{T,U,U}(\mathbf{d}_1, \boldsymbol{\psi}_1)$, i.e. the lower and upper bounds for estimates of expected total costs across all 3 stages of the problem detailed in Section 9.2.

Preliminary Information

Appendix G.4.4 detailed the function Random.Em.Fitter, which is used to fit a randomly drawn version of an emulator model using the set of training data used to fit the emulator model, and a random drawing of the parameters of the polynomial portion of the emulator model, as outlined in Section 5.2.6. For the multi stage problem, it is assumed as a preliminary that the functions Random.Em.Fitter.Stage1, Random.Em.Fitter.Stage2 and Random.Em.Fitter.Stage3 have been defined, which are generalisations of Random.EM.Fitter used to fit randomly drawn versions of the emulator models for mean constraint costs in stages 1, 2 and 3 respectively, for given randomly drawings of the parameters of the polynomial portions of the respective emulator models.

Credible Bounds for Estimates of Expected Total Costs in Stage 3

This sub-subsection will detail the R code for fitting the emulator models $\tilde{G}_{T,3,\boldsymbol{\psi}_3,L}(\mathbf{d}_{T_2}, \boldsymbol{\psi}_3)$ and $\tilde{G}_{T,3,\boldsymbol{\psi}_3,U}(\mathbf{d}_{T_2}, \boldsymbol{\psi}_3)$, i.e. the fitted emulator models which act as lower and upper bounds respectively for $\tilde{G}_{T,3,\boldsymbol{\psi}_3}(\mathbf{d}_{T_2}, \boldsymbol{\psi}_3)$.

Section 9.1.4 notes how these models are fitted by first estimating lower and upper bounds for the expected total costs in stage 3 when making the estimated optimal stage 3 total reinforcement decision, $\mathbf{d}_{3|\theta_{i,3}}$, for each of the sampled stage 2 total reinforcements, $\mathbf{d}_{T_2,\theta_{i,3}}$, and stage 3 scenarios, $\boldsymbol{\psi}_{3,\theta_{i,3}}$, used to fit $\tilde{G}_{T,3,\boldsymbol{\psi}_3}(\mathbf{d}_{T_2}, \boldsymbol{\psi}_3)$.

As noted in Section 9.1.4, such random drawings are calculated by adapting the methodology of Section 5.2.6, the R code for which was detailed in Appendix G.4.4.

An annotated R code to estimate random drawings (and the resulting credible bounds) for $\tilde{F}_{T,3,\theta_{i,3}}$ (the estimate of expected total costs in stage 3 when making the estimated optimal total reinforcement decision, $\mathbf{d}_{3|\theta_{i,3}}$, in stage 3 given that total reinforcement previously made up to stage 2 is $\mathbf{d}_{T_2,\theta_{i,3}}$ and that scenario $\boldsymbol{\psi}_{3,\theta_{i,3}}$ is observed when the

third decision is to be made) is given below. A summary of the code will be given after the code is detailed.

```
RandomDrawSize.Stage3<-200
#Set a number of randomly drawn emulator models to use

Stage3.C.RandomBetasWave1<-mvrnorm(RandomDrawSize.Stage3,
  Stage3.C.Em.Wave1.PolyBeta,Stage3.C.Em.Wave1.PolyBetaCov)
#Randomly draw parameters for the polynomial portion of the stage 3 emulator
 from the multivariate normal distribution

#Stage3.C.RandomBetasWave1 is matrix with RandomDrawSize.Stage3 rows,
 such that the rth row gives the parameters for the polynomial
 portion of the rth randomly drawn model



Stage3.Random.Draws<-matrix(nrow=RandomDrawSize.Stage3,
  ncol=Stage3.G.Em.Sam.Size)
#Create a matrix to store random draws of total stage 3 cost estimates
#The rth row of the ith column will detail the rth random draw
 of the ith decision

Stage3.Random.Draws.Part1<-matrix(nrow=RandomDrawSize.Stage3,
  ncol=Stage3.G.Em.Sam.Size)
#Create a matrix to store random draws of estimates of expected mean
 constraint costs in stage 3
#The rth row of the ith column will detail the rth random draw of
 the ith decision

Stage3.Random.Draws.Part2<-matrix(nrow=1,ncol=Stage3.G.Em.Sam.Size)
#Create a matrix to store the stage 3 reinforcement costs of each decision
#The ith entry of the single row will be the reinforcement costs of
 the ith decision
```

```
#Only a single row is required as the calculation of reinforcement costs
 is assumed to contain no error

for(r in 1:RandomDrawSize.Stage3){

  Temp.Random.Em<-Random.Em.FitterStage3(SampledTrainingInput.Stage3.Wave1.v,
    SampledTrainingInput.Stage3.Wave1.d,SimulatedFullConstraints.Stage3.Wave1,
    Stage3.C.RandomBetasWave1[r,])
  #Fit a randomly drawn emulator model for stage 3 mean constraint costs
   for the rth sample of parameters

  for(i in 1:Stage3.G.Em.Sam.Size){
    sampled.psi3<-Sample.For.Stage3.G.em.psis[i]
    sampled.Stage3.lowers<-c(Stage3.v.lowers.ND,sampled.psi3-0.05)
    sampled.Stage3.uppers<-c(Stage3.v.uppers.ND,sampled.psi3+0.05)
    Stage3.Random.Draws.Part1[r,i]<-ExpectationUnderUncertainty.Psi.m(
      Temp.Random.Em,sampled.Stage3.lowers,sampled.Stage3.uppers,
      Sample.Stage3.G.Opt.Est.decs[i,],Gen.U.Prior.Psi.m,
      RN.Att,sampled.psi3)
  }
  #Estimate expected mean constraint costs for each decision,
   when using the randomly drawn emulator model
}

for(i in 1:Stage3.G.Em.Sam.Size){
  sampled.stage2.r1<-Sample.For.Stage3.G.em.decs[i,1]
  sampled.stage2.r2<-Sample.For.Stage3.G.em.decs[i,2]
  Stage3.Random.Draws.Part2[1,i]<-(Sample.Stage3.G.Opt.Est.decs[i,1]+
    Sample.Stage3.G.Opt.Est.decs[i,2]-sampled.stage2.r1
    -sampled.stage2.r2)*100*AssumedCTR*DiscountFactor^Stage3RStart
}
#Calculate the reinforcement costs of each decision

for(r in 1:RandomDrawSize.Stage3){
```

```
  for(i in 1:Stage3.G.Em.Sam.Size){
    Stage3.Random.Draws[r,i]<-(Stage3.Random.Draws.Part1[r,i]+
      Stage3.Random.Draws.Part2[1,i])
  }
}
#Take the sum of the calculations of reinforcement costs and randomly
 drawn estimates of expected mean constraint costs to calculate
 random drawings of estimates of expected total costs in stage 3



Stage3.Sampled.Opt.Bounds<-CredibleBoundCreator200RD(Stage3.Random.Draws)
#Calculate credible bounds for the estimates of expected total
 costs in stage 3

Stage3.Sampled.Opt.BoundsLB<-Stage3.Sampled.Opt.Bounds[3,]
#Note the lower credible bounds of the 95% credible intervals
Stage3.Sampled.Opt.BoundsUB<-Stage3.Sampled.Opt.Bounds[4,]
#Note the upper credible bounds of the 95% credible intervals
```

In the above code, 200 sets of parameters for the polynomial portion of the emulator model of stage 3 constraint costs are first randomly drawn from a multivariate normal distribution, as Section 5.2.2 describes how beliefs about these variables are represented by a multivariate normal distribution with mean $\hat{\boldsymbol{\beta}}_3$ (denoted Stage3.C.Em.Wave1.PolyBeta in the above R code) described in Equation 5.2.5 and covariance $cov(\hat{\boldsymbol{\beta}}_3)$ (denoted Stage3.C.Em.Wave1.PolyBetaCov in the above R code) described in Equation 5.2.7. These random drawings are subsequently used to estimate random variations of expected total costs in stage 3 as follows.

Stage3.Random.Draws.Part1 represents a matrix where the rth row of the ith column represents the estimate of expected mean constraint costs in stage 3, when using the rth randomly drawn emulator model of stage 3 constraint costs, $\tilde{f}_{c,3,r}(\mathbf{v}_3, \mathbf{d}_{T_3})$, when making total reinforcement decision $\mathbf{d}_{3|\theta_{i,3}}$, in stage 3 (i.e. the estimated optimal stage 3 total reinforcement decision given that total reinforcement $\mathbf{d}_{T_2,\theta_{i,3}}$ was previously made in the second stage and that scenario $\boldsymbol{\psi}_{3,\theta_{i,3}}$ is observed when the third decision

is to be made). That is, Stage3.Random.Draws.Part1[r,i] is

$$\tilde{F}_{c,3,r}(\mathbf{d}_{3|\theta_{i,3}}|\mathbf{d}_{T_2,\theta_{i,3}},\boldsymbol{\psi}_{3,\theta_{i,3}}) = \int_{\mathbf{v}_3} \tilde{f}_{c,3,r}(\mathbf{v}_3,\mathbf{d}_{3|\theta_{i,3}}) \times p(\mathbf{v}_3|\boldsymbol{\psi}_{3,\theta_{i,3}})\mathrm{d}\mathbf{v}_3 \qquad \text{(G.5.14)}$$

Stage3.Random.Draws.Part2 represents a matrix of a single row, where the ith entry in that row represents the reinforcement costs of making total reinforcement decision $\mathbf{d}_{3|\theta_{i,3}}$ in stage 3 given that total reinforcement $\mathbf{d}_{T_2,\theta_{i,3}}$ was previously made in the second stage and that scenario $\boldsymbol{\psi}_{3,\theta_{i,3}}$ is observed when the third decision is to be made, i.e. Stage3.Random.Draws.Part2[1,i] represents $f_{\rho,3}(\mathbf{d}_{3|\theta_{i,3}}|\mathbf{d}_{T_2,\theta_{i,3}},\boldsymbol{\psi}_{3,\theta_{i,3}})$.

Stage3.Random.Draws.Part1 and Stage3.Random.Draws.Part2 are then used to construct Stage3.Random.Draws, which represents the random variations for the estimates of expected total costs in stage 3, such that the rth row of the ith column represents the rth random draw of estimated expected total costs in stage 3 when making the estimated optimal stage 3 total reinforcement decision, $\mathbf{d}_{3|\theta_{i,3}}$, for the ith sampled total stage 2 reinforcement previously made, $\mathbf{d}_{T_2,\theta_{i,3}}$, and the ith sampled stage 3 scenario, $\boldsymbol{\psi}_{3,\theta_{i,3}}$. That is Stage3.Random.Draws[r,i] represents

$$\tilde{F}_{T,3,\theta_{i,3},r} = \tilde{F}_{c,3,r}(\mathbf{d}_{3|\theta_{i,3}}|\mathbf{d}_{T_2,\theta_{i,3}},\boldsymbol{\psi}_{3,\theta_{i,3}}) + f_{\rho,3}(\mathbf{d}_{3|\theta_{i,3}}|\mathbf{d}_{T_2,\theta_{i,3}},\boldsymbol{\psi}_{3,\theta_{i,3}}) \qquad \text{(G.5.15)}$$

The function CredibleBoundCreator200RD is then used to estimate credible bounds of the 95% credible intervals for $\tilde{F}_{T,3,\theta_{i,3},r}$ such that Stage3.Sampled.Opt.BoundsLB denotes the vector of lower bounds (such that the ith entry of Stage3.Sampled.Opt.BoundsLB denotes the estimated lower bound of $\tilde{F}_{T,3,\theta_{i,3},r}$) and Stage3.Sampled.Opt.BoundsUB denotes the vector of upper bounds.

These estimated lower and upper bounds of expected total costs in stage 3 for the sampled stage 2 total reinforcements, $\mathbf{d}_{T_2,\theta_{i,3}}$, and stage 3 scenarios, $\boldsymbol{\psi}_{3,\theta_{i,3}}$, can then be used as a set of N_{θ_3} training runs to fit emulator models $\tilde{G}_{T,3,\boldsymbol{\psi}_3,L}(\mathbf{d}_{T_2},\boldsymbol{\psi}_3)$ and $\tilde{G}_{T,3,\boldsymbol{\psi}_3,U}(\mathbf{d}_{T_2},\boldsymbol{\psi}_3)$ which act as lower and upper bounds respectively for $\tilde{G}_{T,3,\boldsymbol{\psi}_3}(\mathbf{d}_{T_2},\boldsymbol{\psi}_3)$ as outlined in Section 9.1.4. The R code for this is

```
Stage3.G.Em.LB.Wave1.List<-Em.FitterStage3.G(Sample.For.Stage3.G.em.psis,
  Sample.For.Stage3.G.em.decs,Stage3.Sampled.Opt.BoundsLB)
Stage3.G.Em.UB.Wave1.List<-Em.FitterStage3.G(Sample.For.Stage3.G.em.psis,
```

```
  Sample.For.Stage3.G.em.decs,Stage3.Sampled.Opt.BoundsUB)

Stage3.G.Em.LB.Wave1<-Stage3.G.Em.LB.Wave1.List$Fitted.Emulator
Stage3.G.Em.LB.Wave1.PolyBeta<-Stage3.G.Em.LB.Wave1.List$lm.part.beta
Stage3.G.Em.LB.Wave1.PolyBetaCov<-Stage3.G.Em.LB.Wave1.List$lm.part.betacov

Stage3.G.Em.UB.Wave1<-Stage3.G.Em.UB.Wave1.List$Fitted.Emulator
Stage3.G.Em.UB.Wave1.PolyBeta<-Stage3.G.Em.UB.Wave1.List$lm.part.beta
Stage3.G.Em.UB.Wave1.PolyBetaCov<-Stage3.G.Em.UB.Wave1.List$lm.part.betacov
```

such that Stage3.G.Em.LB.Wave1 represents $\tilde{G}_{T,3,\boldsymbol{\psi}_3,L}(\mathbf{d}_{T_2}, \boldsymbol{\psi}_3)$ and Stage3.G.Em.UB.Wave1 represents $\tilde{G}_{T,3,\boldsymbol{\psi}_3,U}(\mathbf{d}_{T_2}, \boldsymbol{\psi}_3)$.

Credible Bounds for Estimates of Expected Total Costs in Stage 2 Onwards

This sub-subsection will detail the R code for fitting the emulator models $\tilde{G}_{T,2,\boldsymbol{\psi}_2,L}(\mathbf{d}_1, \boldsymbol{\psi}_2)$ and $\tilde{G}_{T,2,\boldsymbol{\psi}_2,U}(\mathbf{d}_1, \boldsymbol{\psi}_2)$, i.e. the fitted emulator models which act as lower and upper bounds respectively for $\tilde{G}_{T,2,\boldsymbol{\psi}_2}(\mathbf{d}_1, \boldsymbol{\psi}_2)$.

Section 9.1.4 notes how these models are fitted by first estimating lower and upper bounds for the estimates of expected total costs in stage 2 onwards when making the estimated optimal stage 2 total reinforcement decision, $\mathbf{d}_{2|\theta_{i,2}}$, for each of the sampled stage 1 reinforcements, $\mathbf{d}_{1,\theta_{i,2}}$, and stage 2 scenarios, $\boldsymbol{\psi}_{2,\theta_{i,2}}$, used to fit $\tilde{G}_{T,2,\boldsymbol{\psi}_2}(\mathbf{d}_1, \boldsymbol{\psi}_2)$.

As noted in Section 9.1.4, such random drawings are calculated by adapting the methodology of Section 5.2.6, the R code for which was detailed in Appendix G.4.4.

An annotated R code to estimate random drawings (and the resulting credible bounds) for $\tilde{F}_{T,2,\theta_{i,2}}$ (the estimate of expected total costs in stage 2 onwards when making the estimated optimal total reinforcement decision, $\mathbf{d}_{2|\theta_{i,2}}$, in stage 2 given that the reinforcement made previously in stage 1 is $\mathbf{d}_{1,\theta_{i,2}}$ and that scenario $\boldsymbol{\psi}_{2,\theta_{i,2}}$ is observed when the second decision is to be made) is given below. A summary of the code will be given after the code is detailed.

```
RandomDrawSize.Stage2<-200
#Set a number of randomly drawn emulator models to use
```

```
Stage2.C.RandomBetasWave1<-mvrnorm(RandomDrawSize.Stage2,
  Stage2.C.Em.Wave1.PolyBeta,Stage2.C.Em.Wave1.PolyBetaCov)
#Randomly draw parameters for the polynomial portion of the stage 2 emulator
 from the multivariate normal distribution

#Stage2.C.RandomBetasWave1 is matrix with RandomDrawSize.Stage2 rows,
 such that the rth row gives the parameters for the polynomial
 portion of the rth randomly drawn model

Stage2.Random.Draws.Part1<-matrix(nrow=RandomDrawSize.Stage2,
  ncol=Stage2.G.Em.Sam.Size)
#Create a matrix to store random draws of estimates of expected mean
  constraint costs in stage 2
#The rth row of the ith column will detail the rth random draw of
 the ith decision

Stage2.Random.Draws.Part2<-matrix(nrow=1,ncol=Stage2.G.Em.Sam.Size)
#Create a matrix to store the stage 2 reinforcement costs of each decision
#The ith entry of the single row will be the reinforcement costs
 of the ith decision
#Only a single row is required as the calculation of reinforcement costs
 is assumed to contain no error

Stage2.Random.Draws.Part3L<-matrix(nrow=1,ncol=Stage2.G.Em.Sam.Size)
#Create a matrix to store estimates of expected total costs in stage 3,
 when using the lower bound of the estimate of
 expected stage 3 total costs
#The ith entry of the single row will be the lower bound of the estimate
 of expected total costs in stage 3 when making the
 ith decision in stage 2

Stage2.Random.Draws.Part3U<-matrix(nrow=1,ncol=Stage2.G.Em.Sam.Size)
#Create a matrix to store estimates of expected total costs in stage 3,
```

```
 when using the upper bound of the estimate of
 expected stage 3 total costs
#The ith entry of the single row will be the upper bound of the estimate
 of expected total costs in stage 3 when making the
 ith decision in stage 2

Stage2.Random.DrawsL<-matrix(nrow=1,ncol=Stage2.G.Em.Sam.Size)
#Create a matrix to store random draws of estimates of expected total costs
 in stage 2 onwards when using the lower bound of
 expected total costs in stage 3
#The rth row of the ith column will detail the rth random draw
 of the ith decision

Stage2.Random.DrawsU<-matrix(nrow=1,ncol=Stage2.G.Em.Sam.Size)
#Create a matrix to store random draws of estimates of expected total costs
 in stage 2 onwards when using the upper bound of
 expected total costs in stage 3
#The rth row of the ith column will detail the rth random draw
 of the ith decision

for(r in 1:RandomDrawSize.Stage2){

  Temp.Random.Em<-Random.Em.FitterStage2(
    SampledTrainingInput.Stage2.Wave1.v,SampledTrainingInput.Stage2.Wave1.d,
    SimulatedFullConstraints.Stage2.Wave1,Stage2.C.RandomBetasWave1[r,])
  #Fit a randomly drawn emulator model for mean stage 2 constraint costs
   for the rth sample of parameters

  for(i in 1:Stage2.G.Em.Sam.Size){
    sampled.psi2<-Sample.For.Stage2.G.em.psis[i]
    sampled.Stage2.lowers<-c(Stage2.v.lowers.ND,sampled.psi2-0.05)
    sampled.Stage2.uppers<-c(Stage2.v.uppers.ND,sampled.psi2+0.05)
    Stage2.Random.Draws.Part1[r,i]<-ExpectationUnderUncertainty.Psi.m(
      Temp.Random.Em,sampled.Stage2.lowers,sampled.Stage2.uppers,
```

```
      Sample.Stage2.G.Opt.Est.decs[i,],Gen.U.Prior.Psi.m,
      RN.Att,sampled.psi2)
  }
  #Estimate expected mean constraint costs in stage 2 for each decision,
   when using the randomly drawn emulator model
}


for(i in 1:Stage2.G.Em.Sam.Size){
  sampled.stage1.r1<-Sample.For.Stage2.G.em.decs[i,1]
  sampled.stage1.r2<-Sample.For.Stage2.G.em.decs[i,2]
  Stage2.Random.Draws.Part2[1,i]<-((Sample.Stage2.G.Opt.Est.decs[i,1]+
    Sample.Stage2.G.Opt.Est.decs[i,2]-sampled.stage1.r1-sampled.stage1.r2)*
    100*AssumedCTR*DiscountFactor^Stage2RStart)
}
#Calculate the reinforcement costs of each decision

for(i in 1:Stage2.G.Em.Sam.Size){

  sampled.psi2<-Sample.For.Stage2.G.em.psis[i]
  Stage2.Random.Draws.Part3L[1,i]<-ExpectationUnderUncertainty.Stage.m.G(
    Stage3.G.Em.LB.Wave1,Sample.Stage2.G.Opt.Est.decs[i,],Gen.U.Prior.Psi.m,
    RN.Att,sampled.psi2)

}
#The estimate of expected total costs in stage 3 for each decision,
 using the lower bound of the estimate of expected total costs in stage 3

for(i in 1:Stage2.G.Em.Sam.Size){

  sampled.psi2<-Sample.For.Stage2.G.em.psis[i]
  Stage2.Random.Draws.Part3U[1,i]<-ExpectationUnderUncertainty.Stage.m.G(
    Stage3.G.Em.UB.Wave1,Sample.Stage2.G.Opt.Est.decs[i,],Gen.U.Prior.Psi.m,
    RN.Att,sampled.psi2)
```

```
}
#The estimate of expected total costs in stage 3 for each decision,
 using the upper bound of the estimate of expected total costs in stage 3


for(r in 1:RandomDrawSize.Stage2){
  for(i in 1:Stage2.G.Em.Sam.Size){
    Stage2.Random.DrawsL[r,i]<-(Stage2.Random.Draws.Part1[r,i]+
      Stage2.Random.Draws.Part2[1,i]+Stage2.Random.Draws.Part3L[1,i])
  }
}
#Take the sum of the random draws for expected mean stage 2 constraint
 costs, stage 2 reinforcement costs and the lower bound for expected total
 costs in stage 3


for(r in 1:RandomDrawSize.Stage2){
  for(i in 1:Stage2.G.Em.Sam.Size){
    Stage2.Random.DrawsU[r,i]<-(Stage2.Random.Draws.Part1[r,i]+
      Stage2.Random.Draws.Part2[1,i]+Stage2.Random.Draws.Part3U[1,i])
  }
}
#Take the sum of the random draws for expected mean stage 2 constraint
 costs, stage 2 reinforcement costs and the upper bound for expected total
 costs in stage 3


Stage2.Sampled.Opt.BoundsL<-CredibleBoundCreator200RD(Stage2.Random.DrawsL)
#Calculate credible bounds for the estimates of expected total costs in
 stage 2 onwards when using the lower bound to estimate expected total
 costs in stage 3

Stage2.Sampled.Opt.BoundsU<-CredibleBoundCreator200RD(Stage2.Random.DrawsU)
```

```
#Calculate credible bounds for the estimates of expected total costs in
 stage 2 onwards when using the upper bound to estimate expected total
 costs in stage 3

Stage2.Sampled.Opt.BoundsLLB<-Stage2.Sampled.Opt.BoundsL[3,]
#Note the lower credible bound of the 95% credible intervals of
 Stage2.Sampled.Opt.BoundsL
Stage2.Sampled.Opt.BoundsUUB<-Stage2.Sampled.Opt.BoundsU[4,]
#Note the upper credible bound of the 95% credible intervals of
 Stage2.Sampled.Opt.BoundsU
```

In the above code, 200 sets of parameters for the polynomial portion of the emulator model of stage 2 constraint costs are first randomly drawn from a multivariate normal distribution, as Section 5.2.2 describes how beliefs about these variables are represented by a multivariate normal distribution with mean $\hat{\boldsymbol{\beta}}_2$ (denoted Stage2.C.Em.Wave1.PolyBeta in the above R code) described in Equation 5.2.5 and covariance $cov(\hat{\boldsymbol{\beta}}_2)$ (denoted Stage2.C.Em.Wave1.PolyBetaCov in the above R code) described in Equation 5.2.7. These random drawings are subsequently used to estimate random variations of expected total costs in stage 2 as follows.

Stage2.Random.Draws.Part1 represents a matrix where the rth row of the ith column represents the estimate of expected mean constraint costs in stage 2, when using the rth randomly drawn emulator model of stage 2 constraint costs, $\tilde{f}_{c,2,r}(\mathbf{v}_2, \mathbf{d}_{T_2})$, when making total reinforcement decision $\mathbf{d}_{2|\theta_{i,2}}$, in stage 2 (i.e. the estimated optimal stage 2 total reinforcement decision given that reinforcement decision $\mathbf{d}_{1,\theta_{i,2}}$ was previously made in the first stage and that scenario $\boldsymbol{\psi}_{2,\theta_{i,2}}$ is observed when the second decision is to be made). That is, Stage2.Random.Draws.Part1[r,i] is

$$\tilde{F}_{c,2,r}(\mathbf{d}_{2|\theta_{i,2}}|\mathbf{d}_{1,\theta_{i,2}}, \boldsymbol{\psi}_{2,\theta_{i,2}}) = \int_{\mathbf{v}_2} \tilde{f}_{c,2,r}(\mathbf{v}_2, \mathbf{d}_{2|\theta_{i,2}}) \times p(\mathbf{v}_2|\boldsymbol{\psi}_{2,\theta_{i,2}}) \mathrm{d}\mathbf{v}_2 \qquad \text{(G.5.16)}$$

Stage2.Random.Draws.Part2 represents a matrix of a single row, where the ith entry in that row represents the reinforcement costs of making decision $\mathbf{d}_{2|\theta_{i,2}}$ in stage 2 given that total reinforcement $\mathbf{d}_{1,\theta_{i,2}}$ was previously made in the first stage and that scenario $\boldsymbol{\psi}_{2,\theta_{i,2}}$ is observed when the second decision is to be made,

i.e. Stage2.Random.Draws.Part2[1,i] represents $f_{\rho,2}(\mathbf{d}_{2|\theta_{i,2}}|\mathbf{d}_{1,\theta_{i,2}}, \boldsymbol{\psi}_{2,\theta_{i,2}})$.

Stage2.Random.Draws.Part3L represents a matrix of a single row, detailing estimates of expected total costs in stage 3 of each decision from the emulator model $\tilde{G}_{T,3,\psi_3,L}(\mathbf{d}_{T_2}, \boldsymbol{\psi}_3)$ (the emulator model for the lower bound of the estimates of expected total costs in stage 3). The ith entry in the single row of Stage2.Random.Draws.Part3L represents such an estimate when making the estimated optimal total reinforcement decision $\mathbf{d}_{2|\theta_{i,2}}$ in stage 2 given that the reinforcement decision $\mathbf{d}_{1,\theta_{i,2}}$ was previously made in the first stage and that scenario $\boldsymbol{\psi}_{2,\theta_{i,2}}$ is observed when the second decision is to be made, i.e. Stage2.Random.Draws.Part3L[1,i] represents

$$\tilde{G}_{T,3,\psi_2,L}(\mathbf{d}_{2|\theta_{i,2}}, \boldsymbol{\psi}_{2,\theta_{i,2}}) \;=\; \int_{\boldsymbol{\psi}_3} \tilde{G}_{T,3,\psi_3,L}(\mathbf{d}_{2|\theta_{i,2}}, \boldsymbol{\psi}_3) \times p_{\psi_{3|2}}(\boldsymbol{\psi}_3|\boldsymbol{\psi}_{2,\theta_{i,2}})\mathrm{d}\boldsymbol{\psi}_3 \quad \text{(G.5.17)}$$

Similarly, Stage2.Random.Draws.Part3U represents a matrix of a single row, detailing estimates of expected total costs in stage 3 of each decision from the emulator model $\tilde{G}_{T,3,\psi_3,U}(\mathbf{d}_{T_2}, \boldsymbol{\psi}_3)$ (the emulator model for the lower bound of the estimates of expected total costs in stage 3). The ith entry in the single row of Stage2.Random.Draws.Part3U represents such an estimate when making the estimated optimal total reinforcement decision $\mathbf{d}_{2|\theta_{i,2}}$ in stage 2 given that the reinforcement decision $\mathbf{d}_{1,\theta_{i,2}}$ was previously made in the first stage and that scenario $\boldsymbol{\psi}_{2,\theta_{i,2}}$ is observed when the second decision is to be made, i.e. Stage2.Random.Draws.Part3U[1,i] represents

$$\tilde{G}_{T,3,\psi_2,U}(\mathbf{d}_{2|\theta_{i,2}}, \boldsymbol{\psi}_{2,\theta_{i,2}}) \;=\; \int_{\boldsymbol{\psi}_3} \tilde{G}_{T,3,\psi_3,U}(\mathbf{d}_{2|\theta_{i,2}}, \boldsymbol{\psi}_3) \times p_{\psi_{3|2}}(\boldsymbol{\psi}_3|\boldsymbol{\psi}_{2,\theta_{i,2}})\mathrm{d}\boldsymbol{\psi}_3 \quad \text{(G.5.18)}$$

Stage2.Random.Draws.Part1, Stage2.Random.Draws.Part2, Stage2.Random.Draws.Part3L and Stage2.Random.Draws.Part3U are then used to construct Stage2.Random.DrawsL and Stage2.Random.DrawsU, which represents the random variations for the estimates of expected total costs in stage 2 onwards when using a lower or upper bound to estimate expected total costs in stage 3 respectively, such that the rth row of the ith column represents the rth random draw of estimated expected total costs in stage 2 onwards when making the estimated optimal stage 2 total reinforcement decision, $\mathbf{d}_{2|\theta_{i,2}}$, for the ith sampled stage 1 reinforcement previously made, $\mathbf{d}_{1,\theta_{i,2}}$, and the ith sampled stage 2 scenario, $\boldsymbol{\psi}_{2,\theta_{i,2}}$. That is Stage2.Random.DrawsL[r,i]

represents

$$\tilde{F}_{T,2,\theta_{i,2},L,r} = \tilde{F}_{c,2,r}(\mathbf{d}_{2|\theta_{i,2}}|\mathbf{d}_{1,\theta_{i,2}}, \boldsymbol{\psi}_{2,\theta_{i,2}}) + f_{\rho,2}(\mathbf{d}_{2|\theta_{i,2}}|\mathbf{d}_{1,\theta_{i,2}}, \boldsymbol{\psi}_{2,\theta_{i,2}}) + \tilde{G}_{T,3,\boldsymbol{\psi}_2,L}(\mathbf{d}_{2|\theta_{i,2}}, \boldsymbol{\psi}_{2,\theta_{i,2}}) \tag{G.5.19}$$

and Stage2.Random.DrawsU[r,i] represents

$$\tilde{F}_{T,2,\theta_{i,2},U,r} = \tilde{F}_{c,2,r}(\mathbf{d}_{2|\theta_{i,2}}|\mathbf{d}_{1,\theta_{i,2}}, \boldsymbol{\psi}_{2,\theta_{i,2}}) + f_{\rho,2}(\mathbf{d}_{2|\theta_{i,2}}|\mathbf{d}_{1,\theta_{i,2}}, \boldsymbol{\psi}_{2,\theta_{i,2}}) + \tilde{G}_{T,3,\boldsymbol{\psi}_2,U}(\mathbf{d}_{2|\theta_{i,2}}, \boldsymbol{\psi}_{2,\theta_{i,2}}) \tag{G.5.20}$$

The function CredibleBoundCreator200RD is then used to estimate credible bounds for $\tilde{F}_{T,2,\theta_{i,2},L,r}$ and $\tilde{F}_{T,2,\theta_{i,2},U,r}$ such that Stage2.Sampled.Opt.BoundsL denotes credible bounds for $\tilde{F}_{T,2,\theta_{i,2},L,r}$ and Stage2.Sampled.Opt.BoundsU denotes credible bounds for $\tilde{F}_{T,2,\theta_{i,2},U,r}$. These are in turn used to define Stage2.Sampled.Opt.BoundsLLB, where the ith element of Stage2.Sampled.Opt.BoundsLLB represents the lower credible bound of the 95% credible interval of $\tilde{F}_{T,2,\theta_{i,2},L,r}$, and Stage2.Sampled.Opt.BoundsUUB, where the ith element of Stage2.Sampled.Opt.BoundsUUB represents the upper credible bound at the 95% credible interval of $\tilde{F}_{T,2,\theta_{i,2},U,r}$.

These estimated lower and upper bounds of expected total costs in stage 2 onwards for the sampled stage 1 total reinforcements, $\mathbf{d}_{1,\theta_{i,2}}$, and stage 2 scenarios, $\boldsymbol{\psi}_{2,\theta_{i,2}}$, can then be used as a set of N_{θ_2} training runs to fit emulator models $\tilde{G}_{T,2,\boldsymbol{\psi}_2,L}(\mathbf{d}_1, \boldsymbol{\psi}_2)$ and $\tilde{G}_{T,2,\boldsymbol{\psi}_2,U}(\mathbf{d}_1, \boldsymbol{\psi}_2)$ which act as lower and upper bounds respectively for $\tilde{G}_{T,2,\boldsymbol{\psi}_2}(\mathbf{d}_1, \boldsymbol{\psi}_2)$ as outlined in Section 9.1.4. The R code for this is

```
Stage2.G.Em.LB.Wave1.List<-Em.FitterStage2.G(Sample.For.Stage2.G.em.psis,
  Sample.For.Stage2.G.em.decs,Stage2.Sampled.Opt.BoundsLLB)
Stage2.G.Em.UB.Wave1.List<-Em.FitterStage2.G(Sample.For.Stage2.G.em.psis,
  Sample.For.Stage2.G.em.decs,Stage2.Sampled.Opt.BoundsUUB)


Stage2.G.Em.LB.Wave1<-Stage2.G.Em.LB.Wave1.List$Fitted.Emulator
Stage2.G.Em.LB.Wave1.PolyBeta<-Stage2.G.Em.LB.Wave1.List$lm.part.beta
Stage2.G.Em.LB.Wave1.PolyBetaCov<-Stage2.G.Em.LB.Wave1.List$lm.part.betacov

Stage2.G.Em.UB.Wave1<-Stage2.G.Em.UB.Wave1.List$Fitted.Emulator
```

```
Stage2.G.Em.UB.Wave1.PolyBeta<-Stage2.G.Em.UB.Wave1.List$lm.part.beta
Stage2.G.Em.UB.Wave1.PolyBetaCov<-Stage2.G.Em.UB.Wave1.List$lm.part.betacov
```

such that Stage3.G.Em.LB.Wave1 represents $\tilde{G}_{T,2,\boldsymbol{\psi}_2,L}(\mathbf{d}_1, \boldsymbol{\psi}_2)$ and Stage3.G.Em.UB.Wave1 represents $\tilde{G}_{T,2,\boldsymbol{\psi}_2,U}(\mathbf{d}_1, \boldsymbol{\psi}_2)$.

Credible Bounds for the Estimates of Expected Total Costs Across All 3 Stages

This sub-subsection will detail the R code for estimating credible bounds for estimates of expected total costs across all 3 stages using the methodology outlined in Section 9.1.4. First, create vectors detailing the stage 1 decisions which credible intervals are to be estimated for. The R code for this, as detailed in Appendix G.4.3, is given below

```
Rvec1Temp<-seq(Min.Stage1.B6.Val,Max.Stage1.B6.Val,by=100)
Rvec2Temp<-seq(Min.Stage1.B7.Val,Max.Stage1.B7.Val,by=100)
#Create vectors describing the stage 1 decisions that could be made on either
 boundary to the nearest 100 MW

#These vectors are then used to define two matrices to describe every
 possible combination of B6 and B7a reinforcement
WorkingRvec1Mat<-matrix(nrow=length(Rvec1Temp),ncol=length(Rvec2Temp))
WorkingRvec2Mat<-matrix(nrow=length(Rvec1Temp),ncol=length(Rvec2Temp))
#WorkingRvec1Mat will detail reinforcement of the B6 boundary
#WorkingRvec2Mat will detail reinforcement of the B7a boundary

for(i in 1:length(Rvec1Temp)){
  WorkingRvec1Mat[i,]<-c(rep(Rvec1Temp[i],length(Rvec2Temp)))
}
for(j in 1:length(Rvec2Temp)){
  WorkingRvec2Mat[,j]<-c(rep(Rvec2Temp[j],length(Rvec1Temp)))
}
#The above defines WorkingRvec1Mat such that the jth entry of the ith row
```

```
 is the B6 reinforcement made when making reinforcement
 decisions Rvec1Temp[i] and Rvec2Temp[j]
#Similarly, WorkingRvec2Mat is defined such that the jth entry of the ith row
 is the B7a reinforcement made when making reinforcement
 decisions Rvec1Temp[i] and Rvec2Temp[j]

Stage1Rvec1<-as.vector(WorkingRvec1Mat)
Stage1Rvec2<-as.vector(WorkingRvec2Mat)
#Create vectors from these two matrices

Stage1.Dec.Length.Wave1<-length(Stage1Rvec1)
#Note the number of stage 1 decisions initially considered
```

An annotated R code for estimating credible bounds for the expected total costs across all three stages for the reinforcement decisions detailed in Stage1Rvec1 and Stage1Rvec2 is given below. A summary of the code will then be given.

```
Psi.1<-1
#Detail the stage 1 scenario

RandomDrawSize.Stage1<-200
#Set a number of randomly drawn emulator models to use

Stage1.C.RandomBetasWave1<-mvrnorm(RandomDrawSize.Stage1,
  Stage1.C.Em.Wave1.PolyBeta,Stage1.C.Em.Wave1.PolyBetaCov)
#Randomly draw parameters for the polynomial portion of the stage 1 emulator
 from the multivariate normal distribution

#Stage1.C.RandomBetasWave1 is matrix with RandomDrawSize.Stage1 rows,
 such that the rth row gives the parameters for the polynomial
 portion of the rth randomly drawn model


Stage1.Random.Draws.Part1<-matrix(nrow=RandomDrawSize.Stage1,
```

```
  ncol=Stage1.Dec.Length.Wave1)
#Create a matrix to store random draws of estimates of expected mean
 constraint costs in stage 1
#The rth row of the ith column will detail the rth random draw of
 the ith decision

Stage1.Random.Draws.Part2<-matrix(nrow=1,ncol=Stage1.Dec.Length.Wave1)
#Create a matrix to store the stage 1 reinforcement costs of each decision
#The ith entry of the single row will be the reinforcement costs
 of the ith decision
#Only a single row is required as the calculation of reinforcement costs
 is assumed to contain no error

Stage1.Random.Draws.Part3L<-matrix(nrow=1,ncol=Stage1.Dec.Length.Wave1)
#Create a matrix to store estimates of expected total costs
 in stage 2 onwards, when using the lower bound of the estimate
 of expected total costs in stage 2 onwards
#The ith entry of the single row will be the lower bound of the estimate
 of expected total costs in stage 2 onwards when making the
 ith decision in stage 1

Stage1.Random.Draws.Part3U<-matrix(nrow=1,ncol=Stage1.Dec.Length.Wave1)
#Create a matrix to store estimates of expected total costs
in stage 2 onwards, when using the upper bound of the estimate
of expected total costs in stage 2 onwards
#The ith entry of the single row will be the upper bound of the estimate
 of expected total costs in stage 2 onwards when making the
 ith decision in stage 1

Stage1.Random.DrawsL<-matrix(nrow=1,ncol=Stage1.Dec.Length.Wave1)
#Create a matrix to store random draws of estimates of expected total costs
 in stage 1 onwards when using the lower bound of the estimate of
 expected total costs in stage 2 onwards
#The rth row of the ith column will detail the rth random draw
```

```
 of the ith decision

Stage1.Random.DrawsU<-matrix(nrow=1,ncol=Stage1.Dec.Length.Wave1)
#Create a matrix to store random draws of estimates of expected total costs
 in stage 1 onwards when using the upper bound of the estimate of
 expected total costs in stage 2 onwards
#The rth row of the ith column will detail the rth random draw
 of the ith decision

for(r in 1:RandomDrawSize.Stage1){

  Temp.Random.Em<-Random.Em.FitterStage1(SampledTrainingInput.Stage1.Wave1.v,
    SampledTrainingInput.Stage1.Wave1.d,SimulatedFullConstraints.Stage1.Wave1,
    Stage1.C.RandomBetasWave1[r,])
  #Fit a randomly drawn emulator model for mean stage 1 constraint costs
   for the rth sample of parameters

  for(i in 1:Stage1.Dec.Length.Wave1){
    Stage1.Random.Draws.Part1[r,i]<-ExpectationUnderUncertainty(
      Temp.Random.Em,Stage1.v.lowers,Stage1.v.uppers,c(Stage1Rvec1[i],
      Stage1Rvec2[i]),Gen.U.Prior.Psi.m,RN.Att)
  }
  #Estimate expected mean constraint costs in stage 1 for each decision,
   when using the randomly drawn emulator model
}

for(i in 1:Stage1.Dec.Length.Wave1){
  Stage1.Random.Draws.Part2[1,i]<-((Stage1Rvec1[i]+Stage1Rvec2[i])*
    100*AssumedCTR*DiscountFactor^Stage1RStart)
}
#Calculate the reinforcement costs of each decision

for(i in 1:Stage1.Dec.Length.Wave1){
```

```
  Stage1.Random.Draws.Part3L[1,i]<-ExpectationUnderUncertainty.Stage.m.G(
    Stage2.G.Em.LB.Wave1,c(Stage1Rvec1[i],Stage1Rvec2[i]),
    Gen.U.Prior.Psi.m,RN.Att,Psi.1)

}
#The estimate of expected total costs in stage 2 onwards for each decision,
 using the lower bound of the estimate of expected total costs in
 stage 2 onwards

for(i in 1:Stage1.Dec.Length.Wave1){

  Stage1.Random.Draws.Part3U[1,i]<-ExpectationUnderUncertainty.Stage.m.G(
    Stage2.G.Em.UB.Wave1,c(Stage1Rvec1[i],Stage1Rvec2[i]),
    Gen.U.Prior.Psi.m,RN.Att,Psi.1)

}
#The estimate of expected total costs in stage 2 onwards for each decision,
 using the upper bound of the estimate of expected total costs in
 stage 2 onwards


for(r in 1:RandomDrawSize.Stage1){
  for(i in 1:Stage1.Dec.Length.Wave1){
    Stage1.Random.DrawsL[r,i]<-(Stage1.Random.Draws.Part1[r,i]+
      Stage1.Random.Draws.Part2[1,i]+Stage1.Random.Draws.Part3L[1,i])
  }
}
#Take the sum of the random draws for expected mean stage 1 constraint costs,
 stage 1 reinforcement costs and the lower bound for expected total costs in
 stage 2 onwards


for(r in 1:RandomDrawSize.Stage1){
  for(i in 1:Stage1.Dec.Length.Wave1){
```

```
    Stage1.Random.DrawsU[r,i]<-(Stage1.Random.Draws.Part1[r,i]+
      Stage1.Random.Draws.Part2[1,i]+Stage1.Random.Draws.Part3U[1,i])
  }
}
#Take the sum of the random draws for expected mean stage 1 constraint costs,
 stage 1 reinforcement costs and the upper bound for expected total costs in
 stage 2 onwards

Stage1.Sampled.Opt.BoundsL<-CredibleBoundCreator200RD(Stage1.Random.DrawsL)
#Calculate credible bounds for the estimates of expected total costs in
 stage 1 onwards when using the lower bound to estimate expected total costs
 in stage 2 onwards

Stage1.Sampled.Opt.BoundsU<-CredibleBoundCreator200RD(Stage1.Random.DrawsU)
#Calculate credible bounds for the estimates of expected total costs in
 stage 1 onwards when using the upper bound to estimate expected total costs
 in stage 2 onwards

Stage1.Sampled.Opt.BoundsLLB<-Stage1.Sampled.Opt.BoundsL[3,]
#Note the lower credible bound of the 95% credible intervals of
 Stage1.Sampled.Opt.BoundsL
Stage1.Sampled.Opt.BoundsUUB<-Stage1.Sampled.Opt.BoundsU[4,]
#Note the upper credible bound of the 95% credible intervals of
 Stage1.Sampled.Opt.BoundsU
```

In the above code, 200 sets of parameters for the polynomial portion of the emulator model of stage 1 constraint costs are first randomly drawn from a multivariate normal distribution, as Section 5.2.2 describes how beliefs about these variables are represented by a multivariate normal distribution with mean $\hat{\boldsymbol{\beta}}_1$ (denoted Stage1.C.Em.Wave1.PolyBeta in the above R code) described in Equation 5.2.5 and covariance $cov(\hat{\boldsymbol{\beta}}_1)$ (denoted Stage1.C.Em.Wave1.PolyBetaCov in the above R code) described in Equation 5.2.7. These random drawings are subsequently used to estimate random variations of expected total costs in stage 1 as follows.

Stage1.Random.Draws.Part1 represents a matrix where the rth row of the ith column

represents the estimate of expected mean constraint costs in stage 1, when using the rth randomly drawn emulator model of stage 1 constraint costs, $\tilde{f}_{c,1,r}(\mathbf{v}_1, \mathbf{d}_1)$, when making the ith stage 1 decision detailed in Stage1Rvec1 and Stage1Rvec2. That is Stage1.Random.Draws.Part1[r,i] is

$$\tilde{F}_{c,1,r}(\mathbf{d}^*_{1,i}|\boldsymbol{\psi}_1) = \int_{\mathbf{v}_1} \tilde{f}_{c,1,r}(\mathbf{v}_1, \mathbf{d}^*_{1,i}) \times p(\mathbf{v}_1|\boldsymbol{\psi}_1)\mathrm{d}\mathbf{v}_1 \tag{G.5.21}$$

$\mathbf{d}^*_{1,i}$ represents the first stage decisions defined by Stage1Rvec1[i] (B6 reinforcement magnitude) and Stage1Rvec2[i] (B7a reinforcement magnitude). As noted in Appendix G.5.5, in the first stage it is assumed that there is a single scenario, $\boldsymbol{\psi}_1 = 1$, where beliefs about peak demand magnification in stage 1 are represented by a uniform distribution between 0.95 and 1.05.

Stage1.Random.Draws.Part2 represents a matrix of a single row, where the ith entry in that row represents the reinforcement costs of making decision $\mathbf{d}^*_{1,i}$ in stage 1, i.e. Stage1.Random.Draws.Part2[1,i] represents $f_{\rho,1}(\mathbf{d}^*_{1,i}|\boldsymbol{\psi}_1)$.

Stage1.Random.Draws.Part3L represents a matrix of a single row, where the ith entry of the row details the estimate of expected total costs in stage 2 onwards when making decision $\mathbf{d}^*_{1,i}$ in stage 1 and using the emulator model $\tilde{G}_{T,2,\boldsymbol{\psi}_2,L}(\mathbf{d}_1, \boldsymbol{\psi}_2)$ (the emulator model for the lower bound of the estimates of expected total costs in stage 2 onwards). That is, Stage1.Random.Draws.Part3L[1,i] represents

$$\tilde{G}_{T,2,\boldsymbol{\psi}_1,L}(\mathbf{d}^*_{1,i}, \boldsymbol{\psi}_1) = \int_{\boldsymbol{\psi}_2} \tilde{G}_{T,2,\boldsymbol{\psi}_2,L}(\mathbf{d}^*_{1,i}, \boldsymbol{\psi}_2) \times p_{\boldsymbol{\psi}_{2|1}}(\boldsymbol{\psi}_2|\boldsymbol{\psi}_1)\mathrm{d}\boldsymbol{\psi}_2 \tag{G.5.22}$$

Similarly, Stage1.Random.Draws.Part3U represents a matrix of a single row, where the ith entry of the row details the estimate of expected total costs in stage 2 onwards when making decision $\mathbf{d}^*_{1,i}$ in stage 1 and using the emulator model $\tilde{G}_{T,2,\boldsymbol{\psi}_2,U}(\mathbf{d}_1, \boldsymbol{\psi}_2)$ (the emulator model for the upper bound of the estimates of expected total costs in stage 2 onwards). That is, Stage1.Random.Draws.Part3U[1,i] represents

$$\tilde{G}_{T,2,\boldsymbol{\psi}_1,U}(\mathbf{d}^*_{1,i}, \boldsymbol{\psi}_1) = \int_{\boldsymbol{\psi}_2} \tilde{G}_{T,2,\boldsymbol{\psi}_2,U}(\mathbf{d}^*_{1,i}, \boldsymbol{\psi}_2) \times p_{\boldsymbol{\psi}_{2|1}}(\boldsymbol{\psi}_2|\boldsymbol{\psi}_1)\mathrm{d}\boldsymbol{\psi}_2 \tag{G.5.23}$$

Stage1.Random.Draws.Part1, Stage1.Random.Draws.Part2, Stage1.Random.Draws.Part3L and Stage1.Random.Draws.Part3U are then used to construct Stage1.Random.DrawsL and Stage1.Random.DrawsU, which represents the ran-

dom variations for the estimates of expected total costs across all three stages when using a lower or upper bound to estimate expected total costs in stage 2 onwards respectively, such that the rth row of the ith column represents the rth random draw of estimated expected total costs across all three stages when making the decision $\mathbf{d}^*_{1,i}$. That is Stage1.Random.DrawsL[r,i] represents

$$\tilde{F}_{T,L,r}(\mathbf{d}^*_{1,i}|\boldsymbol{\psi}_1) = \tilde{F}_{c,1,r}(\mathbf{d}^*_{1,i}|\boldsymbol{\psi}_1) + f_{\rho,1}(\mathbf{d}^*_{1,i}|\boldsymbol{\psi}_1) + \tilde{G}_{T,2,\psi_1,L}(\mathbf{d}^*_{1,i}, \boldsymbol{\psi}_1) \tag{G.5.24}$$

and Stage1.Random.DrawsU[r,i] represents

$$\tilde{F}_{T,U,r}(\mathbf{d}^*_{1,i}|\boldsymbol{\psi}_1) = \tilde{F}_{c,1,r}(\mathbf{d}^*_{1,i}|\boldsymbol{\psi}_1) + f_{\rho,1}(\mathbf{d}^*_{1,i}|\boldsymbol{\psi}_1) + \tilde{G}_{T,2,\psi_1,U}(\mathbf{d}^*_{1,i}, \boldsymbol{\psi}_1) \tag{G.5.25}$$

The function CredibleBoundCreator200RD is then used to estimate 95% credible bounds for $\tilde{F}_{T,L,r}(\mathbf{d}^*_{1,i}|\boldsymbol{\psi}_1)$ and $\tilde{F}_{T,U,r}(\mathbf{d}^*_{1,i}|\boldsymbol{\psi}_1)$ such that Stage1.Sampled.Opt.BoundsL denotes credible bounds for $\tilde{F}_{T,L,r}(\mathbf{d}^*_{1,i}|\boldsymbol{\psi}_1)$ and Stage1.Sampled.Opt.BoundsU denotes credible bounds for $\tilde{F}_{T,U,r}(\mathbf{d}^*_{1,i}|\boldsymbol{\psi}_1)$. These are in turn used to define Stage1.Sampled.Opt.BoundsLLB, where the ith element of Stage1.Sampled.Opt.BoundsLLB represents the lower credible bound of the 95% credible interval of $\tilde{F}_{T,L,r}(\mathbf{d}^*_{1,i}|\boldsymbol{\psi}_1)$, and Stage1.Sampled.Opt.BoundsUUB, where the ith element of Stage1.Sampled.Opt.BoundsUUB represents the upper credible bound of the 95% credible interval of $\tilde{F}_{T,U,r}(\mathbf{d}^*_{1,i}|\boldsymbol{\psi}_1)$.

The ith elements of Stage1.Sampled.Opt.BoundsLLB and Stage1.Sampled.Opt.BoundsUUB thus represent the estimated credible bounds for the estimate of expected total costs across all three stages when making decision $\mathbf{d}^*_{1,i}$ in stage 1, using the methodology of Section 9.1.4. These credible bounds could subsequently be used to eliminate stage 1 decisions from consideration, using the methodology of Section 8.2.7, adapting the R code detailed in Appendix G.4.4.